

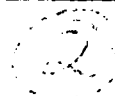
MICROCOPY RESOLUTION TEST CHART
NATIONAL BUREAU OF STANDARDS 1963-A



INSTITUTE
FOR
AEROSPACE STUDIES

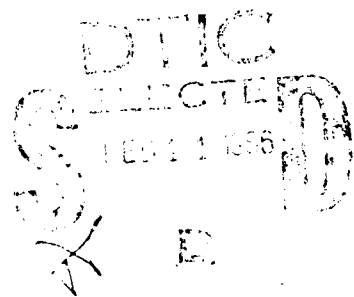
UNIVERSITY OF TORONTO

AFOSR-TR. 85-1231



TABULAR AND GRAPHICAL SOLUTIONS OF REGULAR AND MACH REFLECTIONS
IN PSEUDO-STATIONARY FROZEN AND VIBRATIONAL-EQUILIBRIUM FLOWS

PART 2



by

T. C. J. Hu and M. Shirouzu

AD-A164 047

Approved for public release;
distribution unlimited.

June 1985

UTIAS Report No. 283
CN ISSN 0082-5255

86 2 11 034

UNCLASSIFIED

SECURITY CLASSIFICATION OF THIS PAGE

A-D-116-407

REPORT DOCUMENTATION PAGE

1a. REPORT SECURITY CLASSIFICATION Unclassified		1b. RESTRICTIVE MARKINGS	
2a. SECURITY CLASSIFICATION AUTHORITY		3. DISTRIBUTION/AVAILABILITY OF REPORT Approved for public release; distribution unlimited.	
2b. DECLASSIFICATION/DOWNGRADING SCHEDULE			
4. PERFORMING ORGANIZATION REPORT NUMBER(S) UTIAS Report No. 283 (in two parts)		5. MONITORING ORGANIZATION REPORT NUMBER(S) AFOSR-TR- 87-128	
6a. NAME OF PERFORMING ORGANIZATION University of Toronto, Inst. for Aerospace Studies	6b. OFFICE SYMBOL (If applicable)	7a. NAME OF MONITORING ORGANIZATION AFOSR/NA	
6c. ADDRESS (City, State and ZIP Code) 4925 Dufferin Street, Downsview, Ontario, Canada M3H 5T6		7b. ADDRESS (City, State and ZIP Code) Building 410 Bolling AFB, DC 20332-6448	
8a. NAME OF FUNDING/SPONSORING ORGANIZATION Air Force Office of Scientific Research/NA	8b. OFFICE SYMBOL (If applicable) AFOSR/NA	9. PROCUREMENT INSTRUMENT IDENTIFICATION NUMBER AF-AFOSR 82-0096	
8c. ADDRESS (City, State and ZIP Code) Bldg. 410, Bolling Air Force Base, DC 20332, U.S.A.		10. SOURCE OF FUNDING NOS.	
		PROGRAM ELEMENT NO. 61102F	PROJECT NO. 2307
		TASK NO. A1	WORK UNIT NO.
11. TITLE (Include Security Classification) Tabular and Graphical Solutions of Regular and Mach Reflections in			
12. PERSONAL AUTHOR(S) Pseudo-Stationary Frozen and Vibrational-Equilibrium Flows, Part 2 T. C. J. Hu and M. Shirouzu			
13a. TYPE OF REPORT Interim	13b. TIME COVERED FROM _____ TO _____	14. DATE OF REPORT (Yr., Mo., Day) 1985, June	15. PAGE COUNT 352
16. SUPPLEMENTARY NOTATION			
17. COSATI CODES		18. SUBJECT TERMS (Continue on reverse if necessary and identify by block number)	
FIELD	GROUP	SUB. GR.	
		Oblique-shock-wave reflections; regular reflection; Mach reflection; numerical and graphical solutions; frozen and equilibrium flows.	
19. ABSTRACT (Continue on reverse if necessary and identify by block number)			
Flow properties of pseudo-stationary oblique-shock-wave reflections are given as solutions of two-shock and three-shock theories. The calculations were performed for Ar, air, CO ₂ and SF ₆ using both frozen and vibrational equilibrium gas assumptions. The flow properties are tabulated for initial shock Mach numbers $1.2 < M_s < 10.0$ and wedge angles $1^\circ < \theta_w < 85^\circ$. The flow properties are plotted as a function of the incident shock Mach number for a series of wedge angles for both regular and Mach reflections. Another set of graphs is presented for Mach reflection with the flow properties plotted against the effective wedge angle θ_w' for a series of shock Mach numbers. The latter set is used when the effective wedge angle is chosen as the parameter for comparison. The second triple-point system, which exists only in double-Mach reflection, is solved numerically for the first time, and the solutions are presented both in tabular and graphical forms. The tables and graphs are designed to serve the analyst and experimenter working on oblique-shock-wave reflections.			
20. DISTRIBUTION/AVAILABILITY OF ABSTRACT UNCLASSIFIED/UNLIMITED <input checked="" type="checkbox"/> SAME AS RPT. <input type="checkbox"/> RIC USERS <input type="checkbox"/>		21. ABSTRACT SECURITY CLASSIFICATION Unclassified	
22a. NAME OF RESPONSIBLE INDIVIDUAL JAMES D WILSON		22b. TELEPHONE NUMBER (Include Area Code) (202) 767-4935	22c. OFFICE SYMBOL AFOSR/NA

DD FORM 1473, 83 APR

EDITION OF 1 JAN 73 IS OBSOLETE.

UNCLASSIFIED
SECURITY CLASSIFICATION OF THIS PAGE

TABULAR AND GRAPHICAL SOLUTIONS OF REGULAR AND MACH REFLECTIONS
IN PSEUDO-STATIONARY FROZEN AND VIBRATIONAL-EQUILIBRIUM FLOWS

PART 2

by

T. C. J. Hu and M. Shirouzu

Submitted October 1984

AIR FORCE OFFICE OF SCIENTIFIC RESEARCH (AFOSR)
NOTICE OF CHANGE OF STATUS
This report is the property of the AFOSR
and is loaned to you. It and its contents
are not to be distributed outside your
organization.
DATE: _____
NAME: _____
Chief, Technical Information Division

June 1985

UTIAS Report No. 283
CN ISSN 0082-5255

Table of Contents

PART 1

Acknowledgements ii
Summary iii
Notation v
1. INTRODUCTION 1
2. METHOD OF CALCULATION 1
3. REMARKS 6
4. DISCUSSIONS 7
5. WORKED EXAMPLES 18
6. CONCLUSIONS 19
REFERENCES 21

TABLE 1. γ_0 , T_k and n_k of Relevant Gases

FIG. 1. Regions and angles in RR and MR

FIG. 2. The Analogy between the Two Triple-Point Wave System
in a Double-Mach Reflection

LIST OF TABLES

LIST OF FIGURES

TABLES: T-1 to T-120

FIGURES: F-1 to F-120

PART 2

FIGURES: F-121 to F-320

APPENDIX A : Actual Sidewall Pressure Histories and Numerical Results; *1.1*

APPENDIX B : Computer-Program Listing for the Analytical Solution of
Regular and Mach Reflections. *(1.1)*

1.1-15-A164046

1.1-15-A164046

Notation

Notations used in tables are shown in parentheses.

a	sound speed (A)
Ar	argon
CO ₂	carbon dioxide
h	specific enthalpy
K	kink
M	Mach number (relative to P or T unless otherwise indicated) (MACH)
m	molecular weight
MR	Mach reflection
M _s	incident shock Mach number (MACHS)
n _k	number of modes in mode k
N ₂	nitrogen
O ₂	oxygen
P	reflection point
p	pressure (P)
R	universal gas constant
RR	regular reflection
SF ₆	sulphur hexafluoride
T	temperature
T	triple point
T'	second triple point
T _k	characteristic temperature of mode k
u	flow velocity
γ	specific heat ratio
γ _p	specific heat ratio of perfect gas
γ _o	specific heat ratio of frozen gas

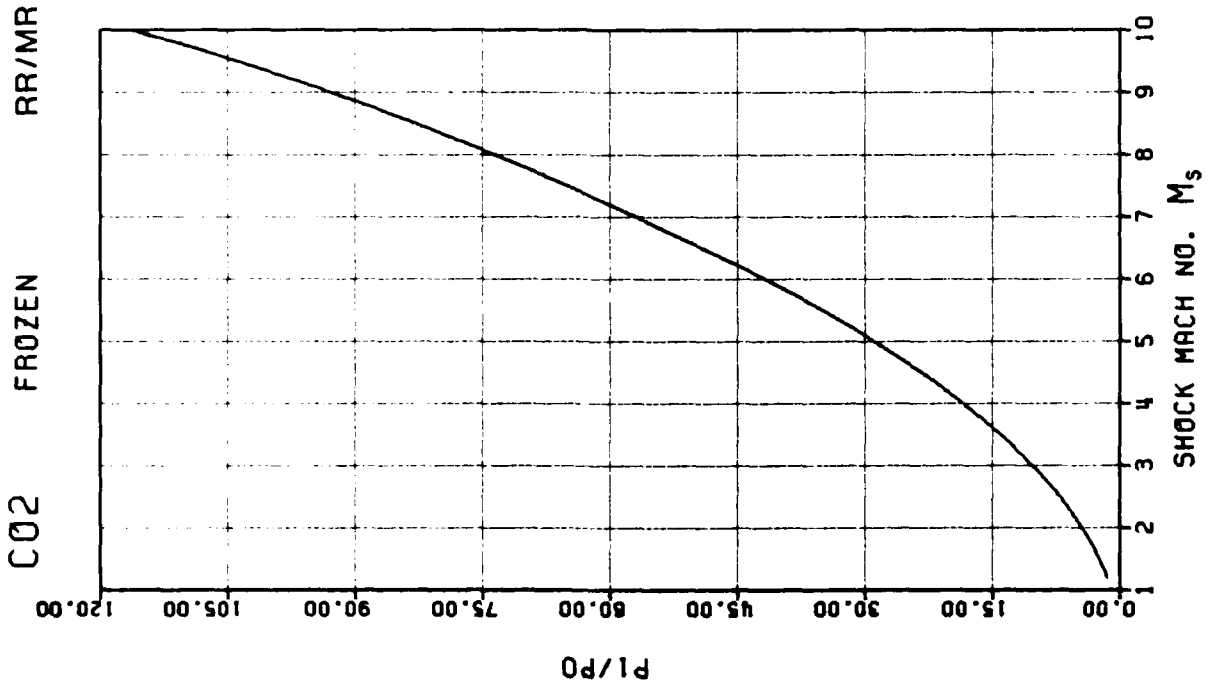
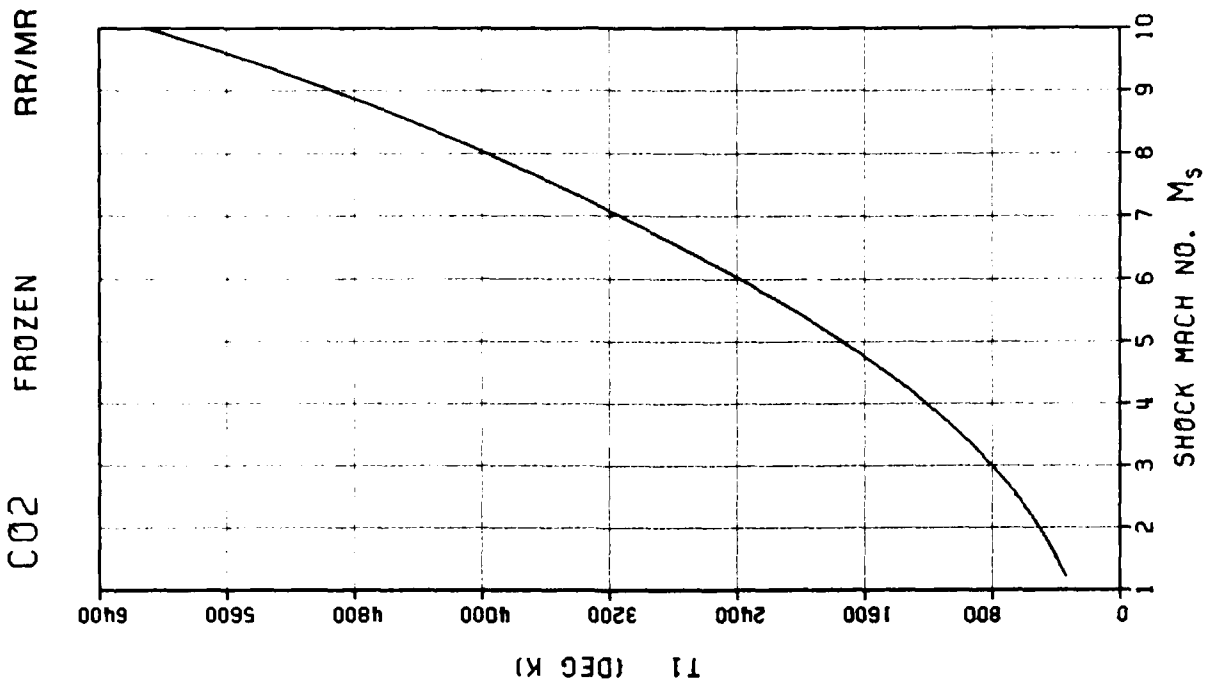
Accession For	
NTIS CRA&I	<input checked="" type="checkbox"/>
DTIC TAB	<input type="checkbox"/>
Unannounced	<input type="checkbox"/>
Justification	
By	
Distribution /	
Availability Codes	
Dist	Avail and/or Special
A-1	

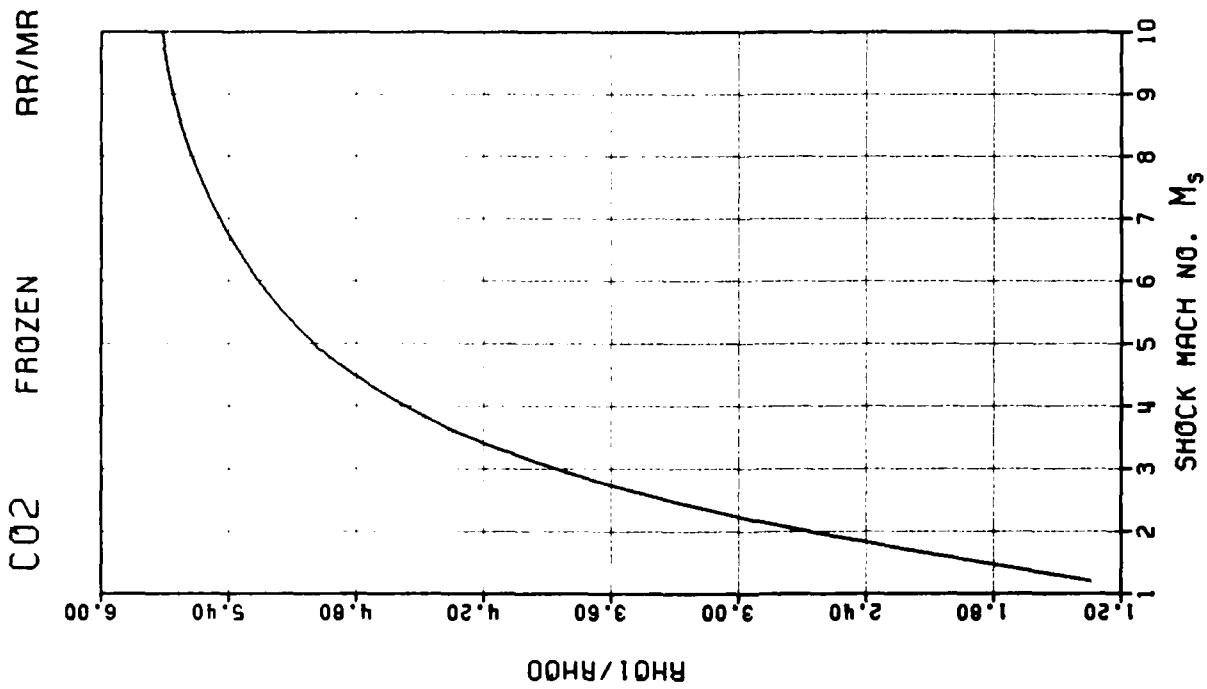
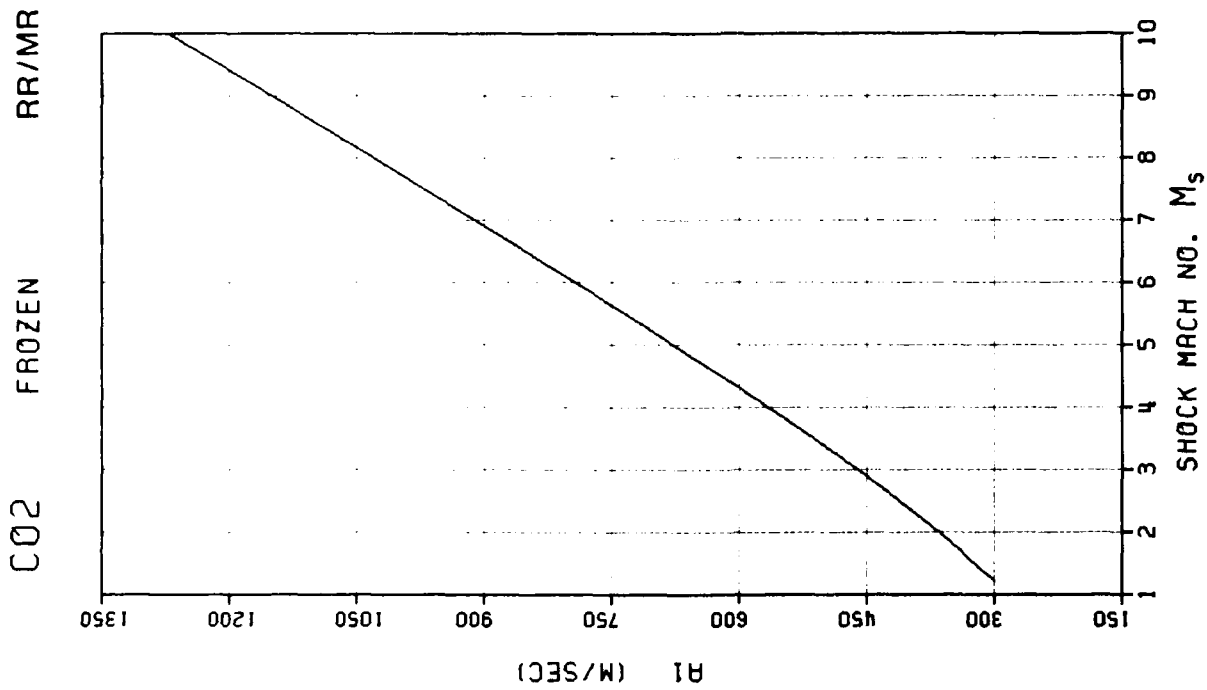


ξ angle between incident shock wave and reflected shock wave at triple point (DELTA)
 η angle between reflected shock wave and second Mach stem (ETA)
 θ deflection angle of flow from its original direction while passing through a shock wave (THETA)
 θ_w actual wedge angle (THETA WALL)
 θ'_w effective wedge angle (THETA WALL PRIME)
 ξ angle between the two reflected shock waves R and R' in region (1) (XI)
 ρ density (RHO)
 ϕ incident wave angle (PHI)
 χ triple-point-trajectory angle (CHI)
 χ' second-triple-point-trajectory angle (CHI PRIME)
 ω' angle between reflected shock wave and wedge surface (in RR) or triple-point-trajectory (in MR) (OMEGA PRIME)

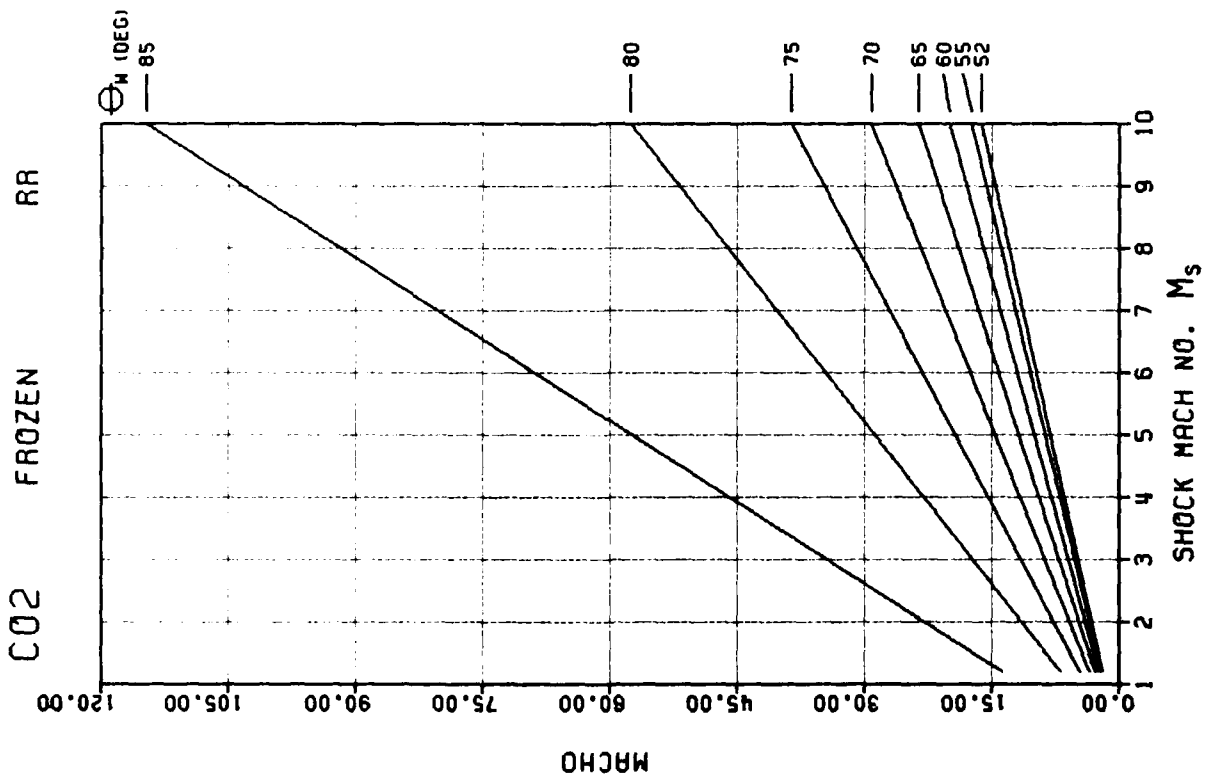
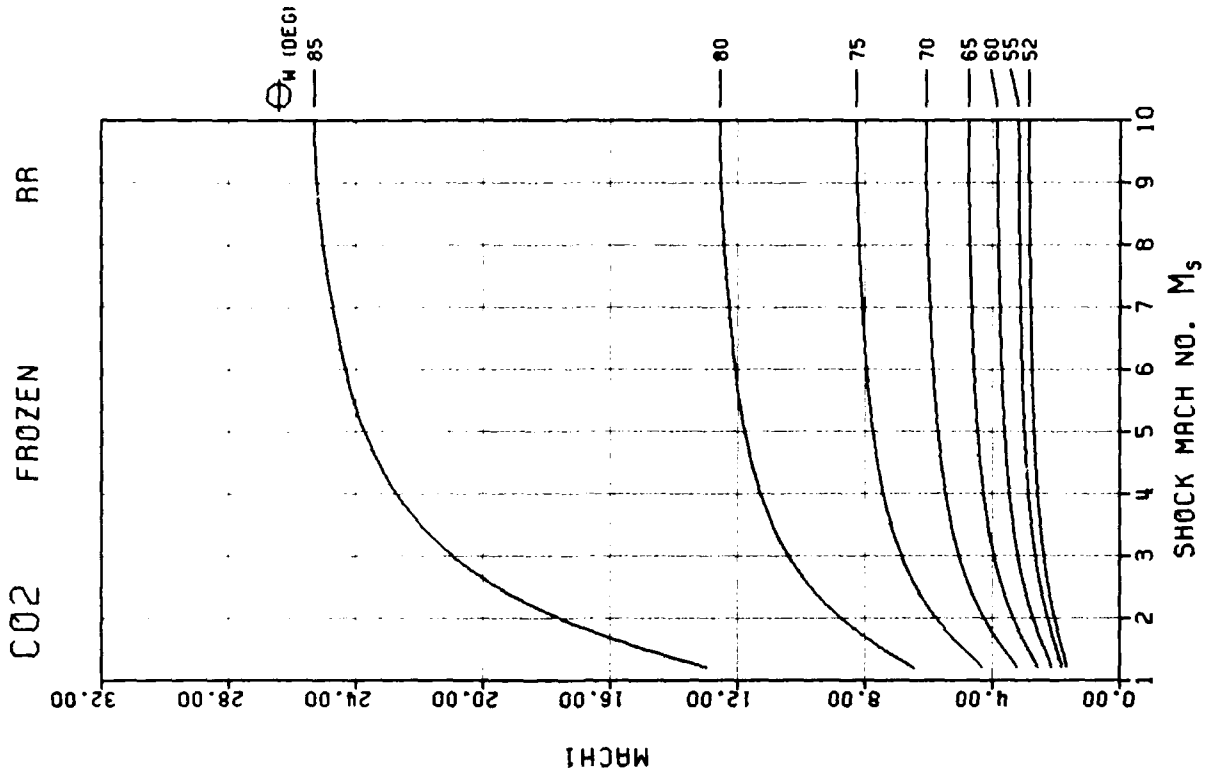
Subscripts

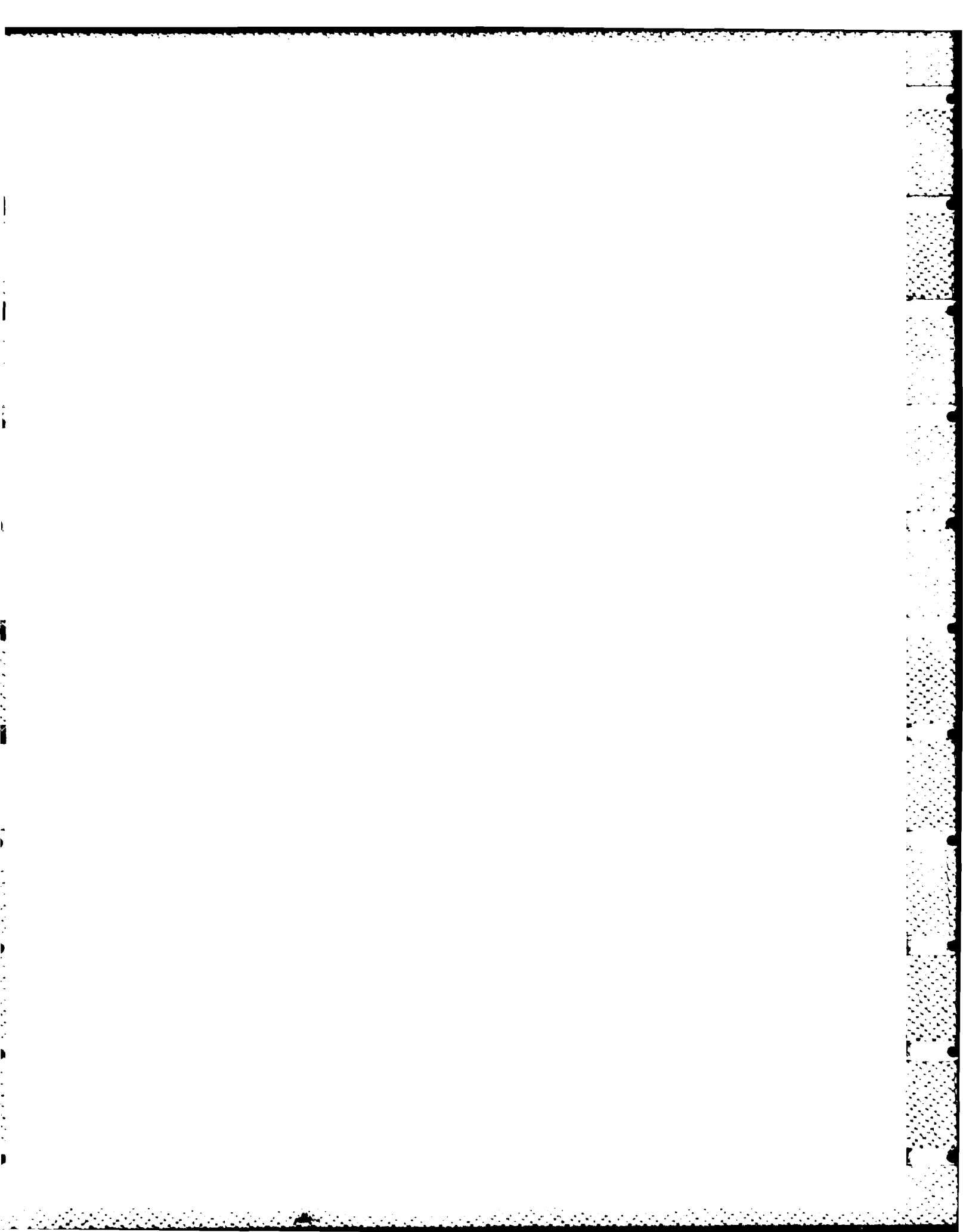
0, 1, 2, 3 regions 0, 1, 2, 3 (0, 1, 2, 3)

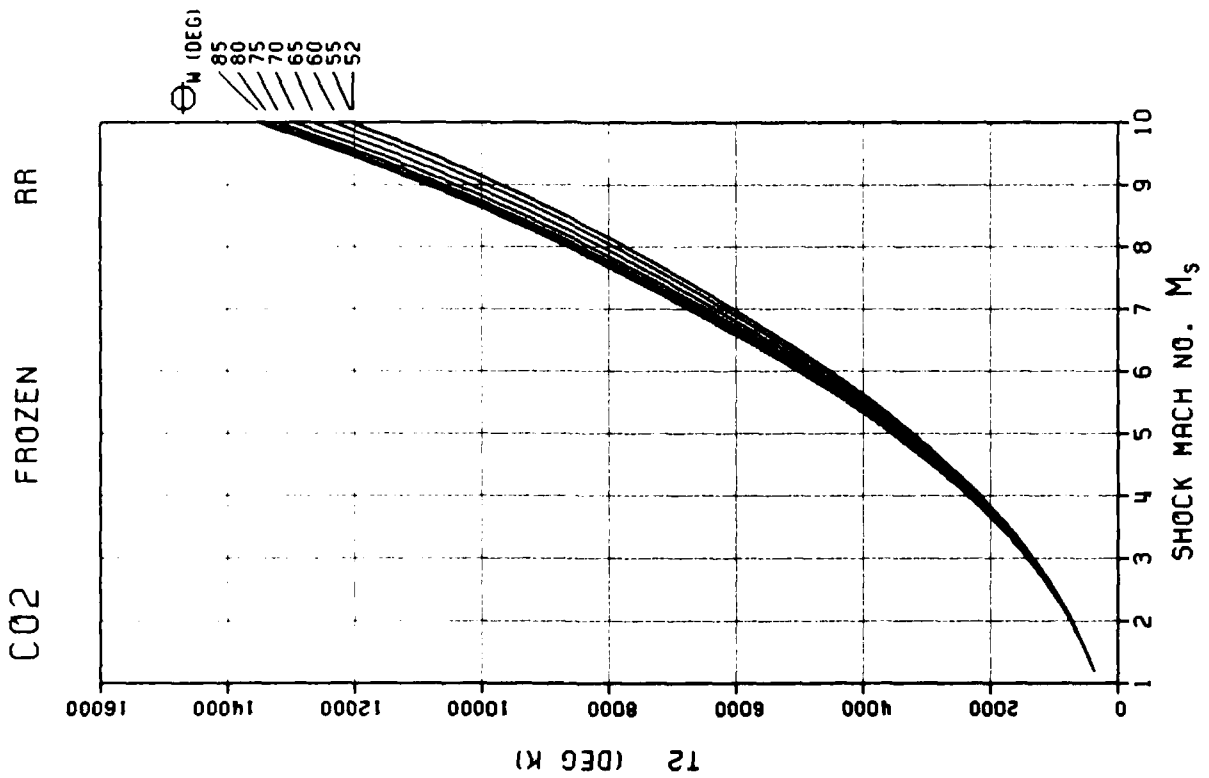
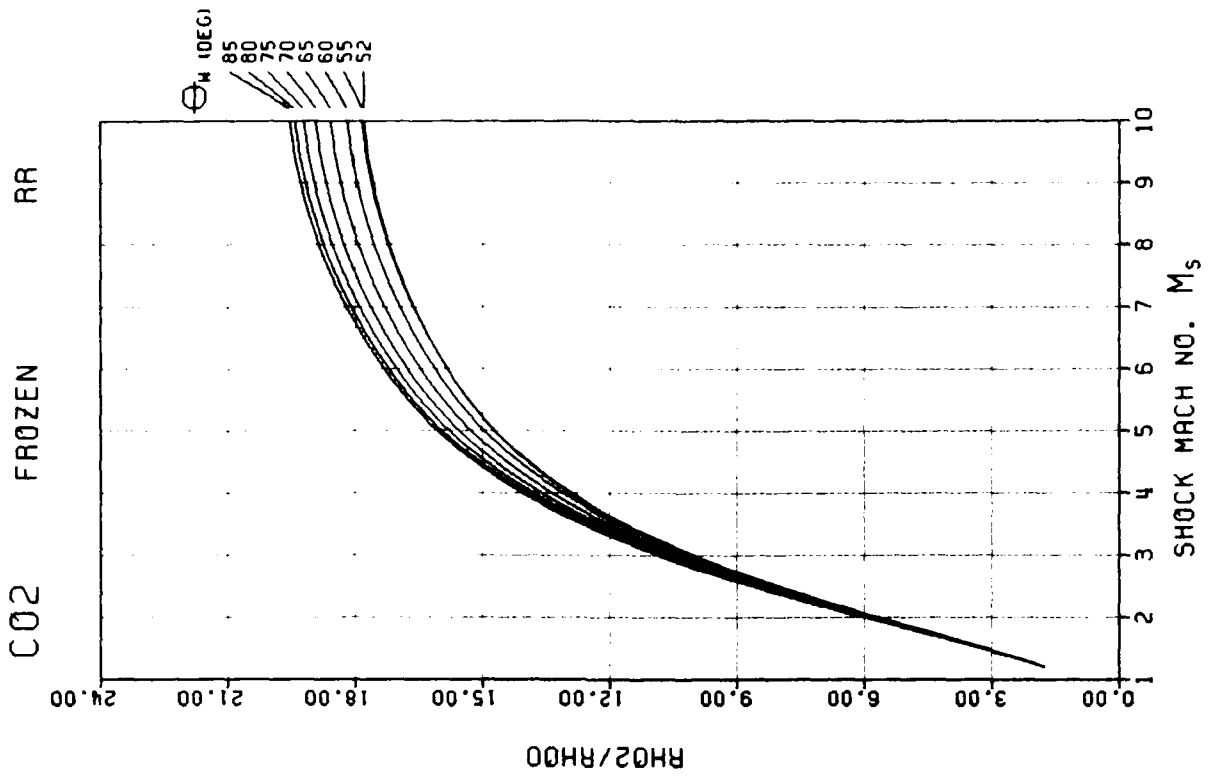


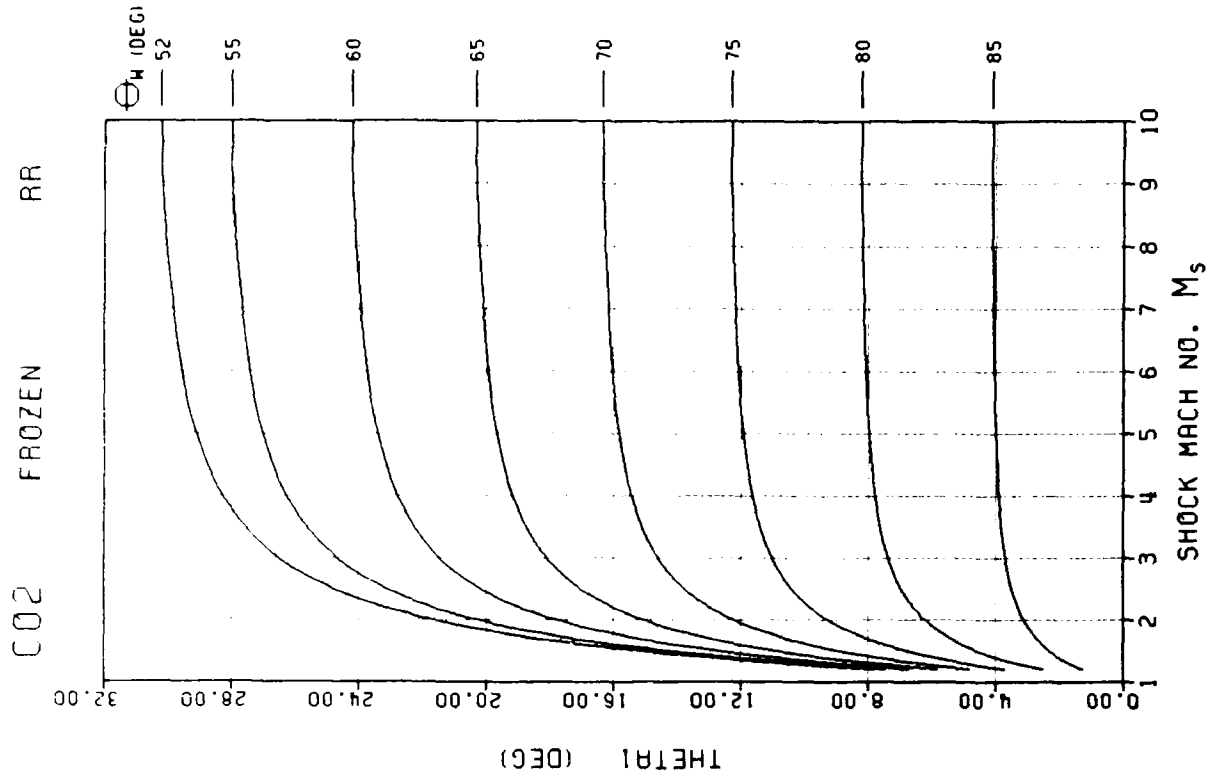
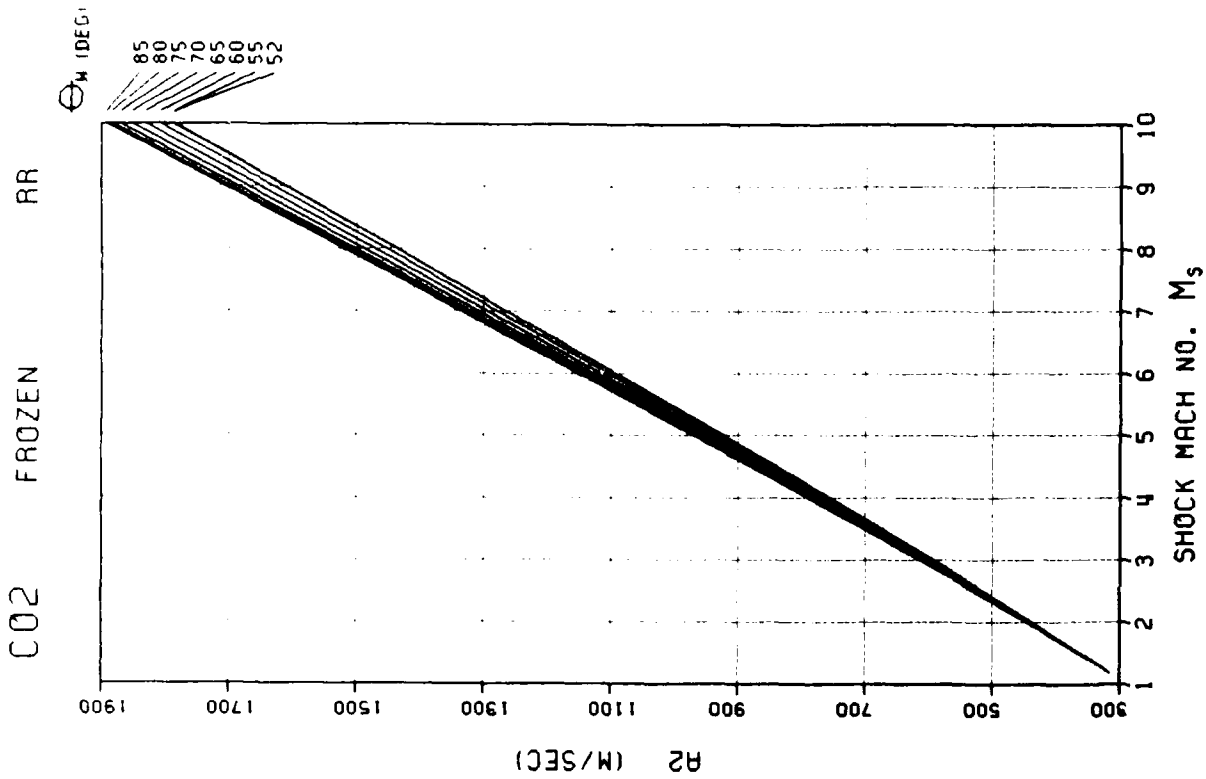


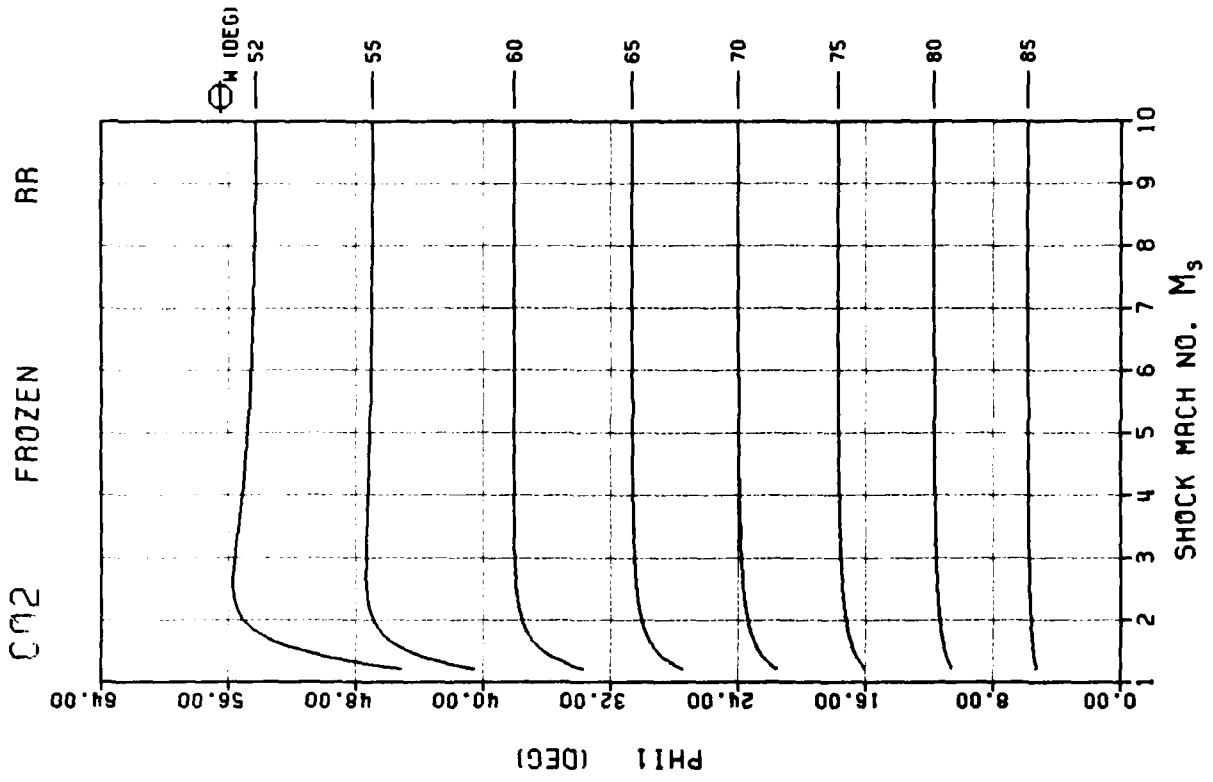
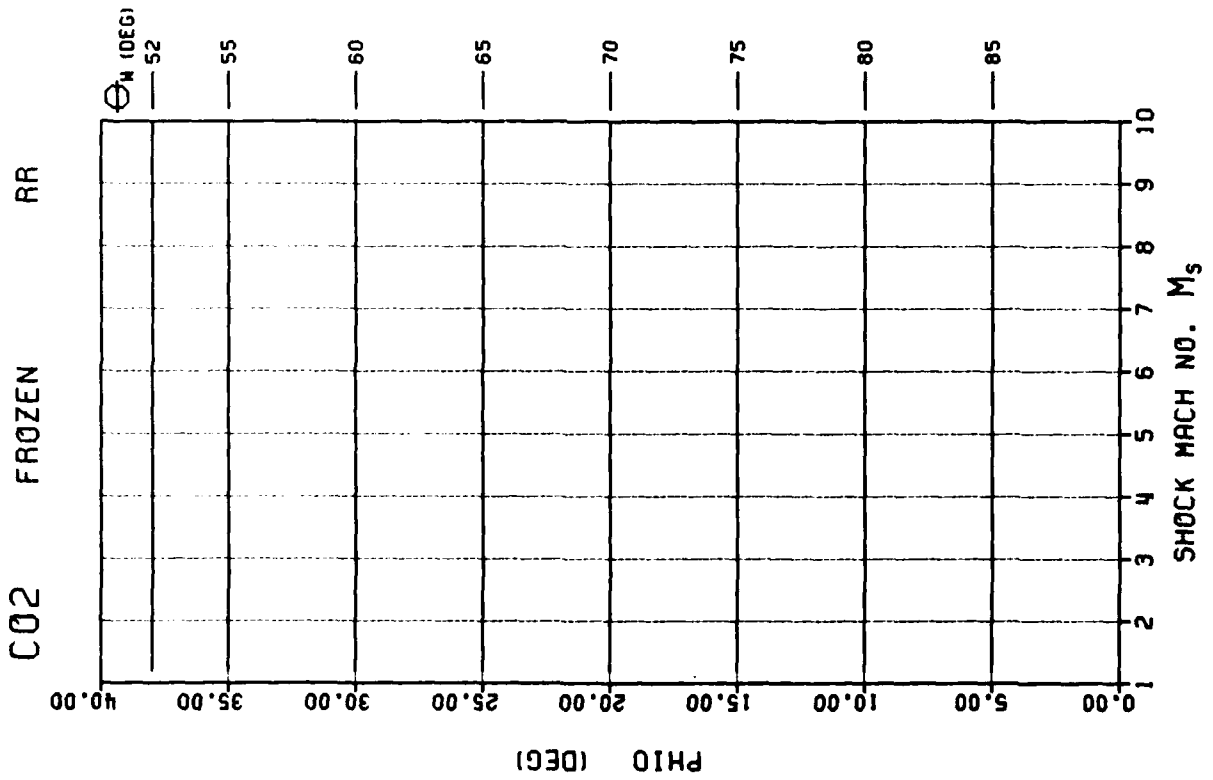
F - 122

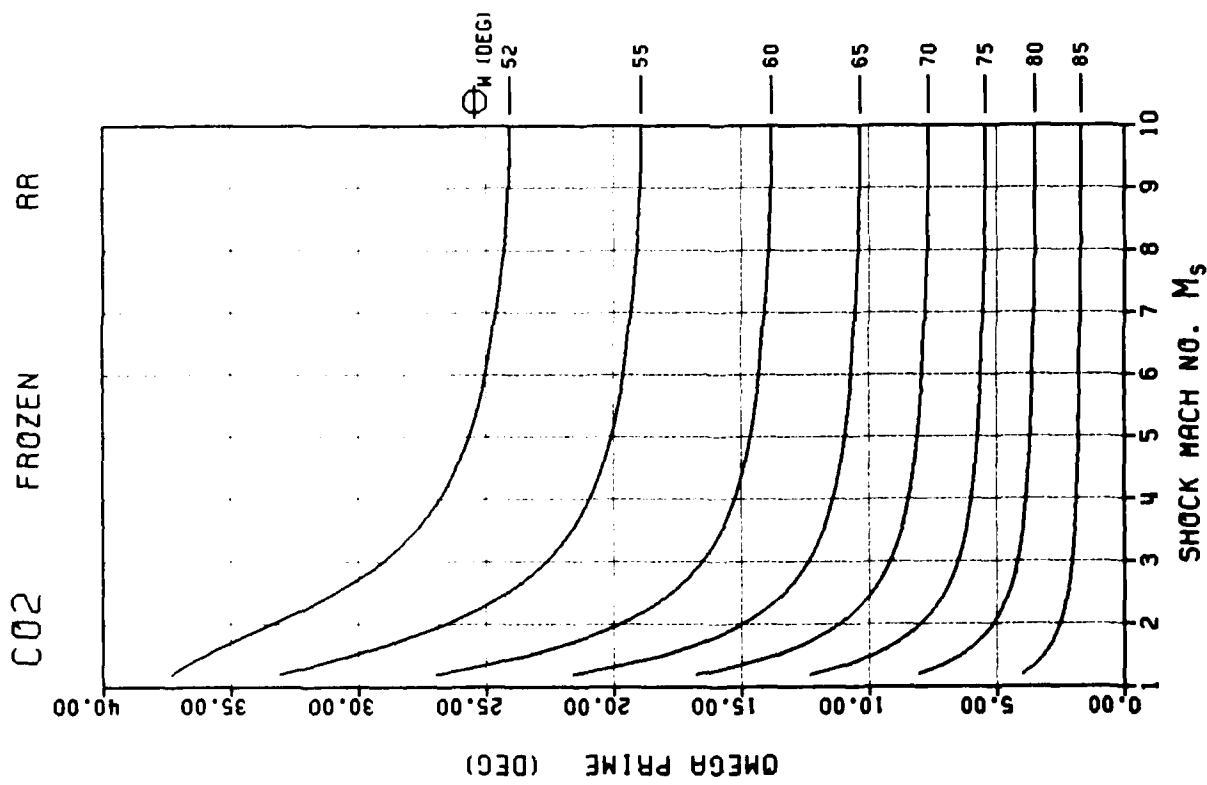
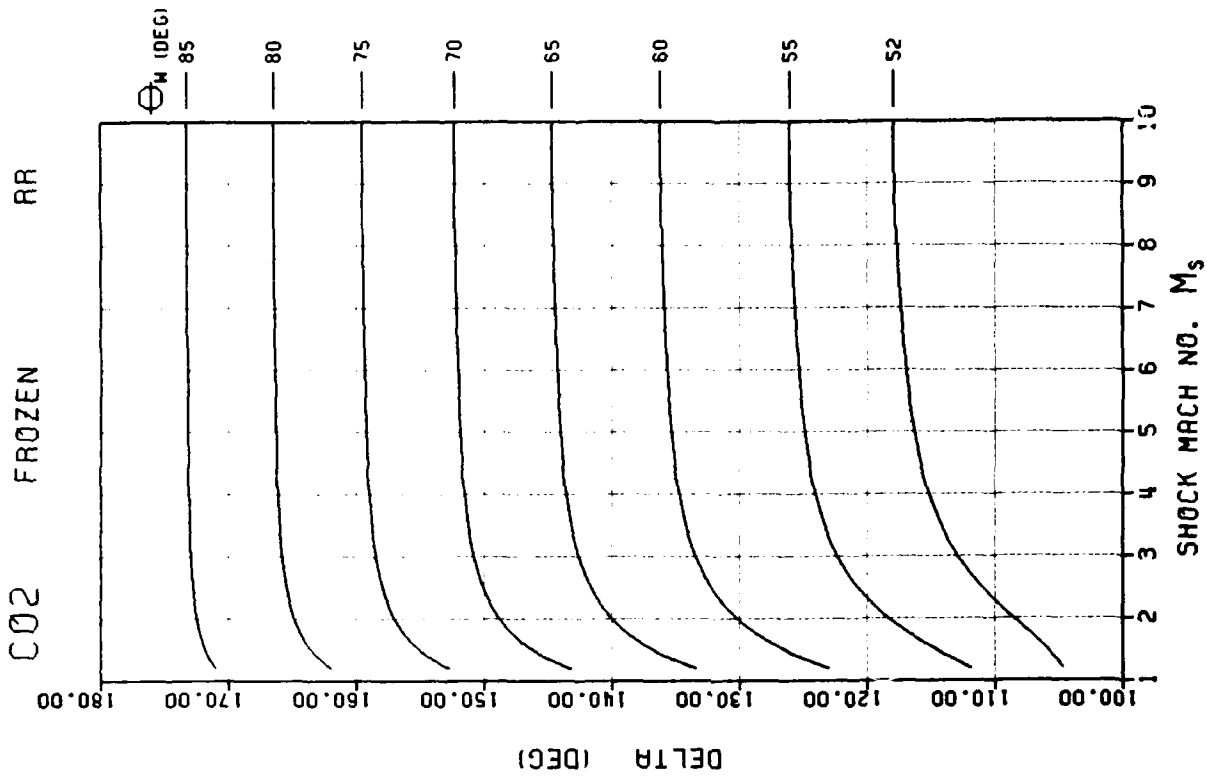


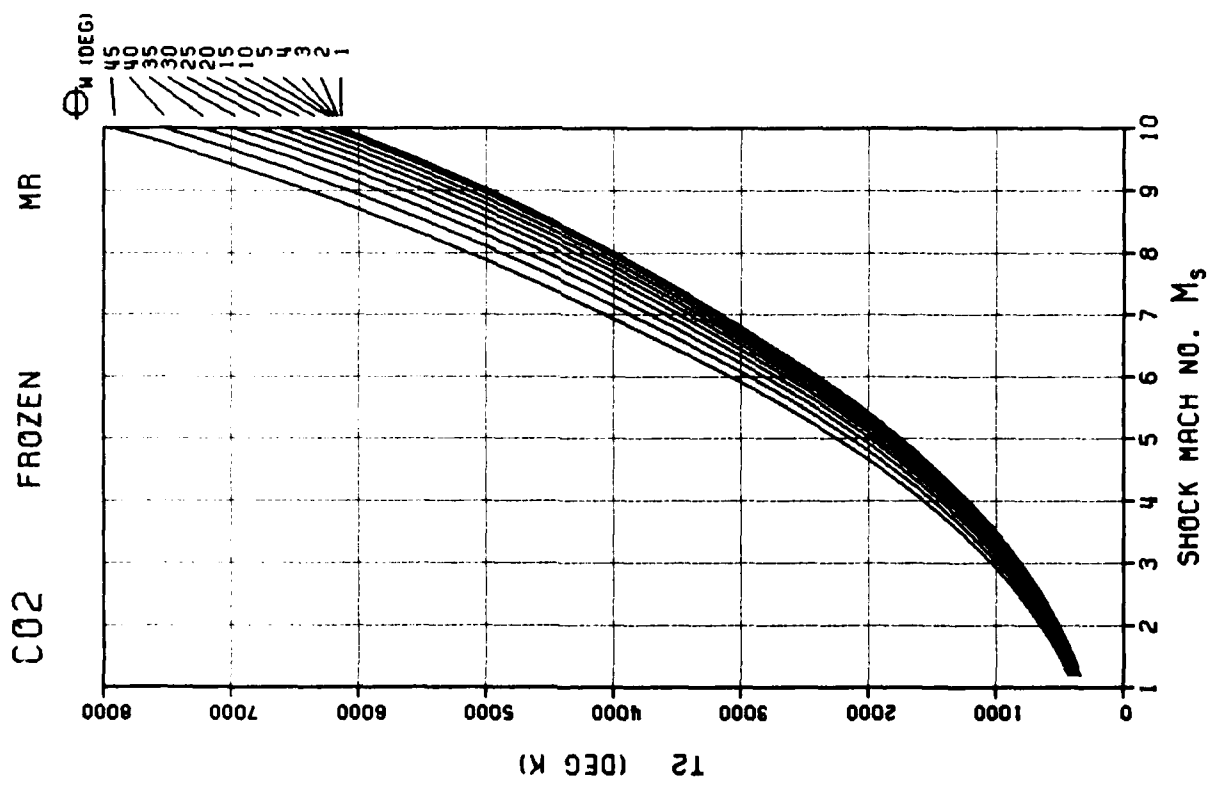
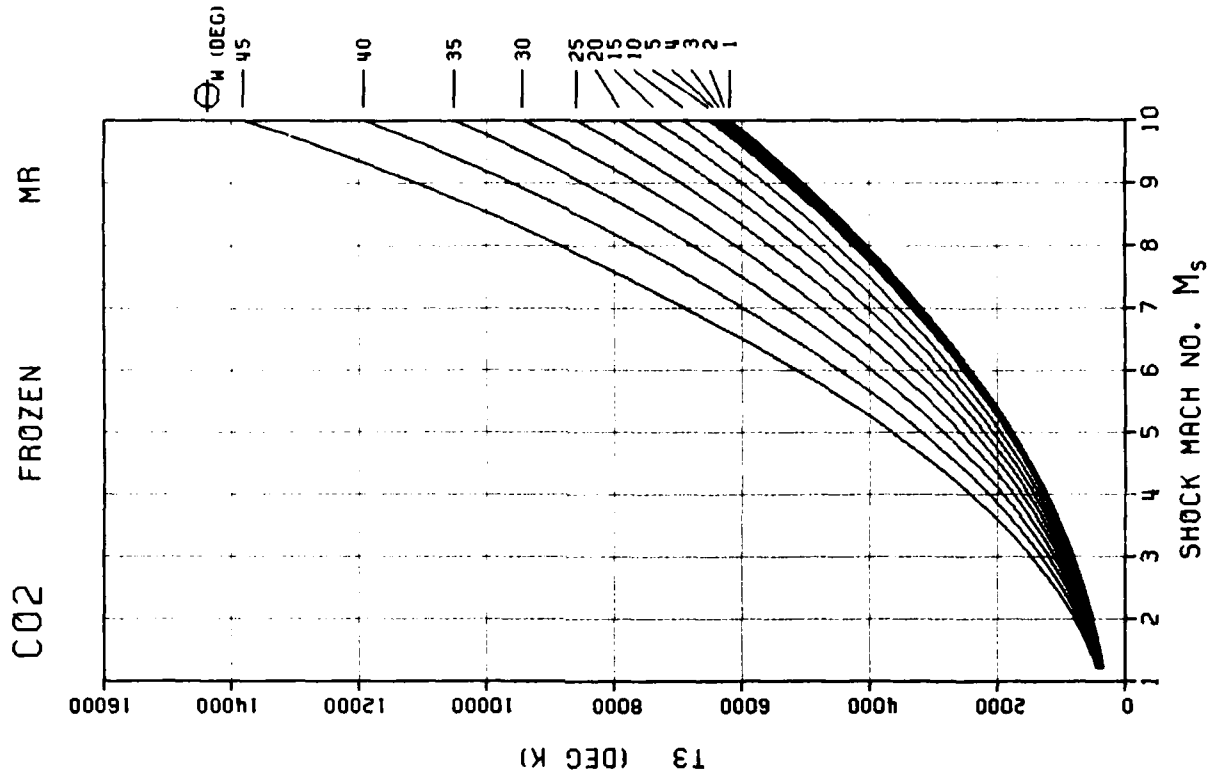


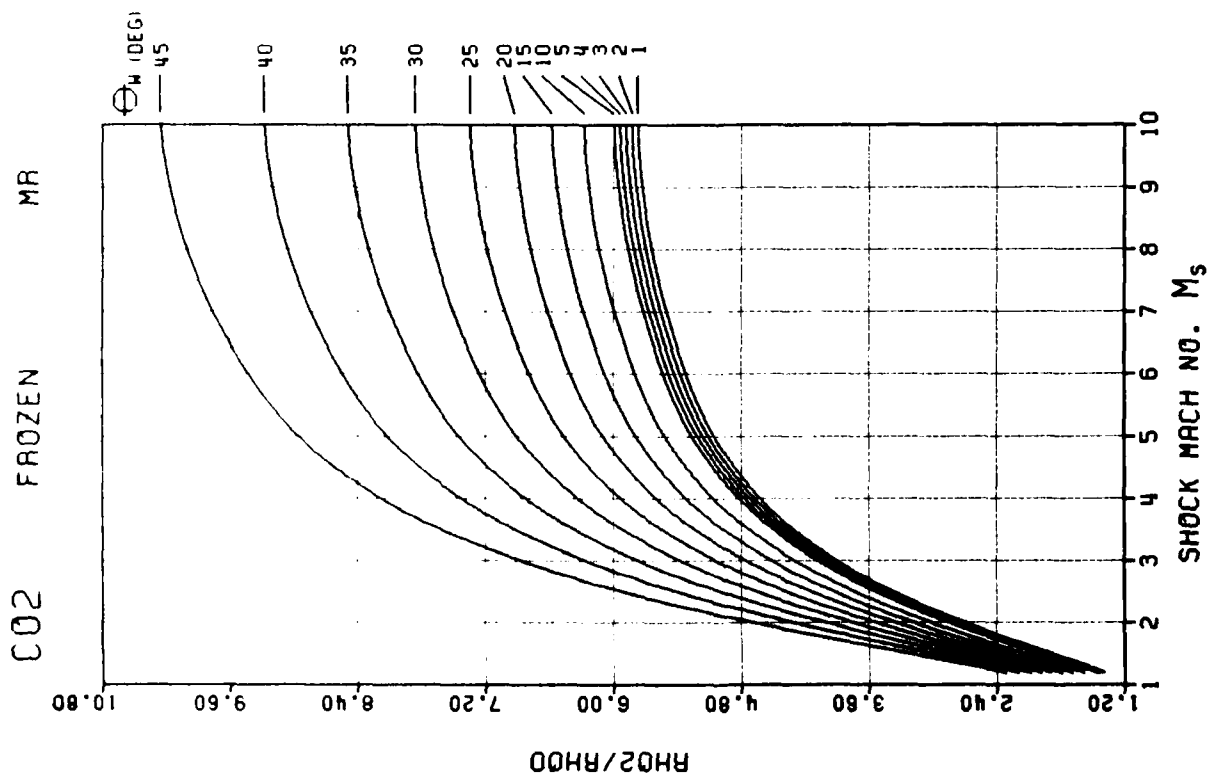
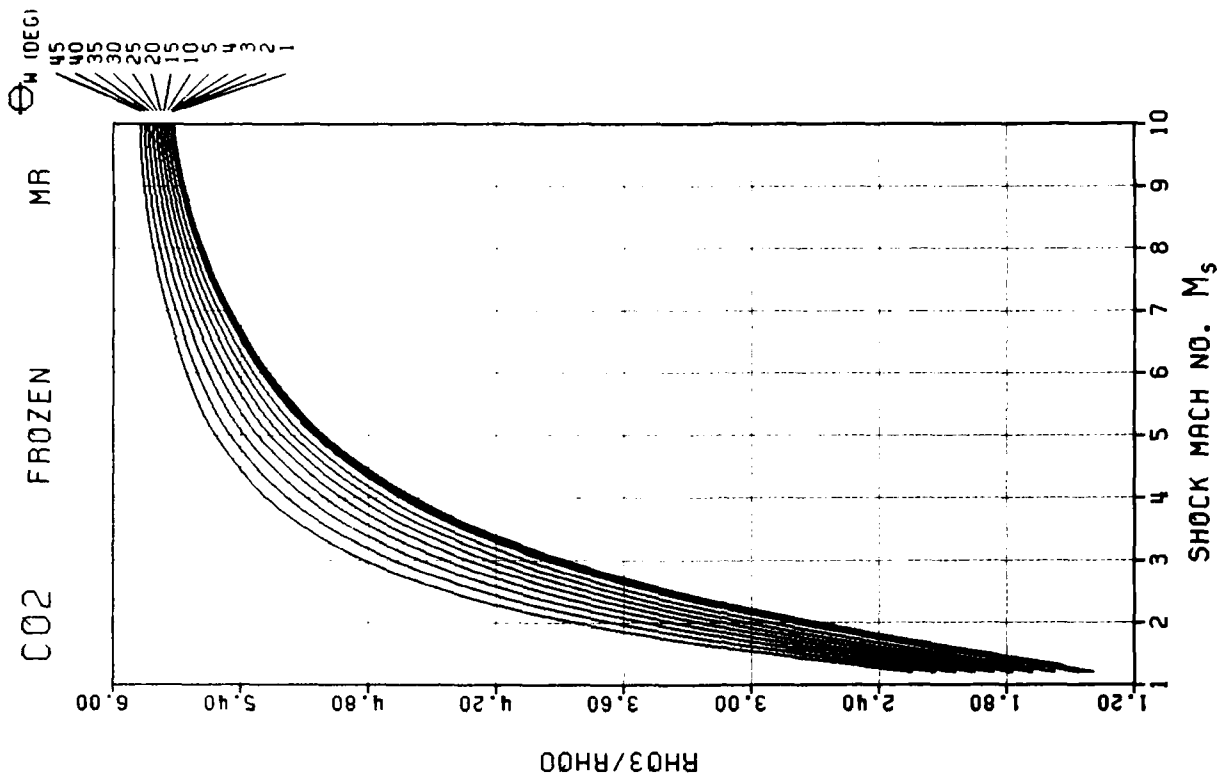


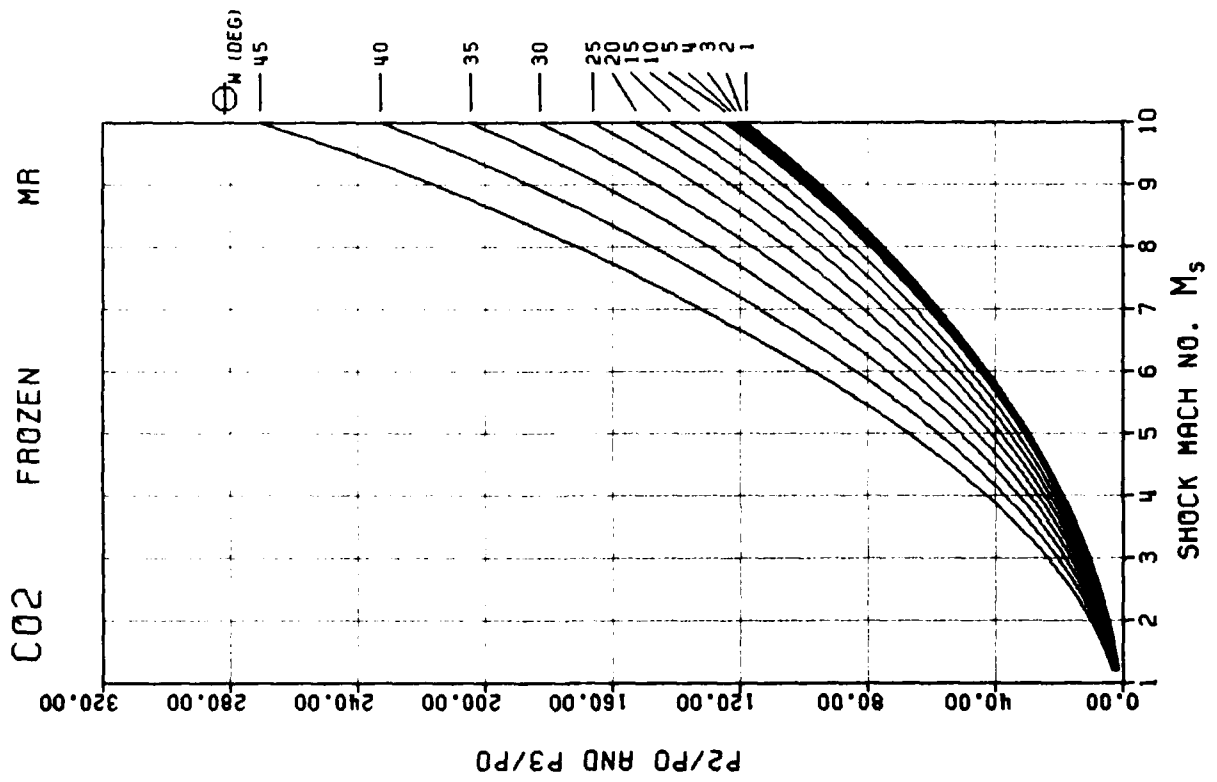
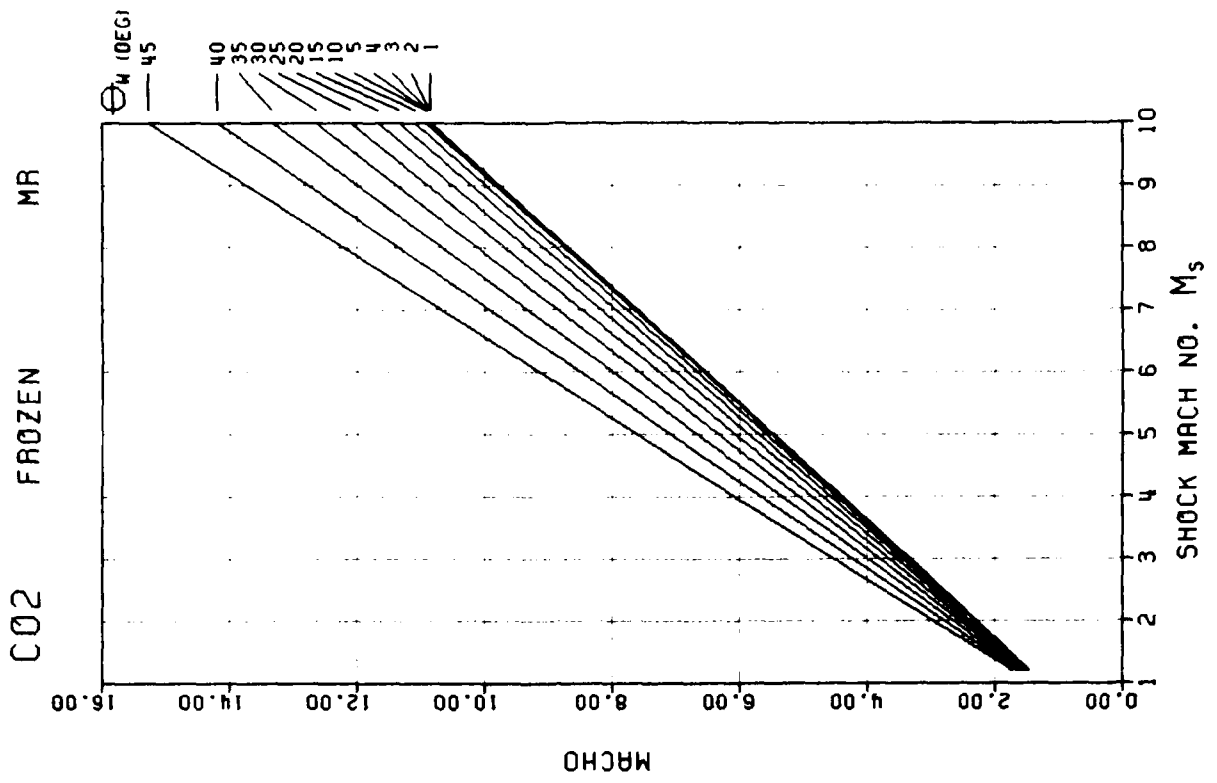


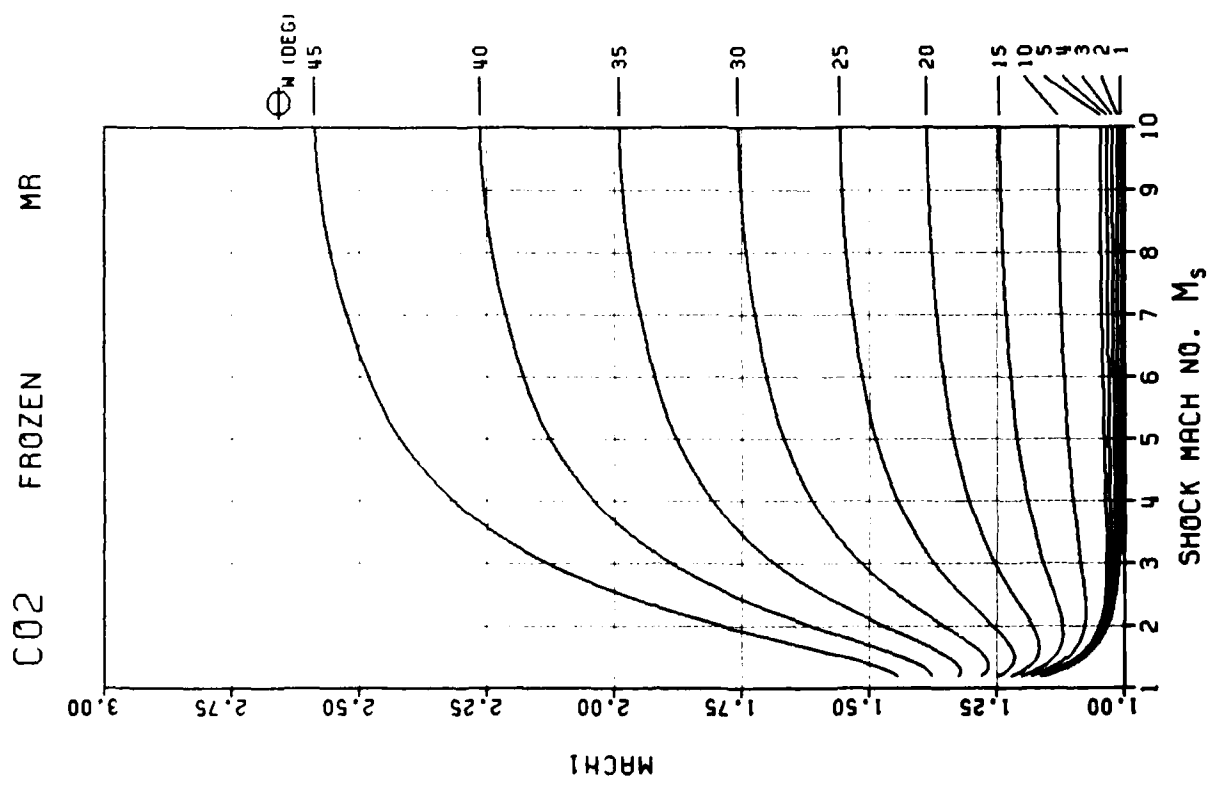
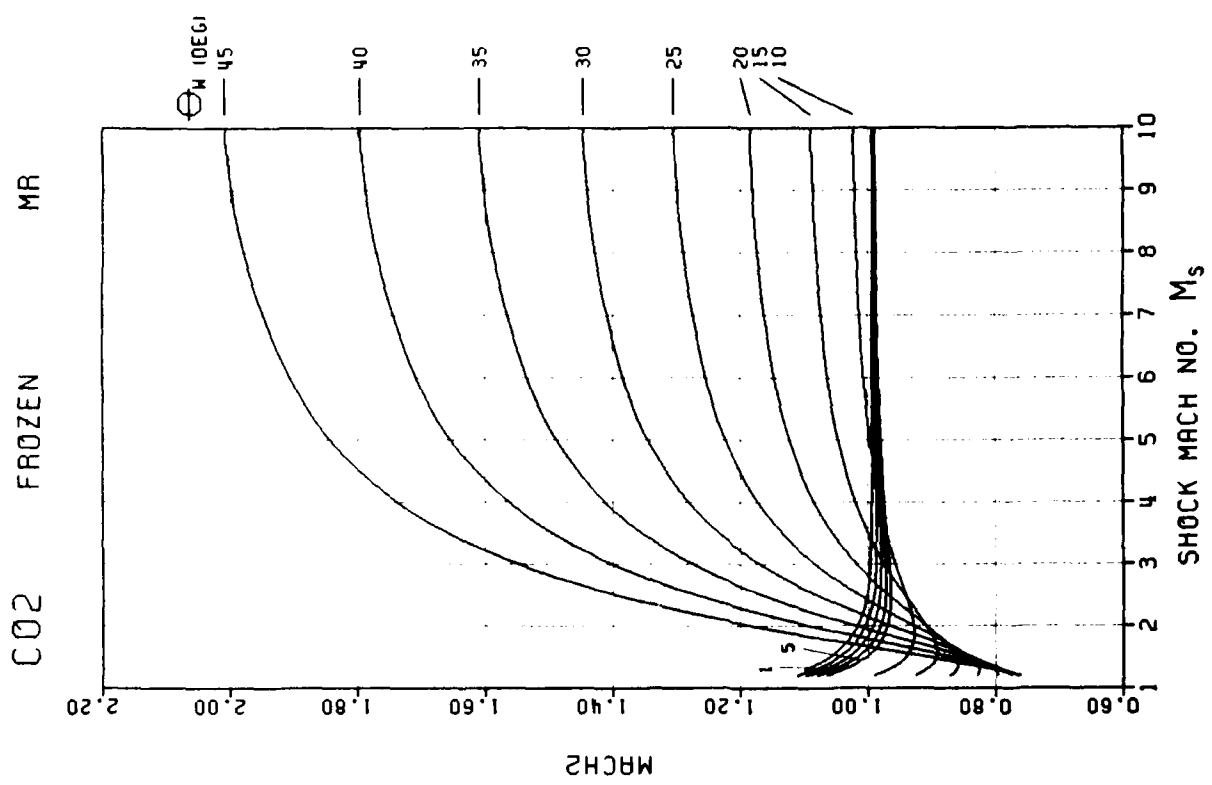


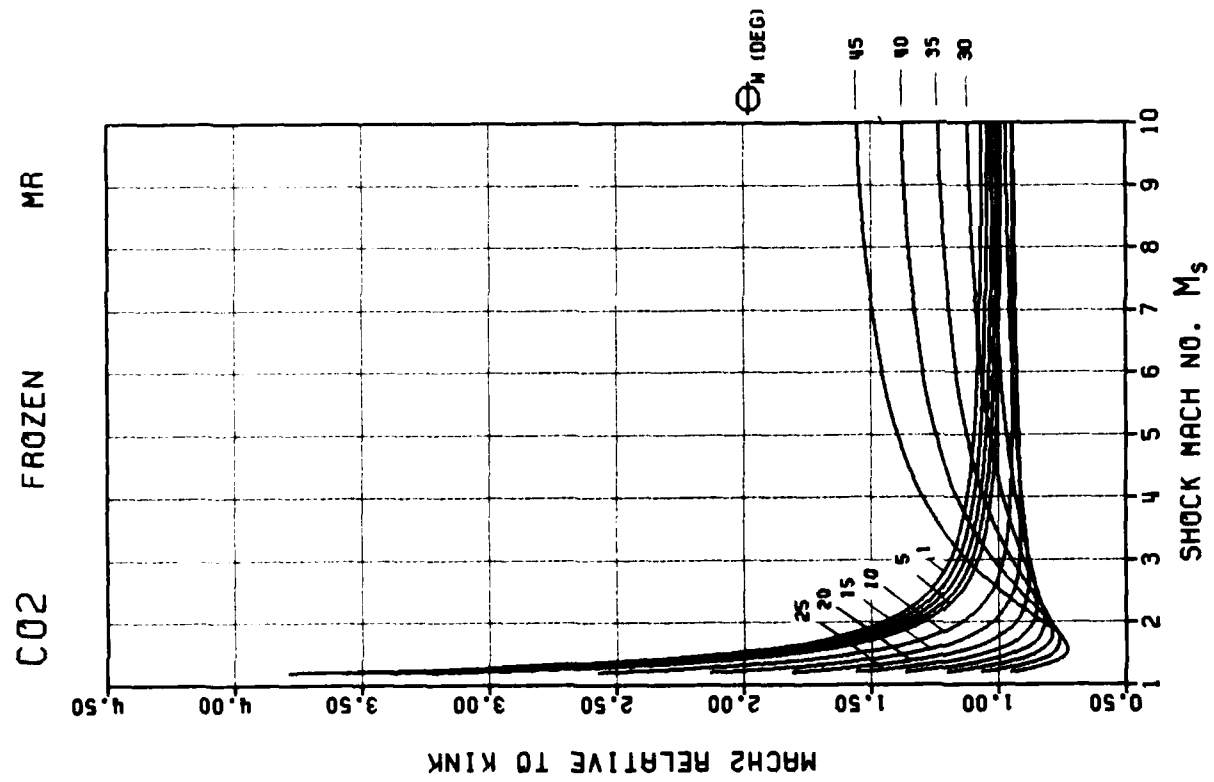
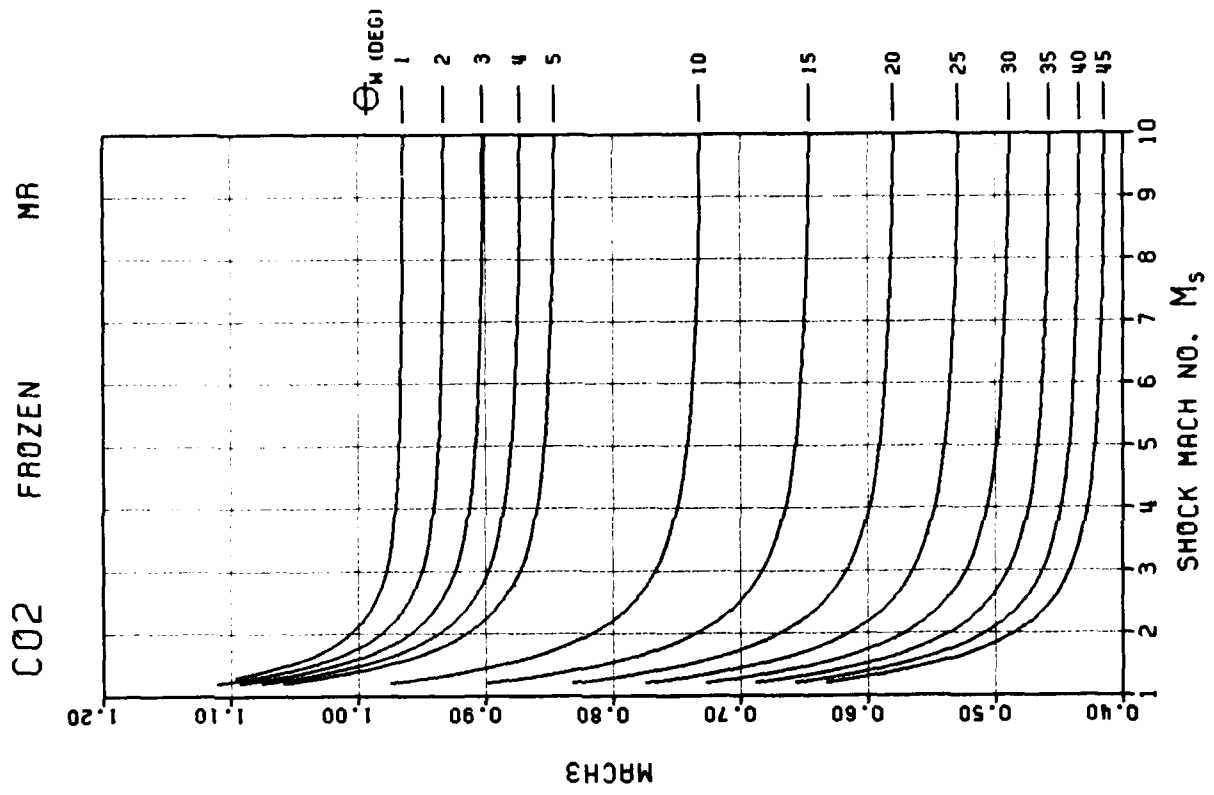


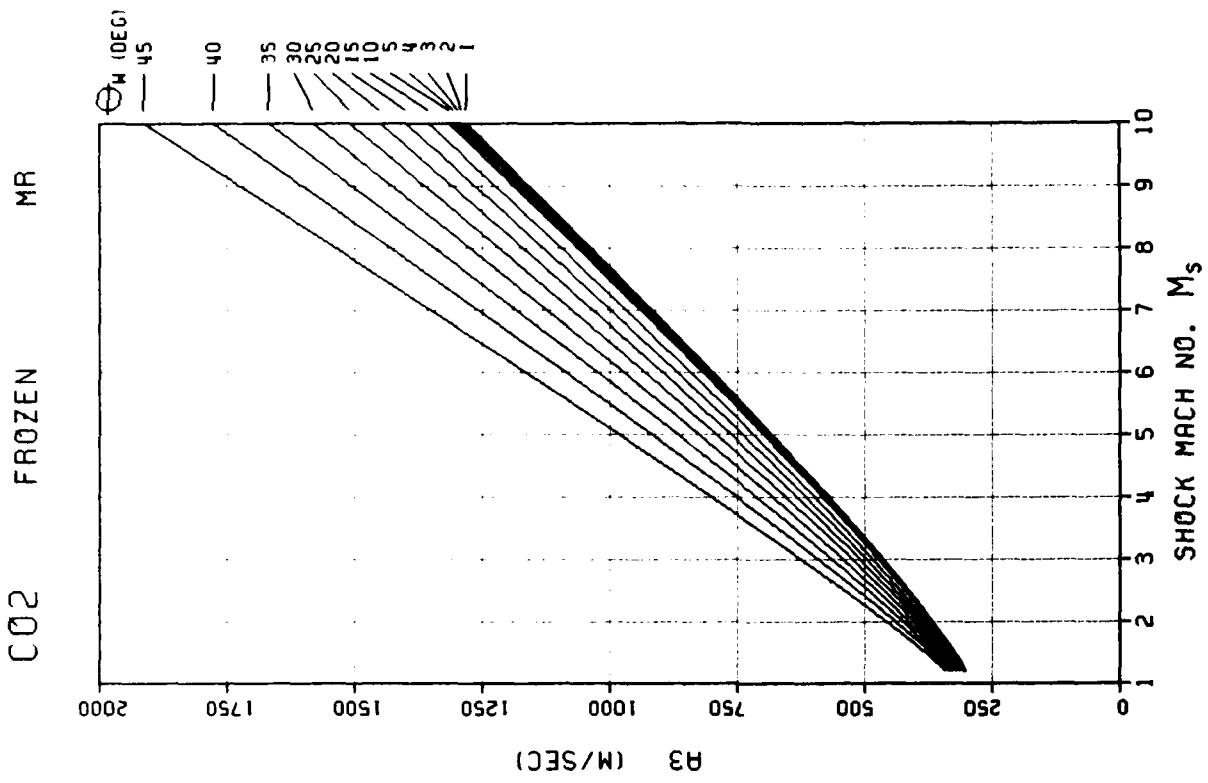
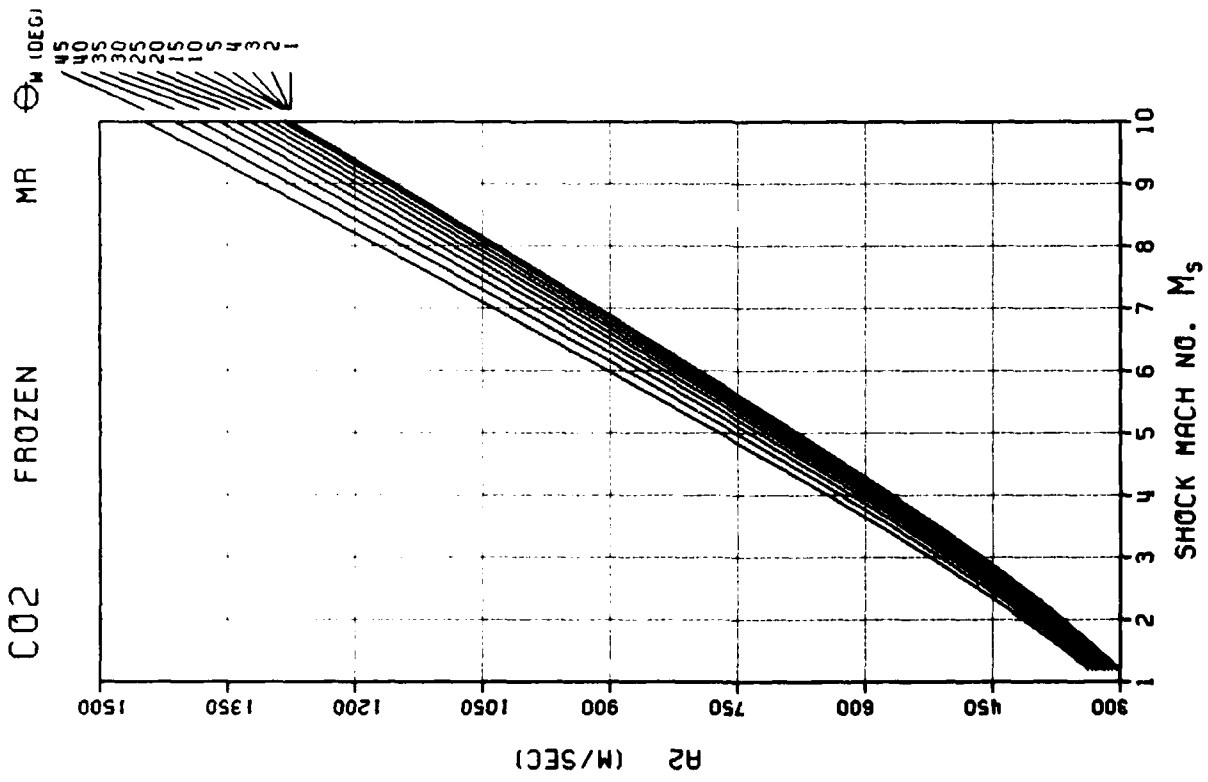


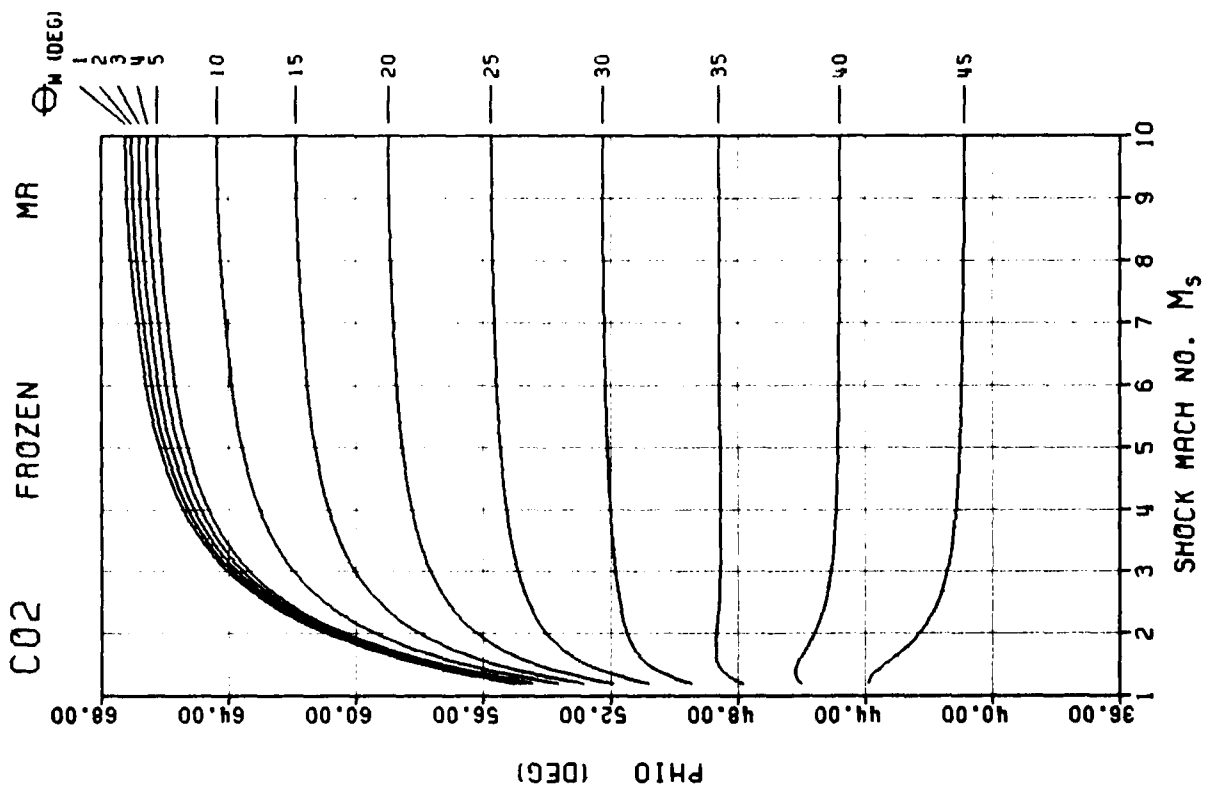
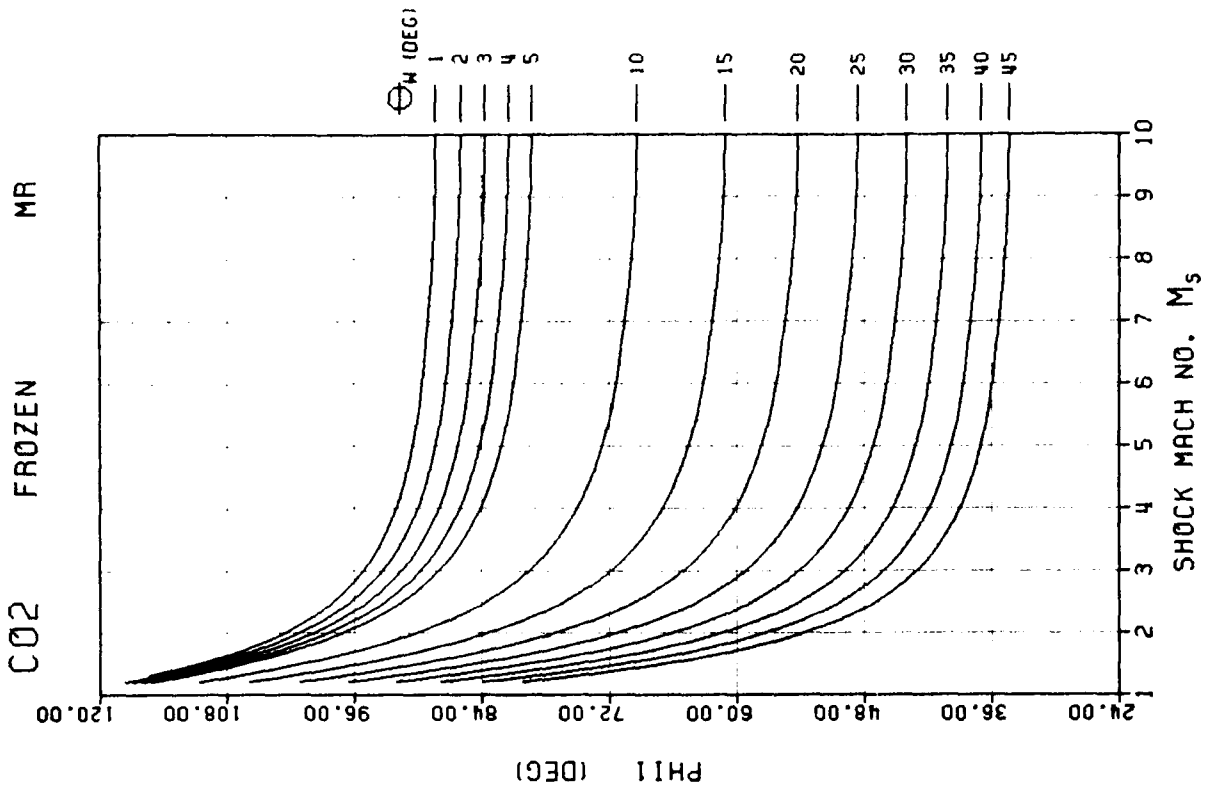


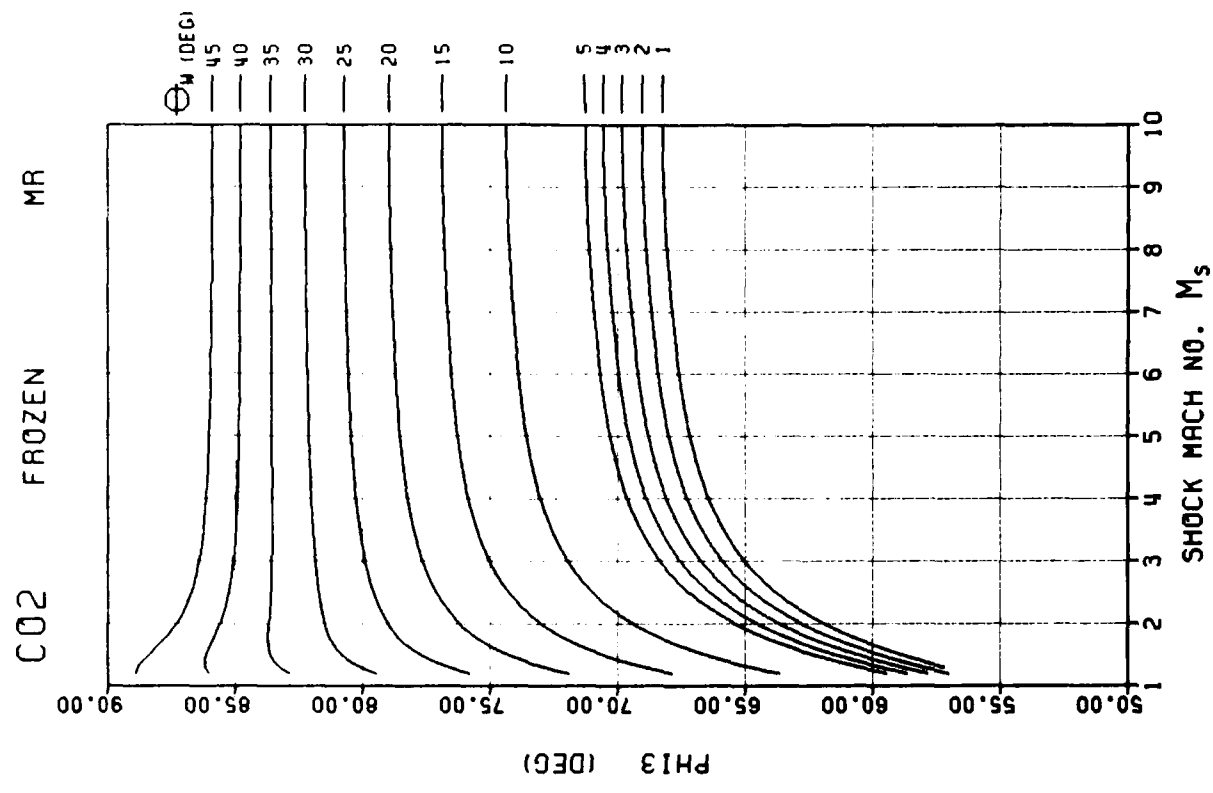
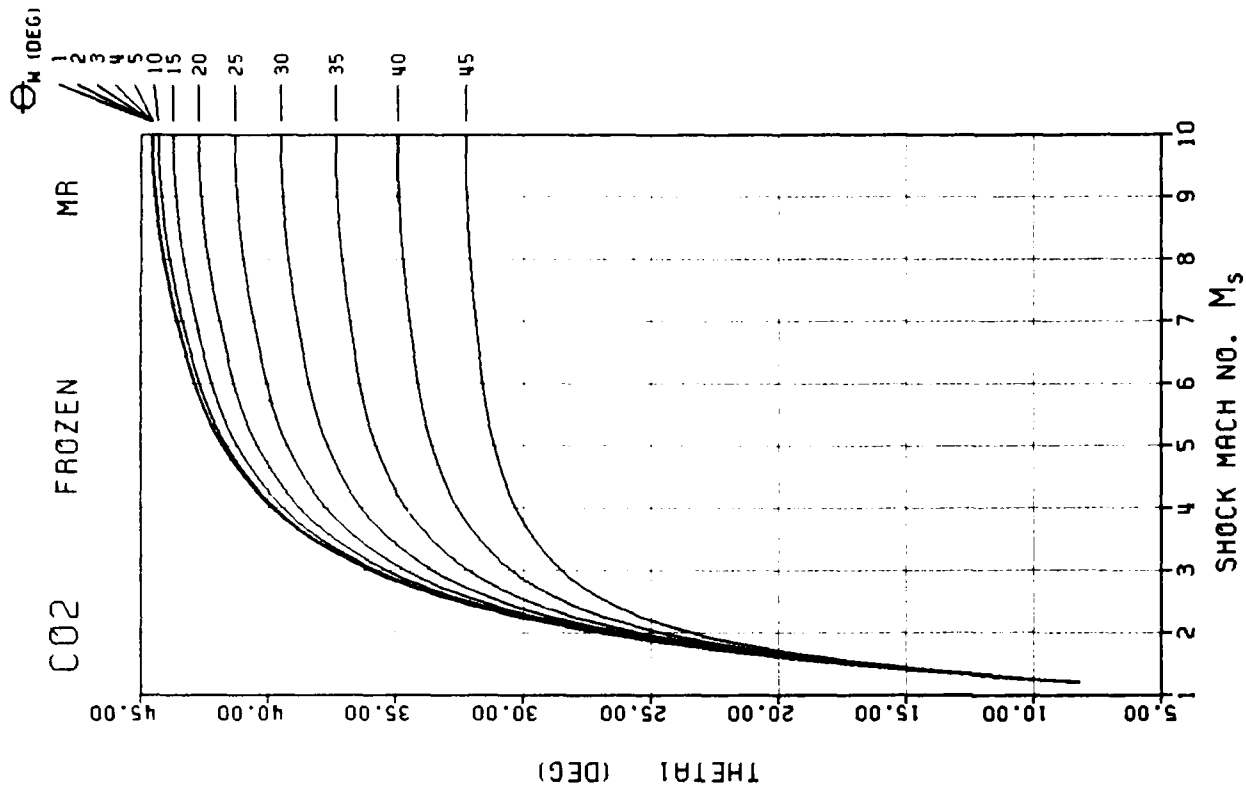


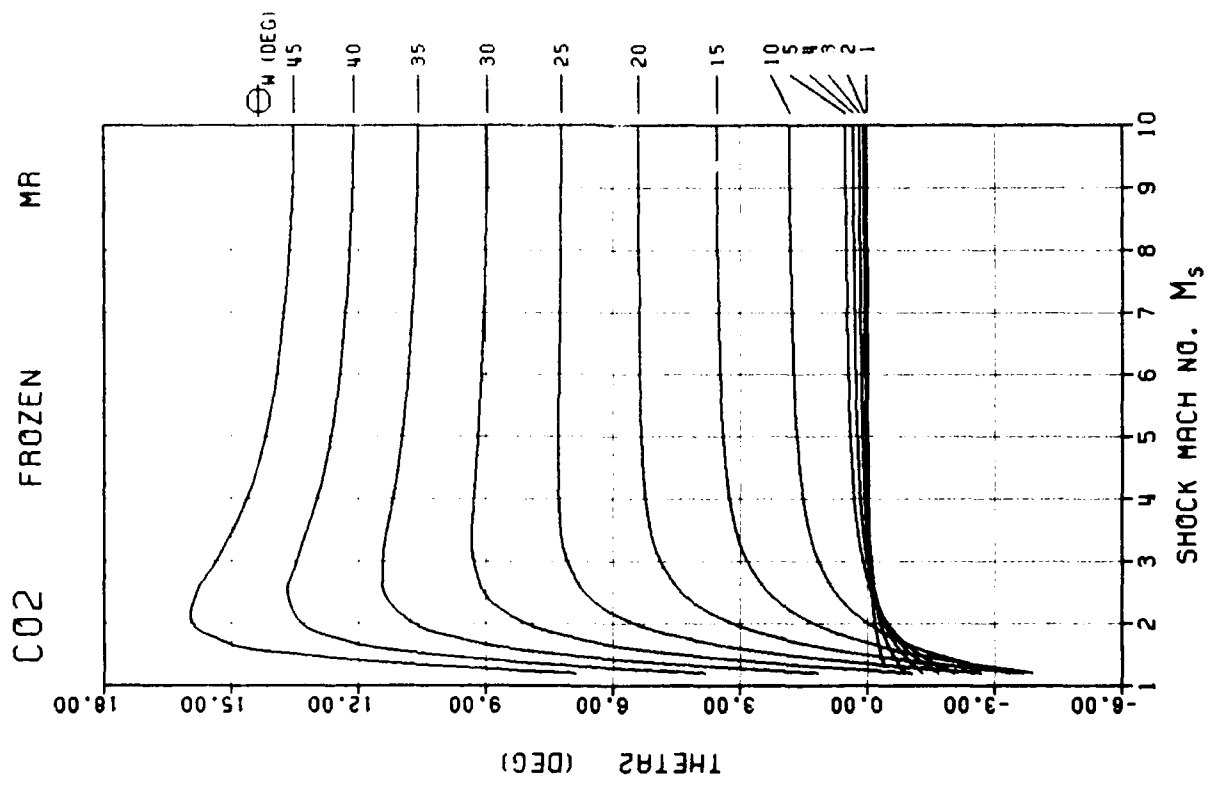
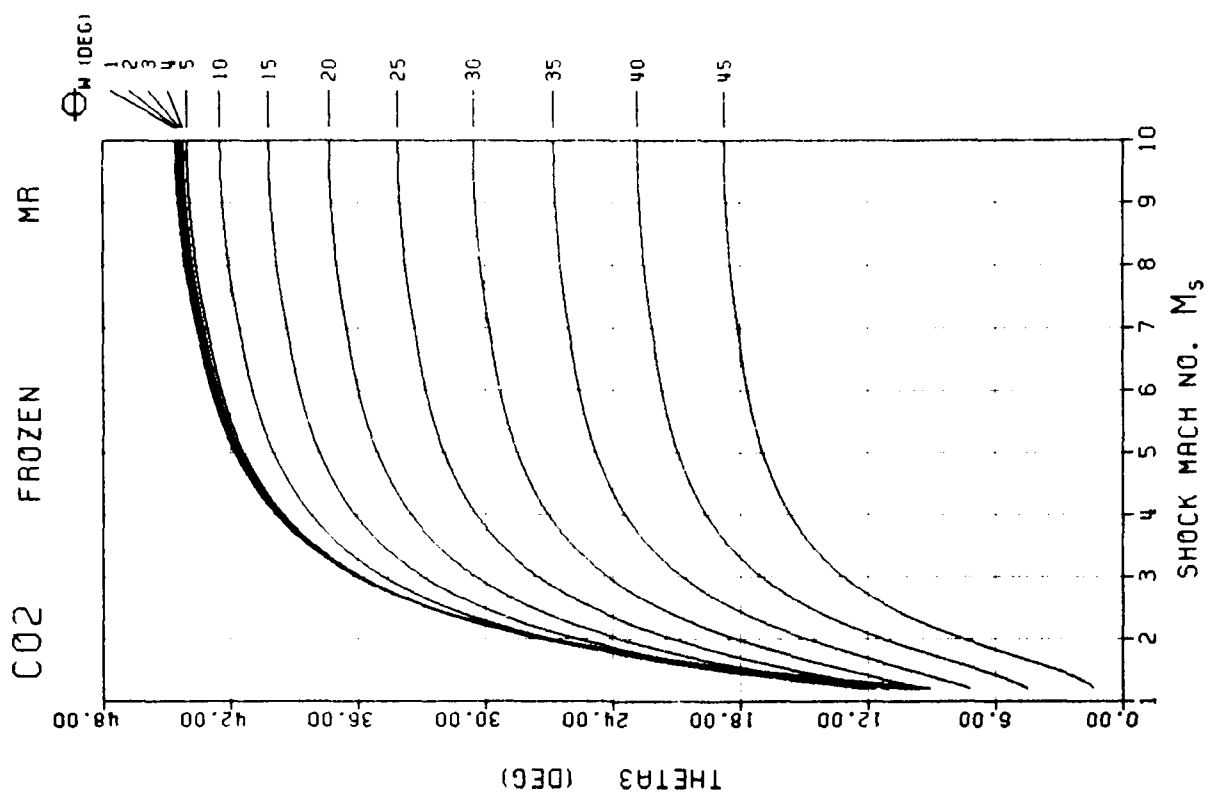


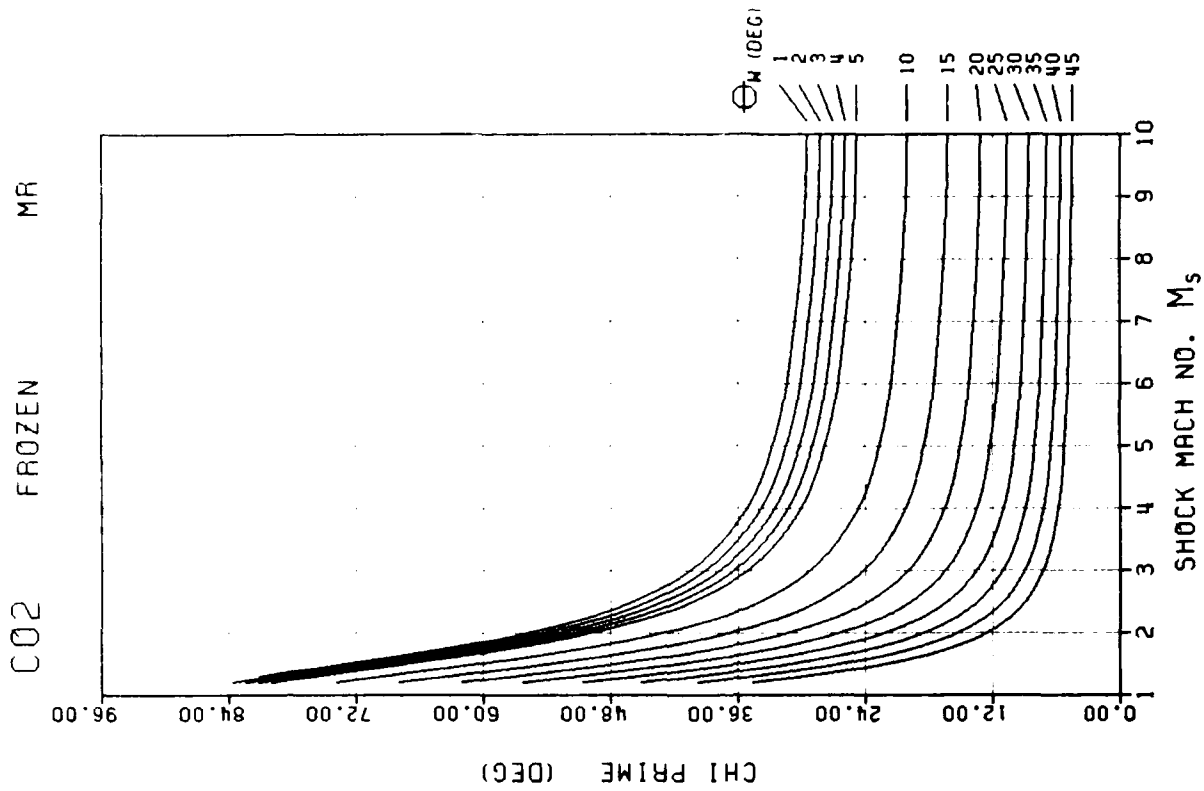
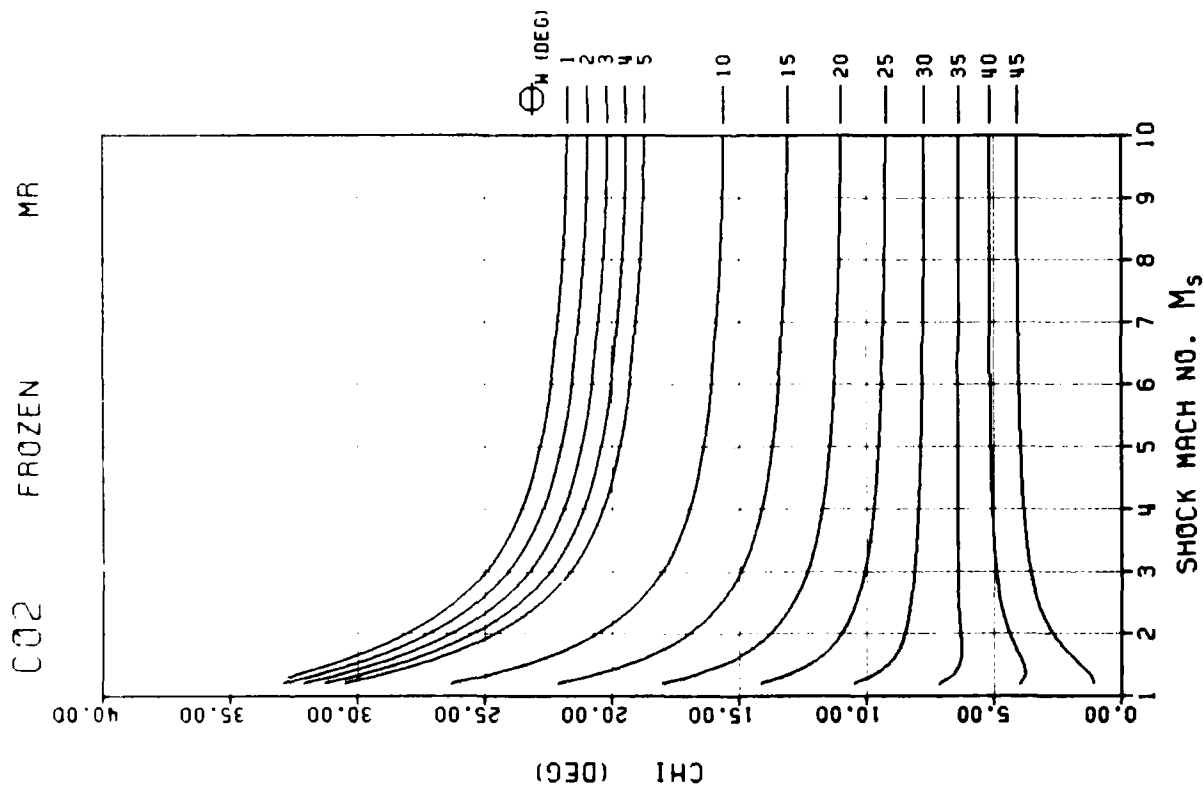


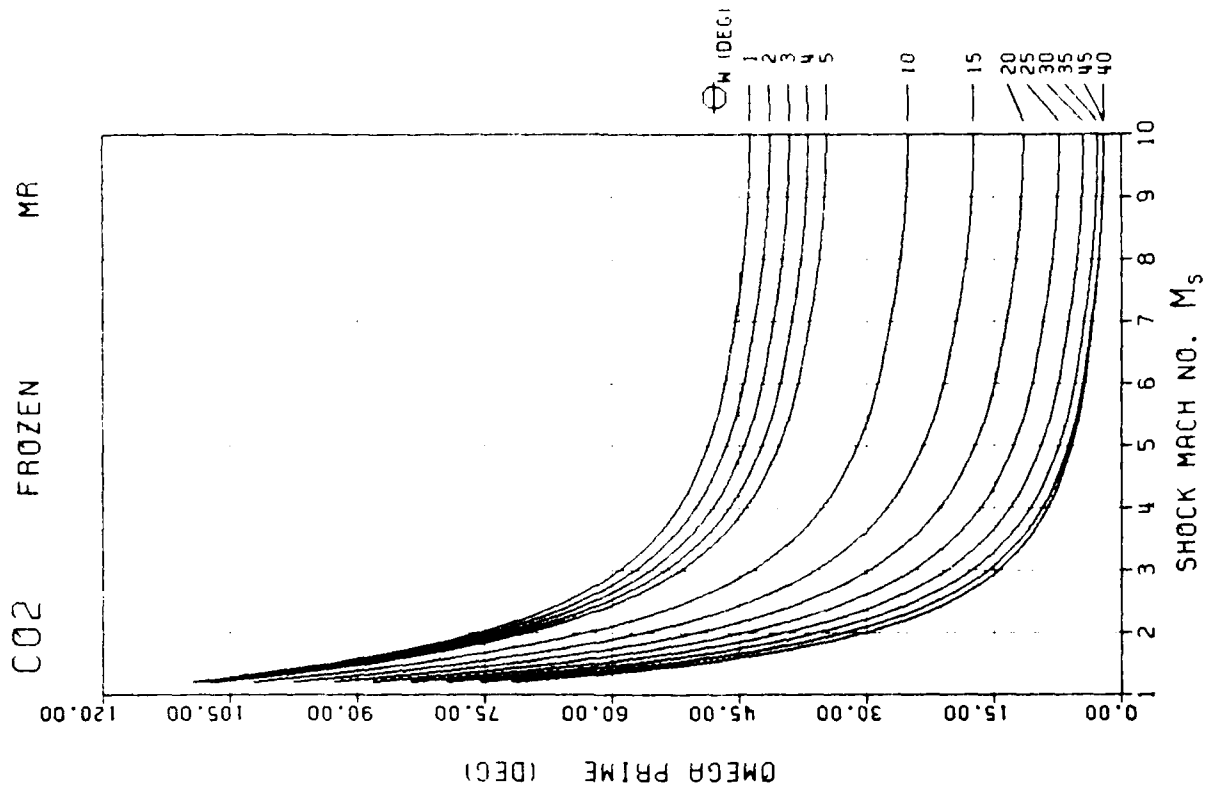
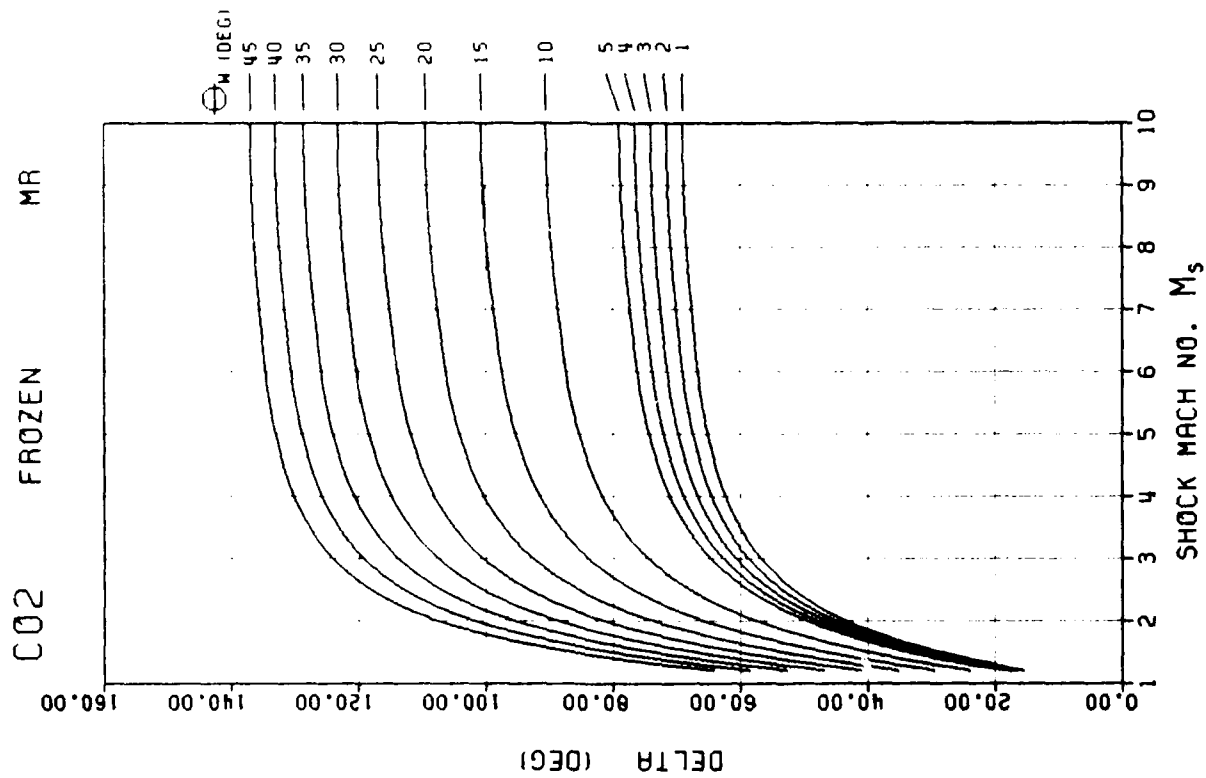


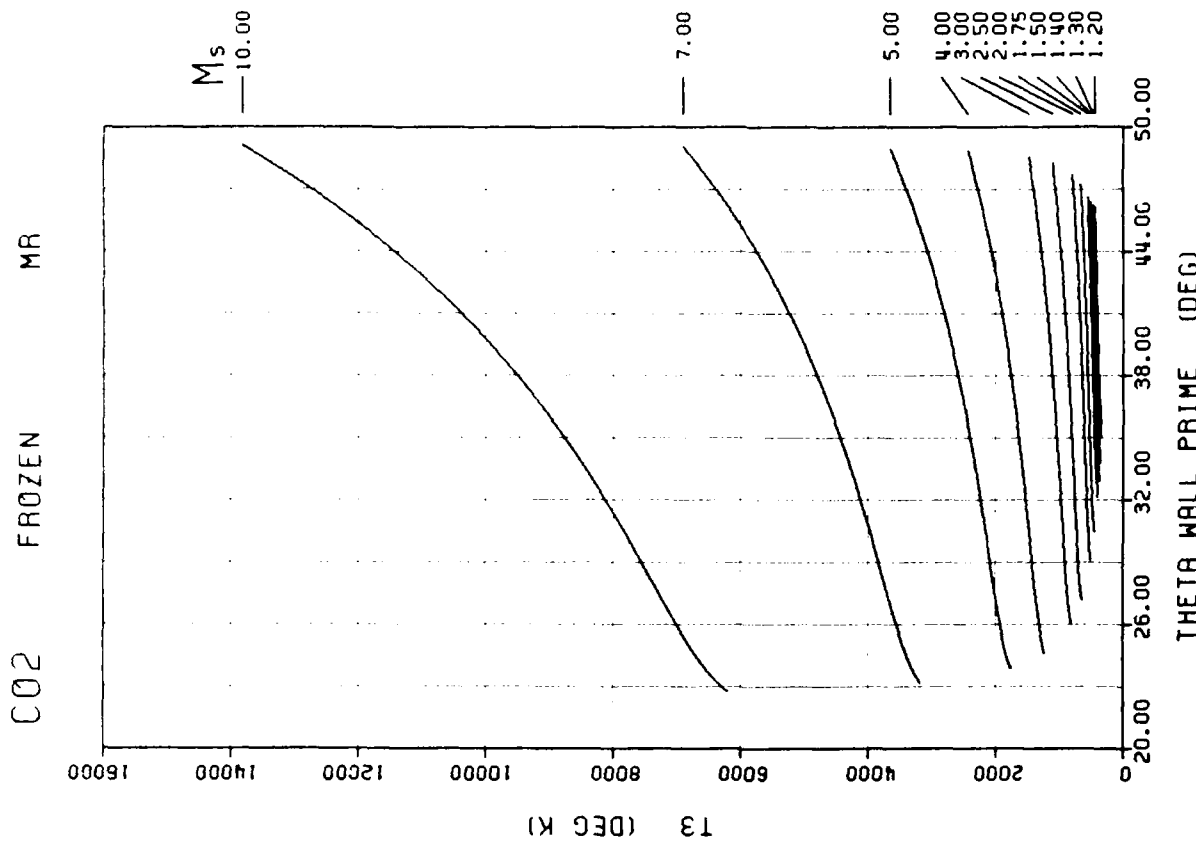
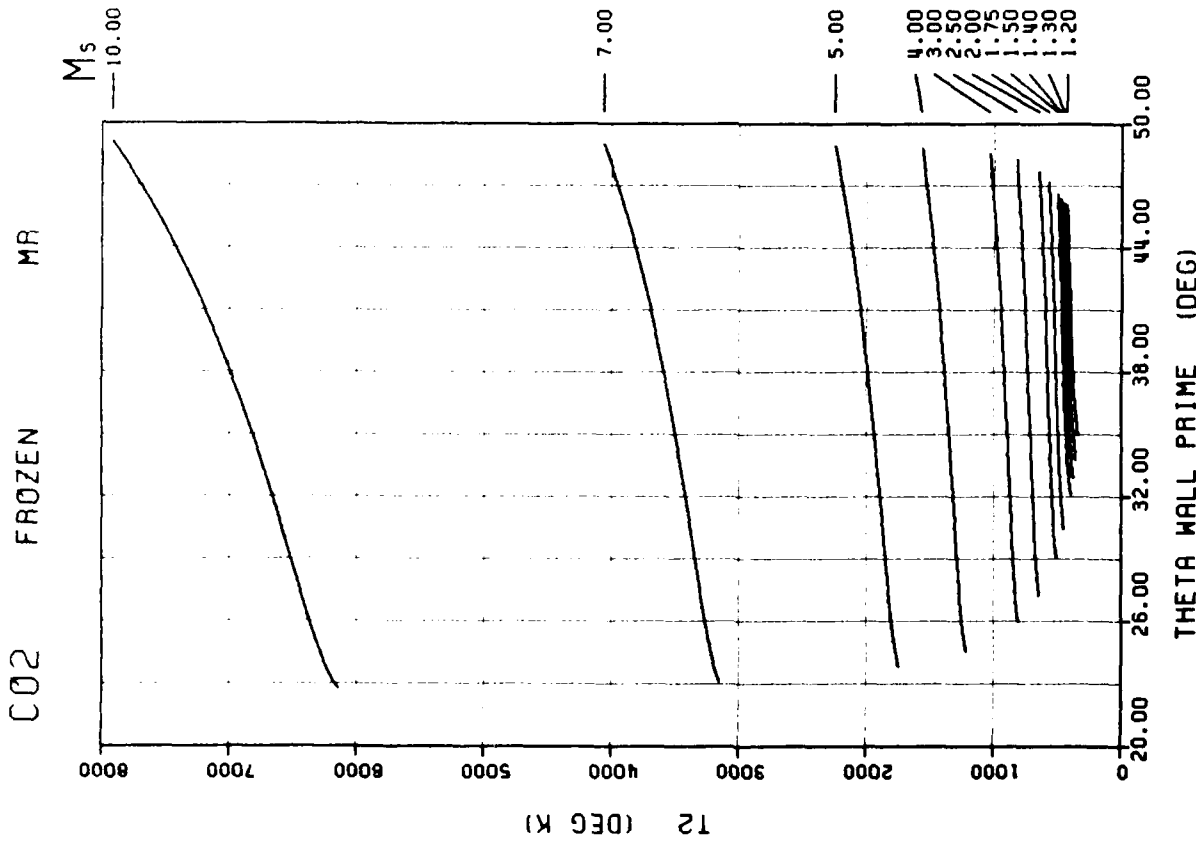


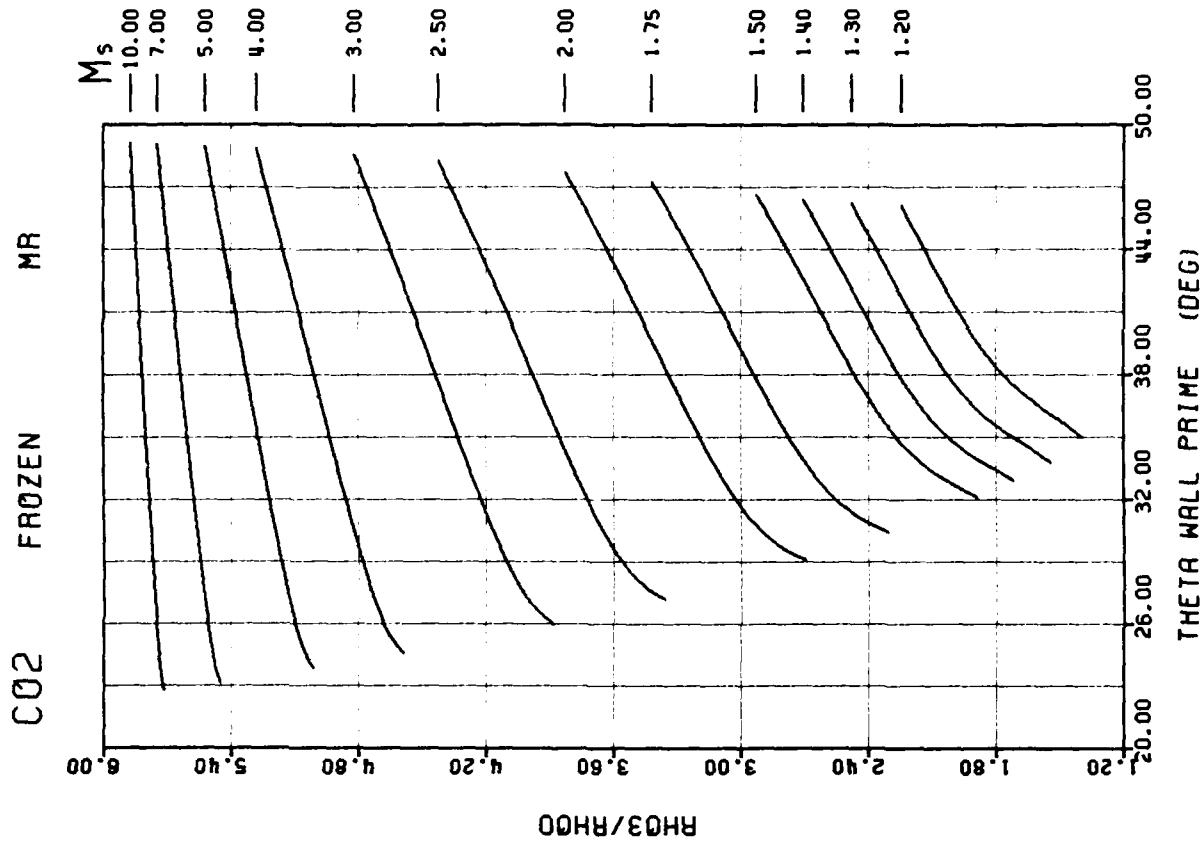
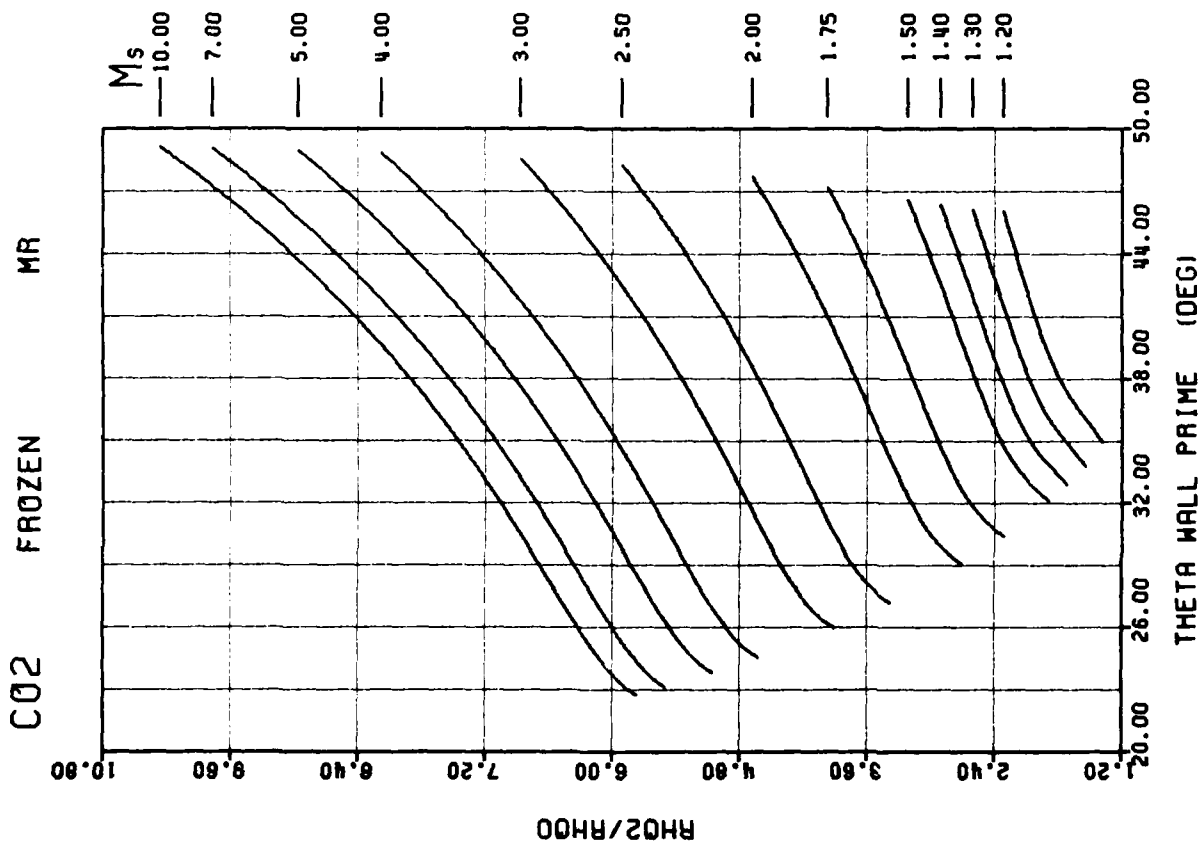


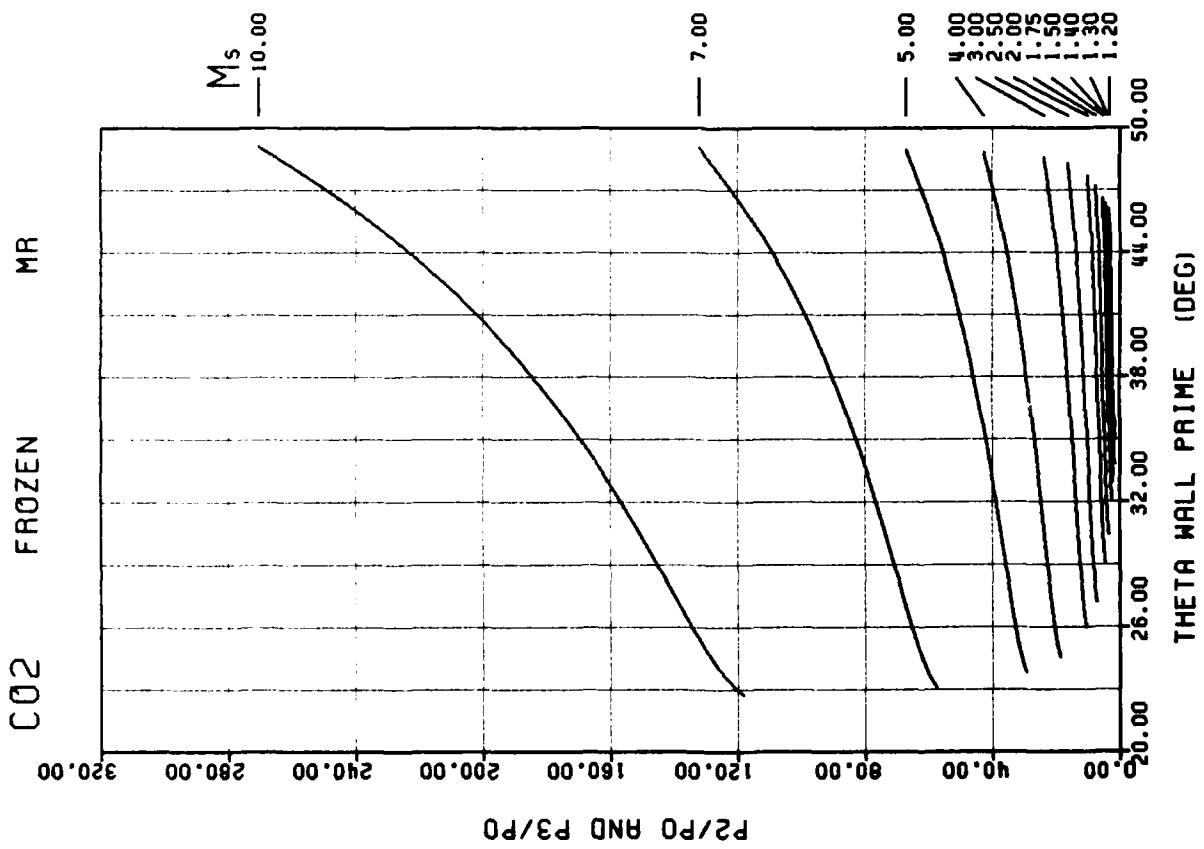
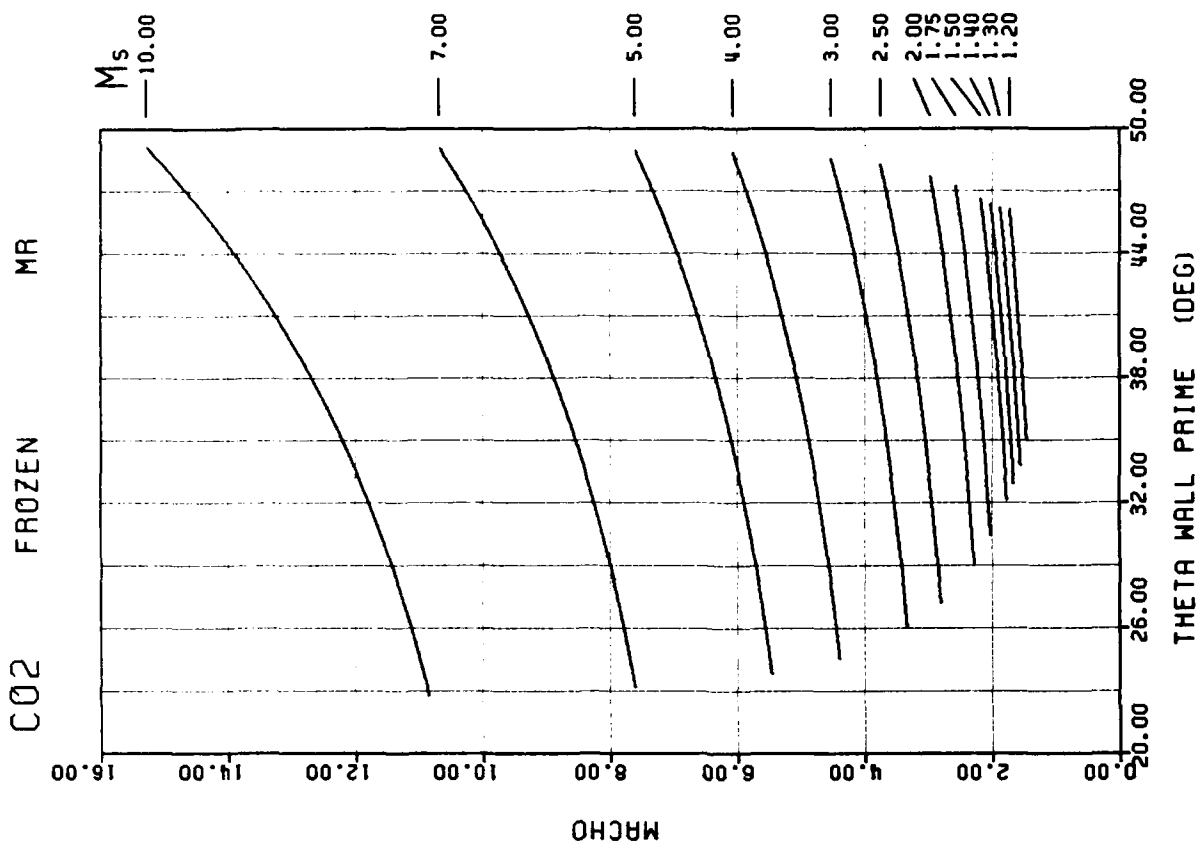


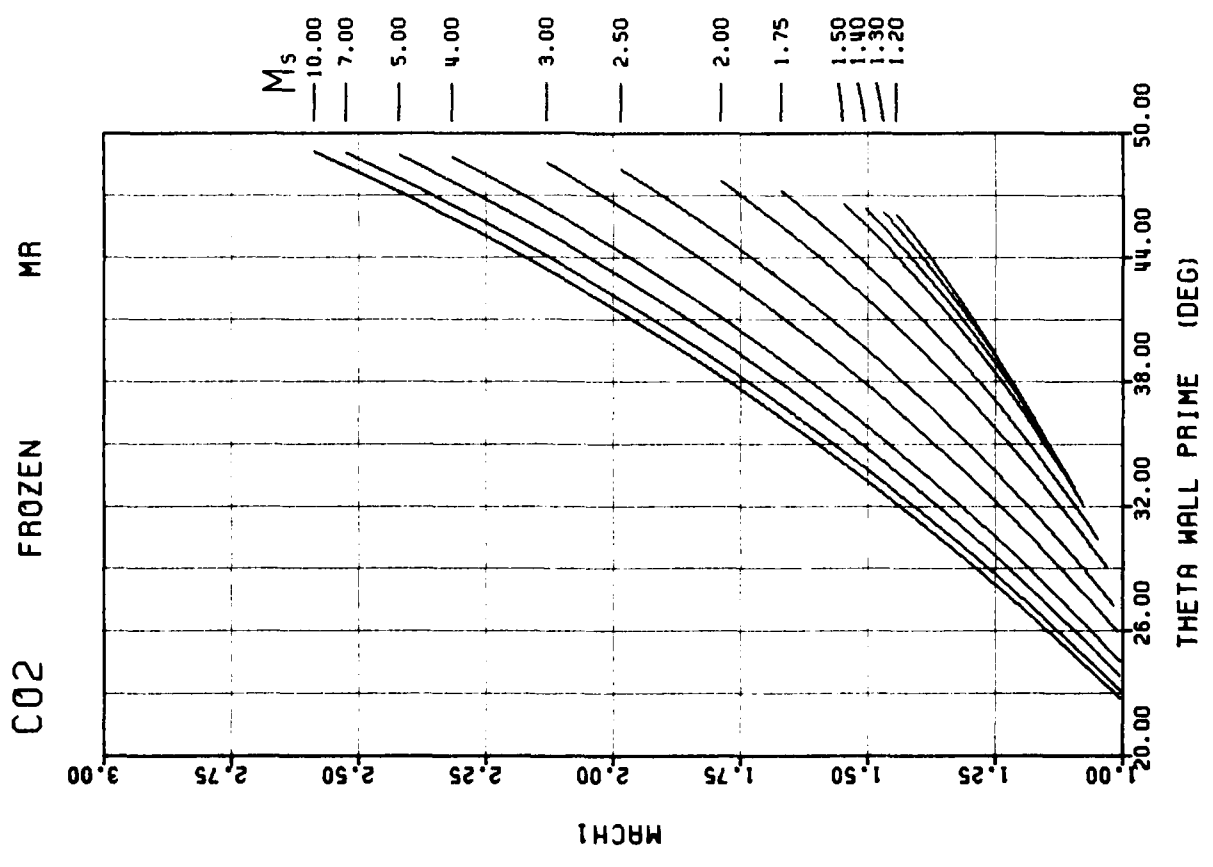
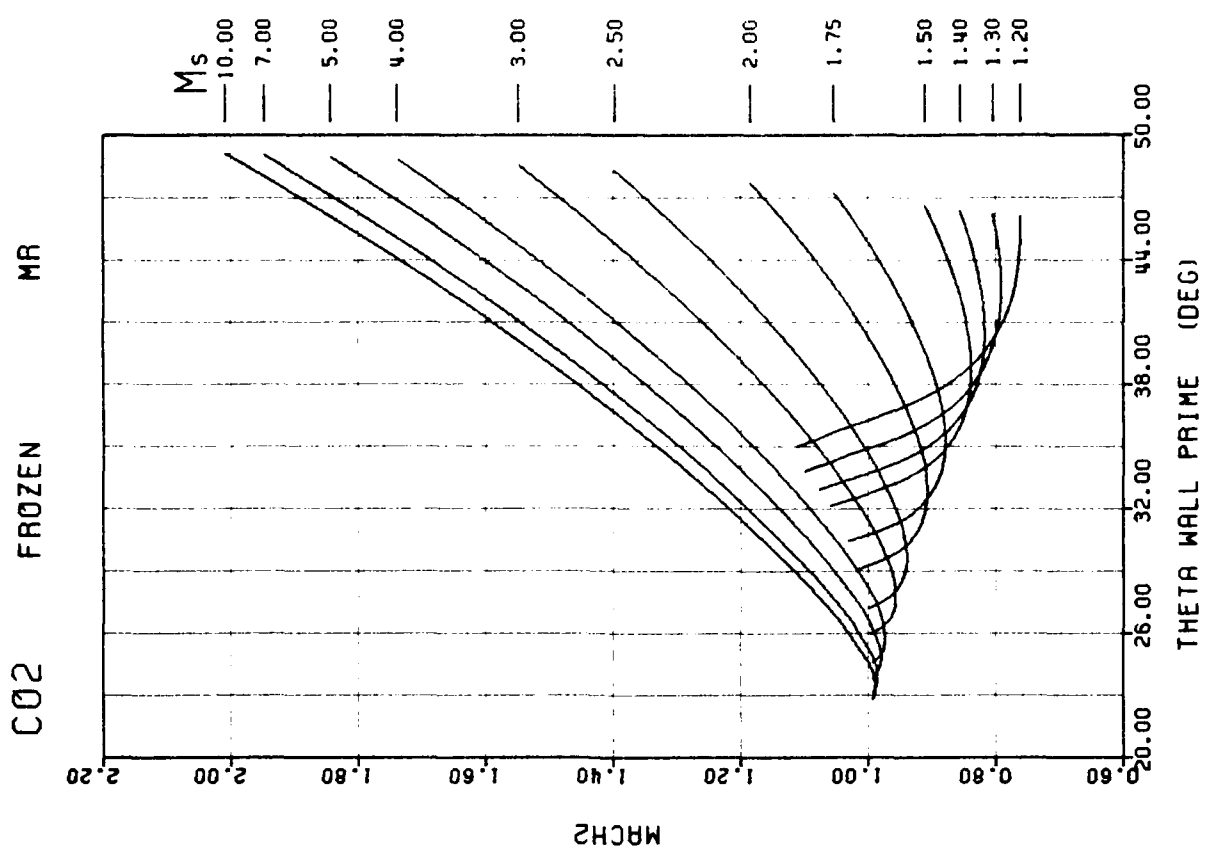


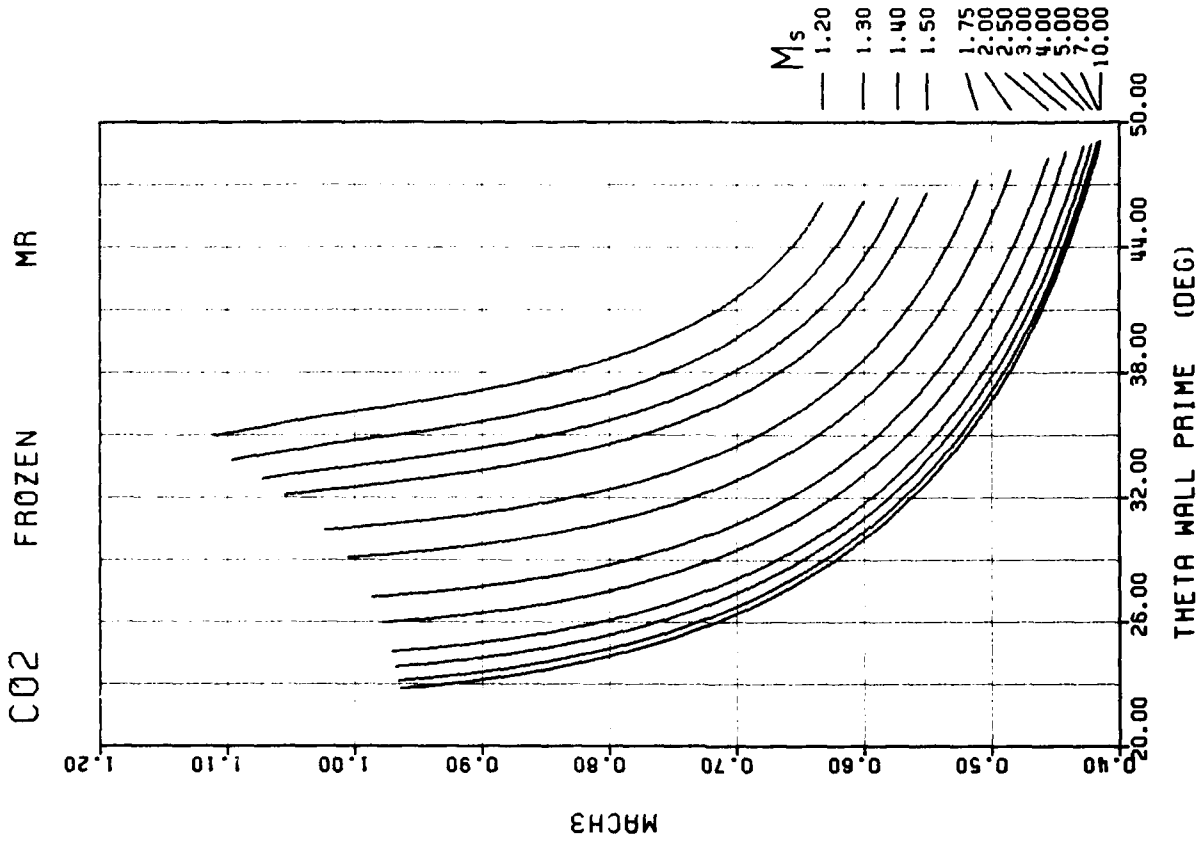
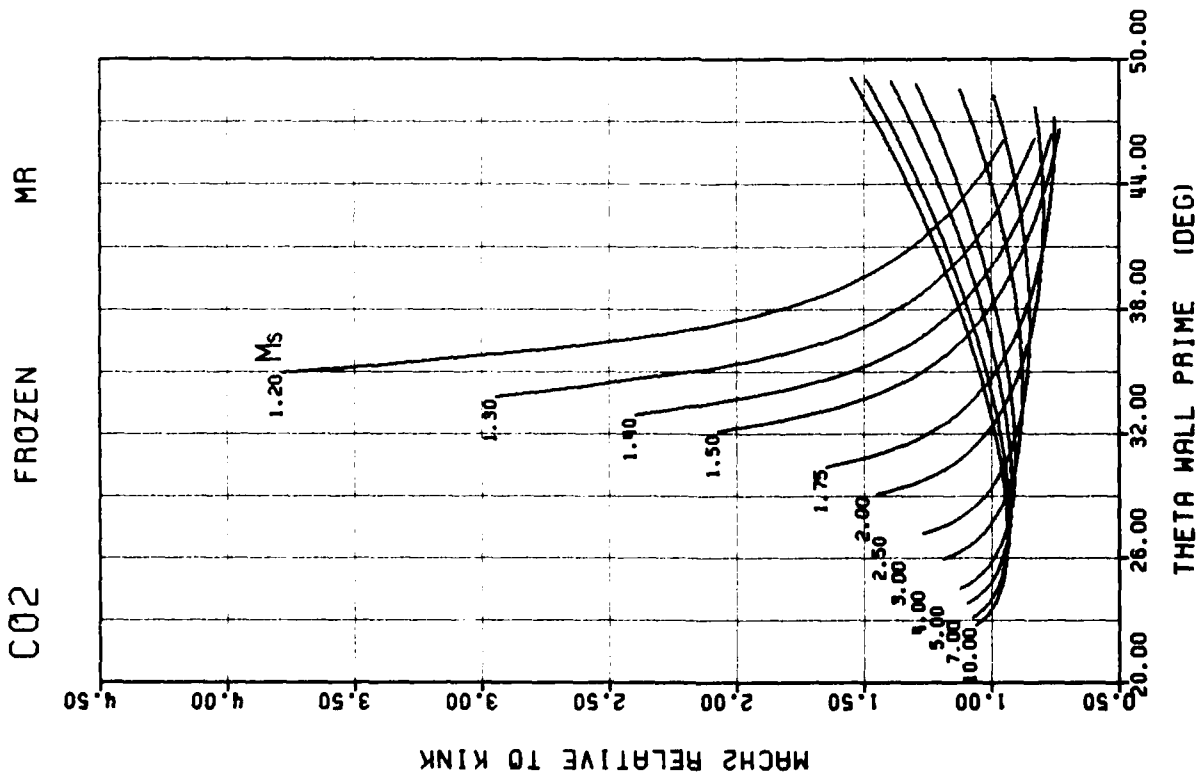


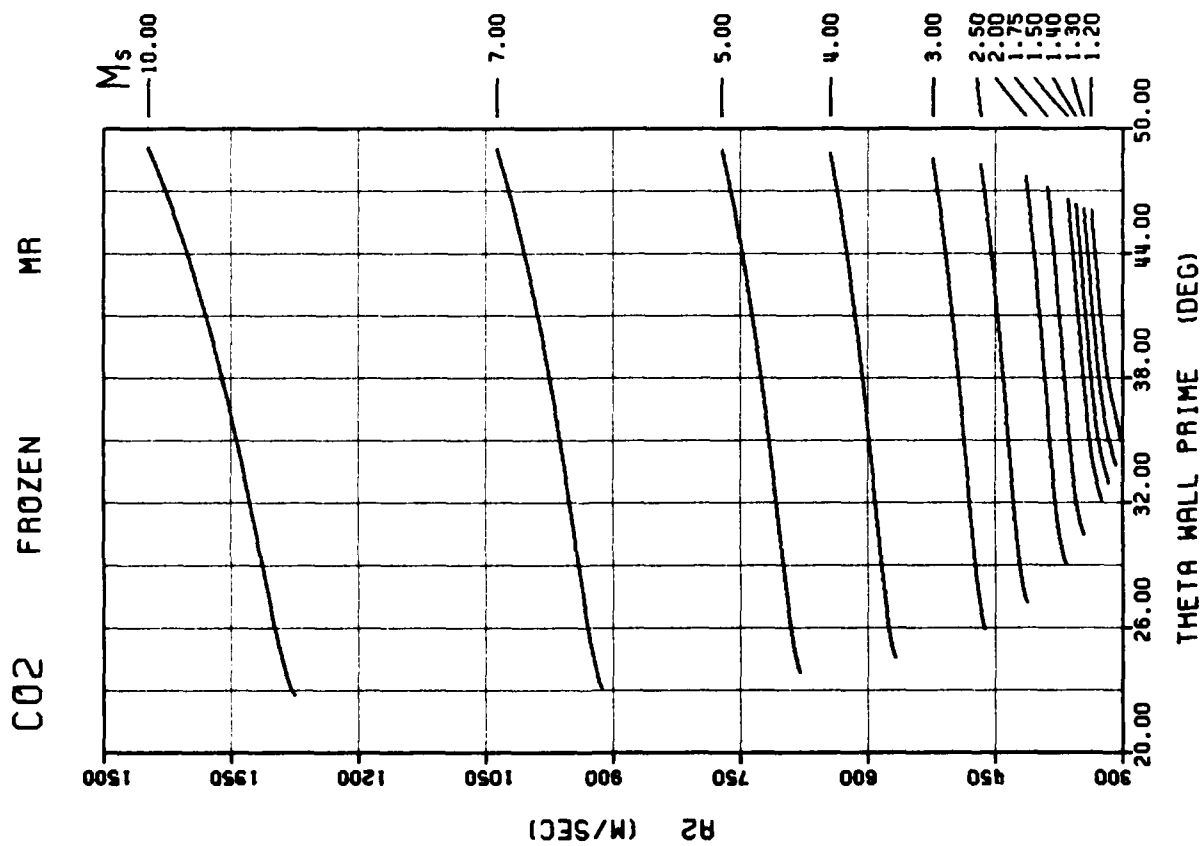
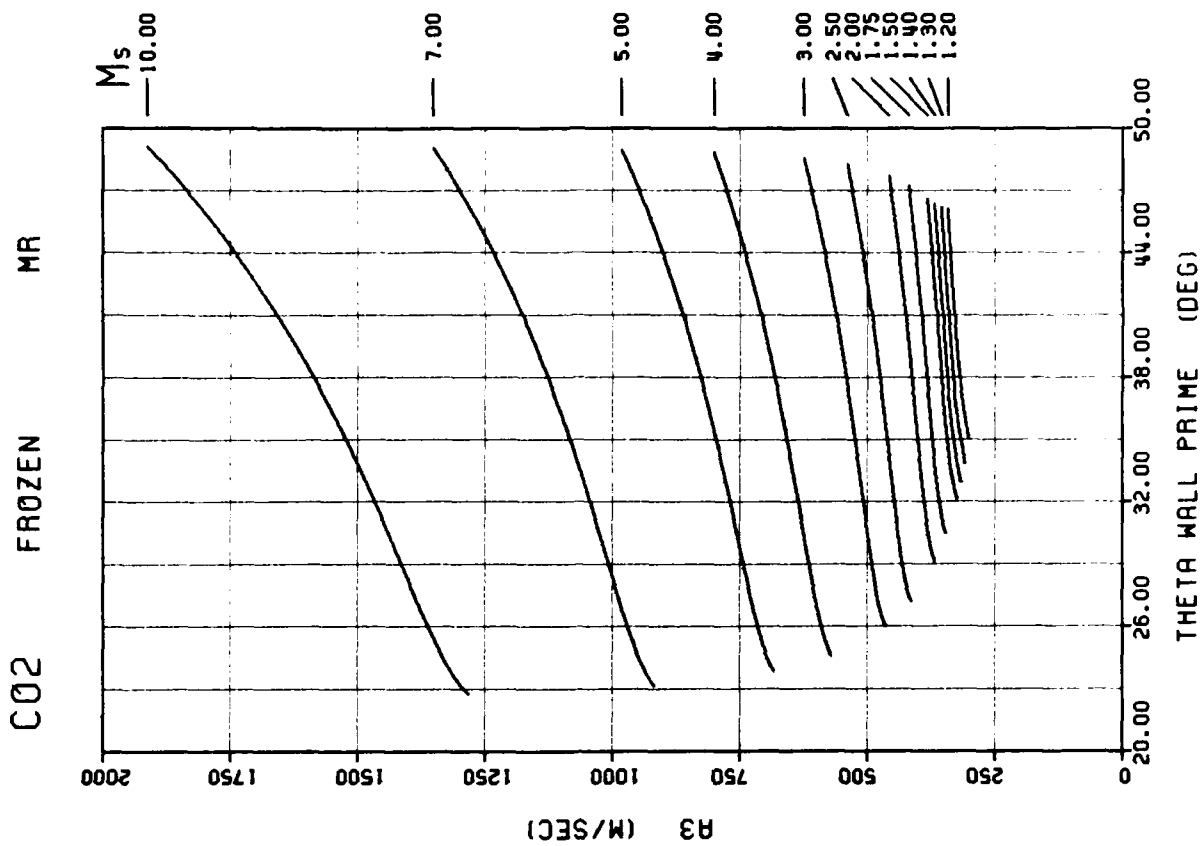


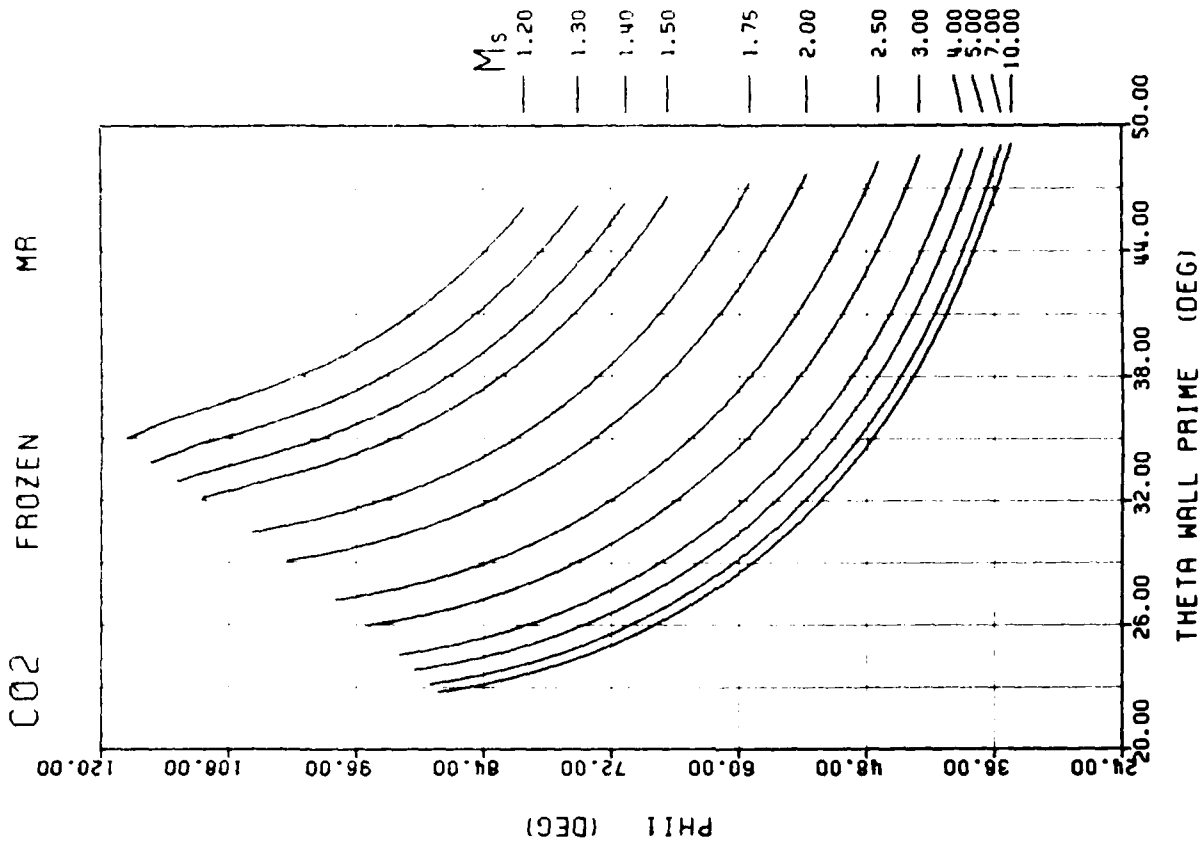
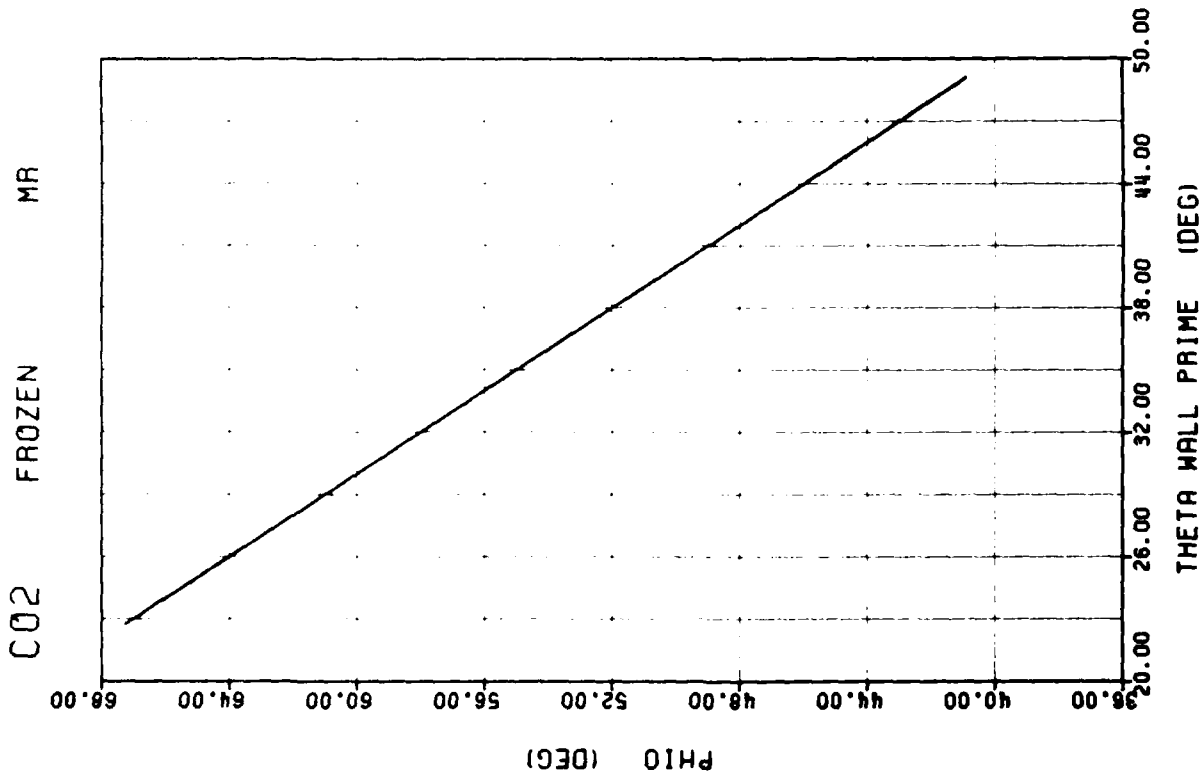


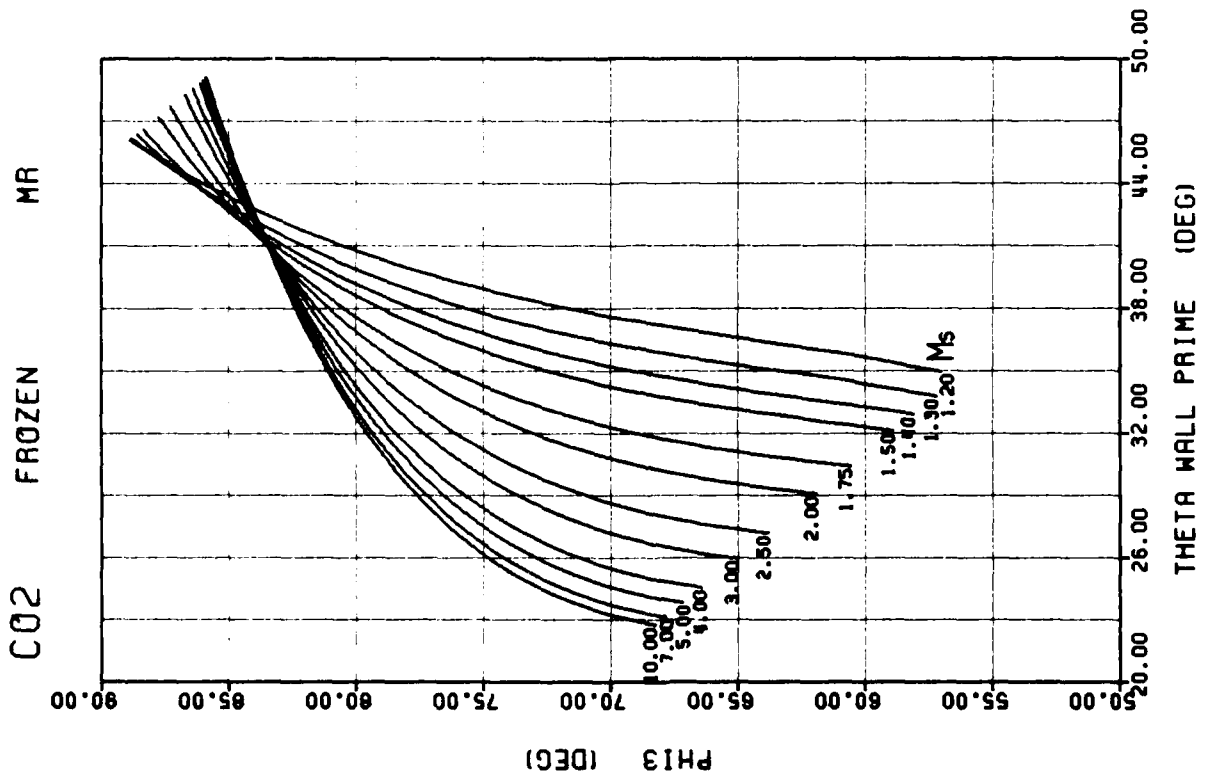
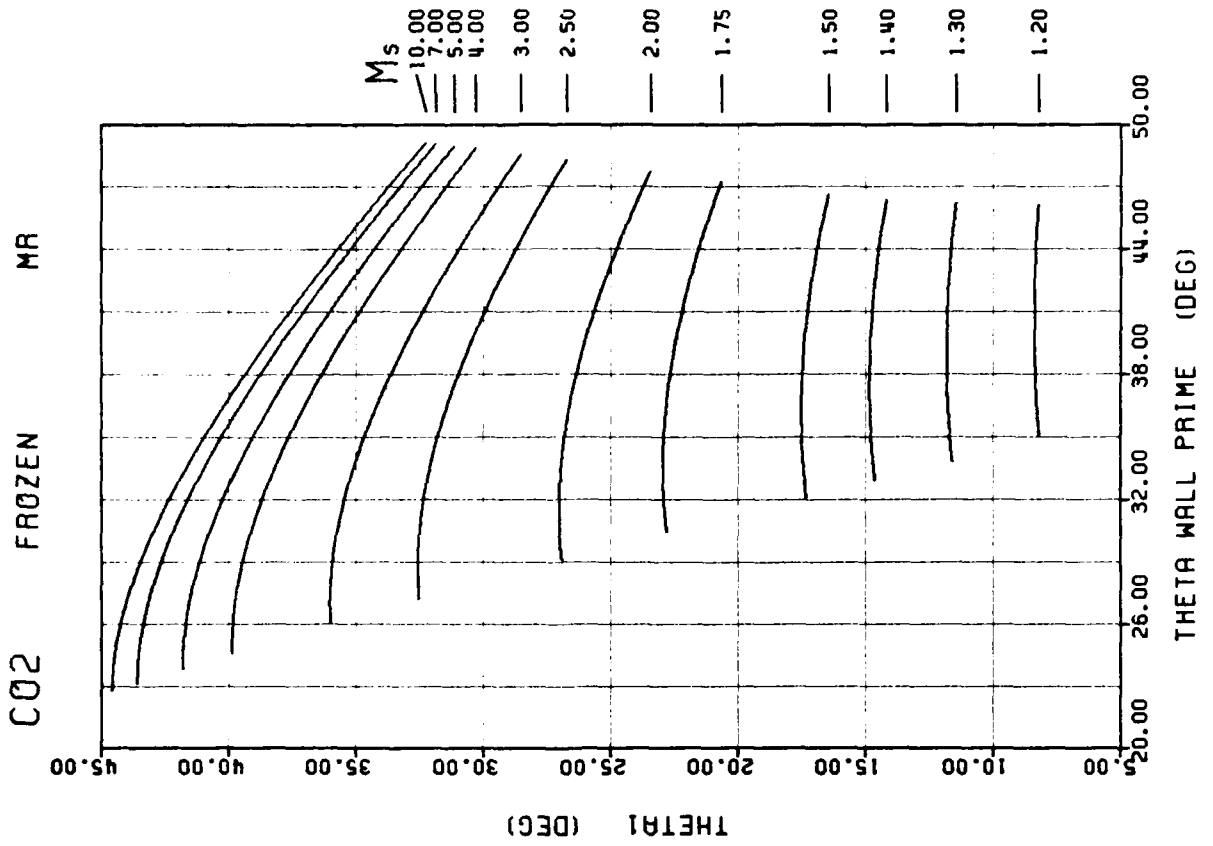


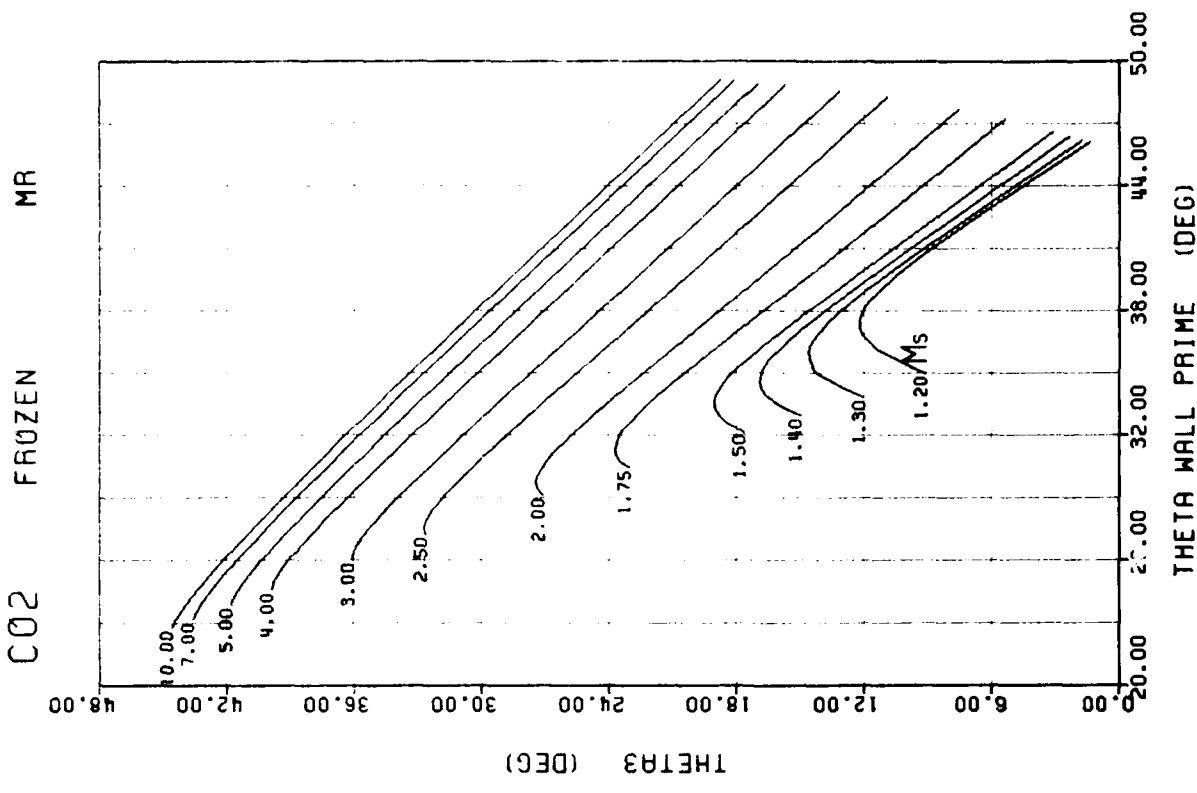
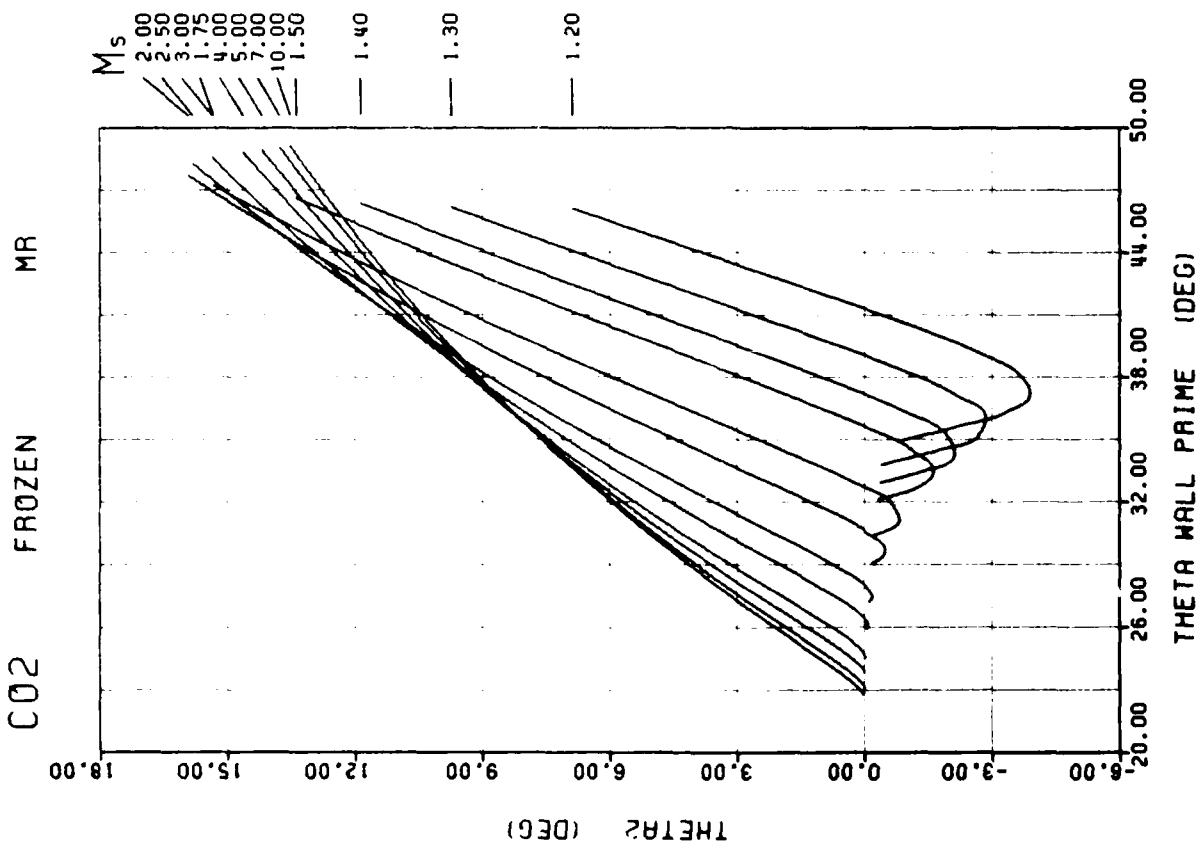


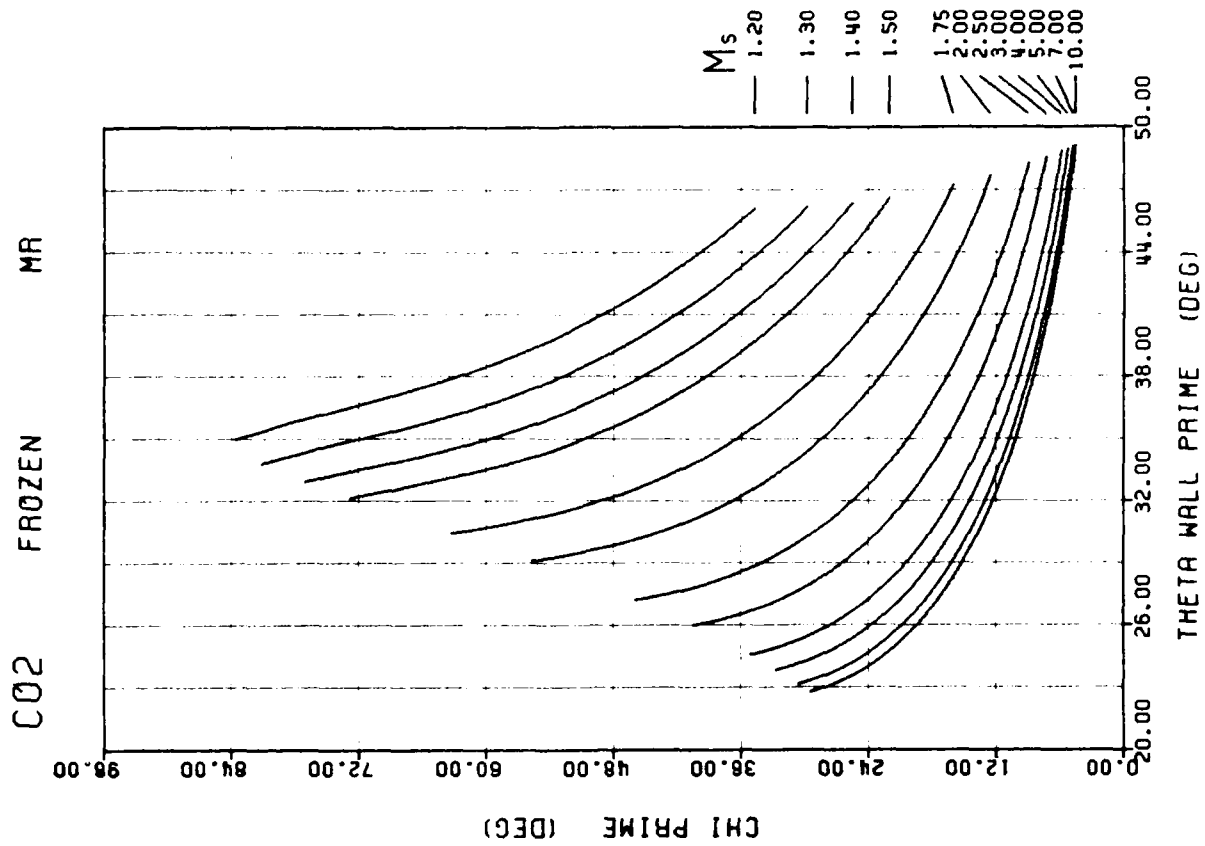
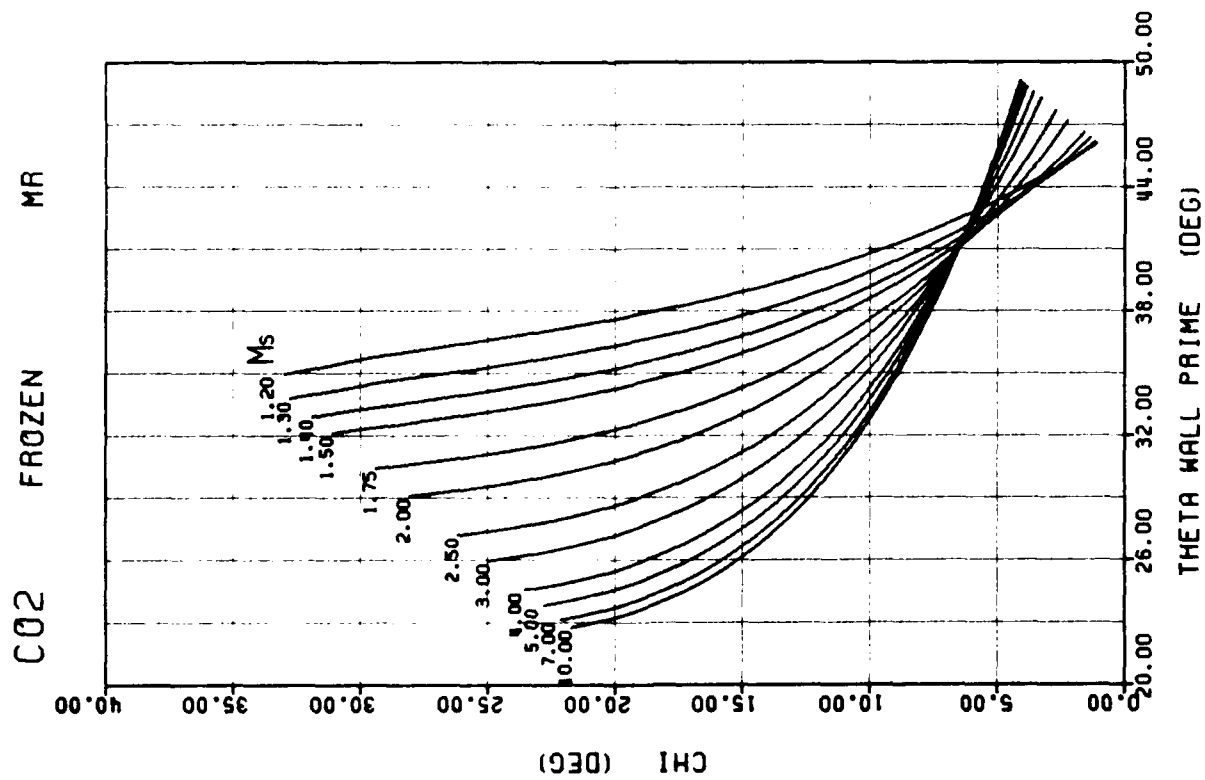


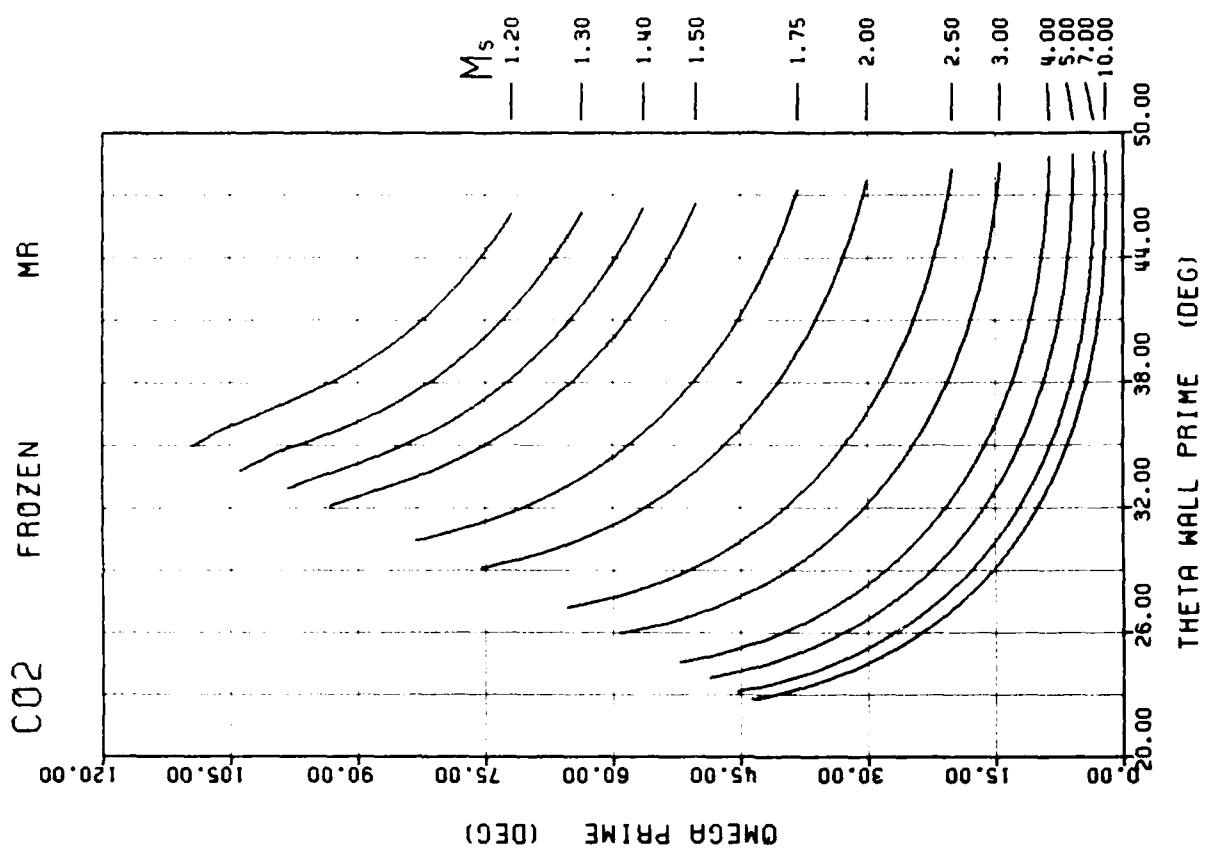
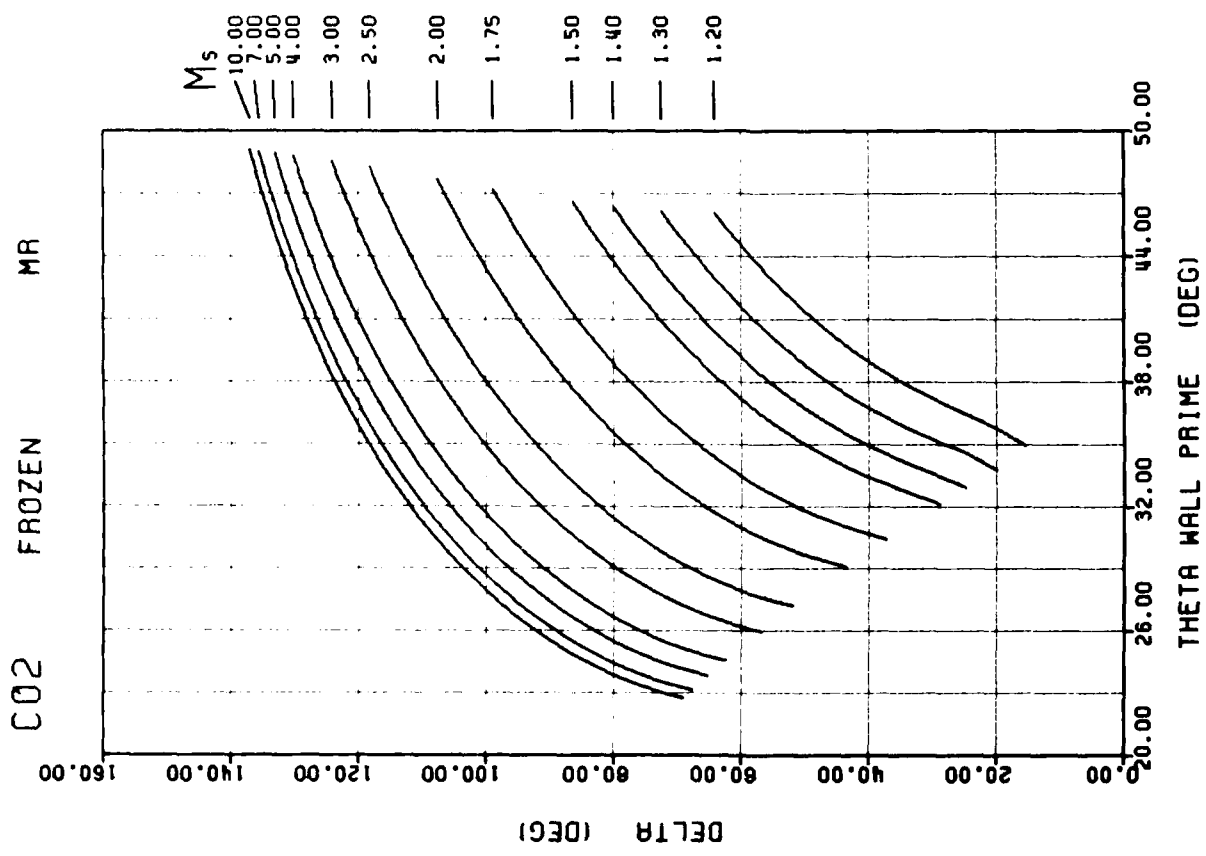


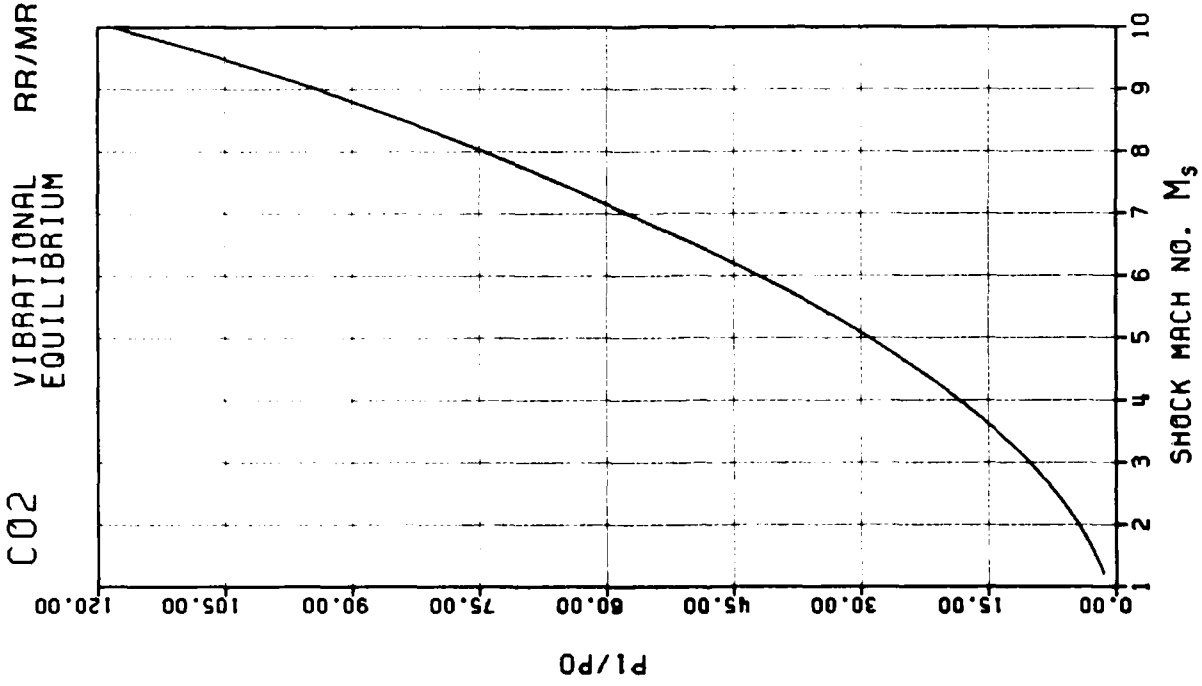
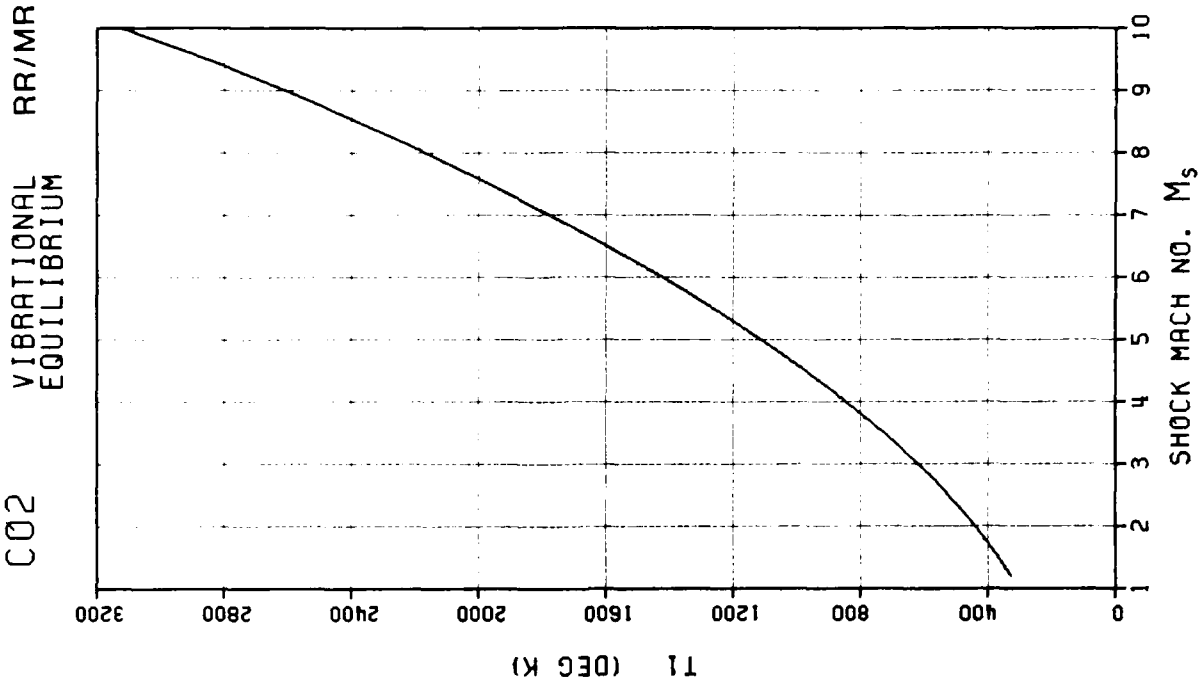


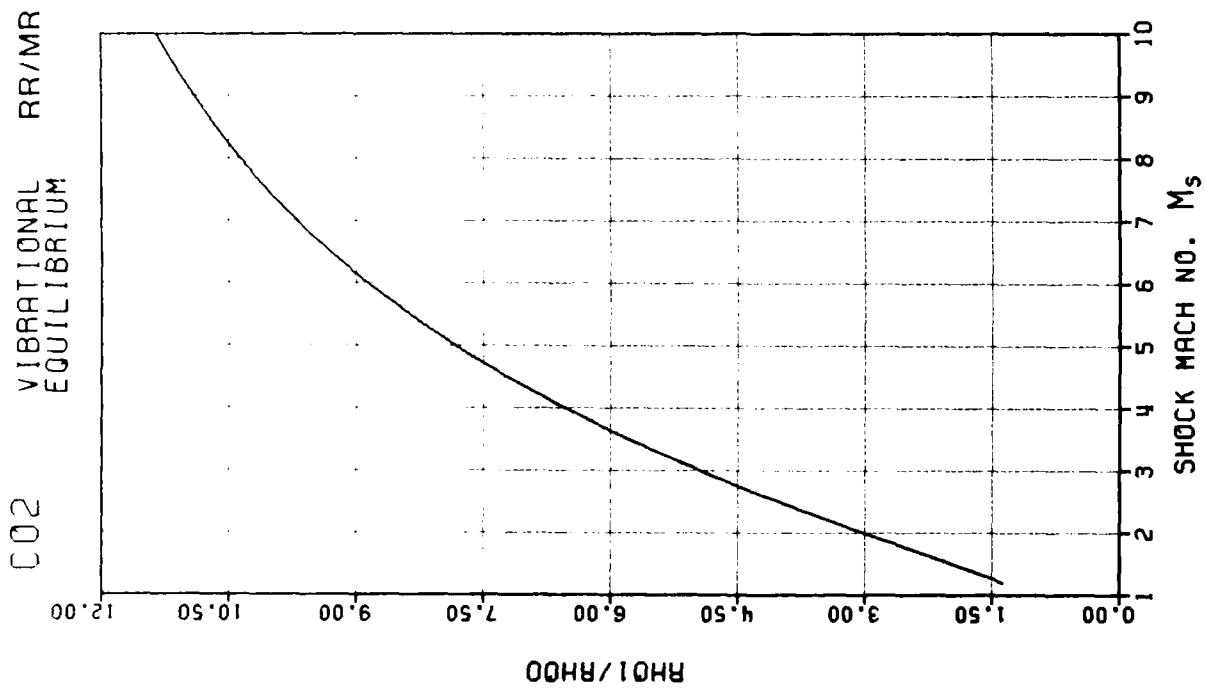
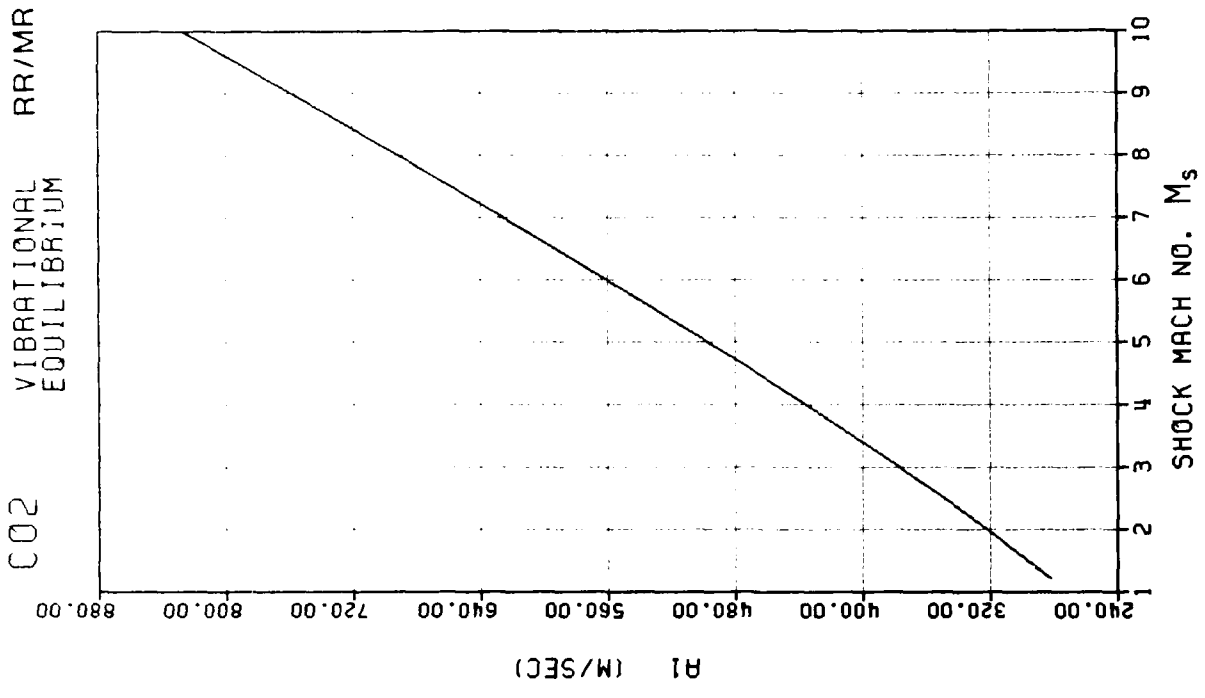


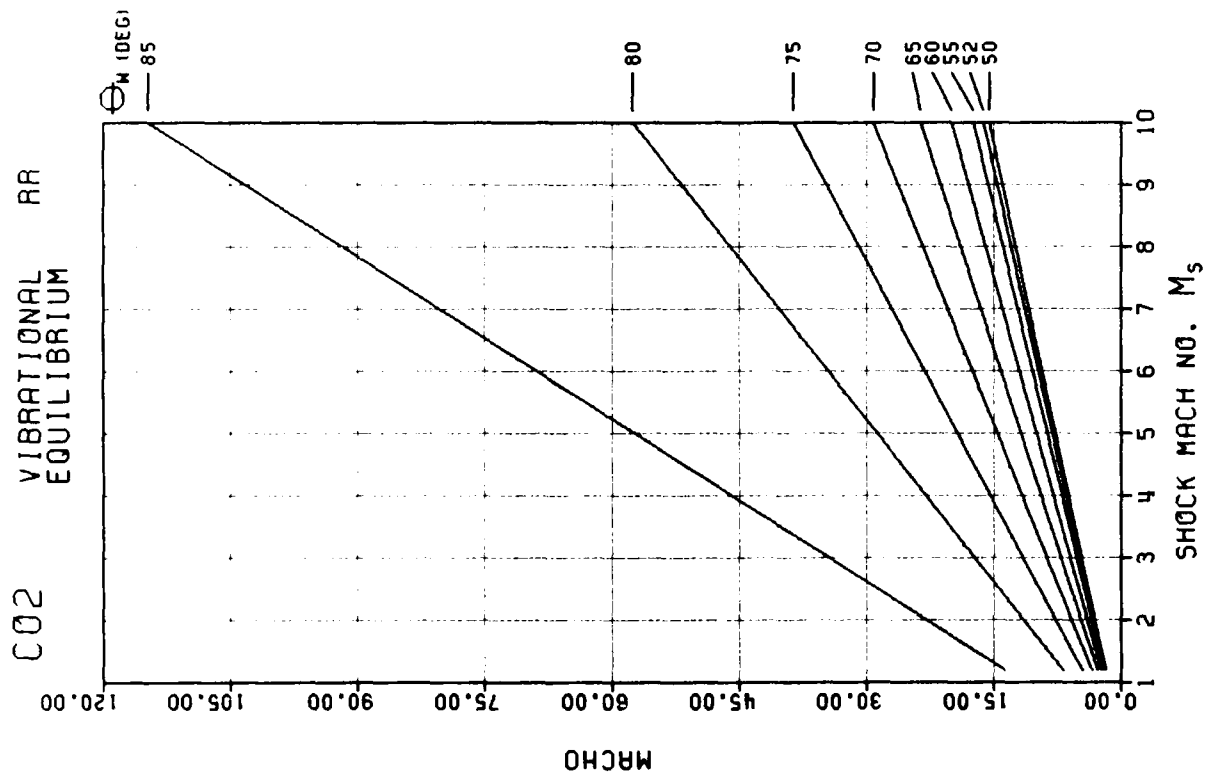
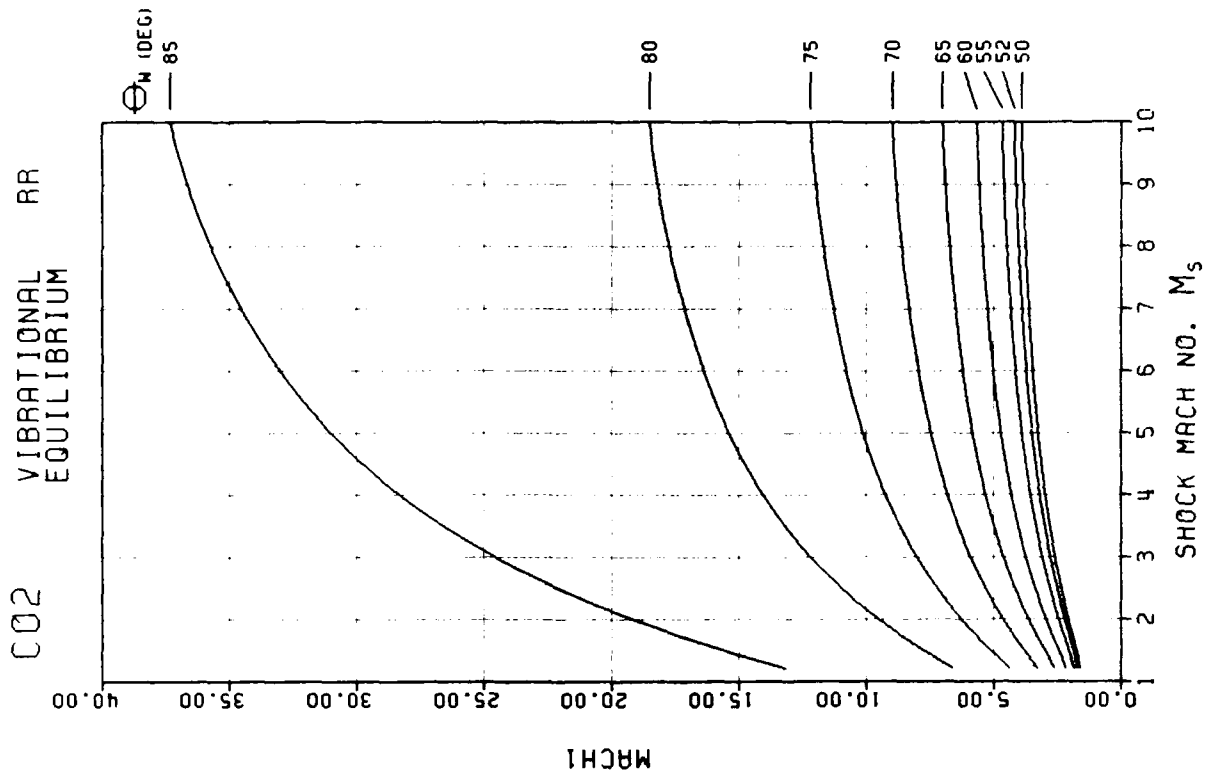


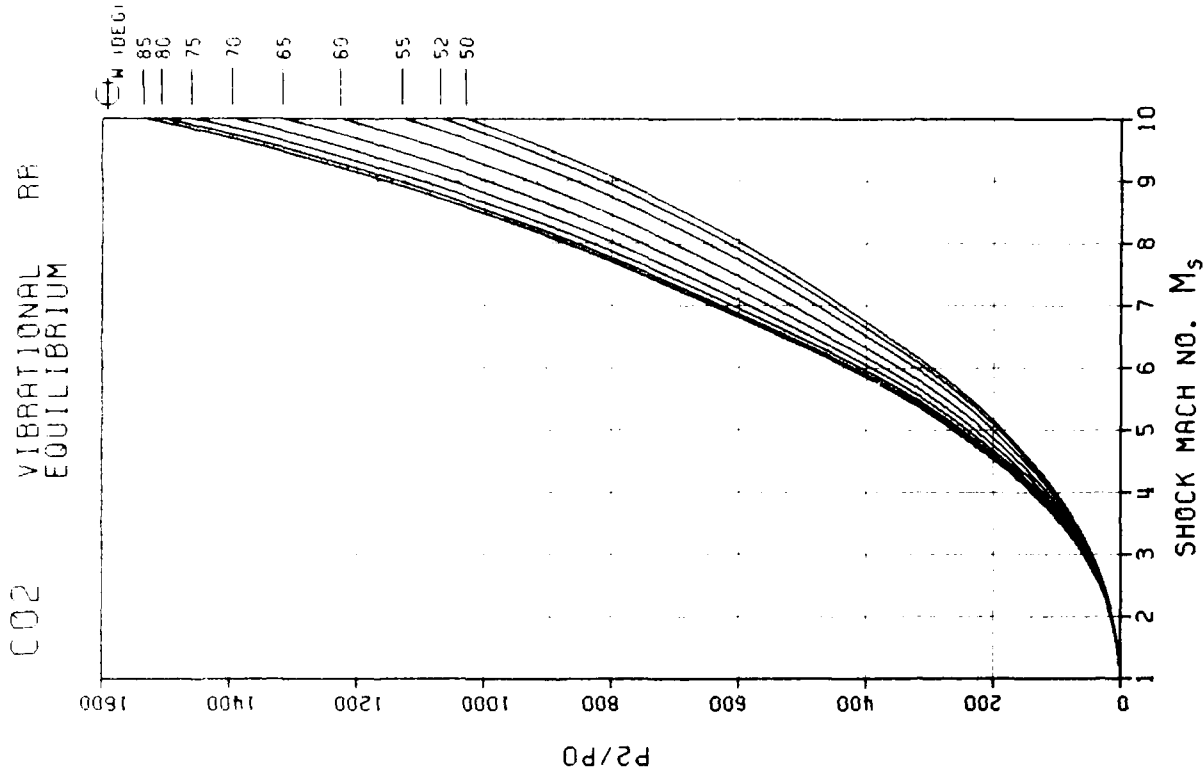
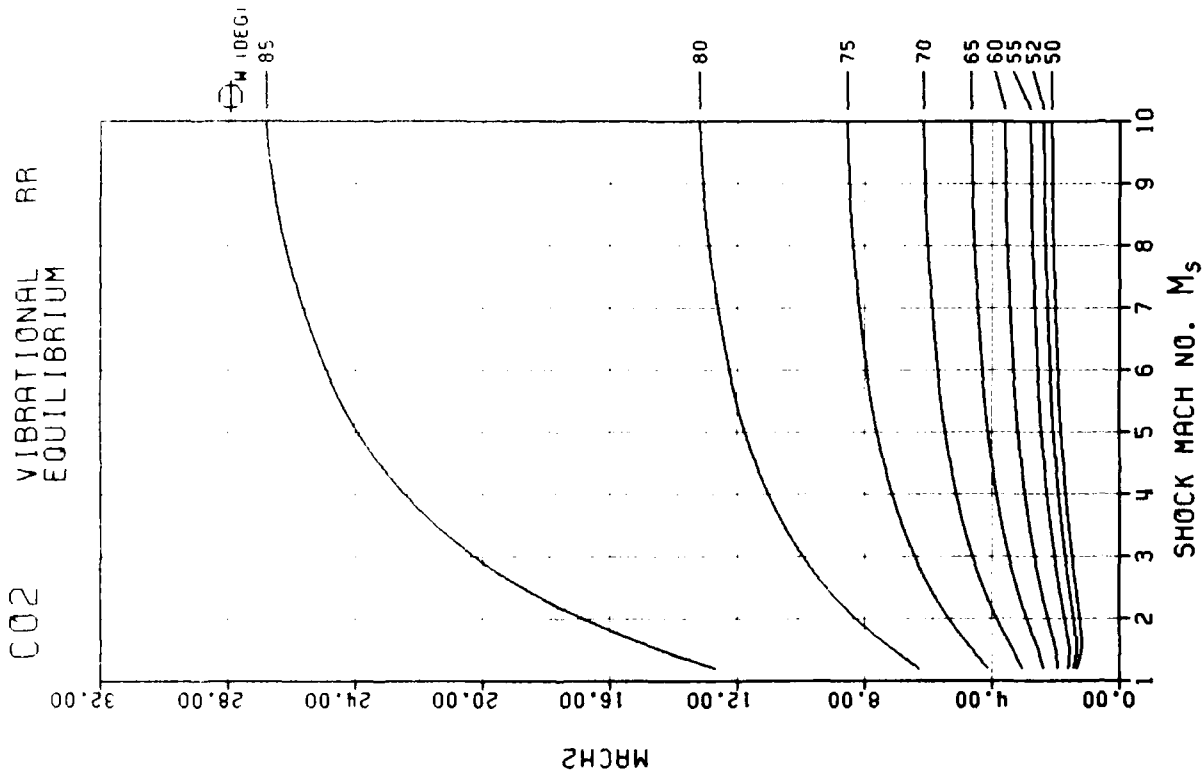


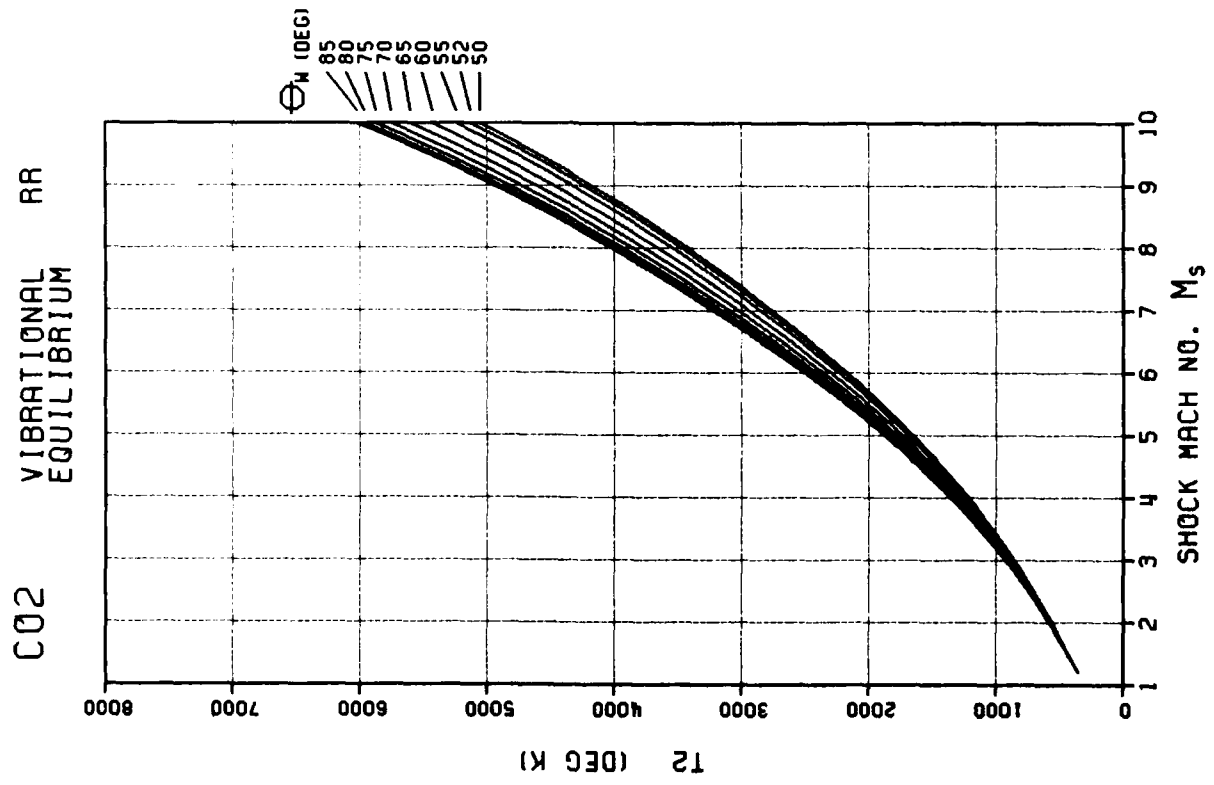
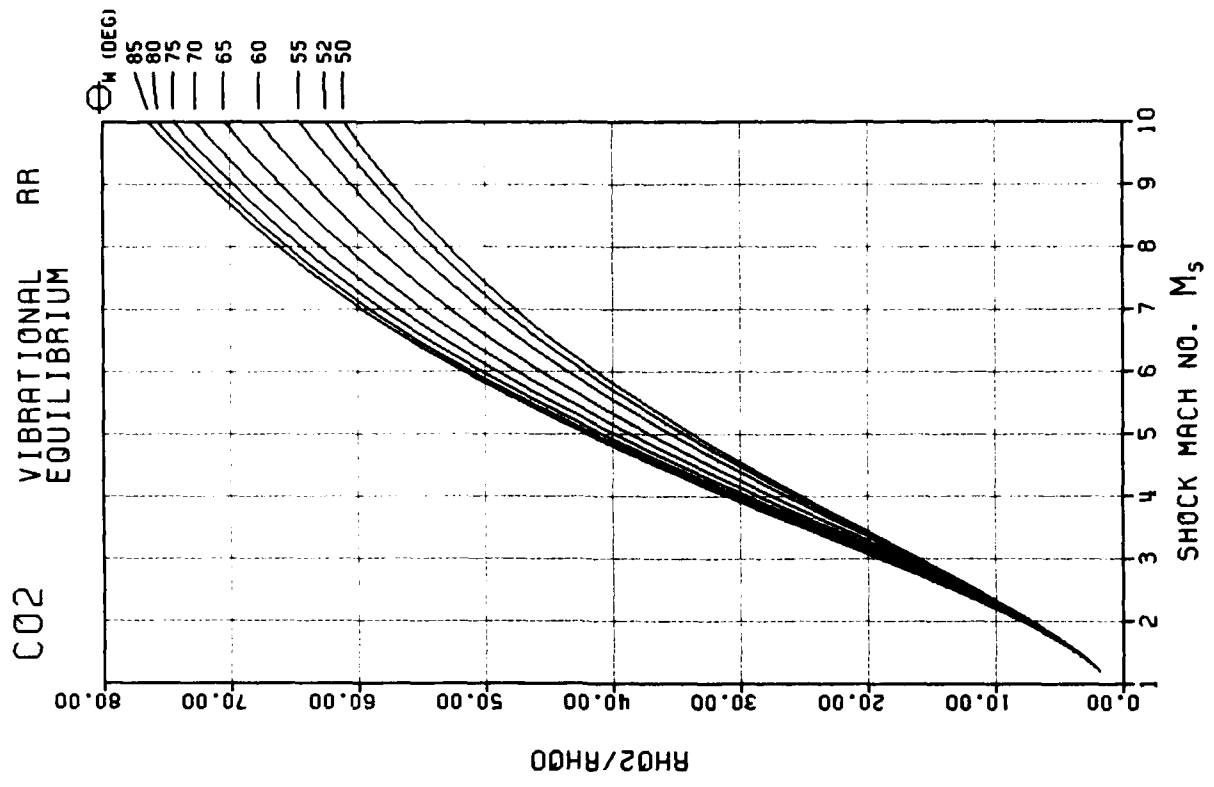


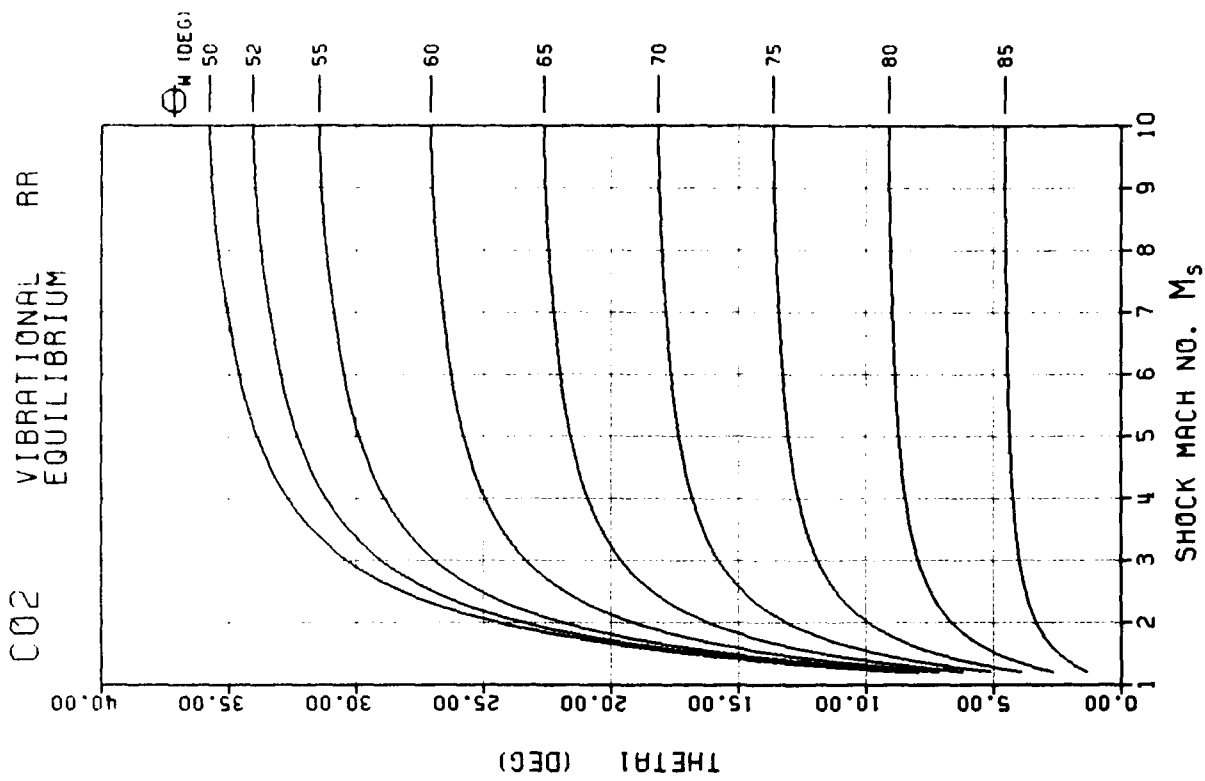
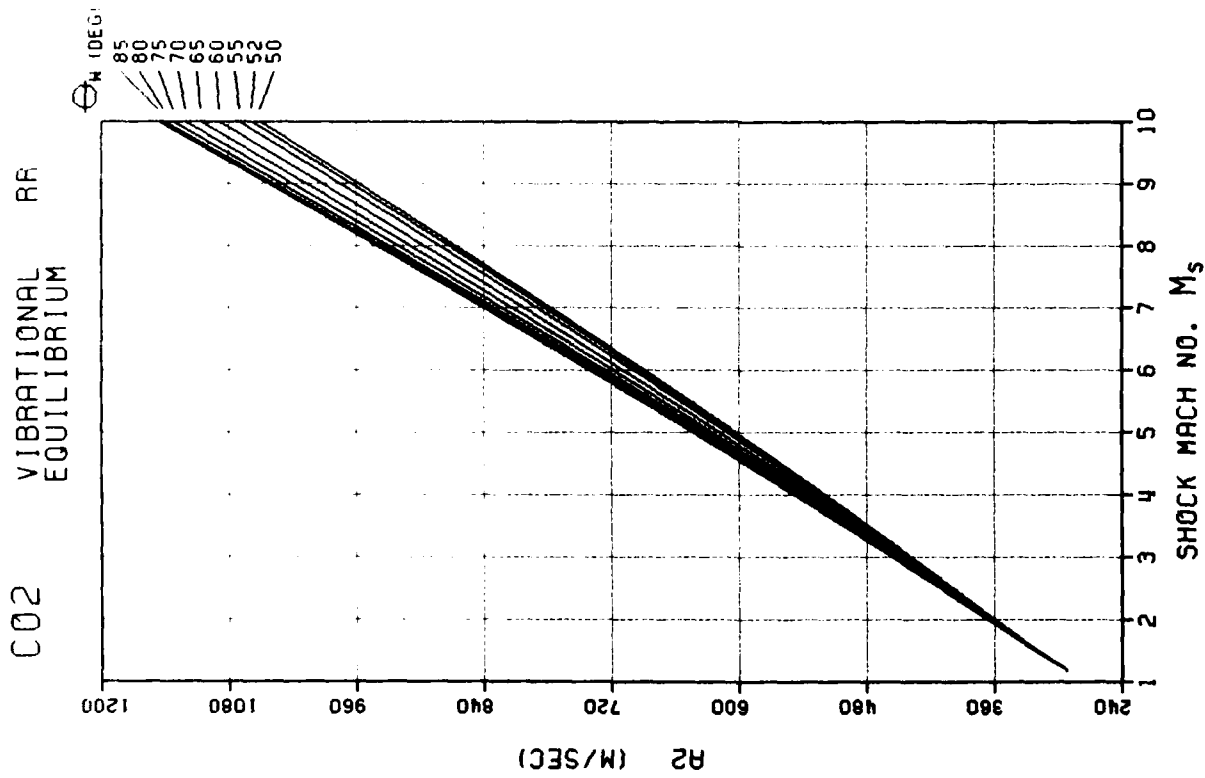


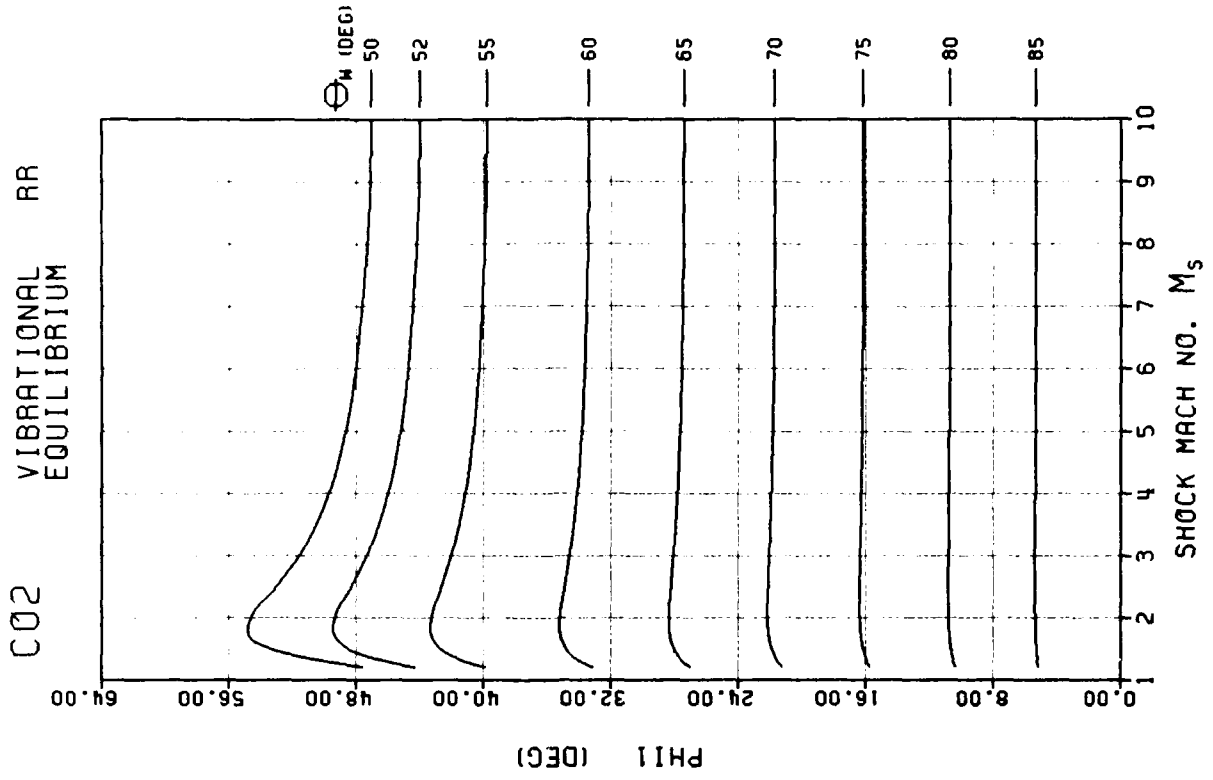
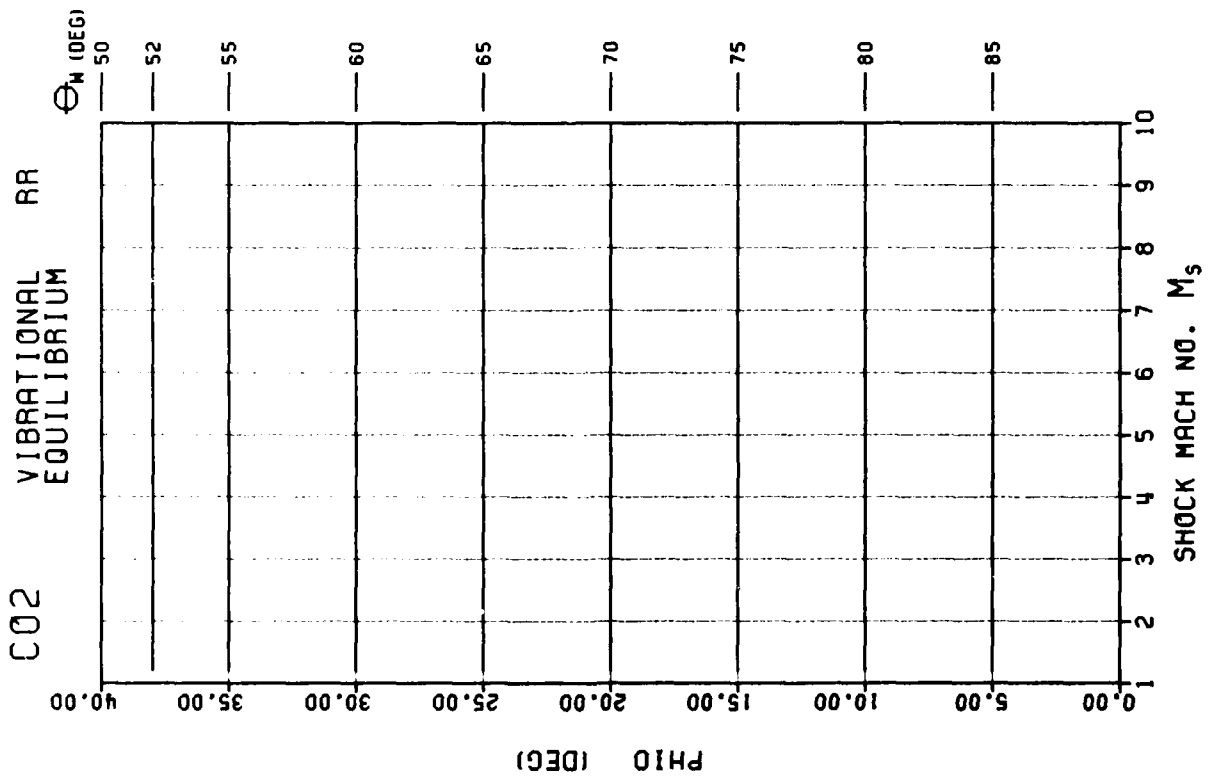


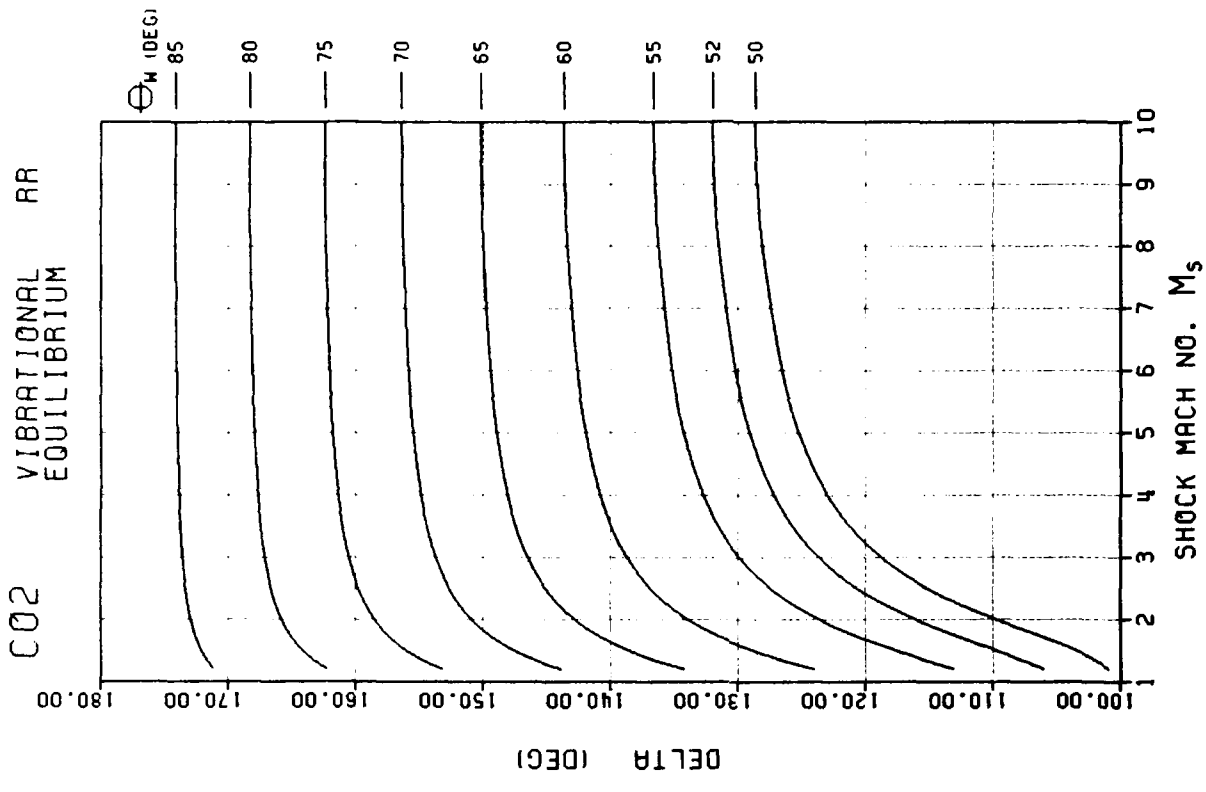
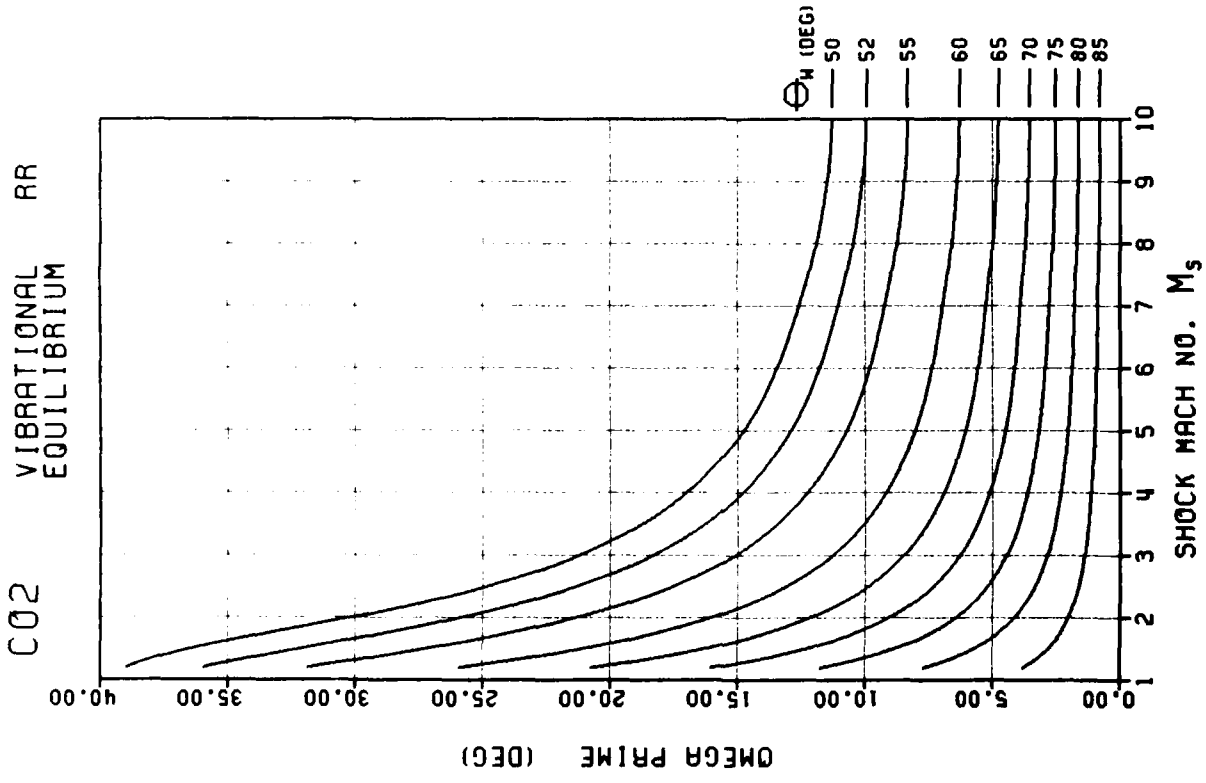


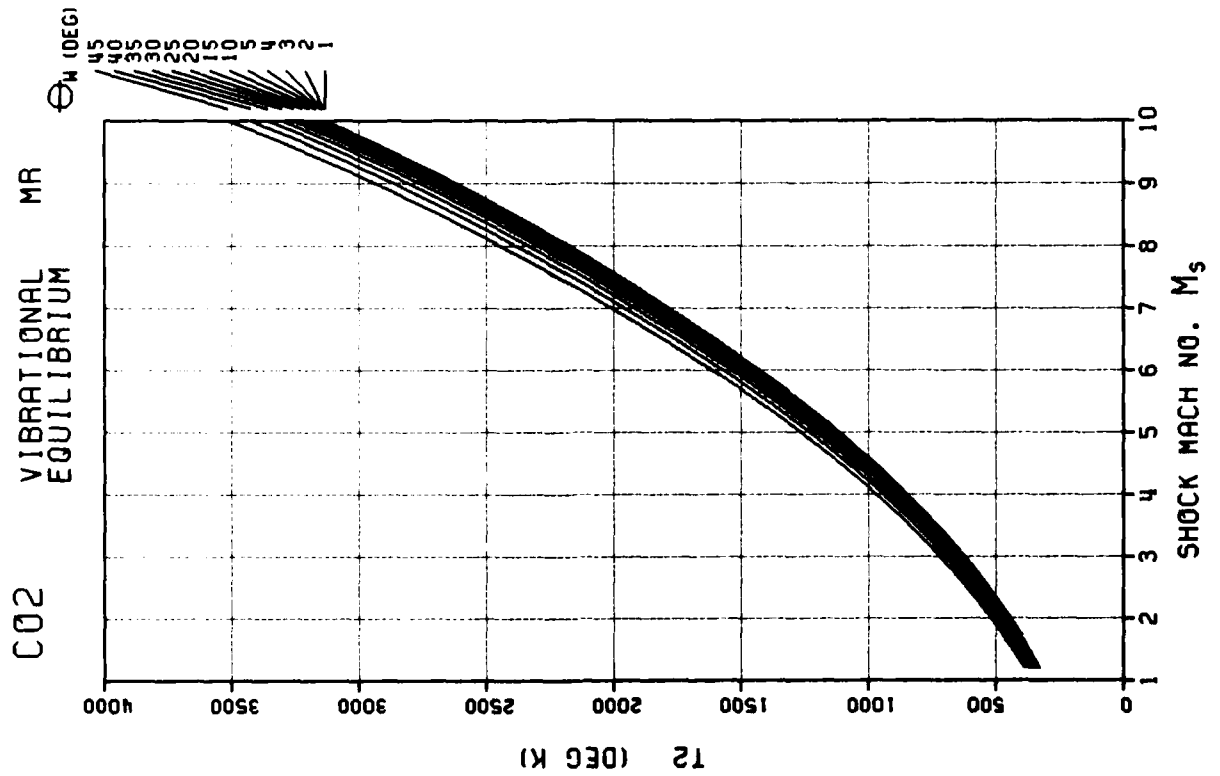
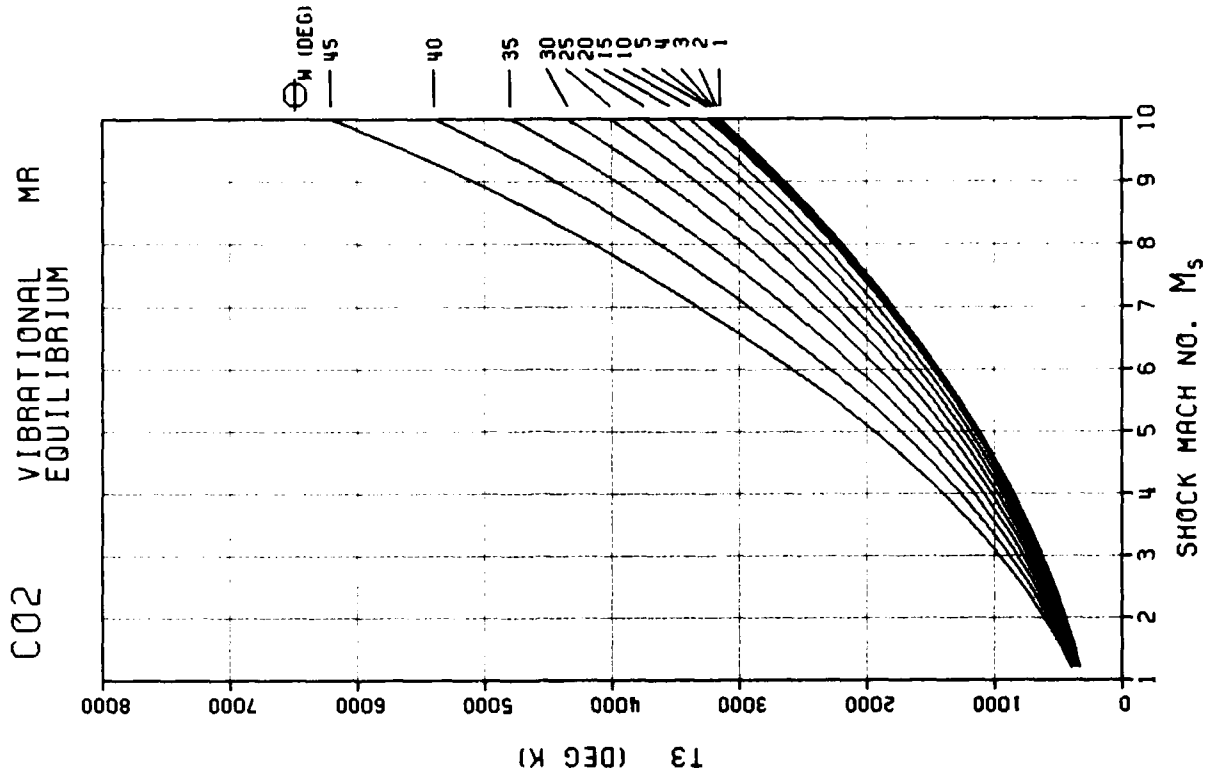


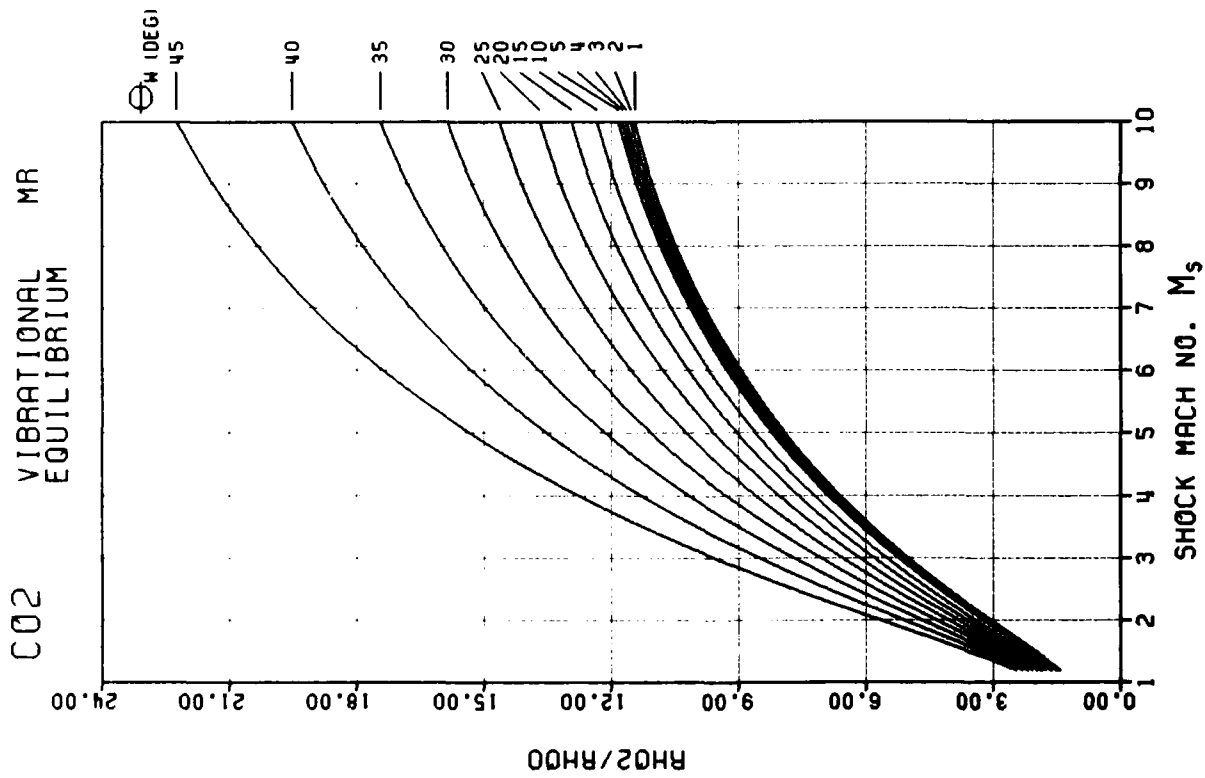
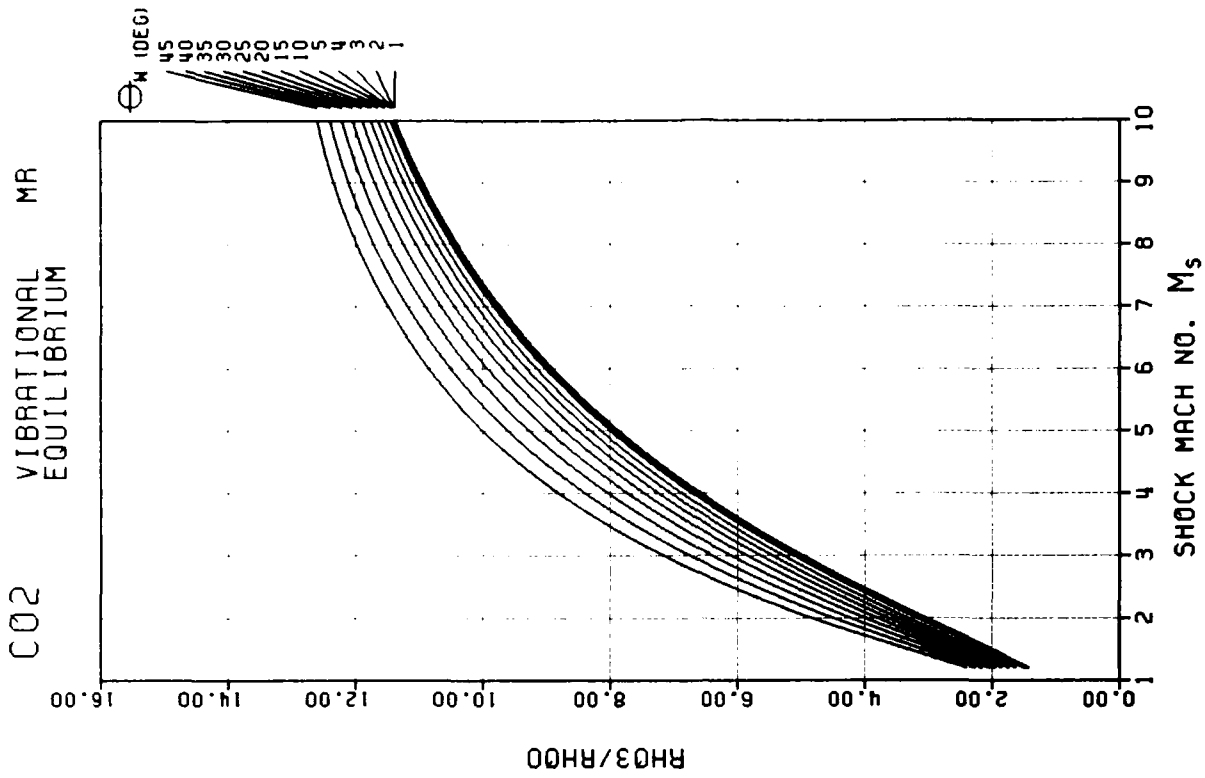


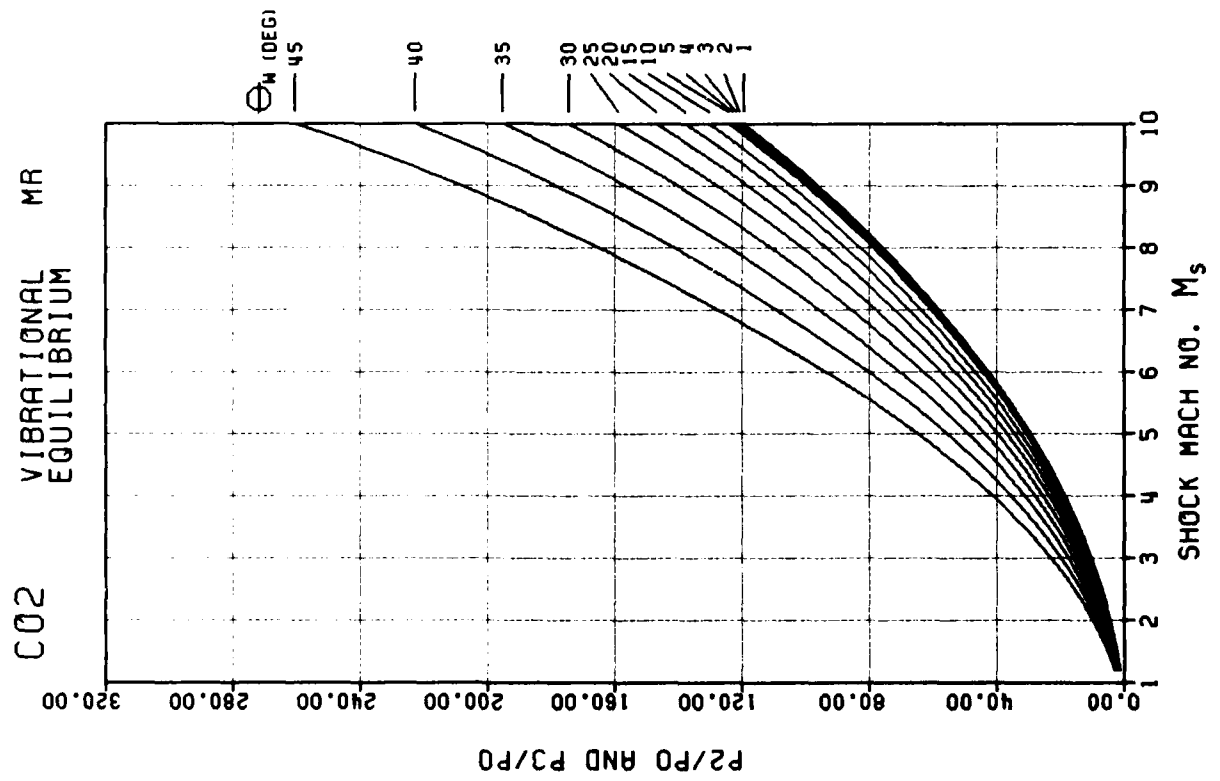
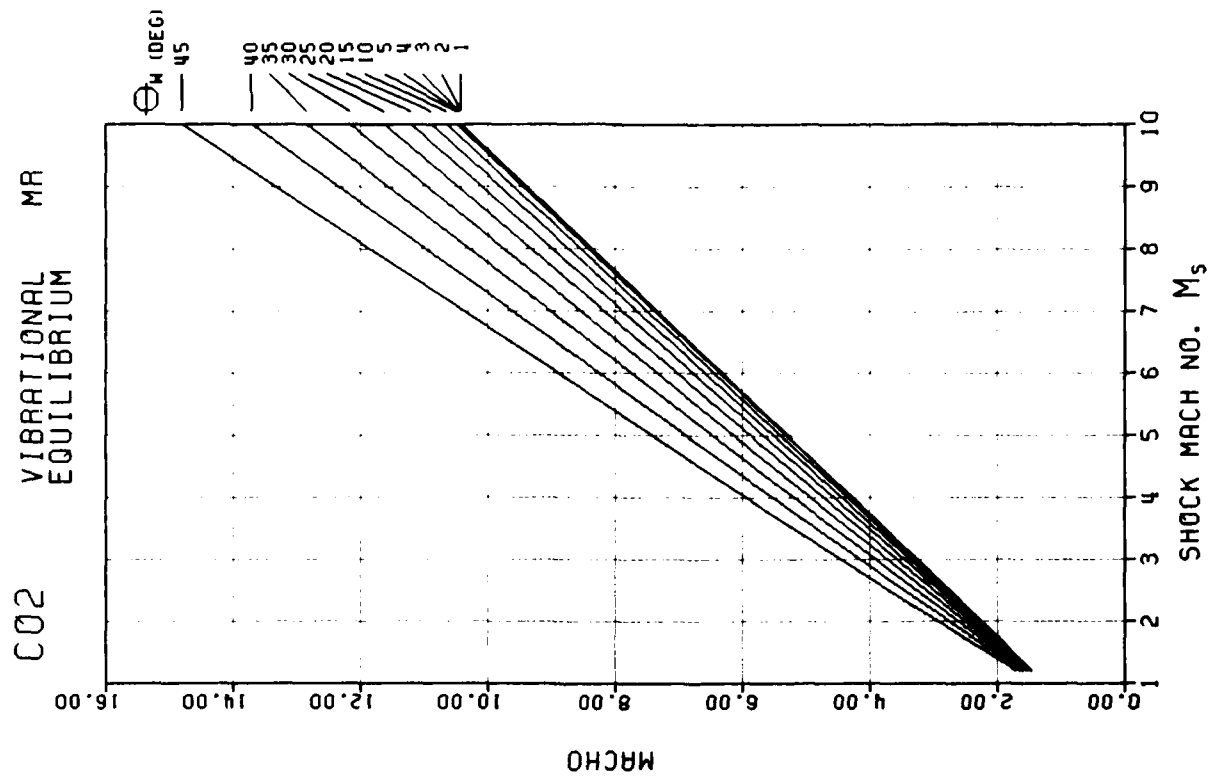


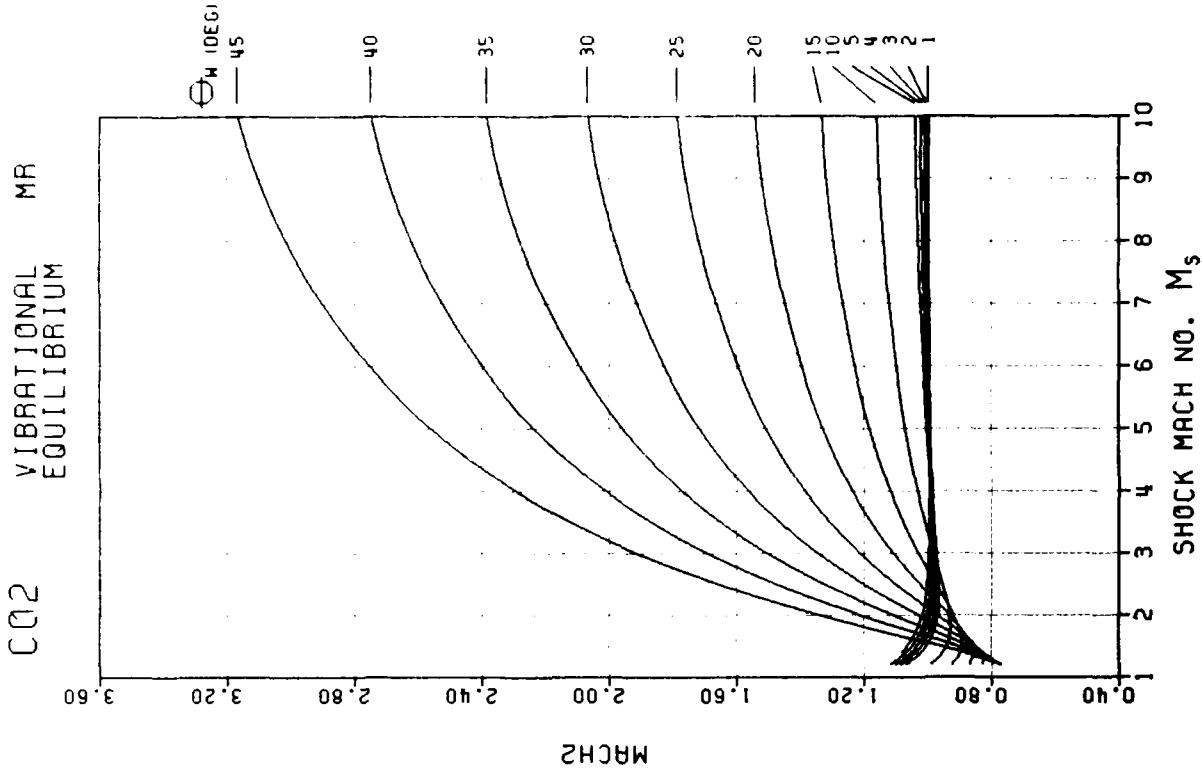
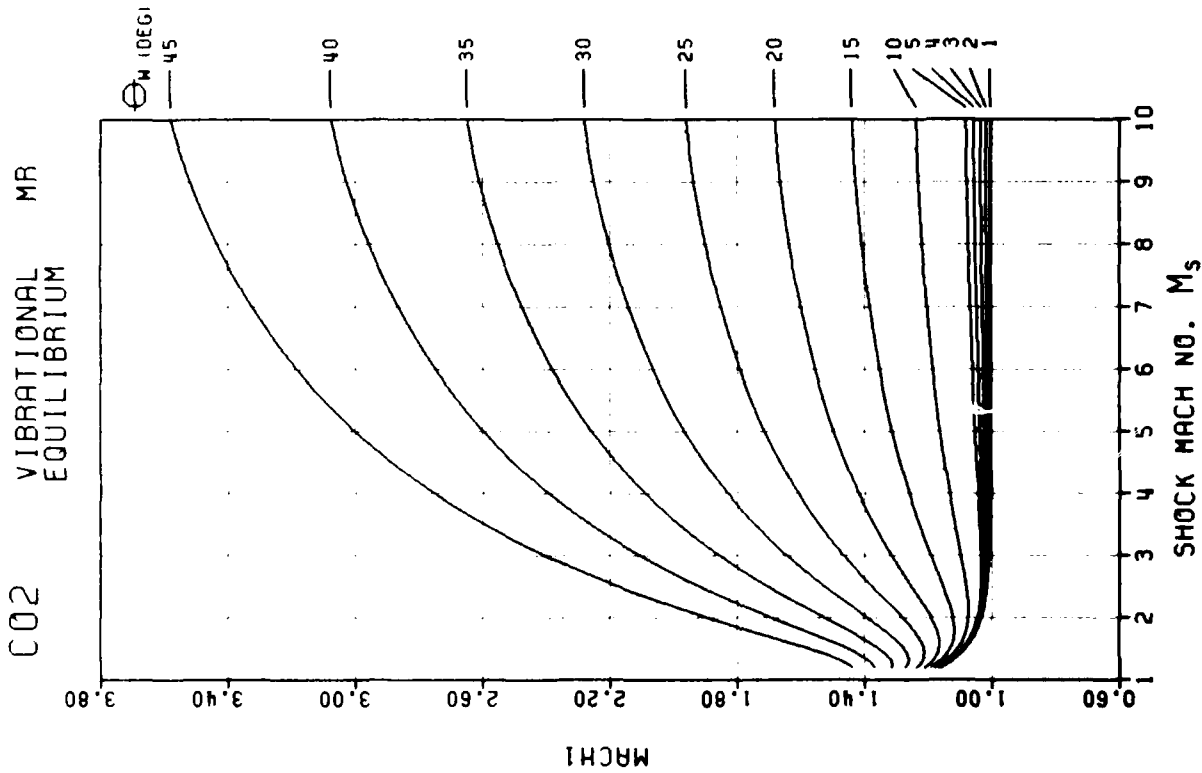


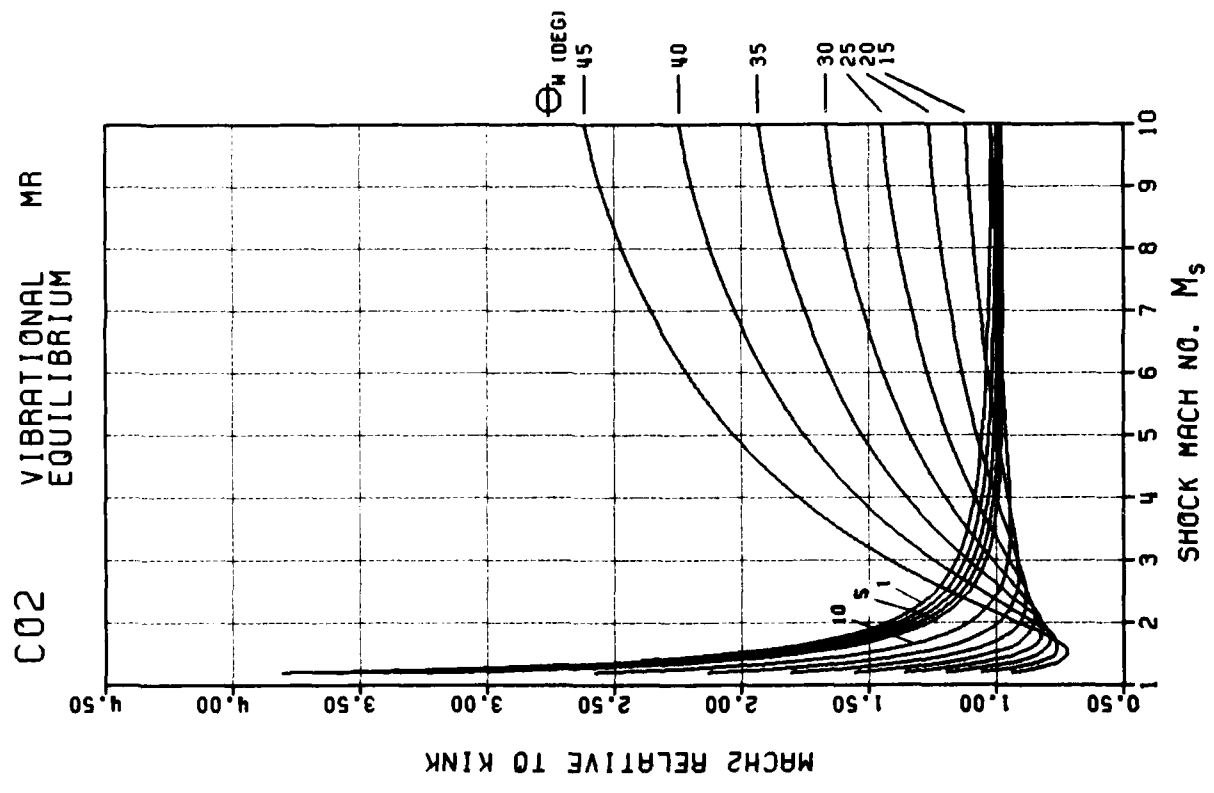
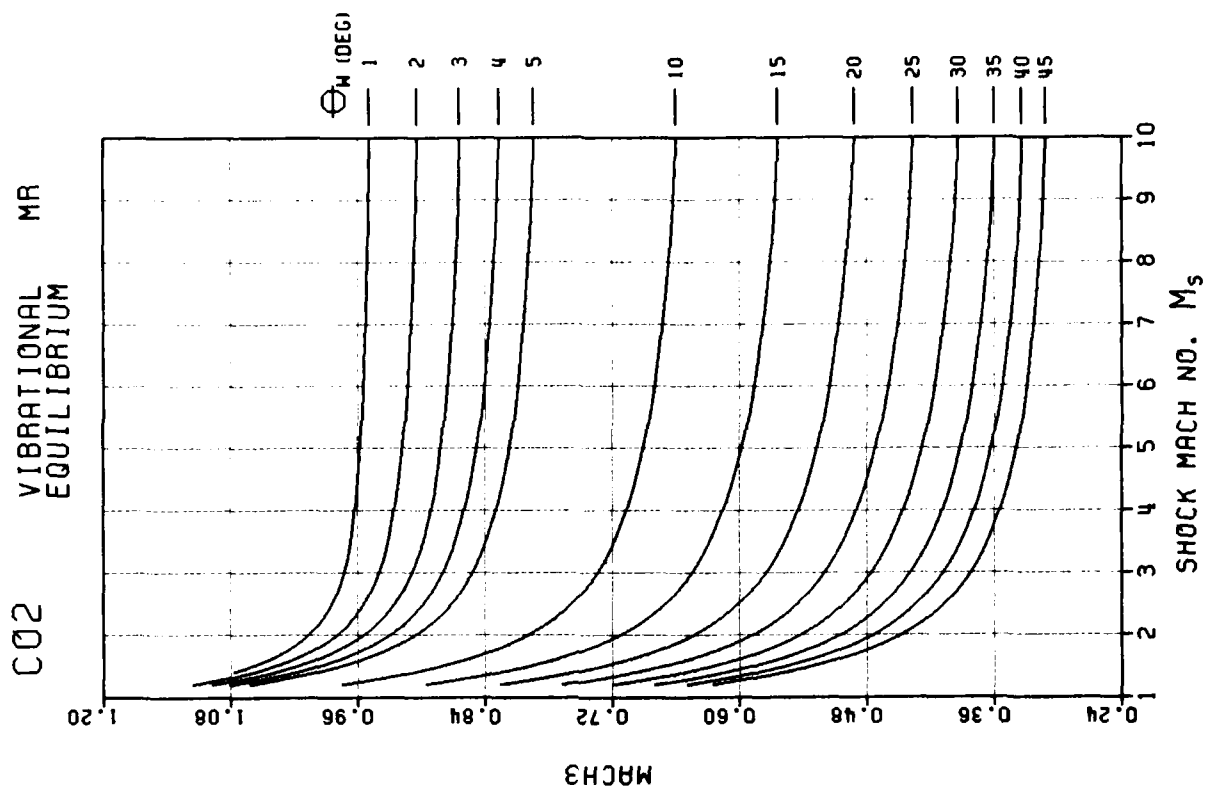


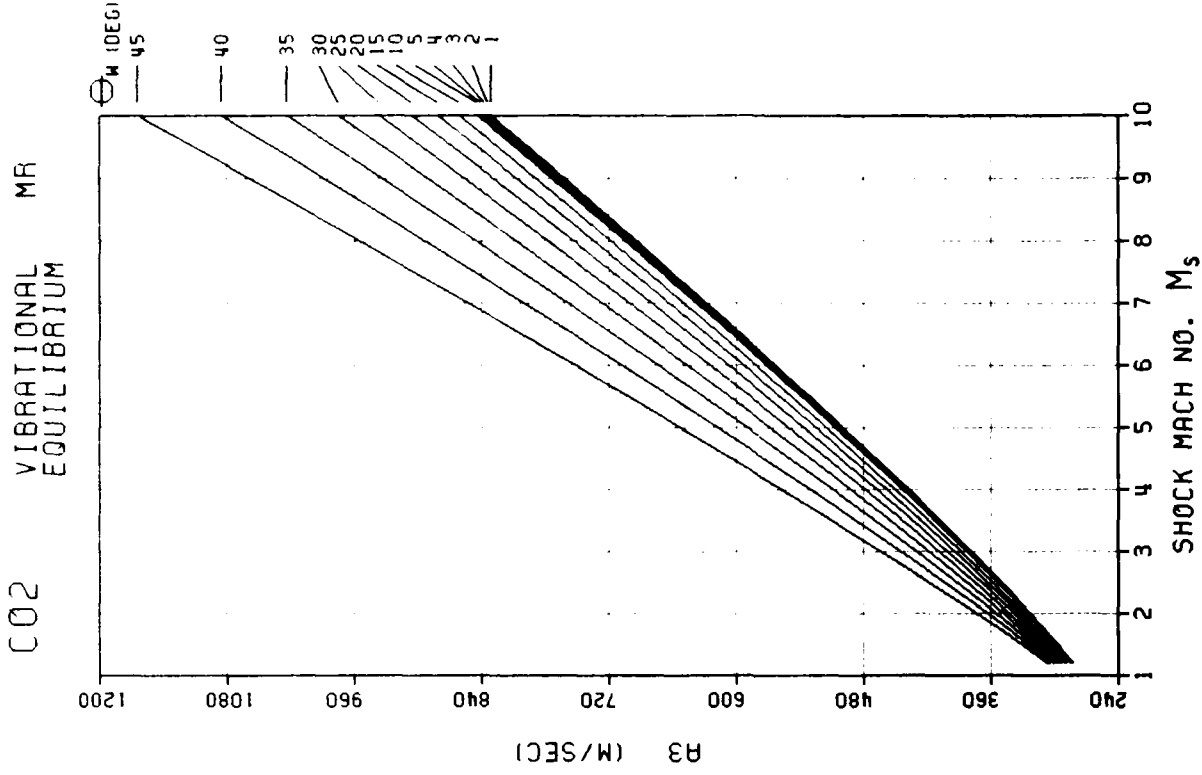
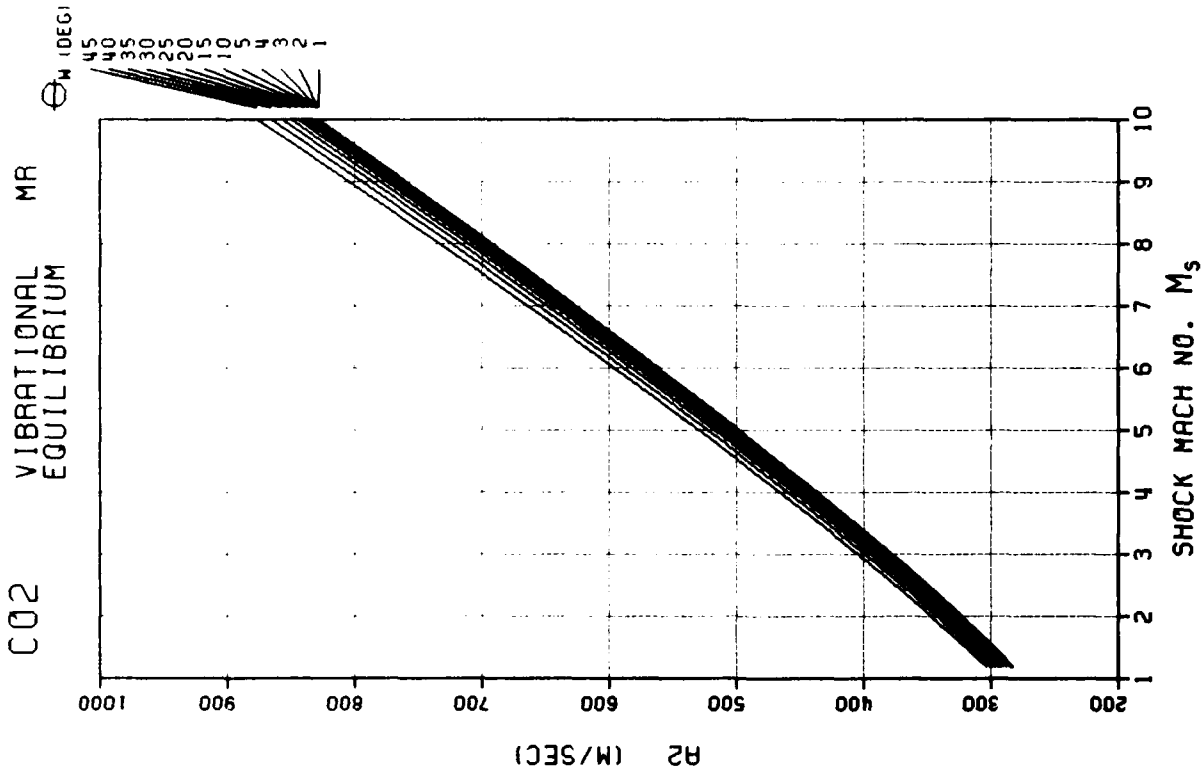


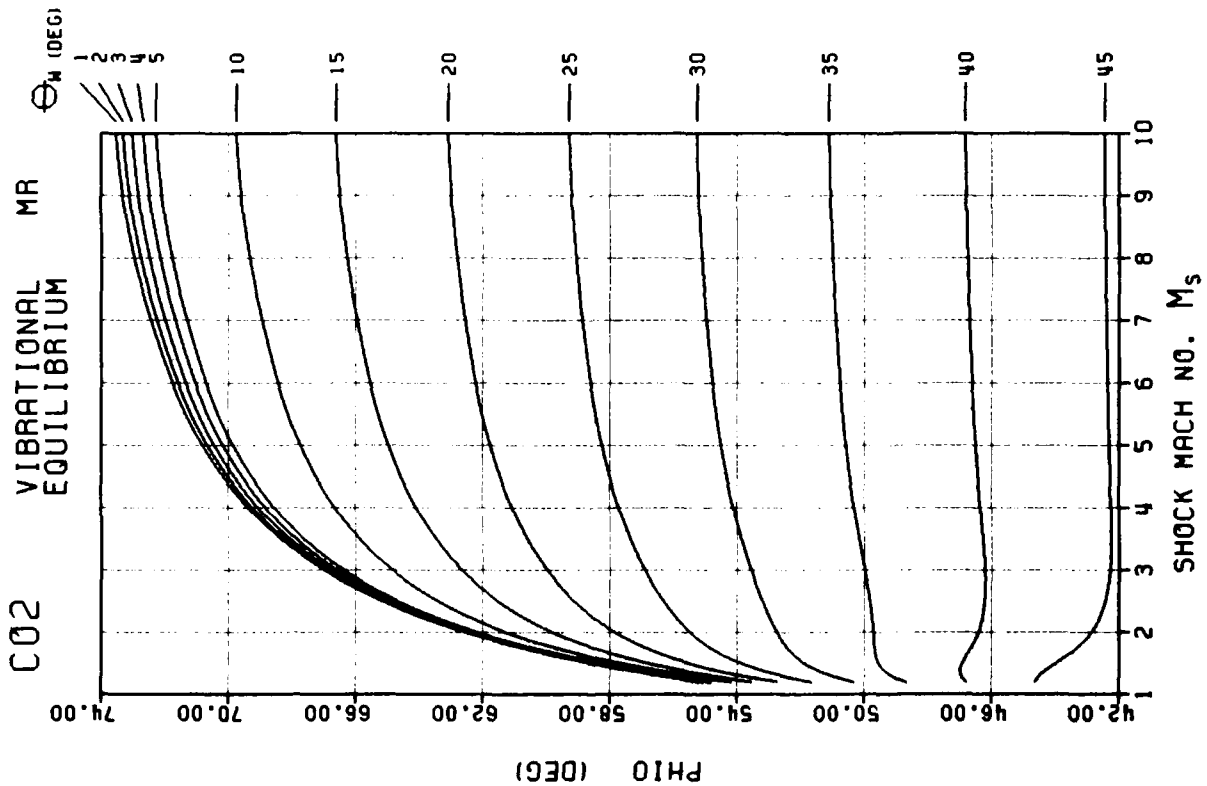
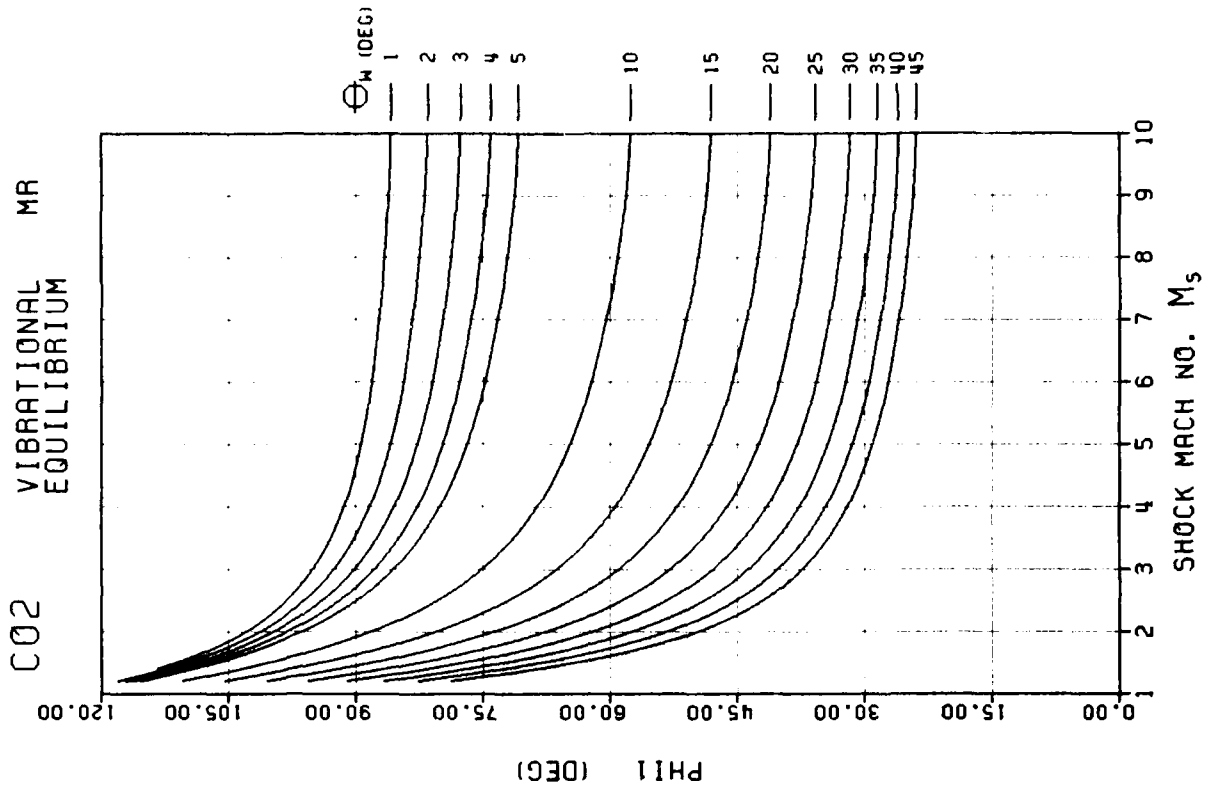


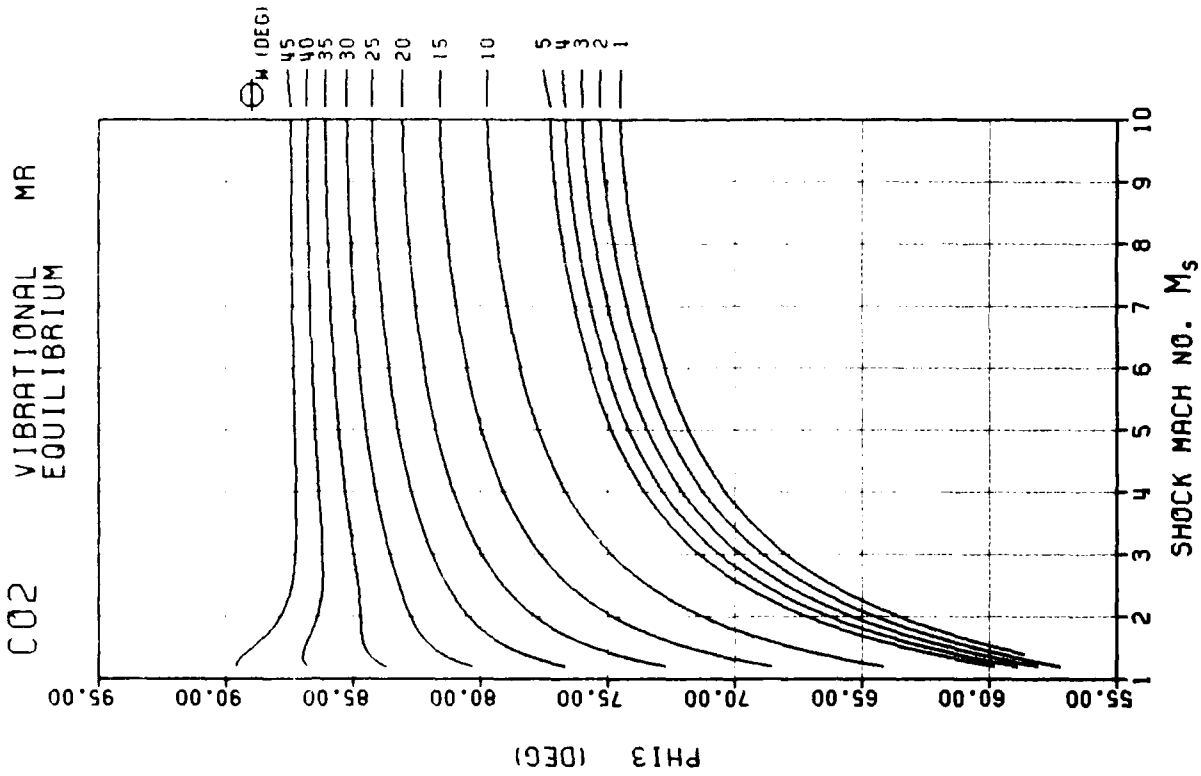
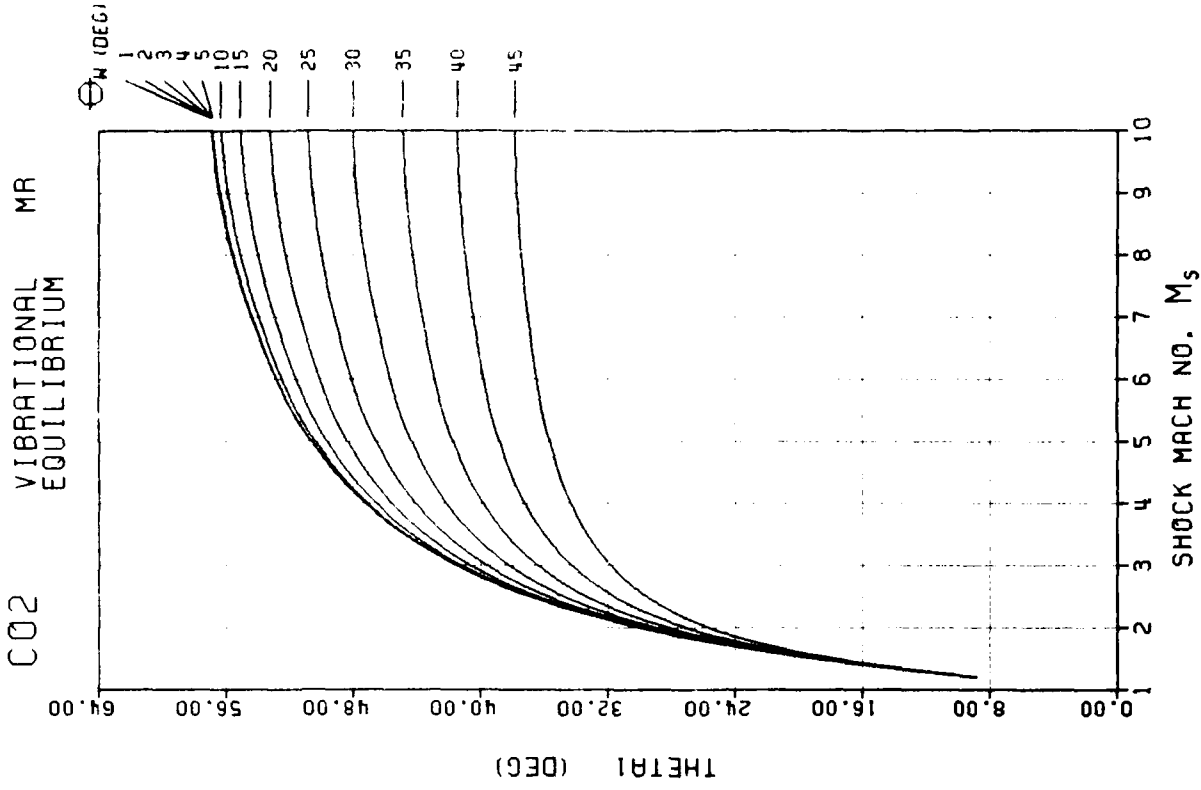


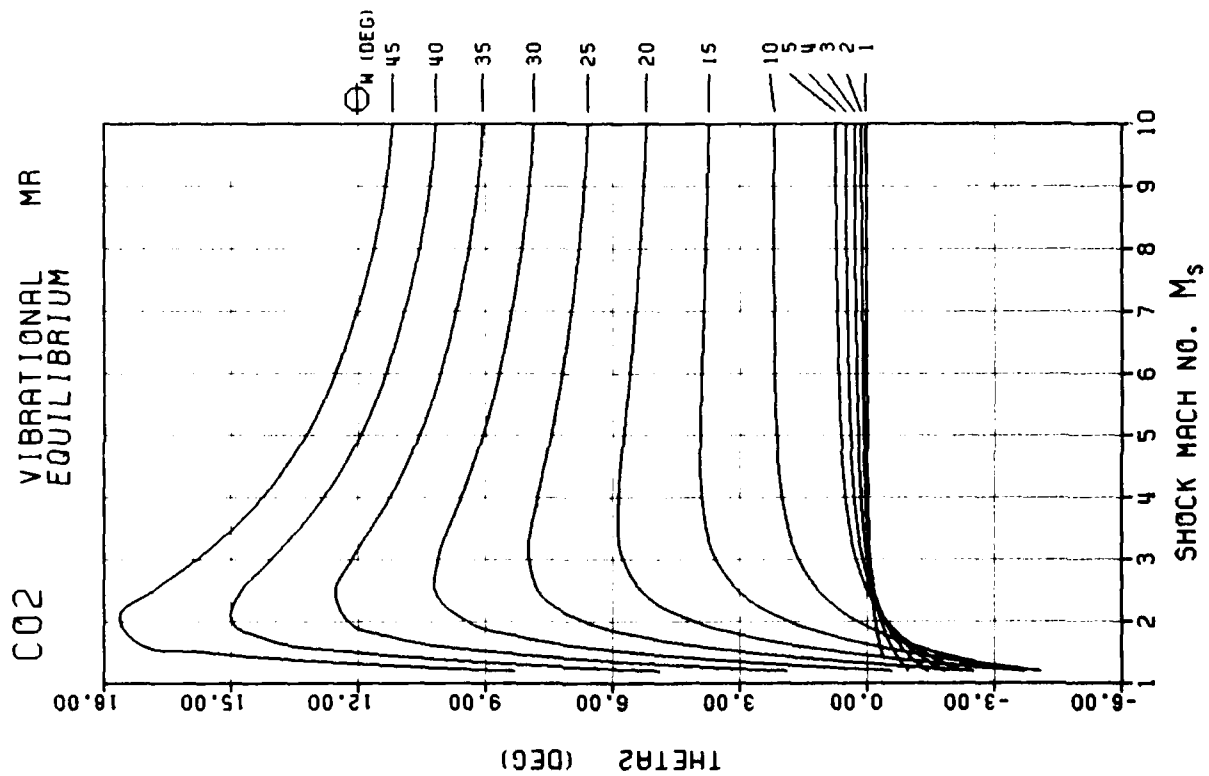
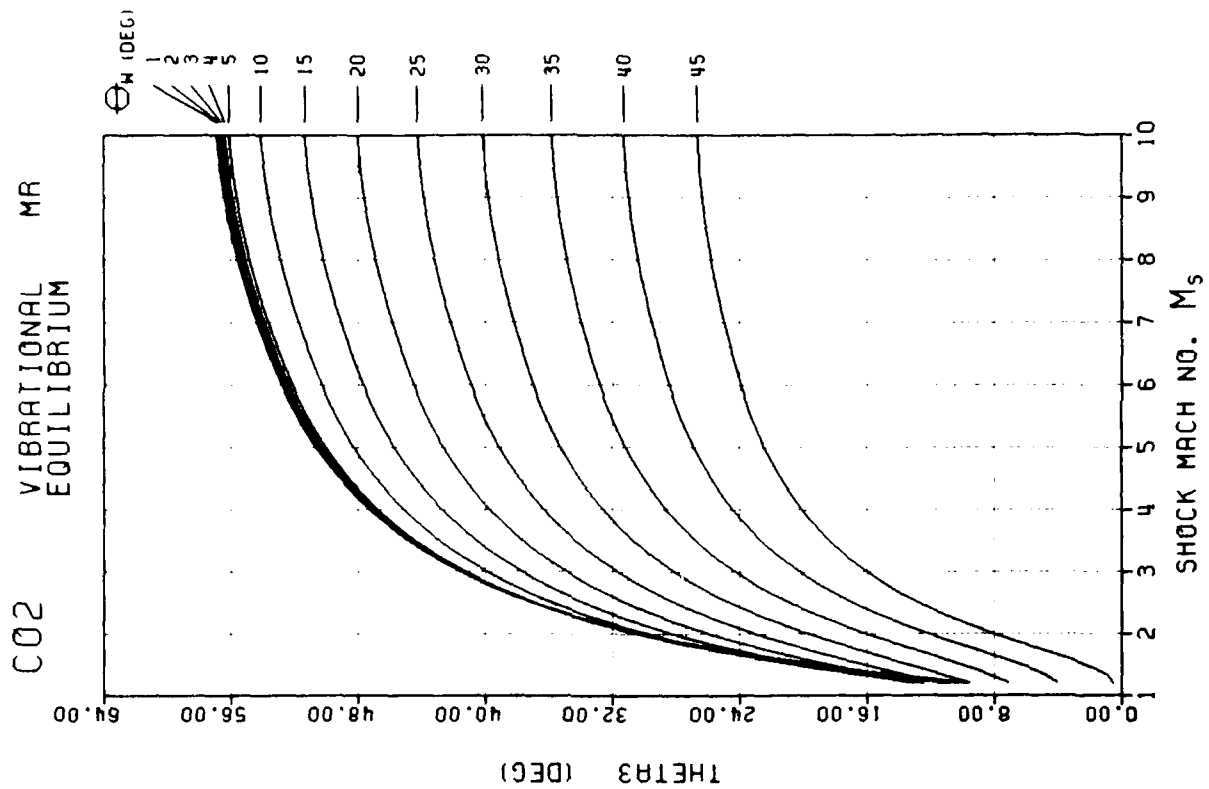


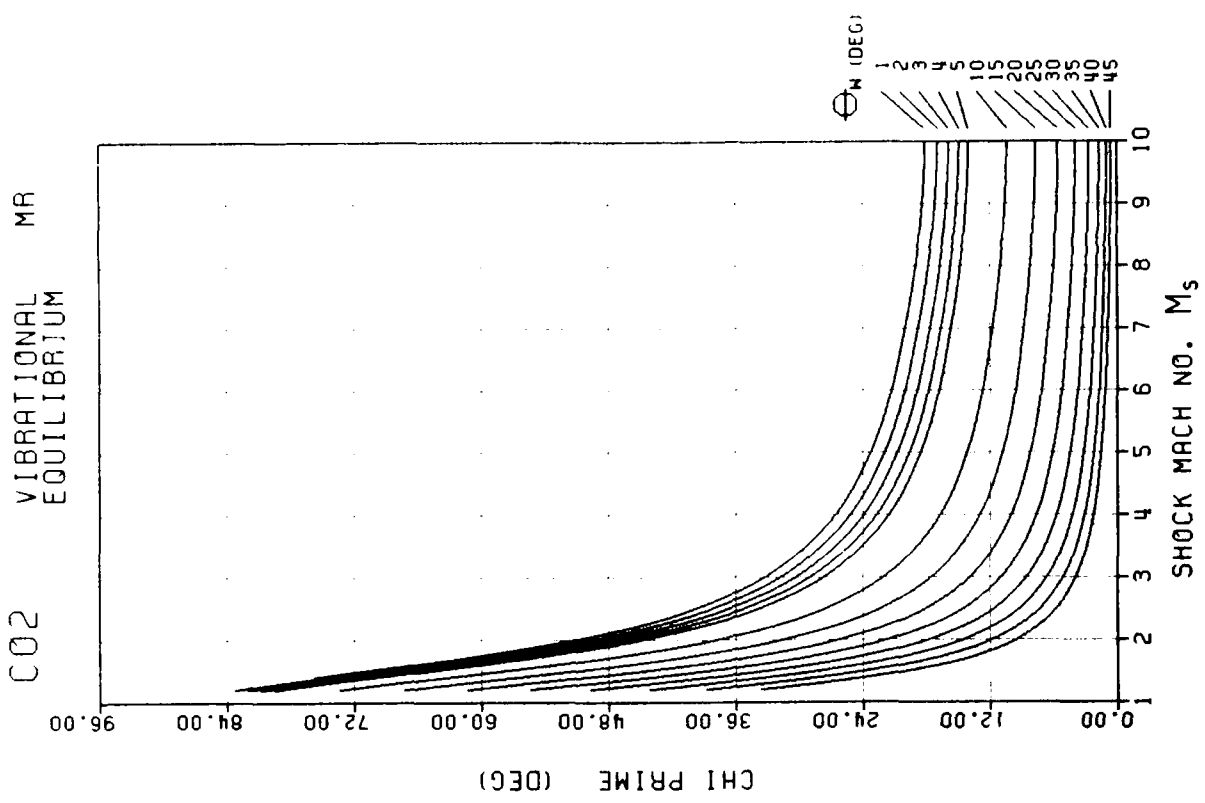
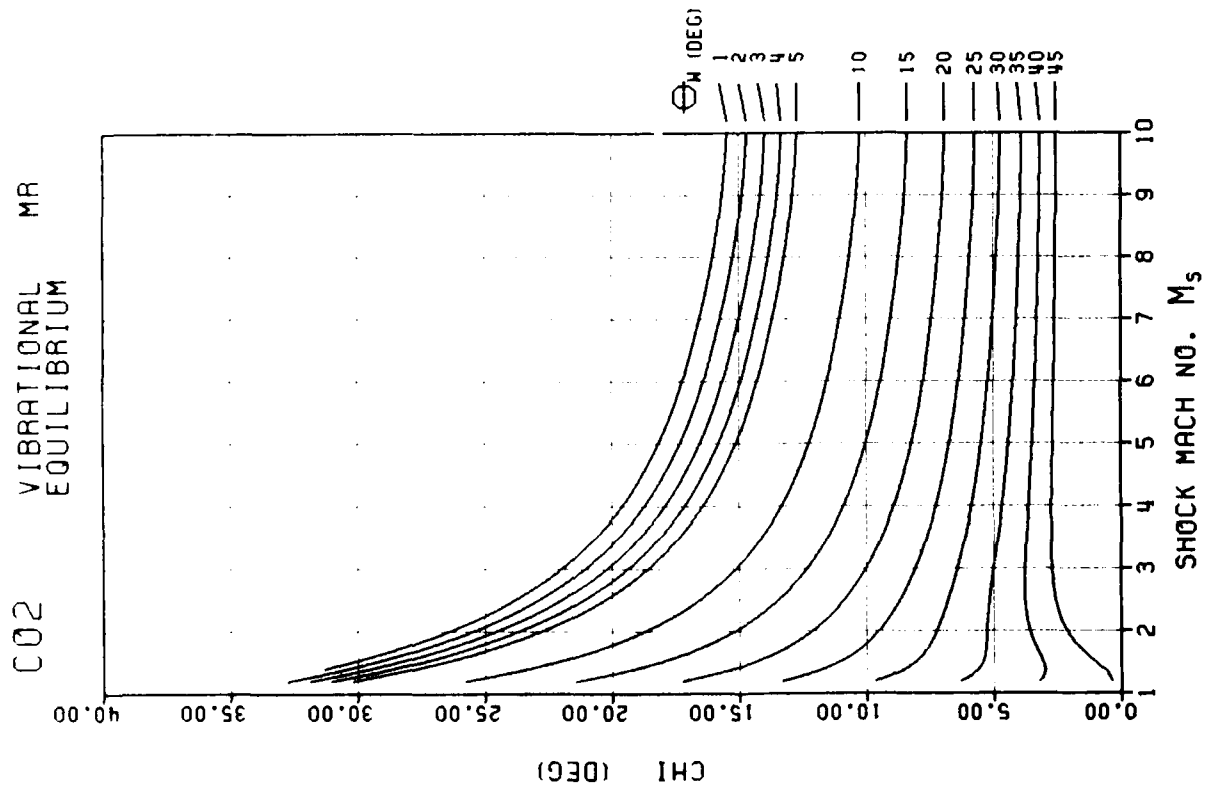


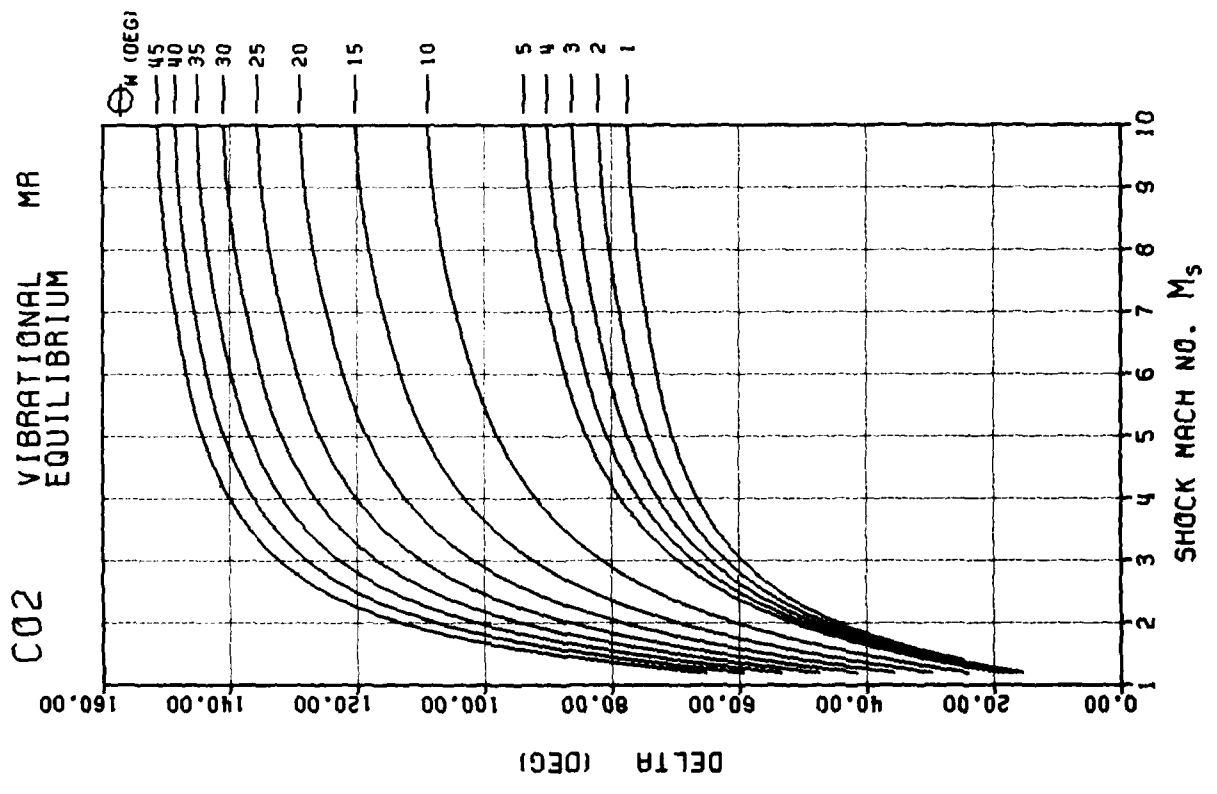
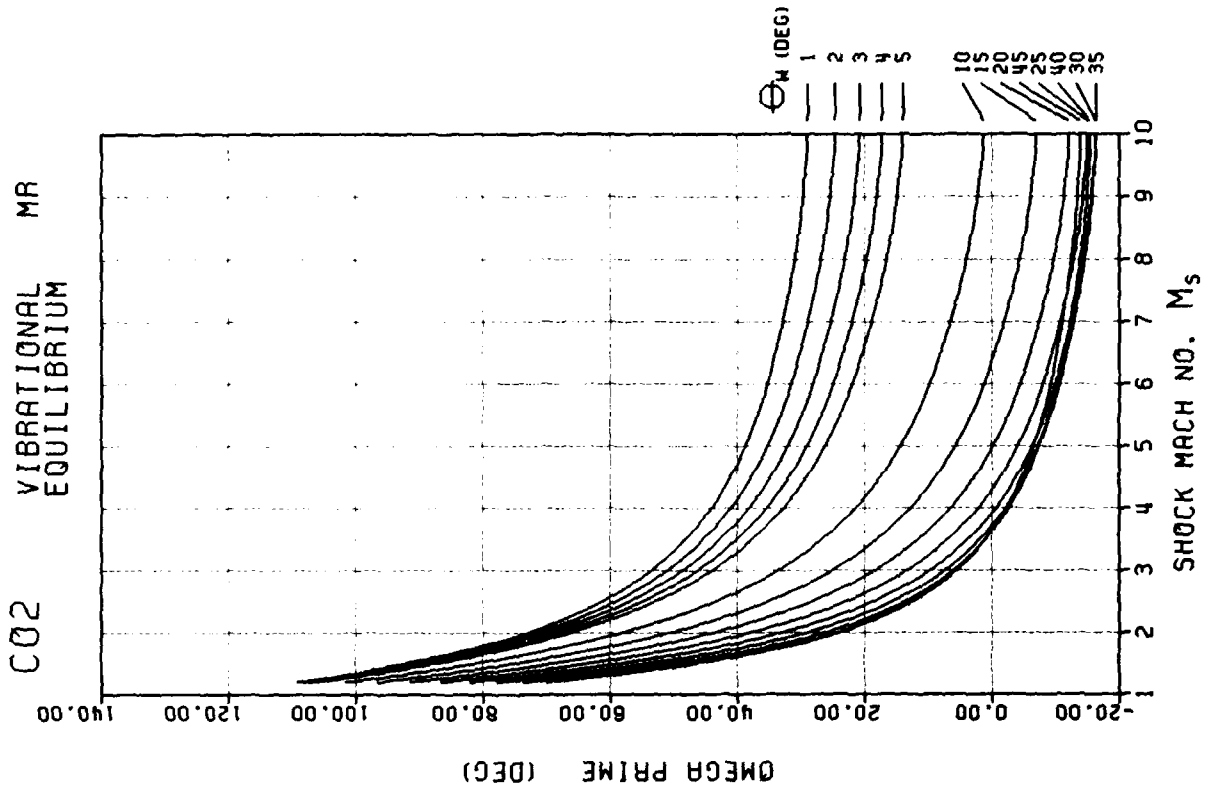


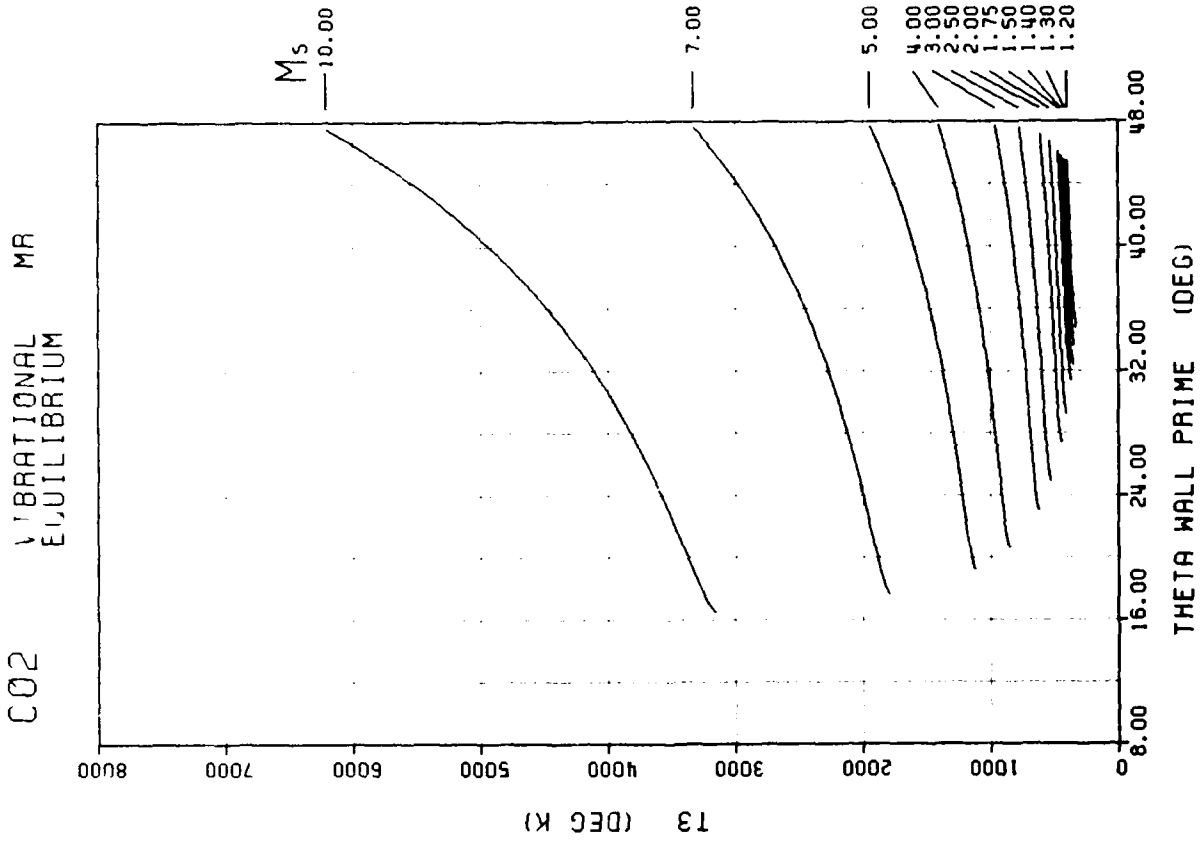
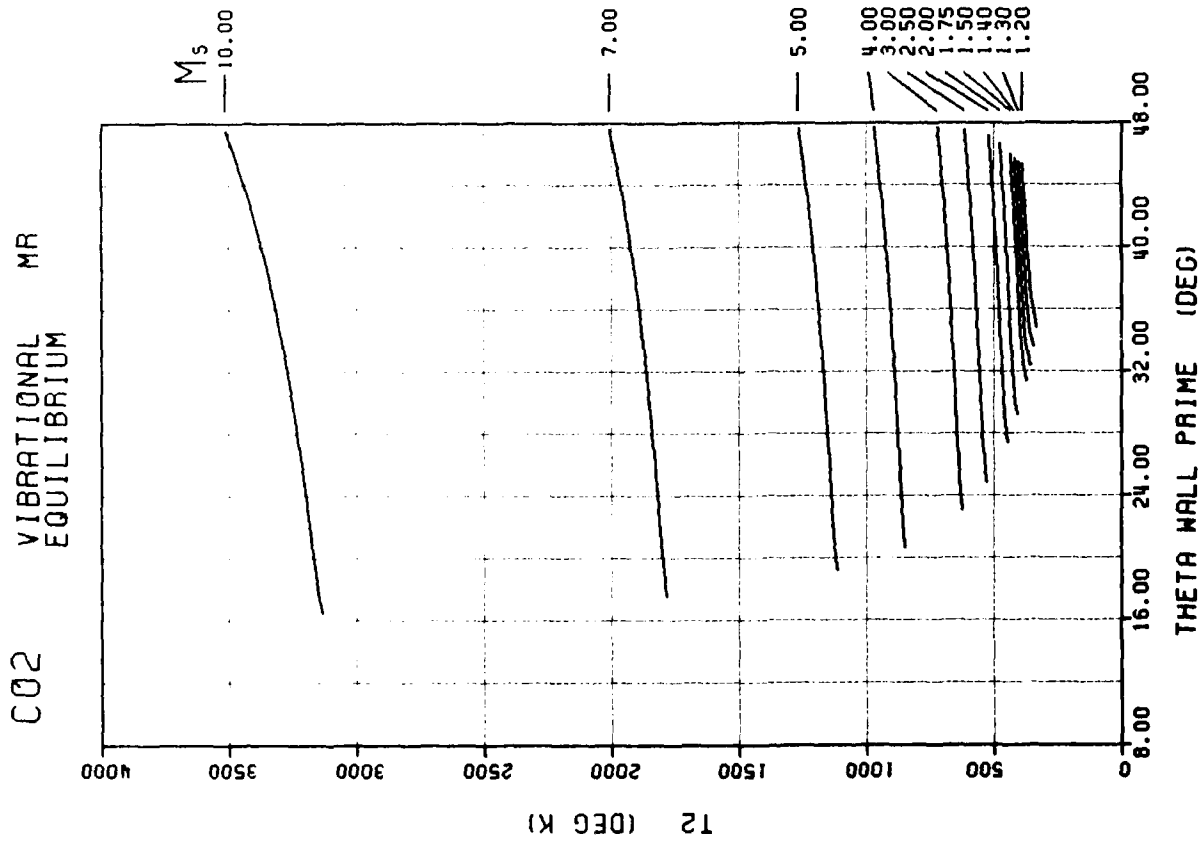


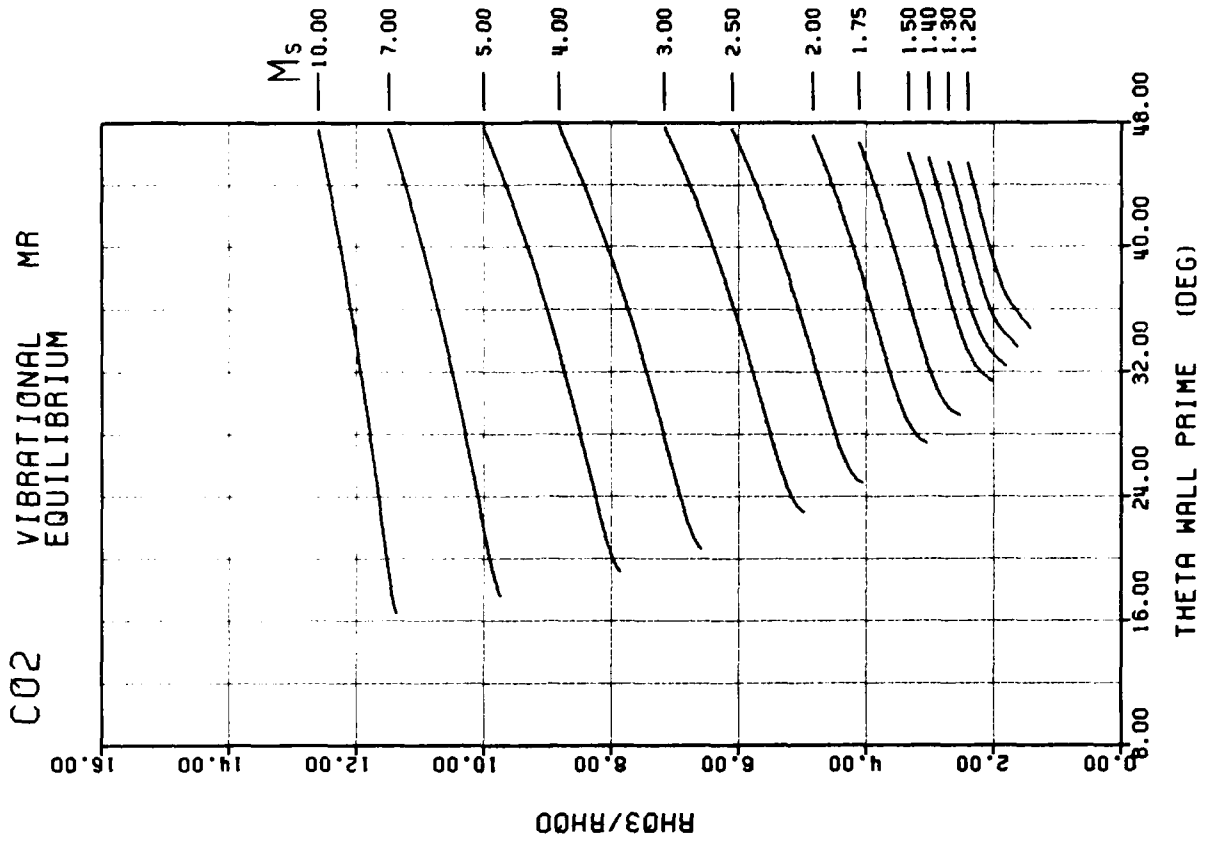
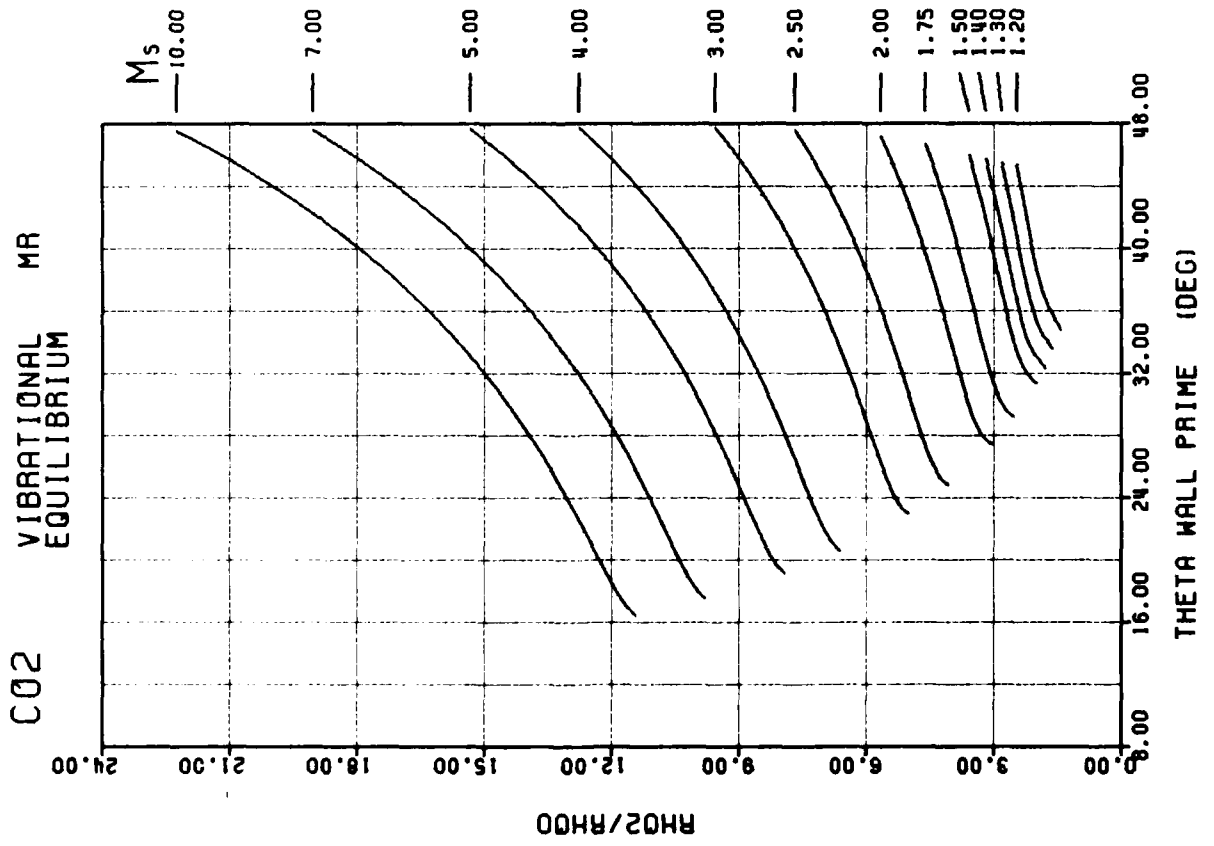


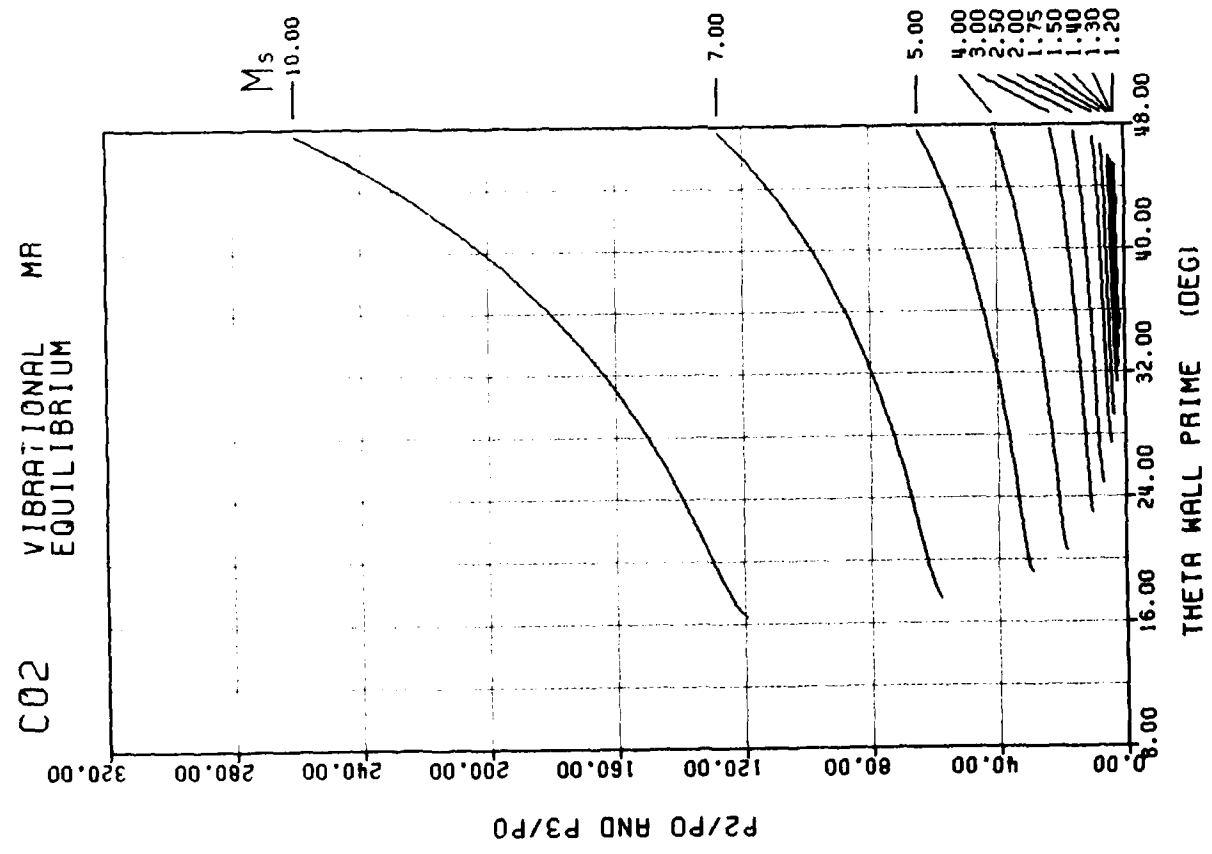
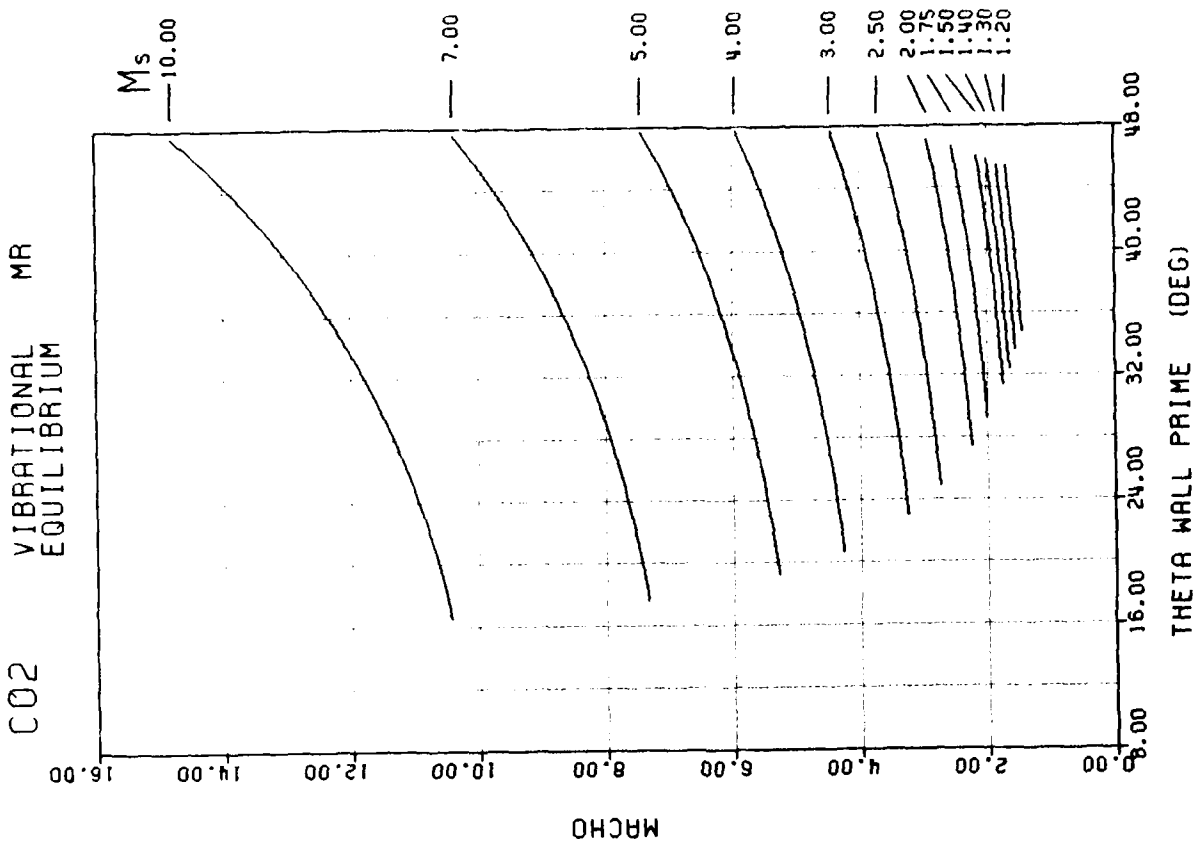


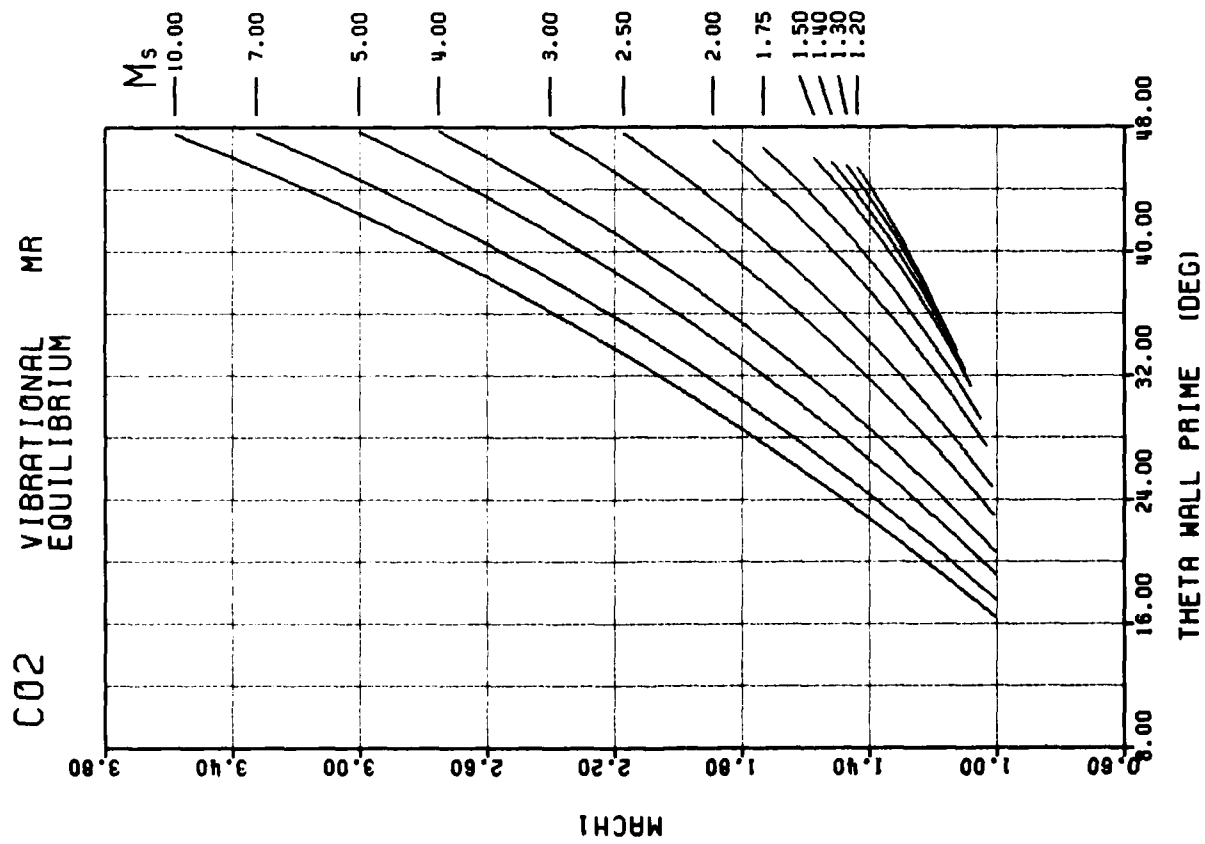
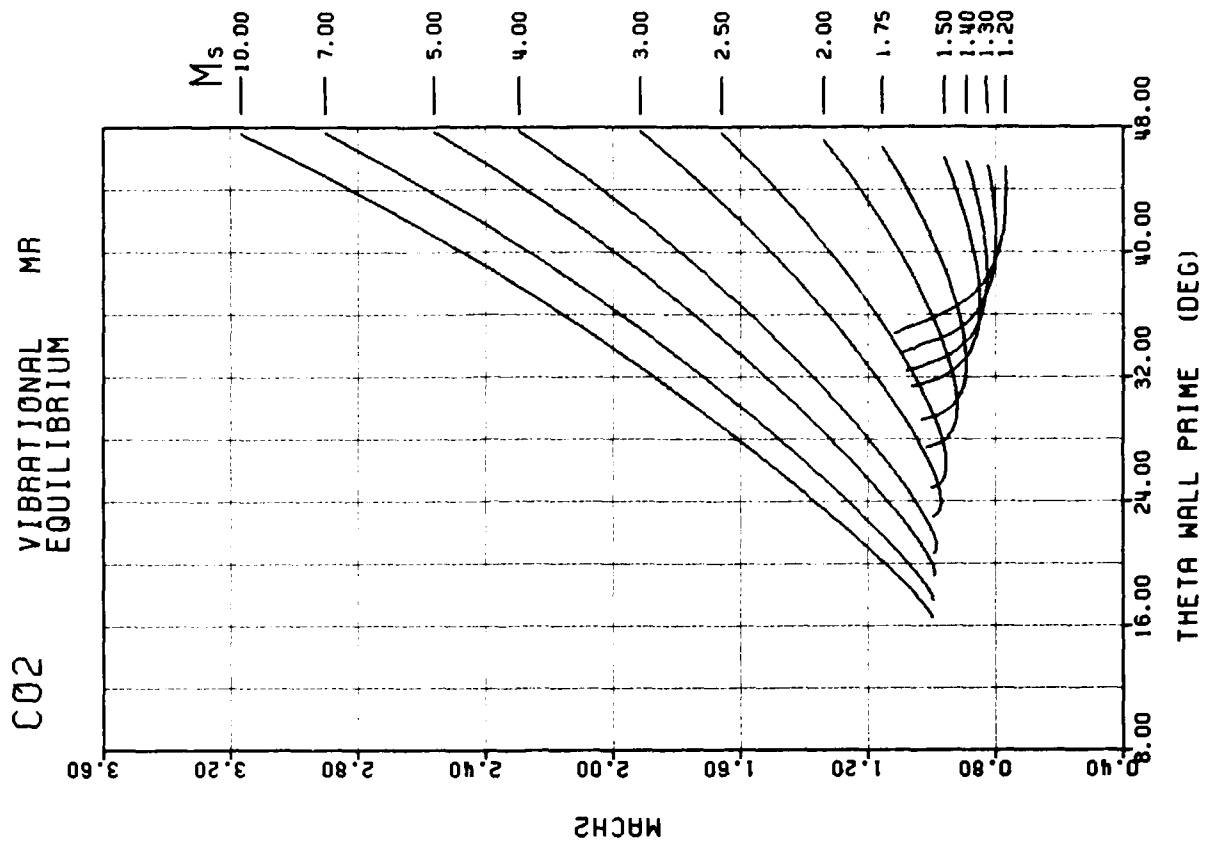




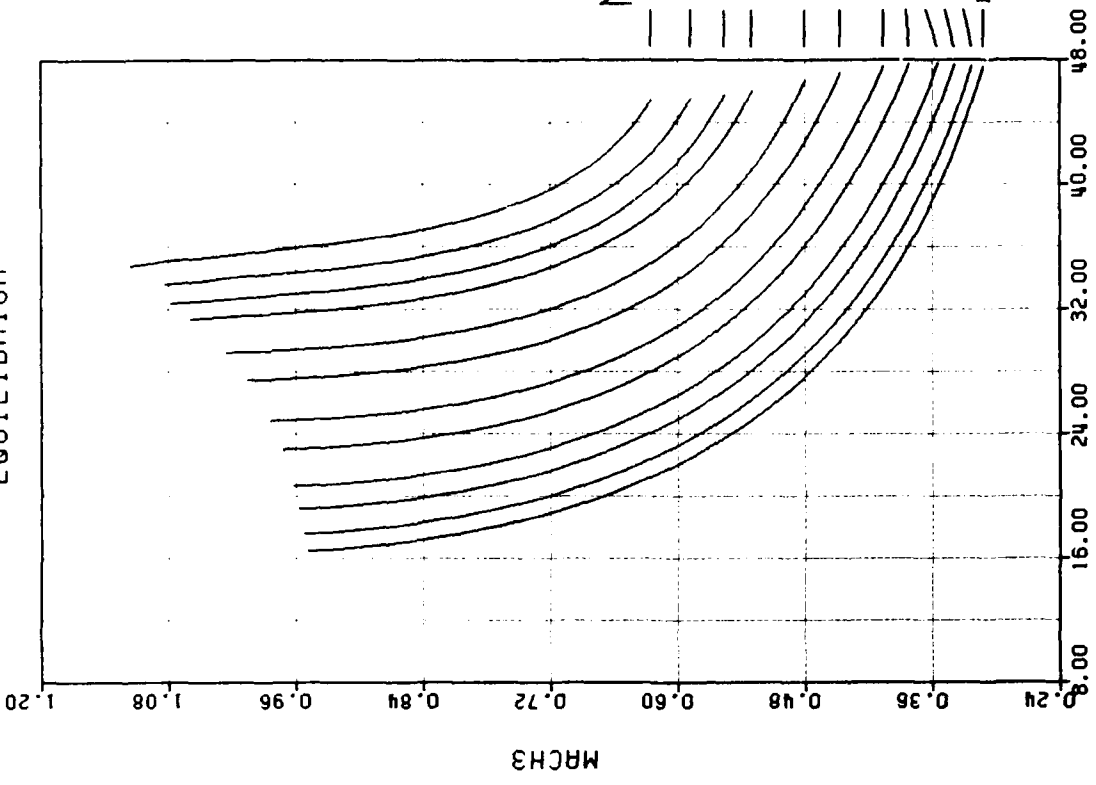




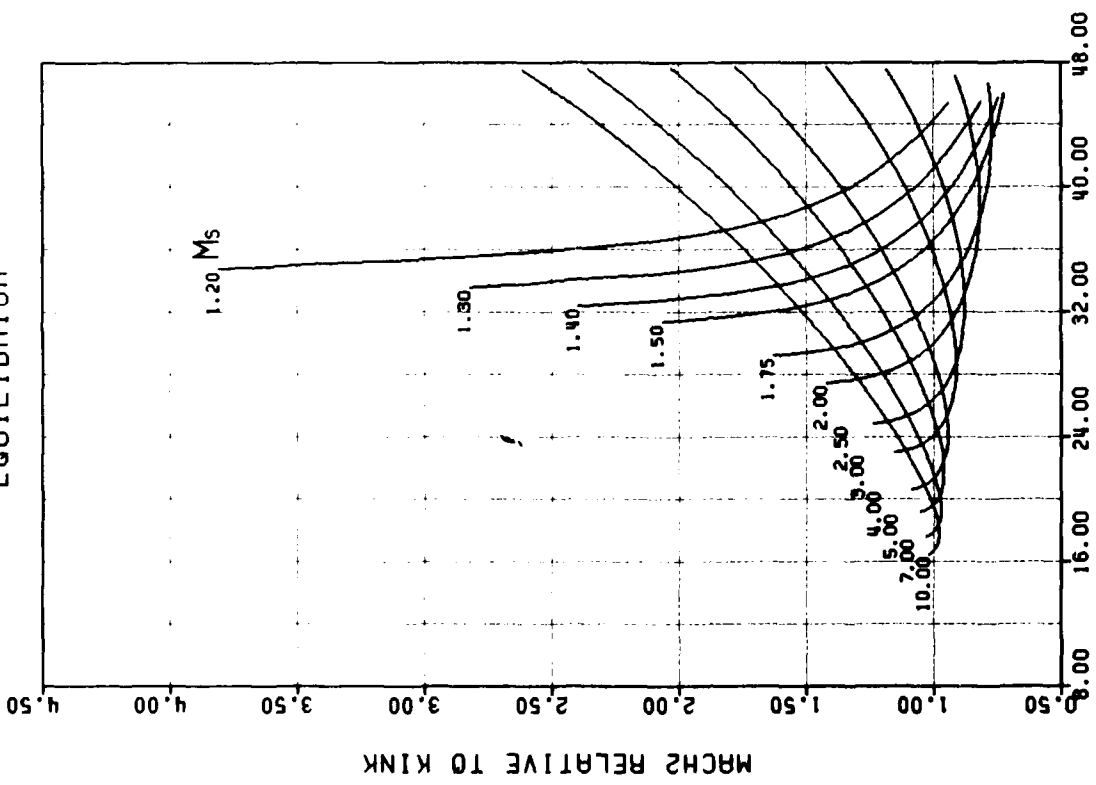




C02 VIBRATIONAL EQUILIBRIUM MR

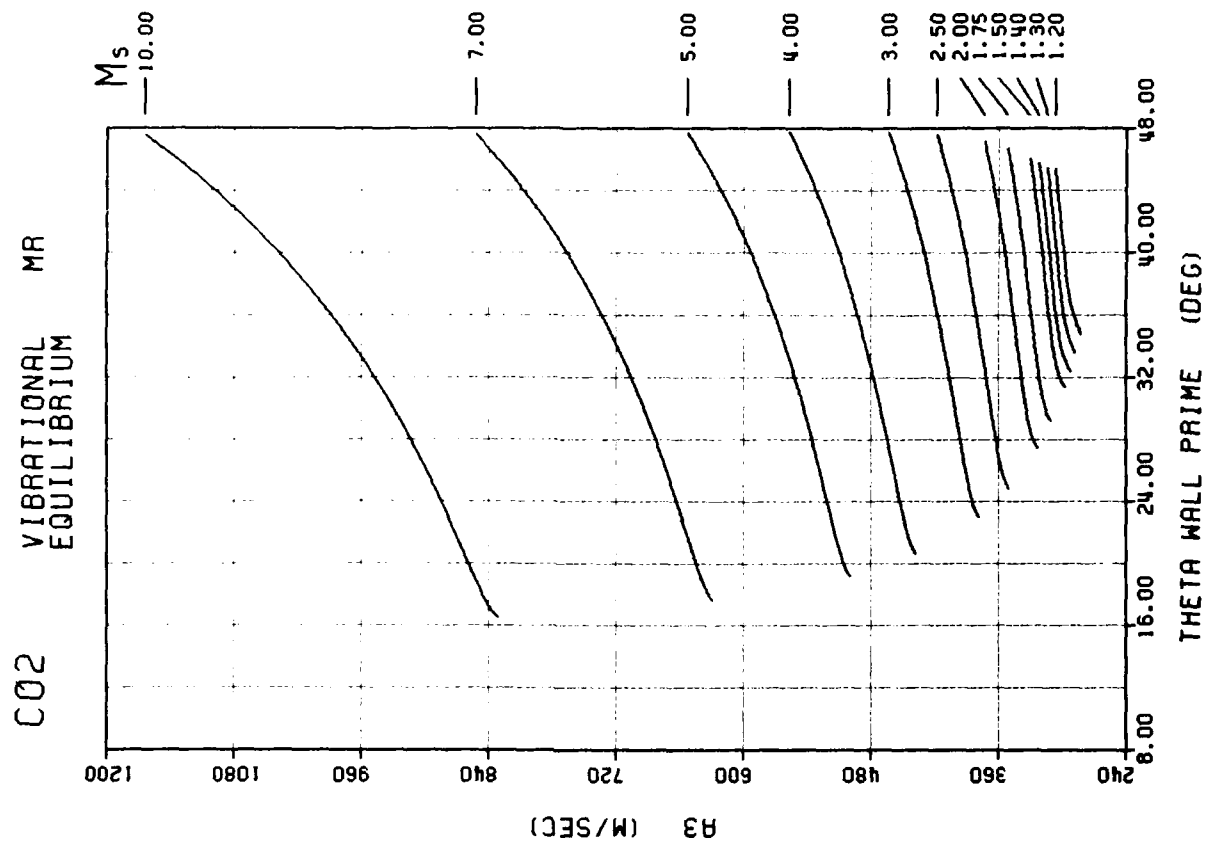
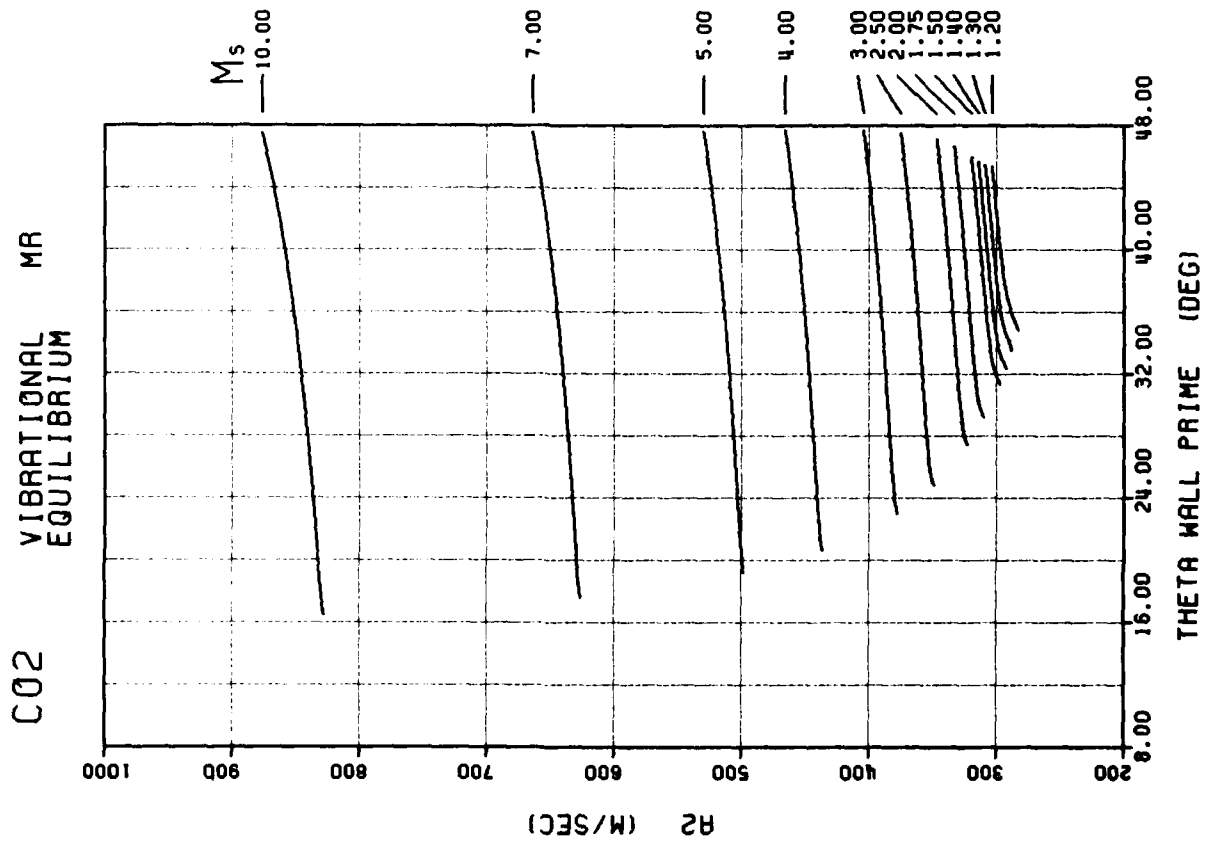


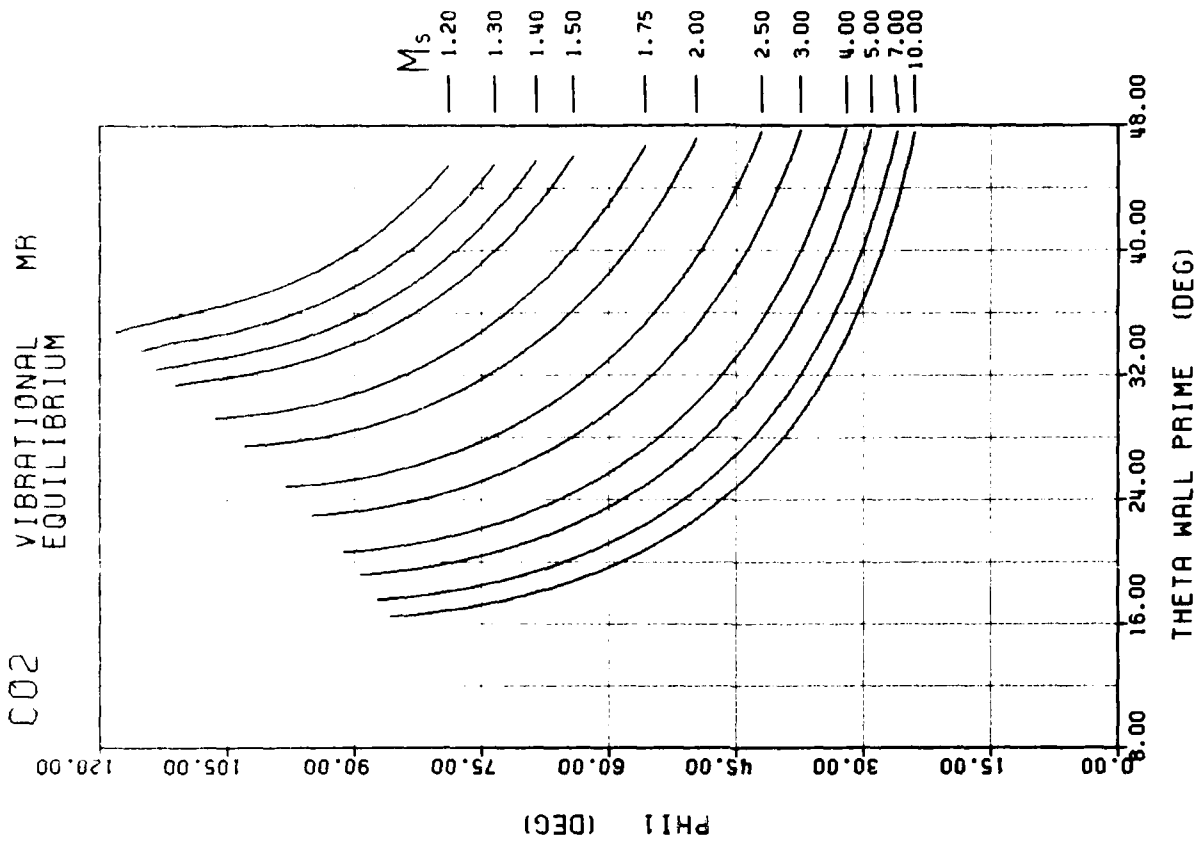
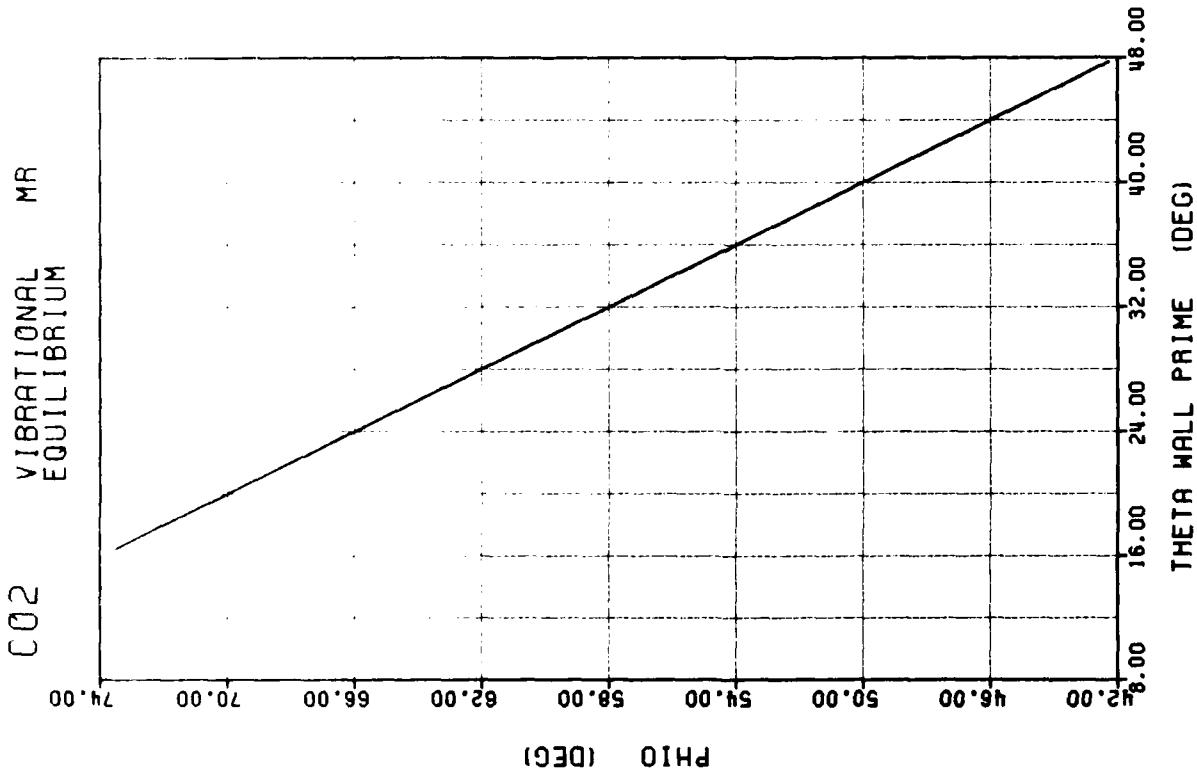
C02 VIBRATIONAL EQUILIBRIUM MR

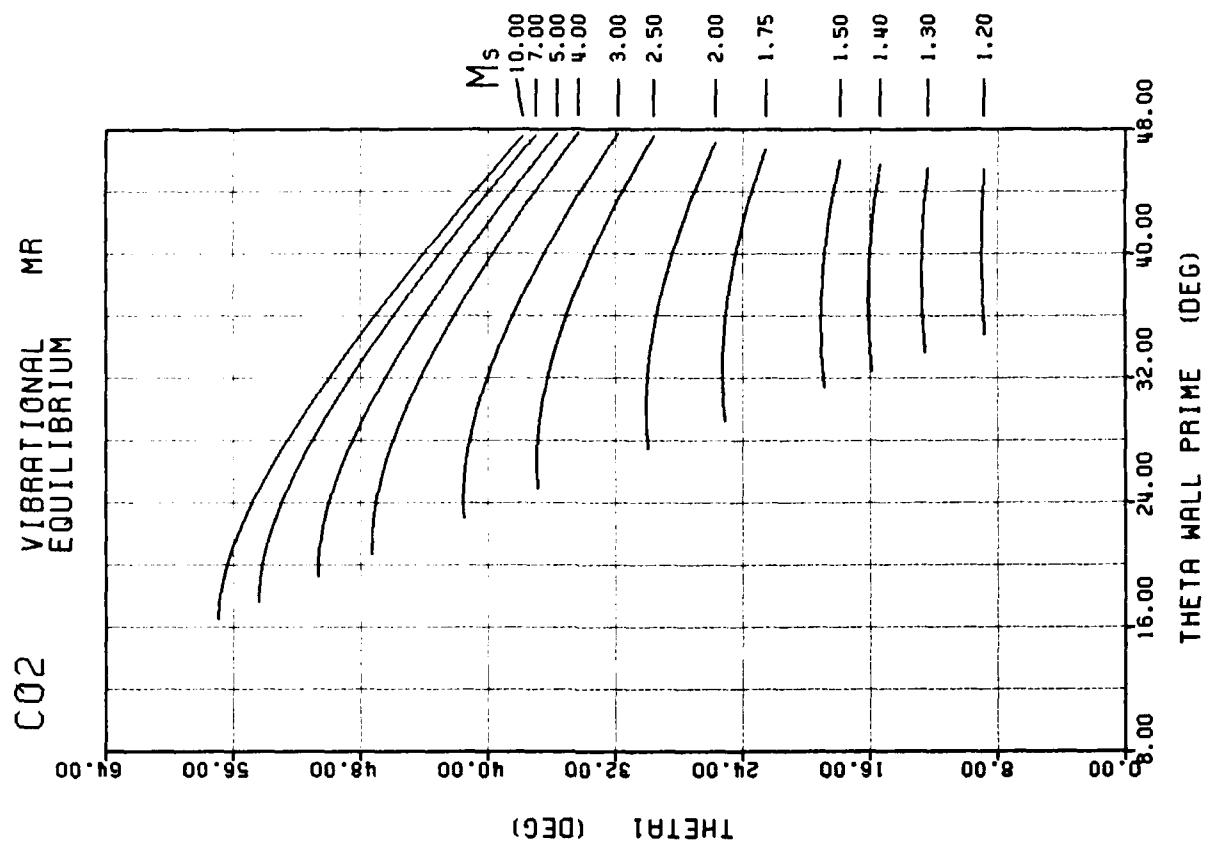
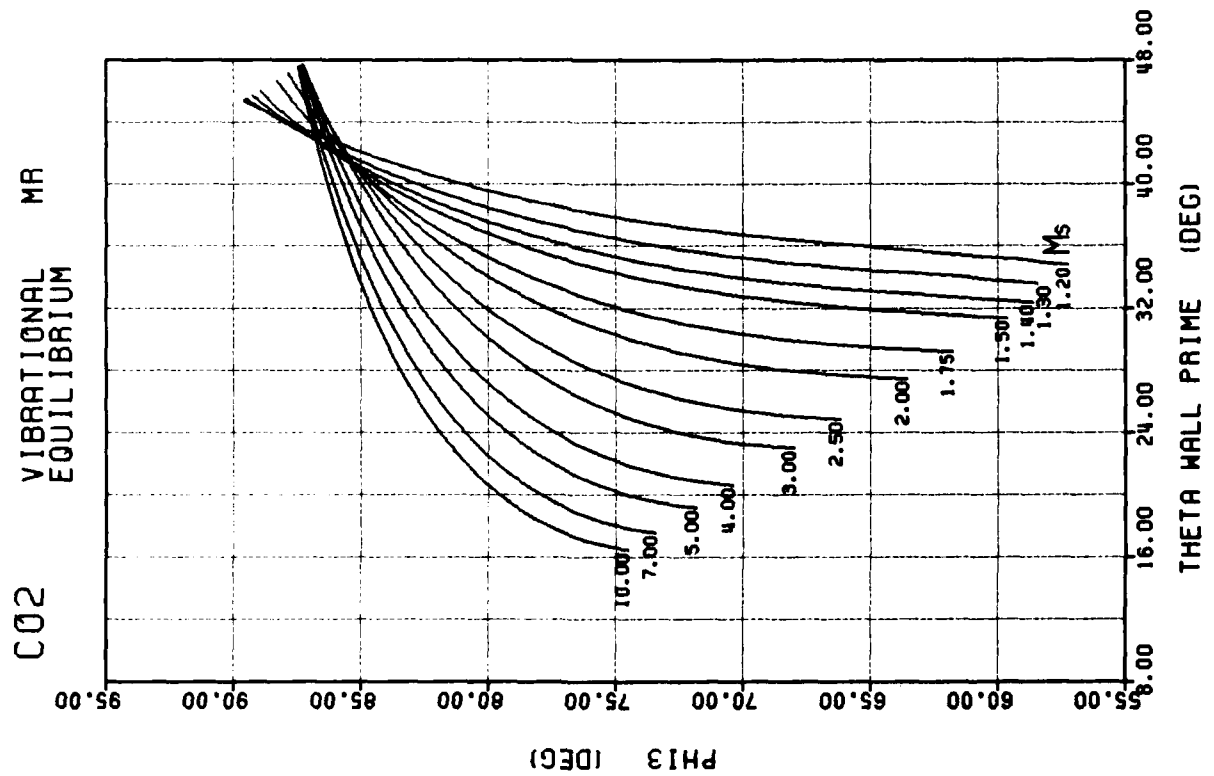


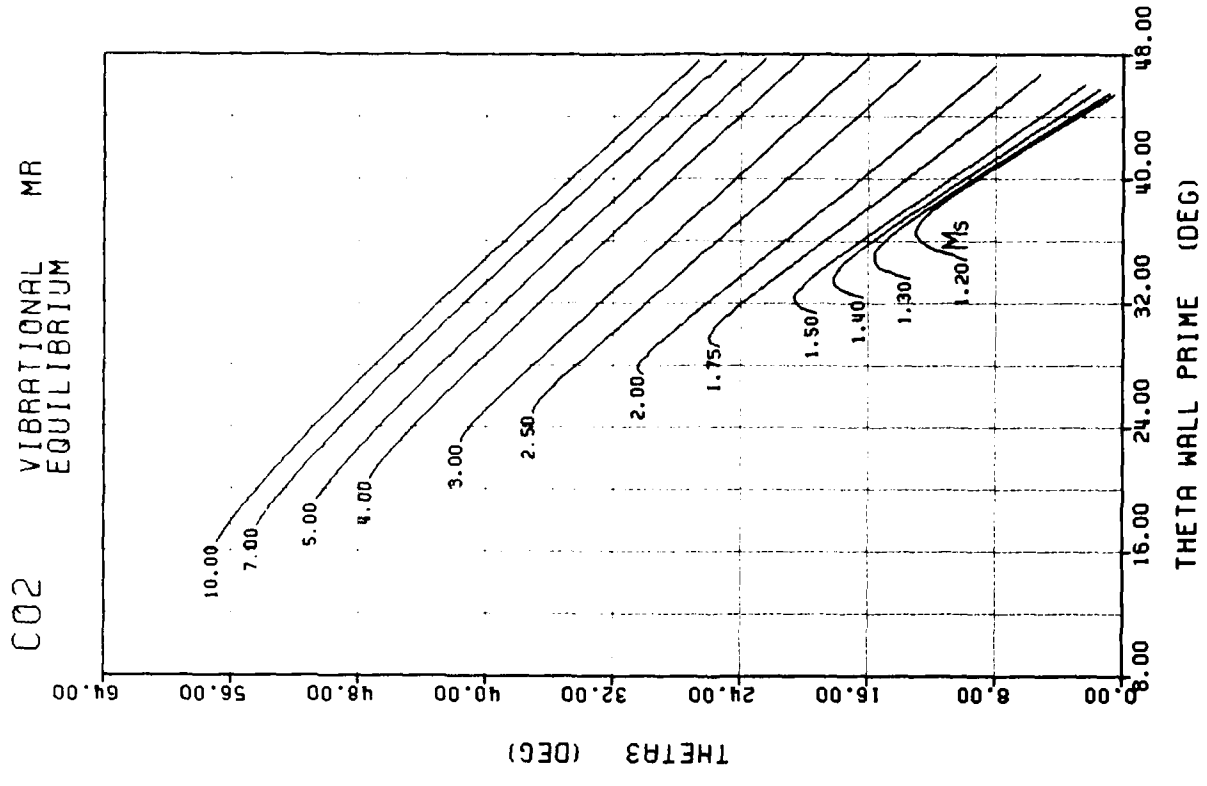
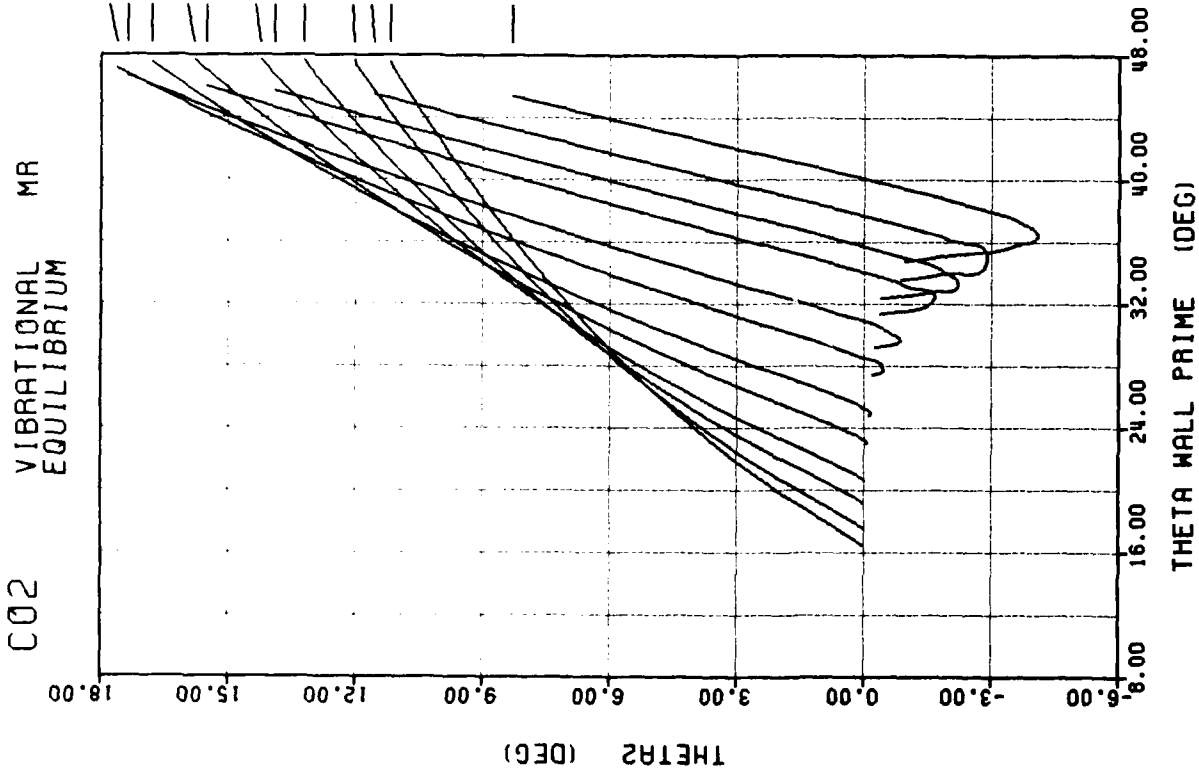
THETA WALL PRIME (DEG)

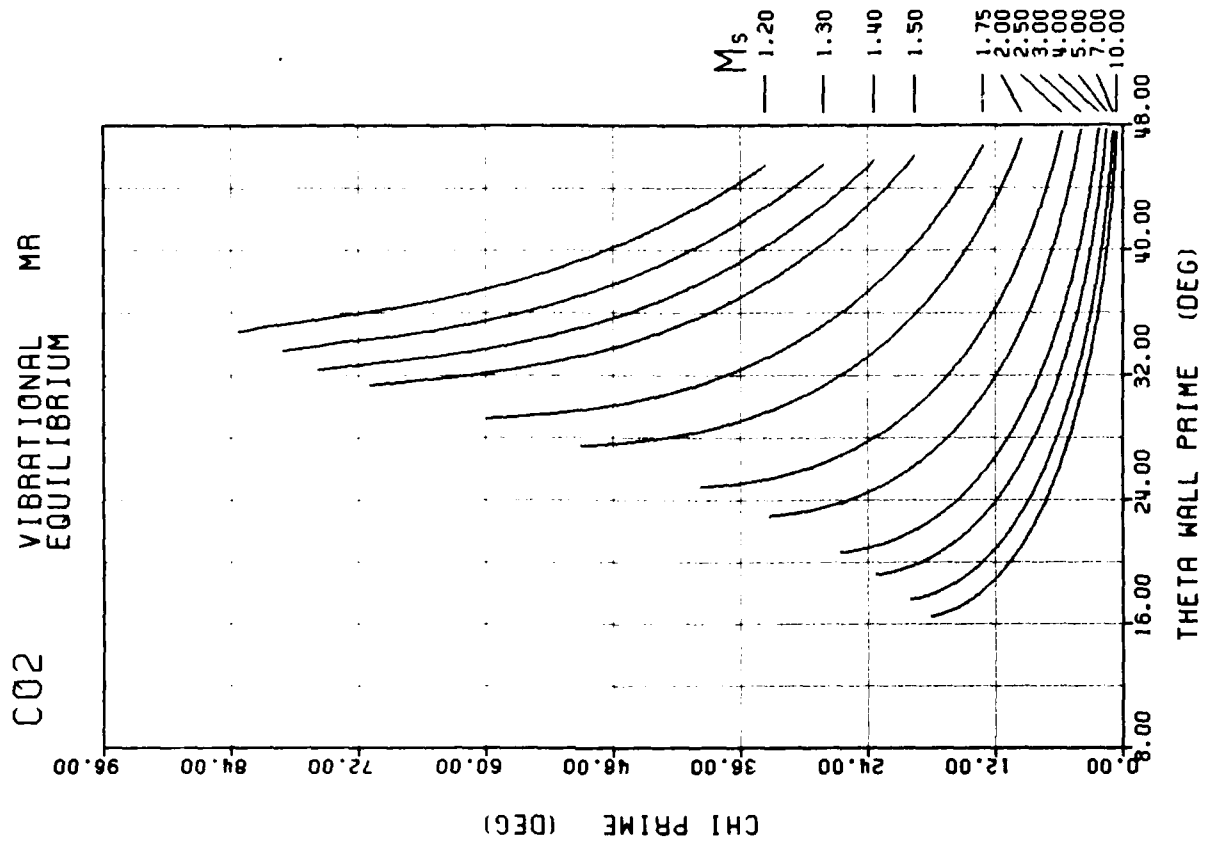
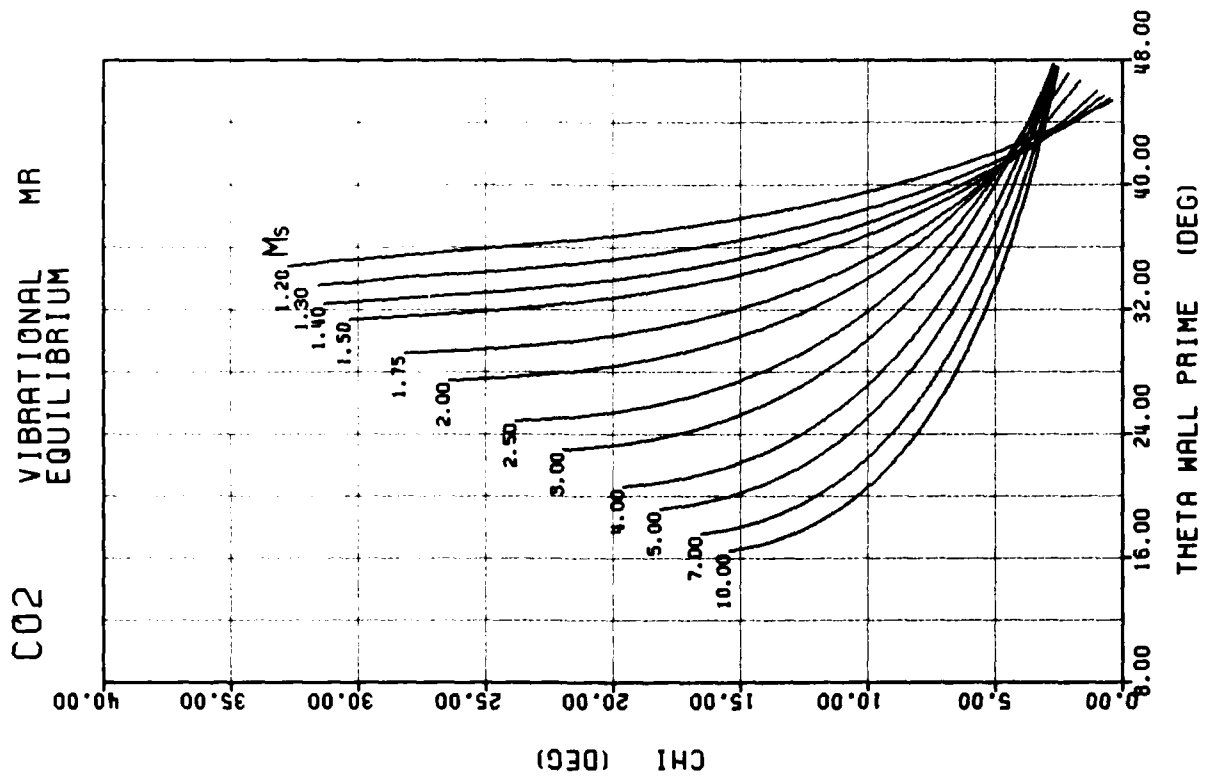
THETA WALL PRIME (DEG)

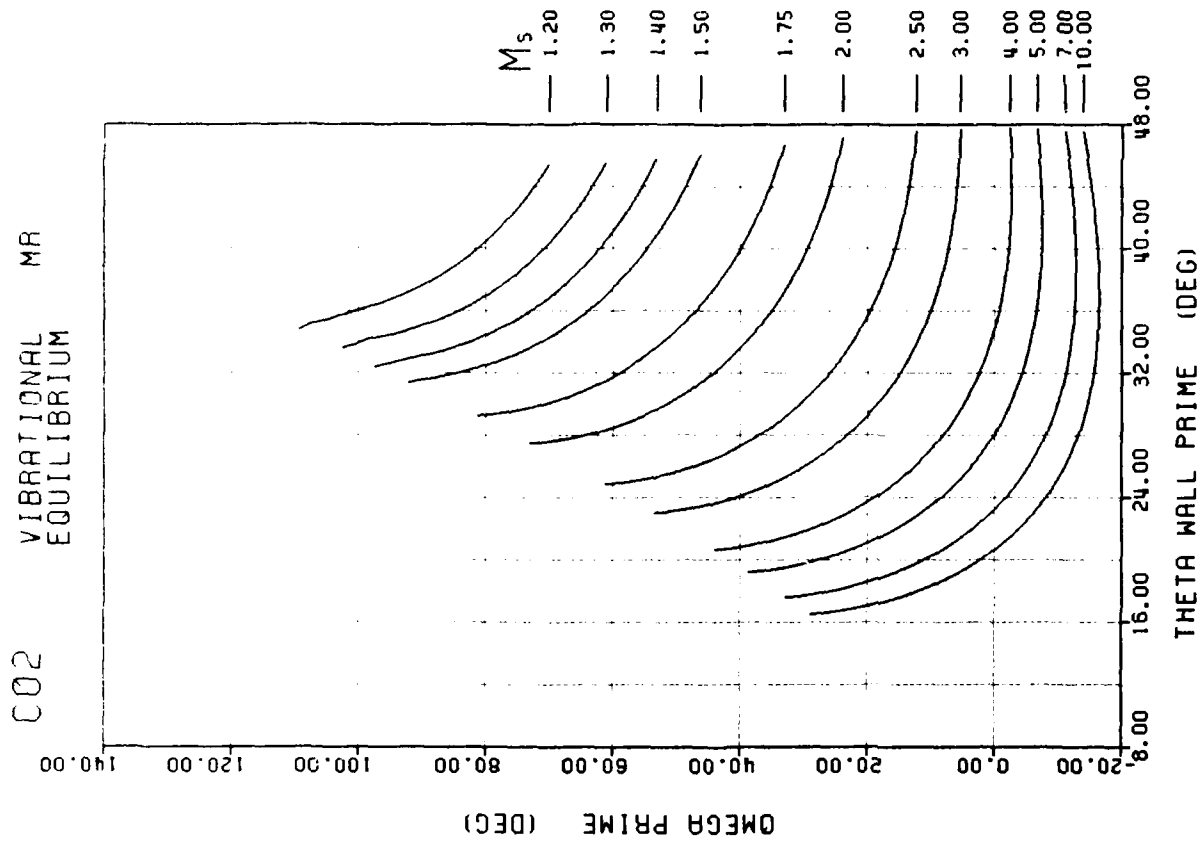
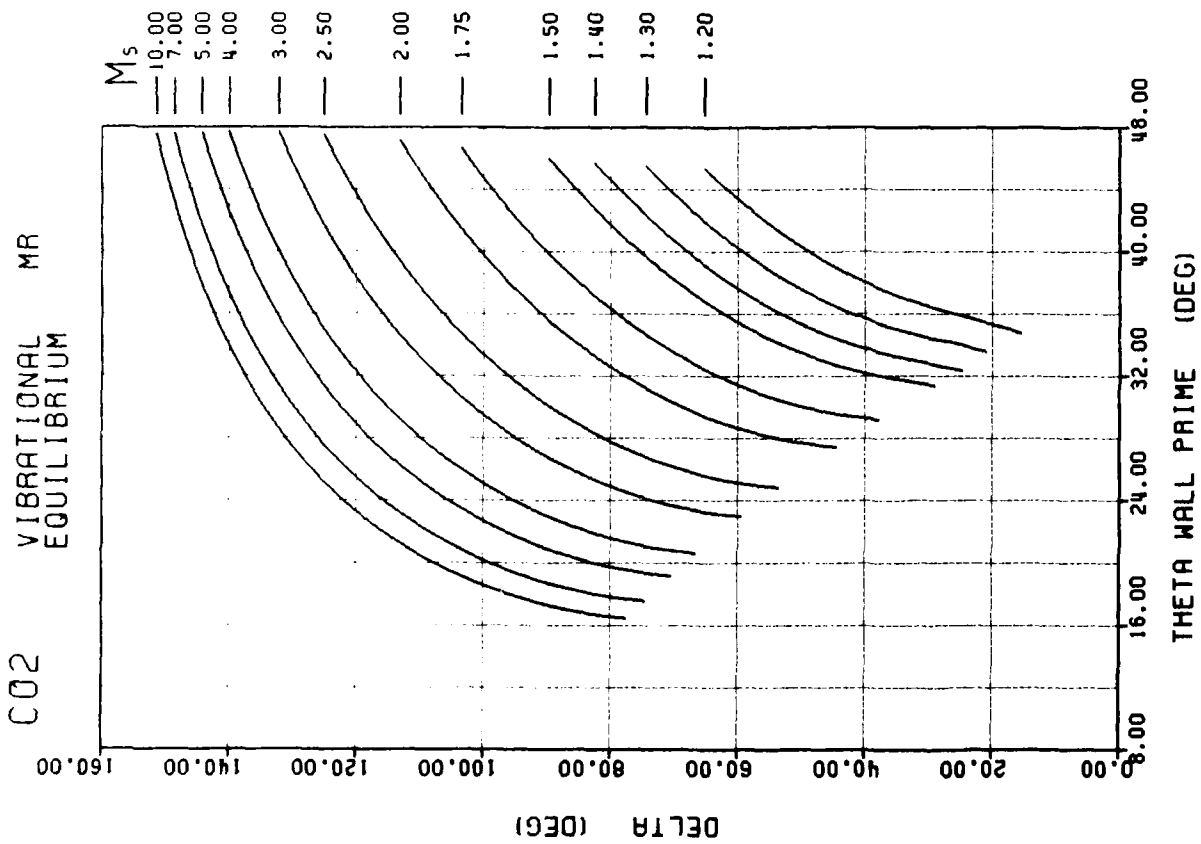


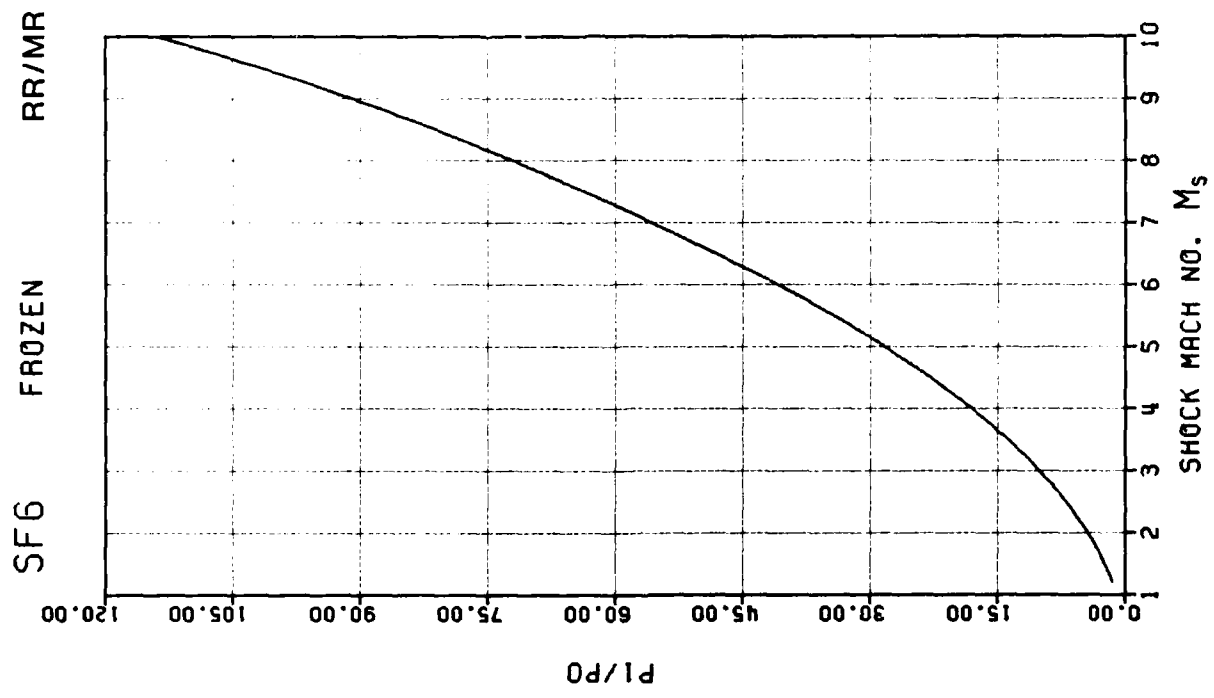
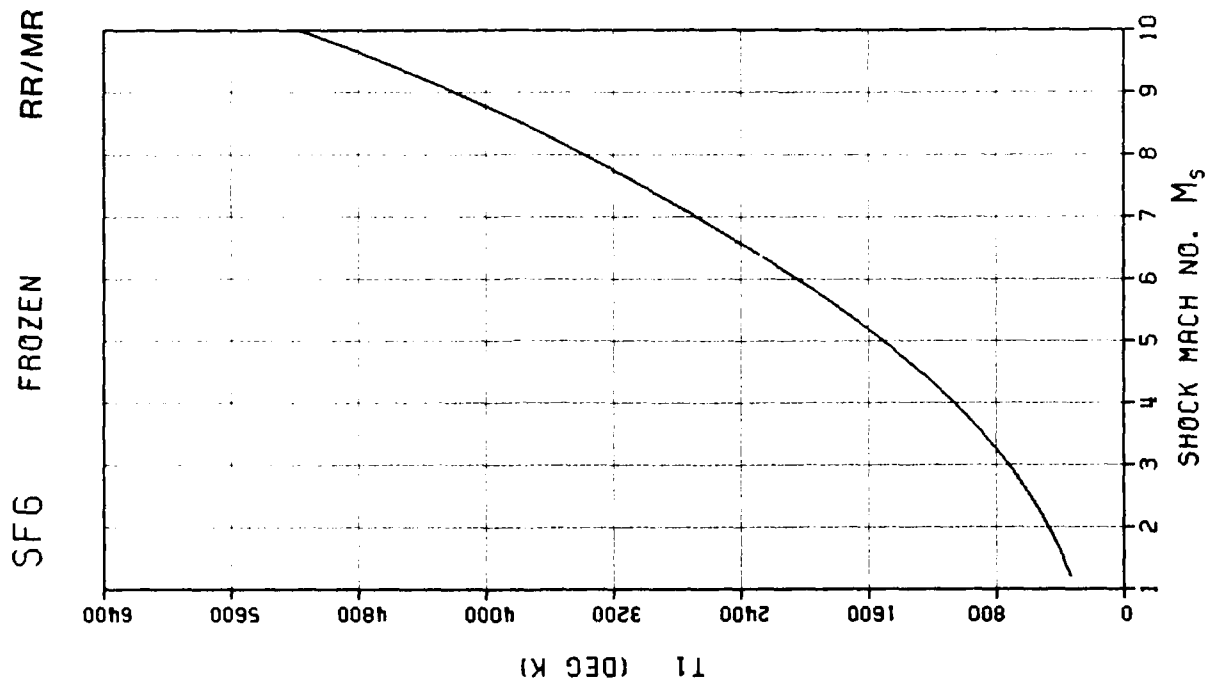


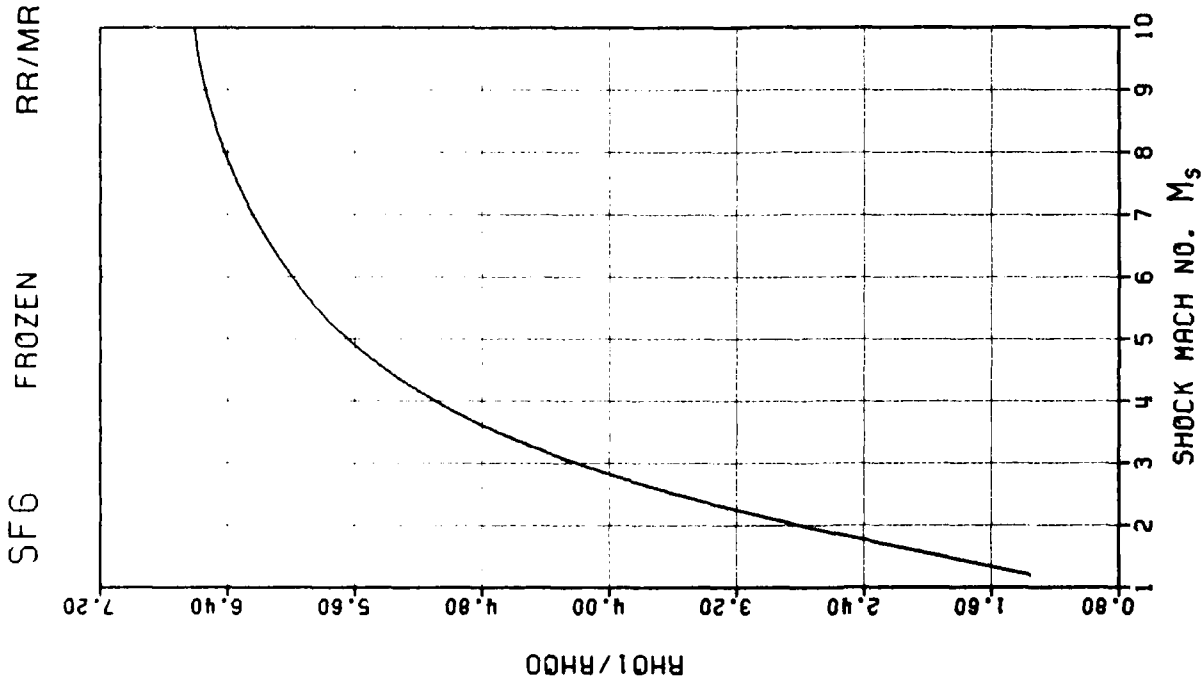
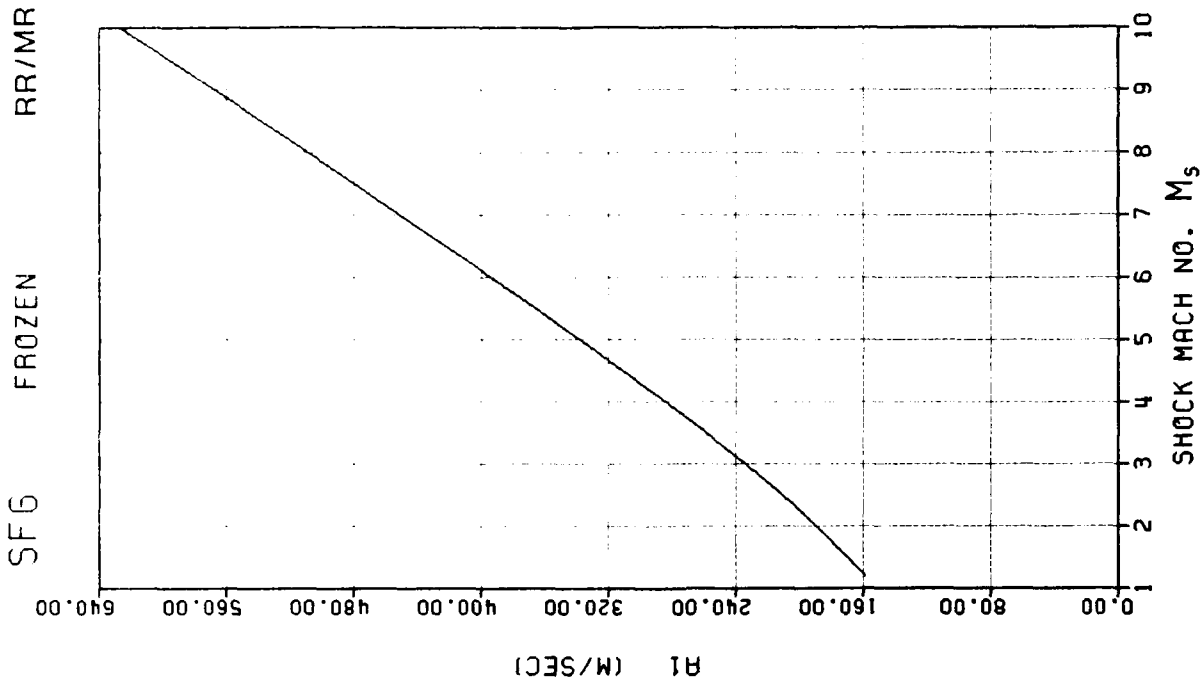


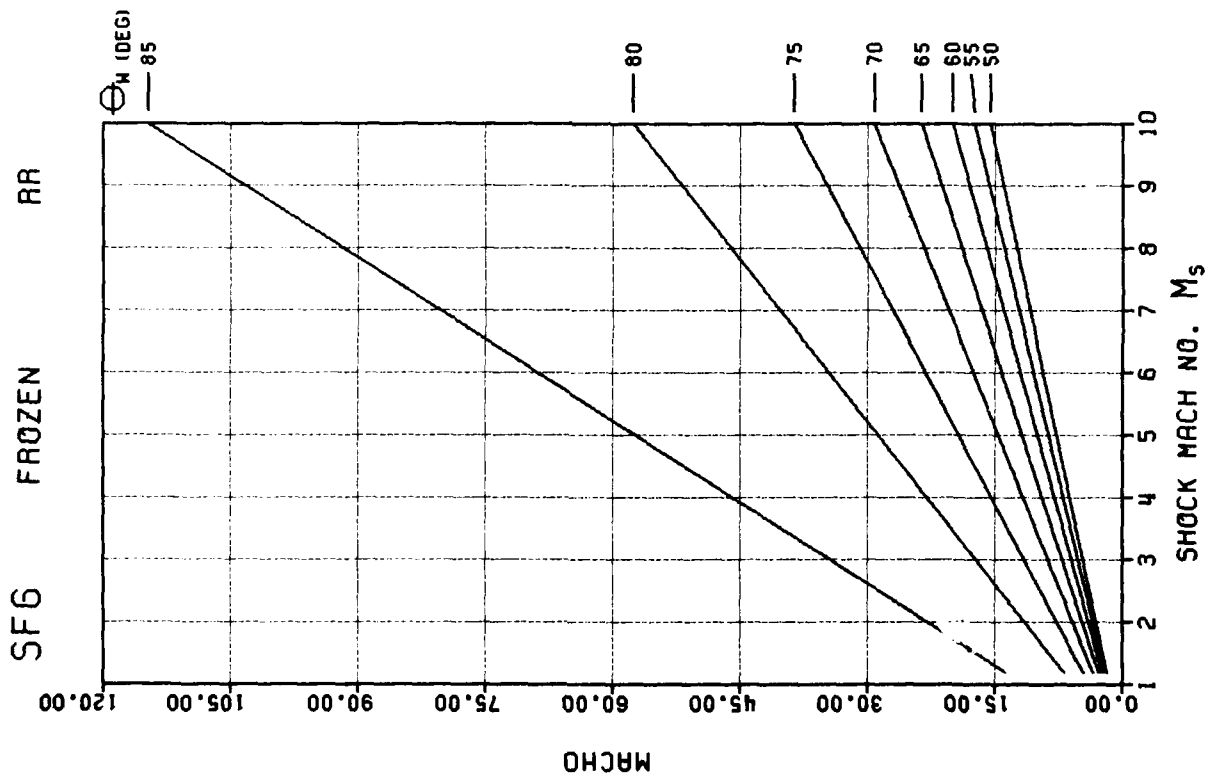
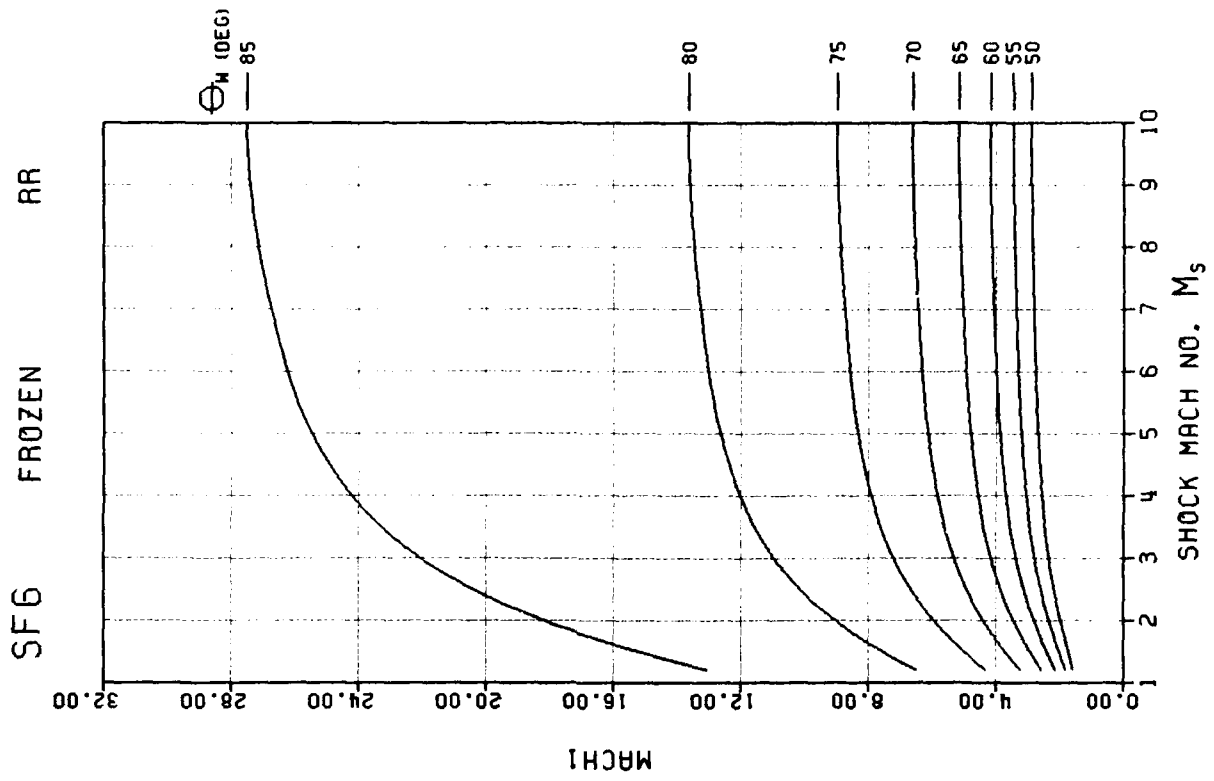


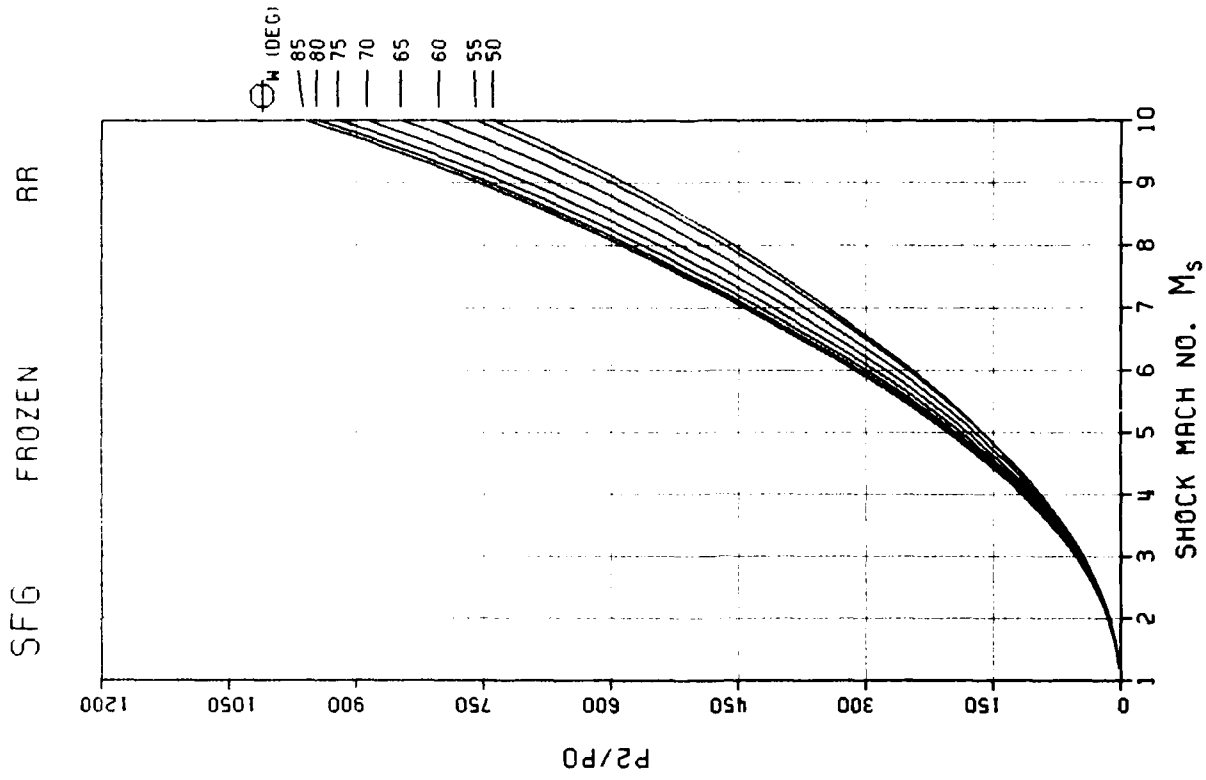
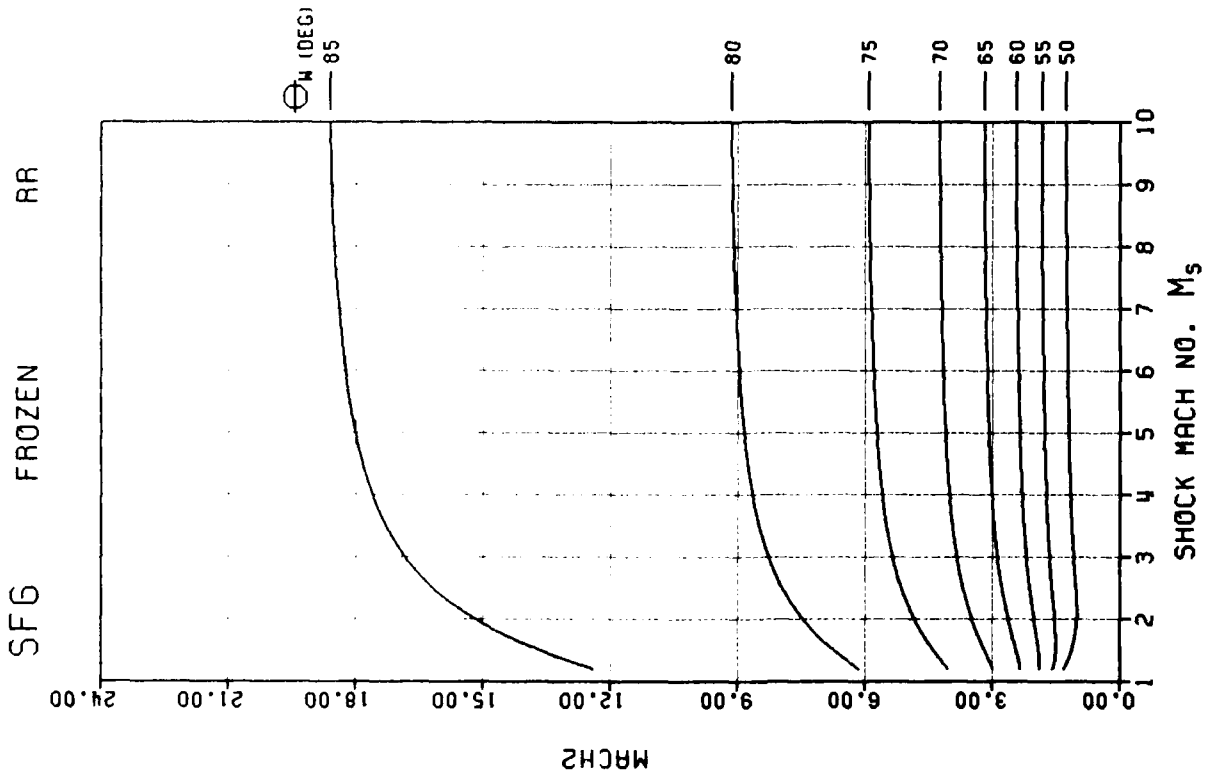


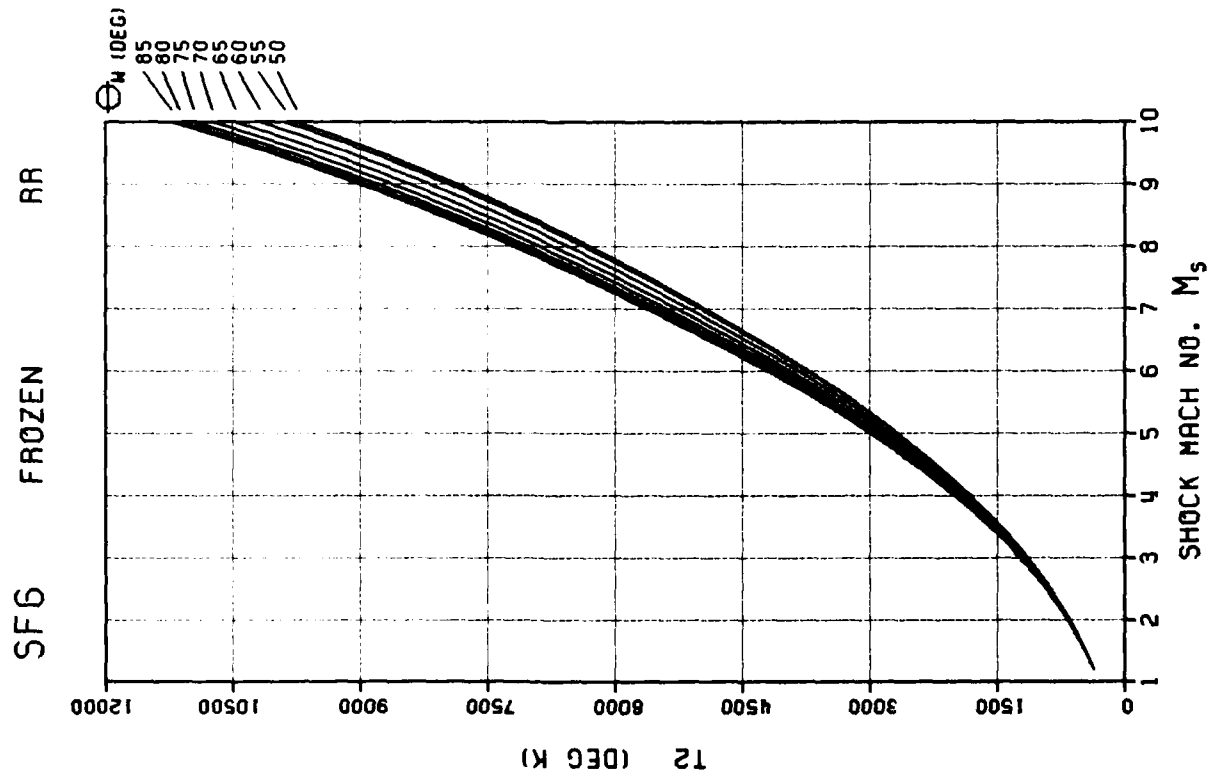
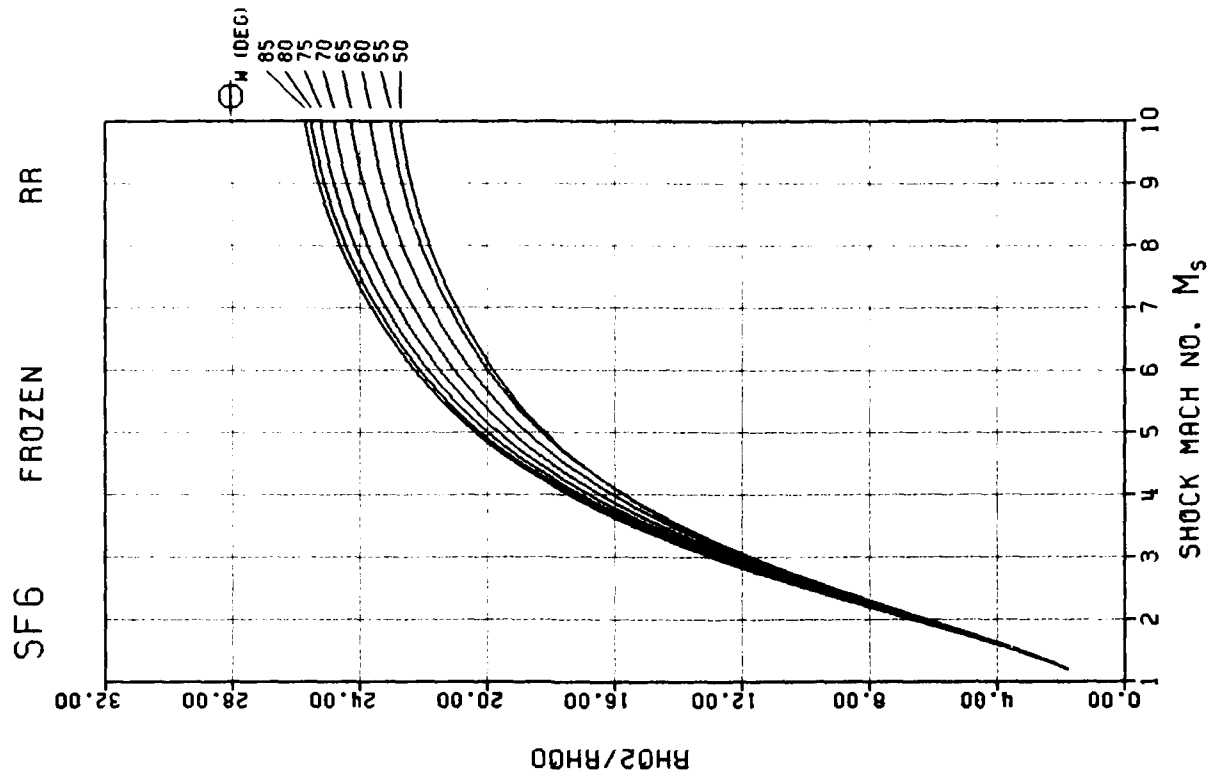


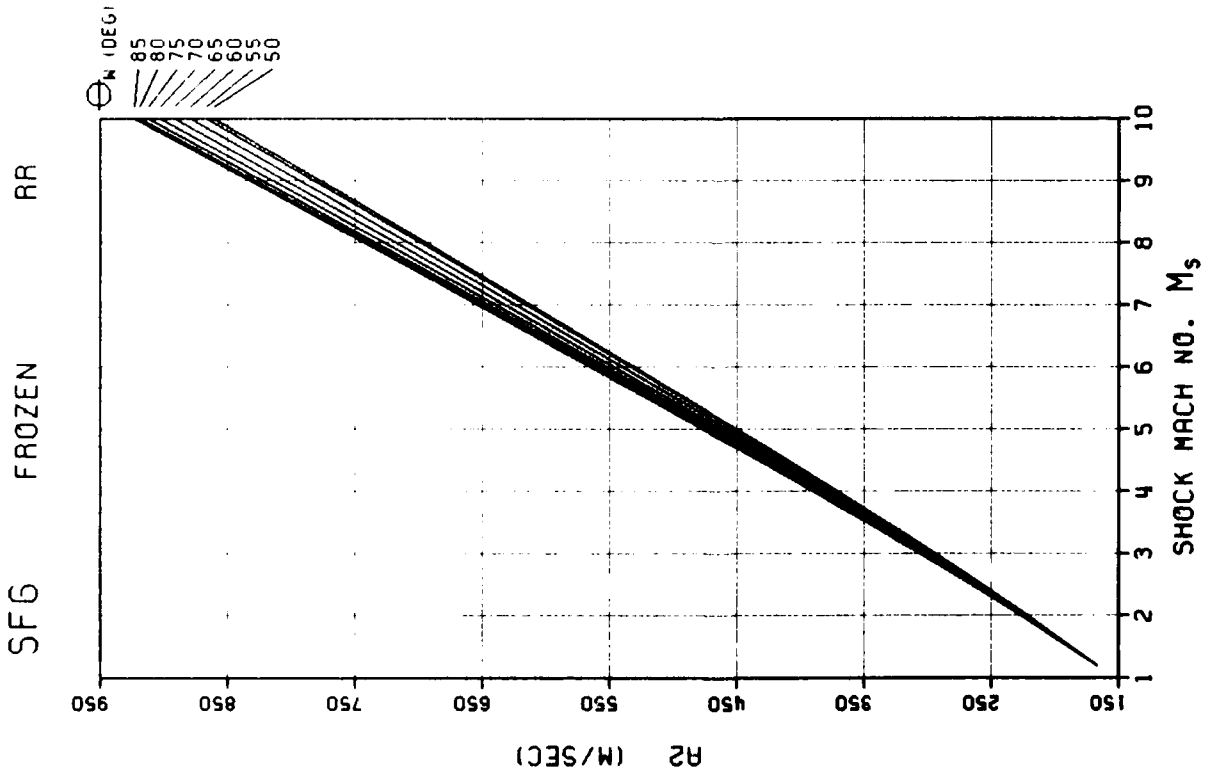
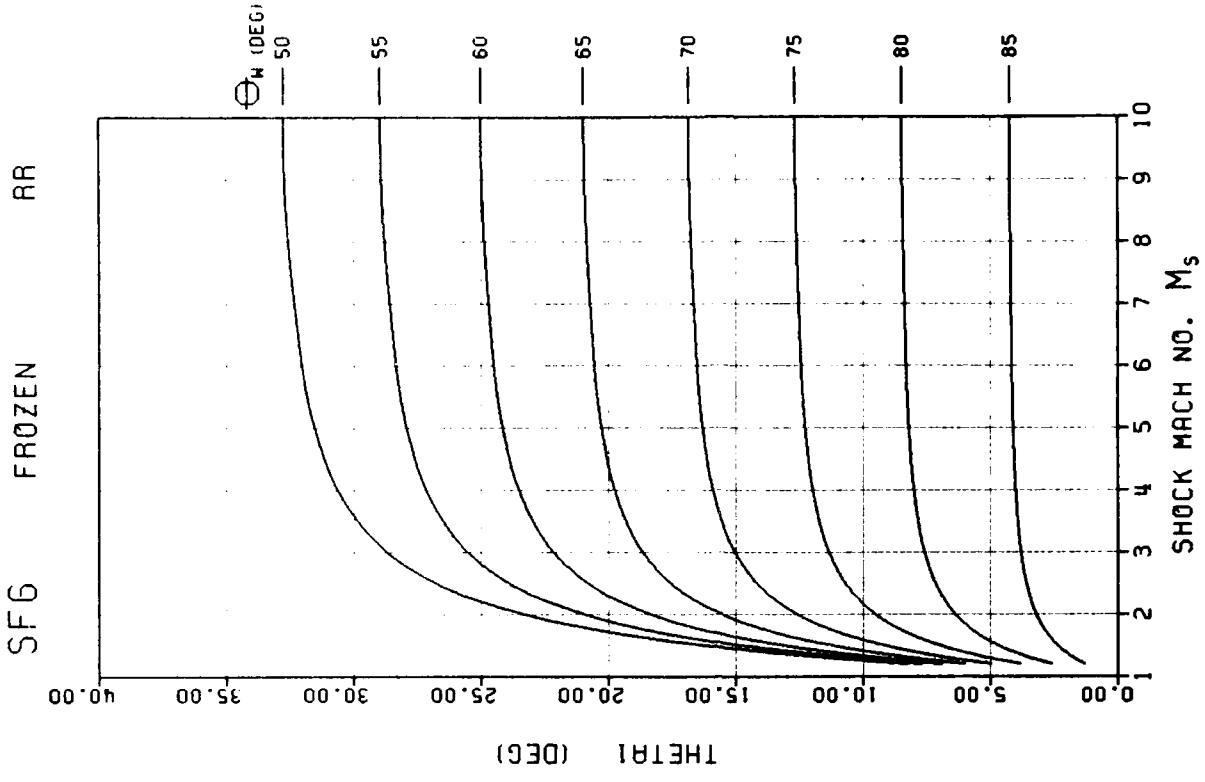


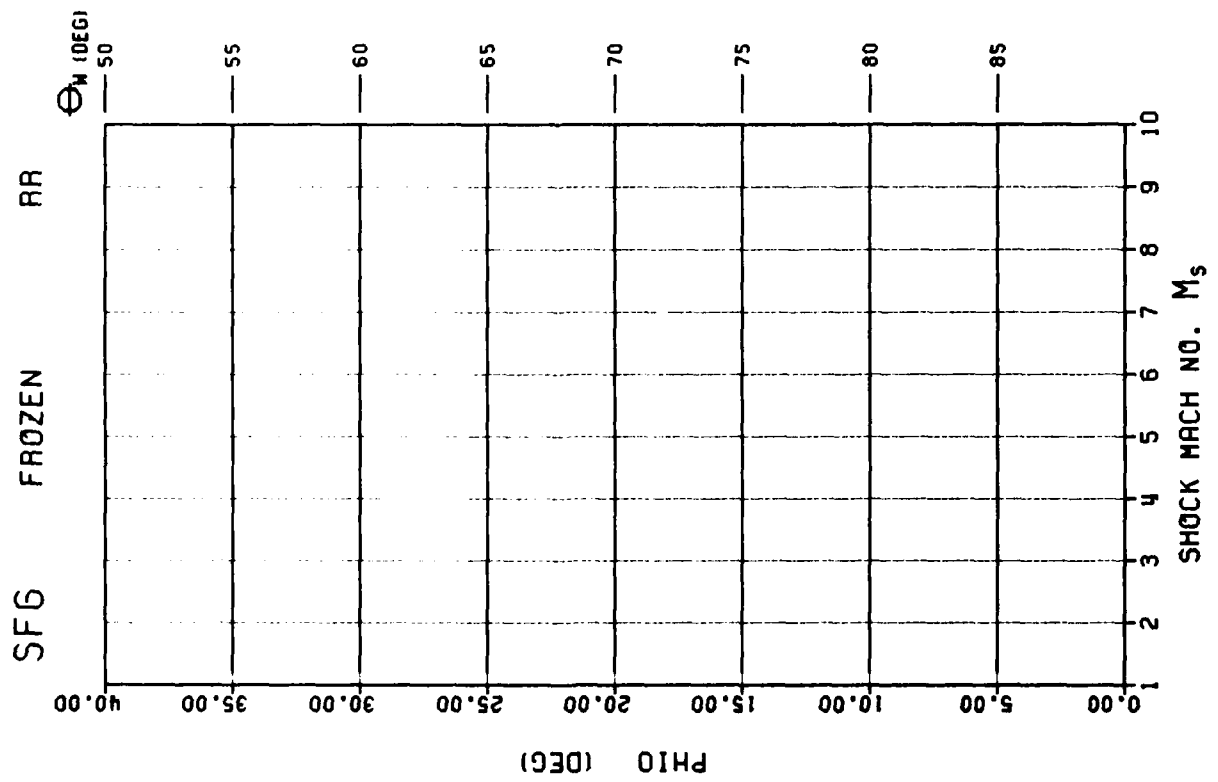
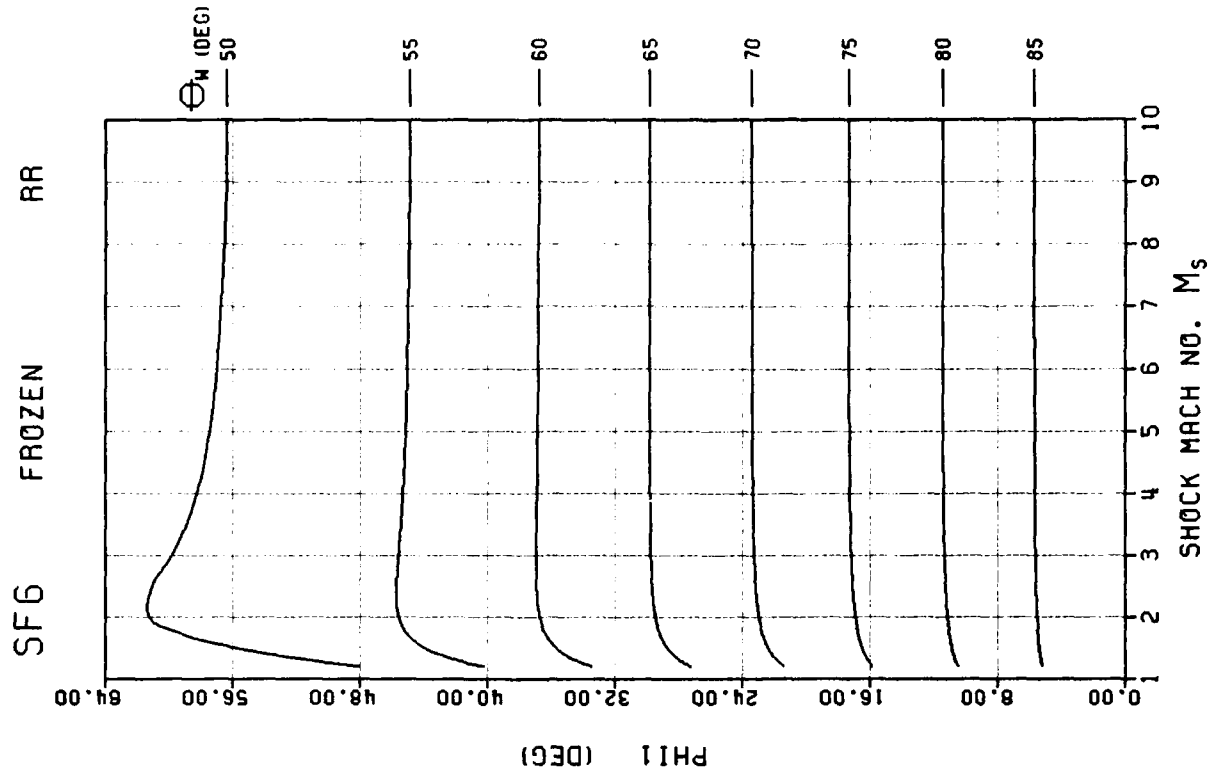


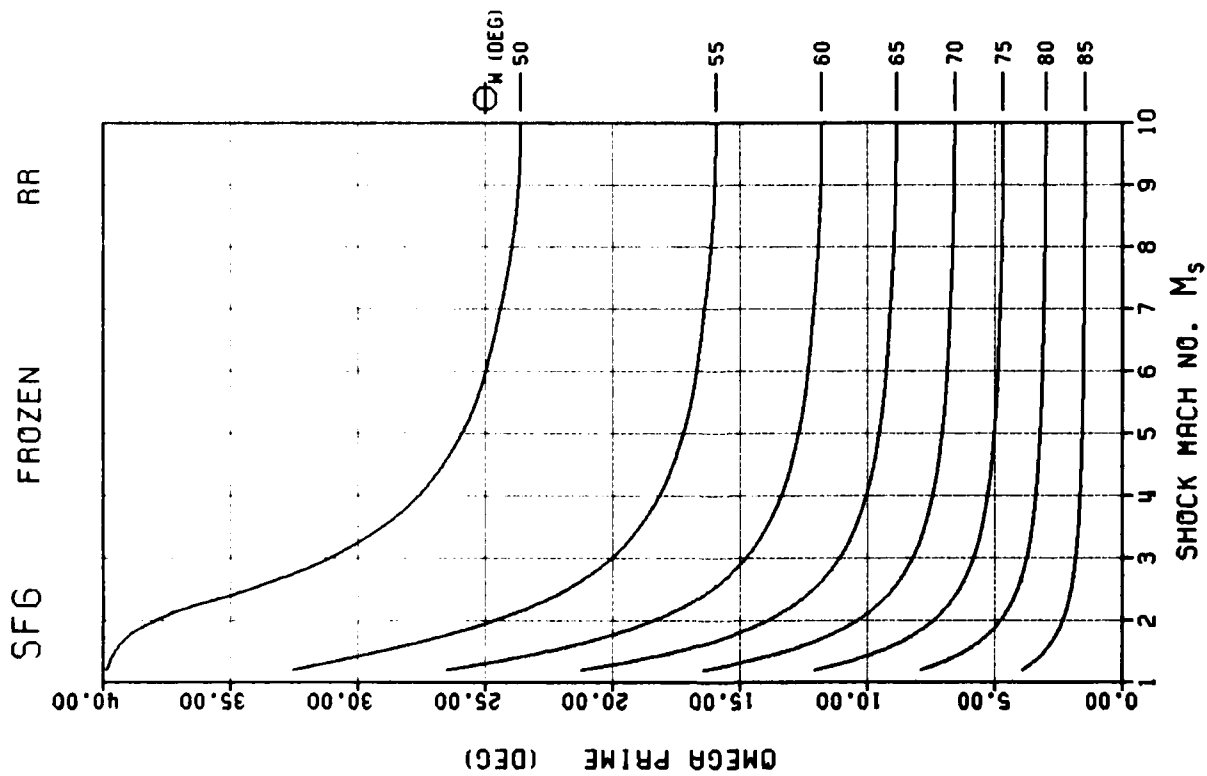
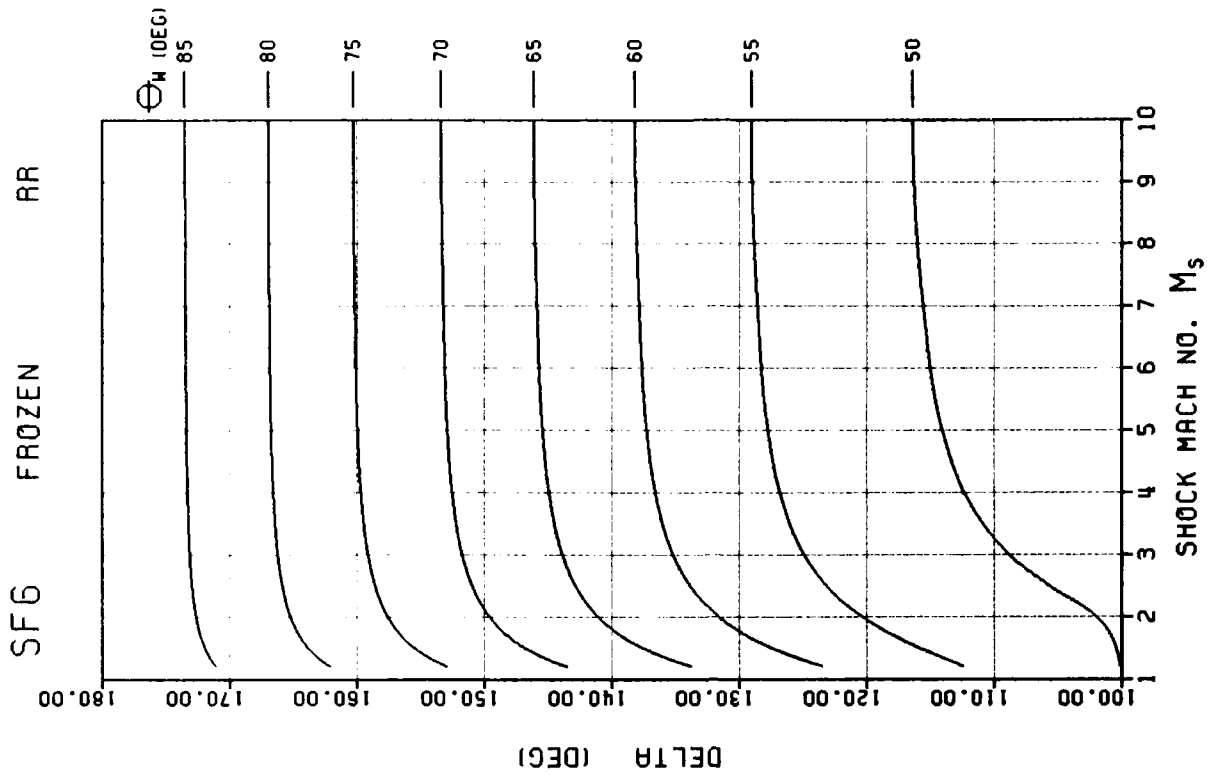


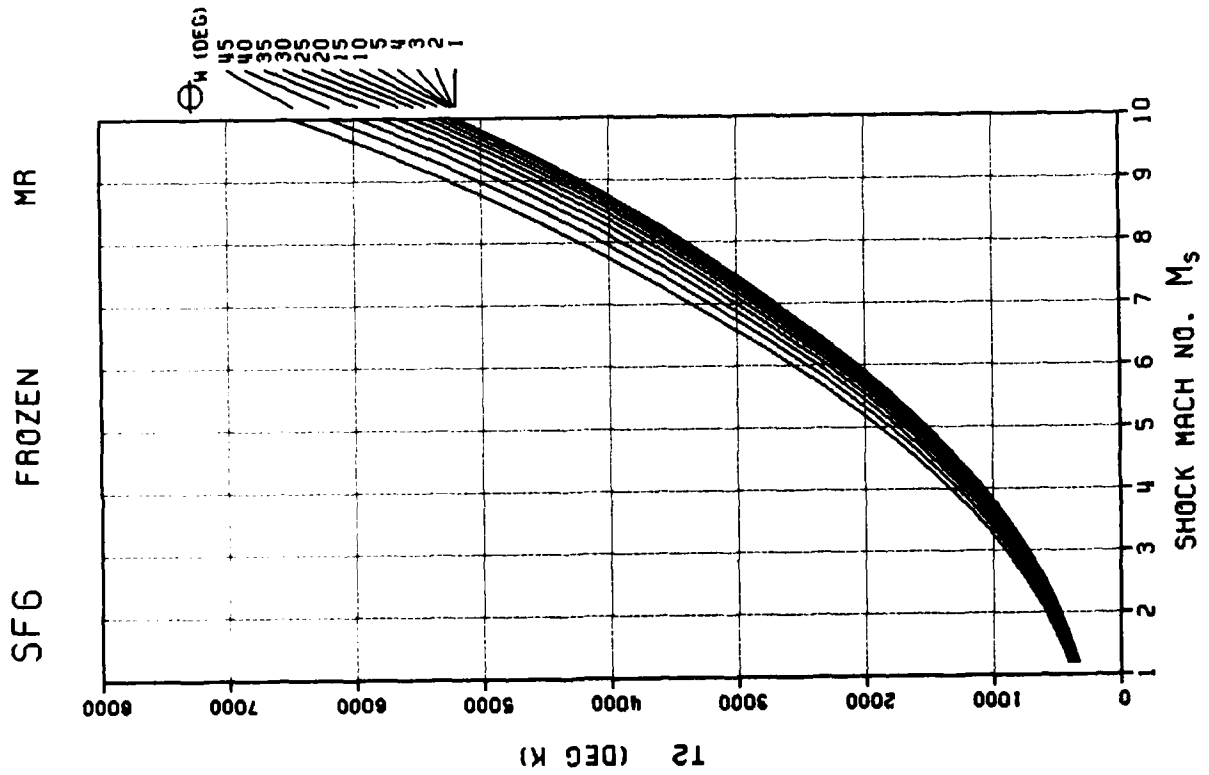
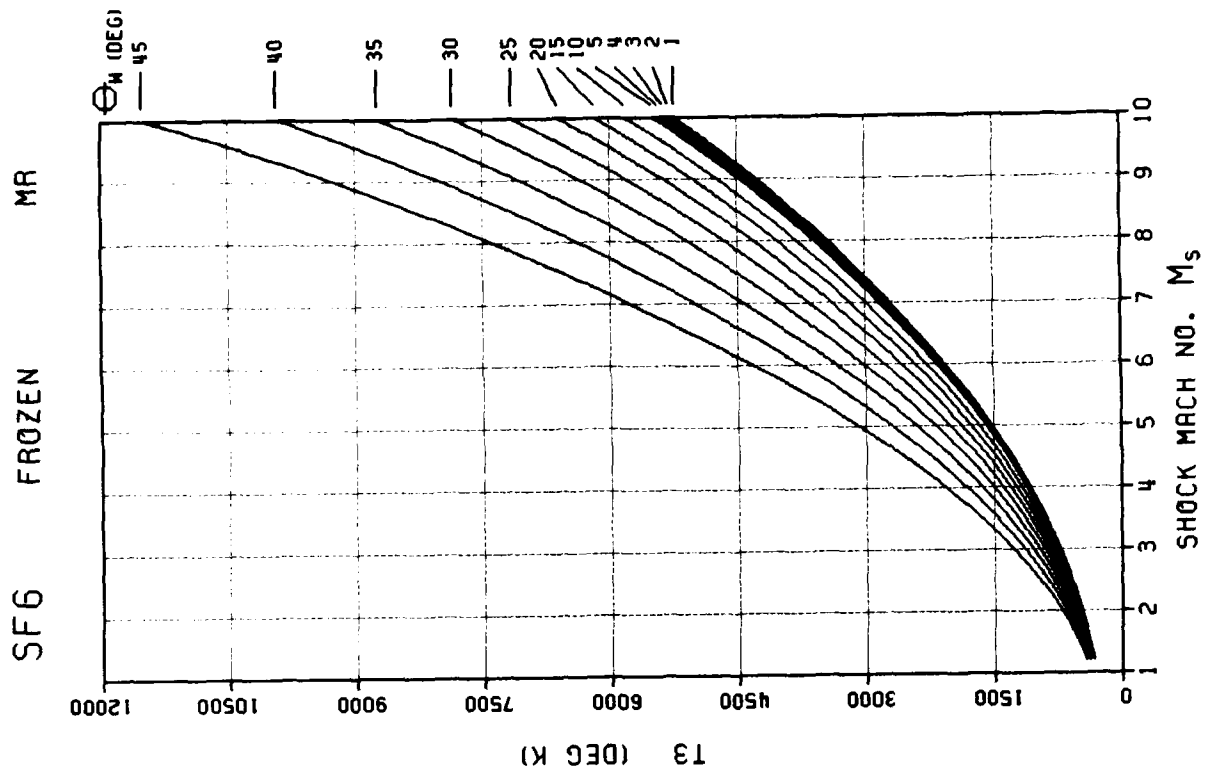


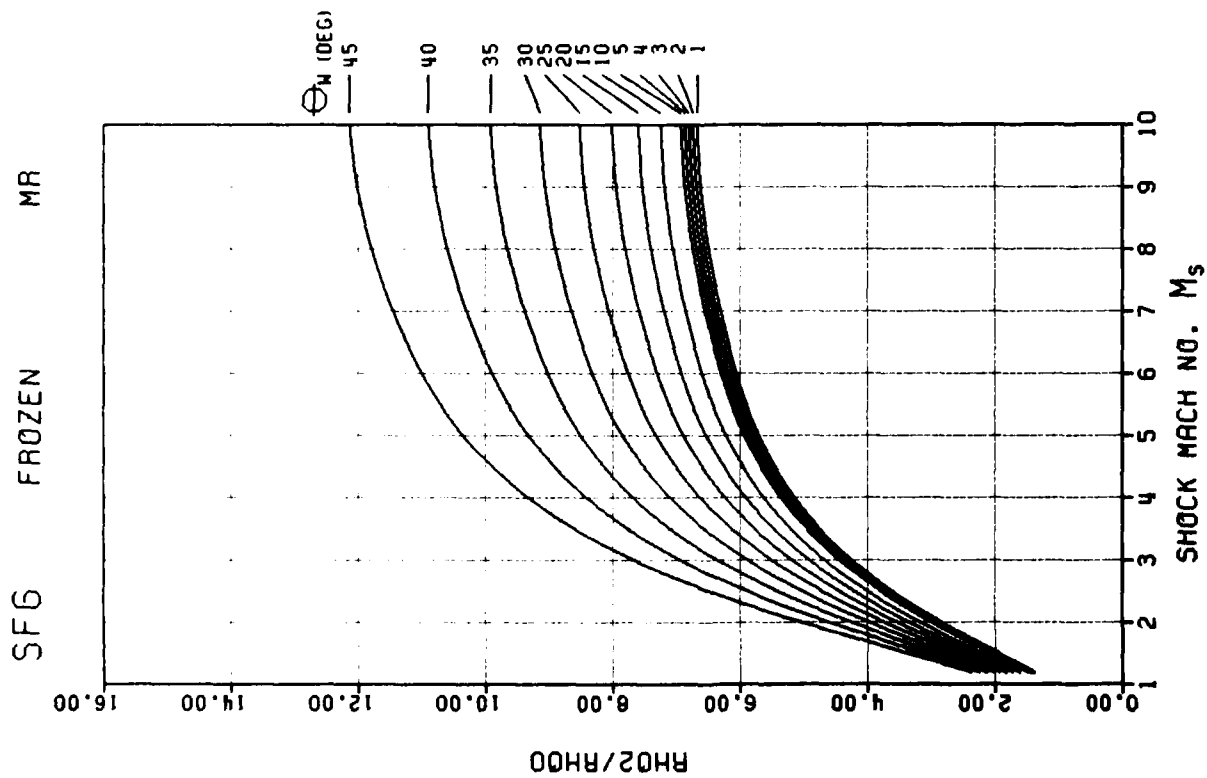
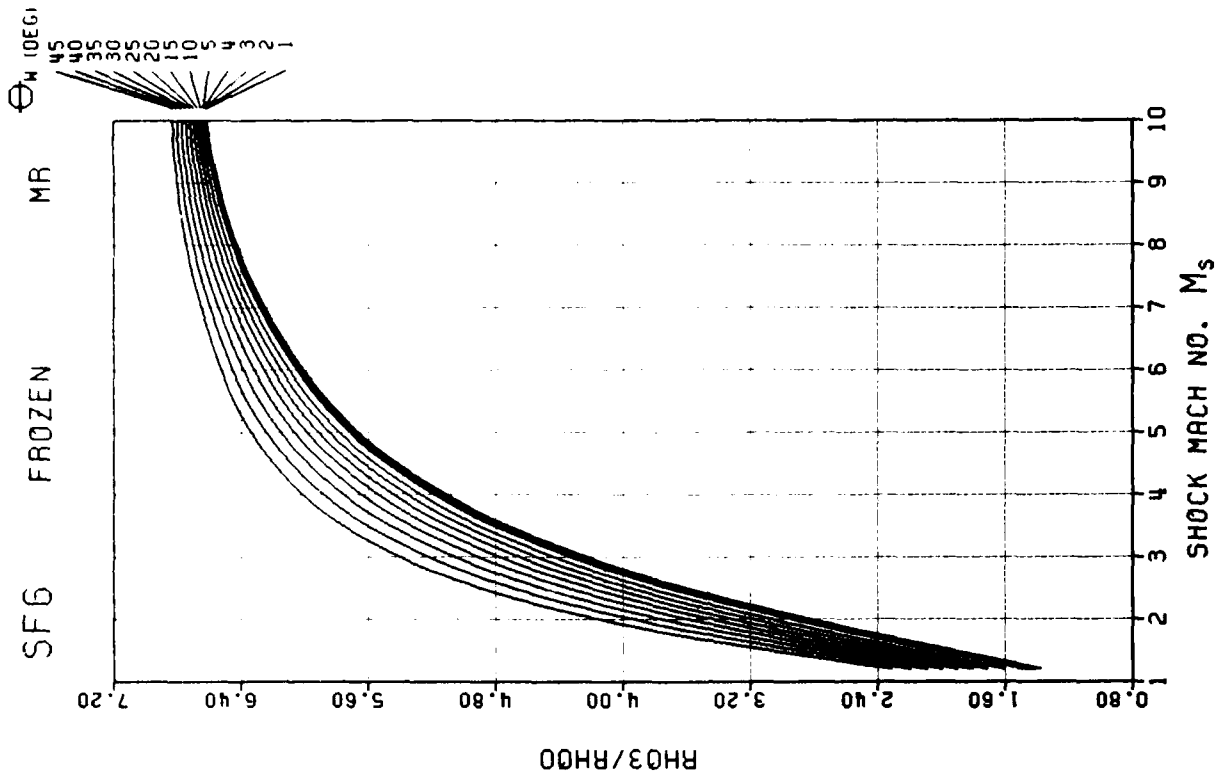


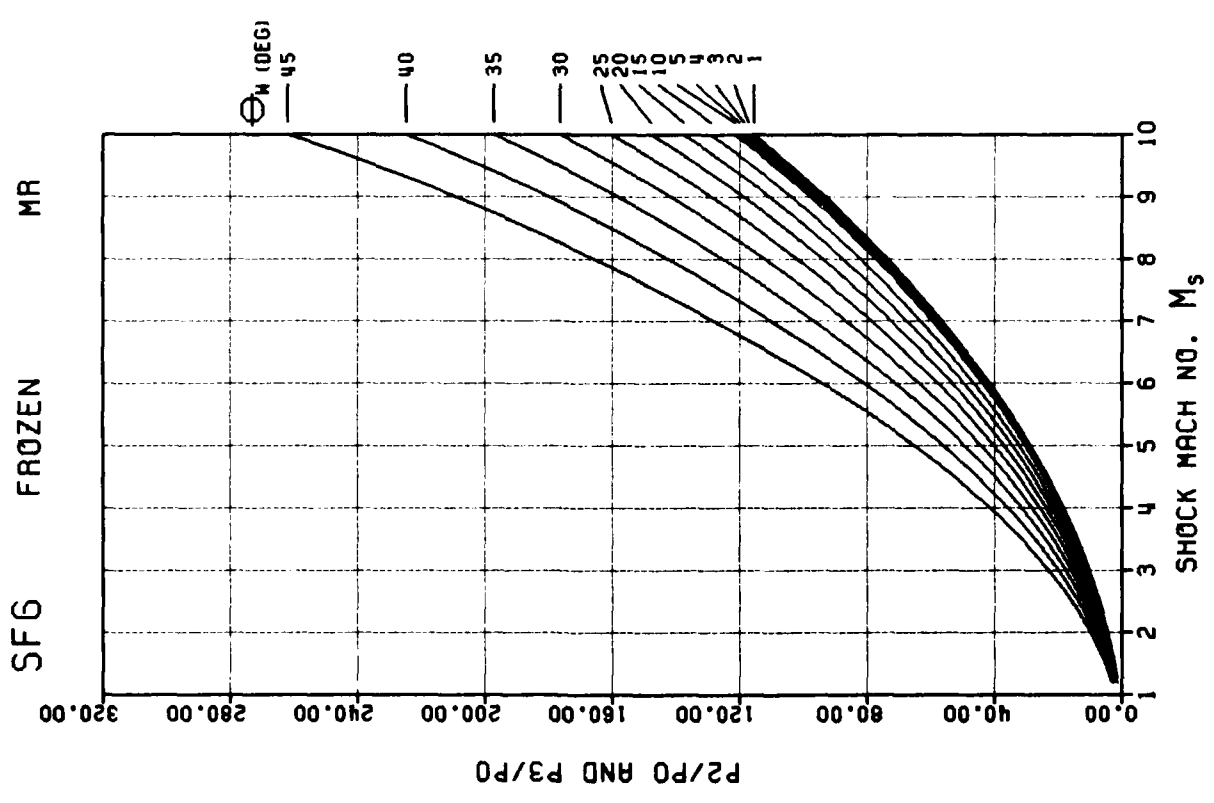
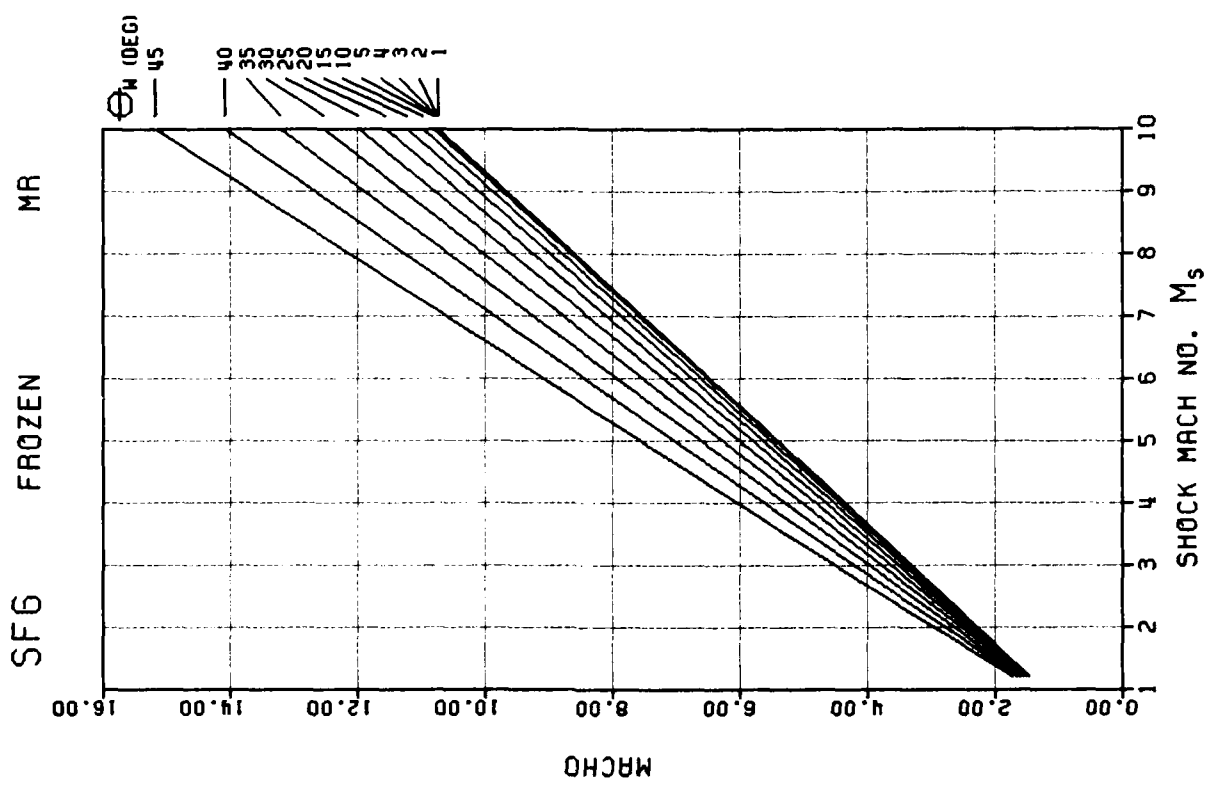


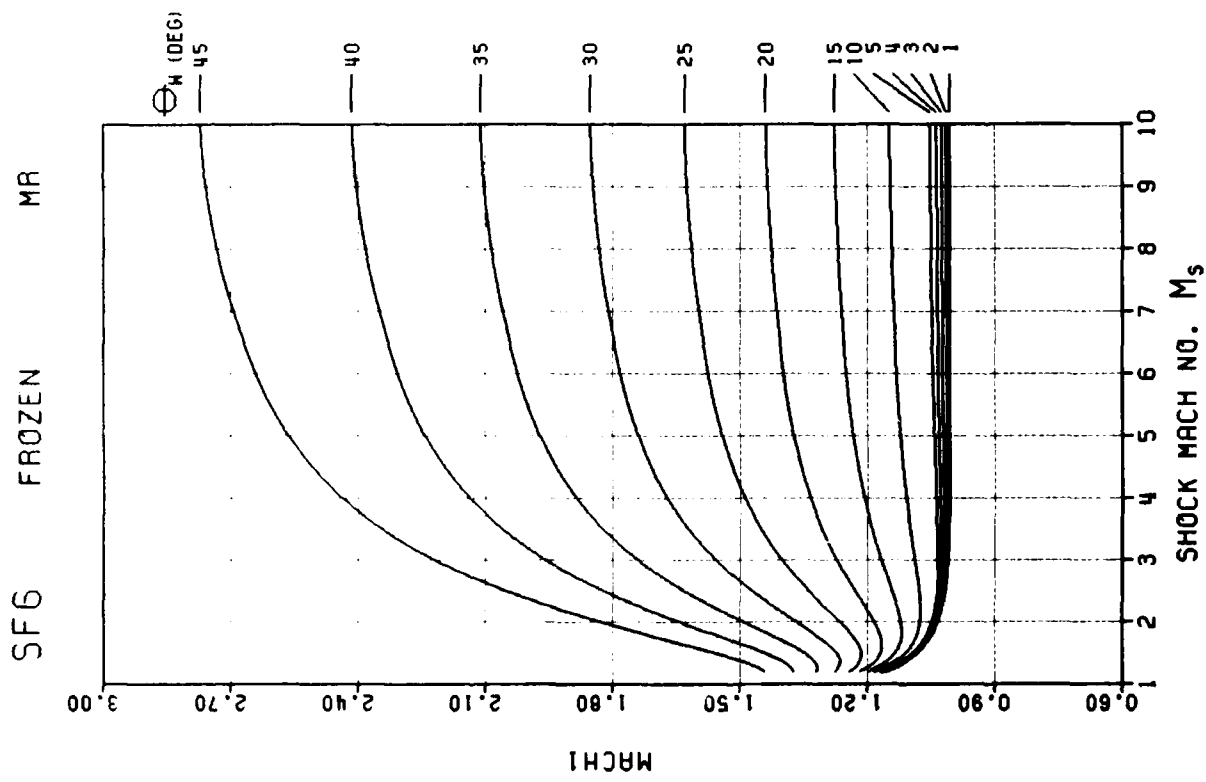
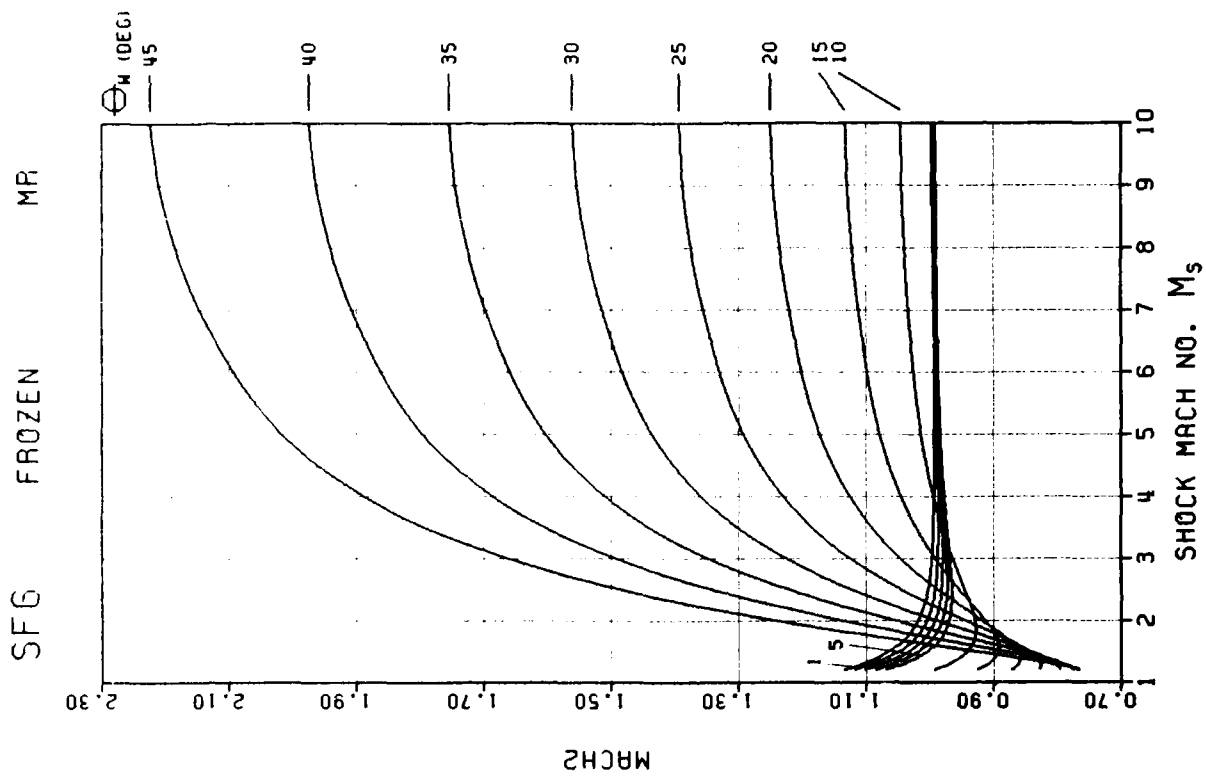


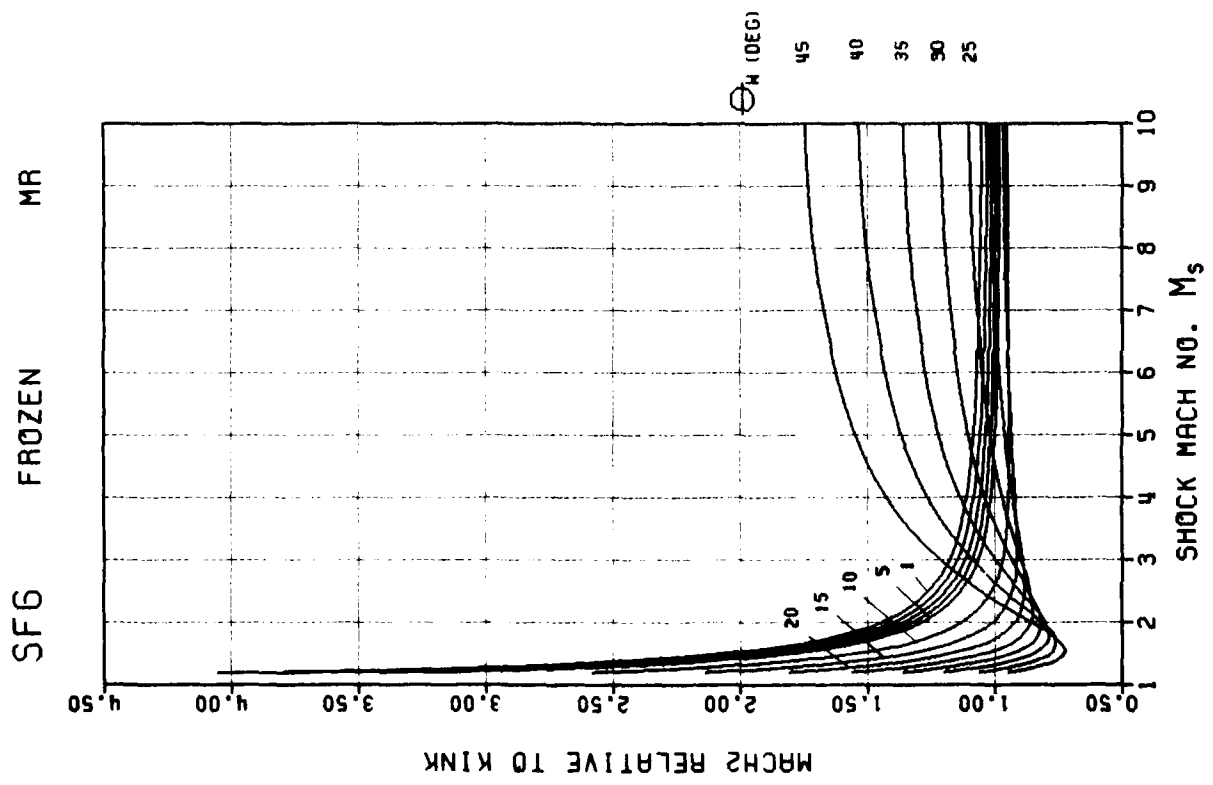
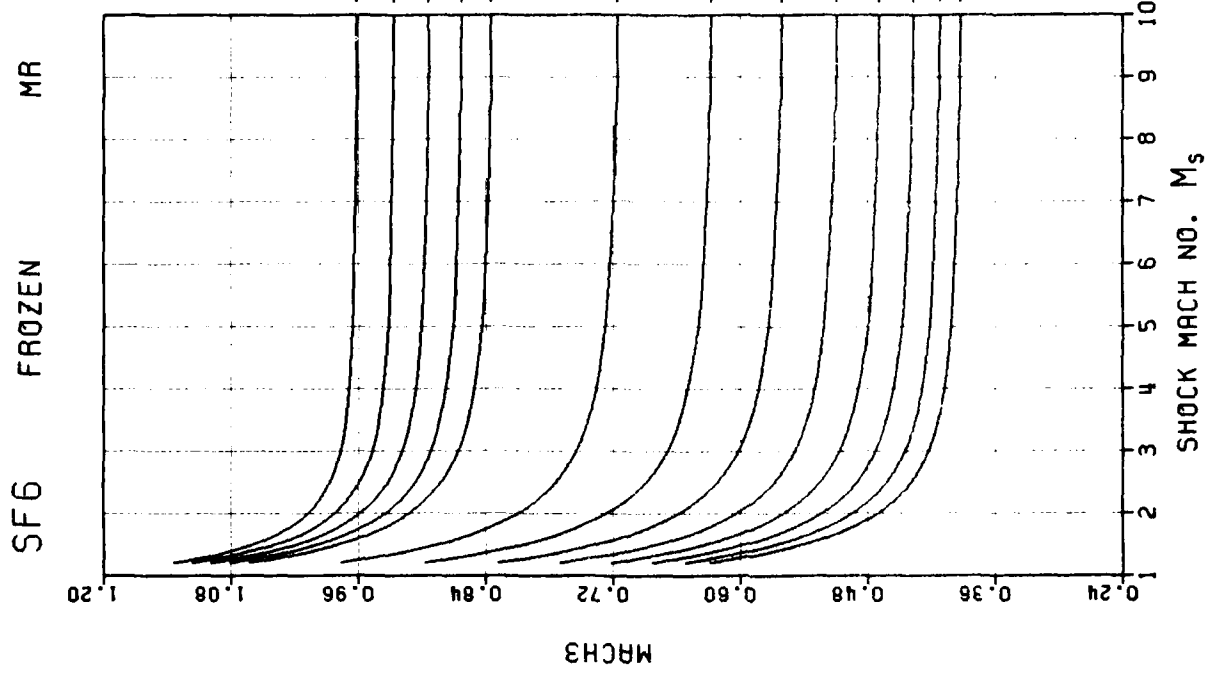


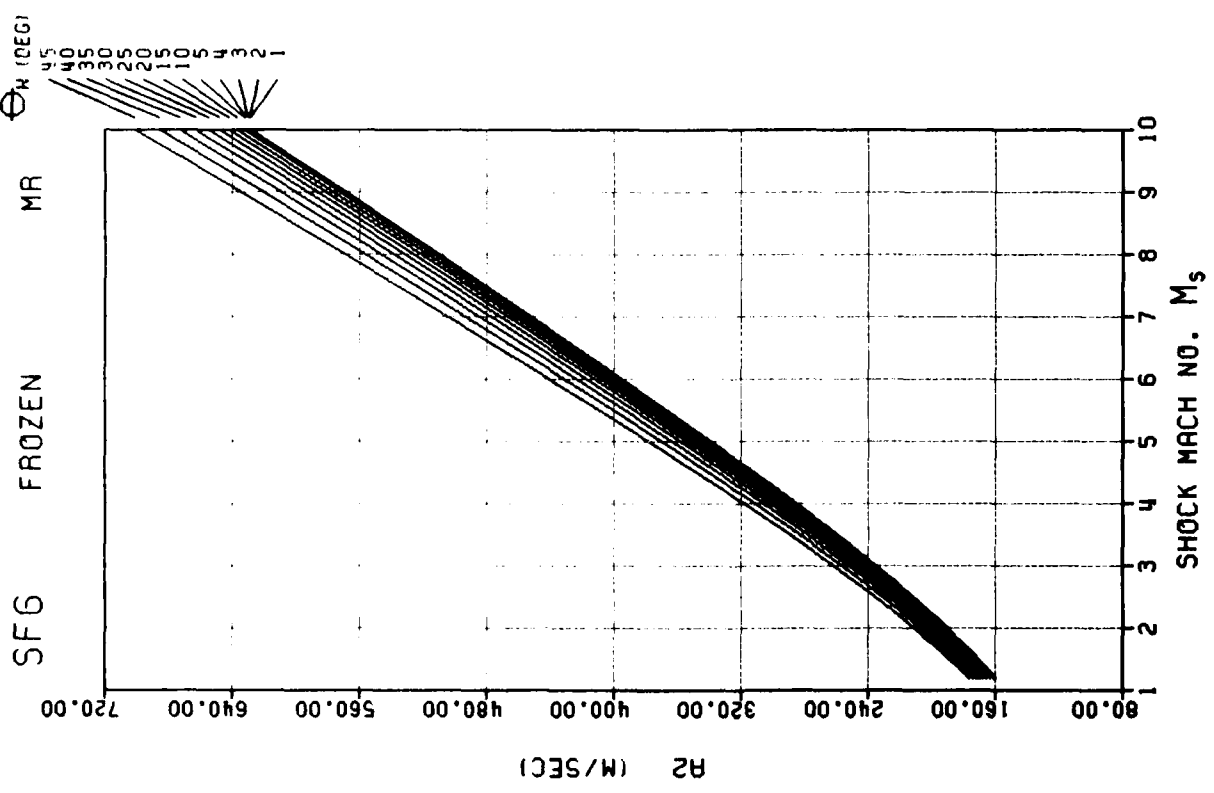
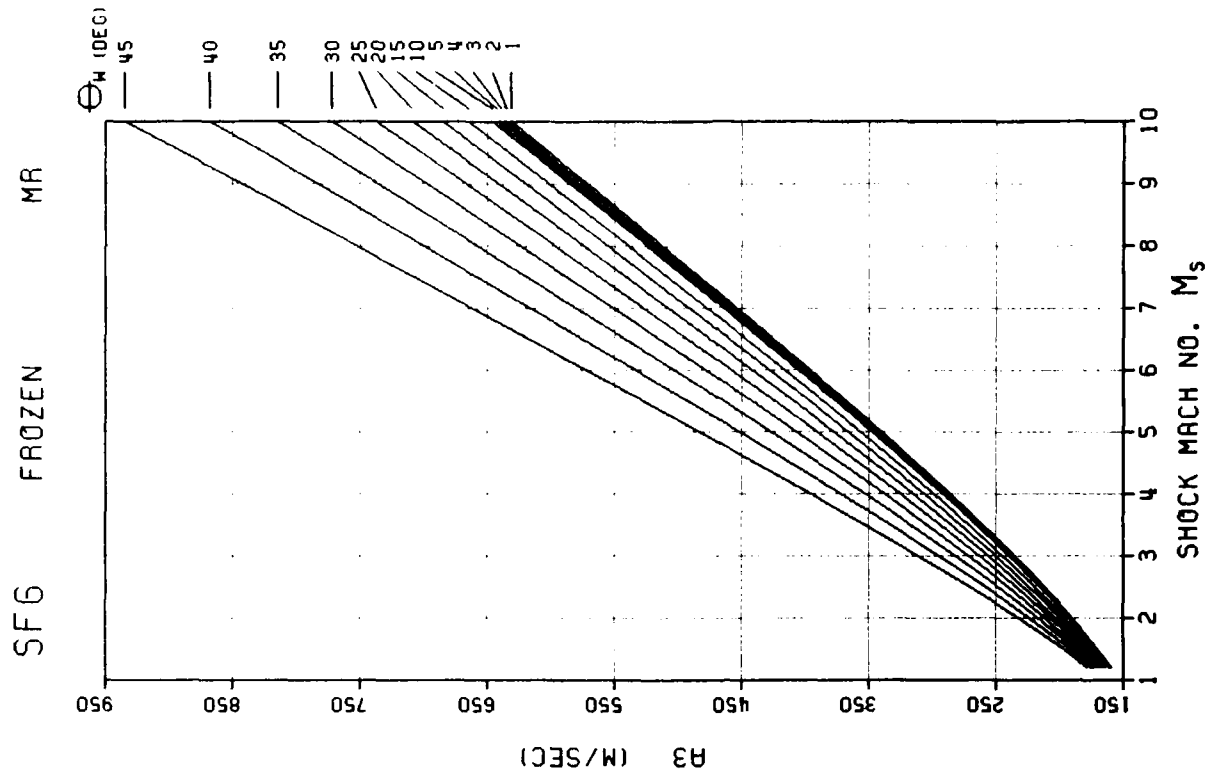


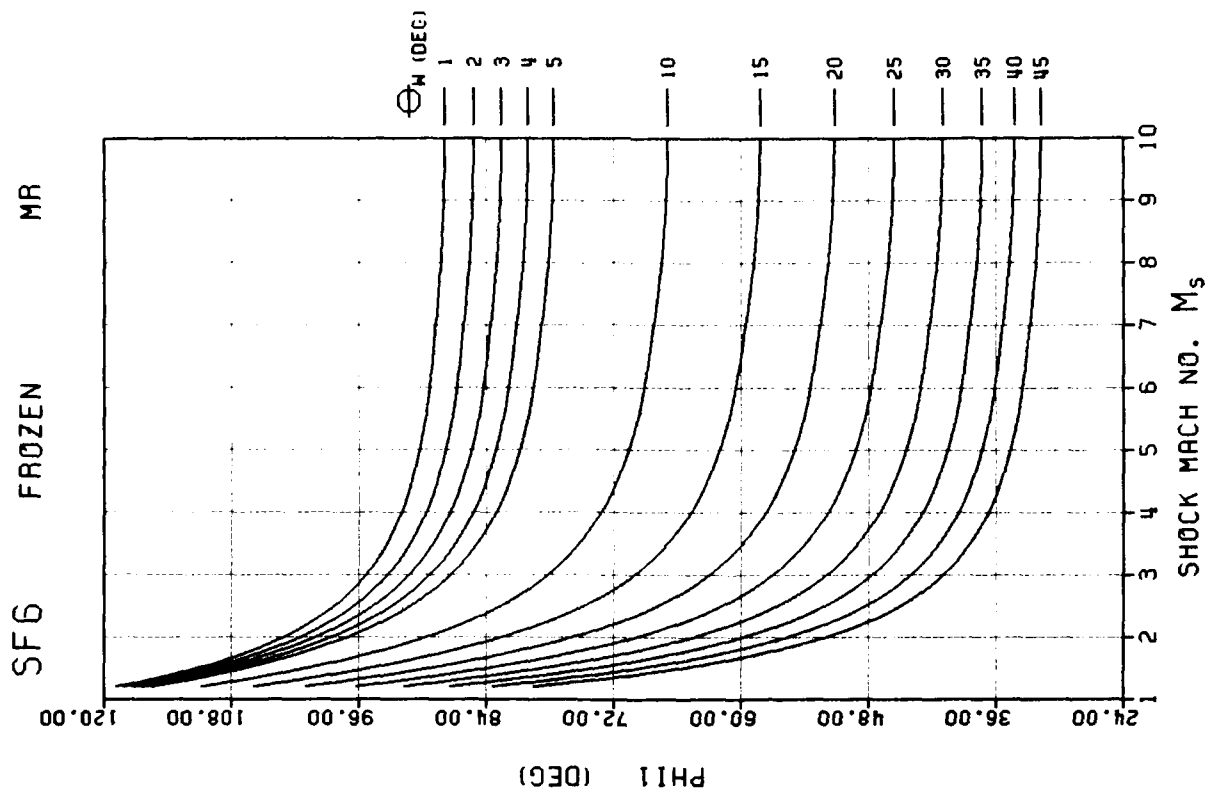
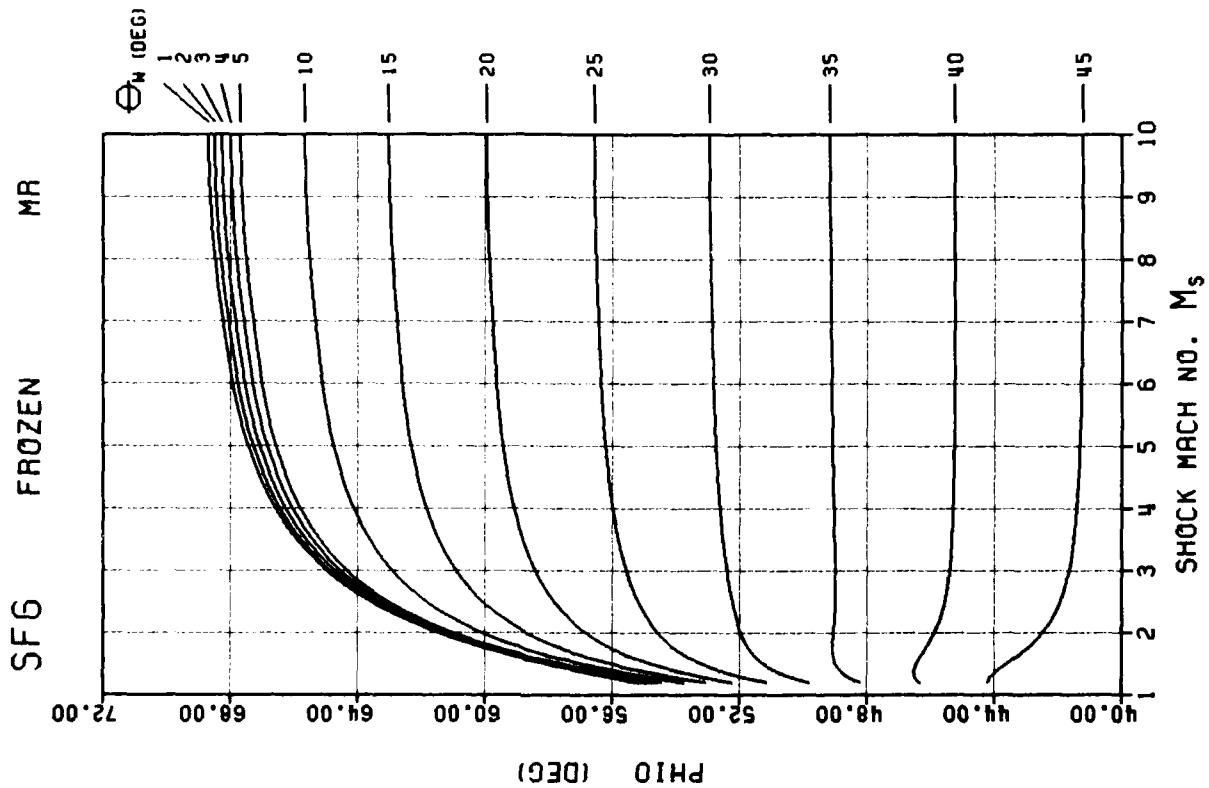


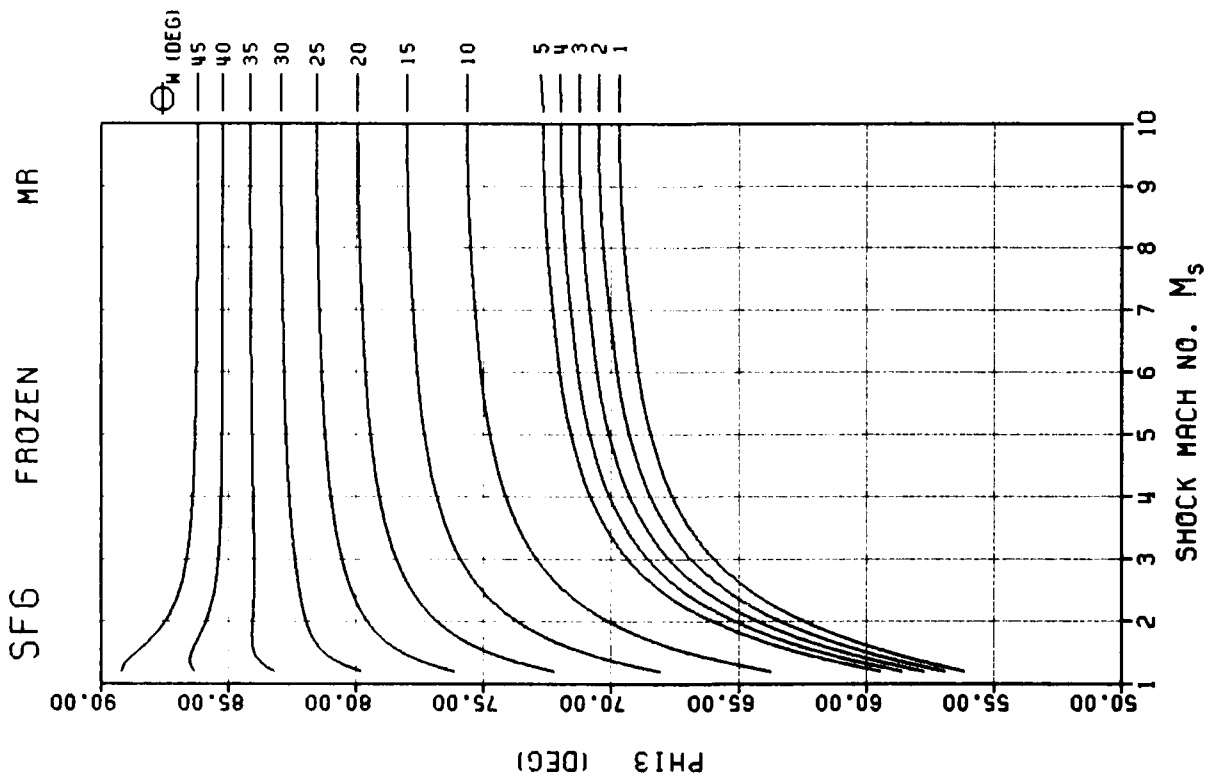
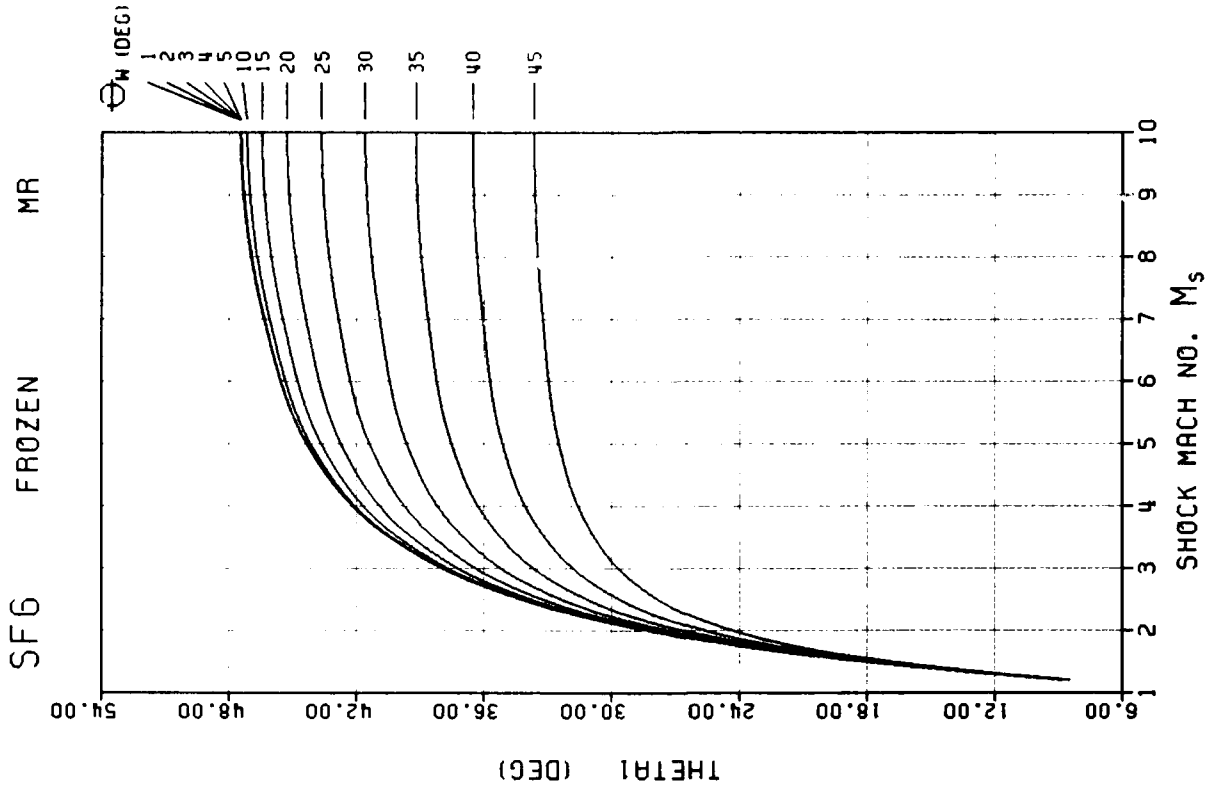


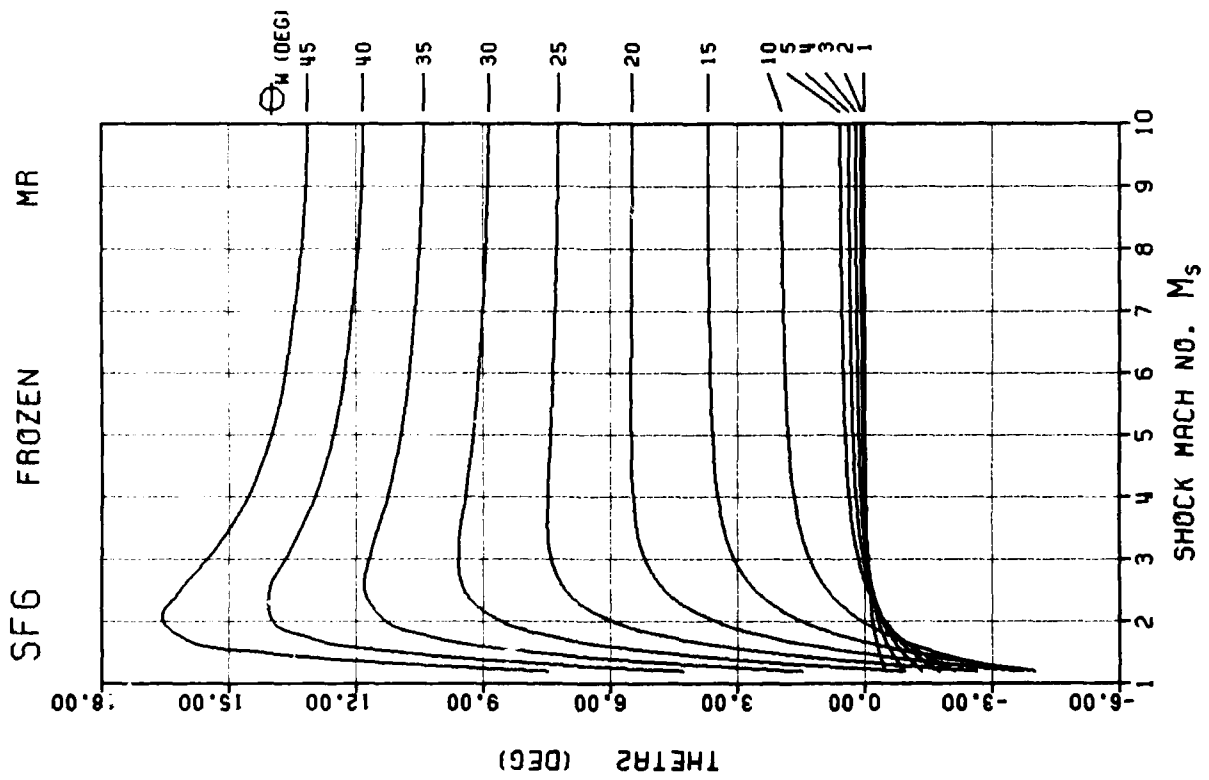
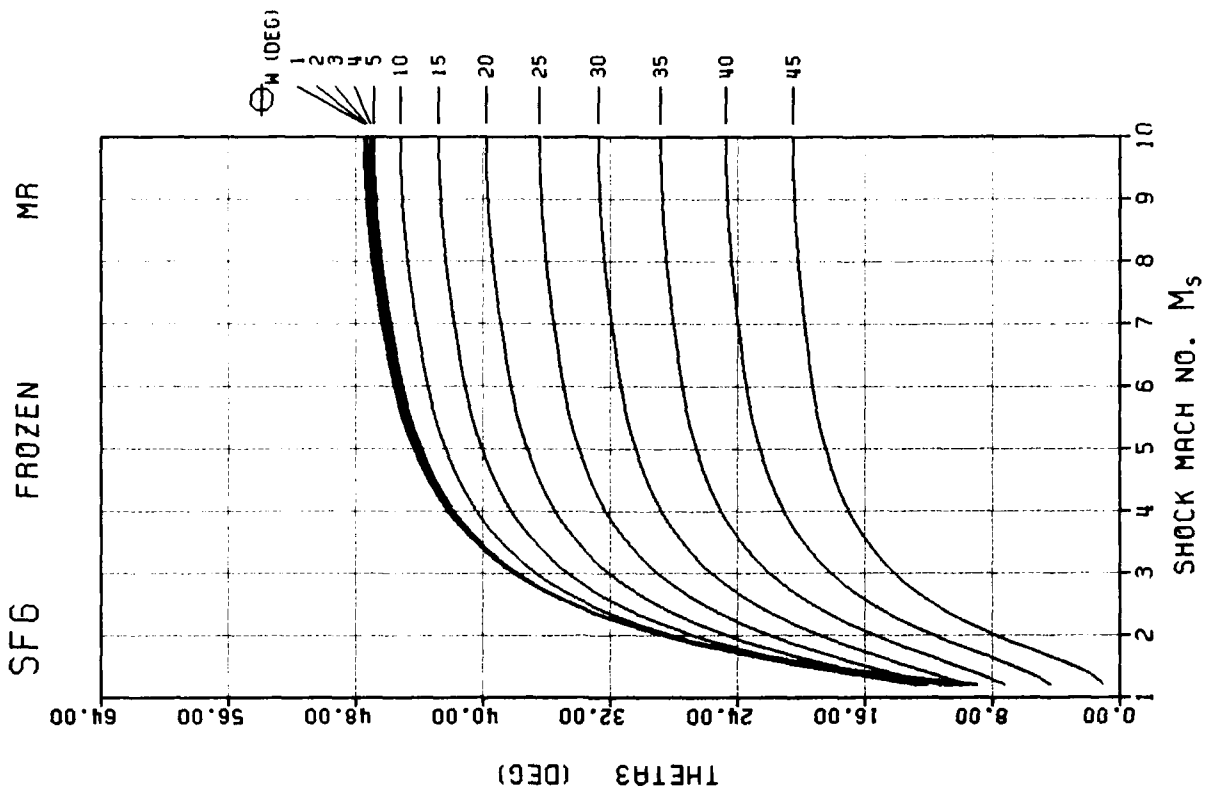


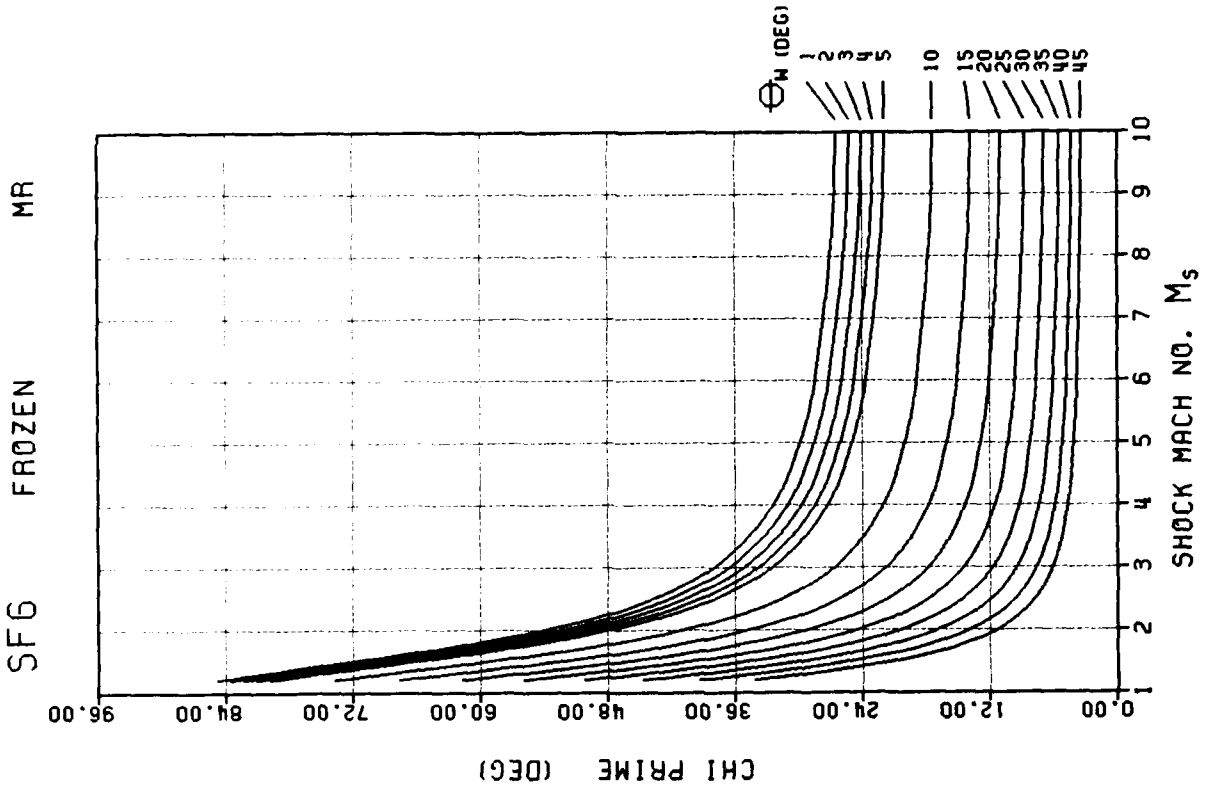
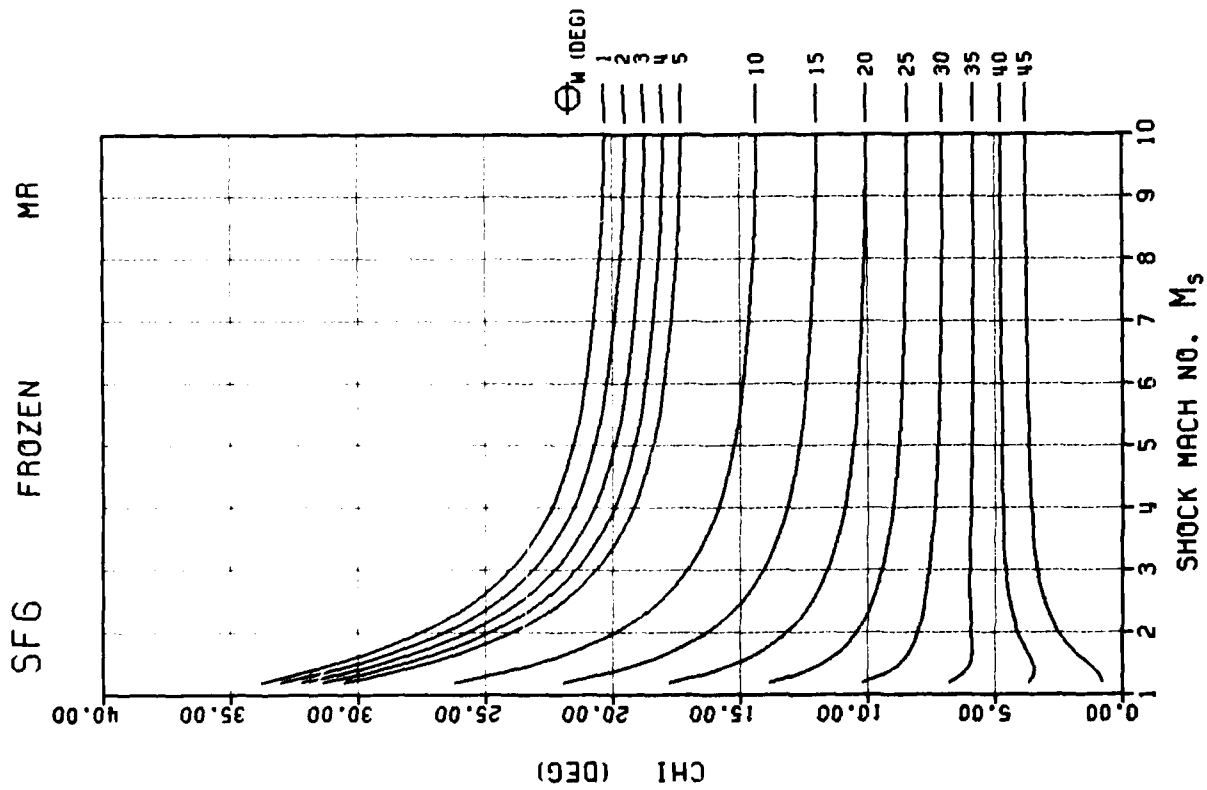


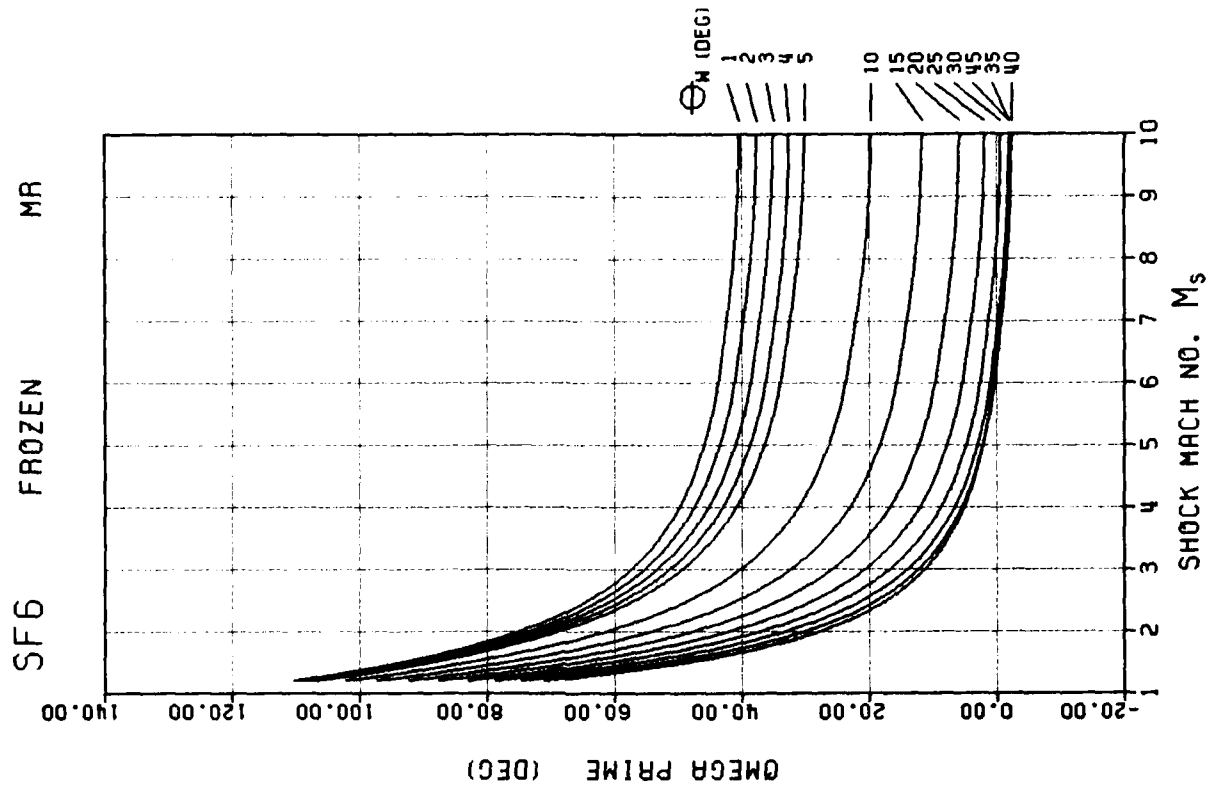
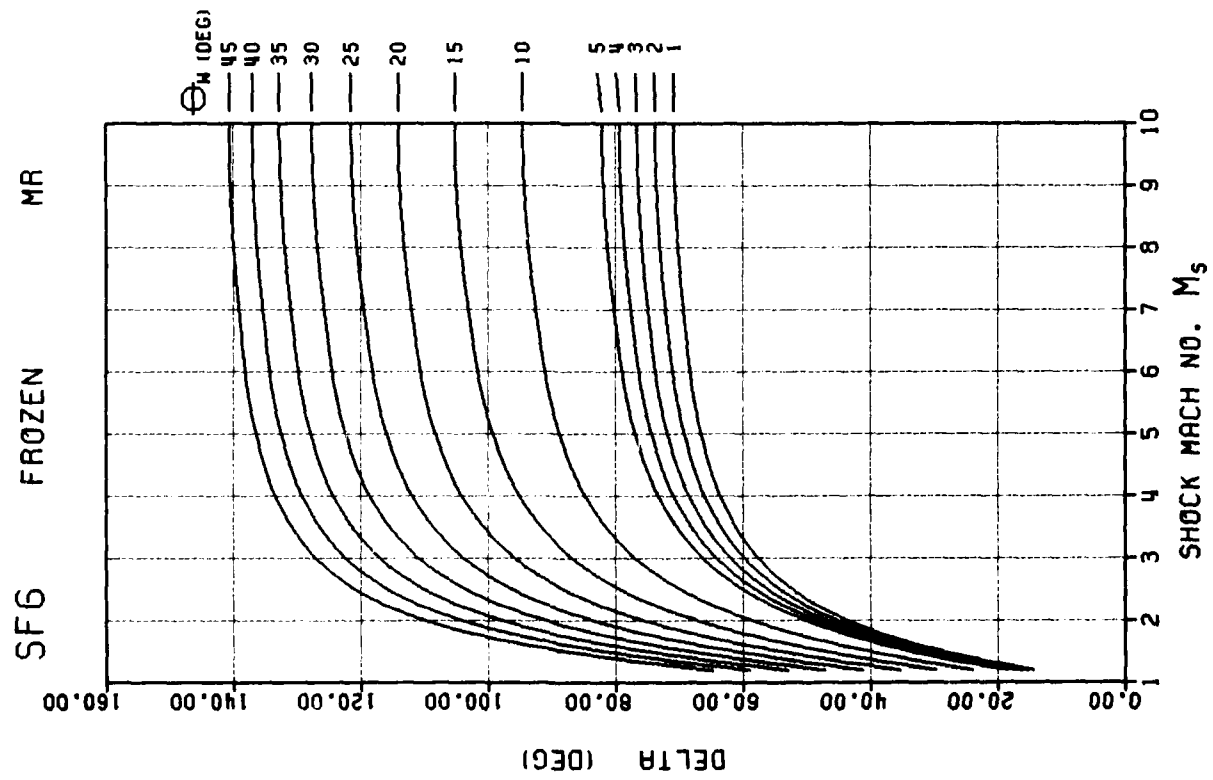


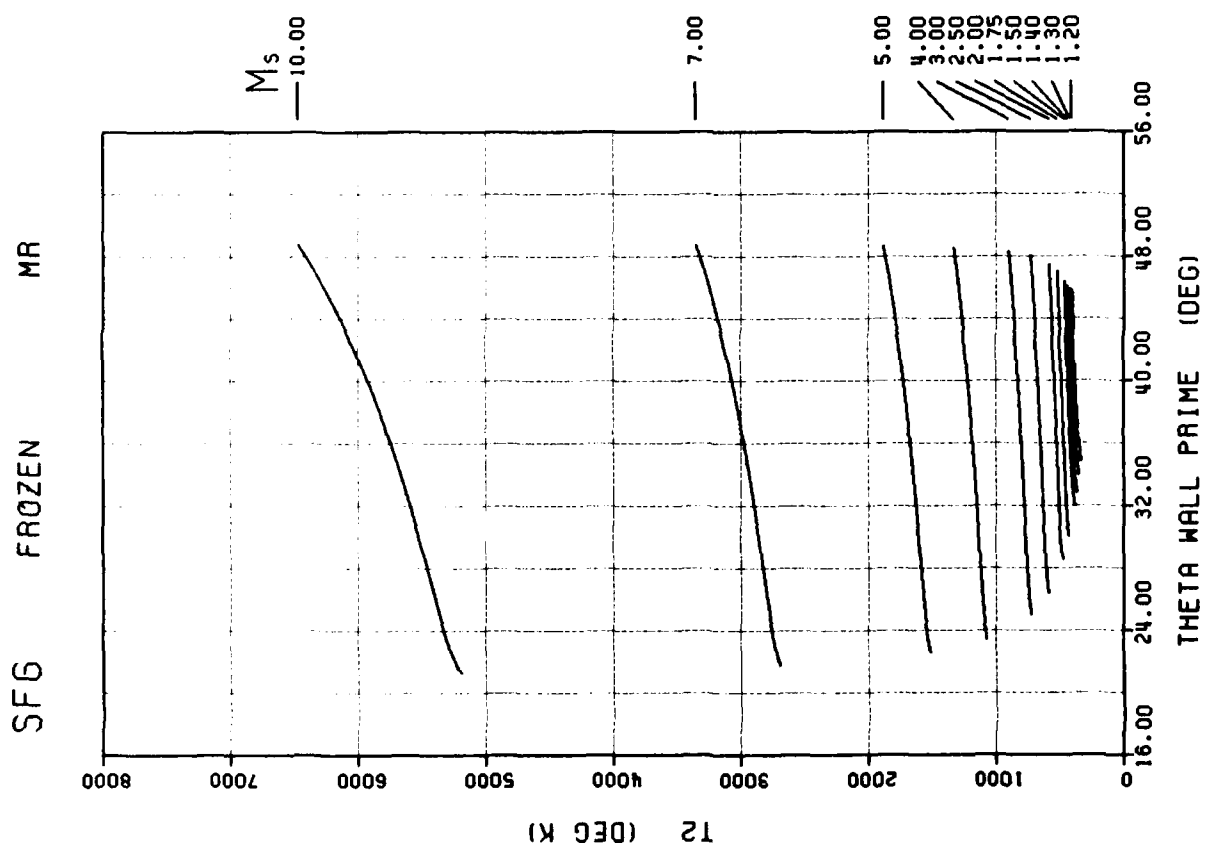
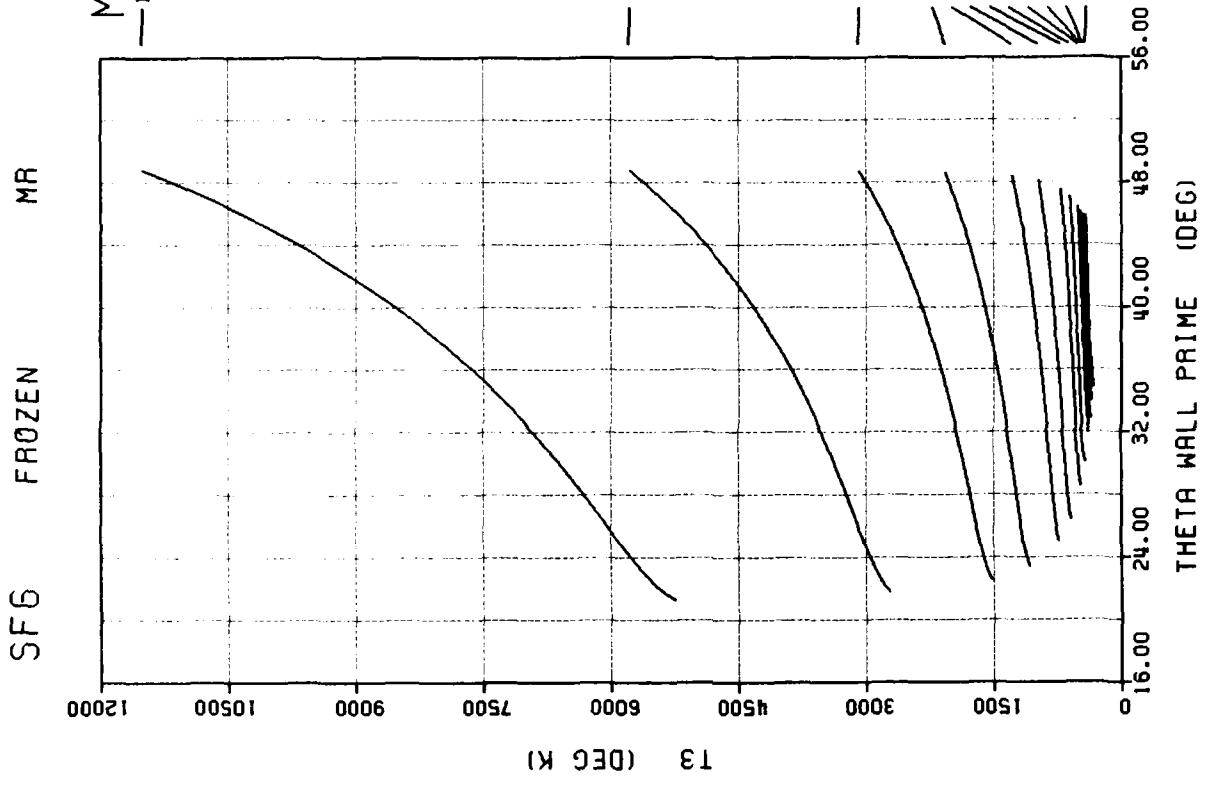


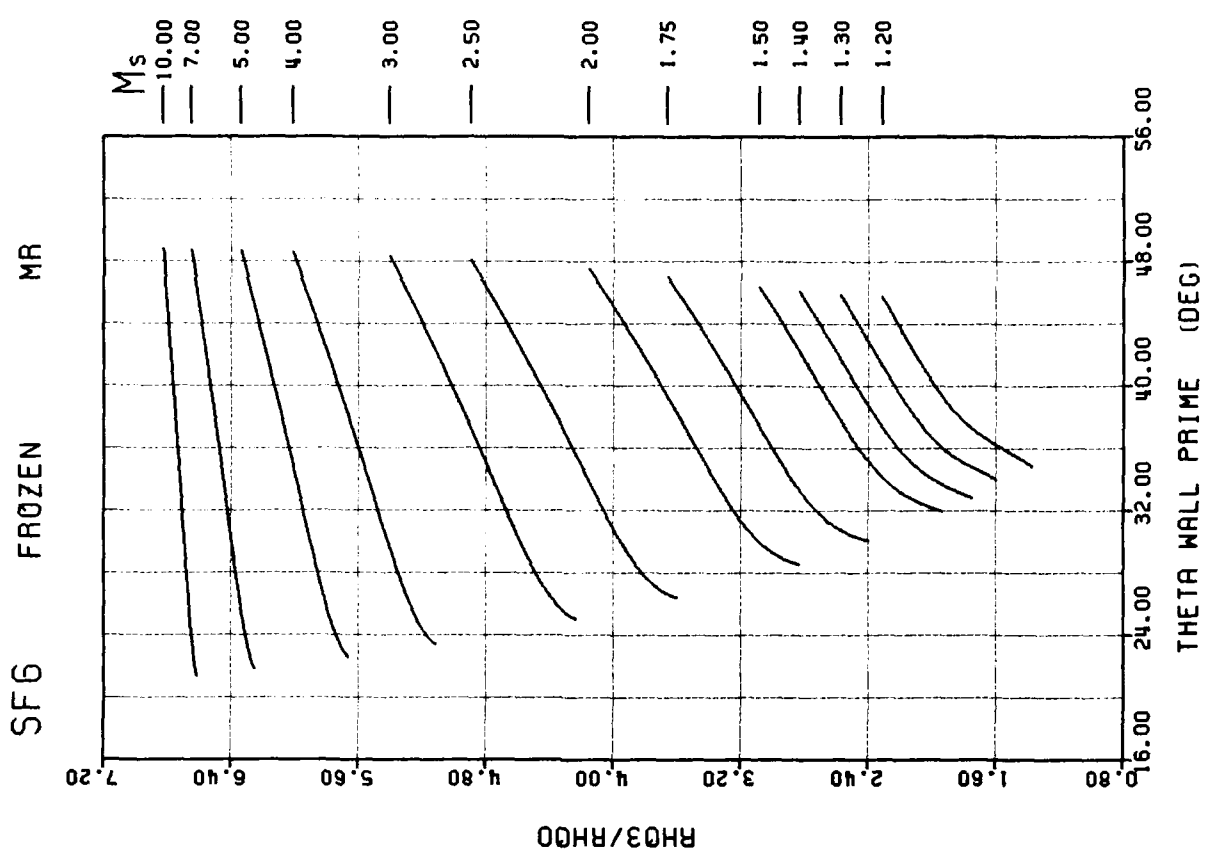
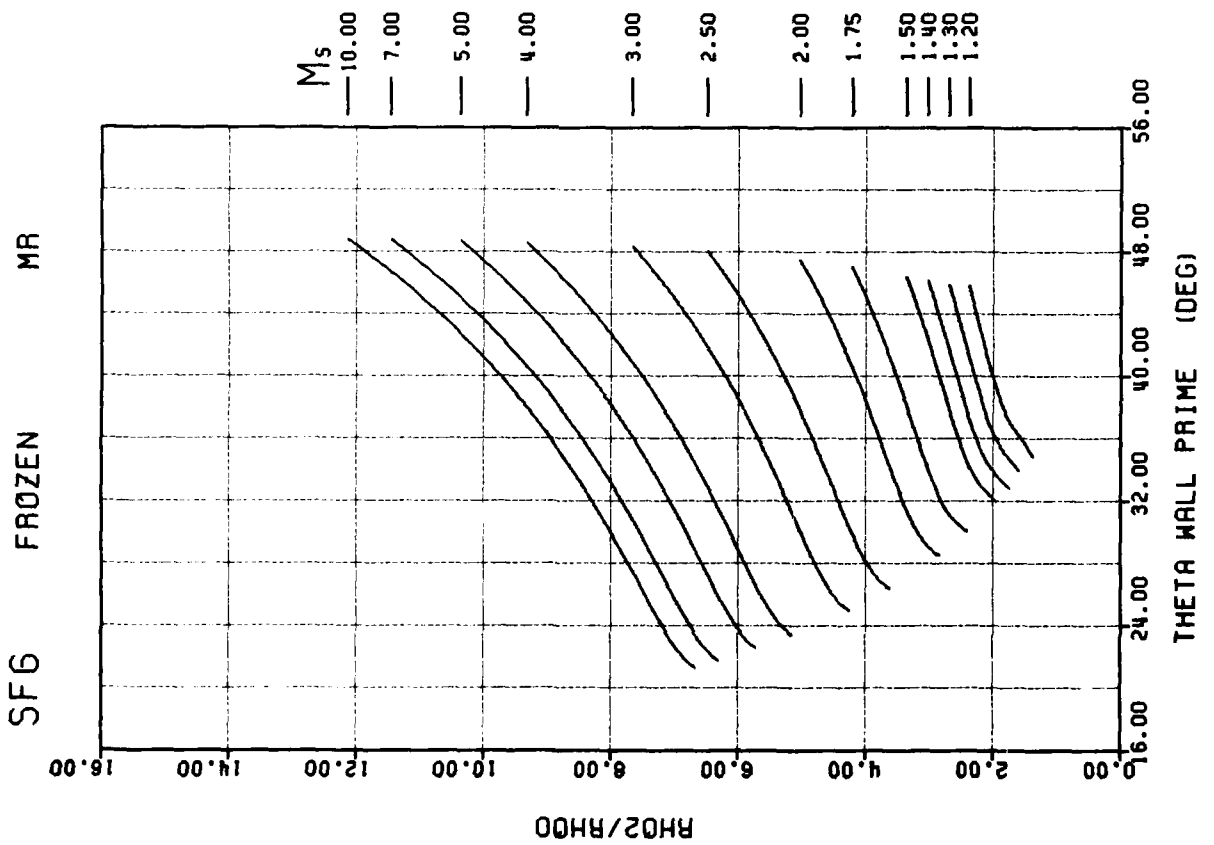


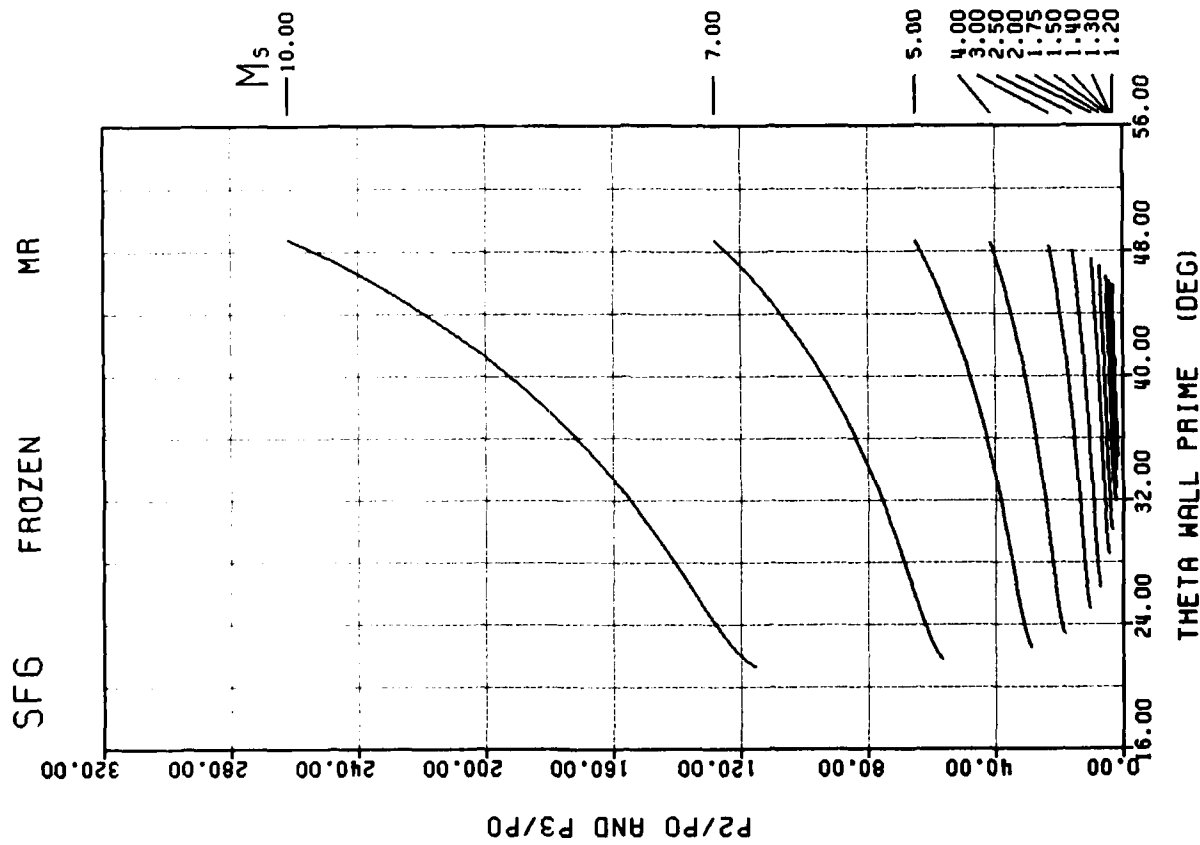
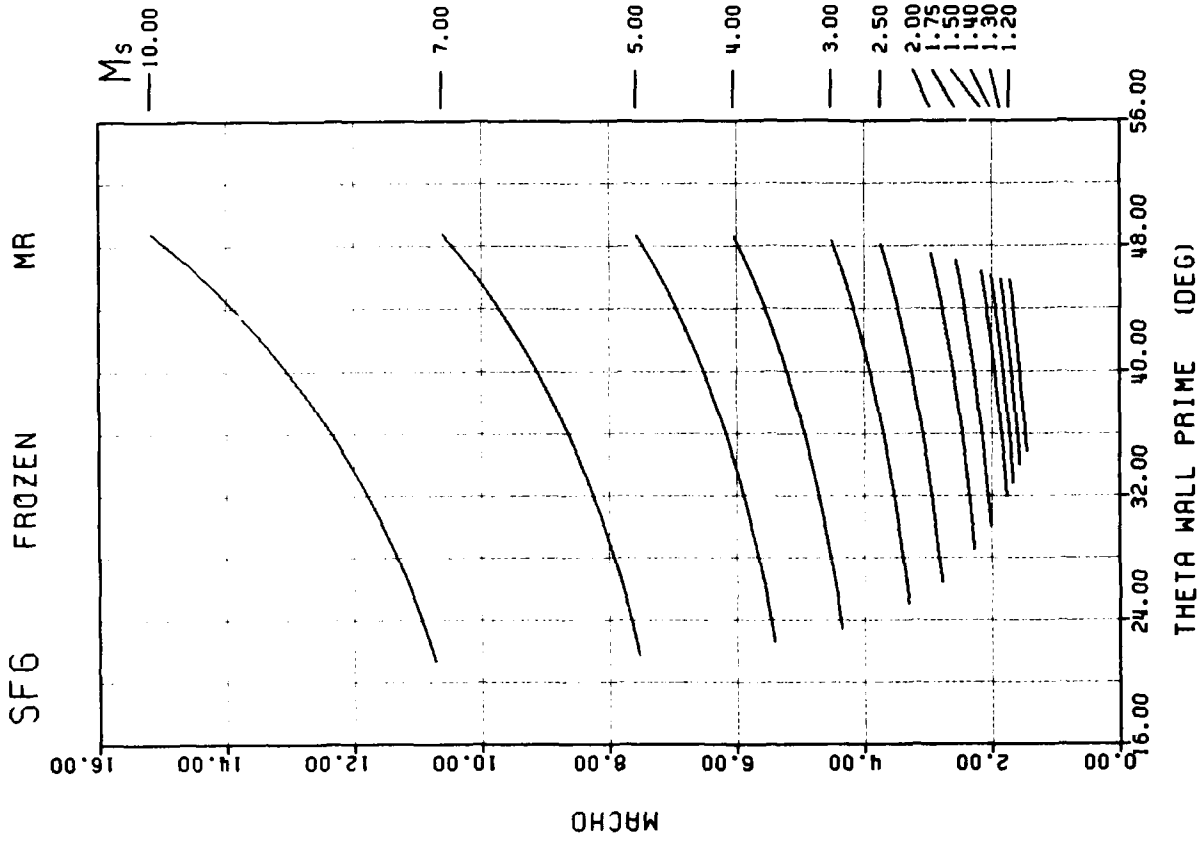


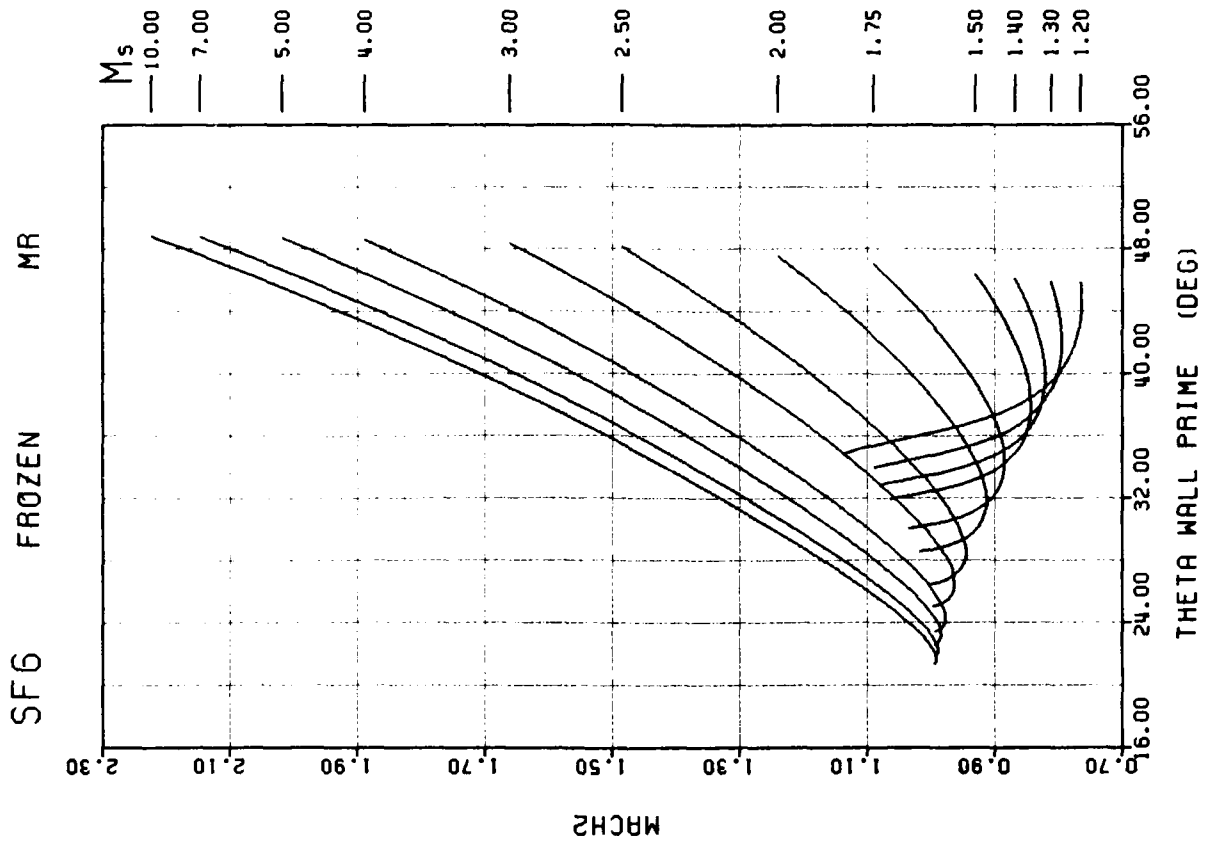
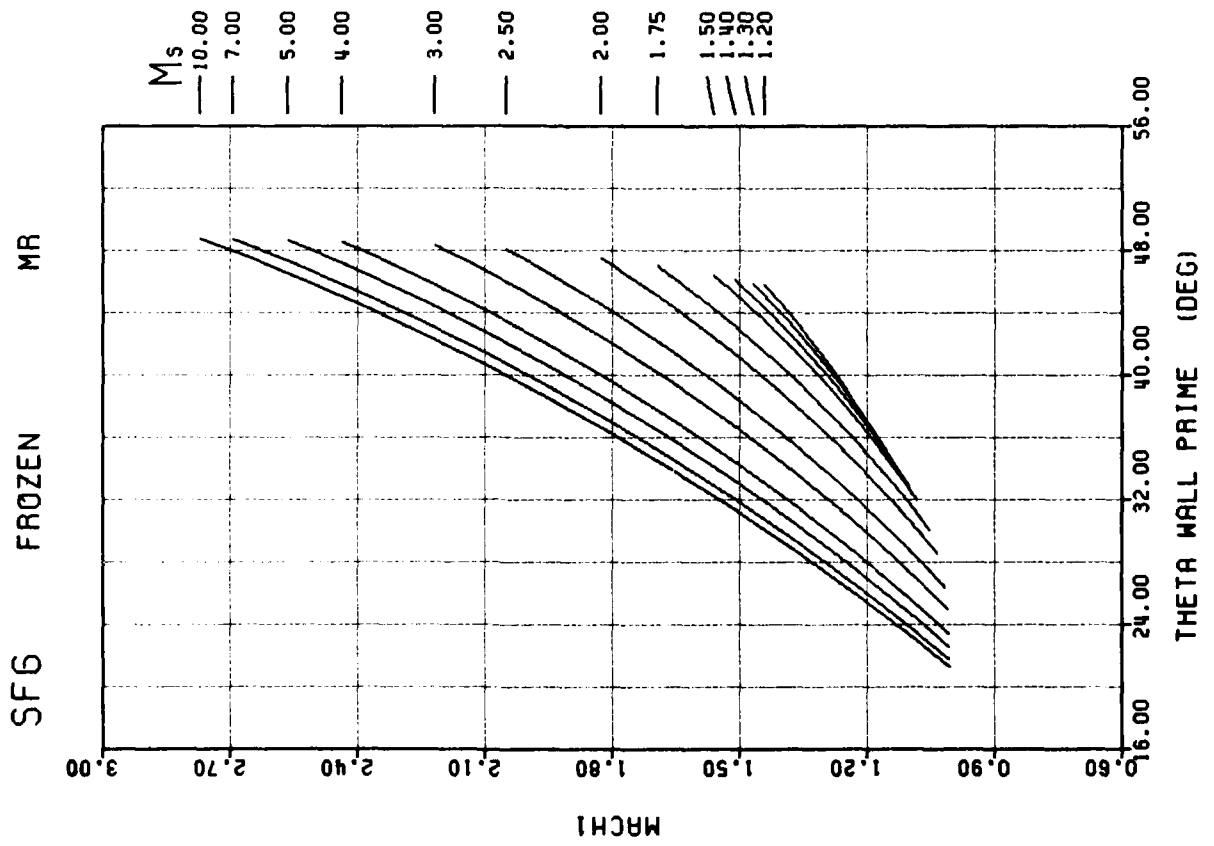


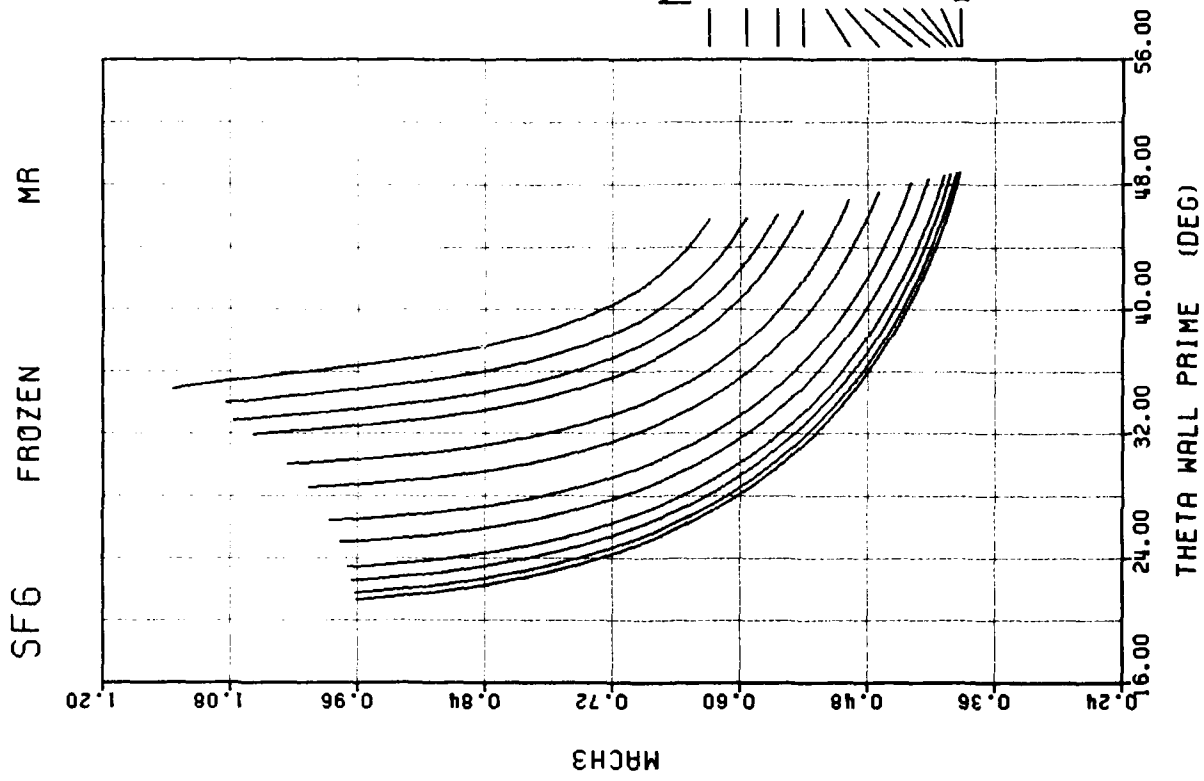
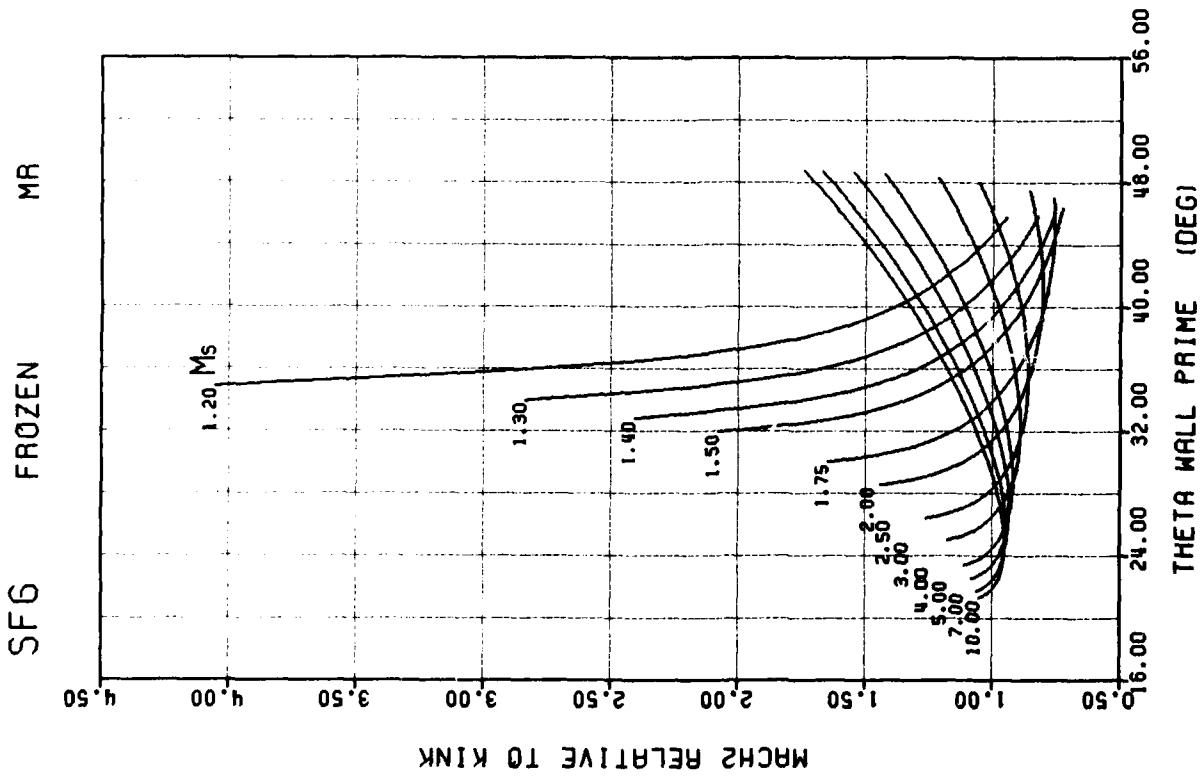


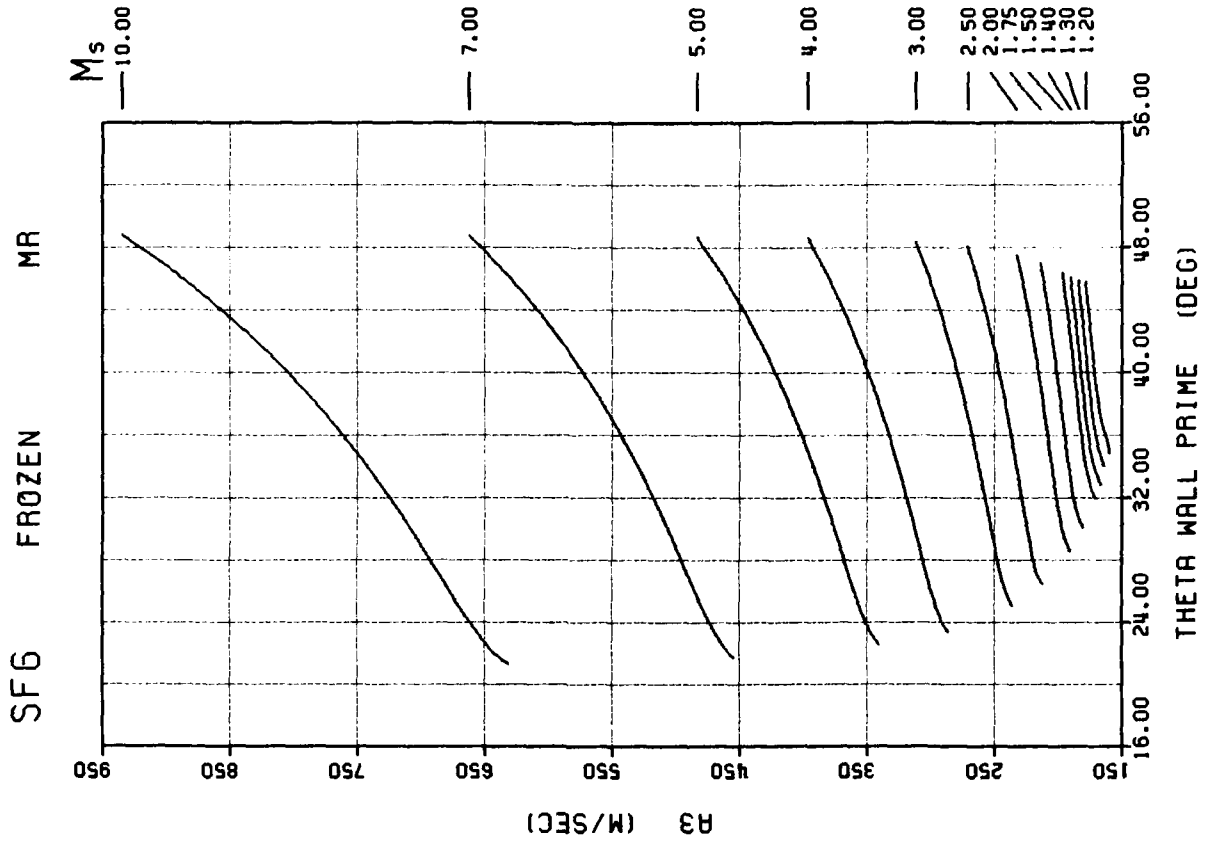
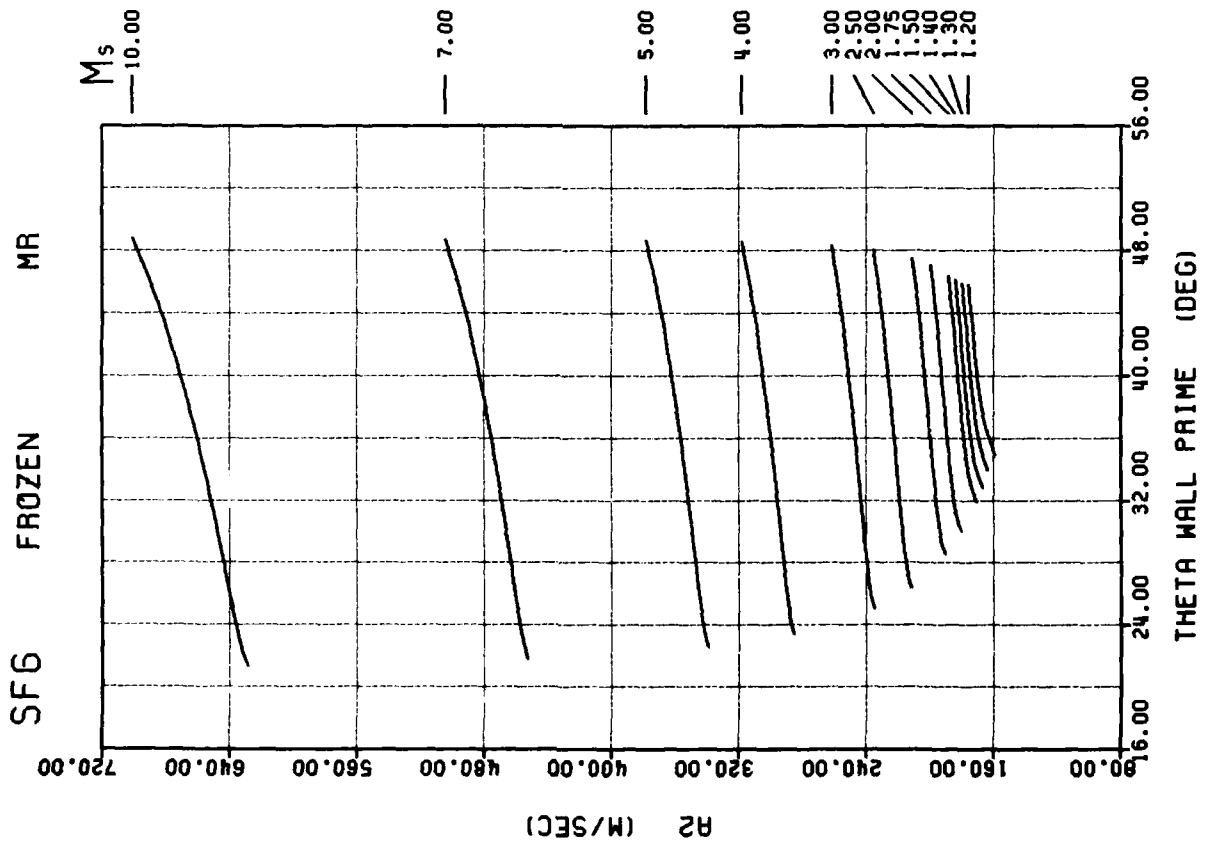


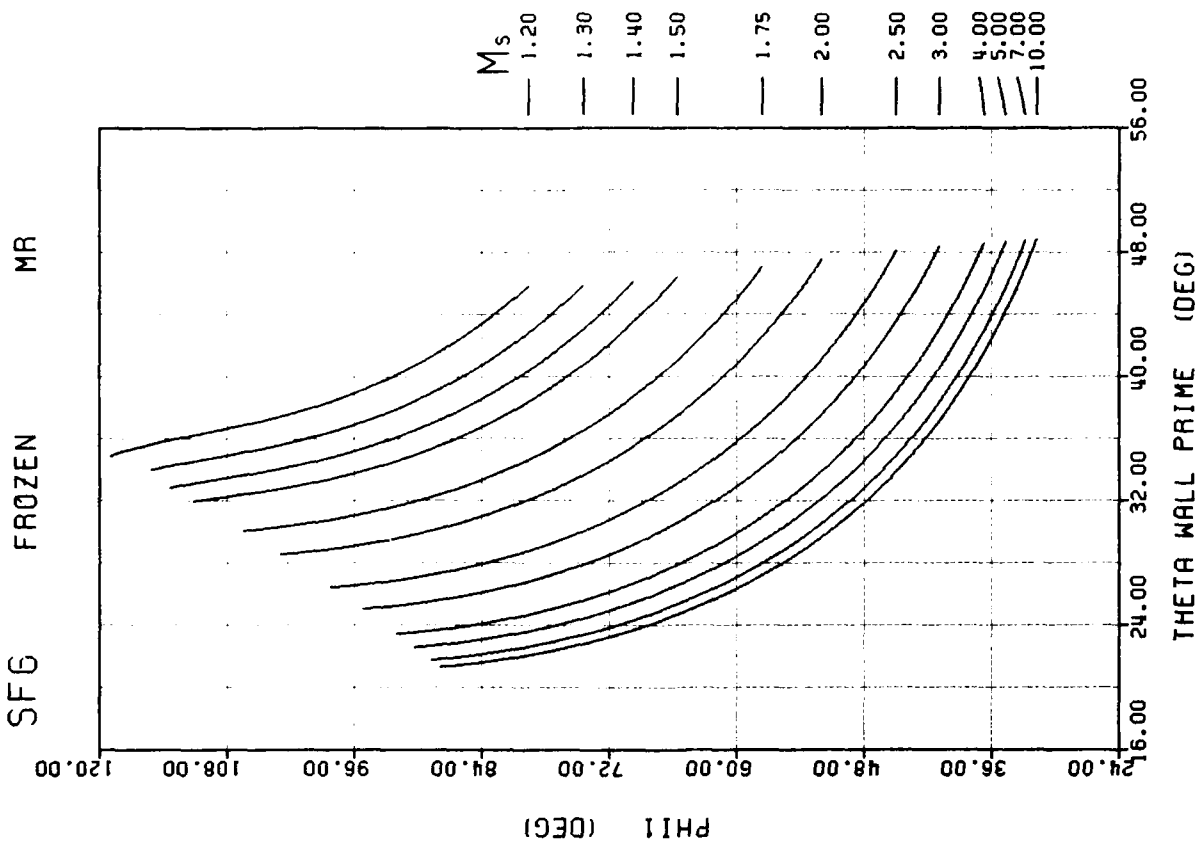
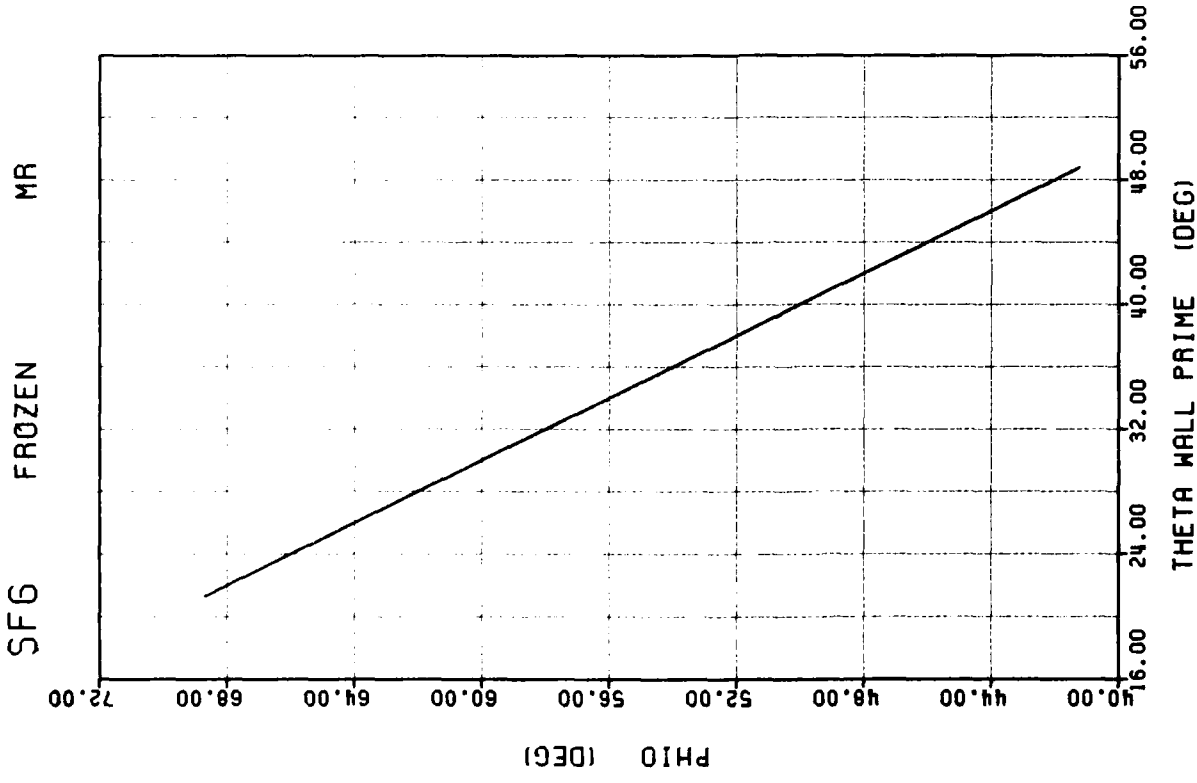


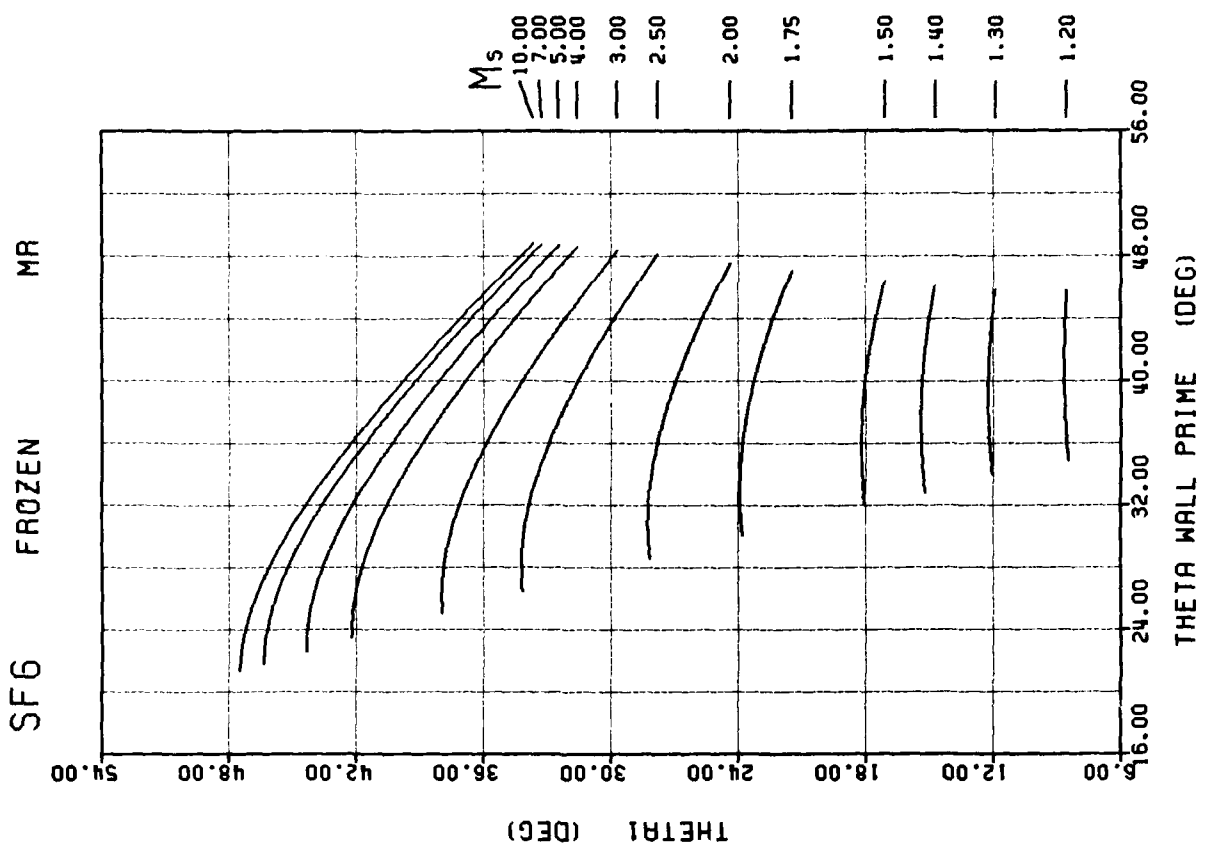
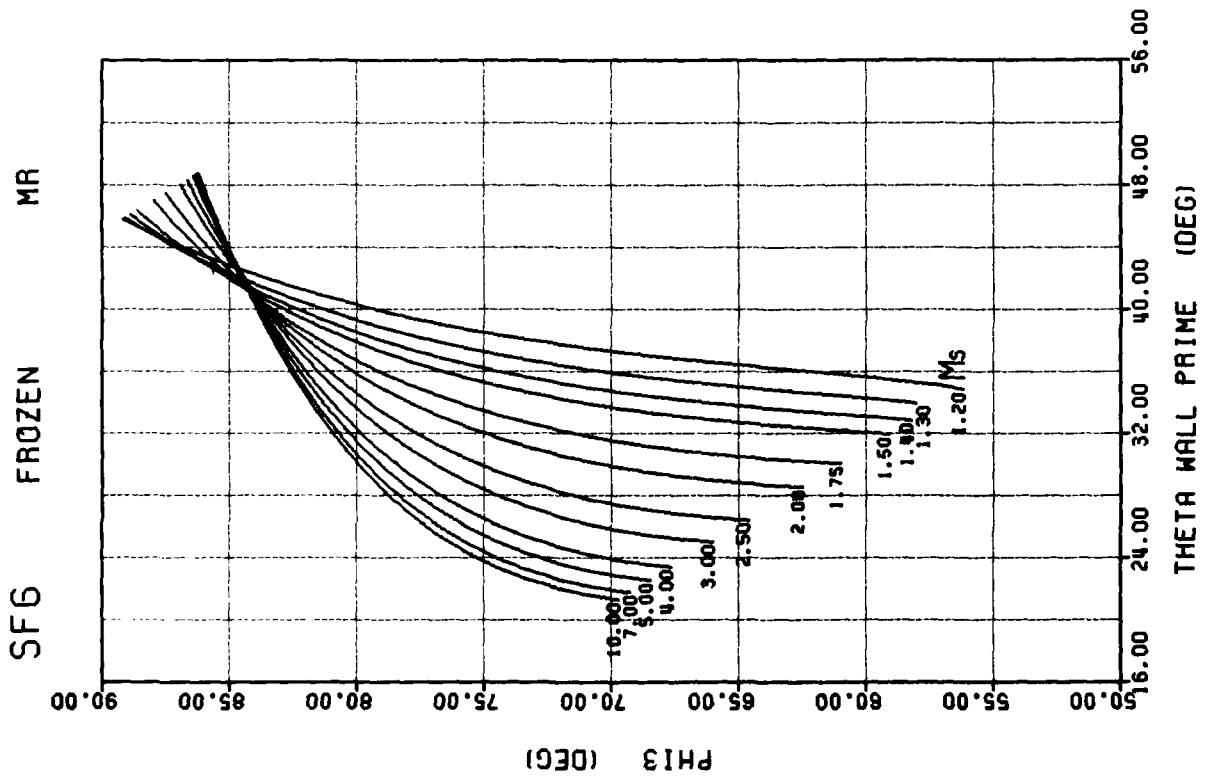




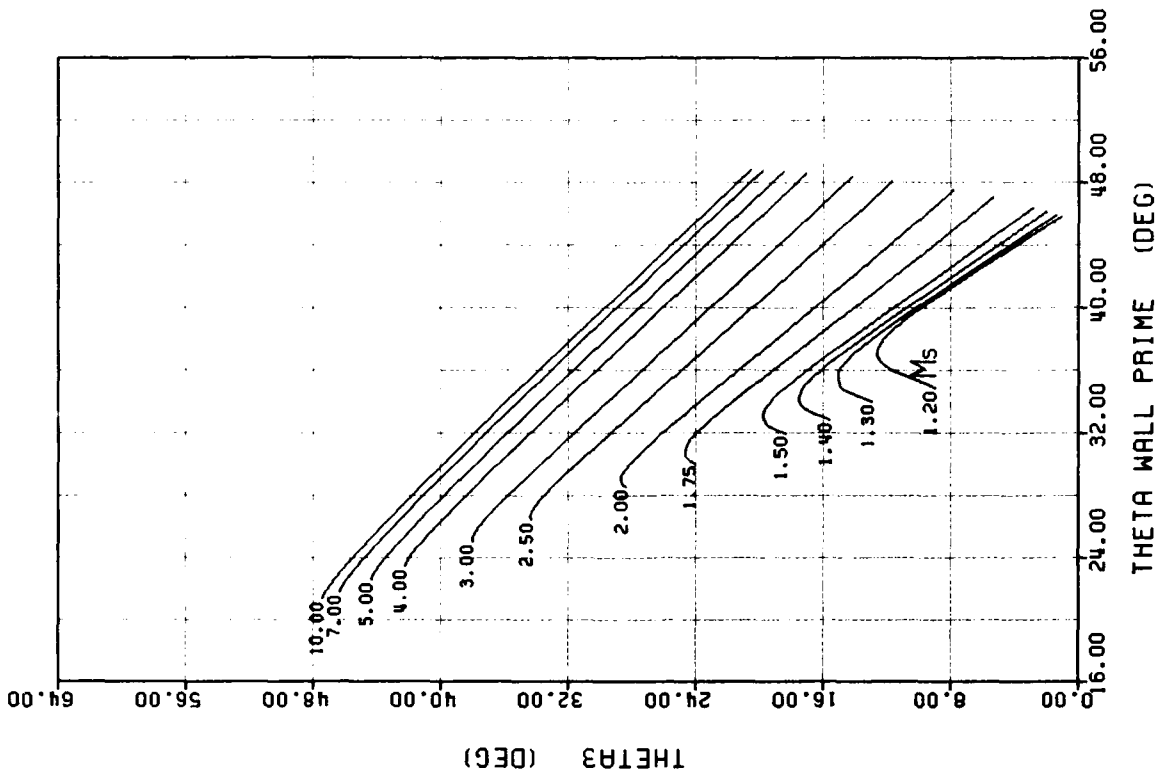




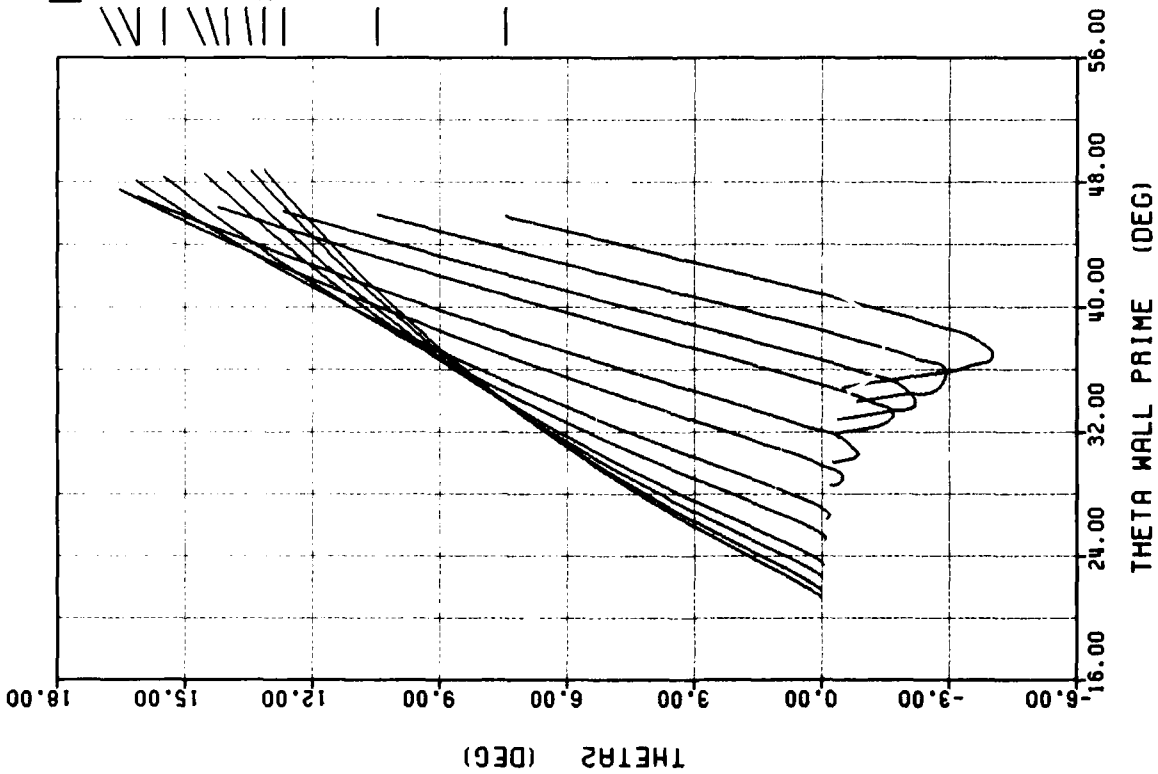




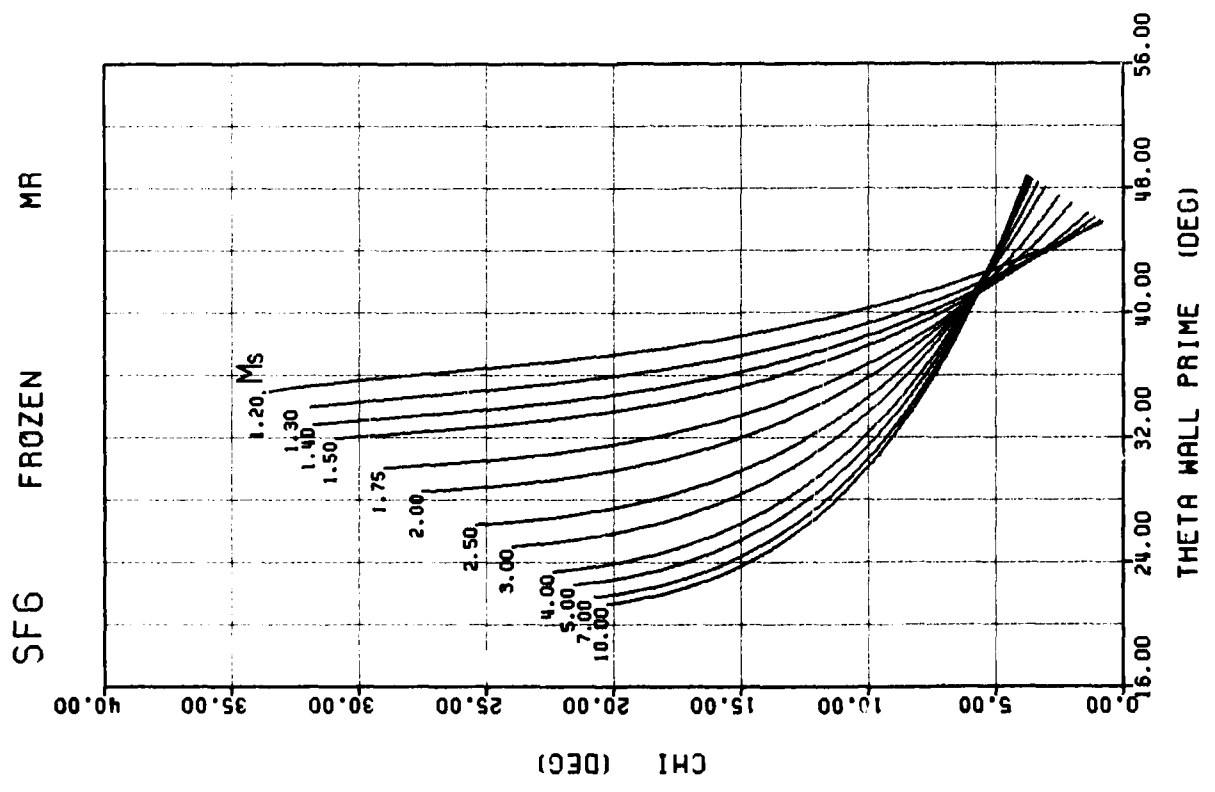
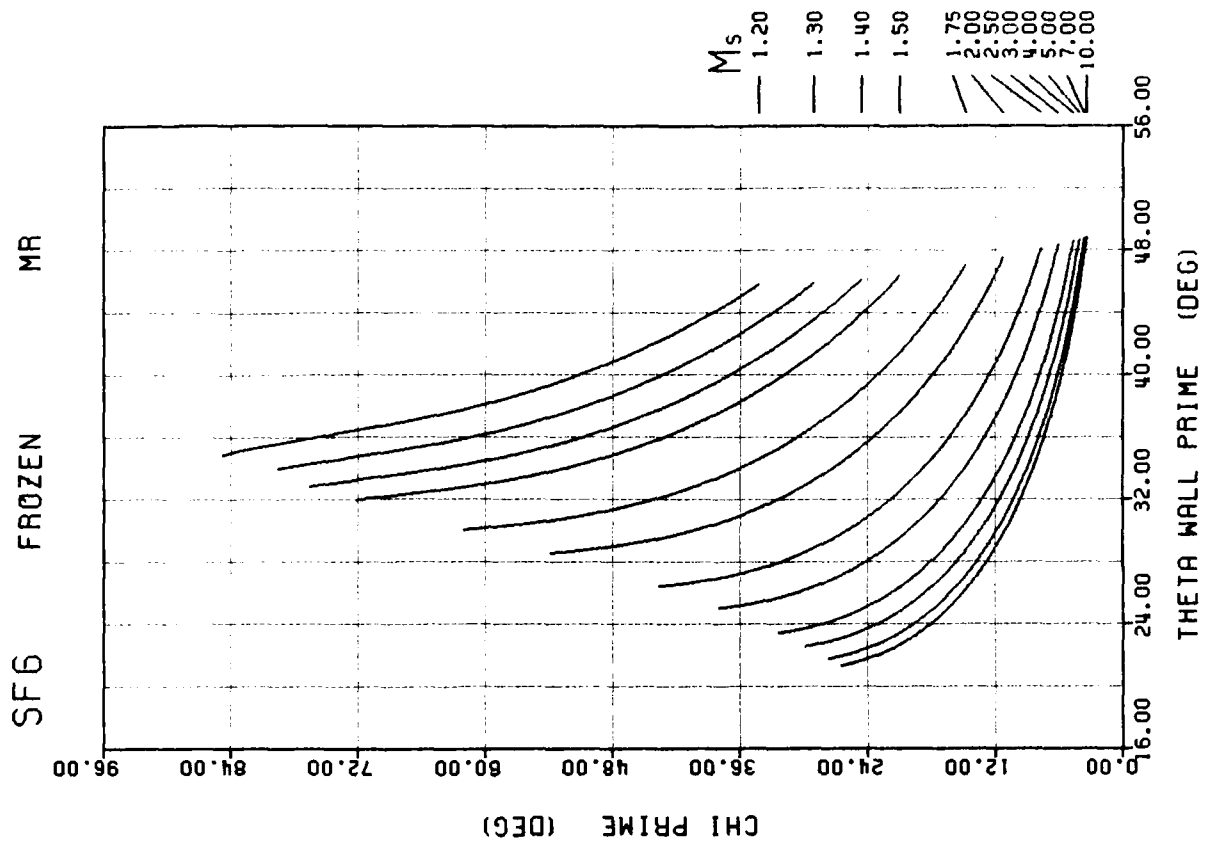
SF6 FROZEN MR

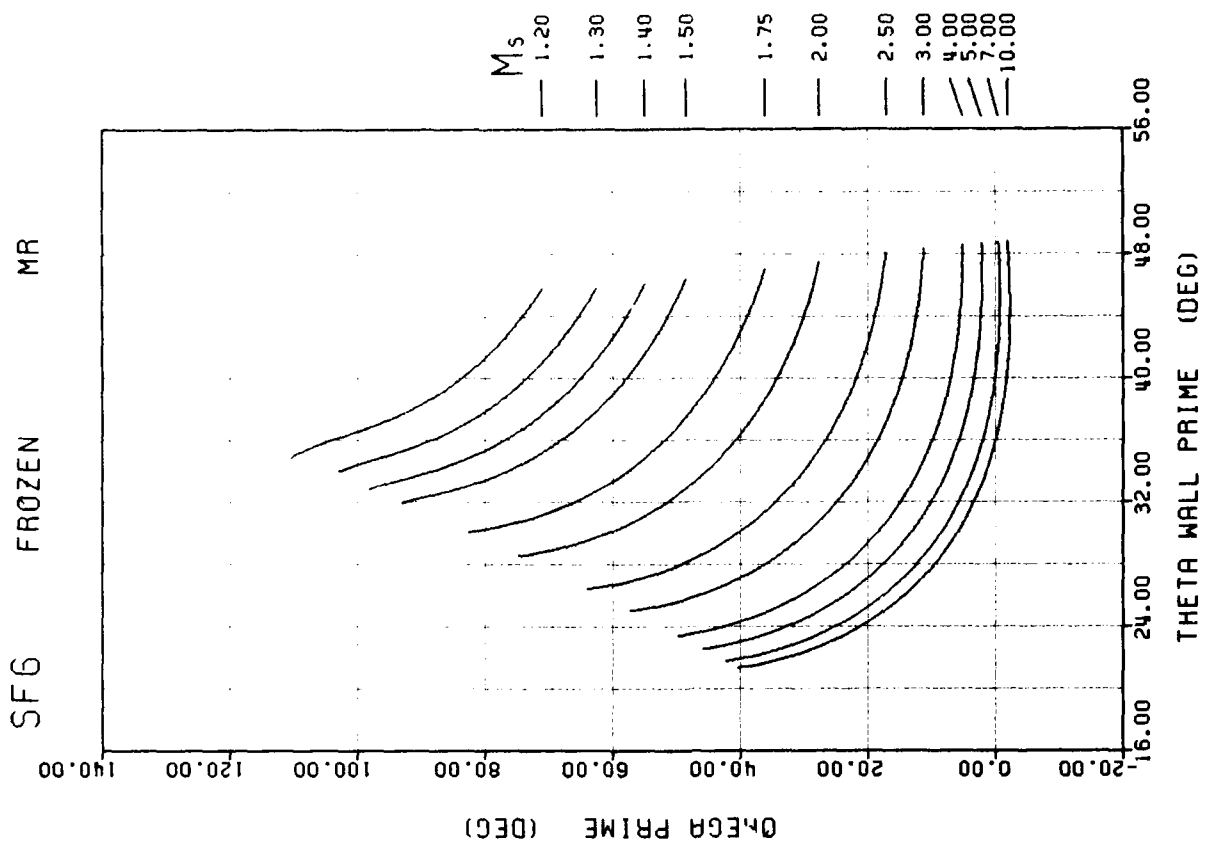
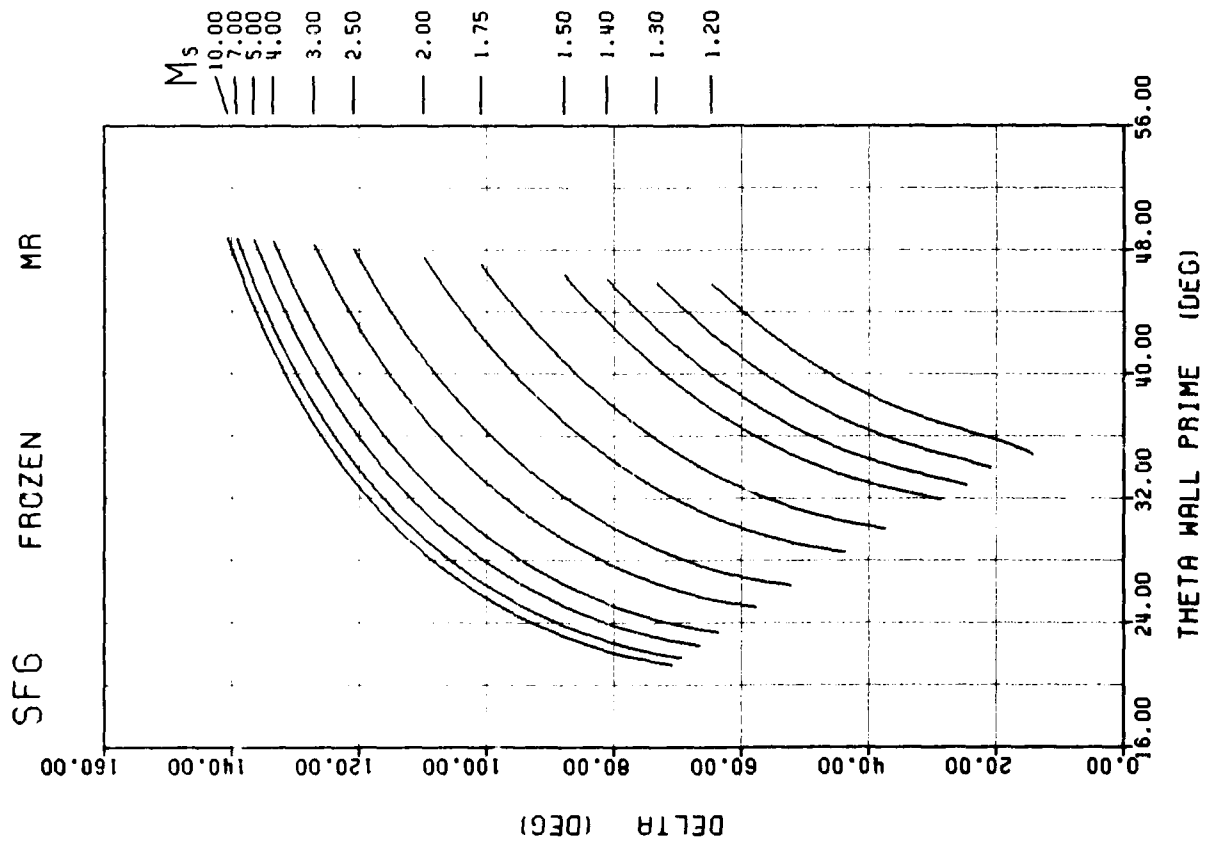


SF6 FROZEN MR



- M_s
- 2.00
 - 2.50
 - 1.75
 - 3.00
 - 4.00
 - 1.50
 - 5.00
 - 7.00
 - 10.00
 - 1.40
 - 1.30
 - 1.20





AD-A164 047

TABULAR AND GRAPHICAL SOLUTIONS OF REGULAR AND MACH
REFLECTIONS IN PSEUDO-. (U) TORONTO UNIV DONMSVIEH
(ONTARIO) INST FOR AEROSPACE STUDIES T C HU ET AL.

2/3

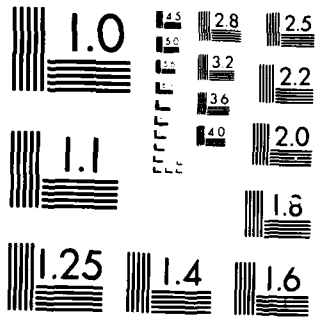
UNCLASSIFIED

JUN 85 UTIAS-283-PT-2 AFOSR-TR-85-1231

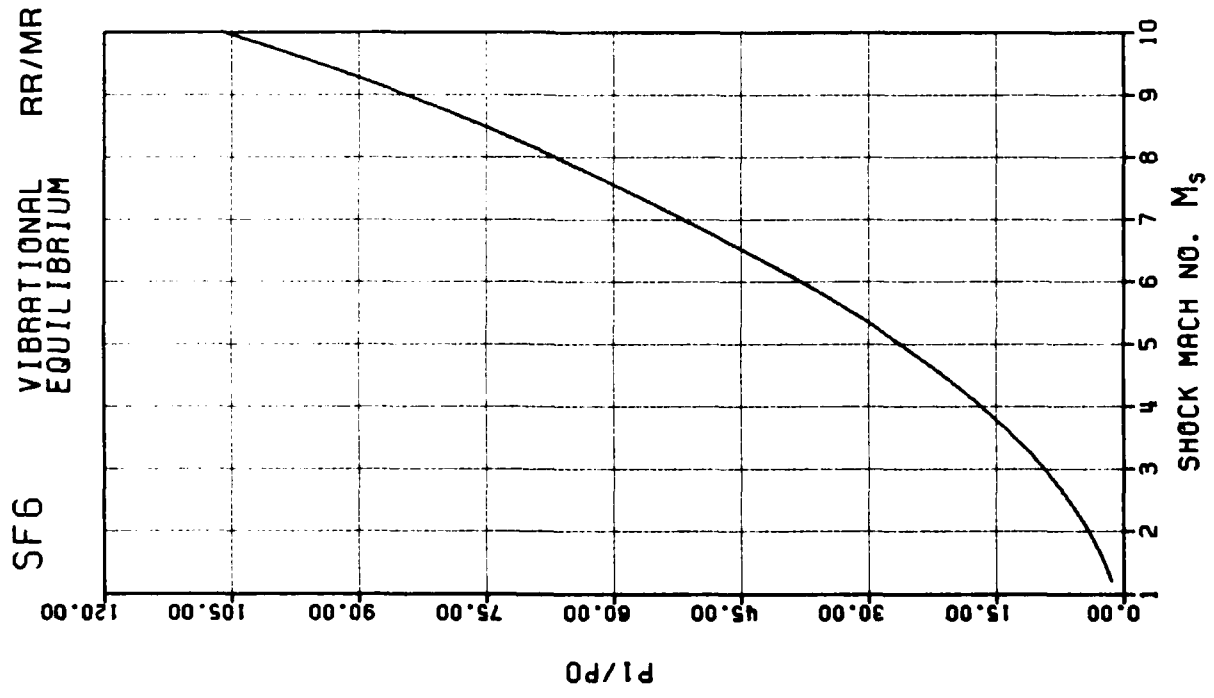
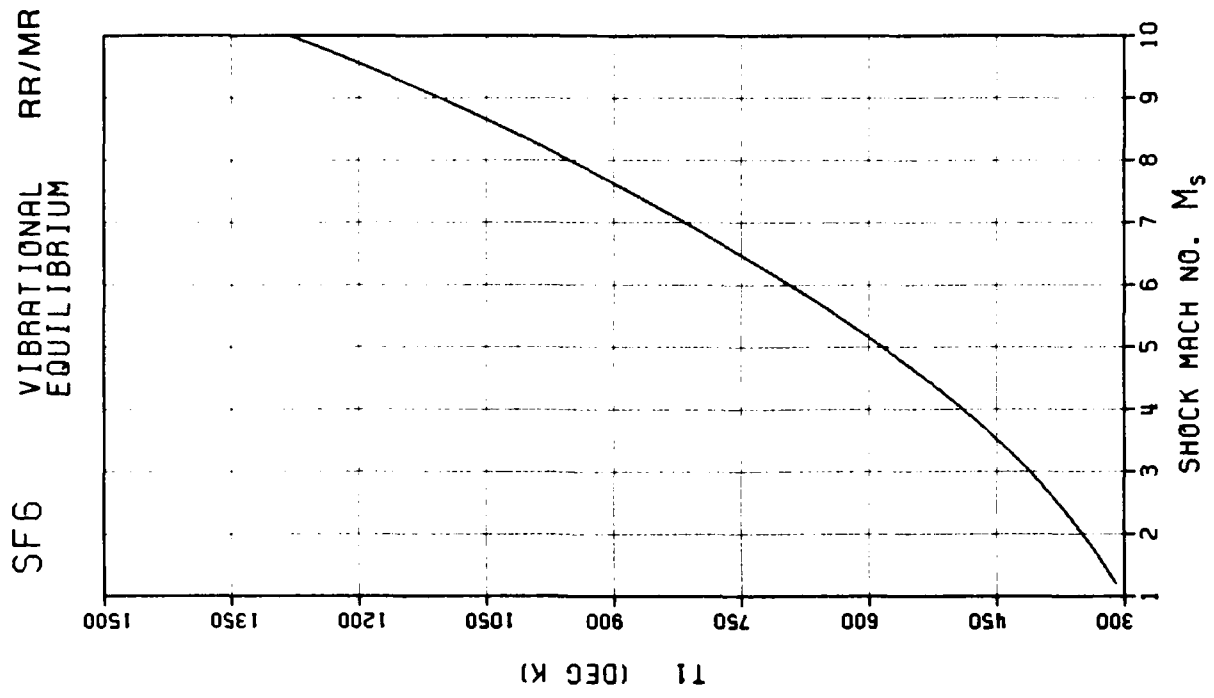
F/G 28/4

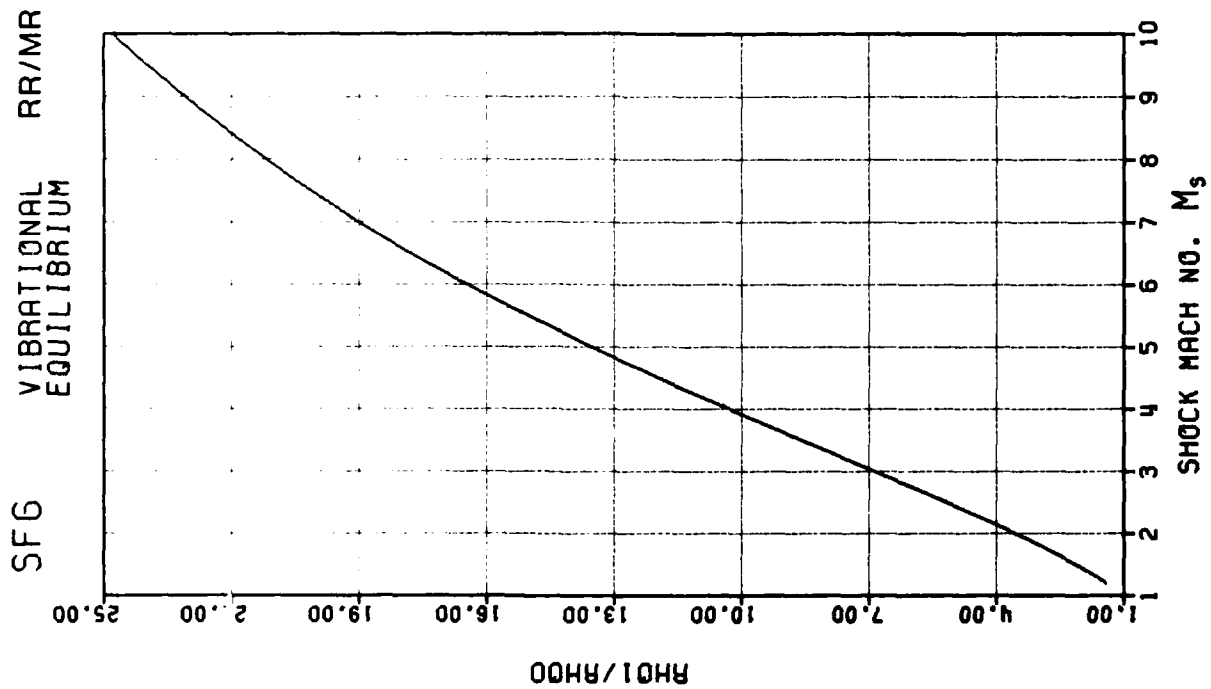
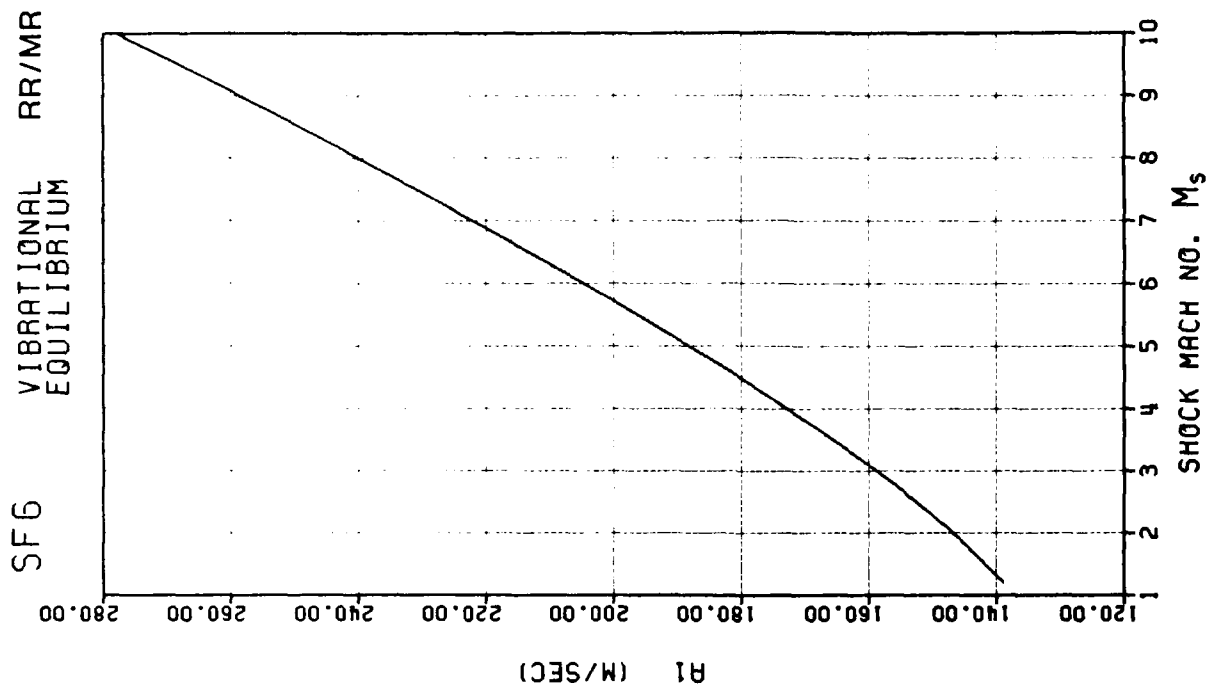
ML

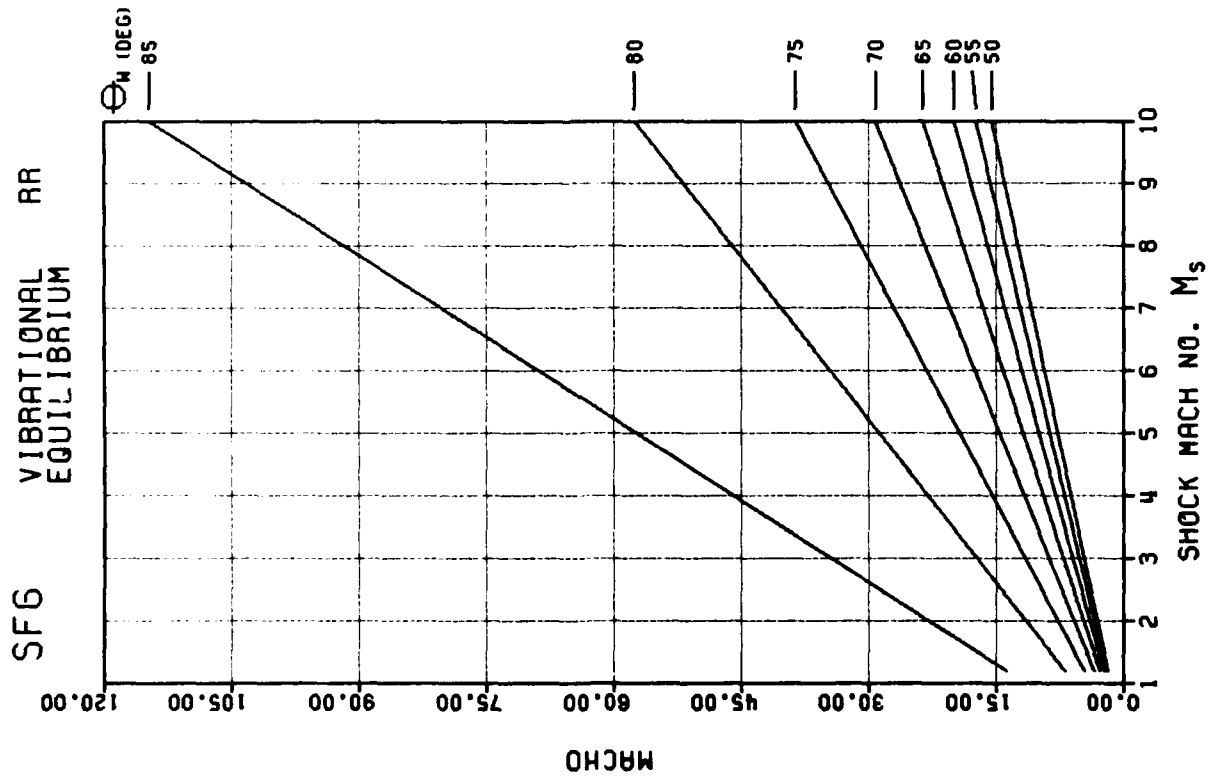
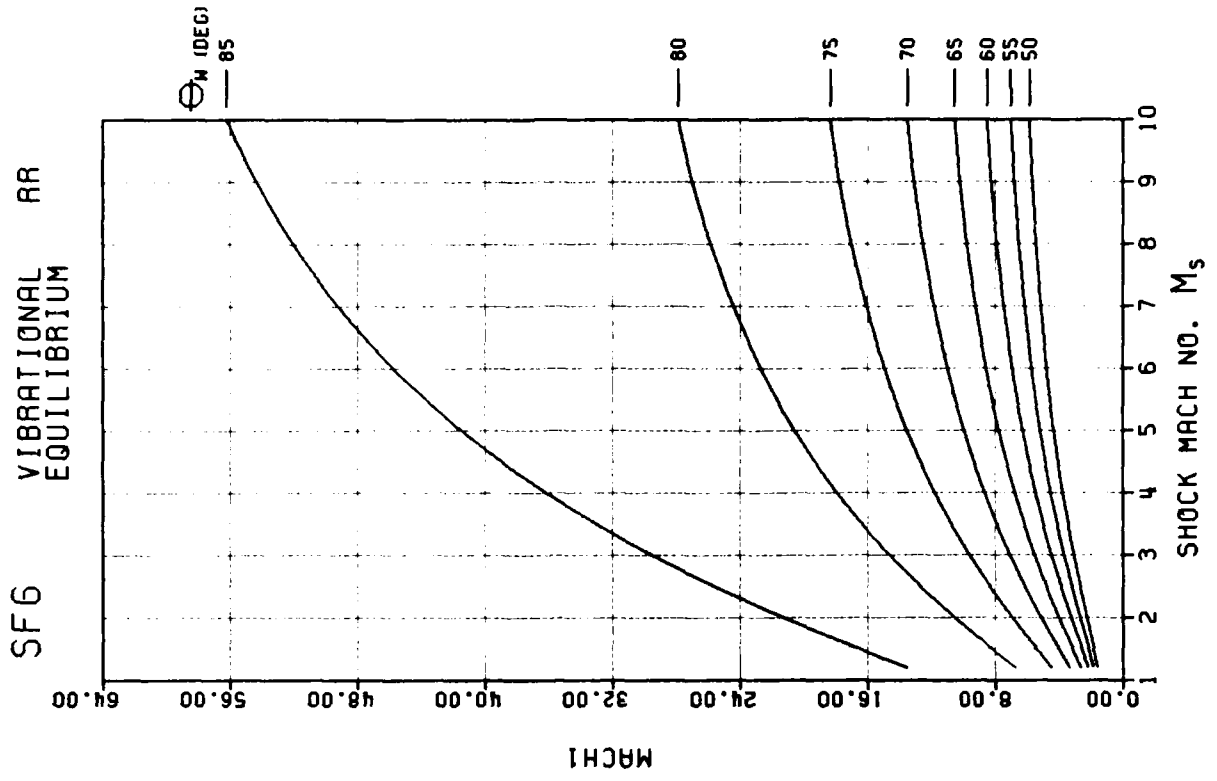
The table consists of 10 columns and 10 rows. The top row contains 10 blacked-out cells. The remaining 9 rows each contain 10 blacked-out cells, forming a 9x10 grid of redacted data.

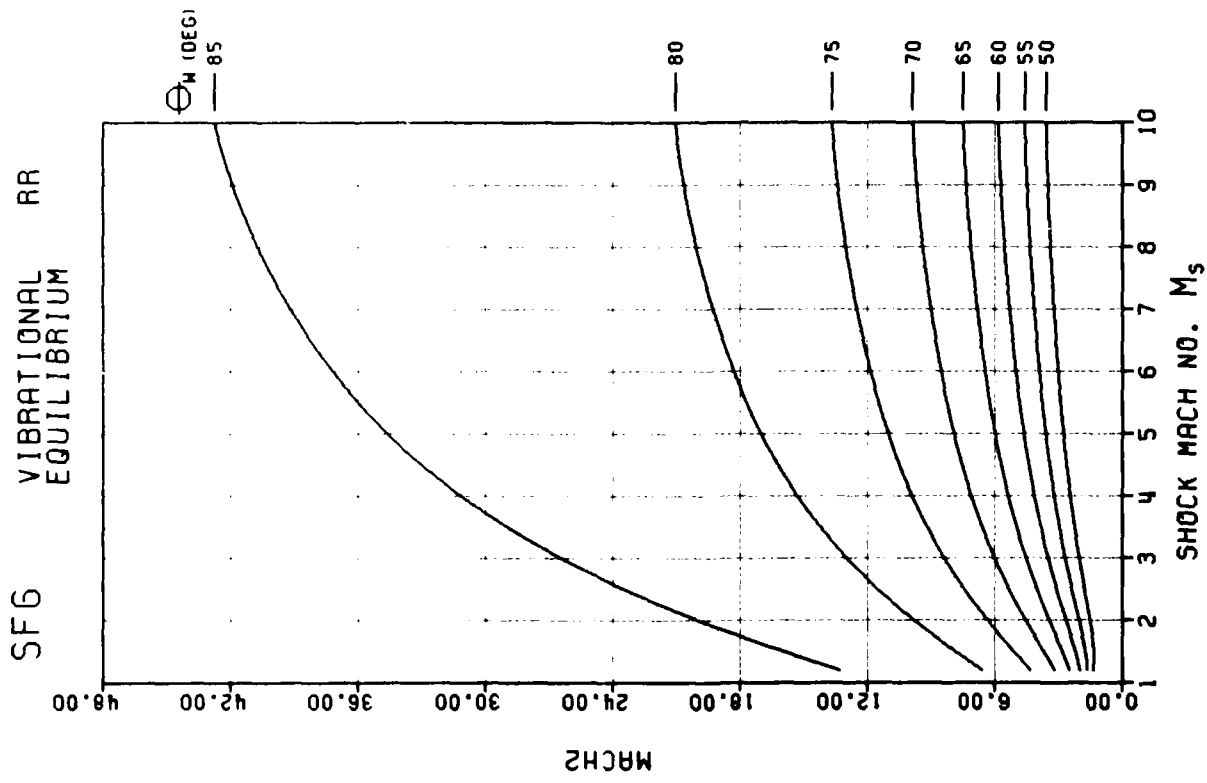
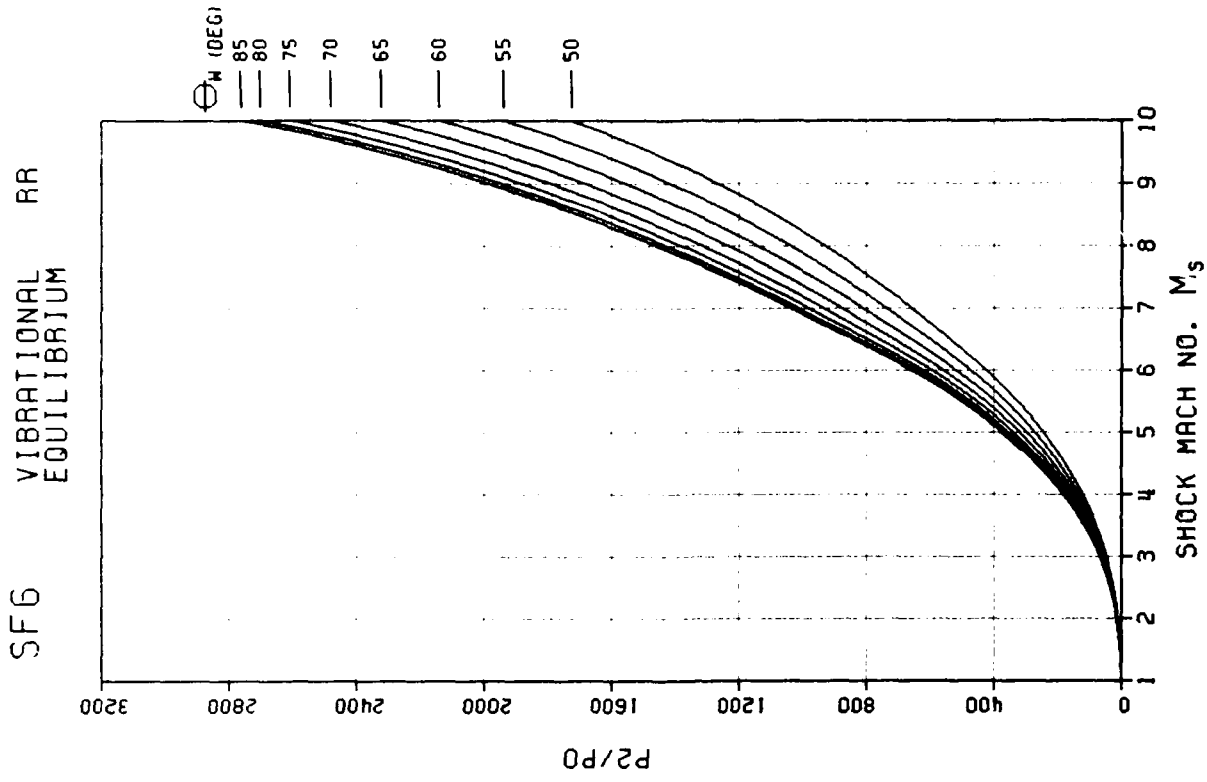


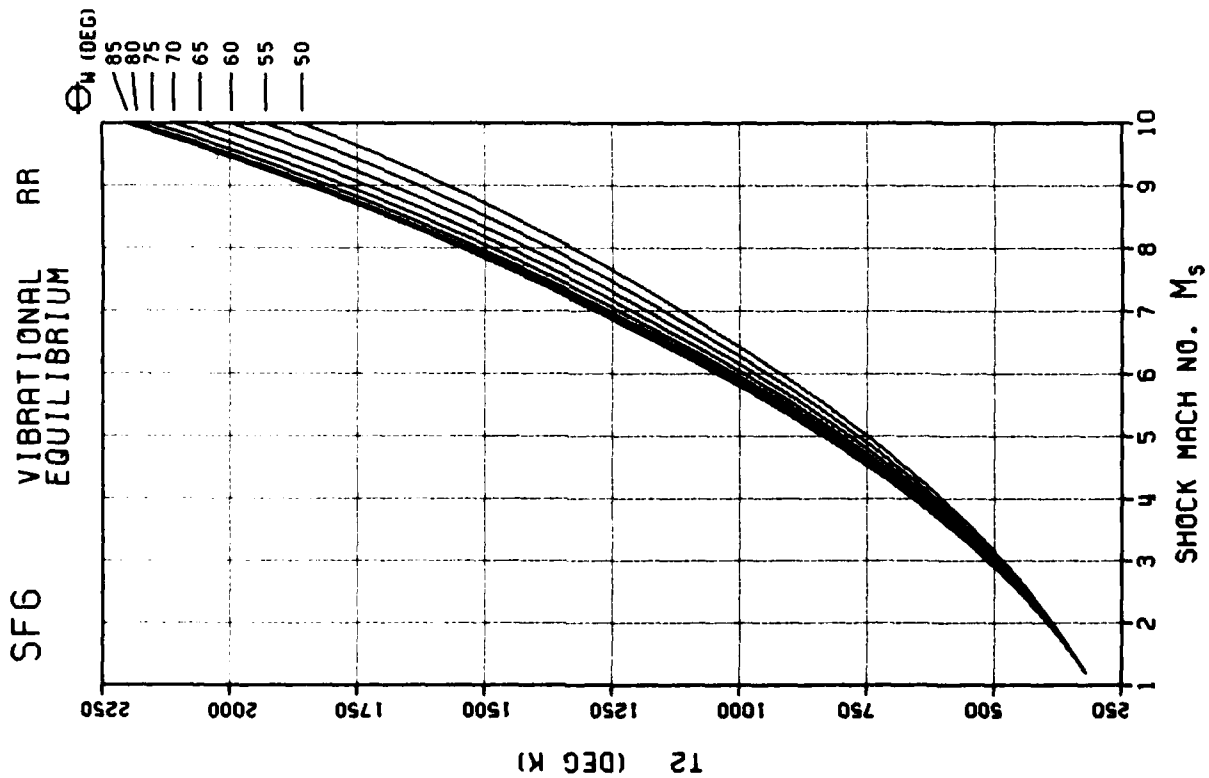
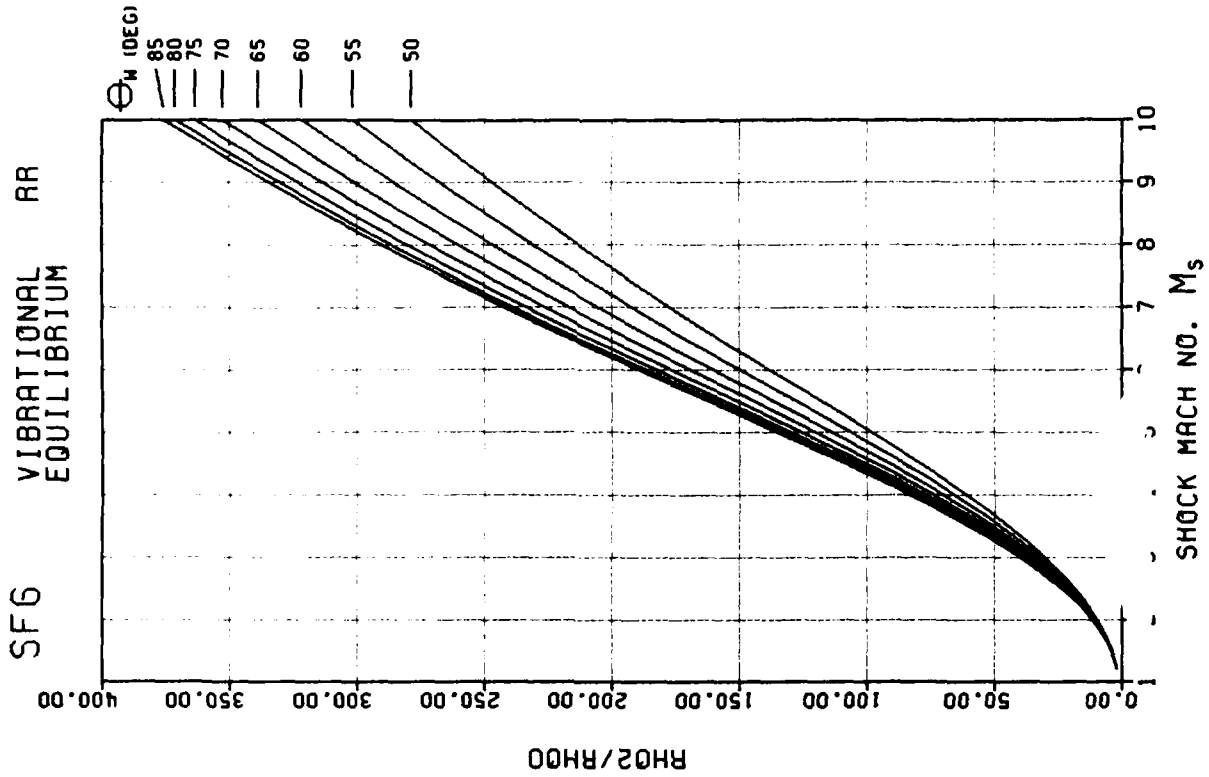
MICROCOPY RESOLUTION TEST CHART
NATIONAL BUREAU OF STANDARDS 1963-A

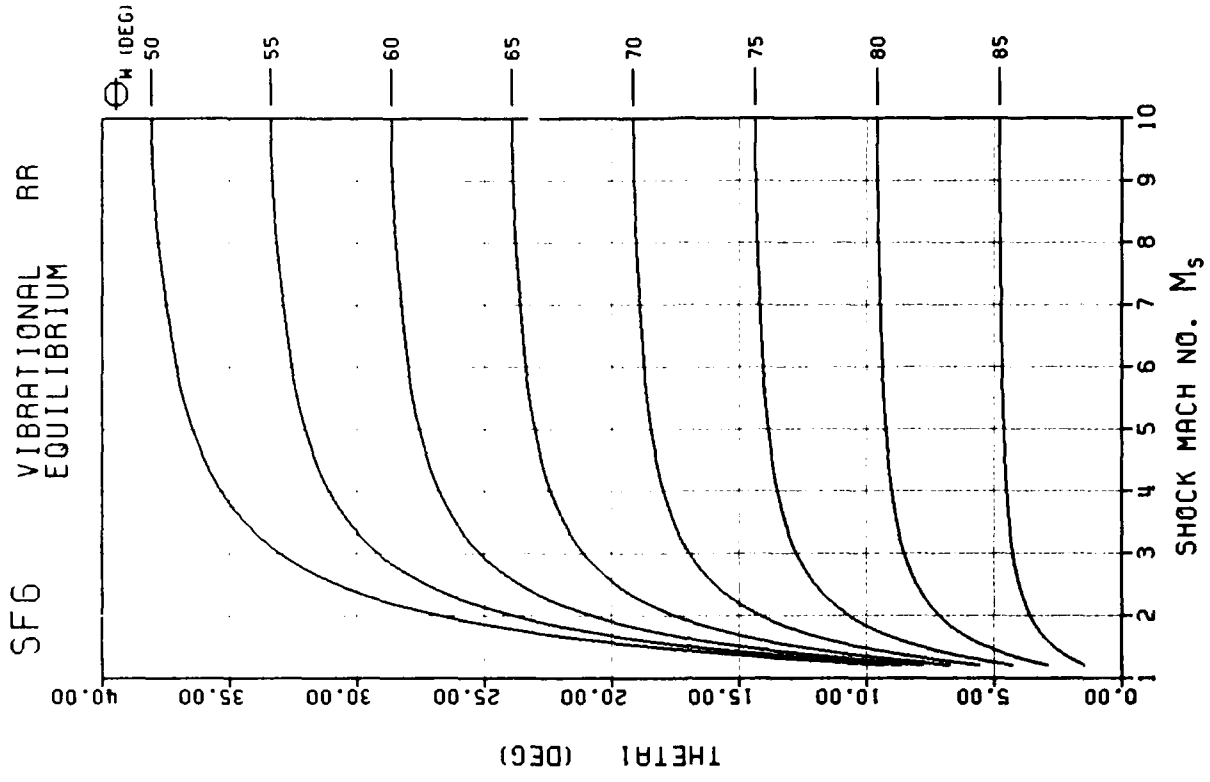
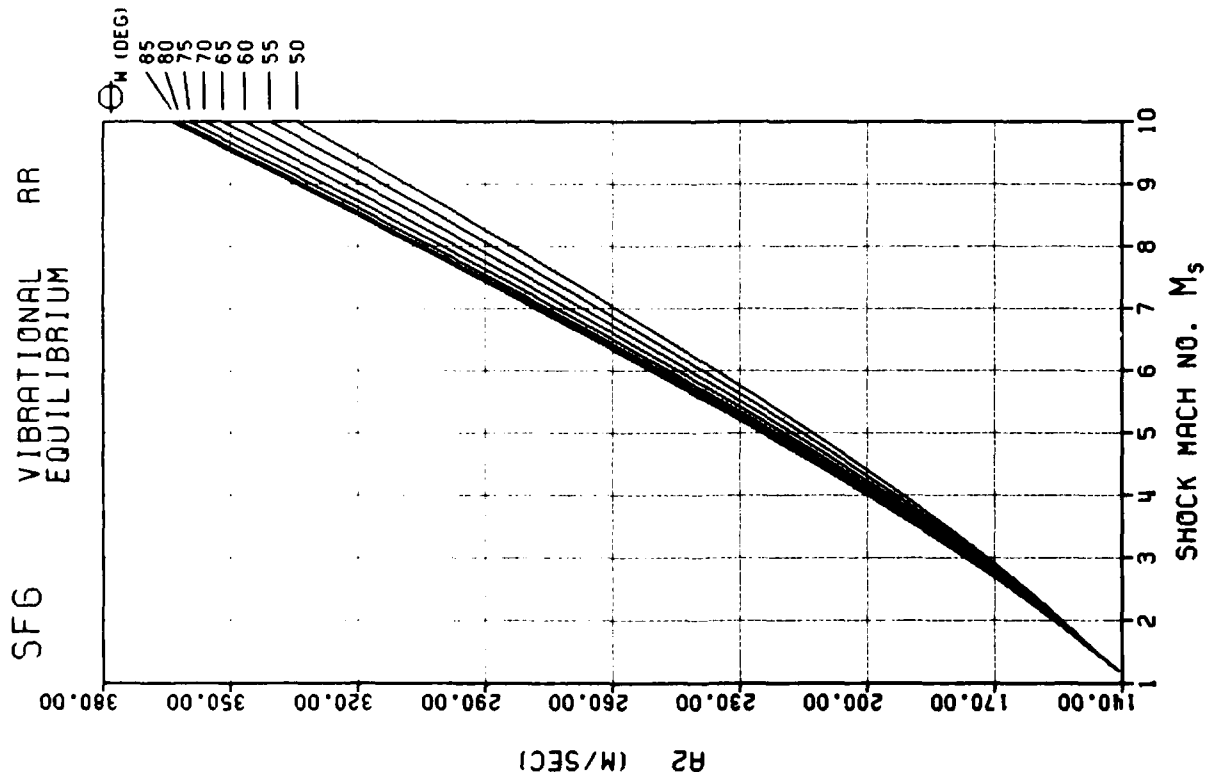


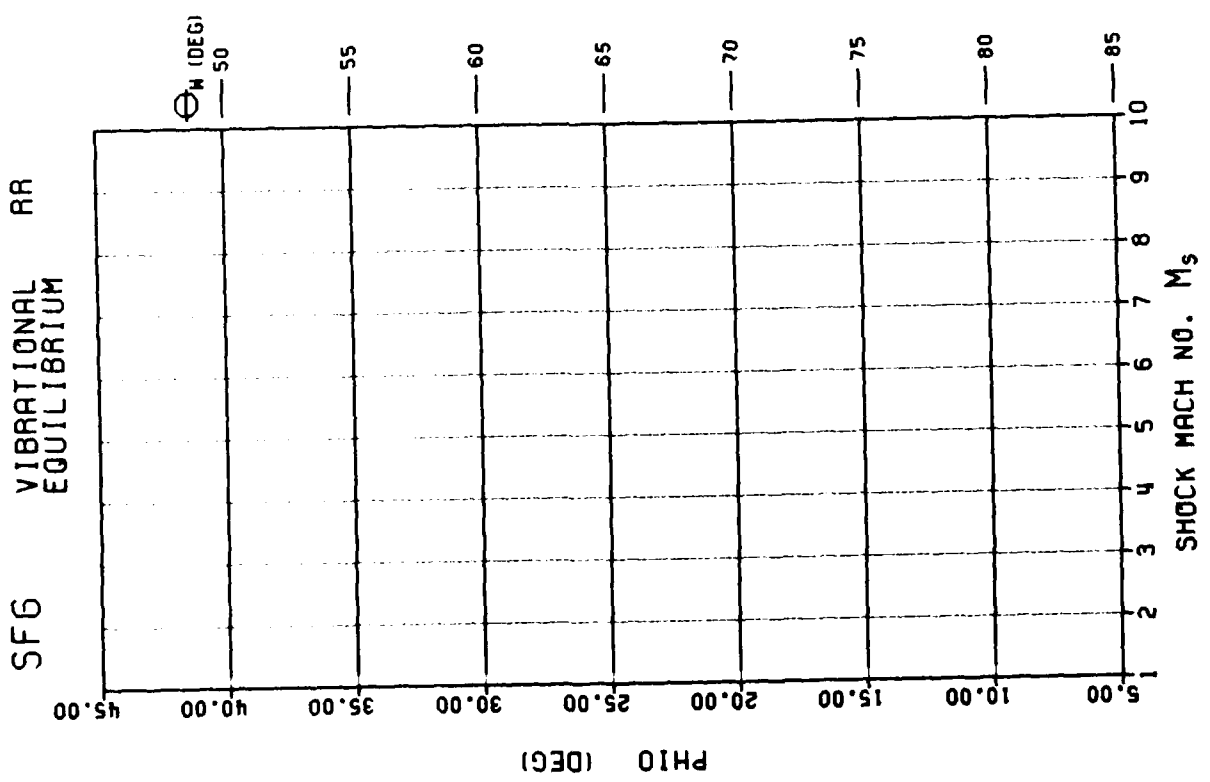
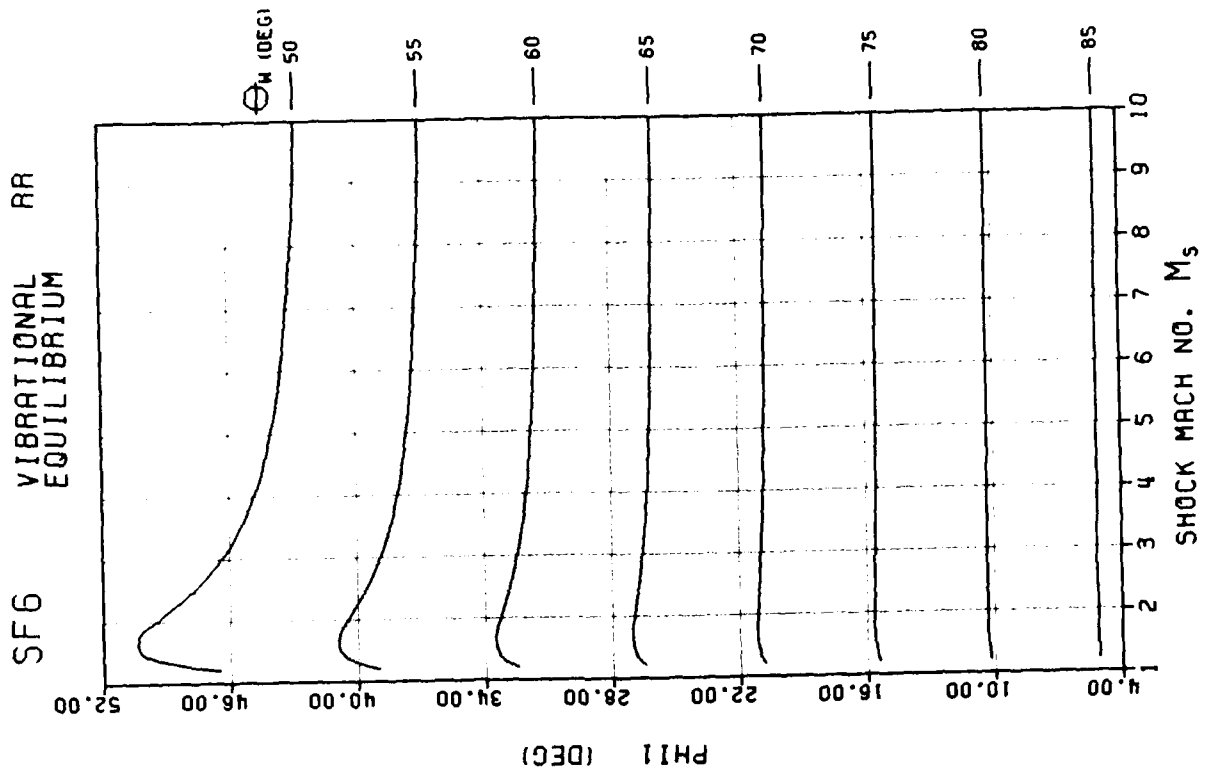


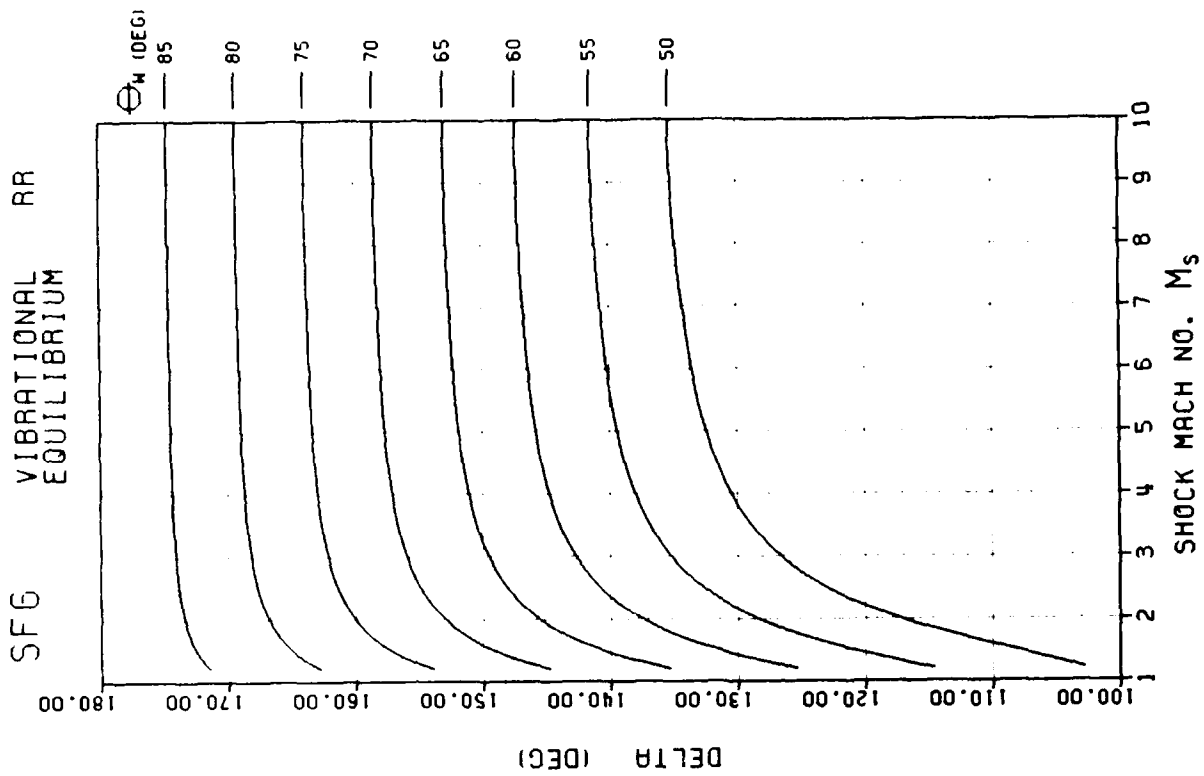
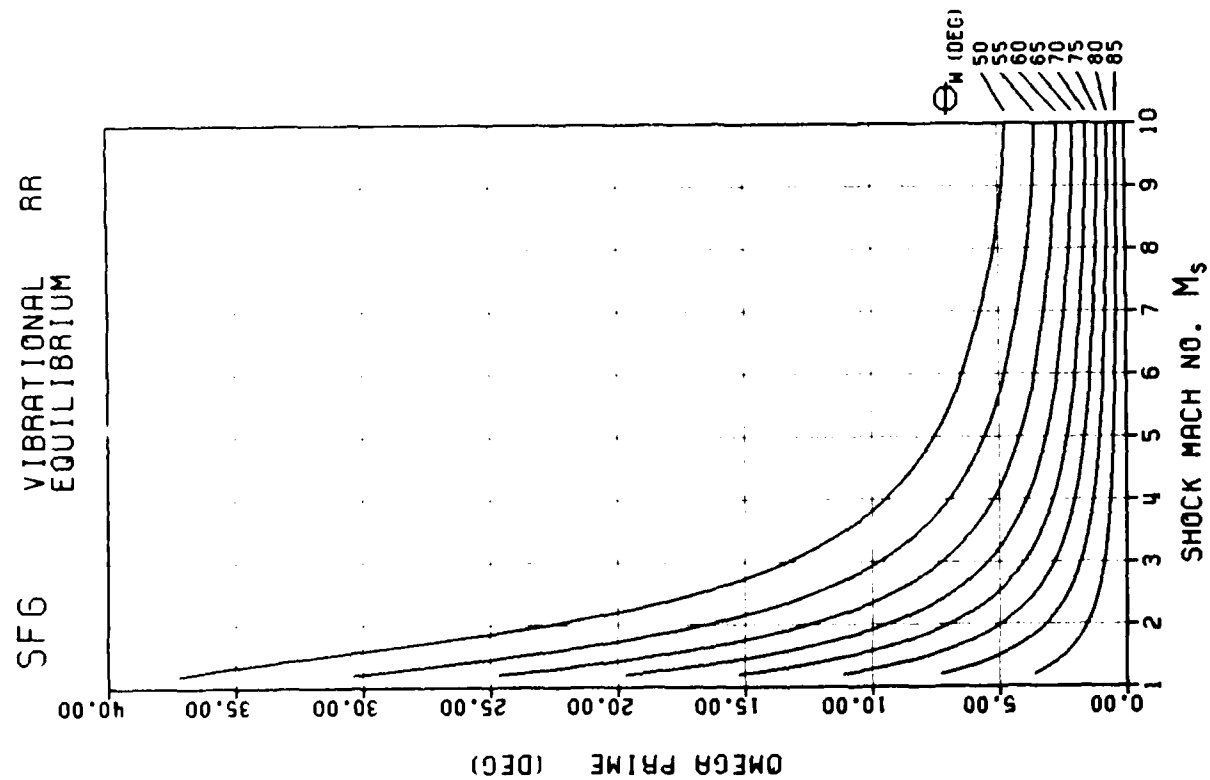


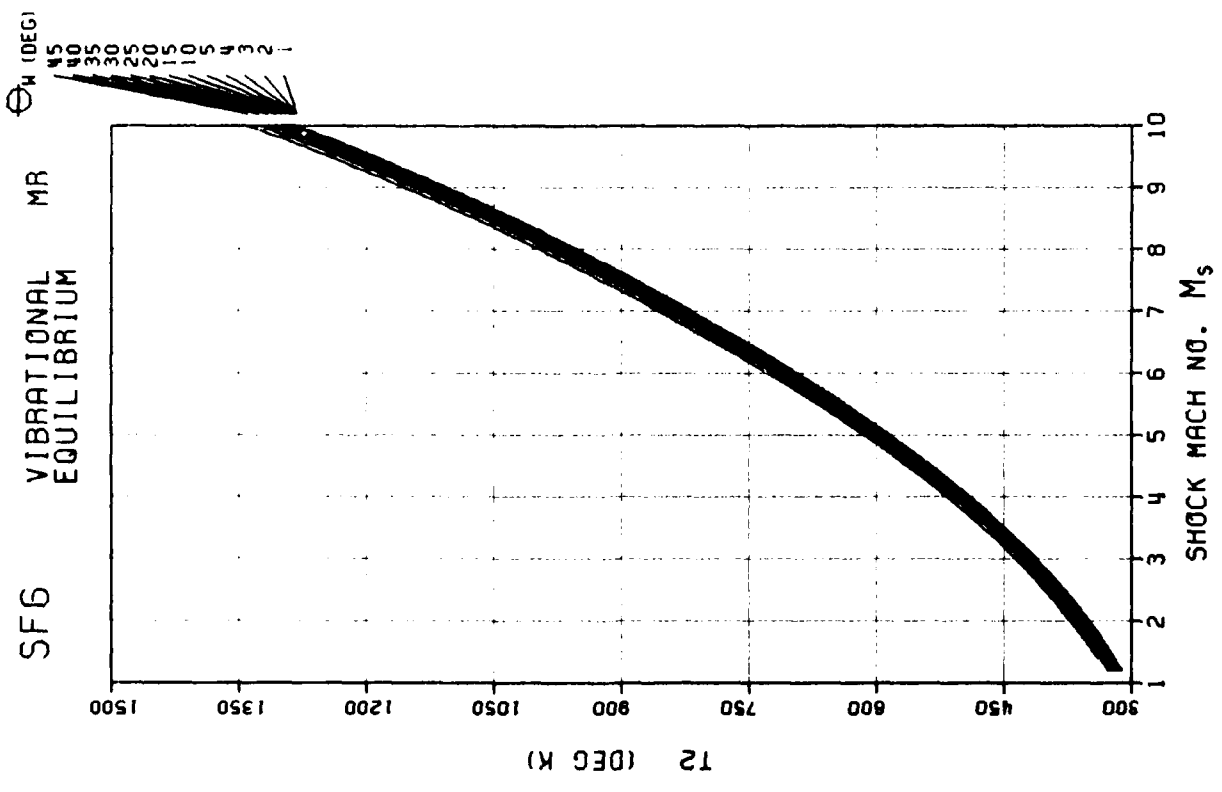
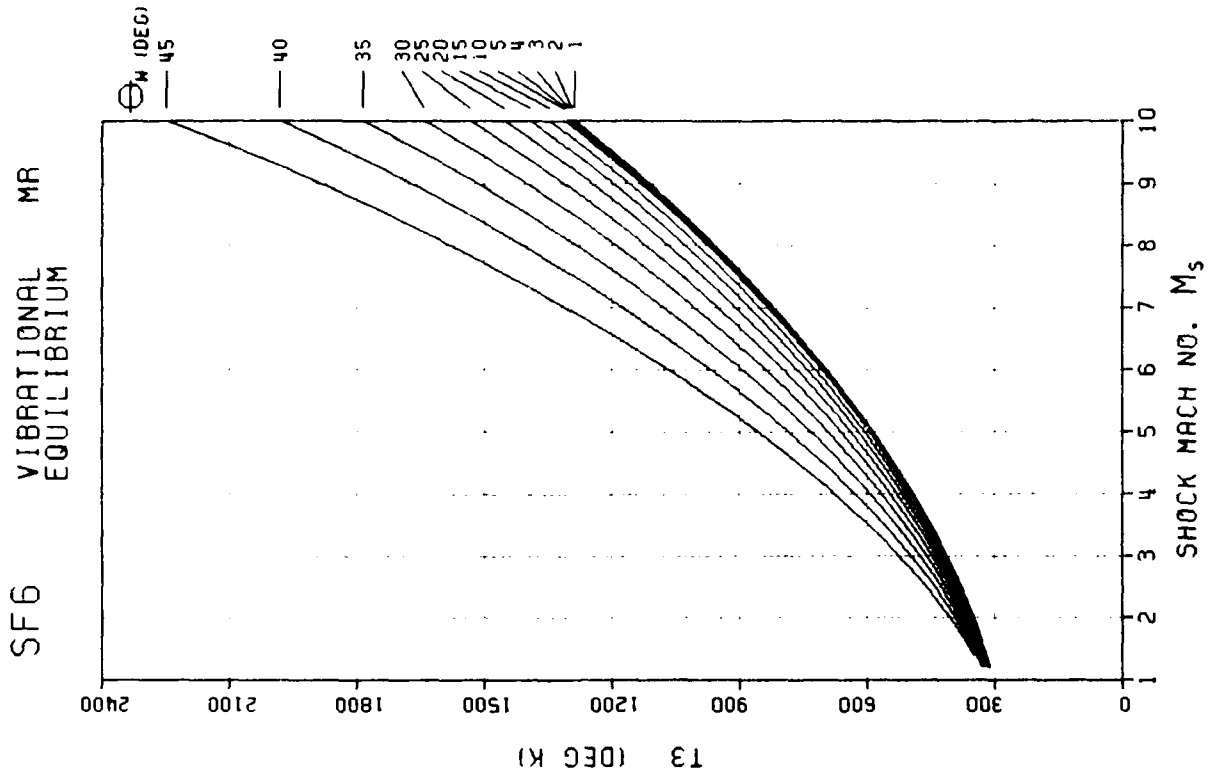


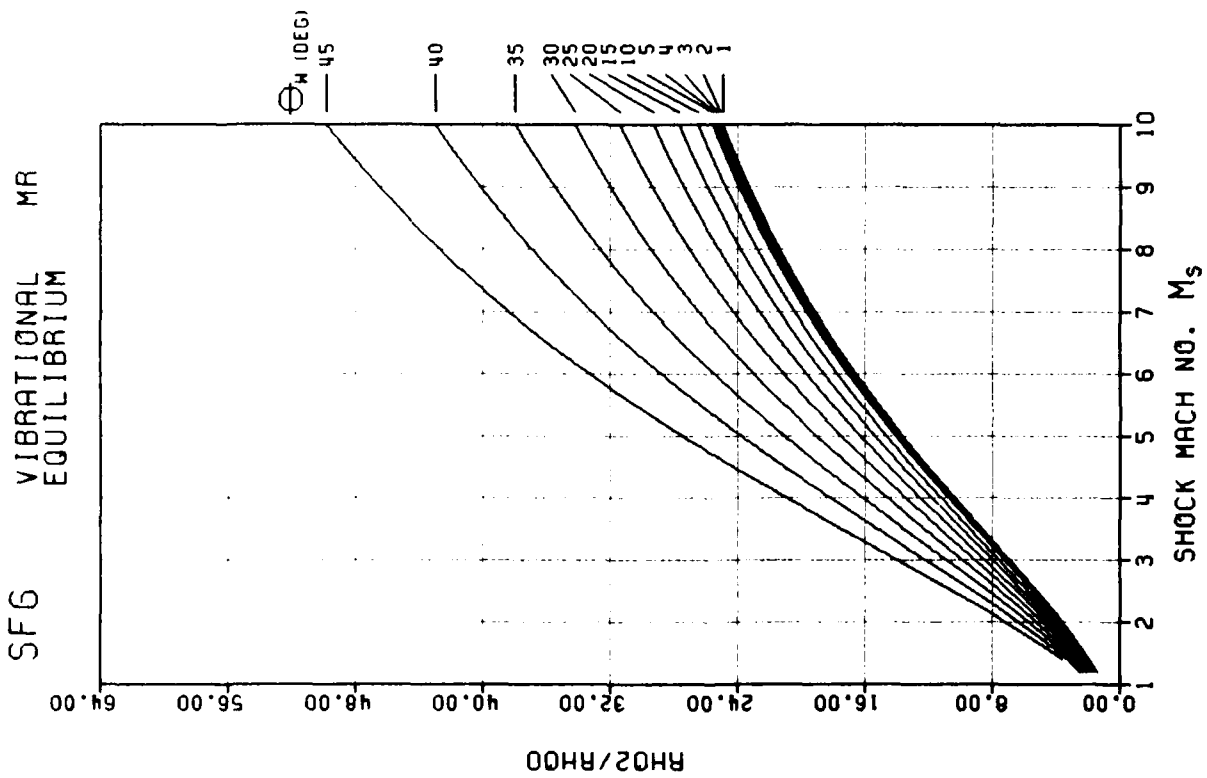
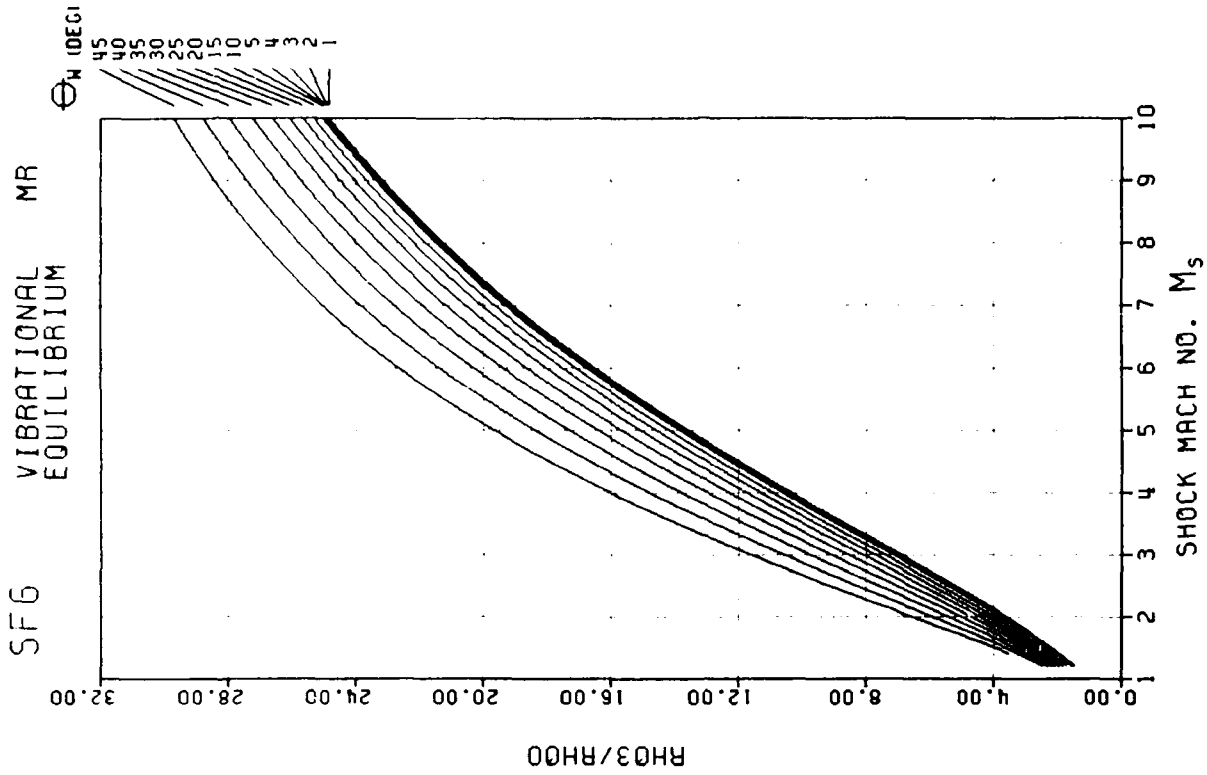




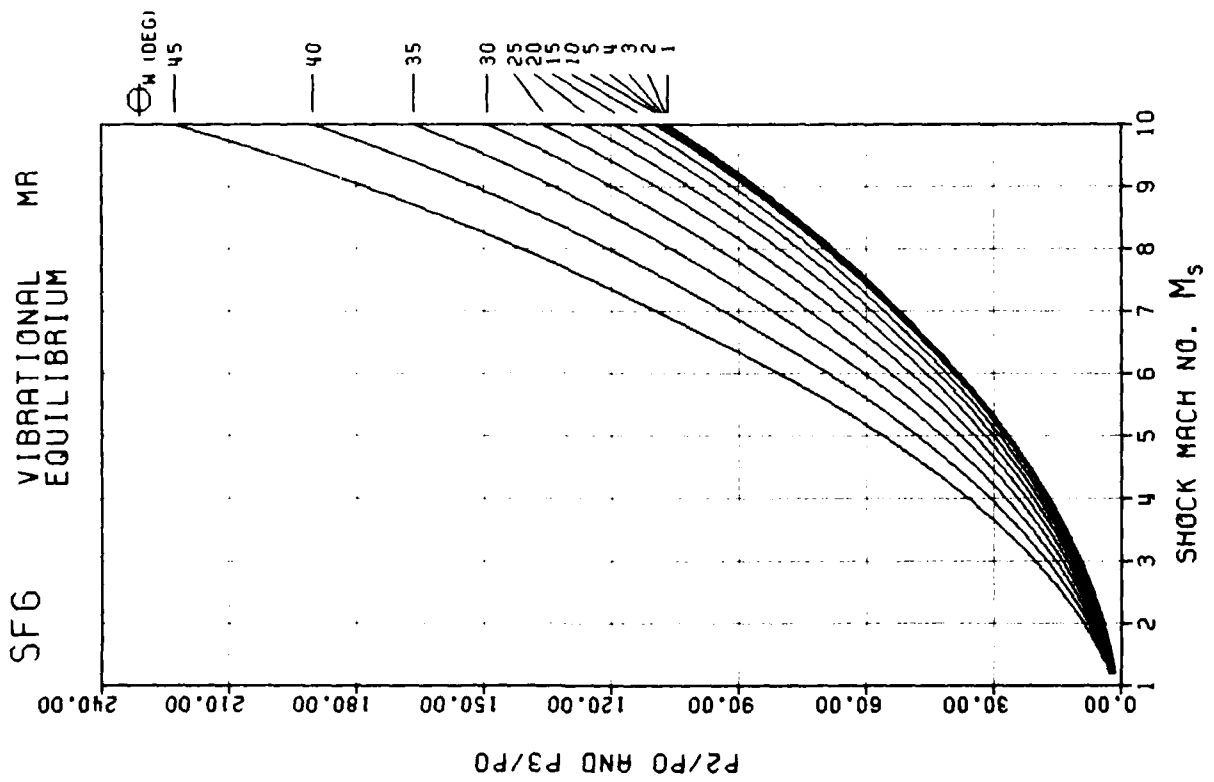
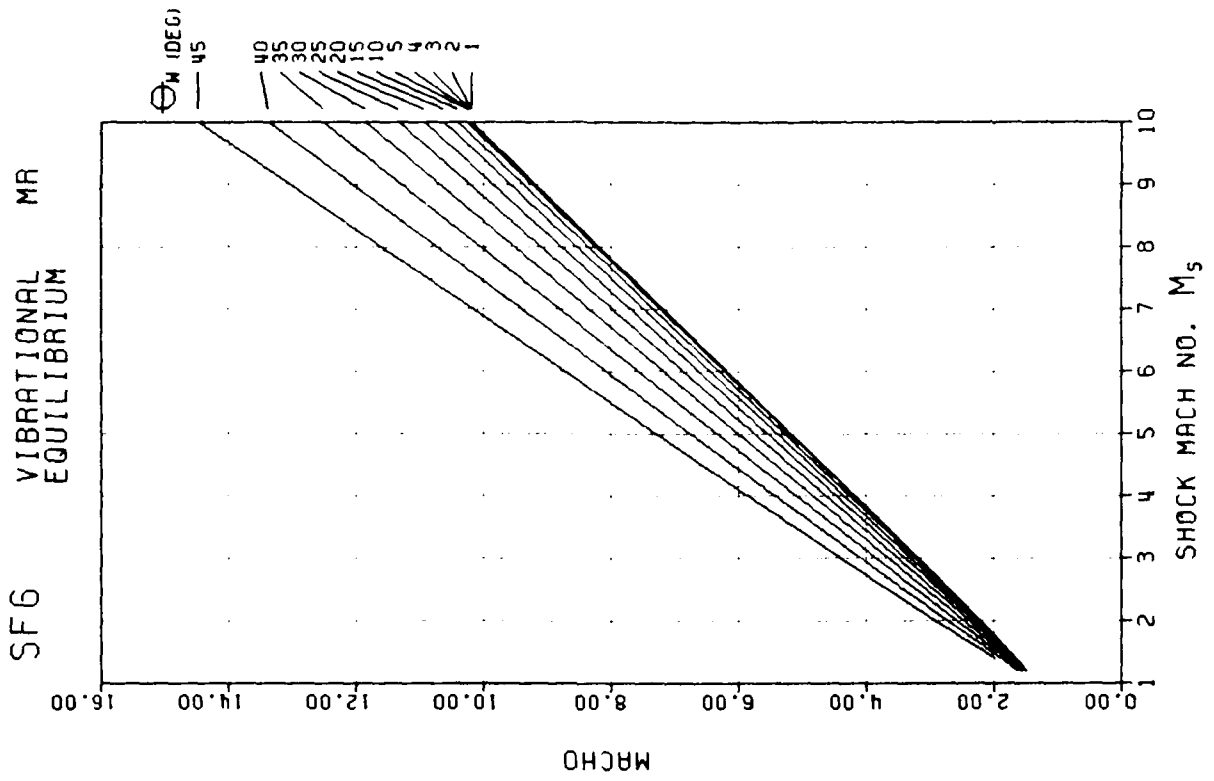


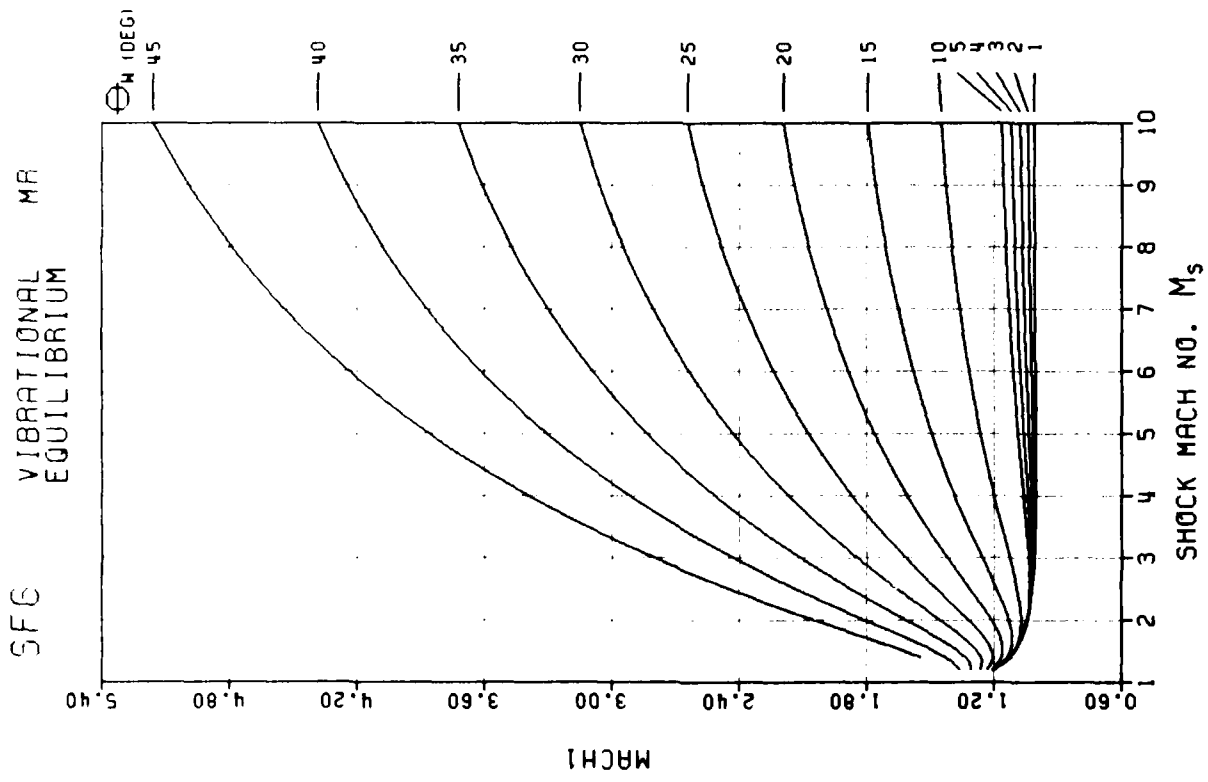
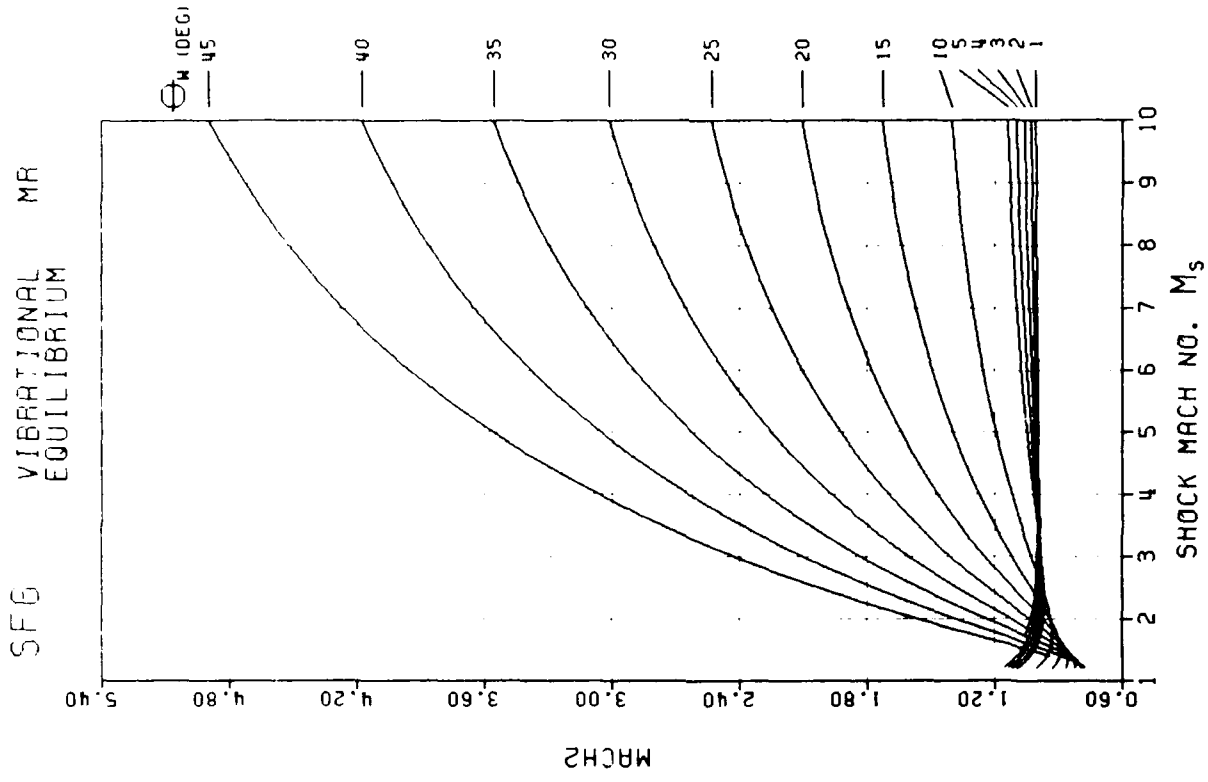


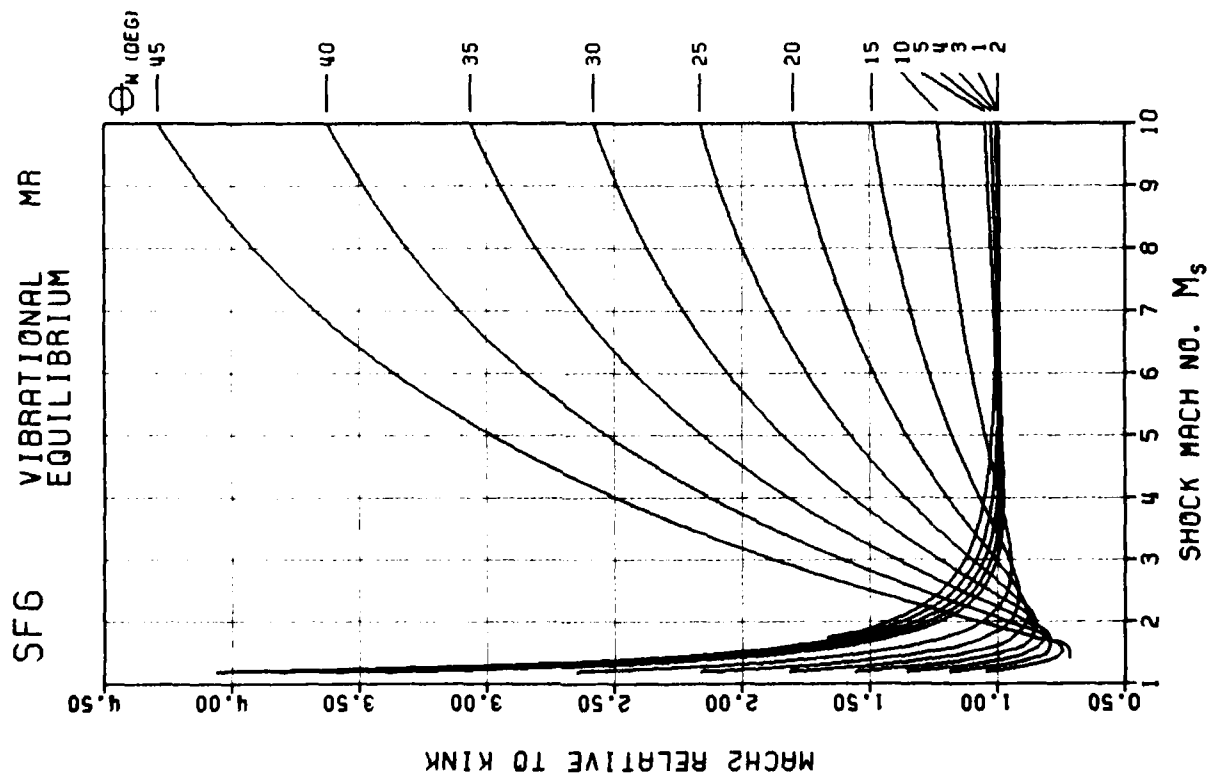
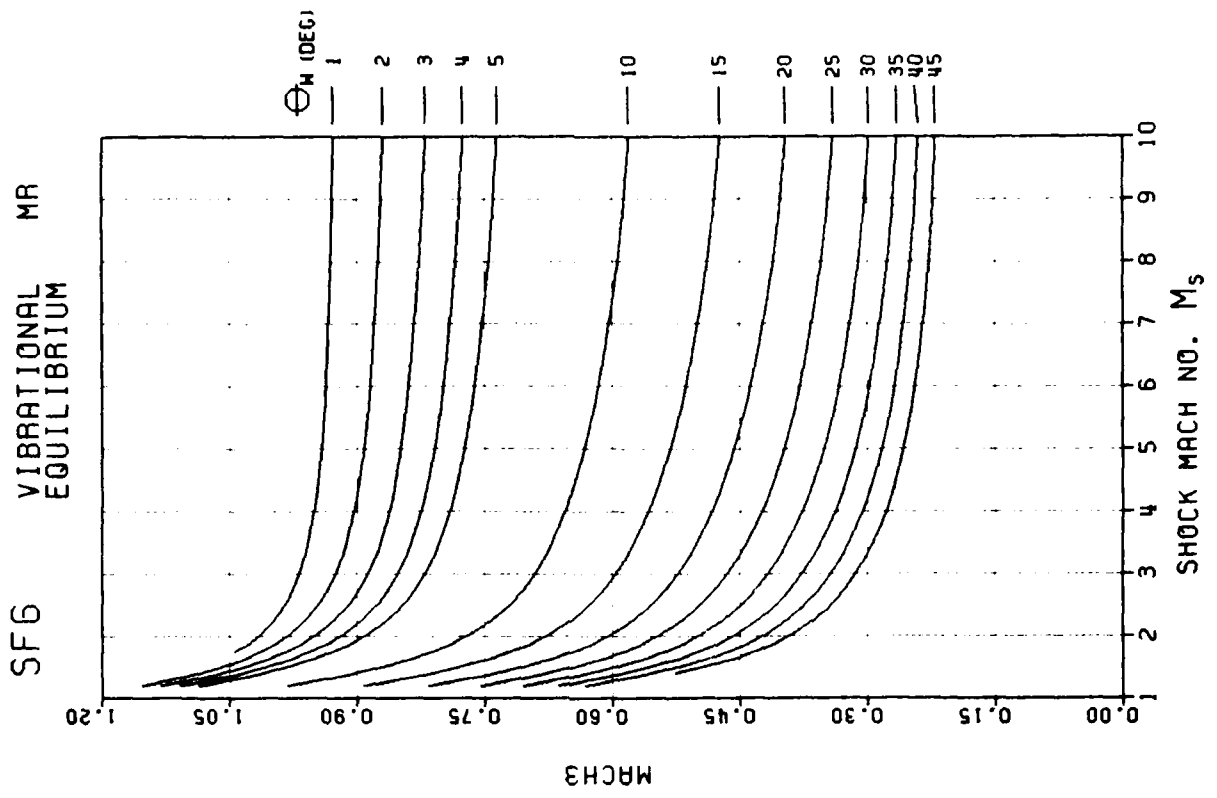


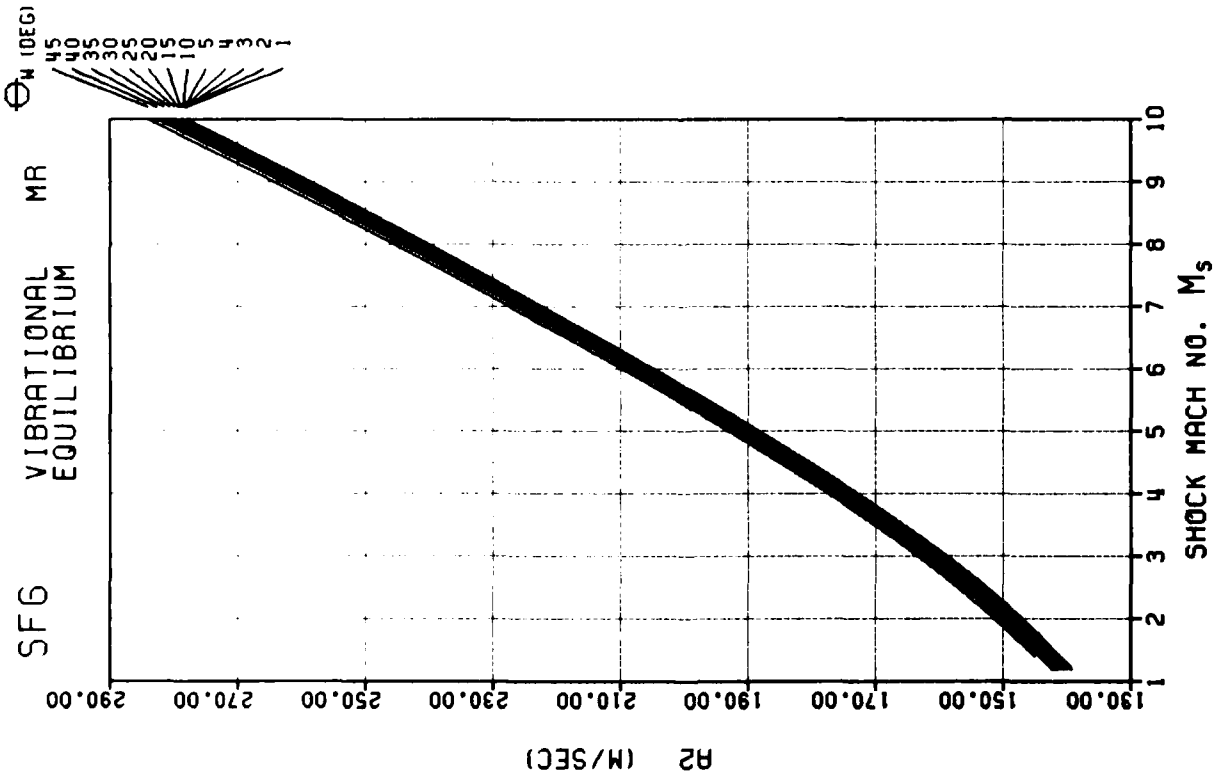
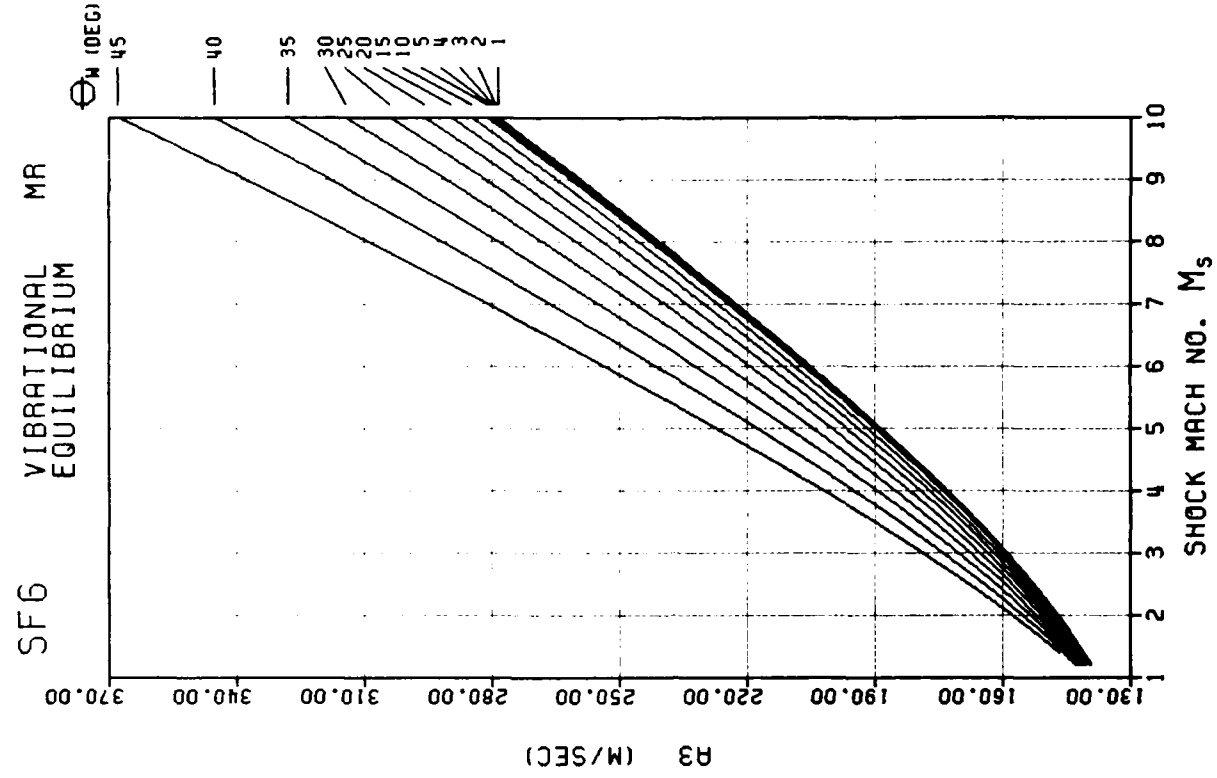


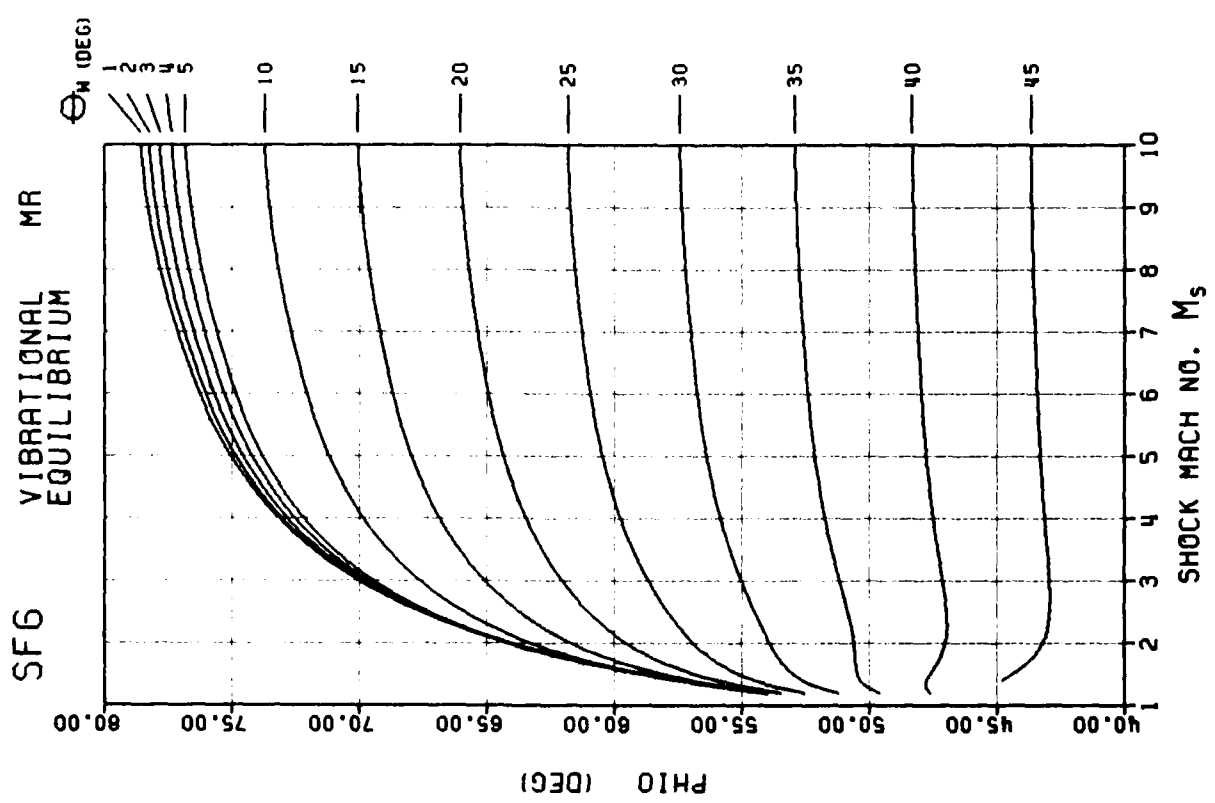
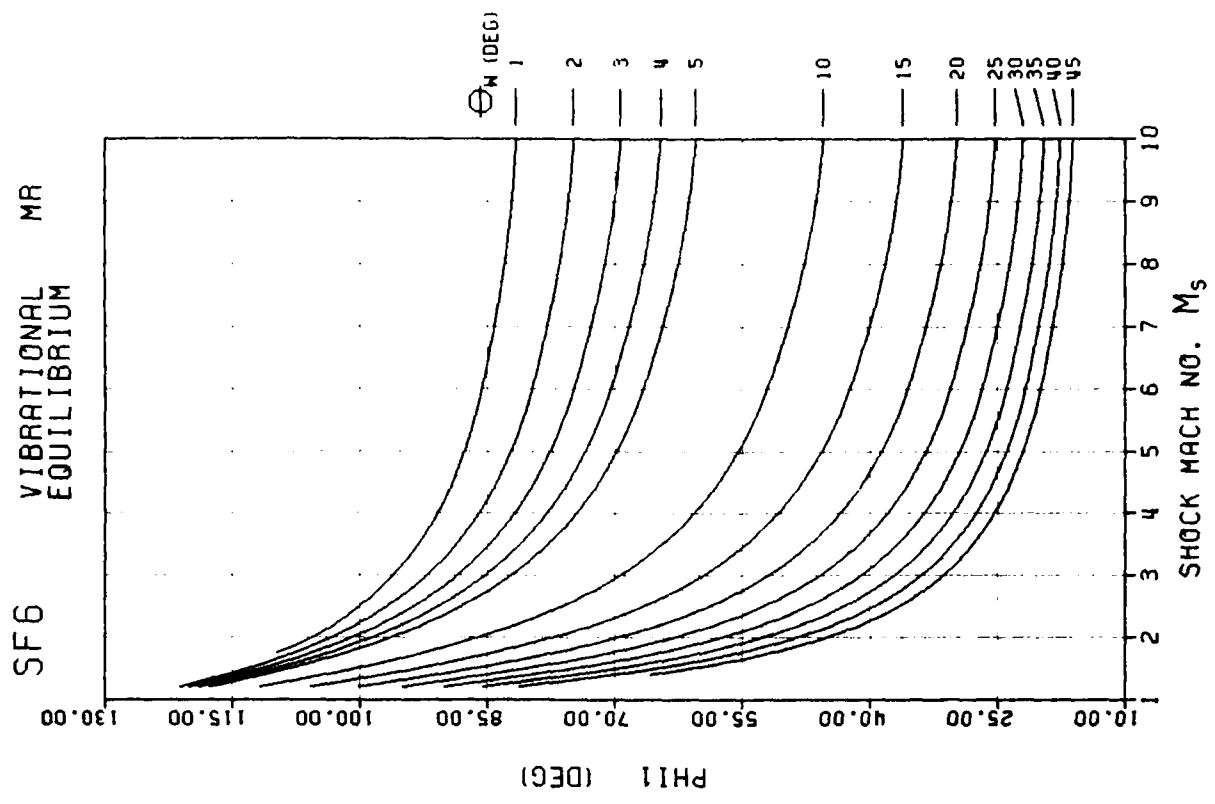
F - 220

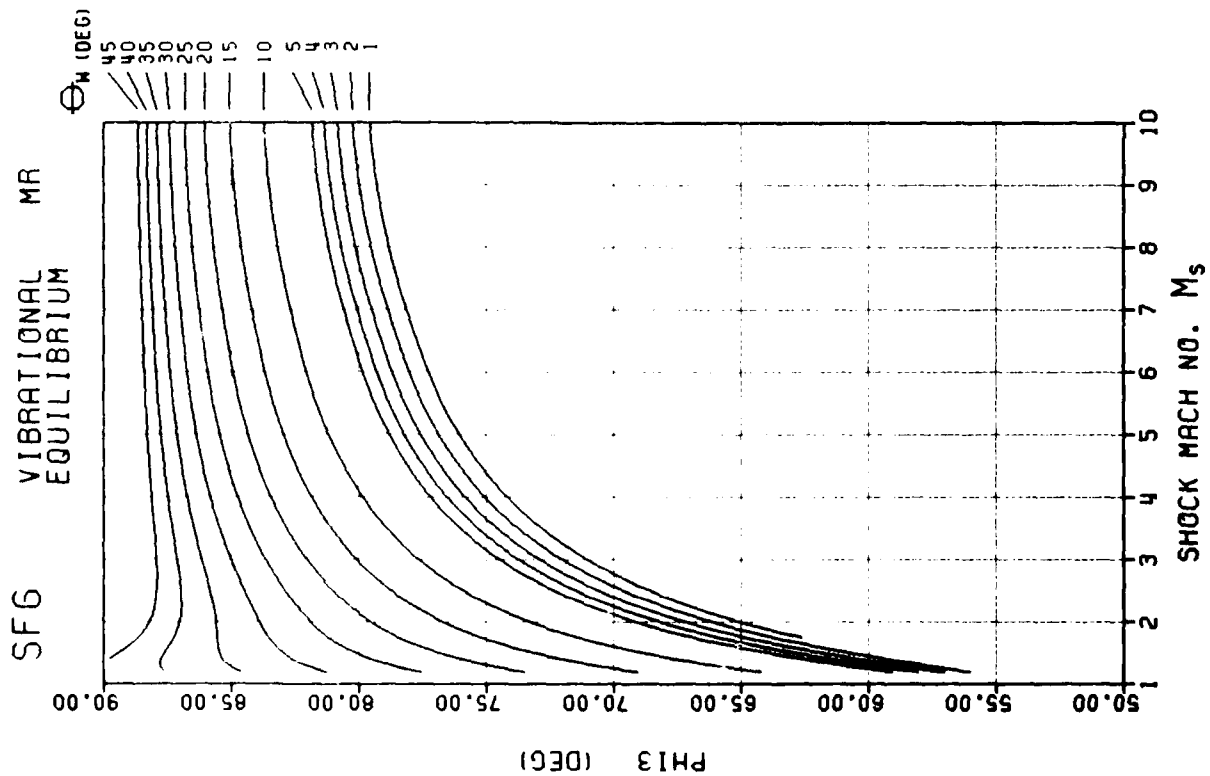
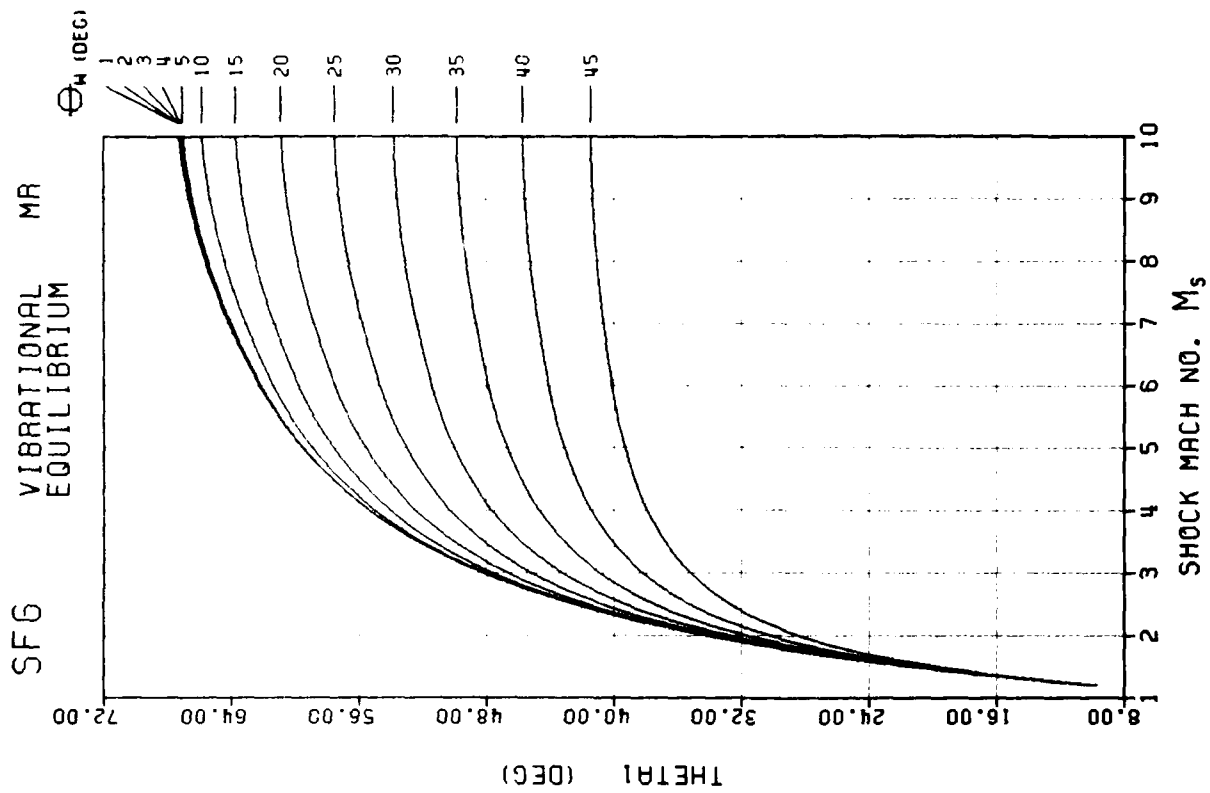


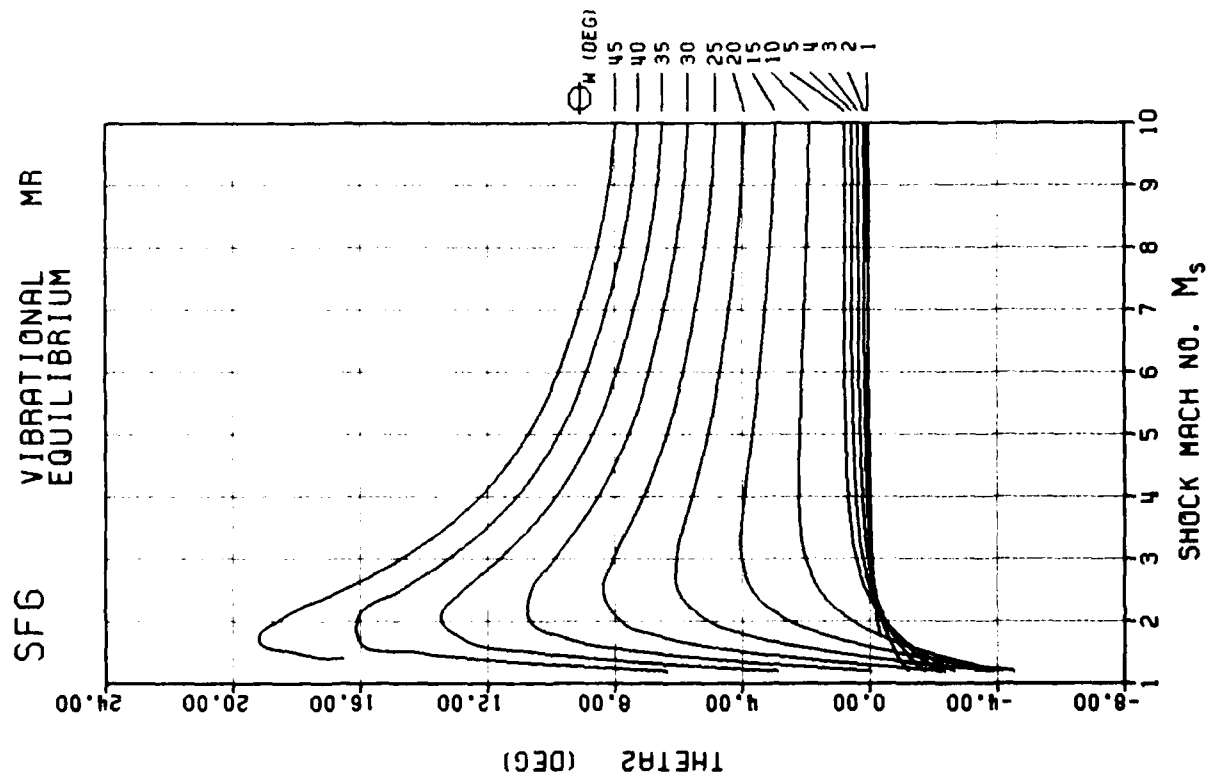
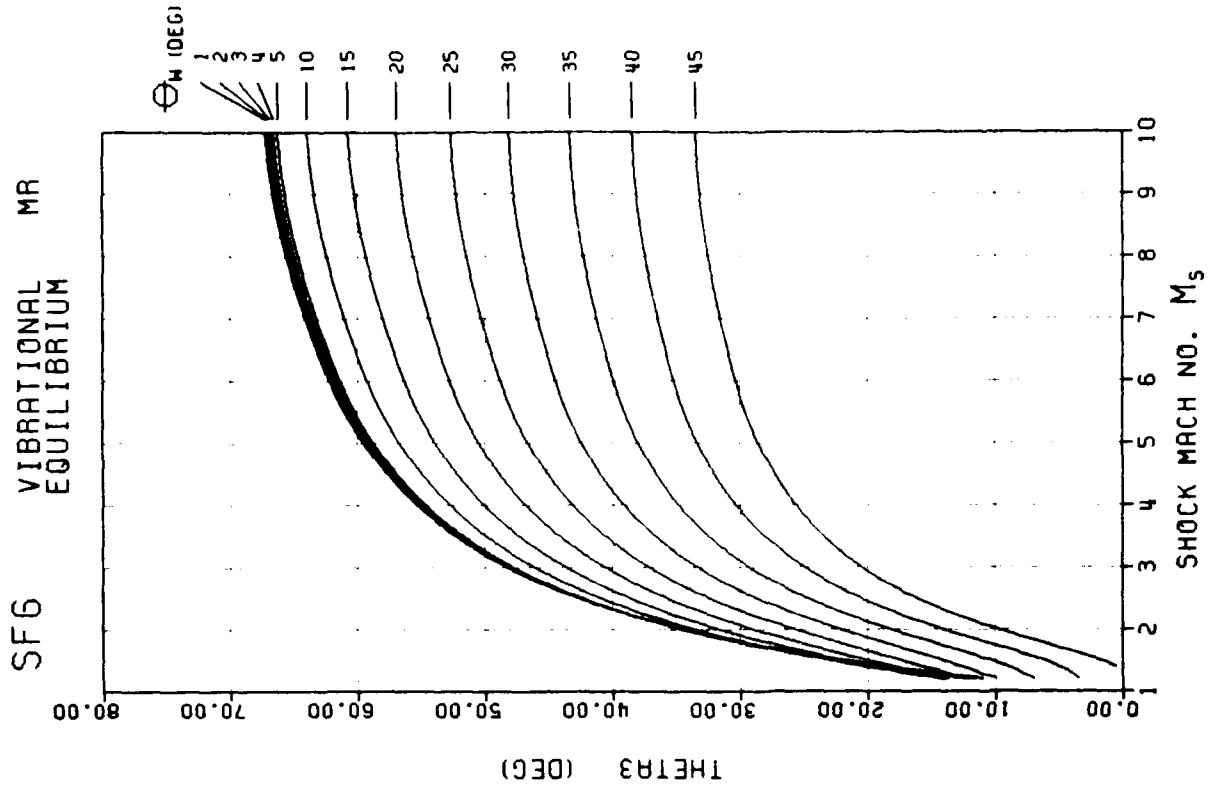


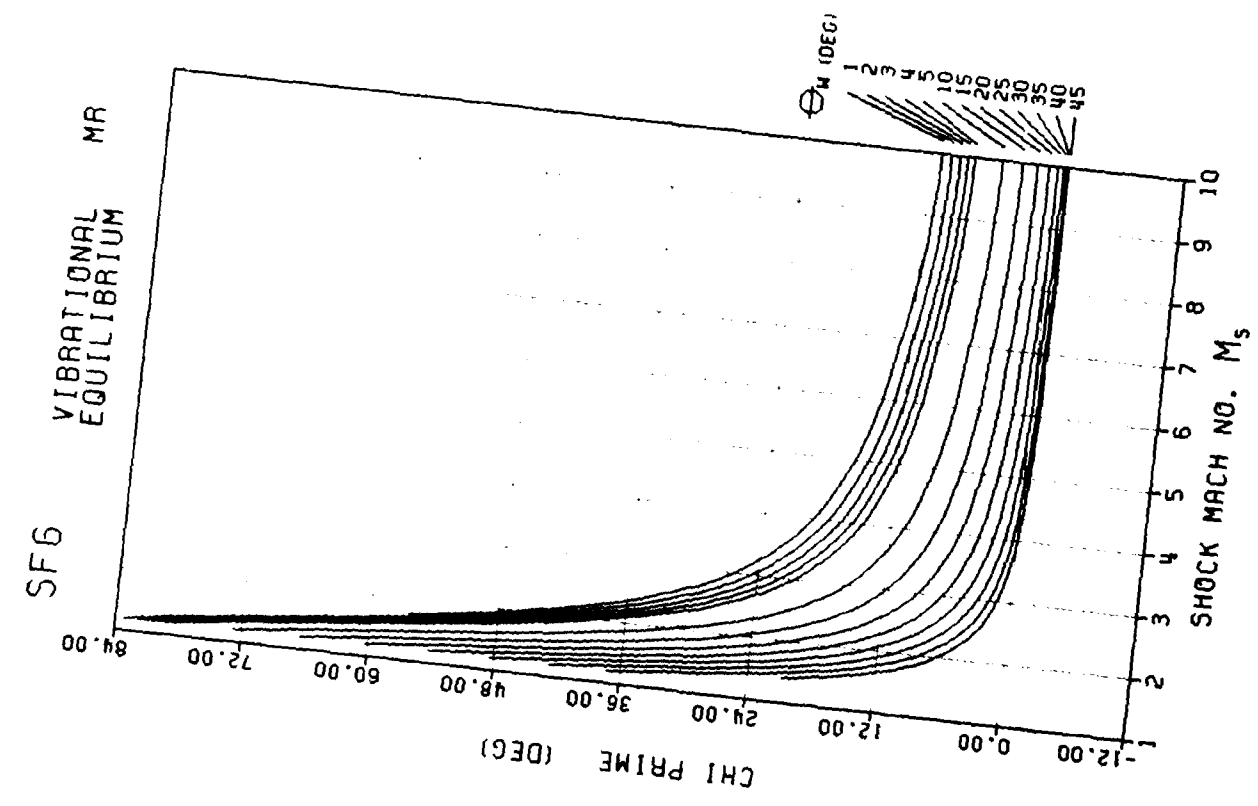
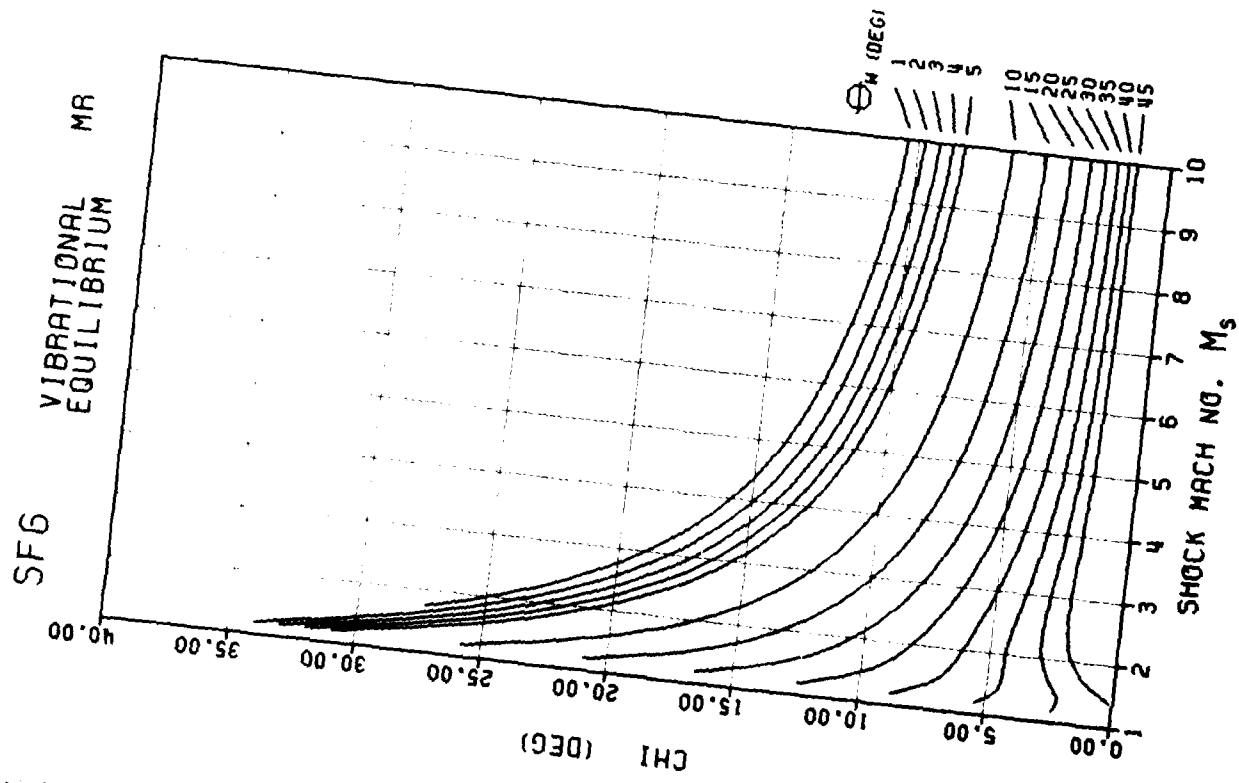




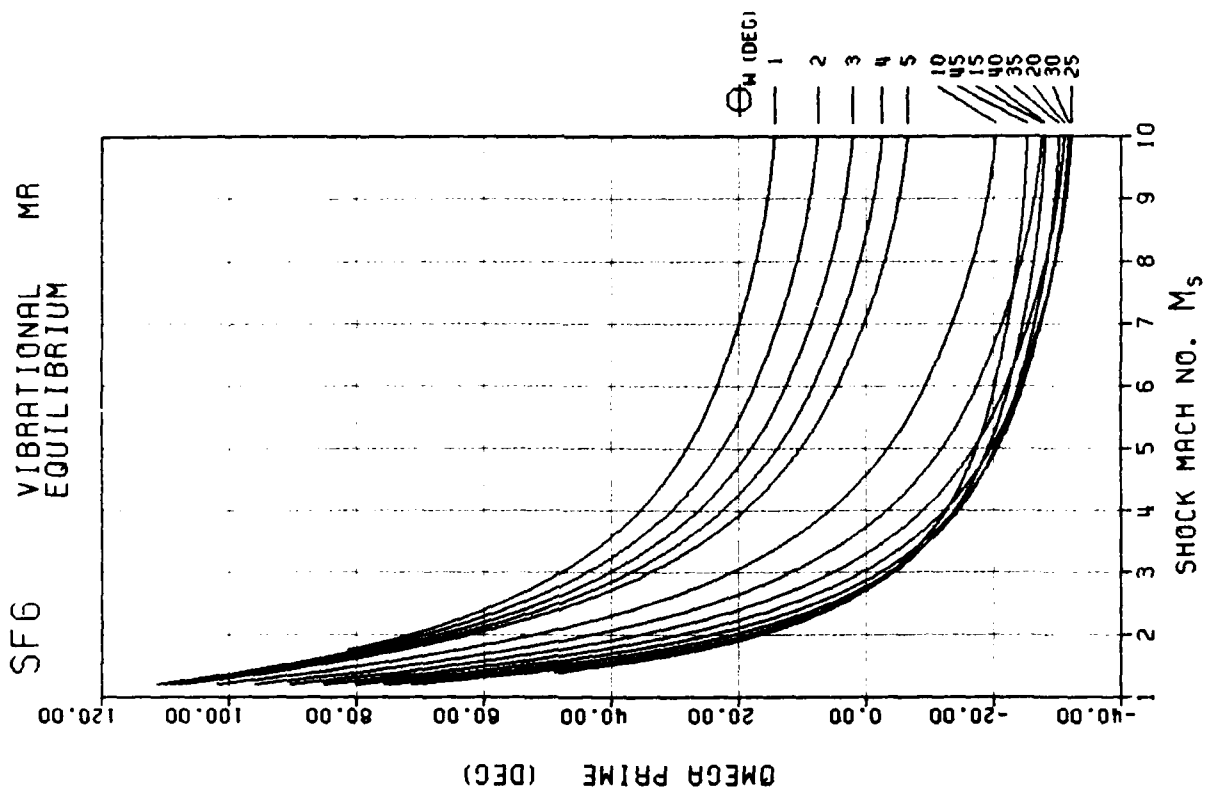
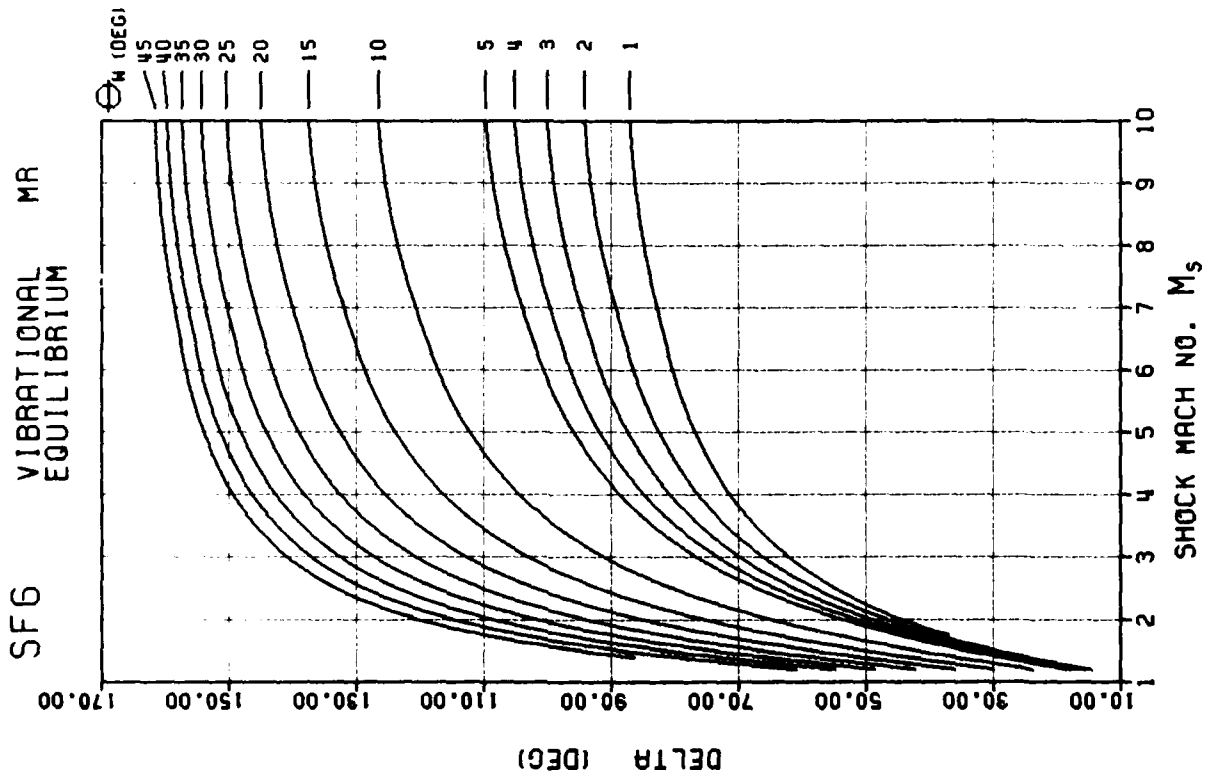




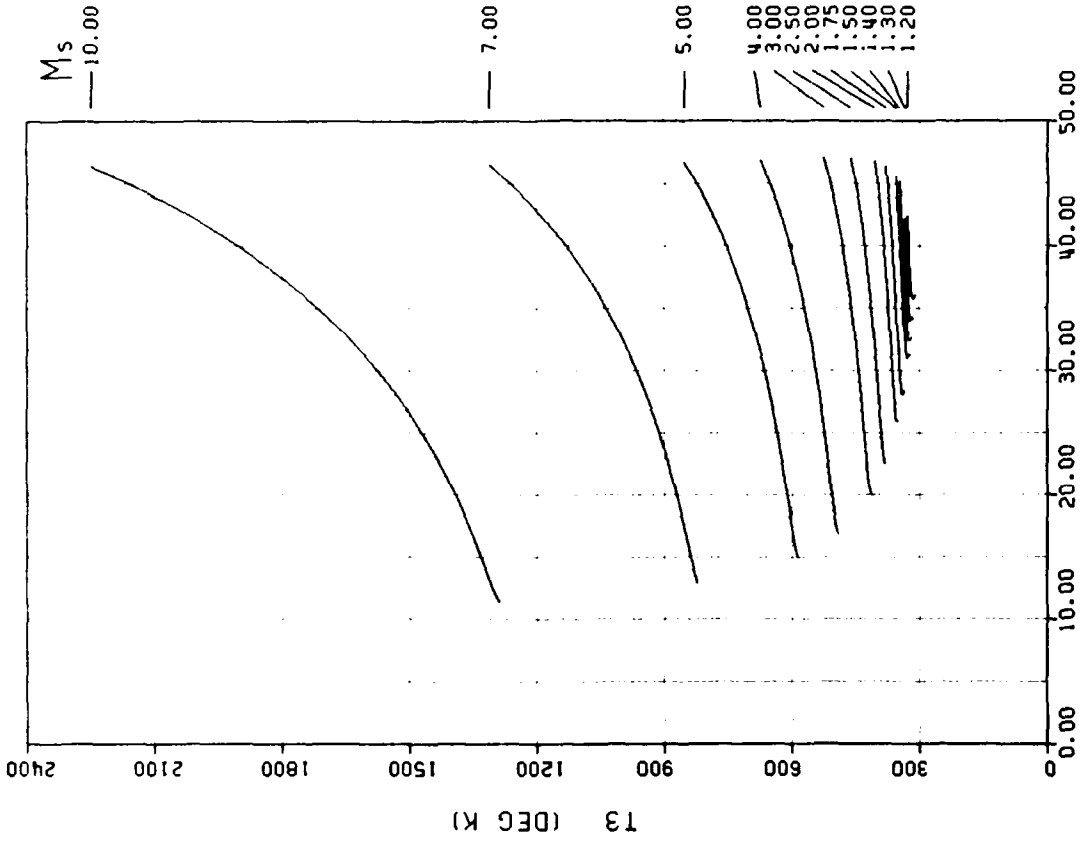




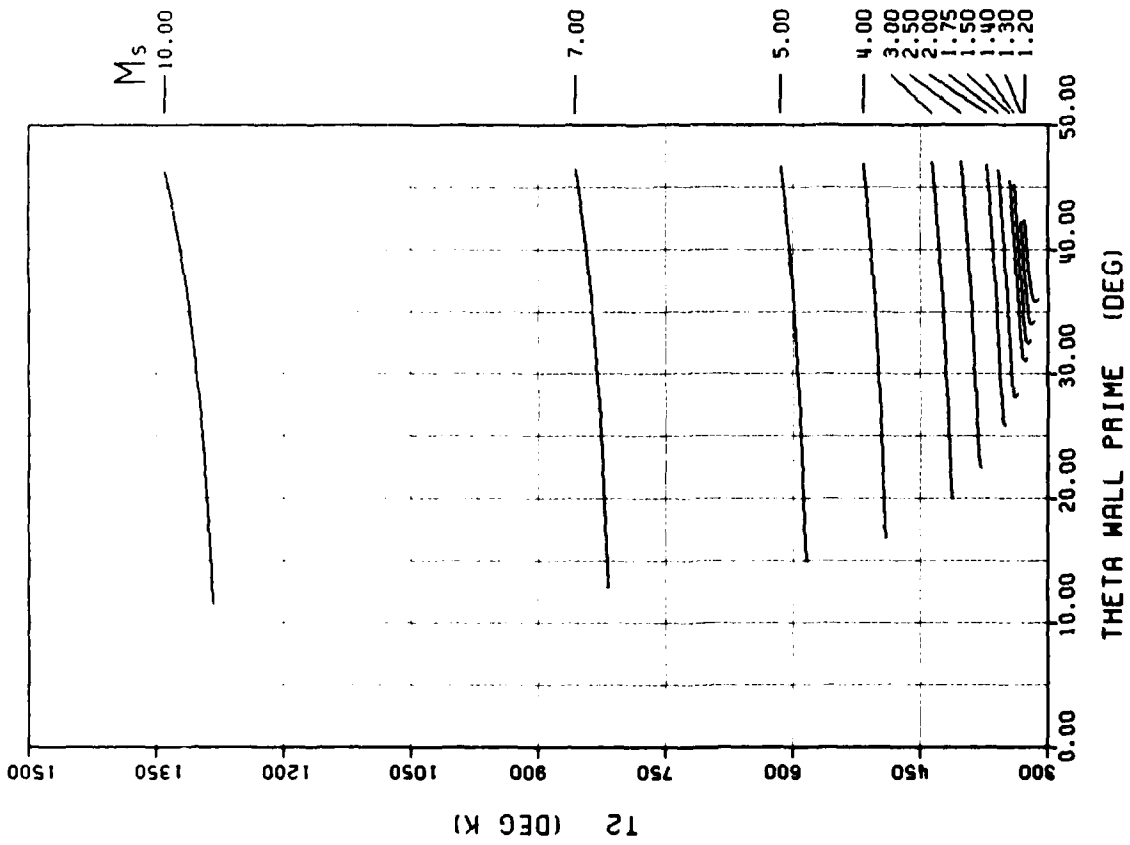
F - 228

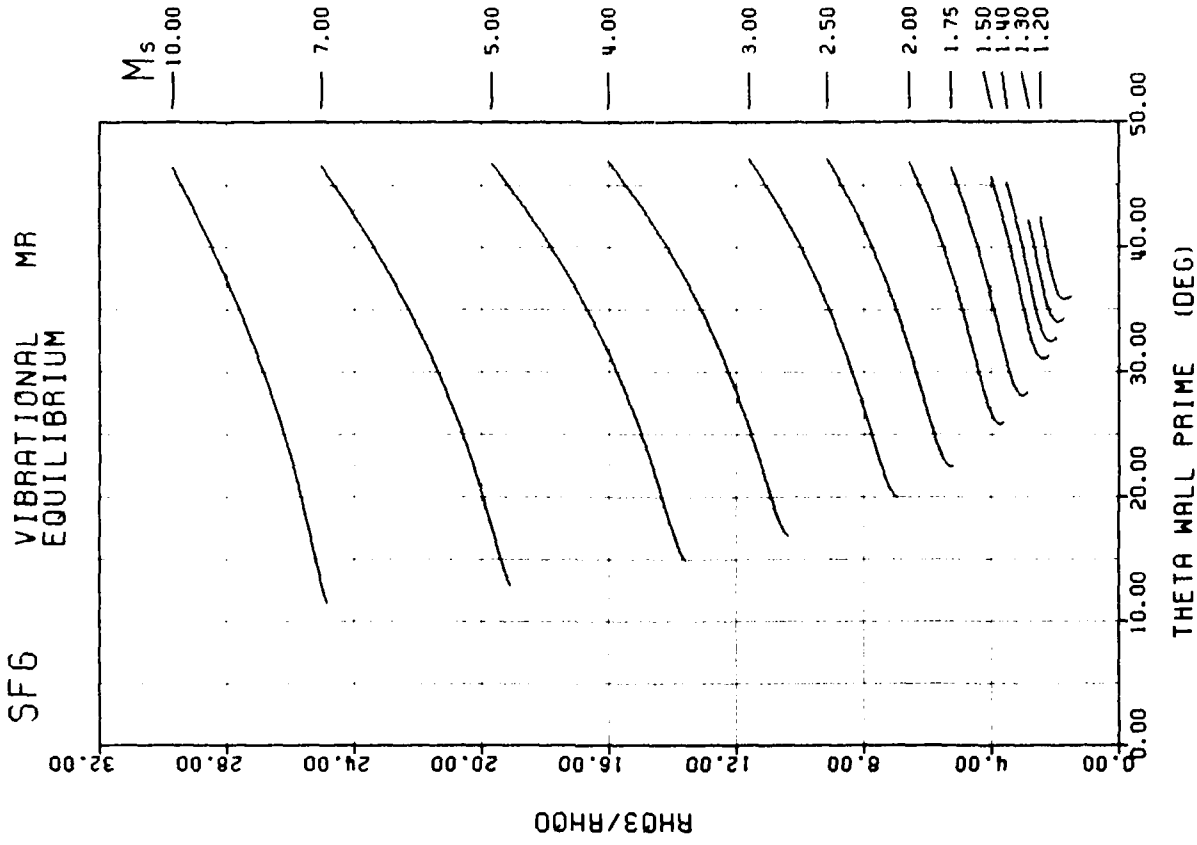
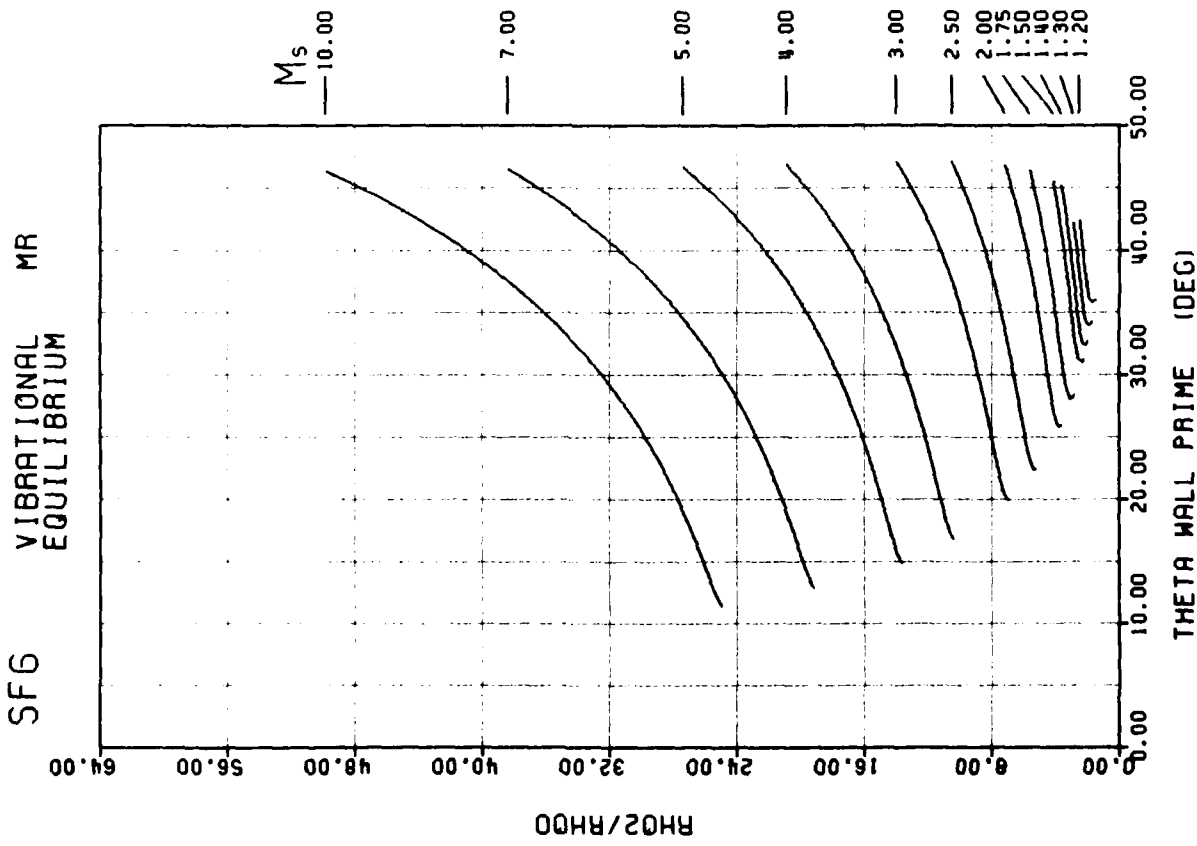


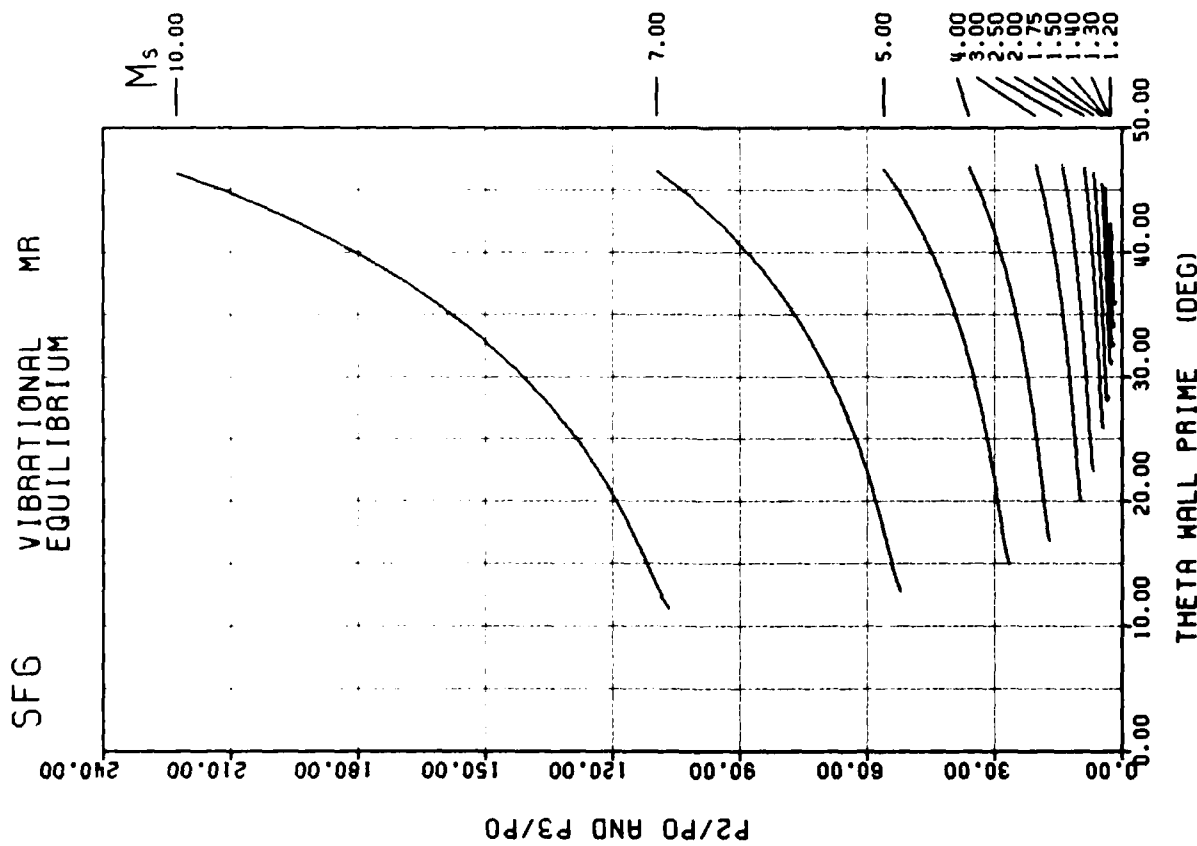
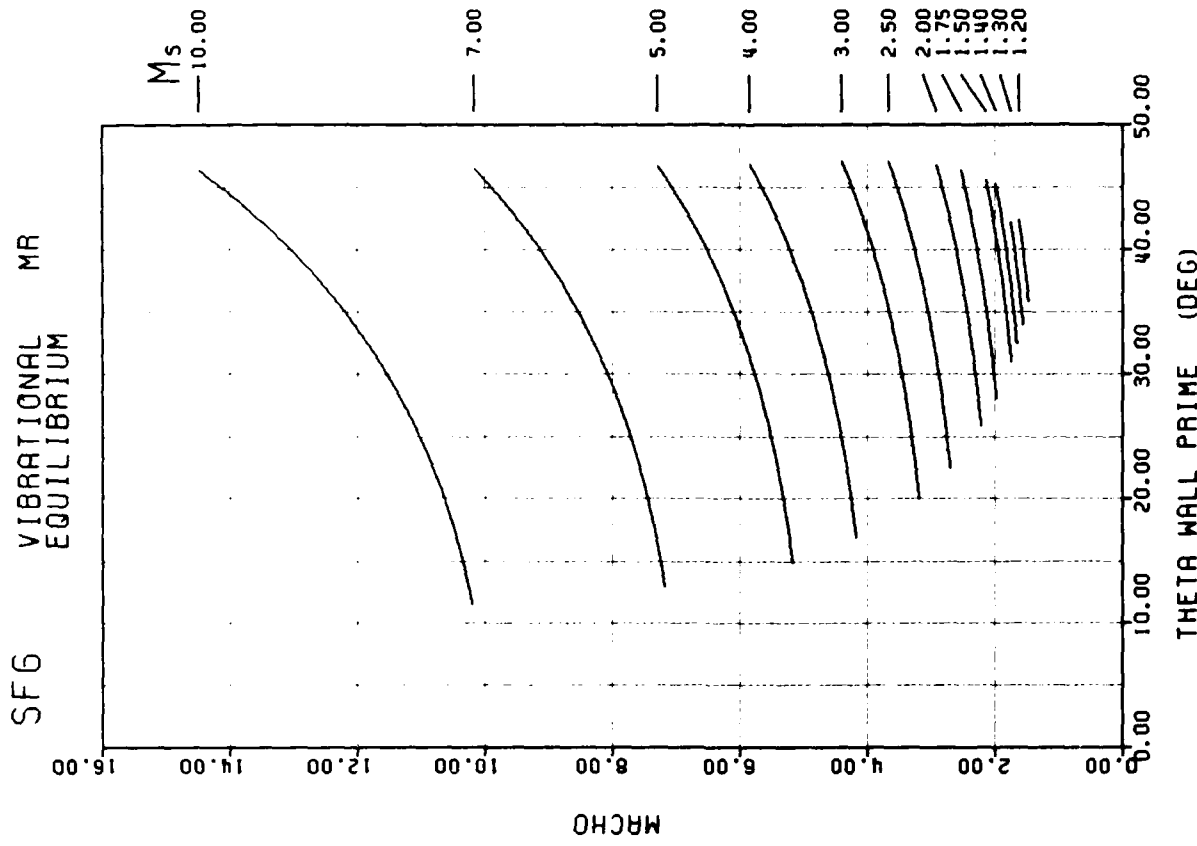
SFG VIBRATIONAL EQUILIBRIUM MR

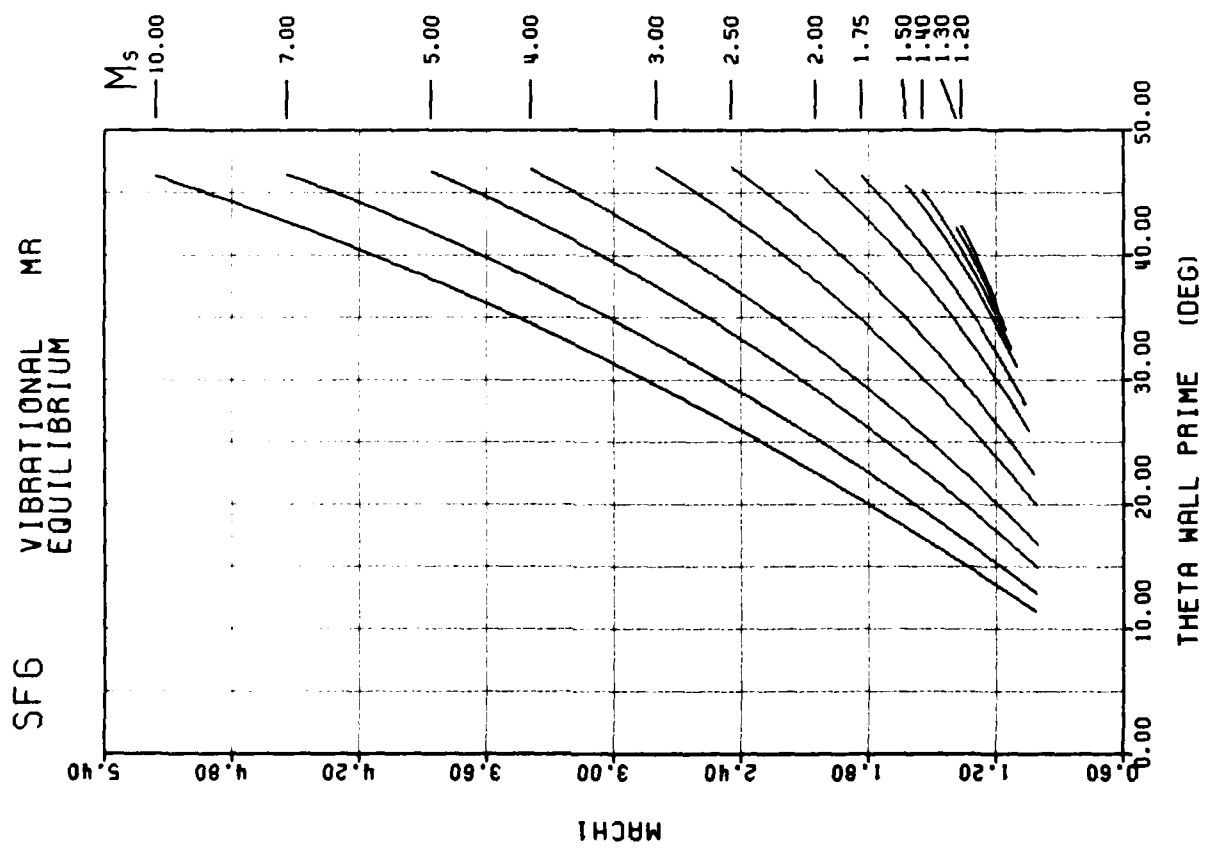
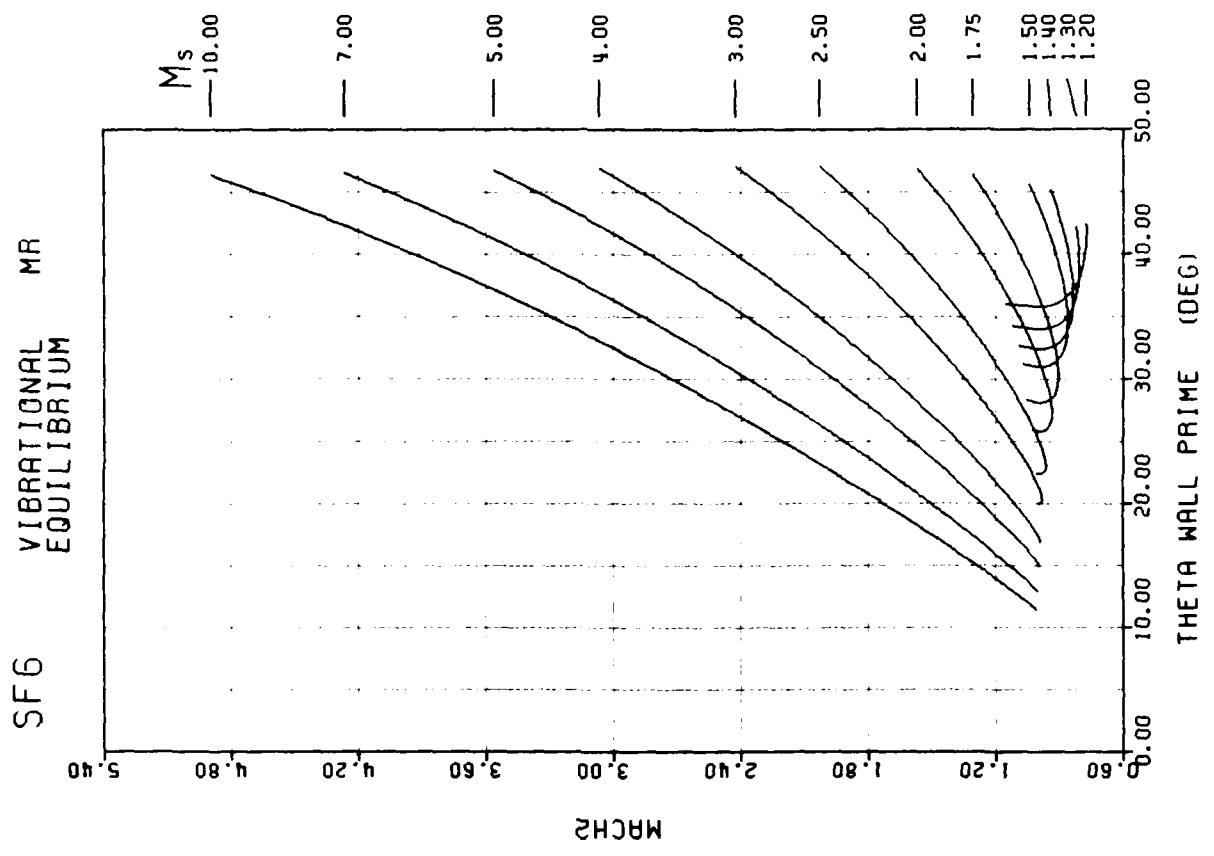


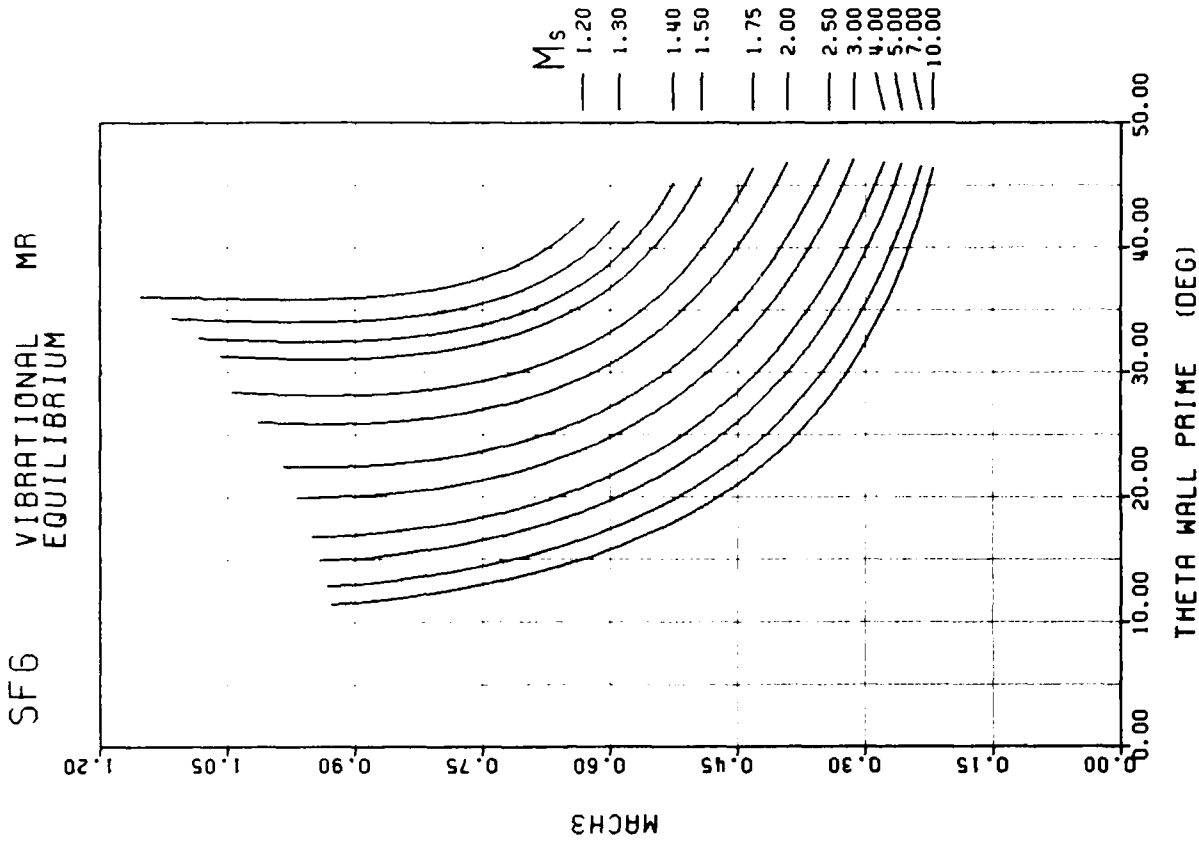
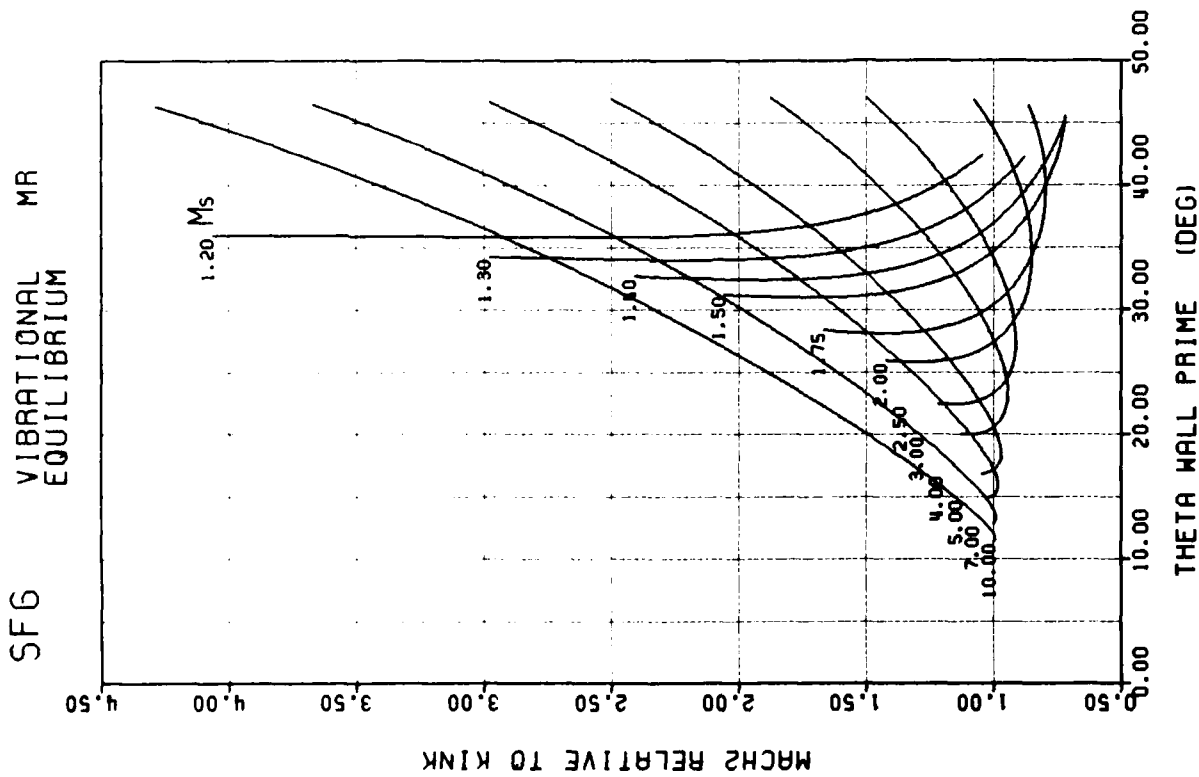
SFG VIBRATIONAL EQUILIBRIUM MR

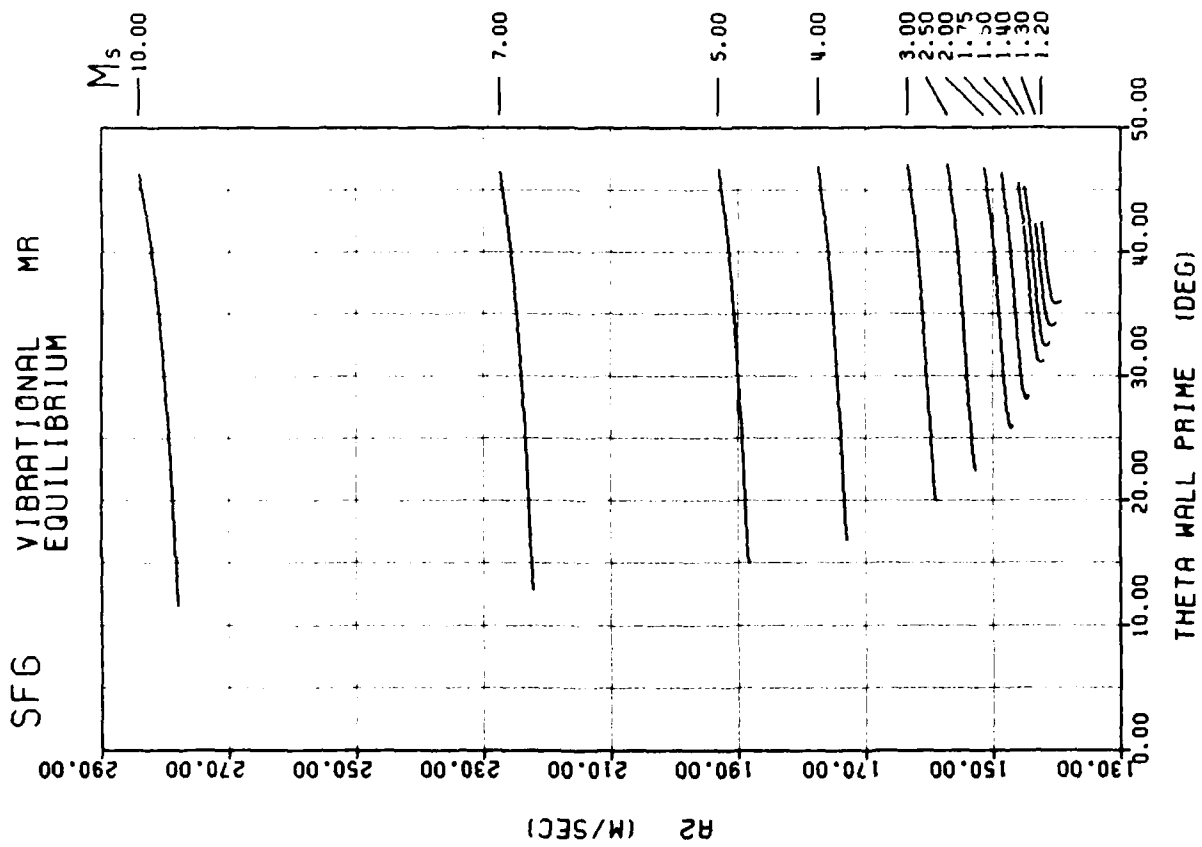
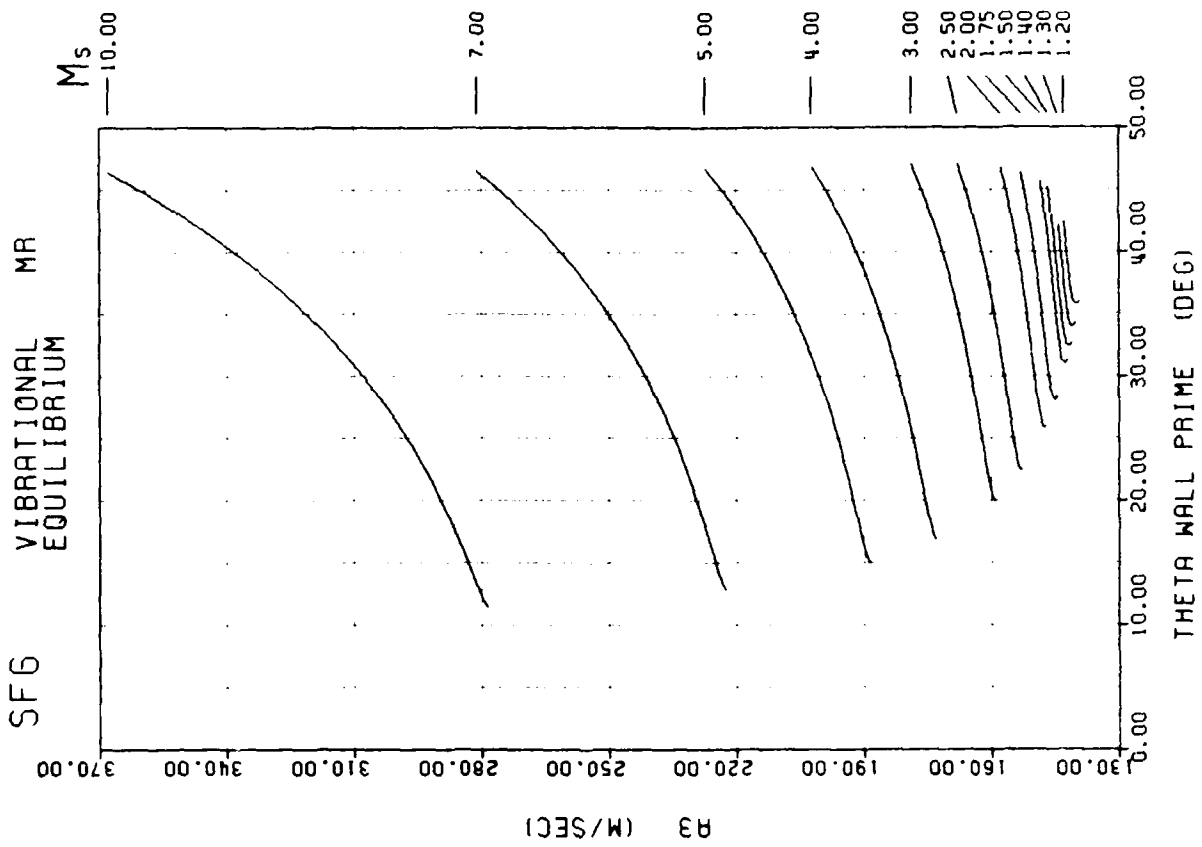


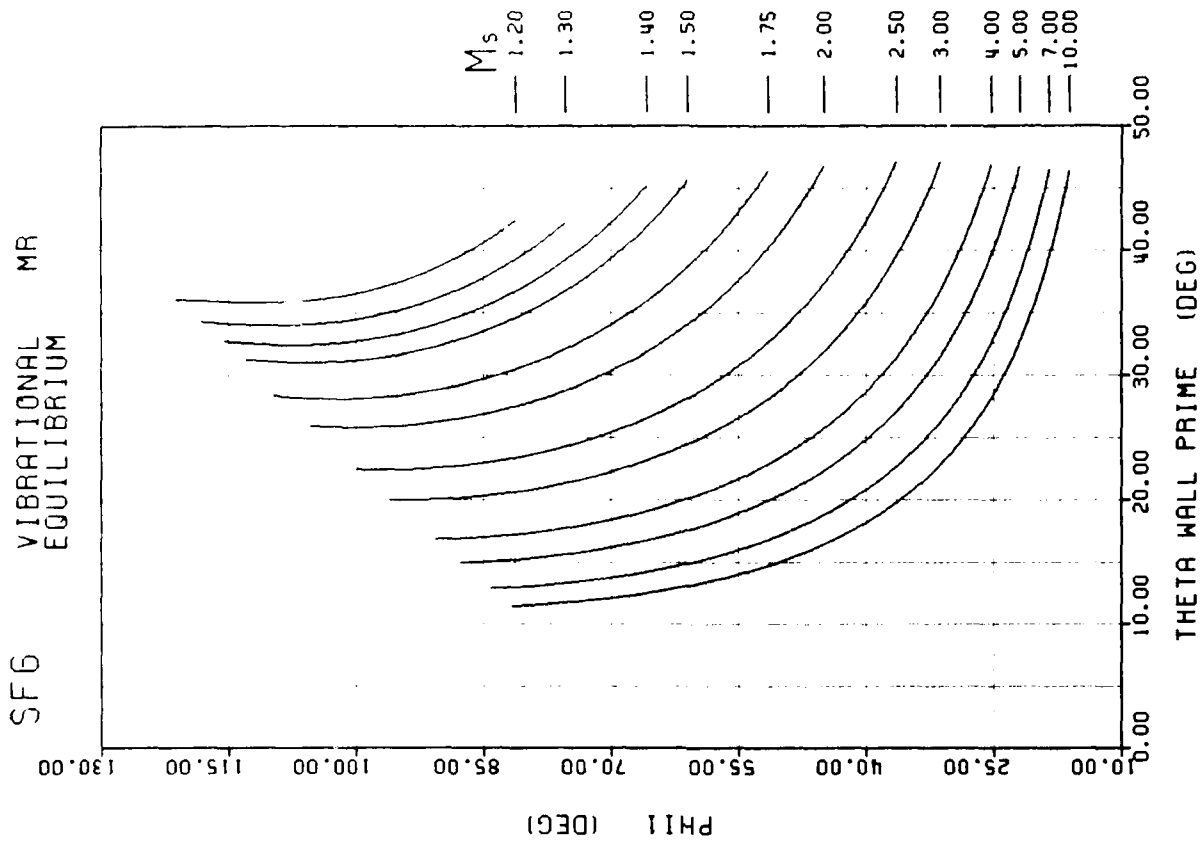
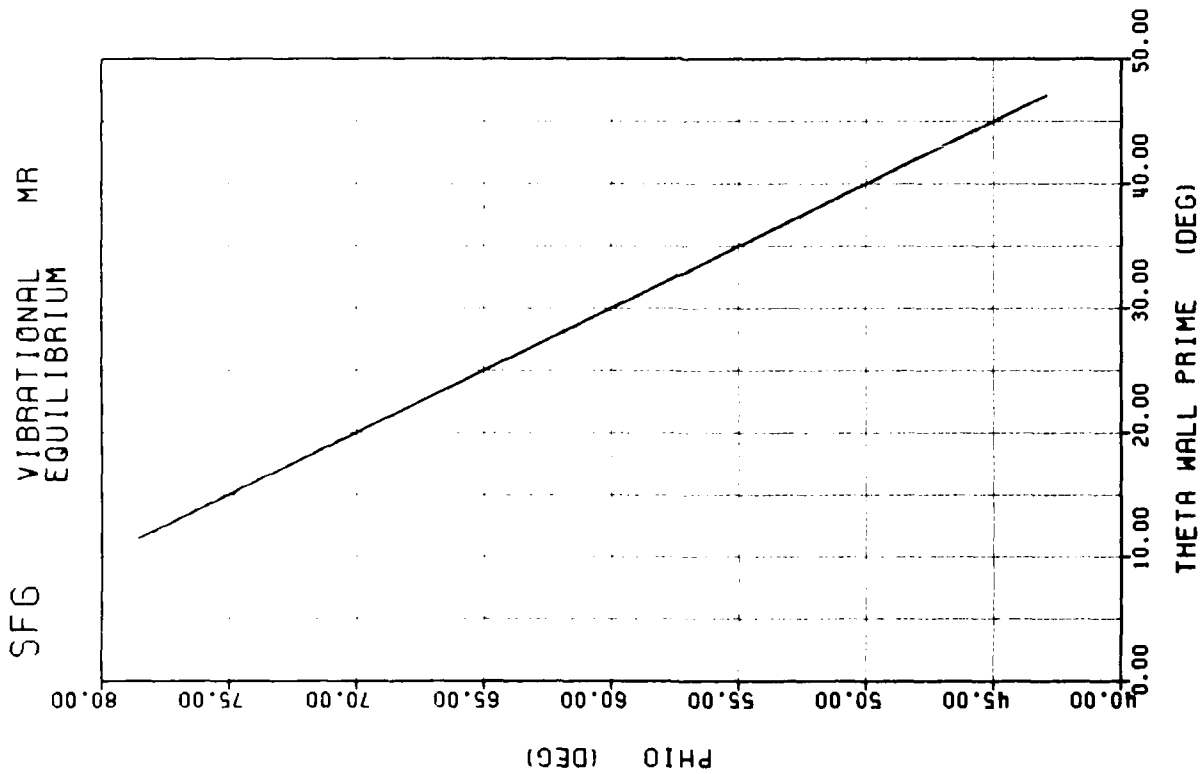


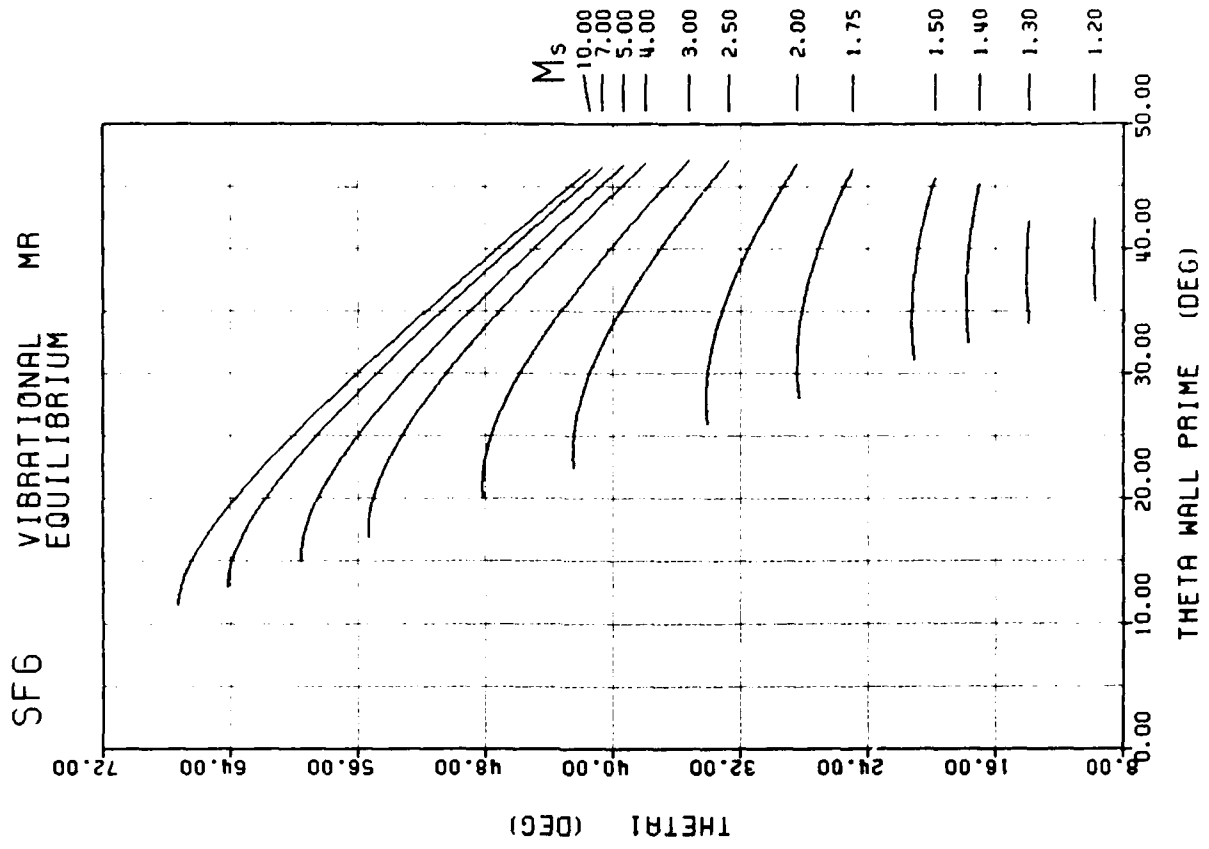
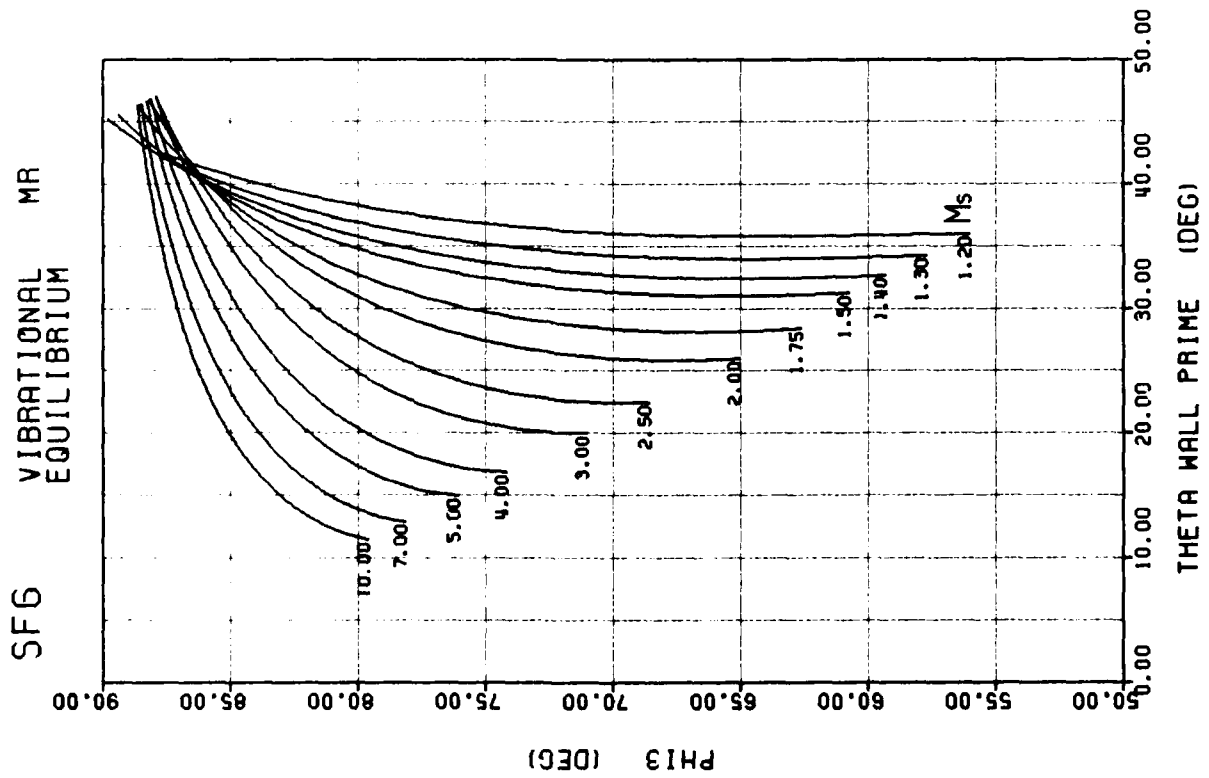


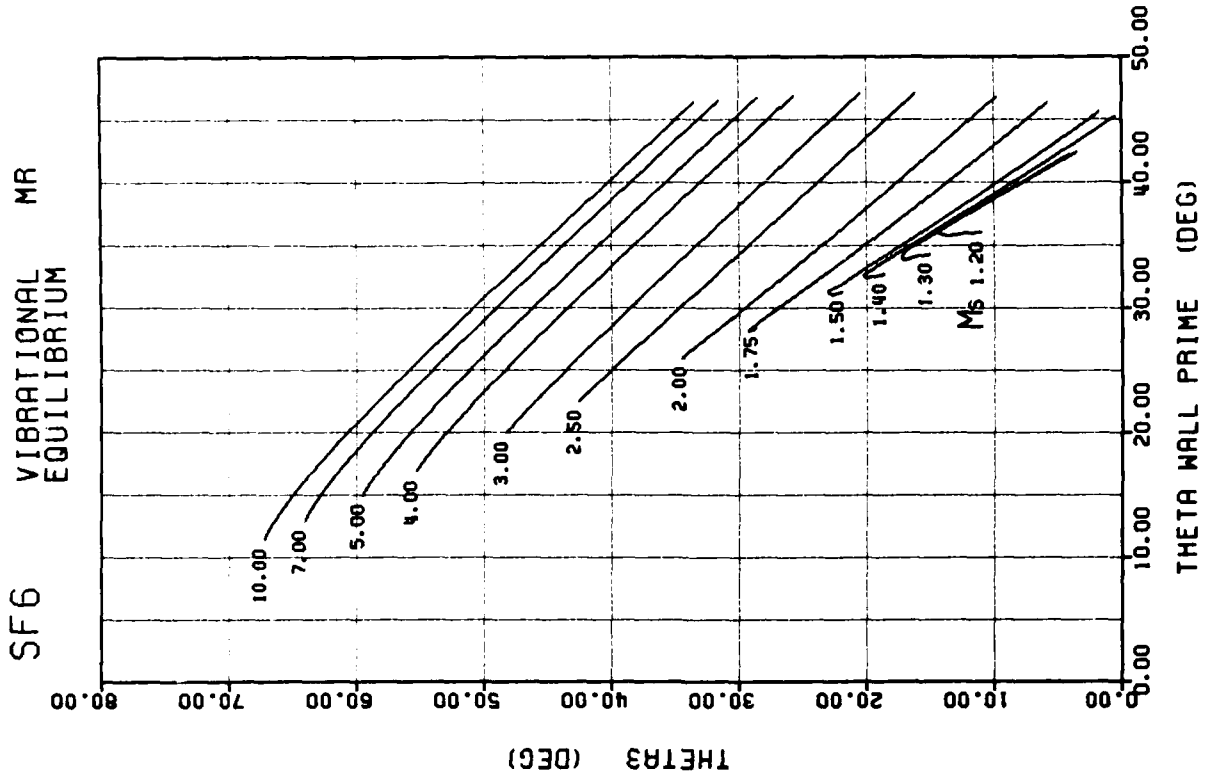
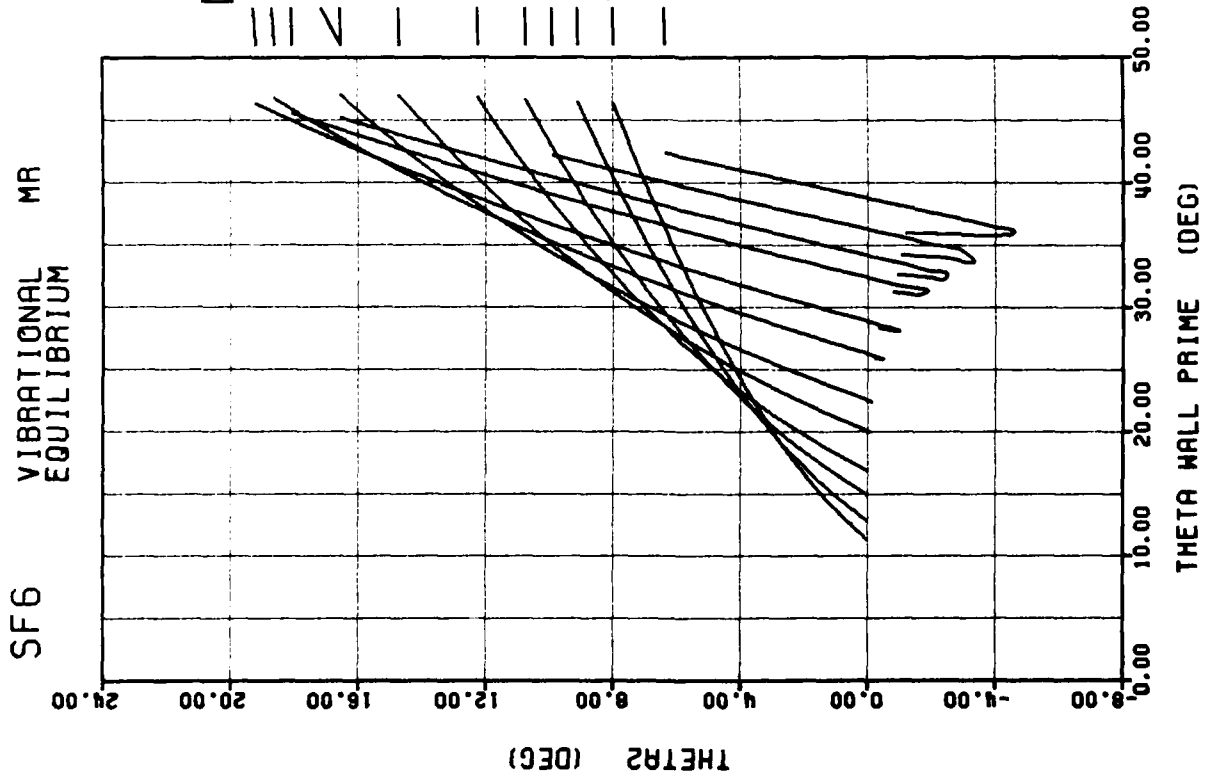


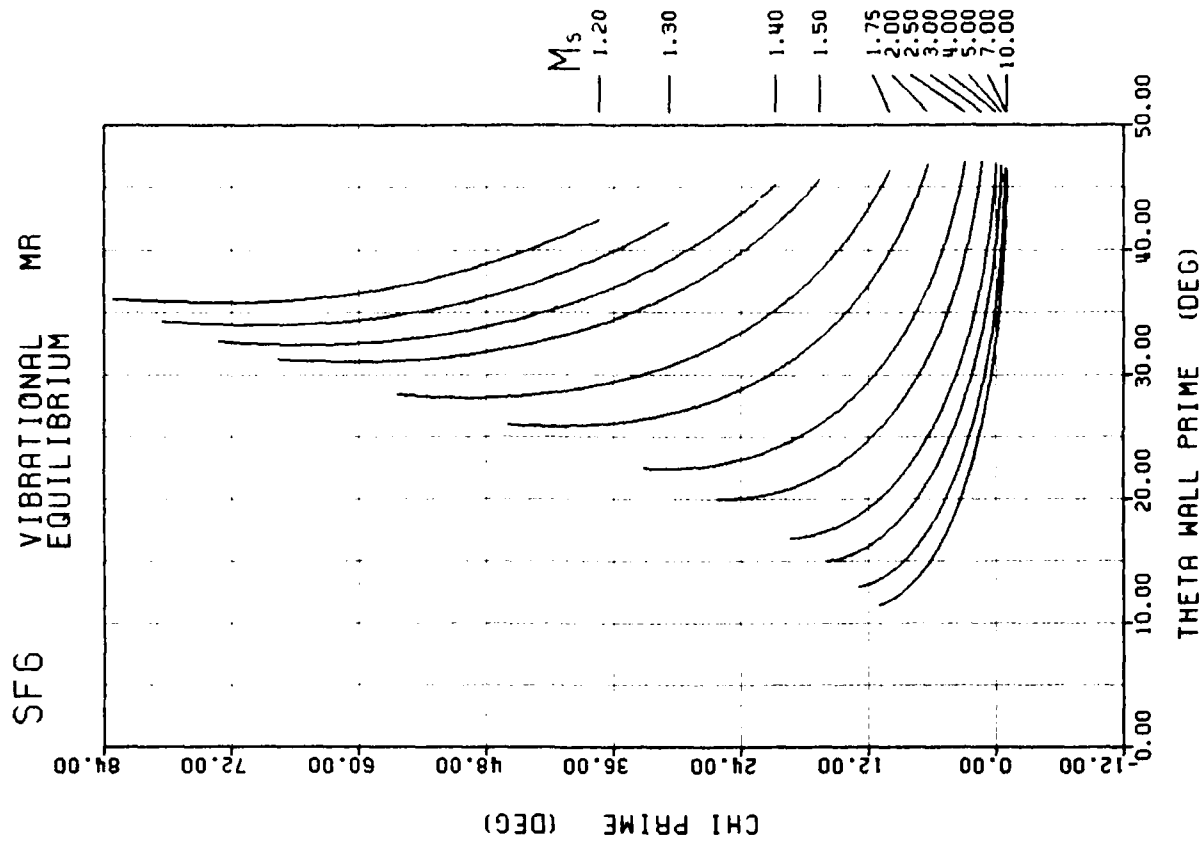
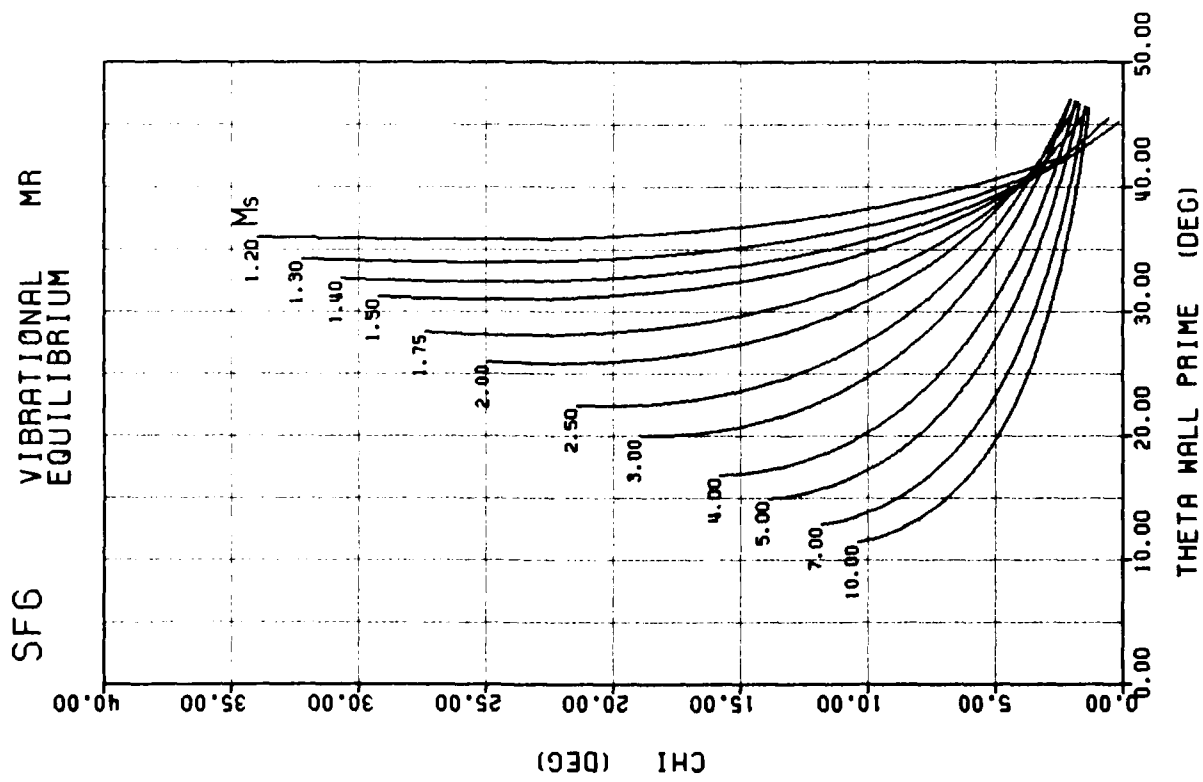


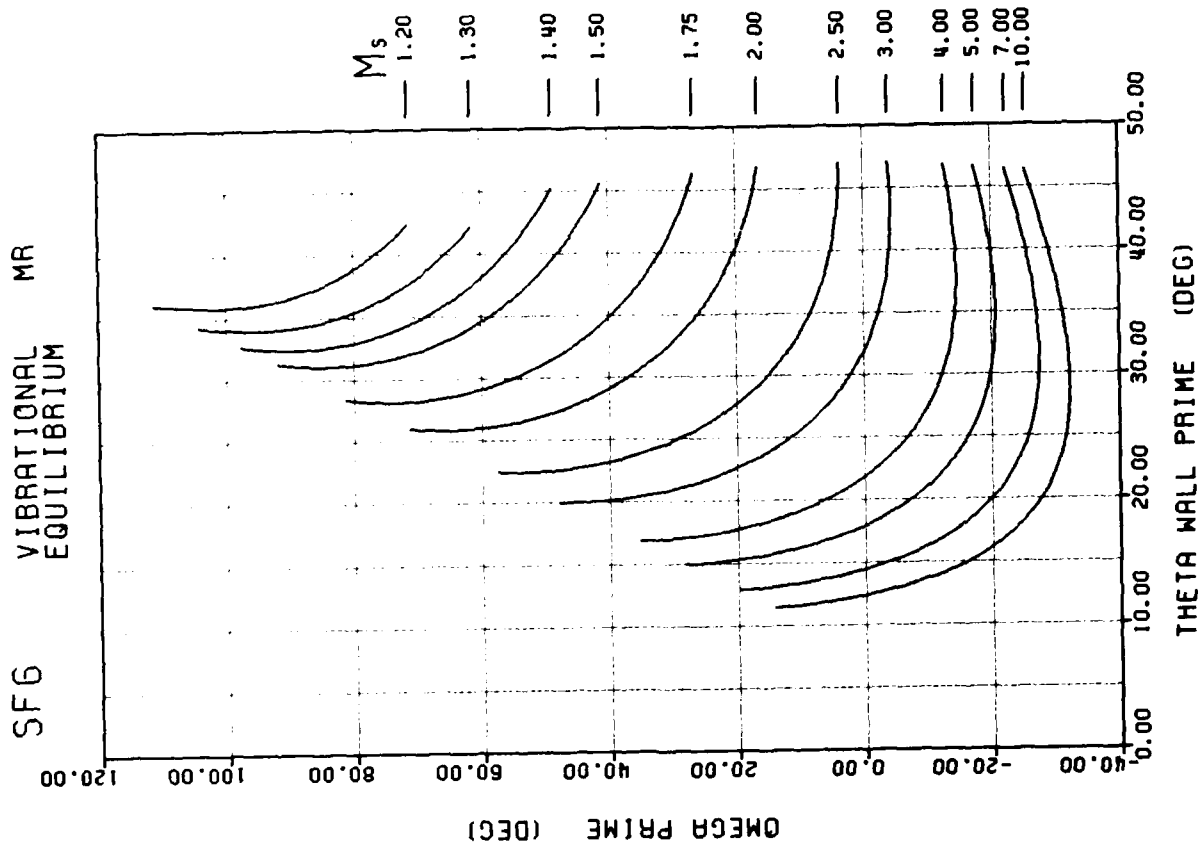
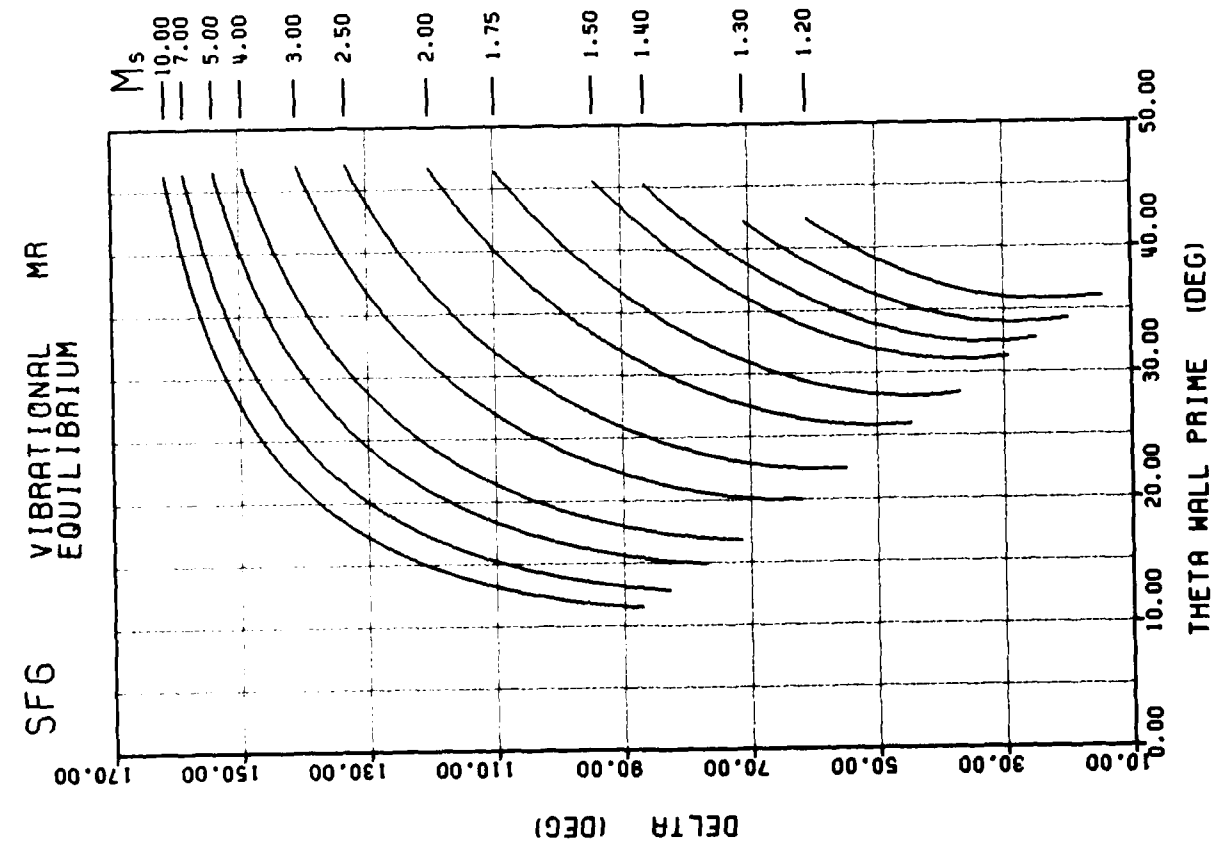


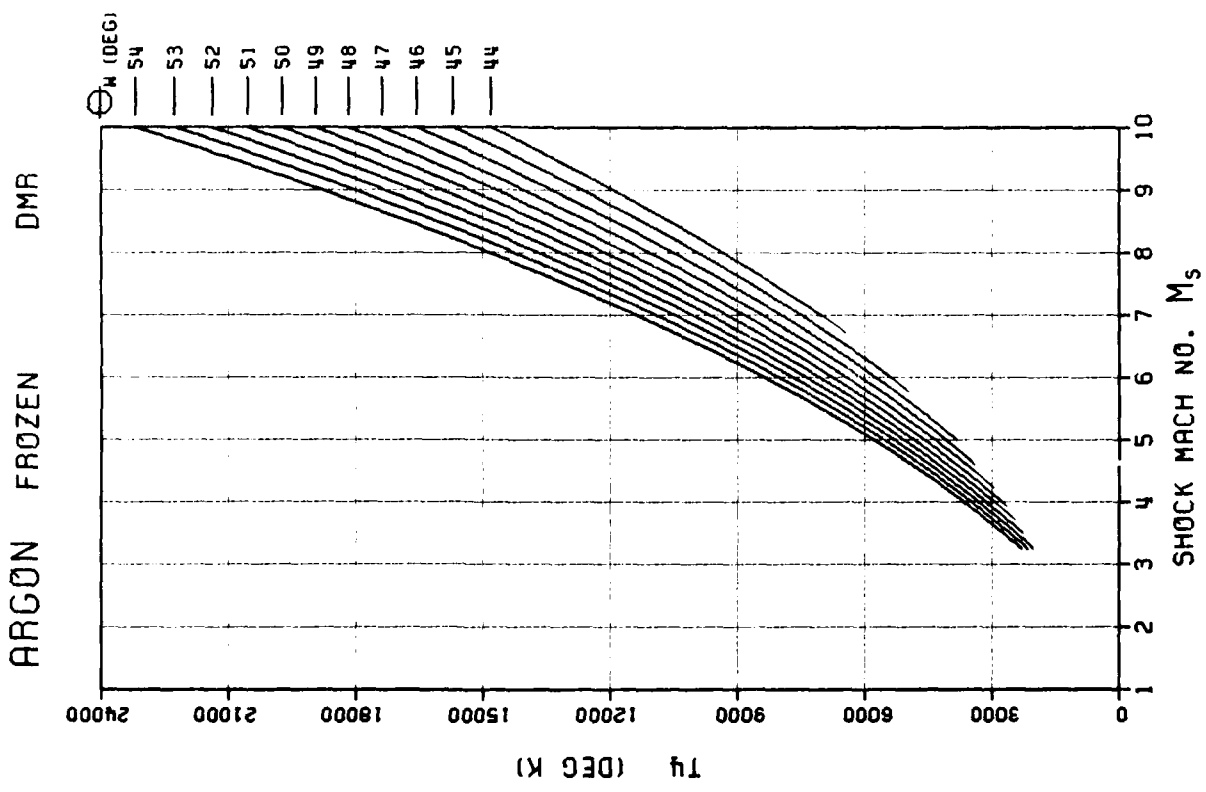
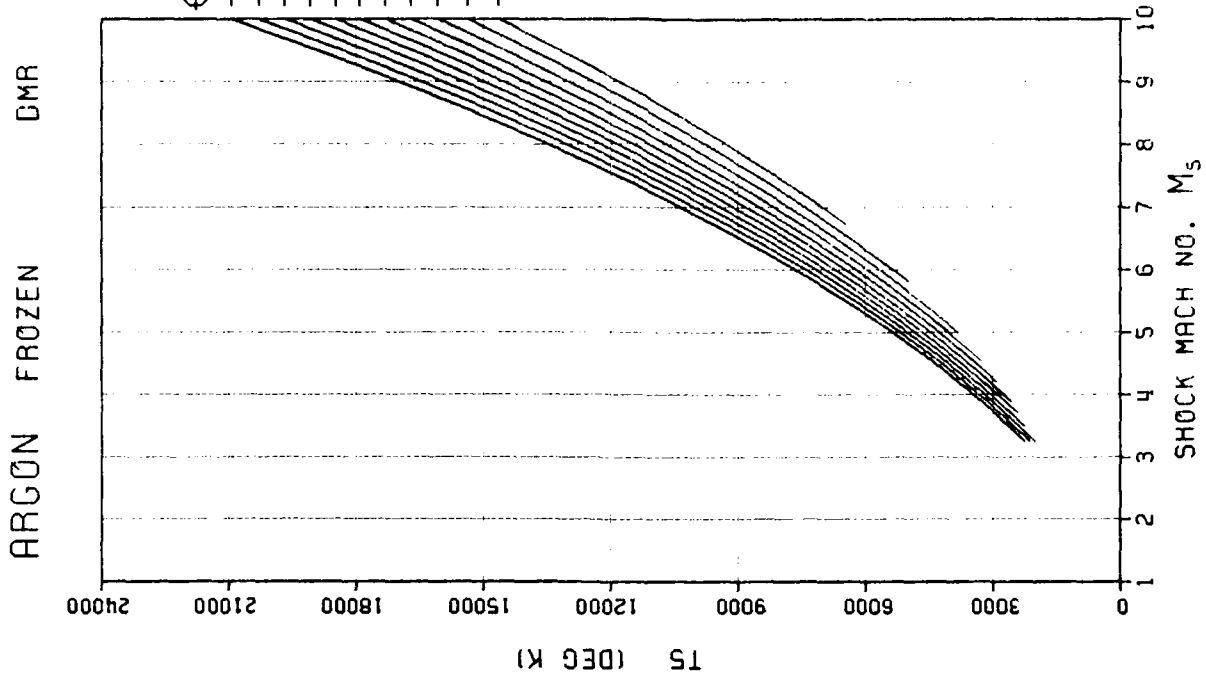


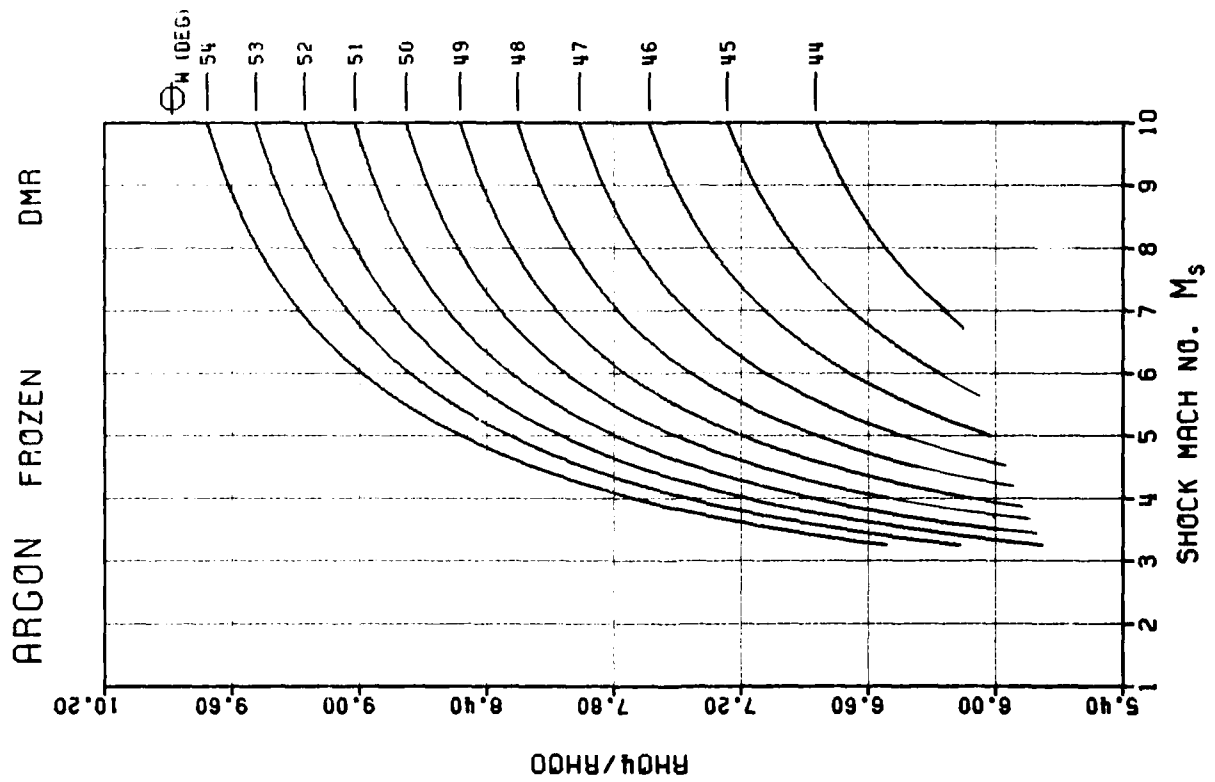
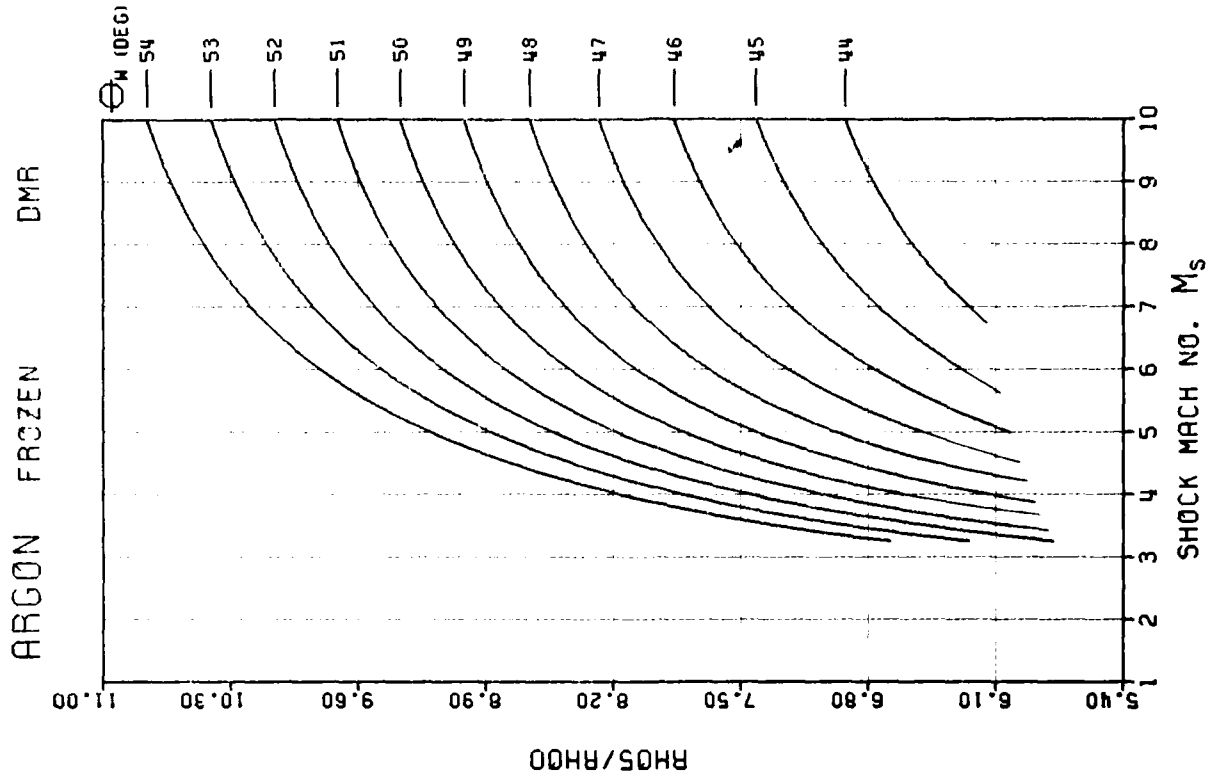


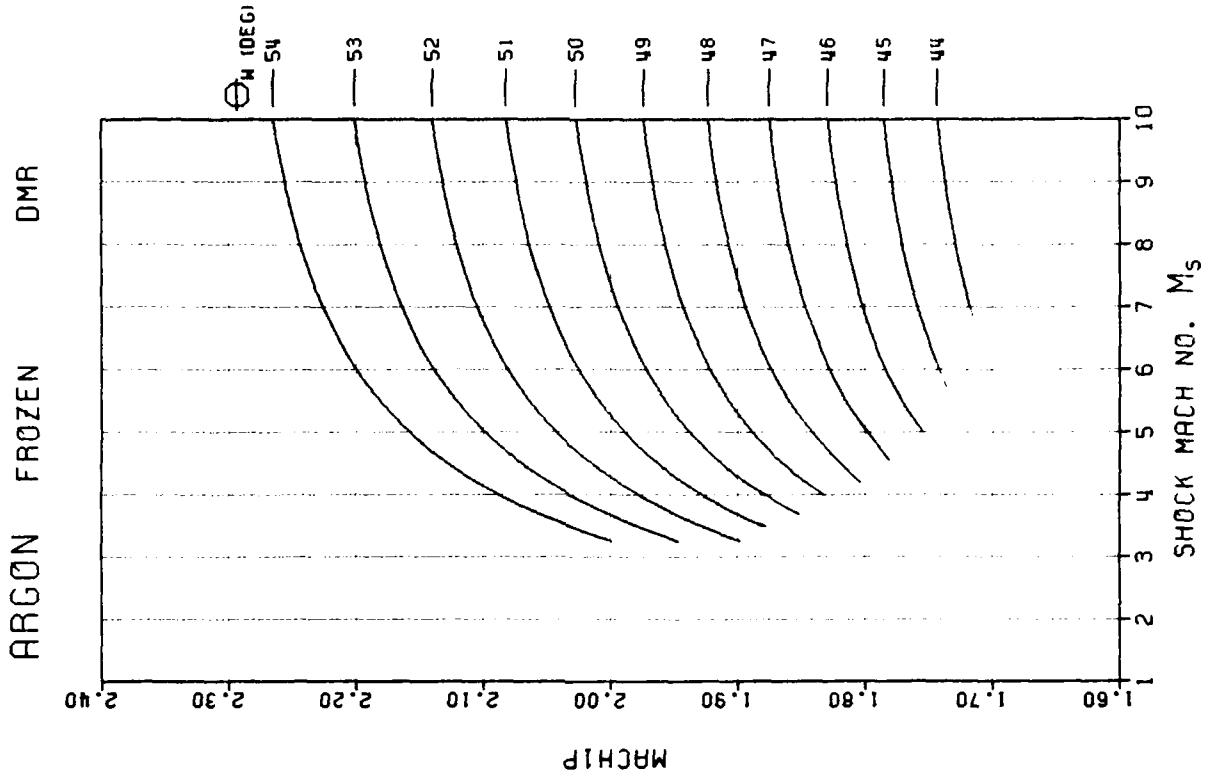
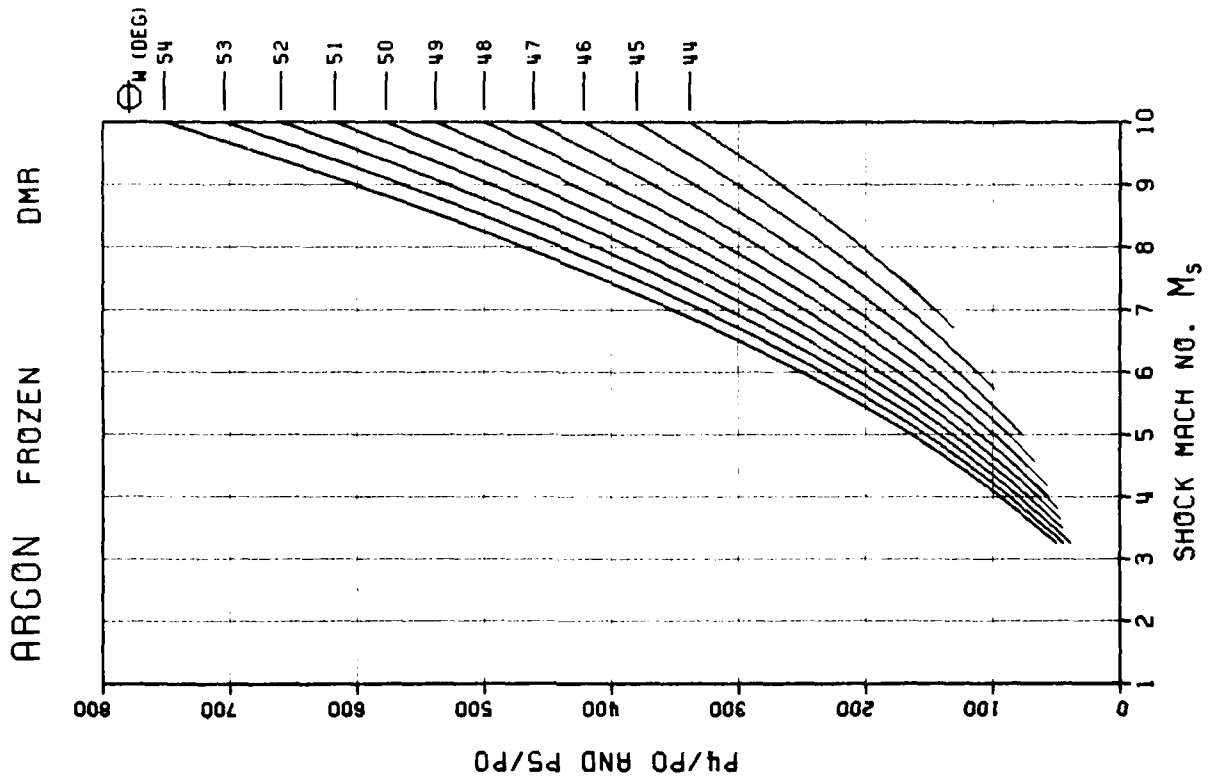




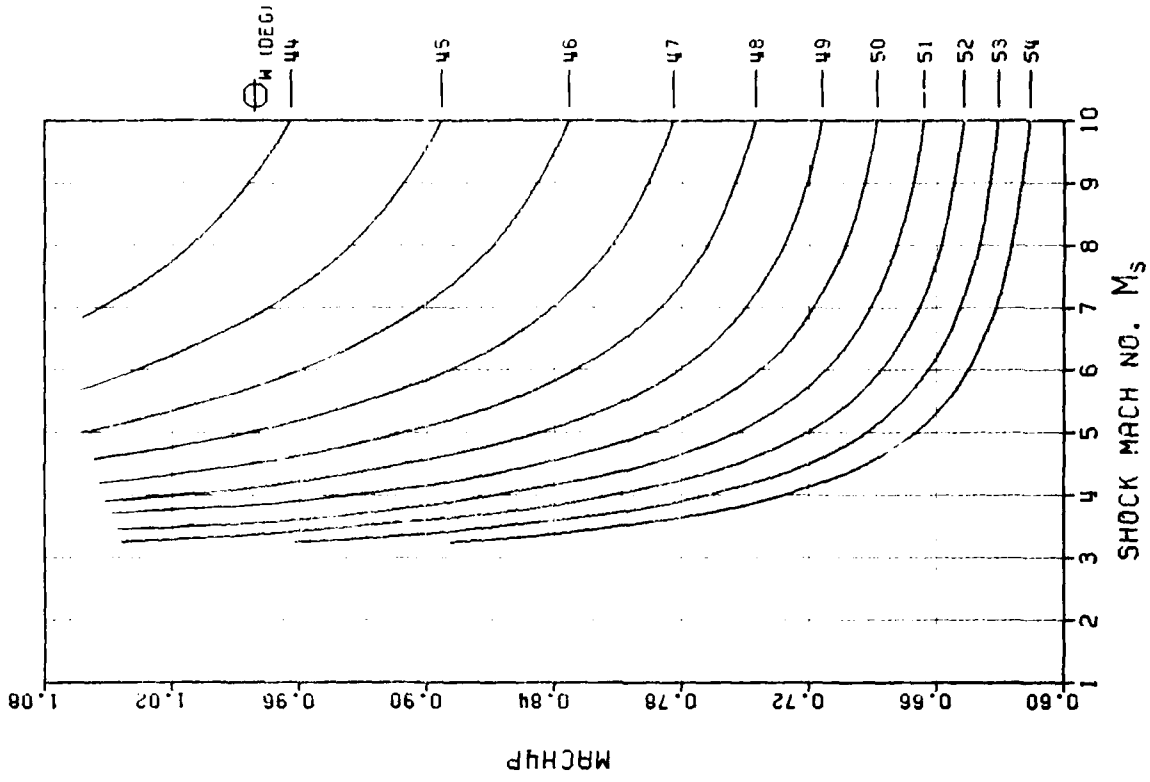




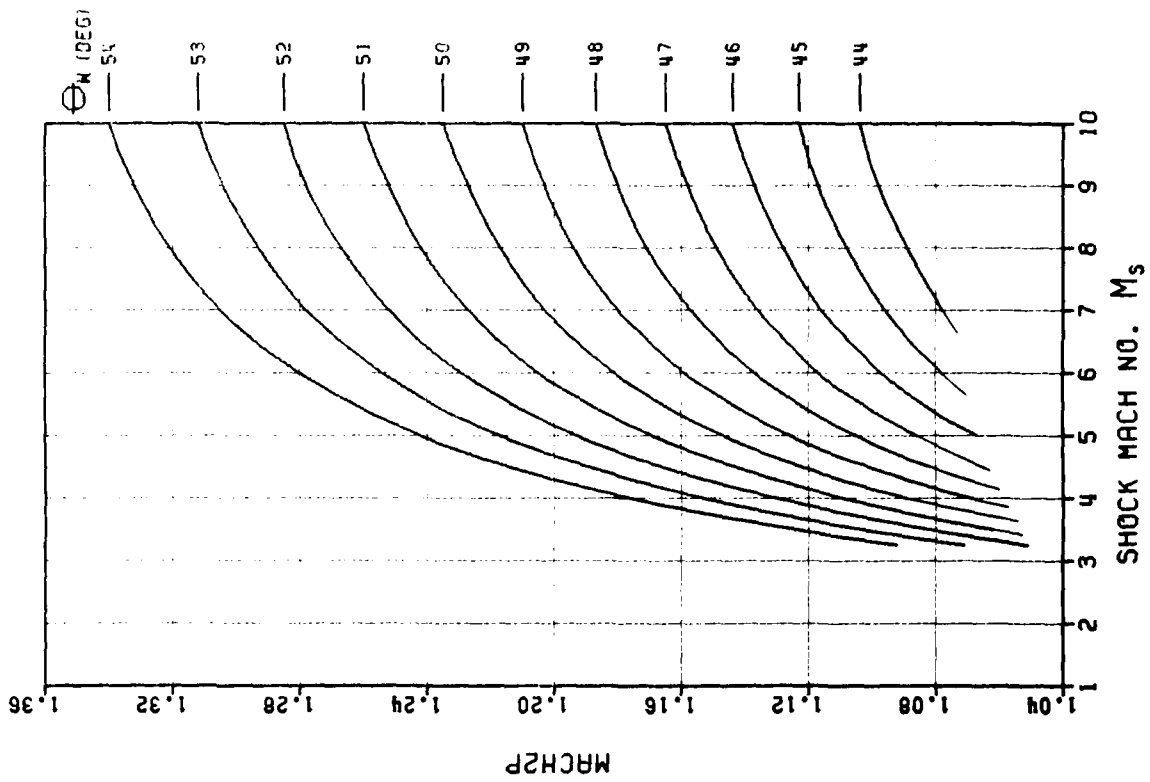


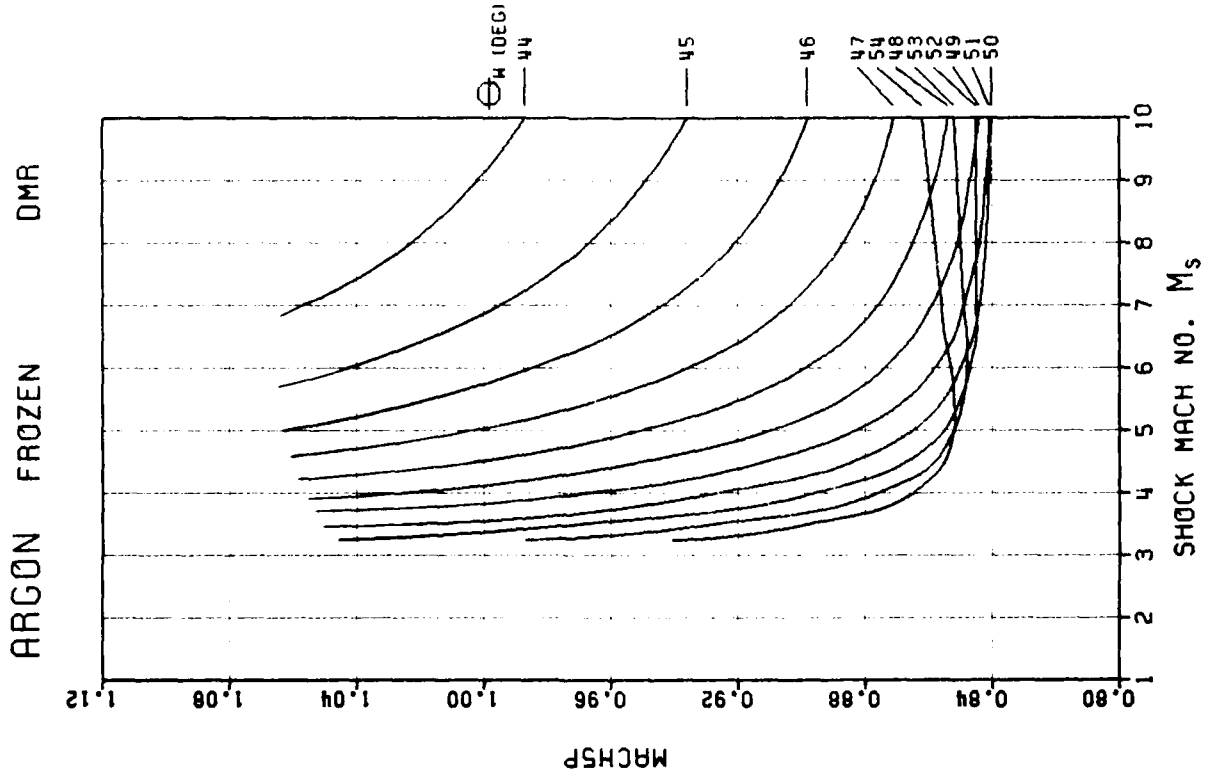
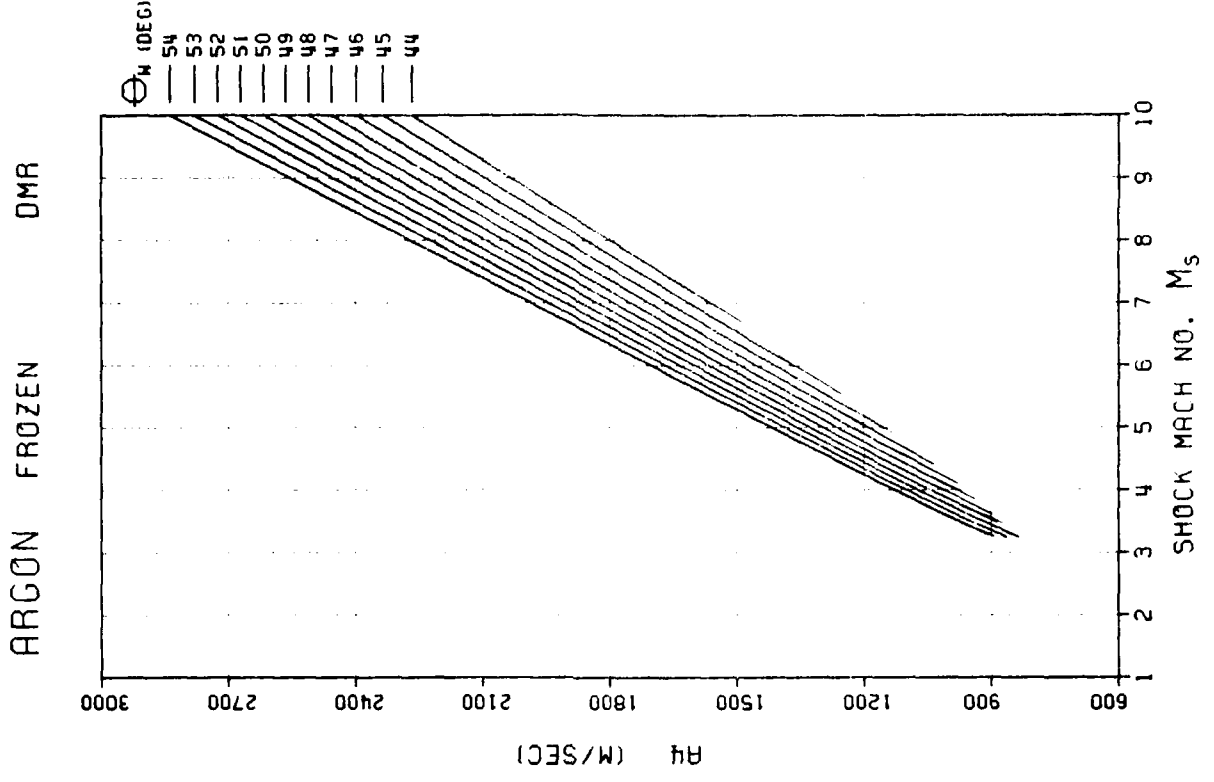


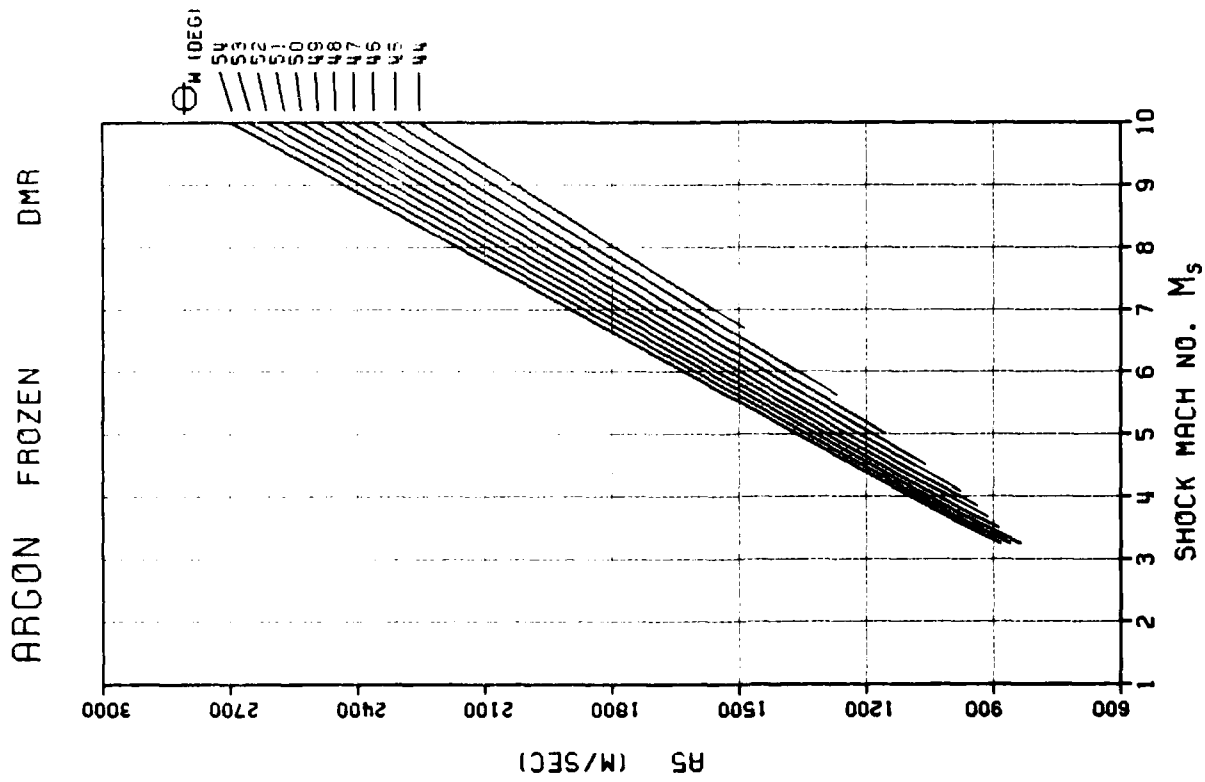
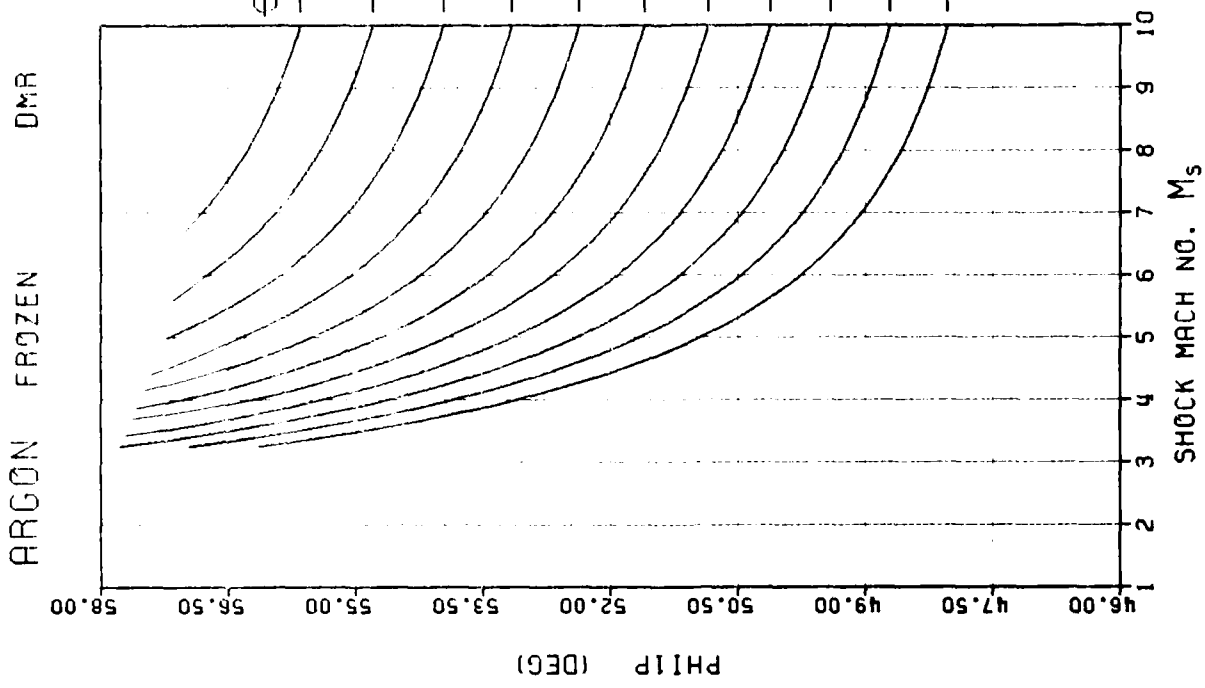
ARGON FROZEN DMR

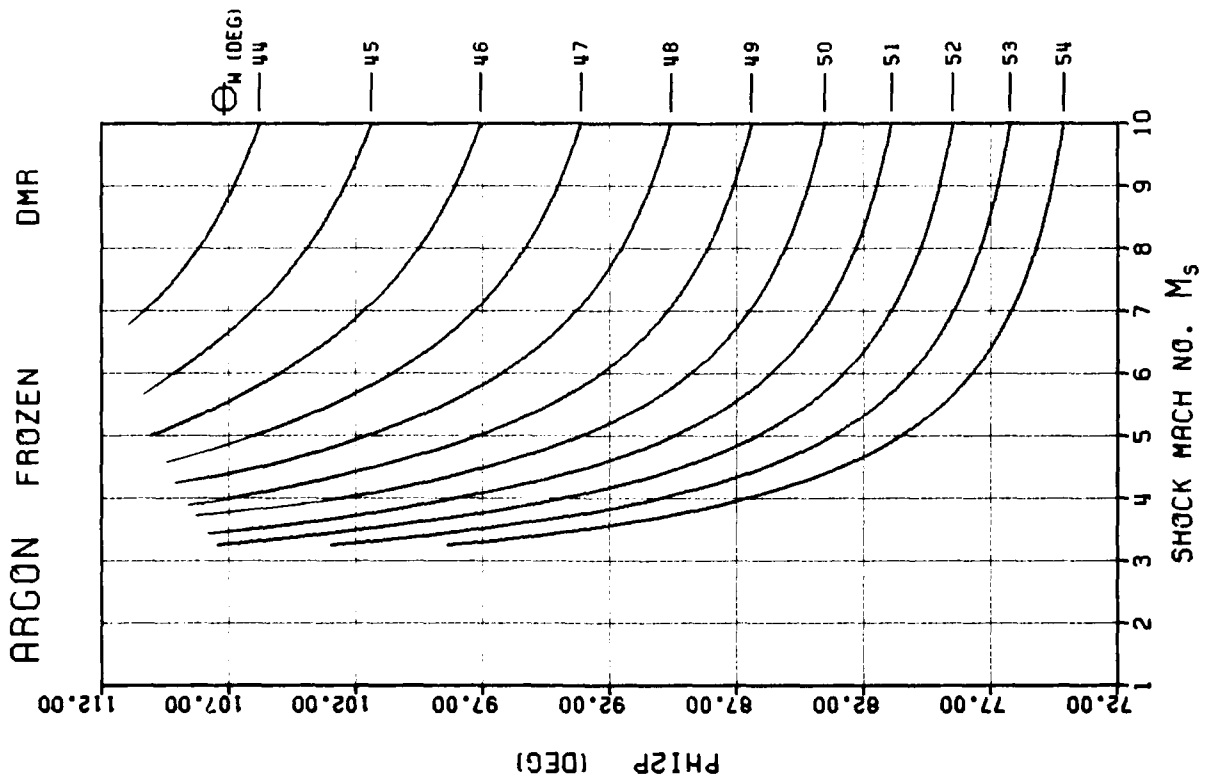
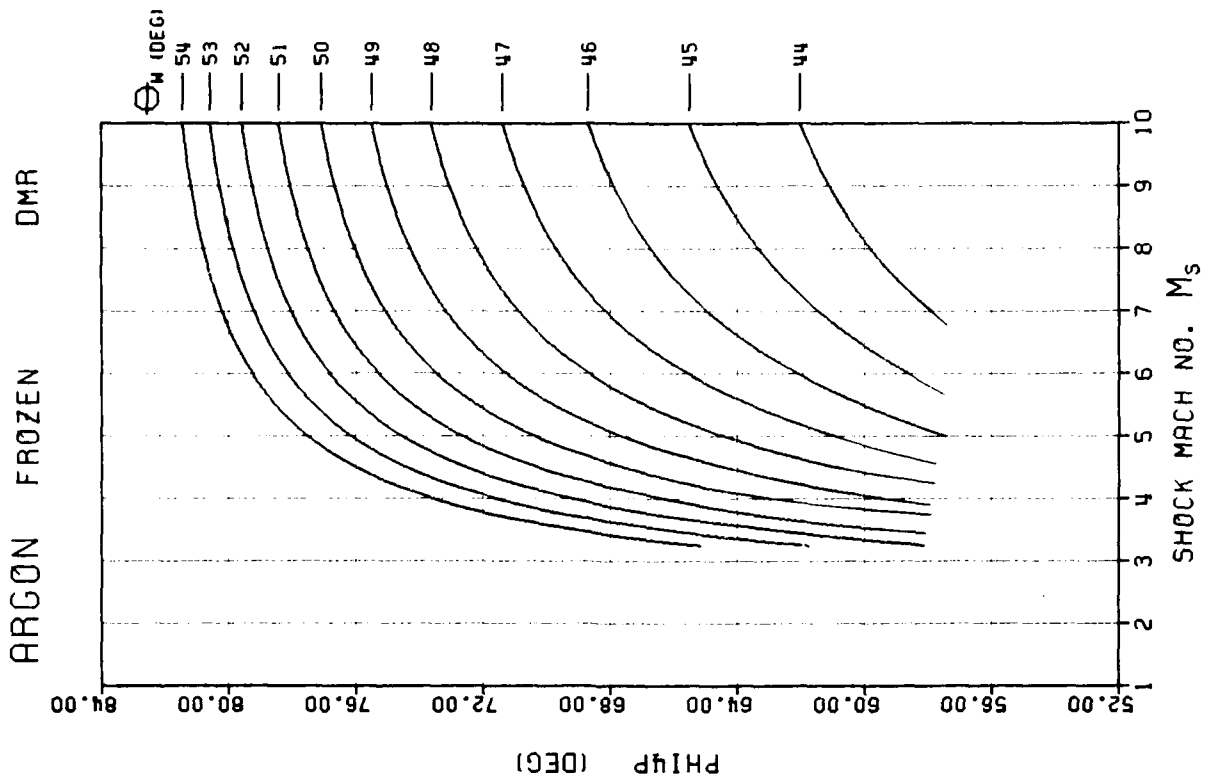


ARGON FROZEN DMR

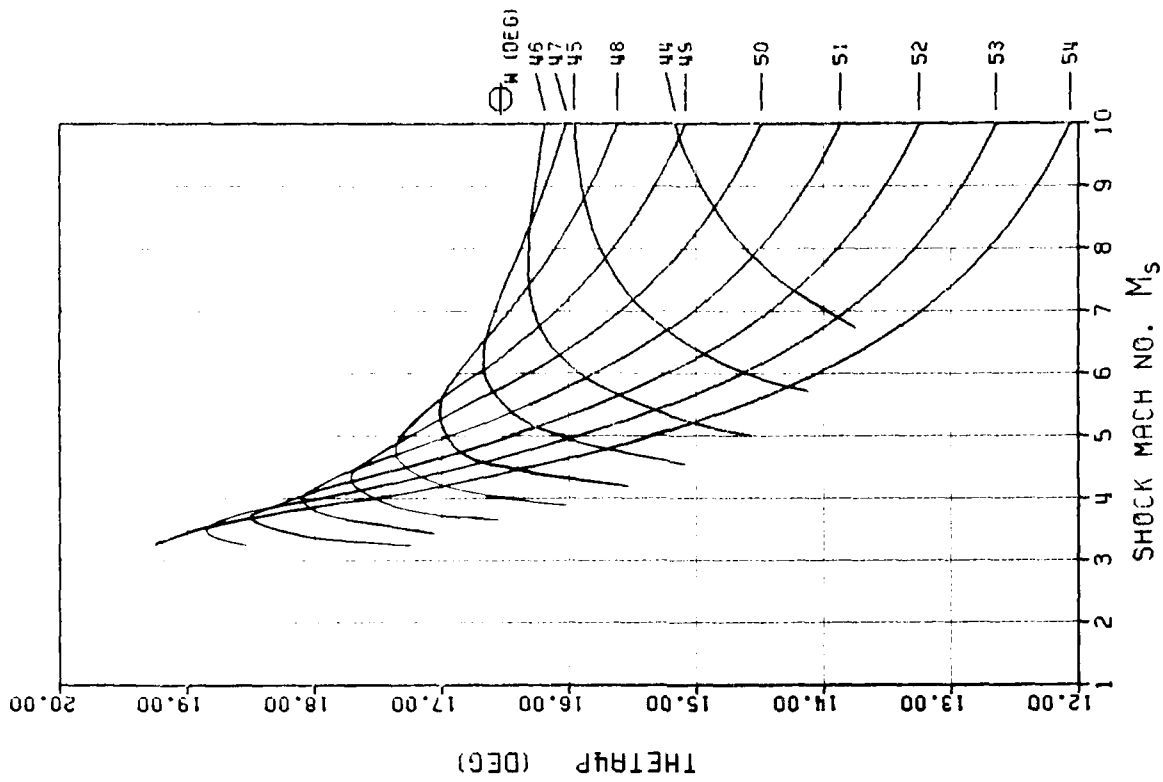




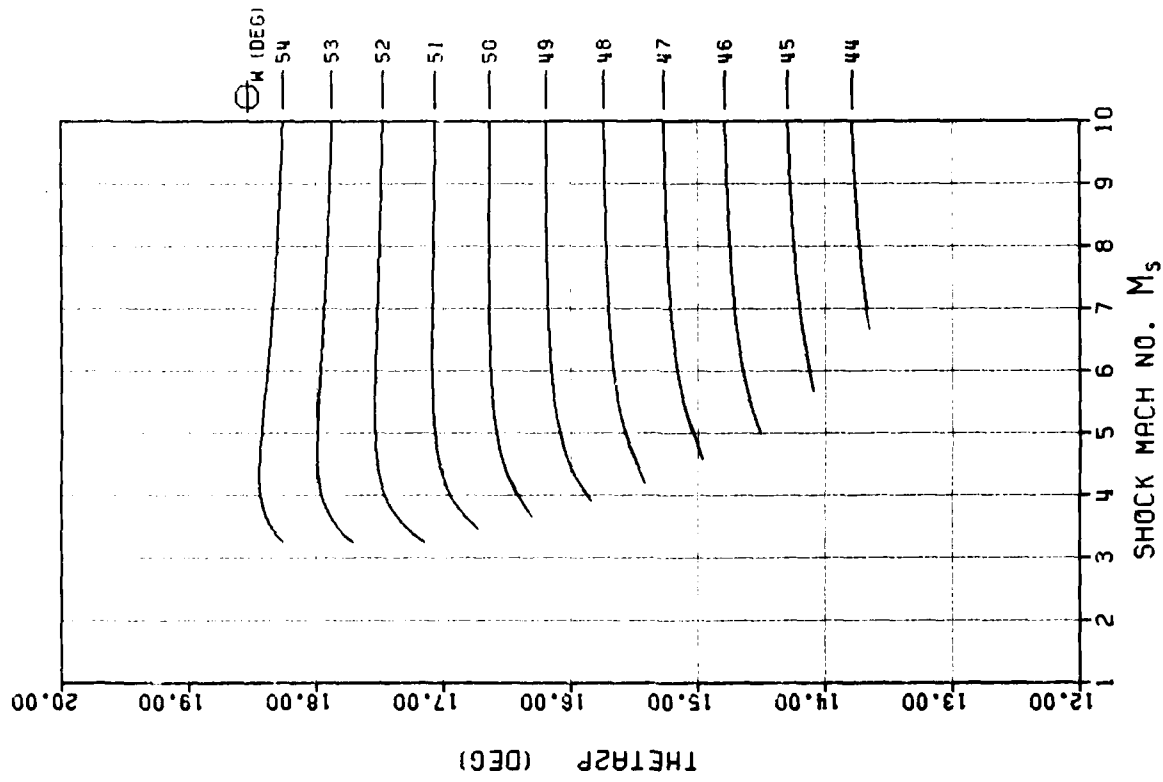


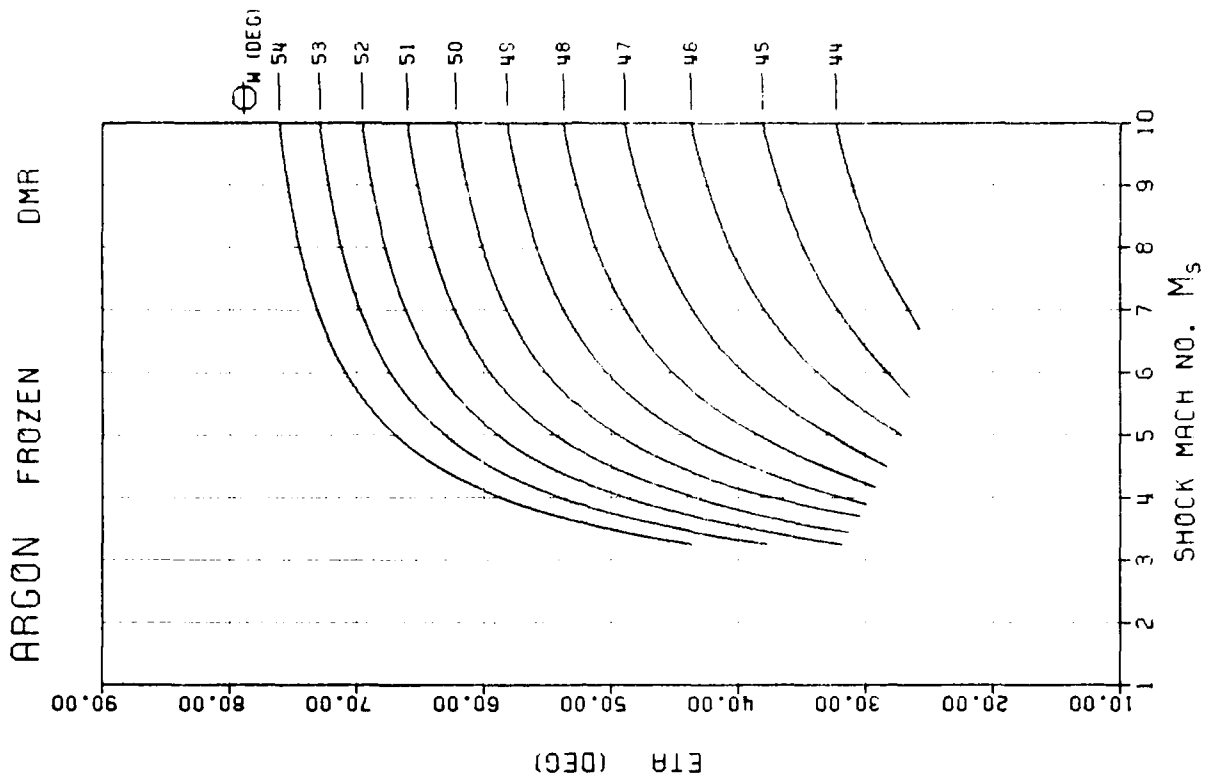
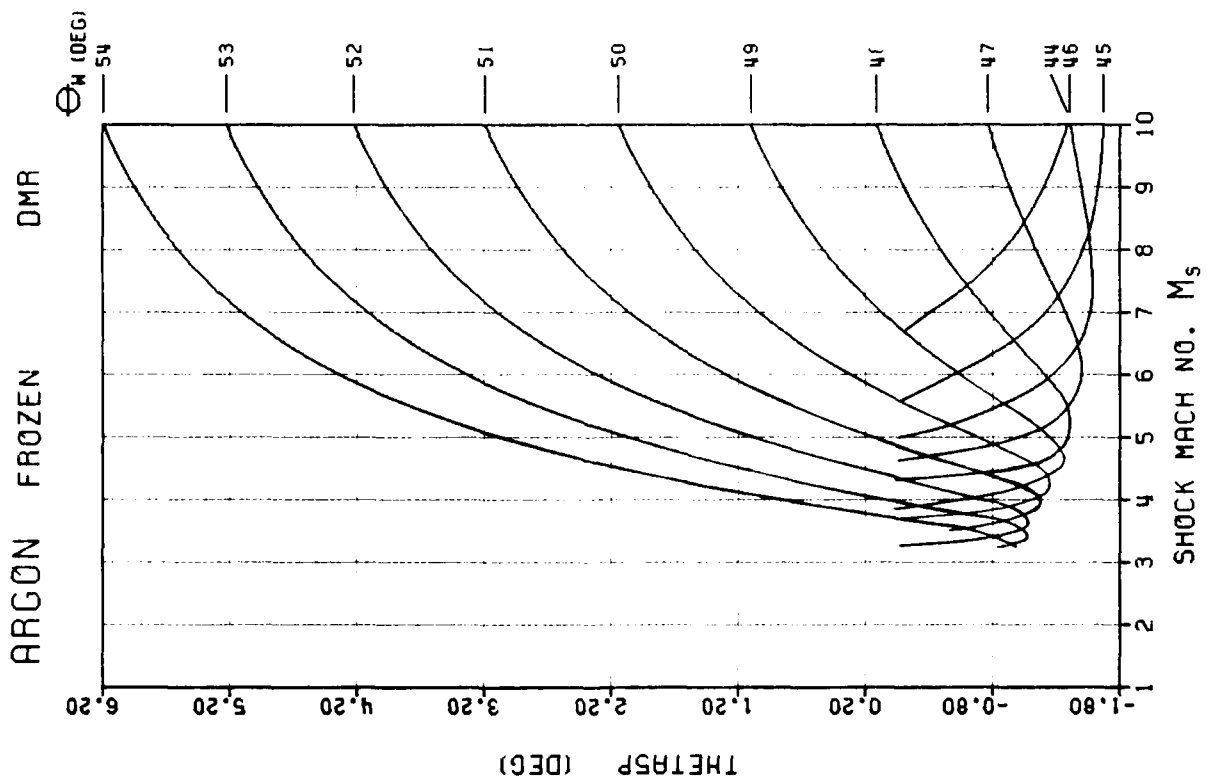


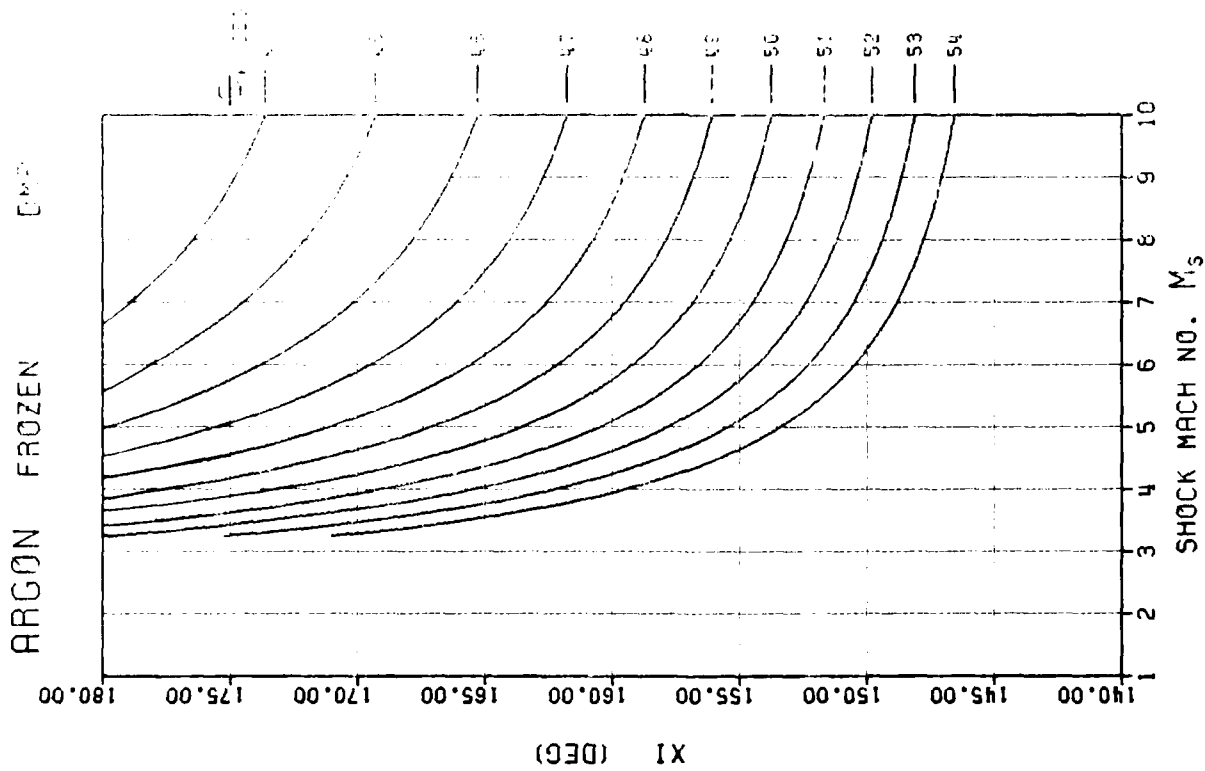
ARGON FROZEN DMP

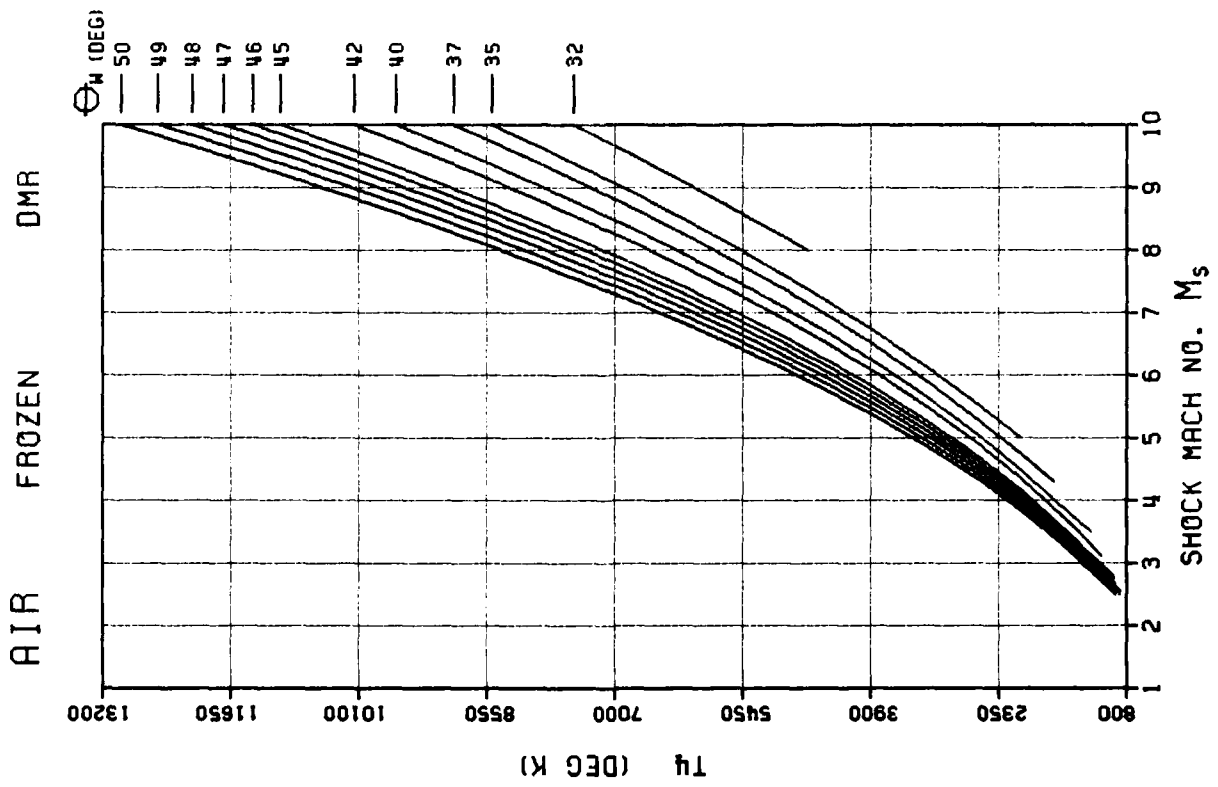
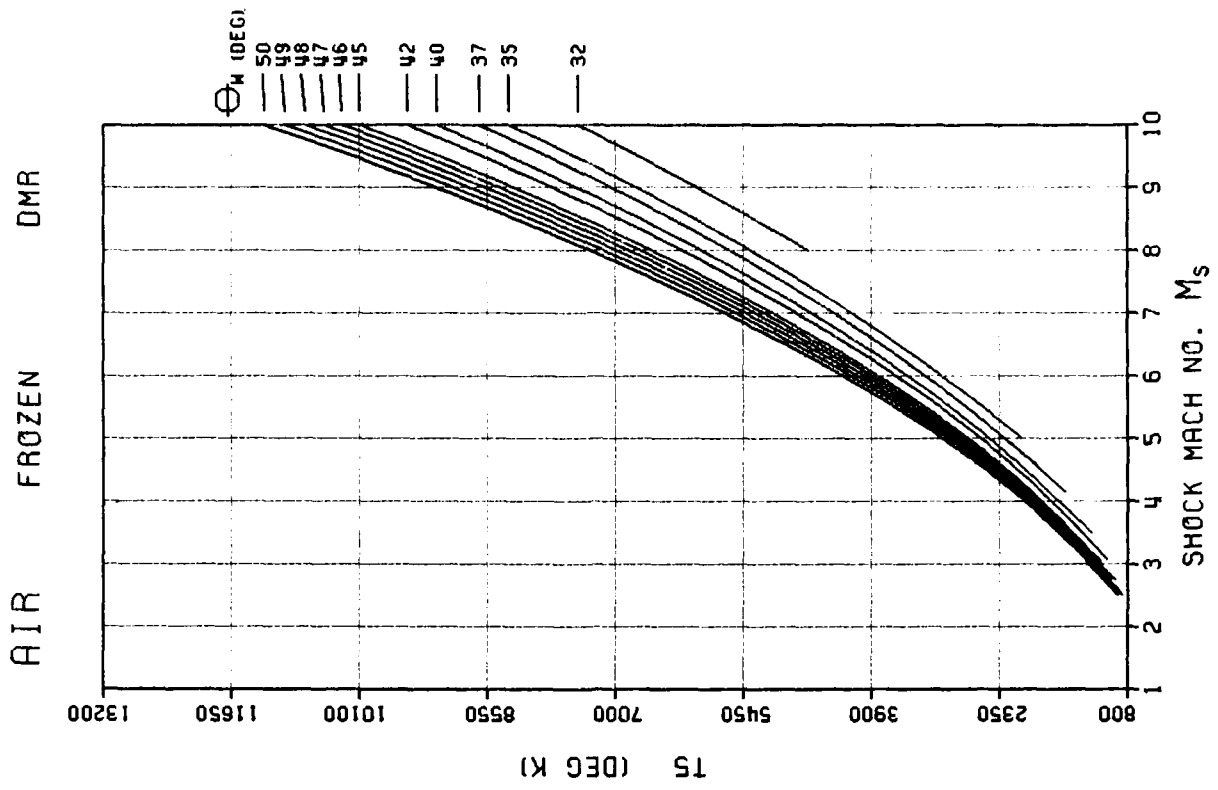


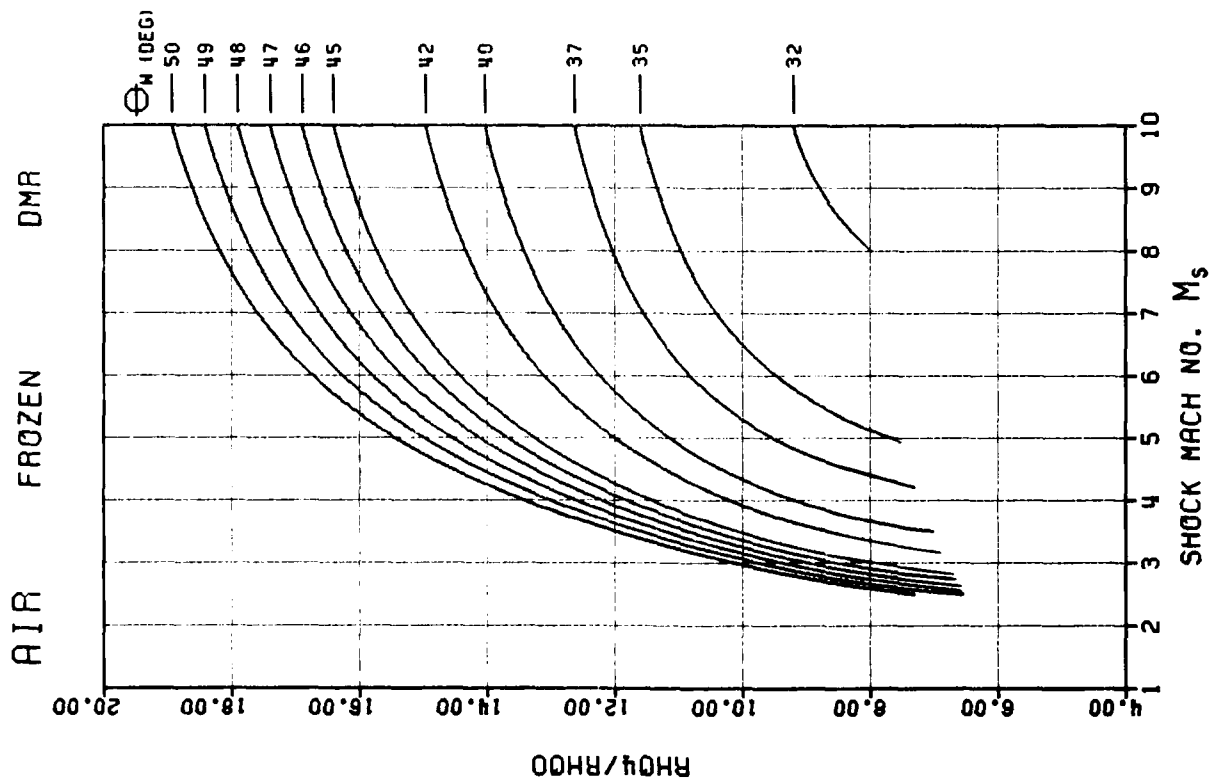
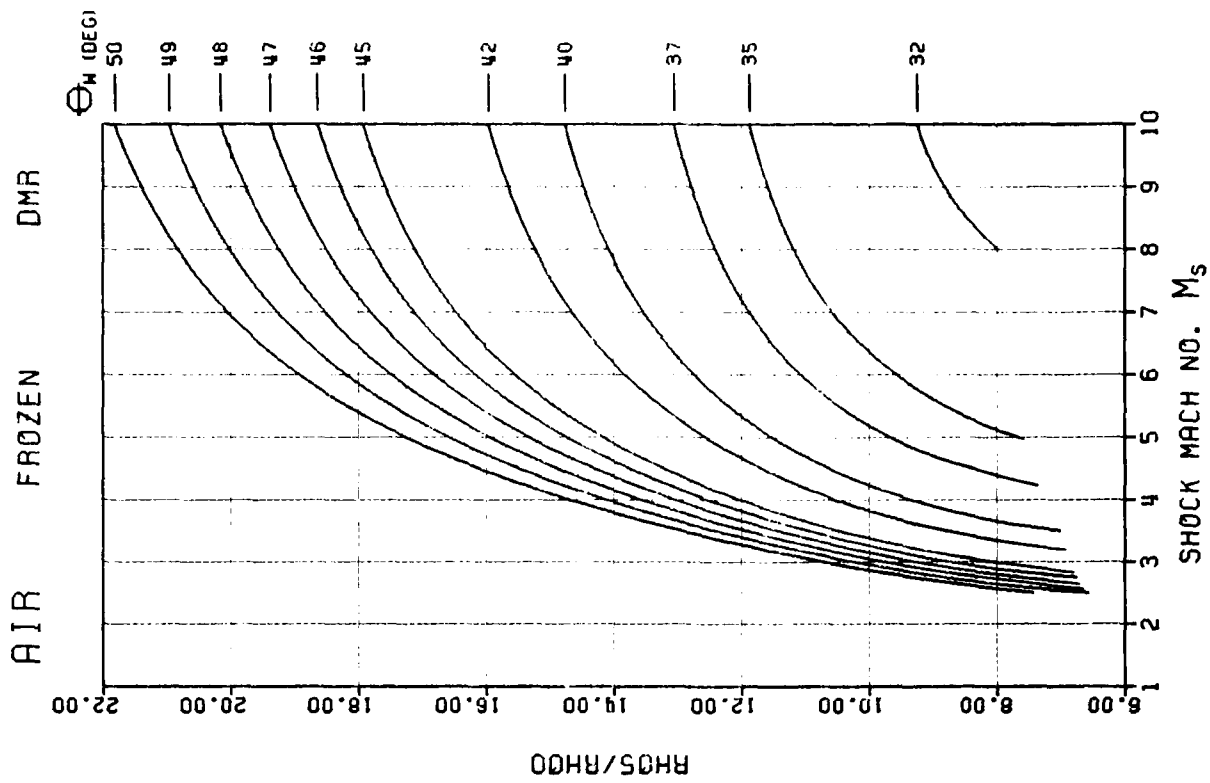
ARGON FROZEN DMP

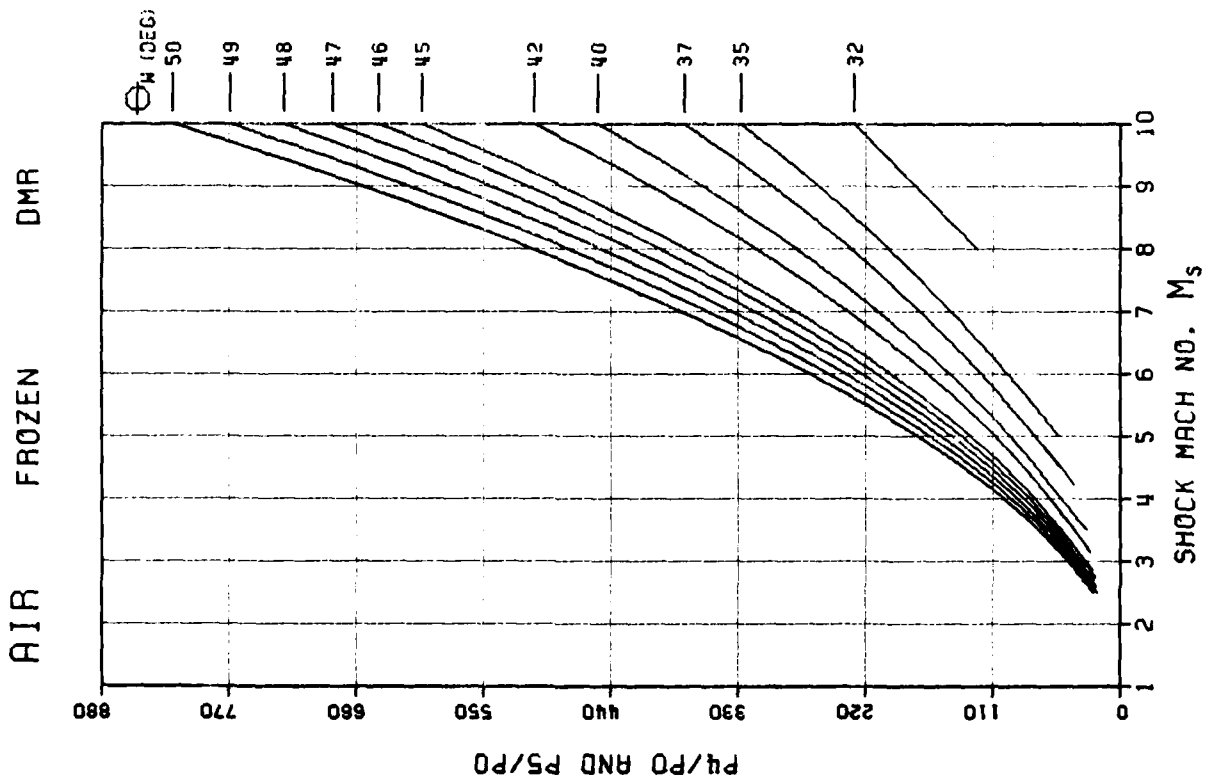
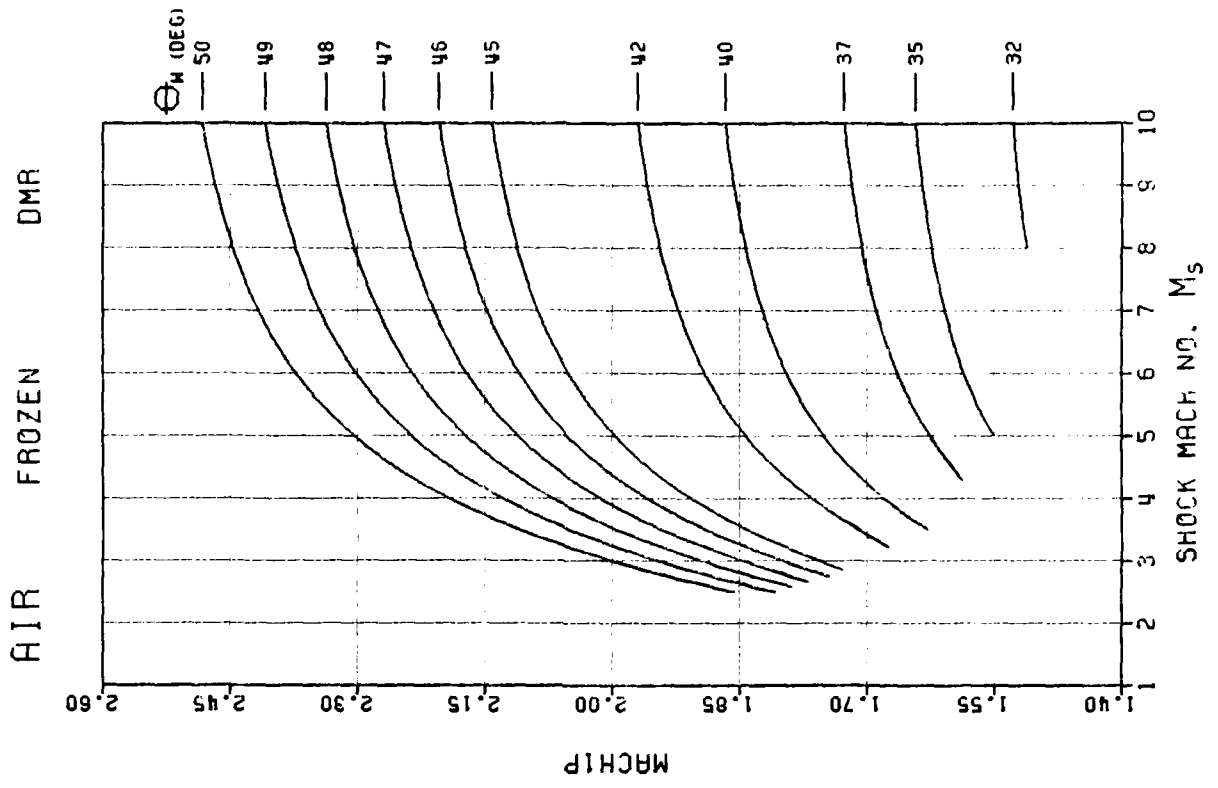


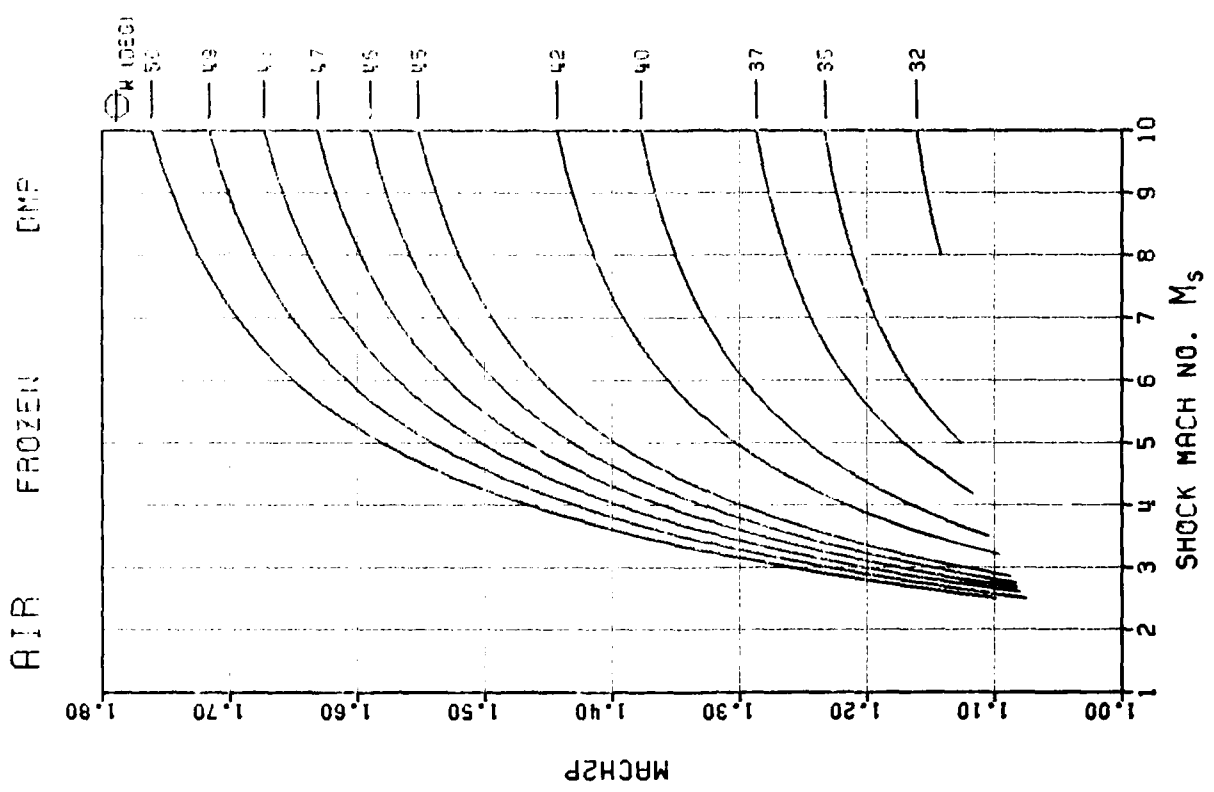
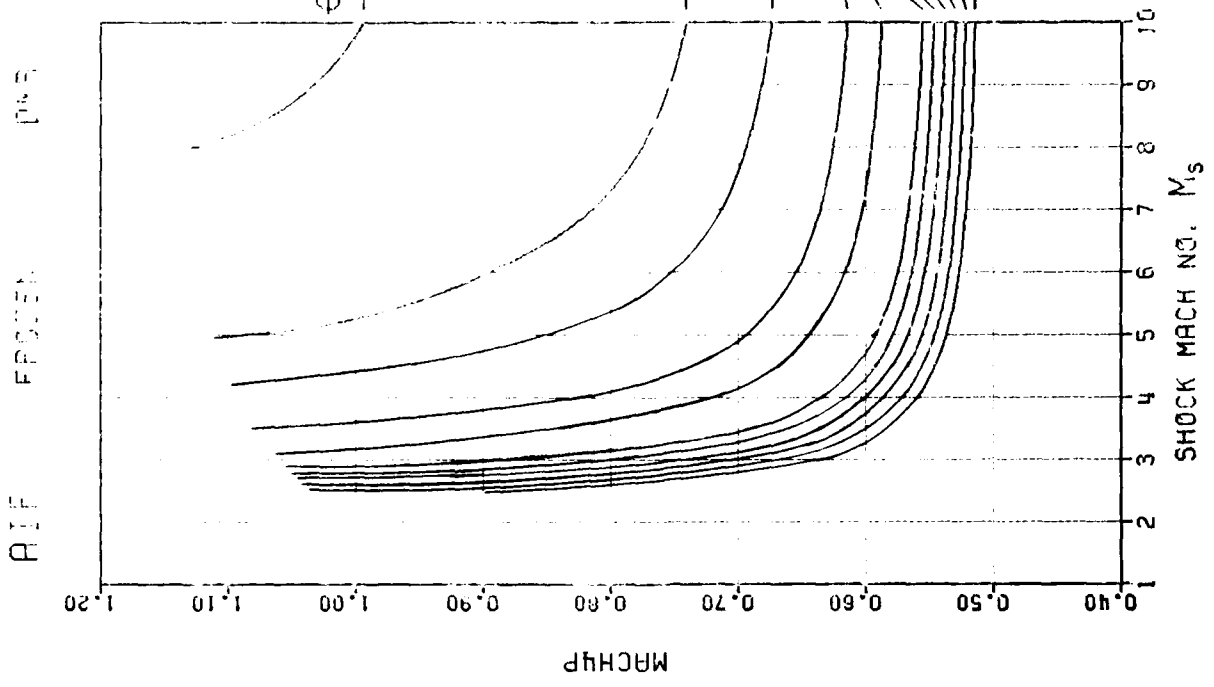


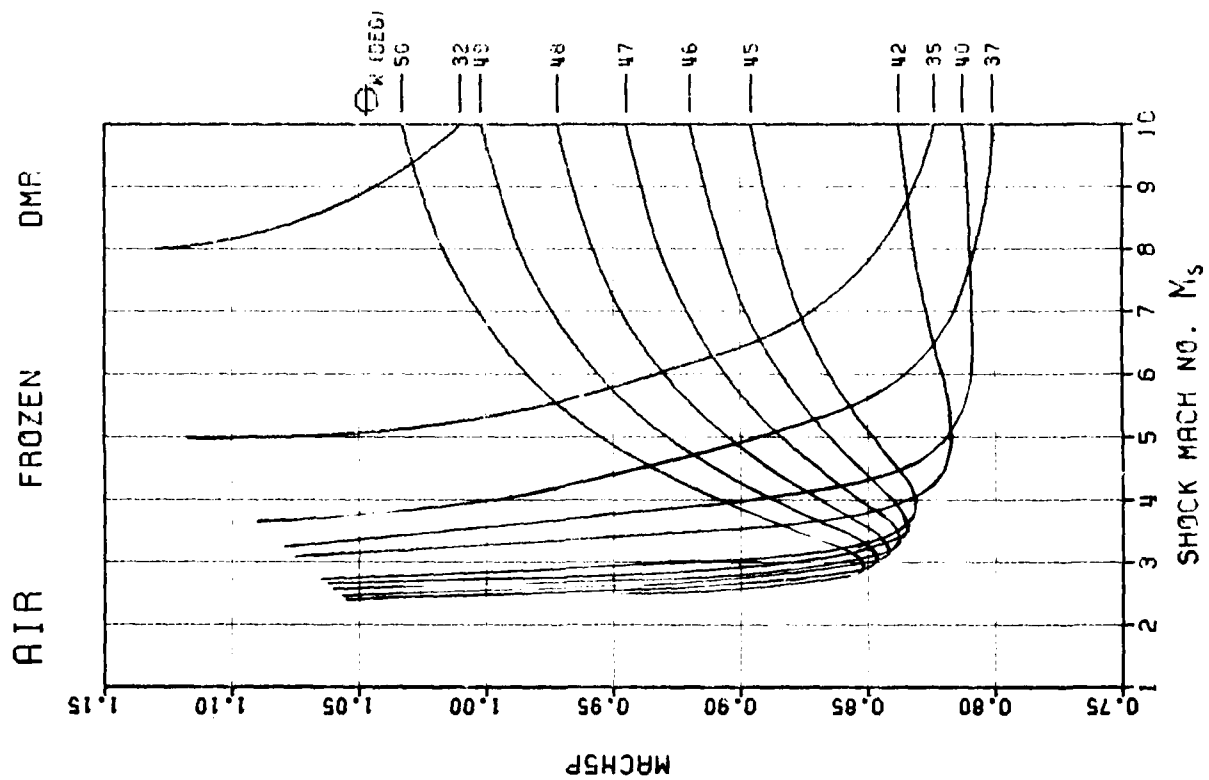
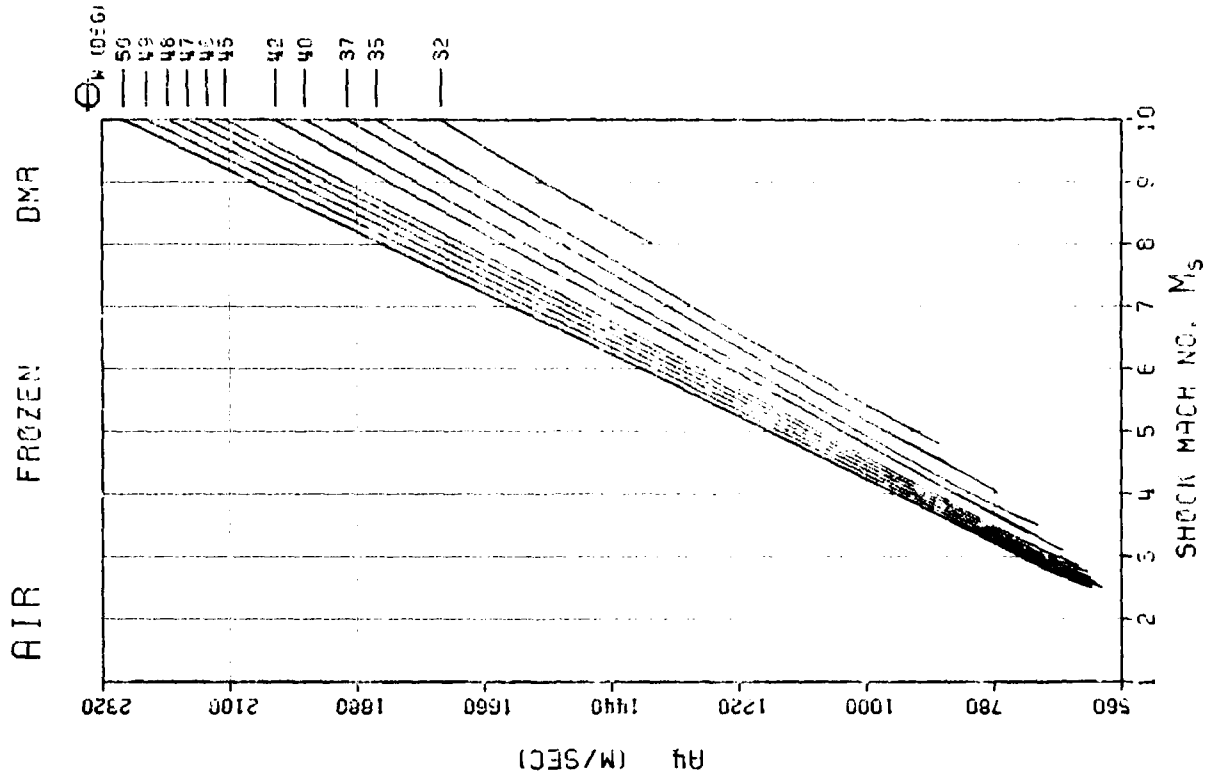


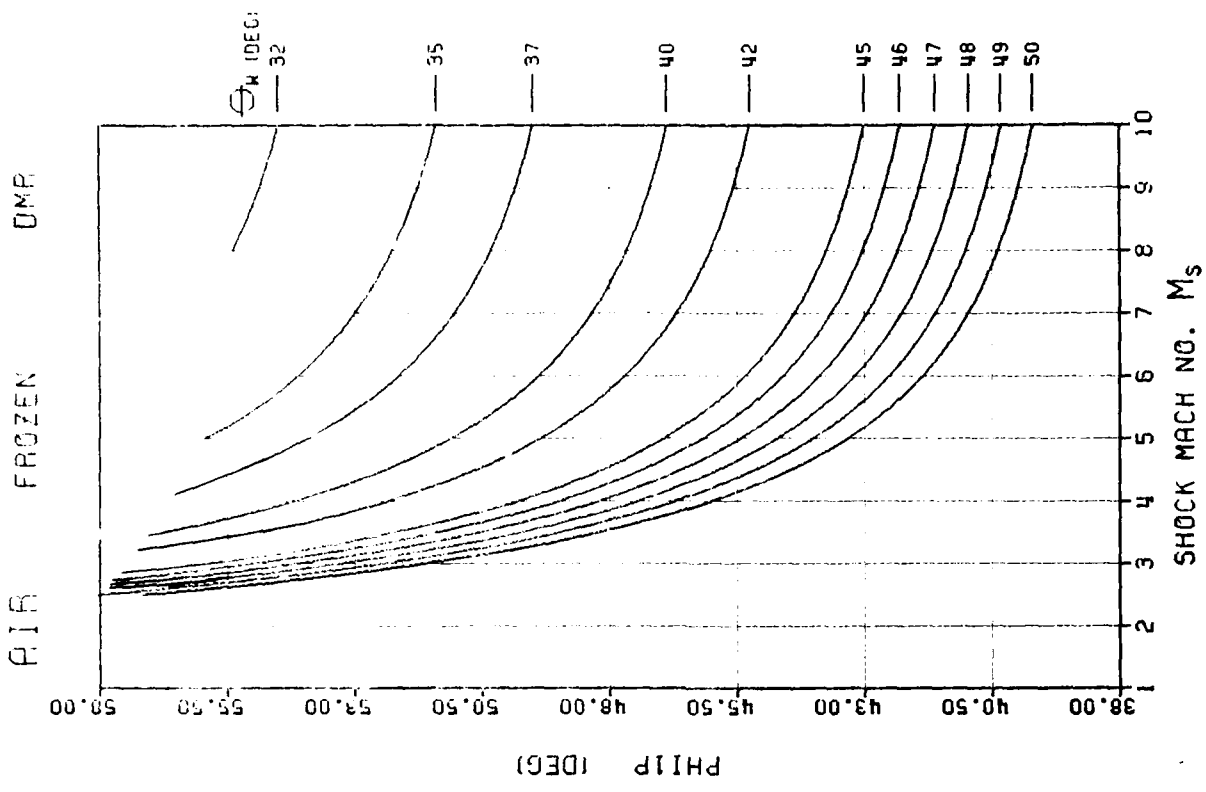
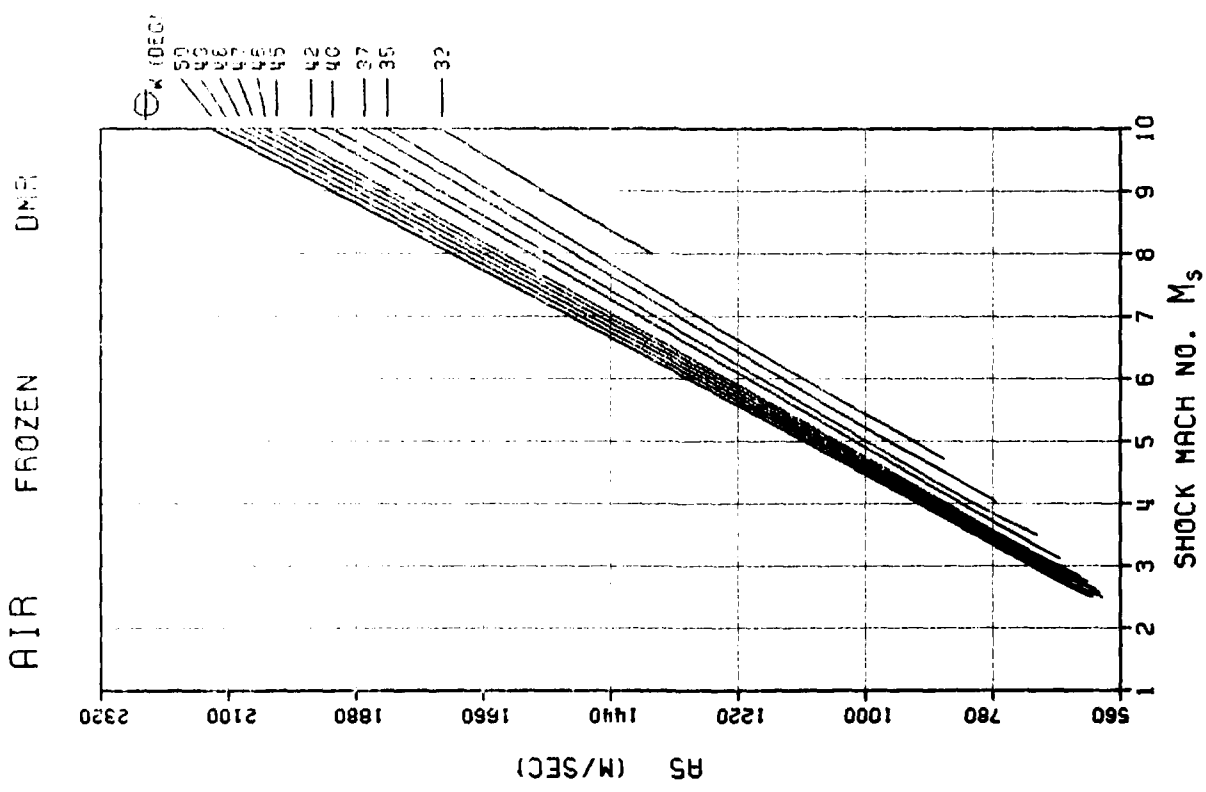


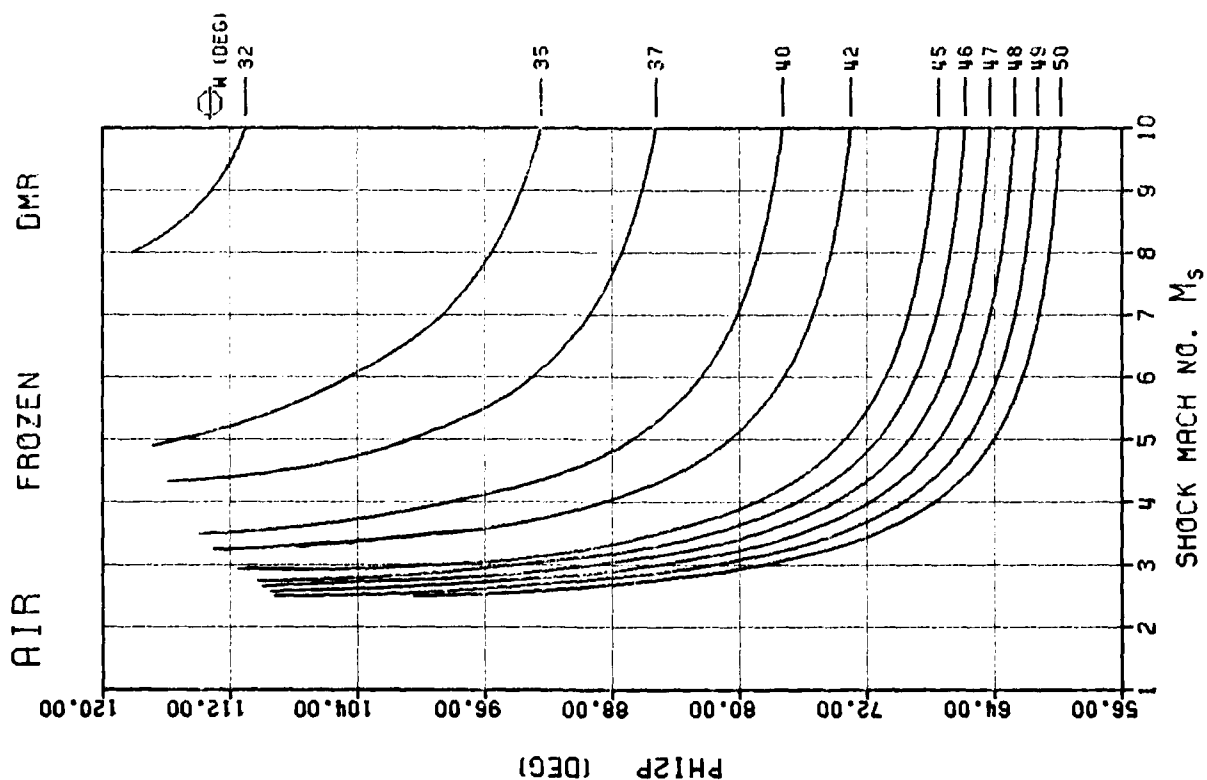
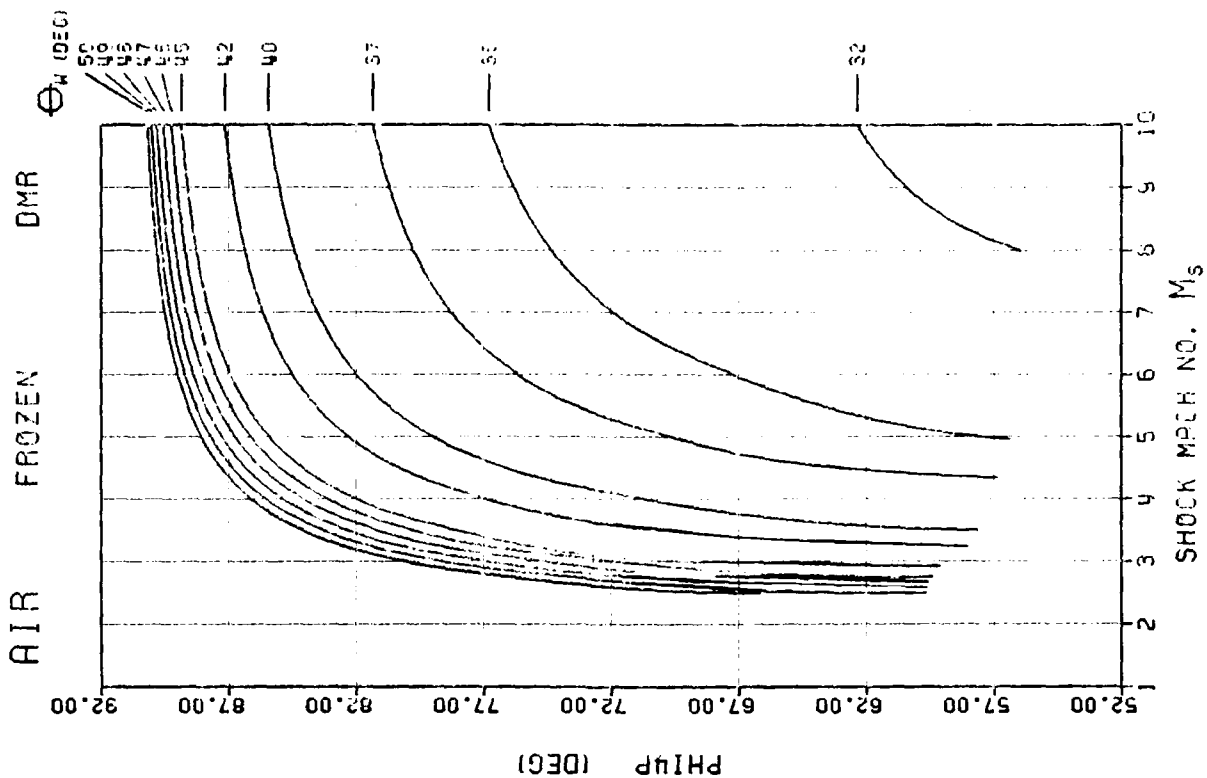


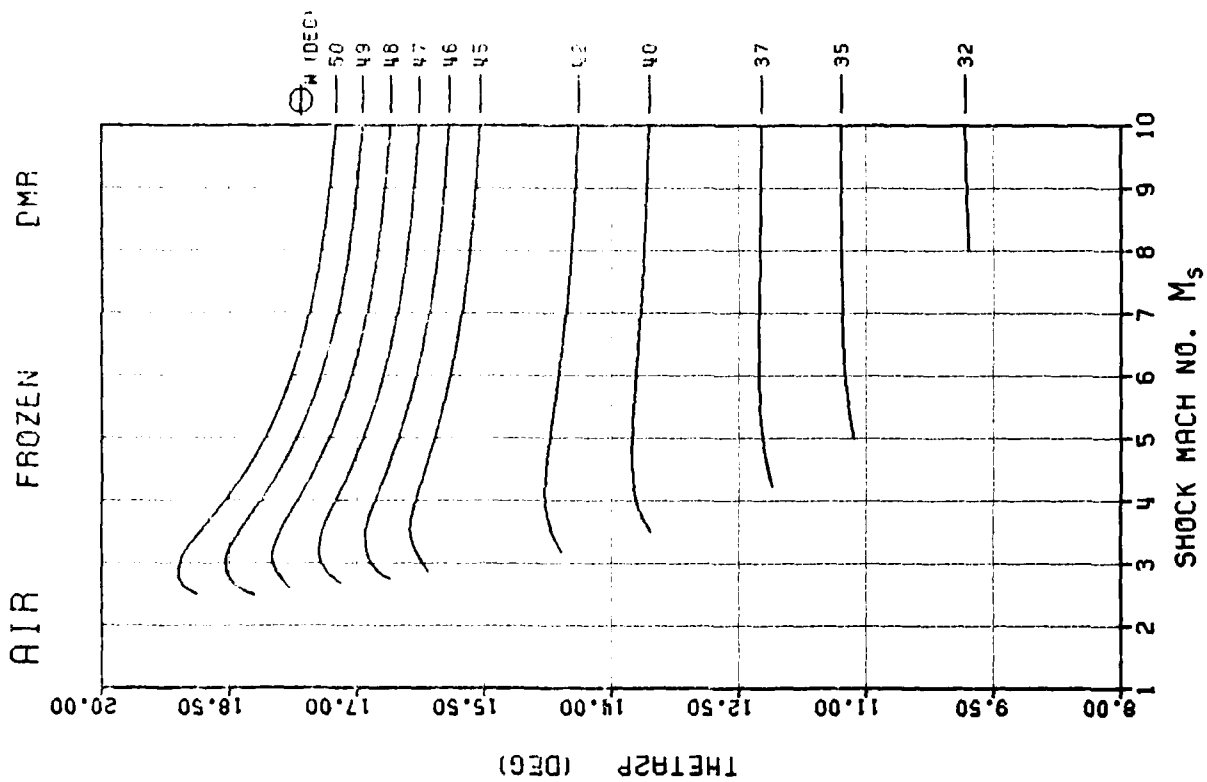
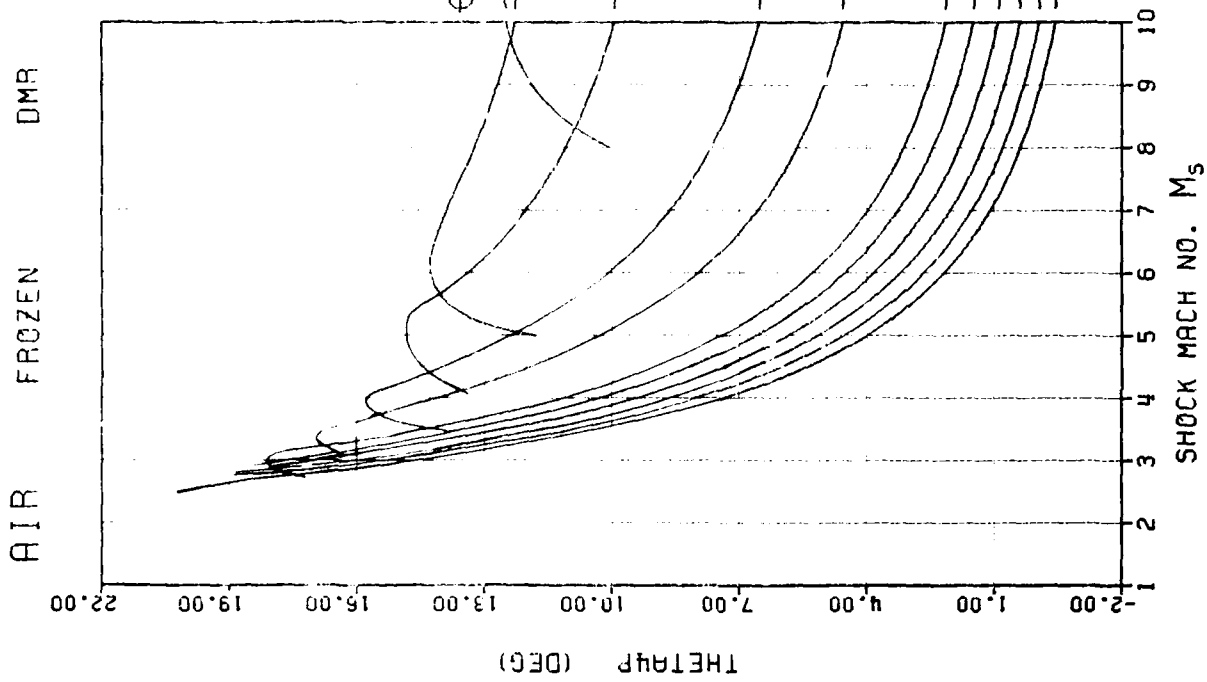


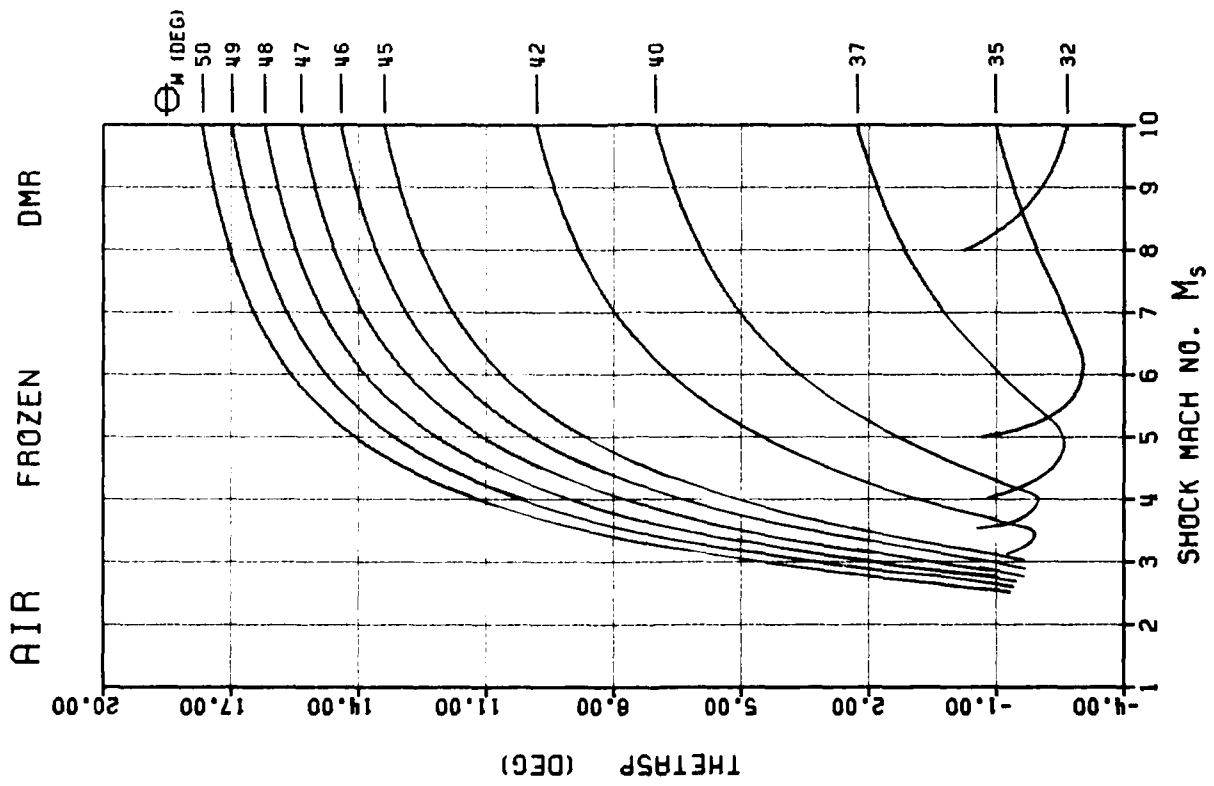
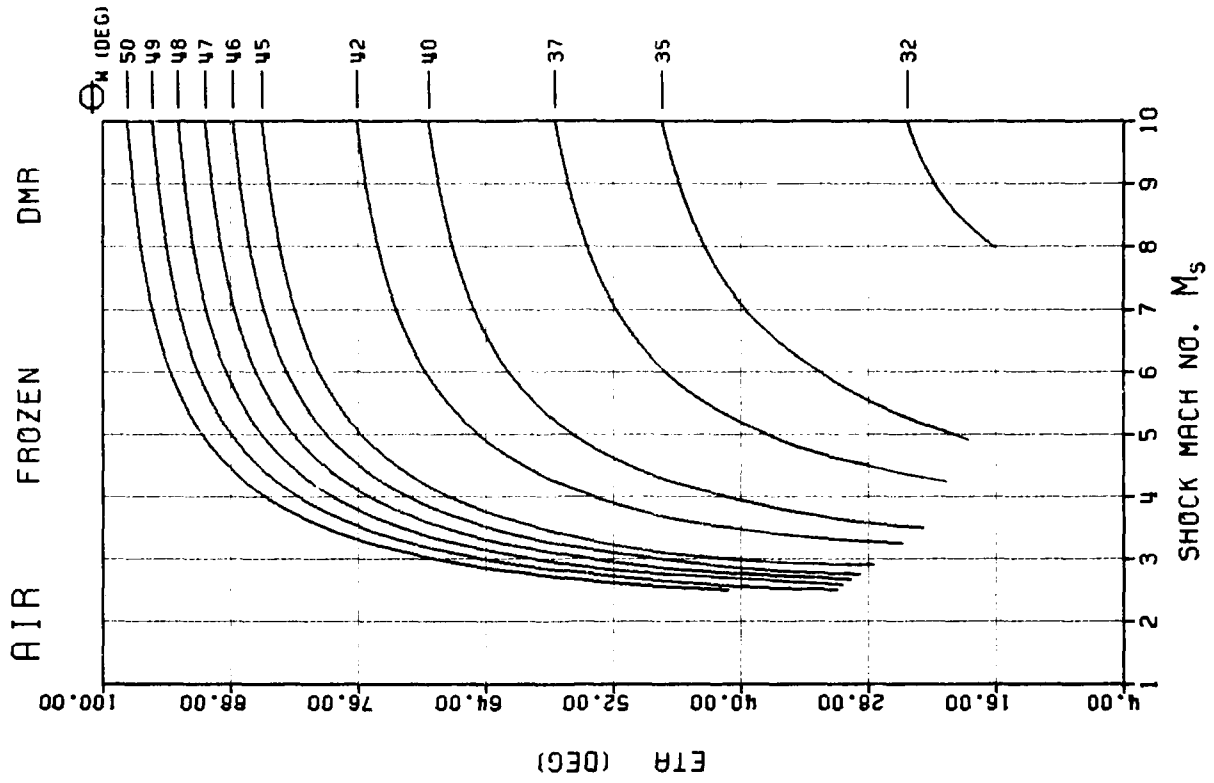


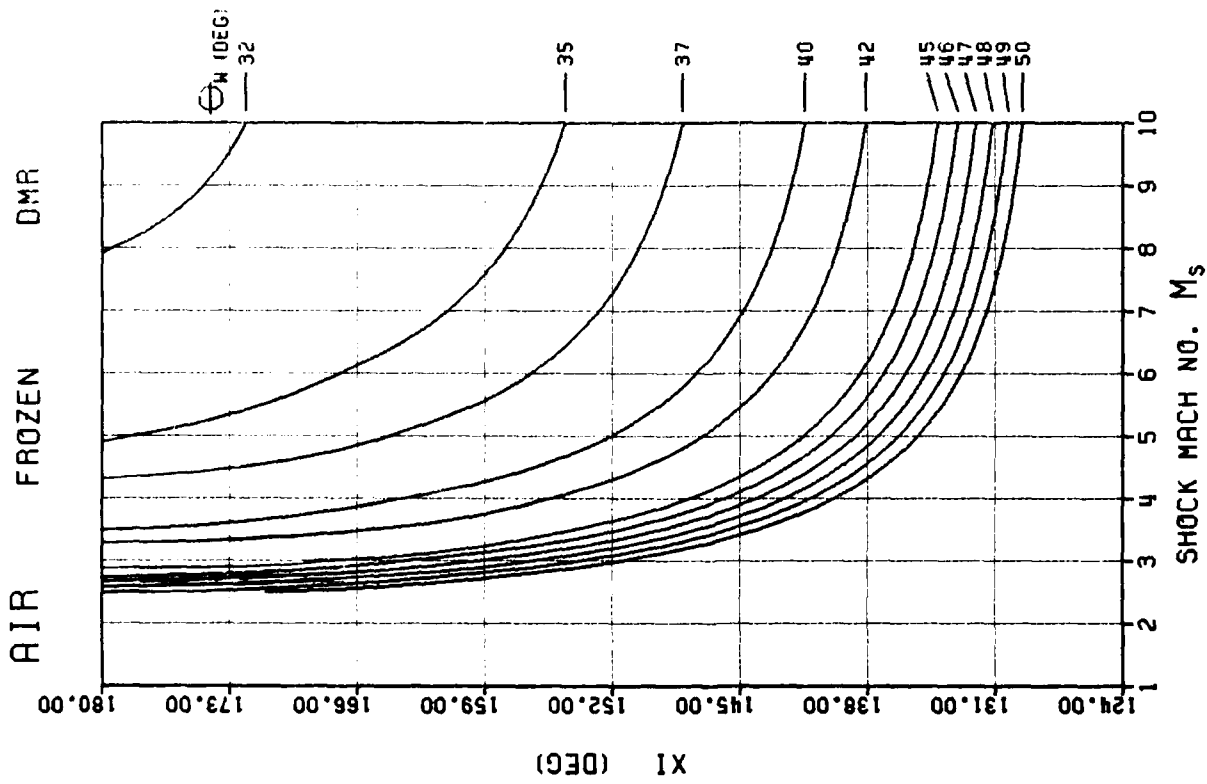


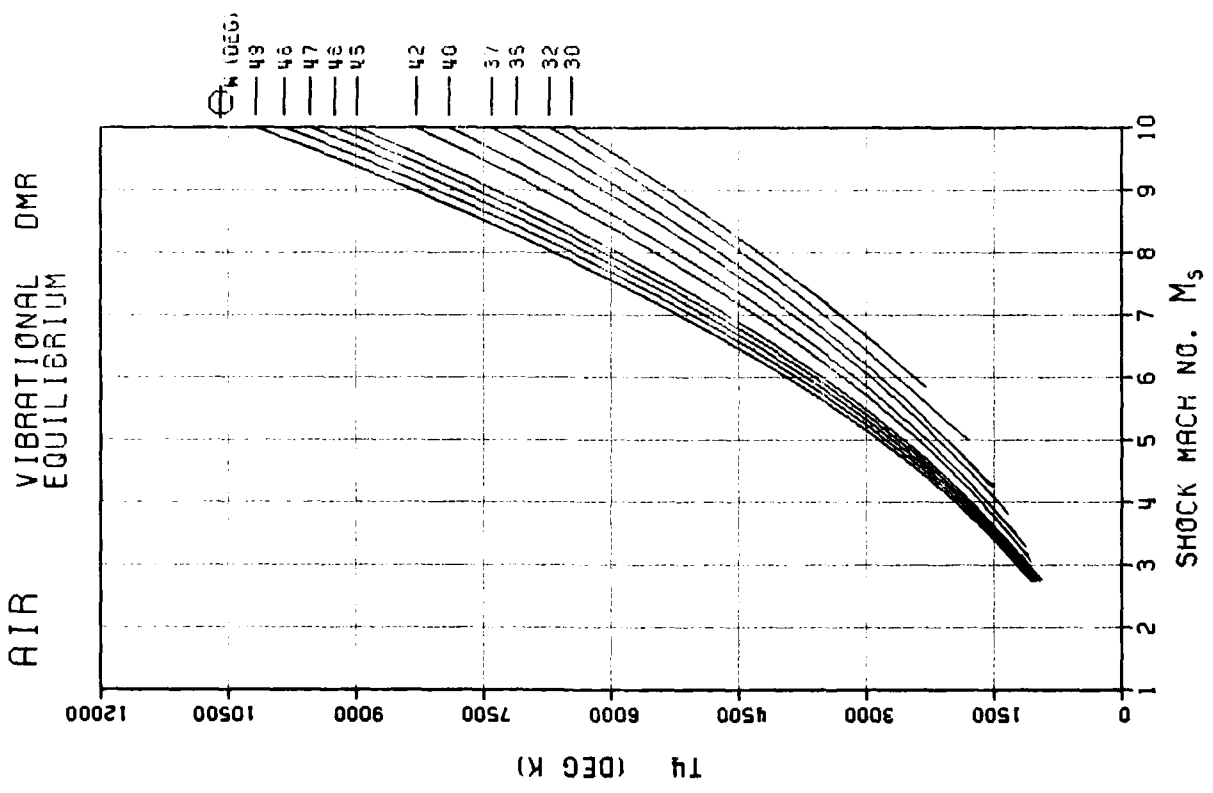
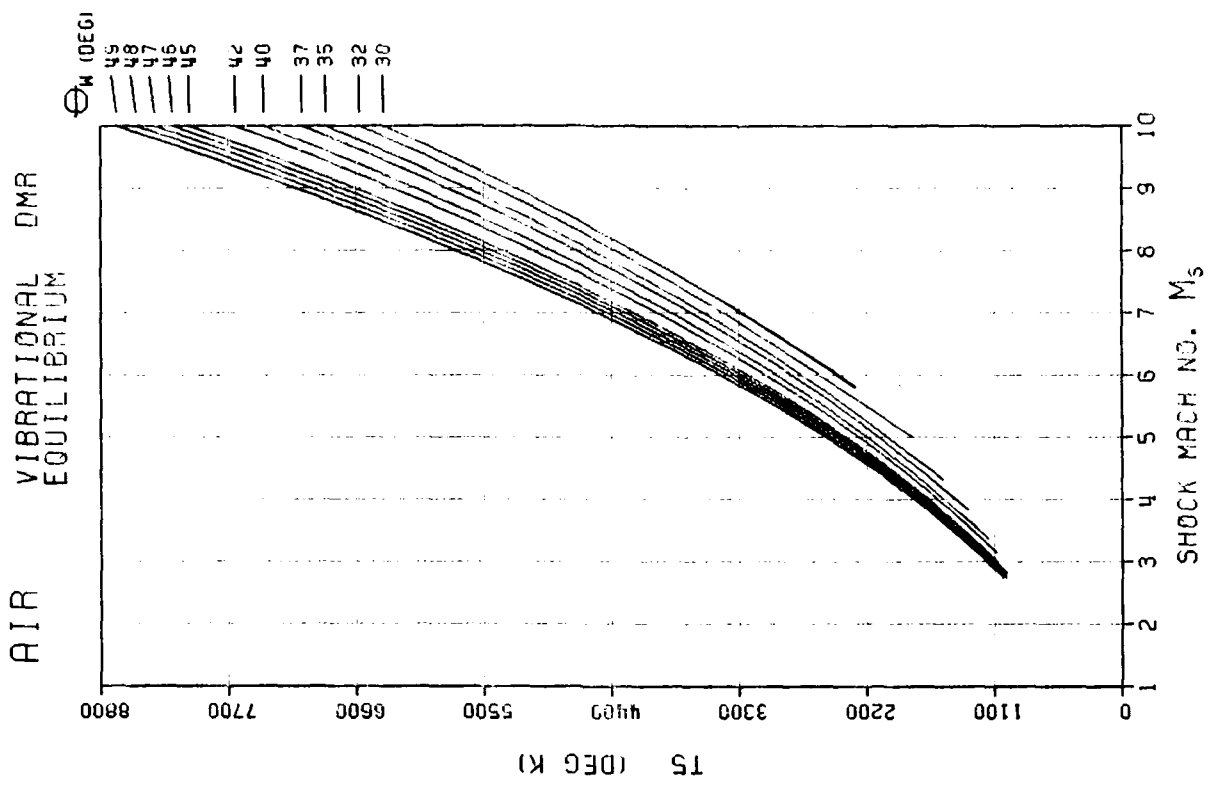


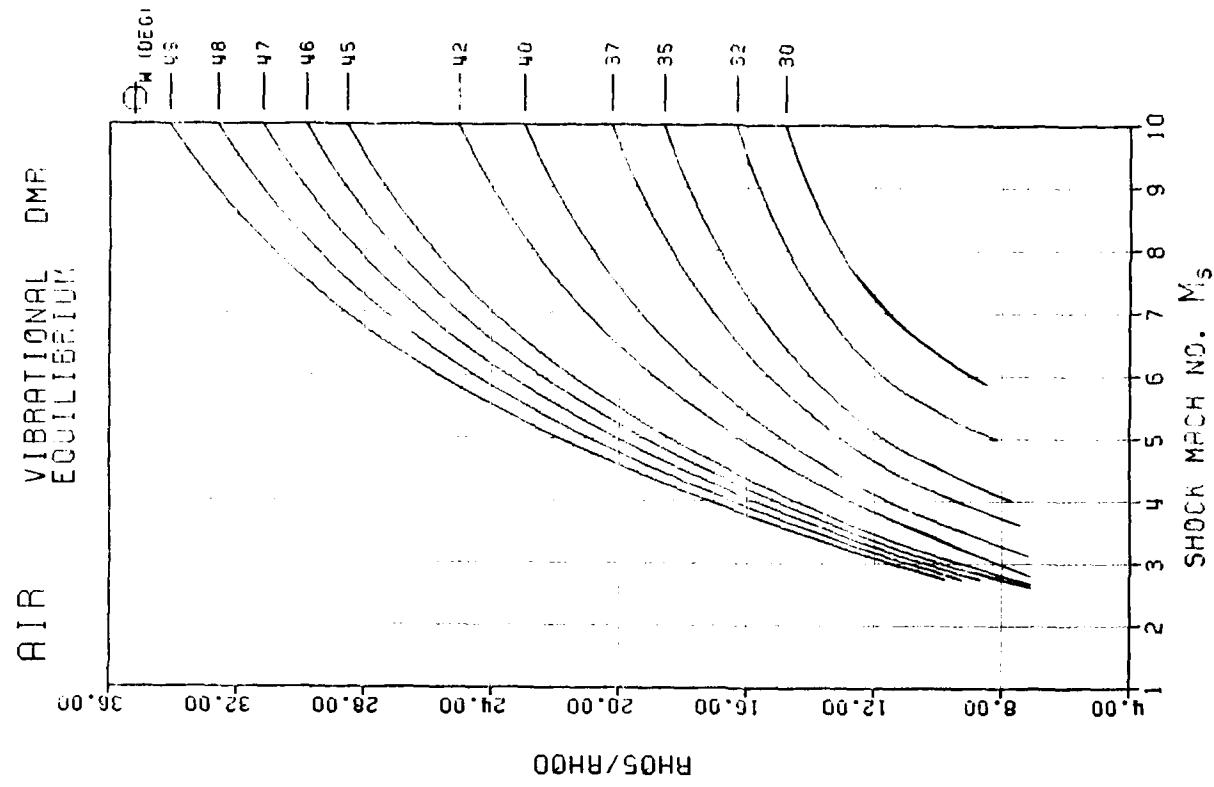
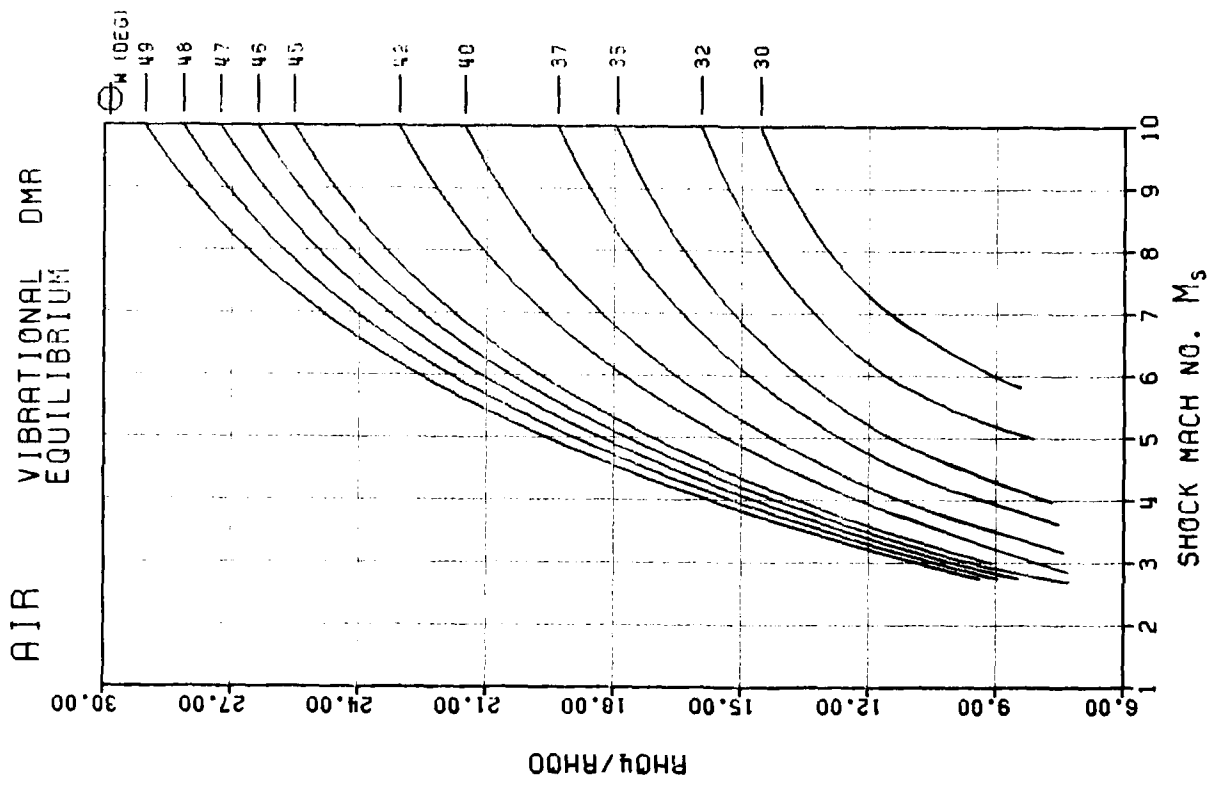


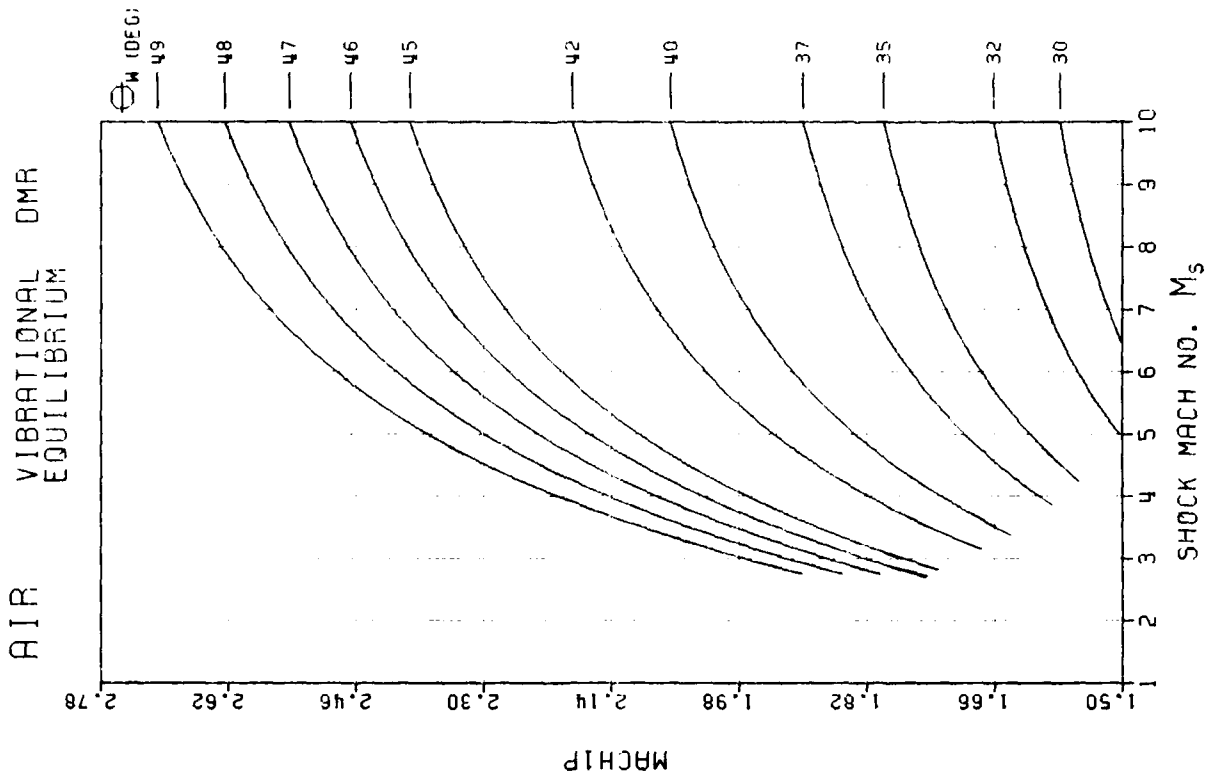
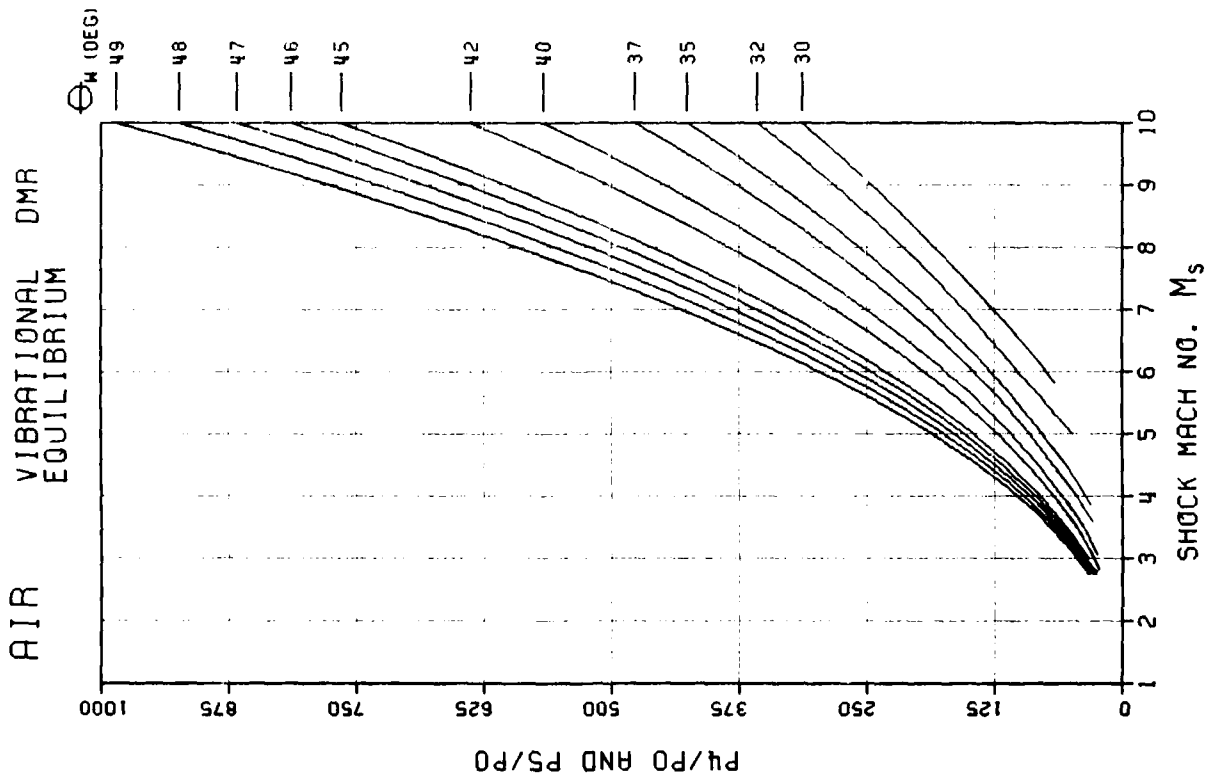


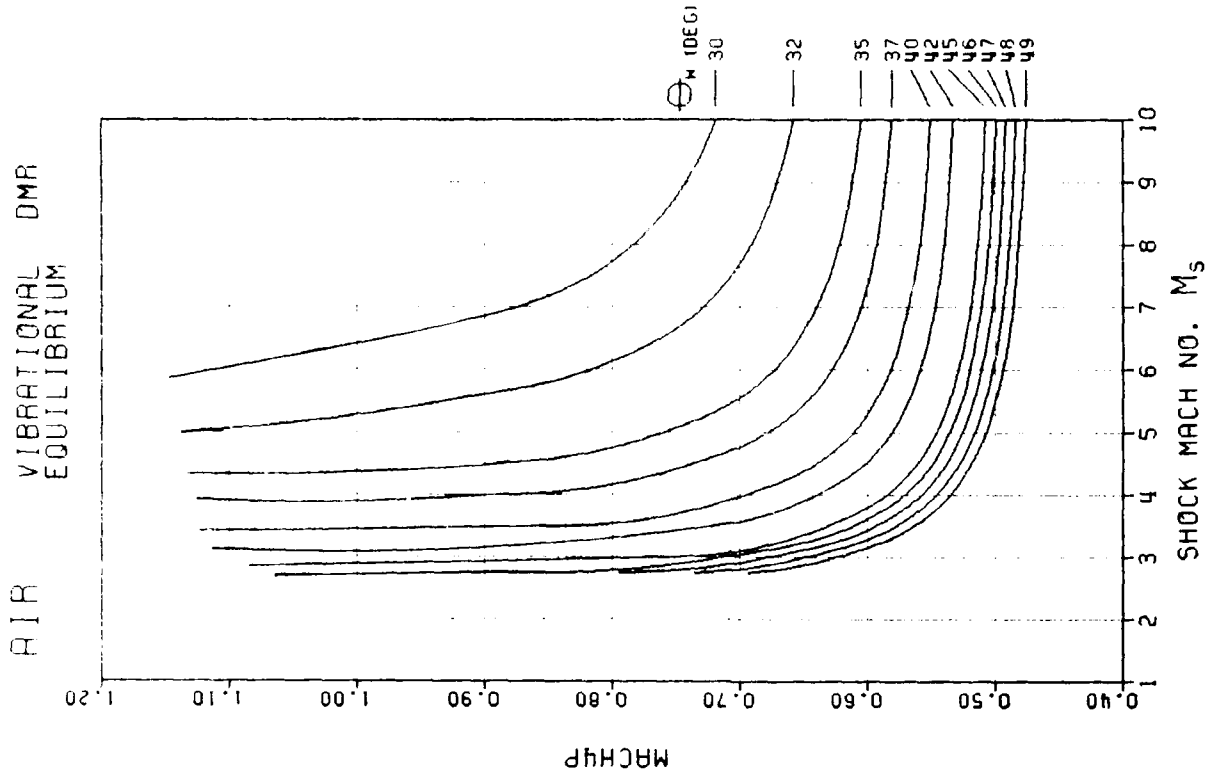
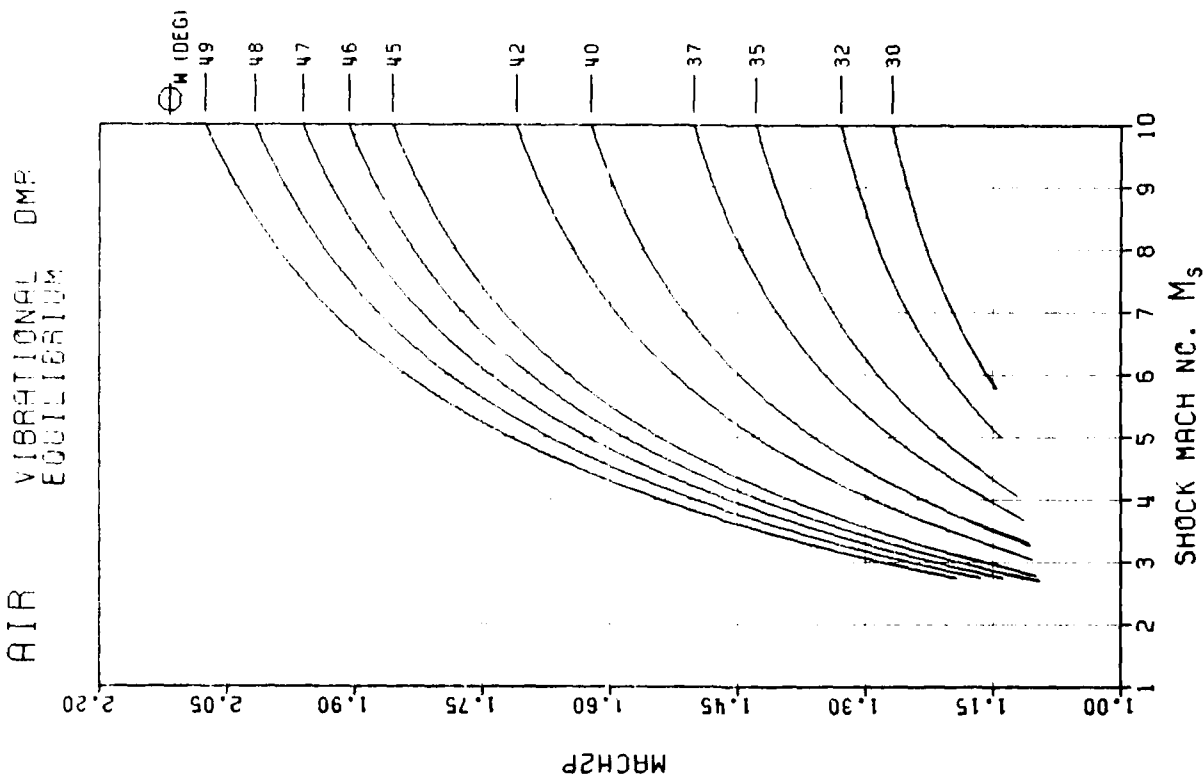


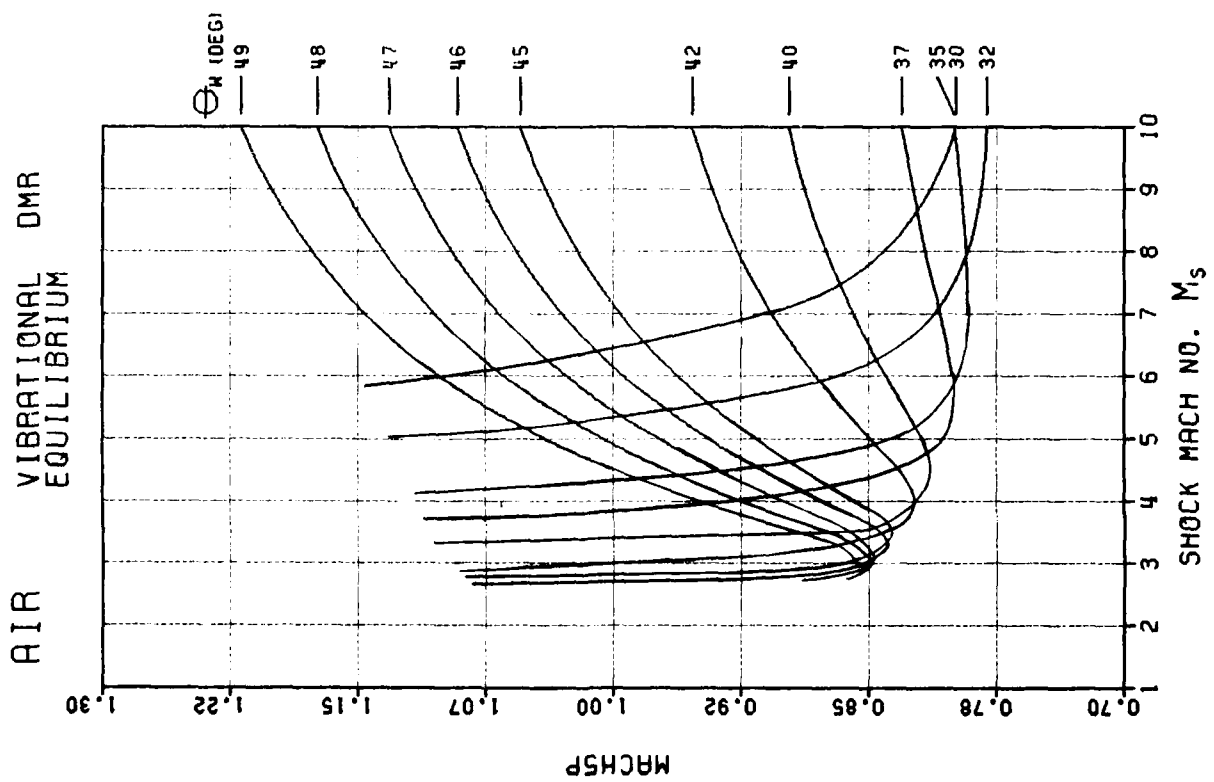
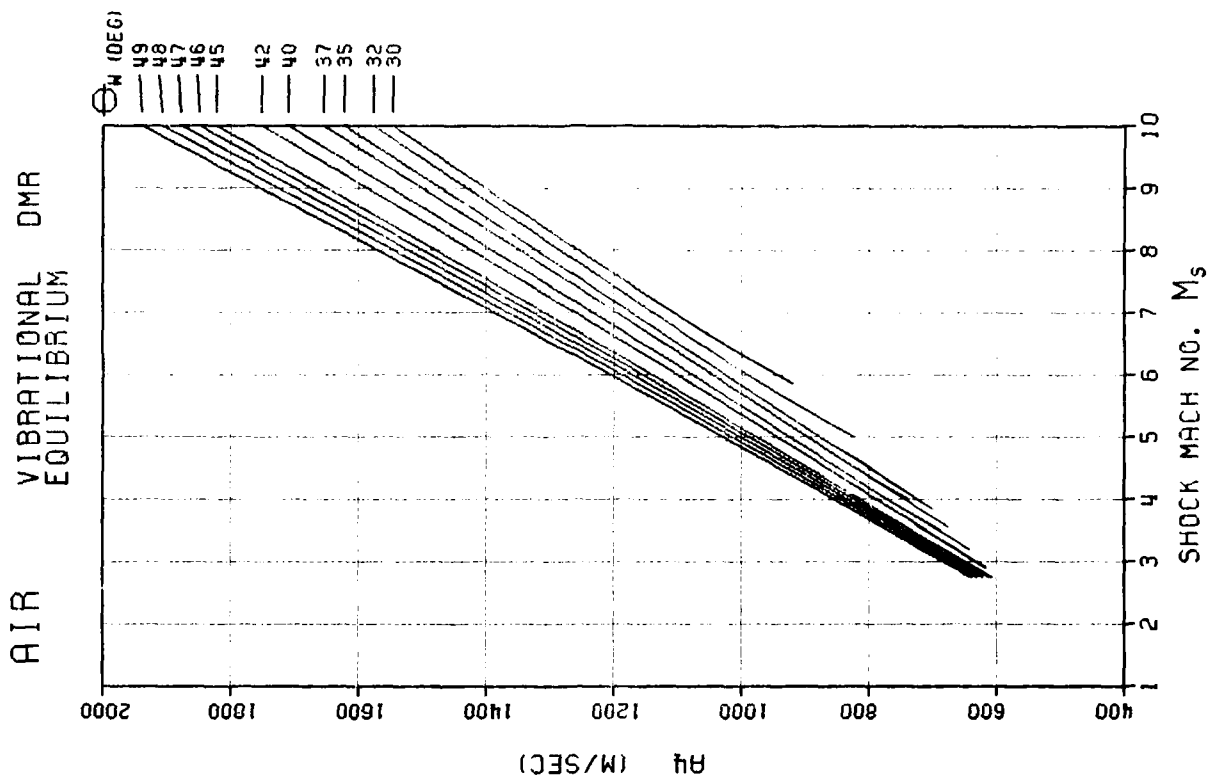


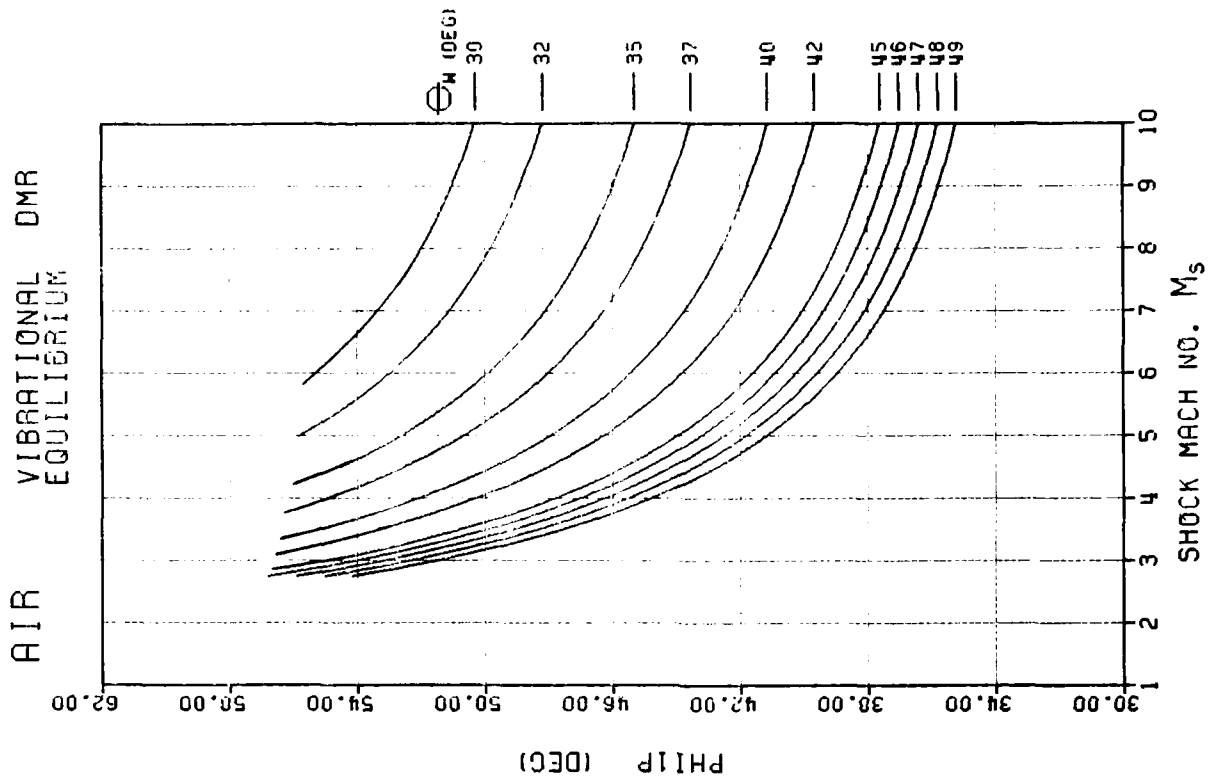
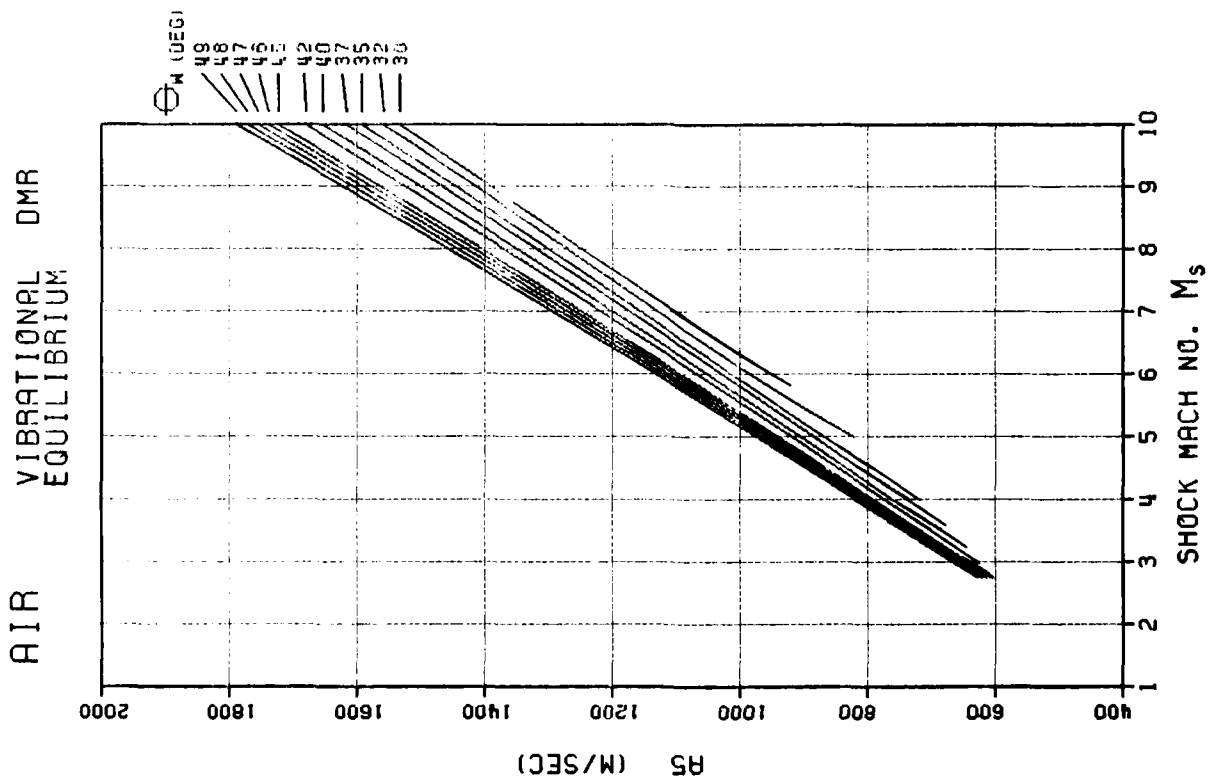


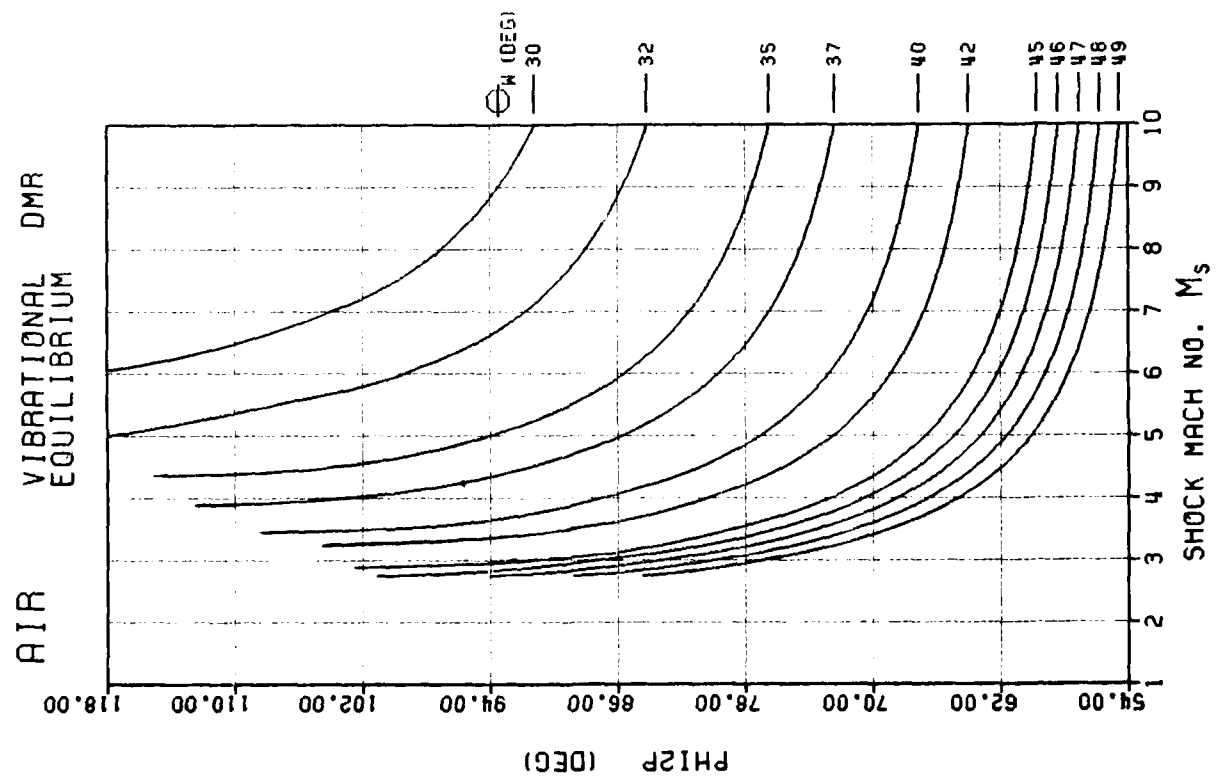
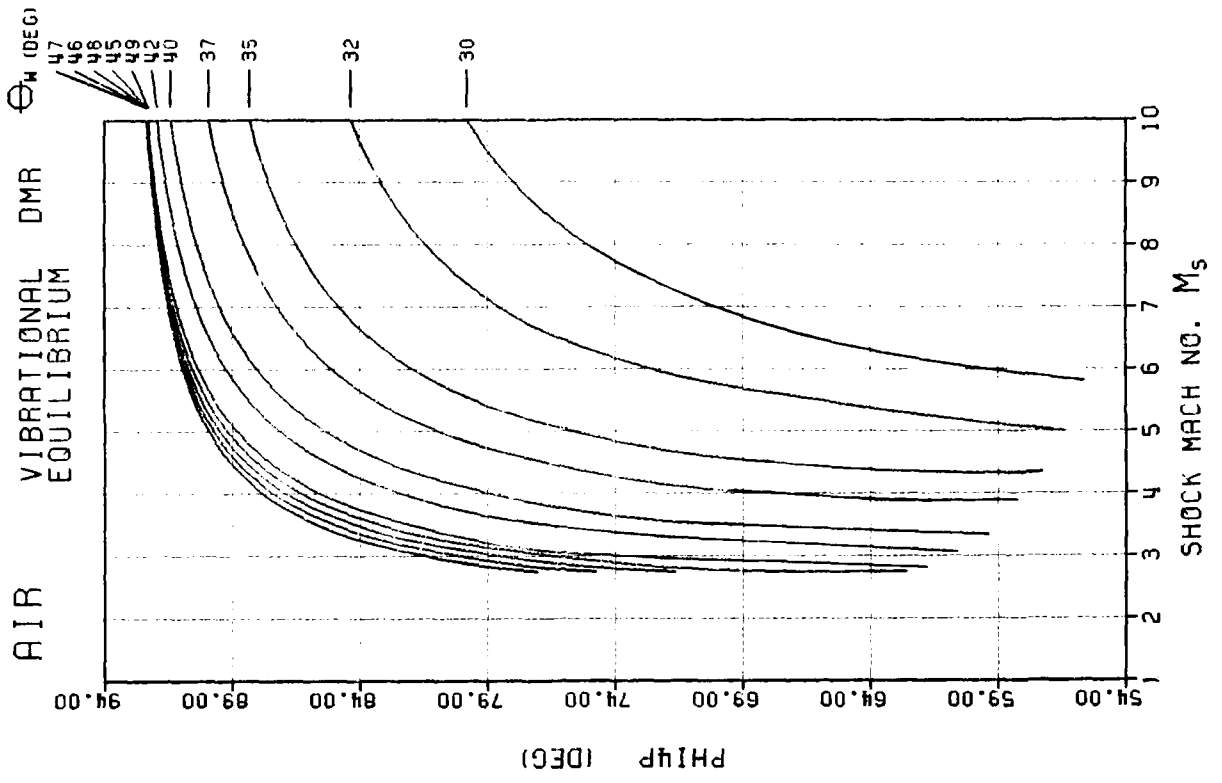


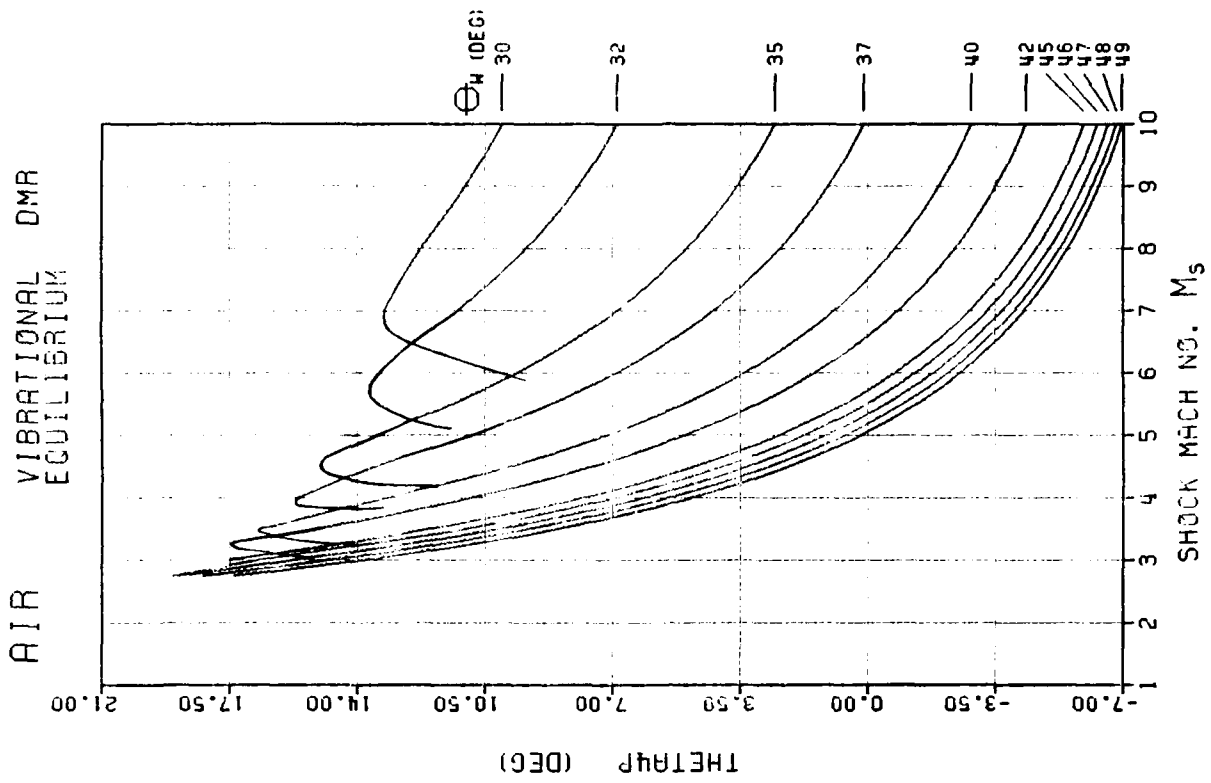
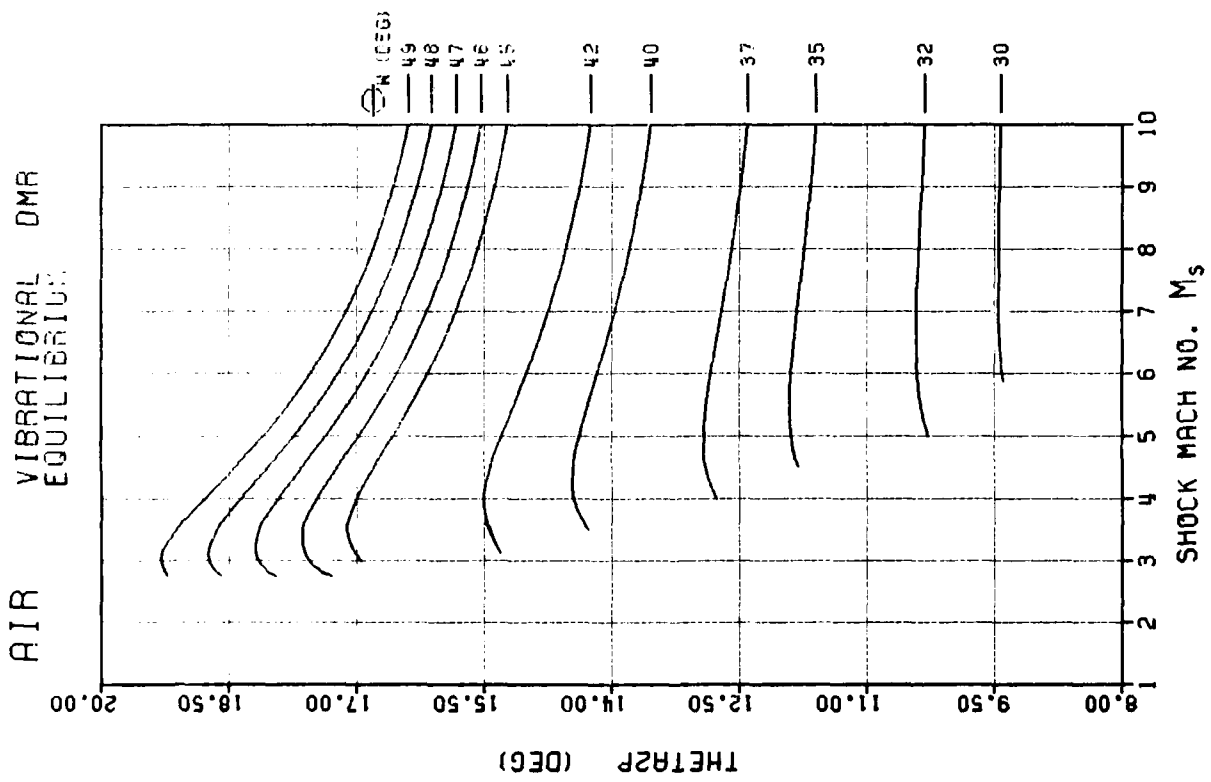


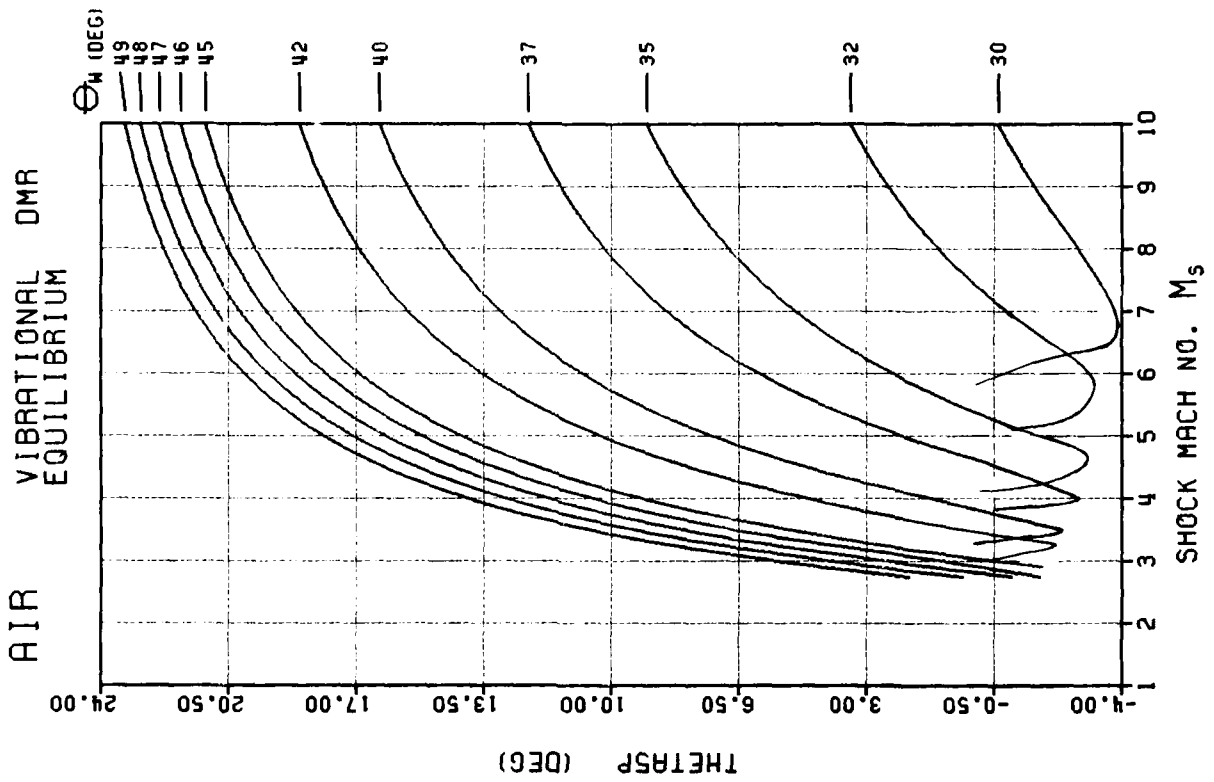
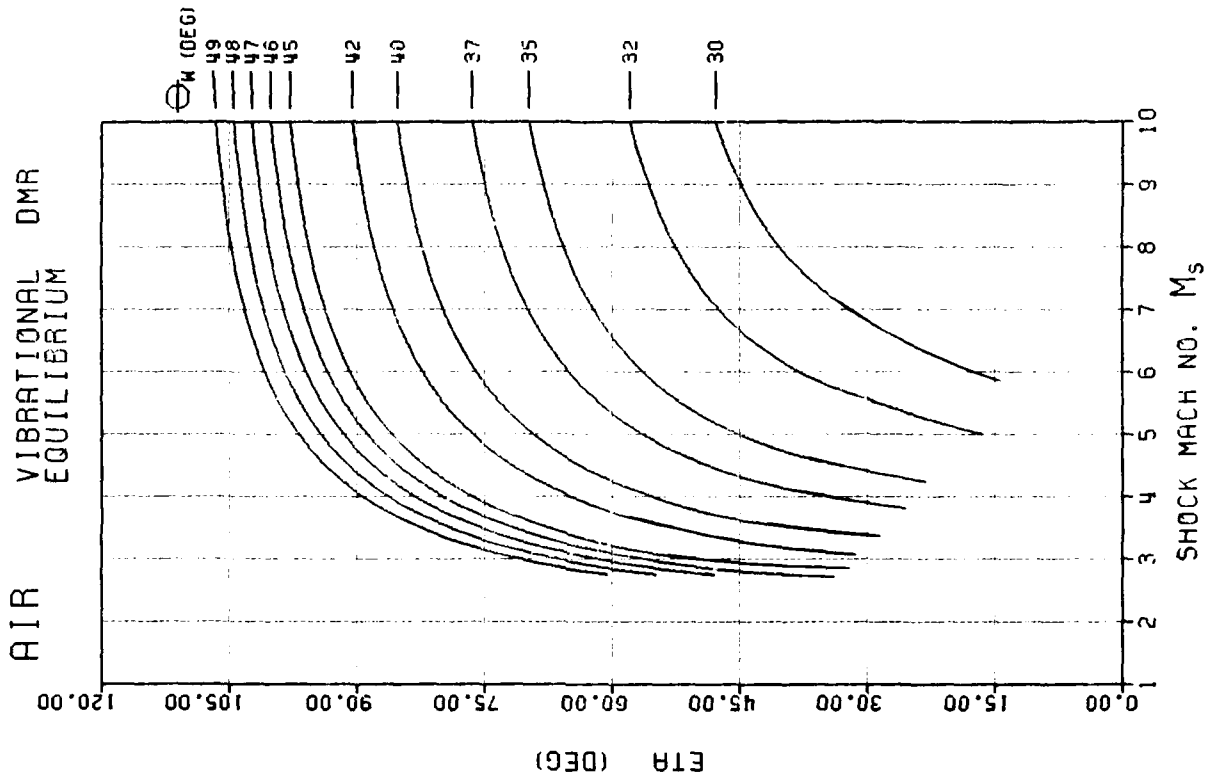


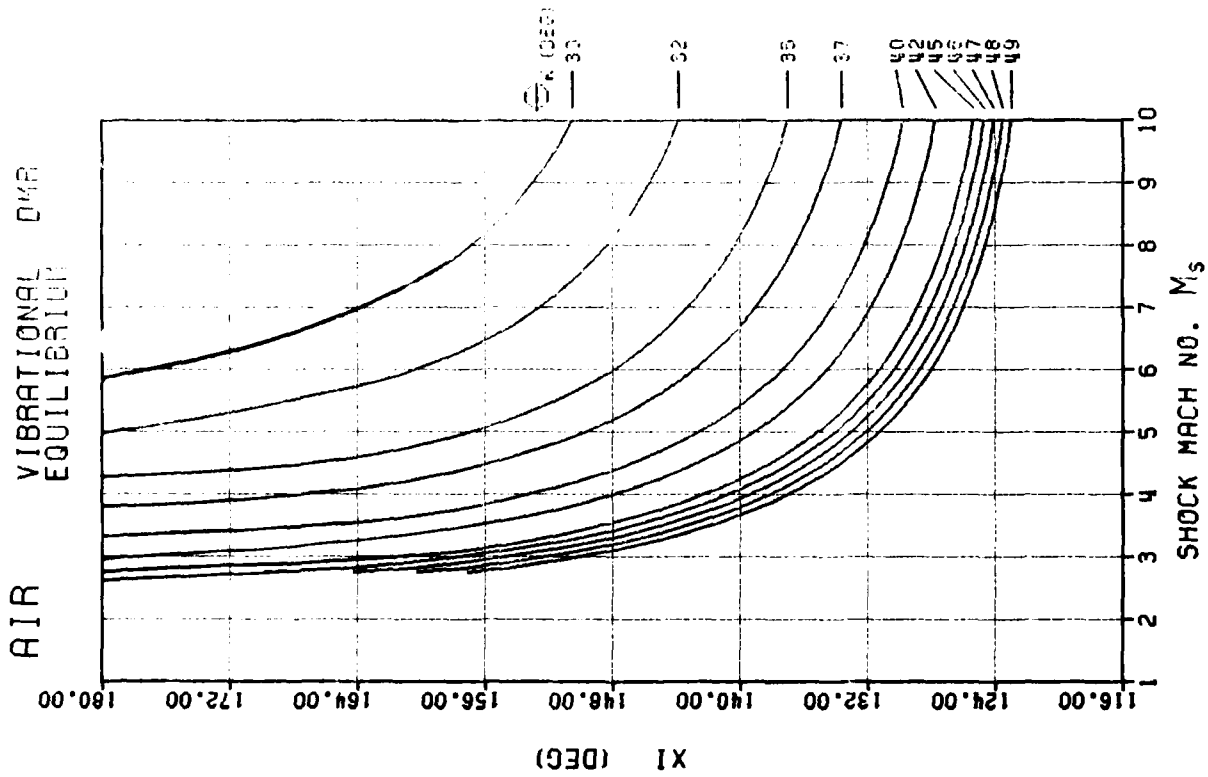




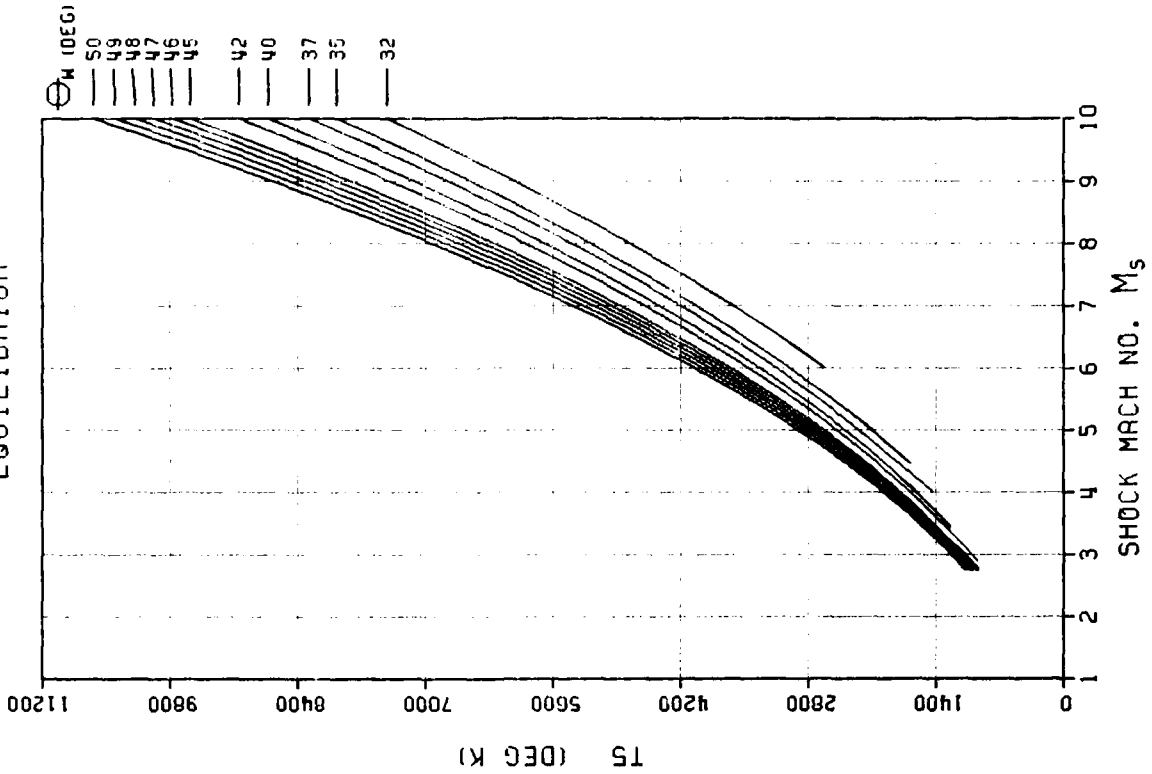




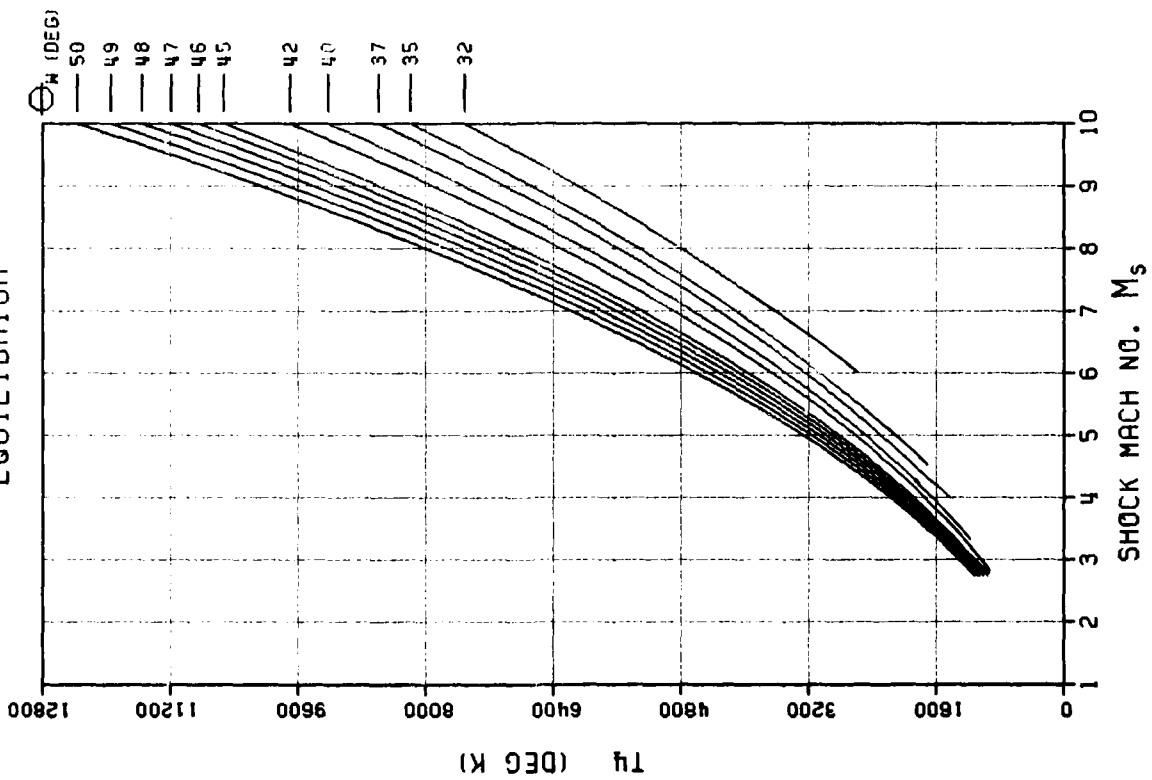




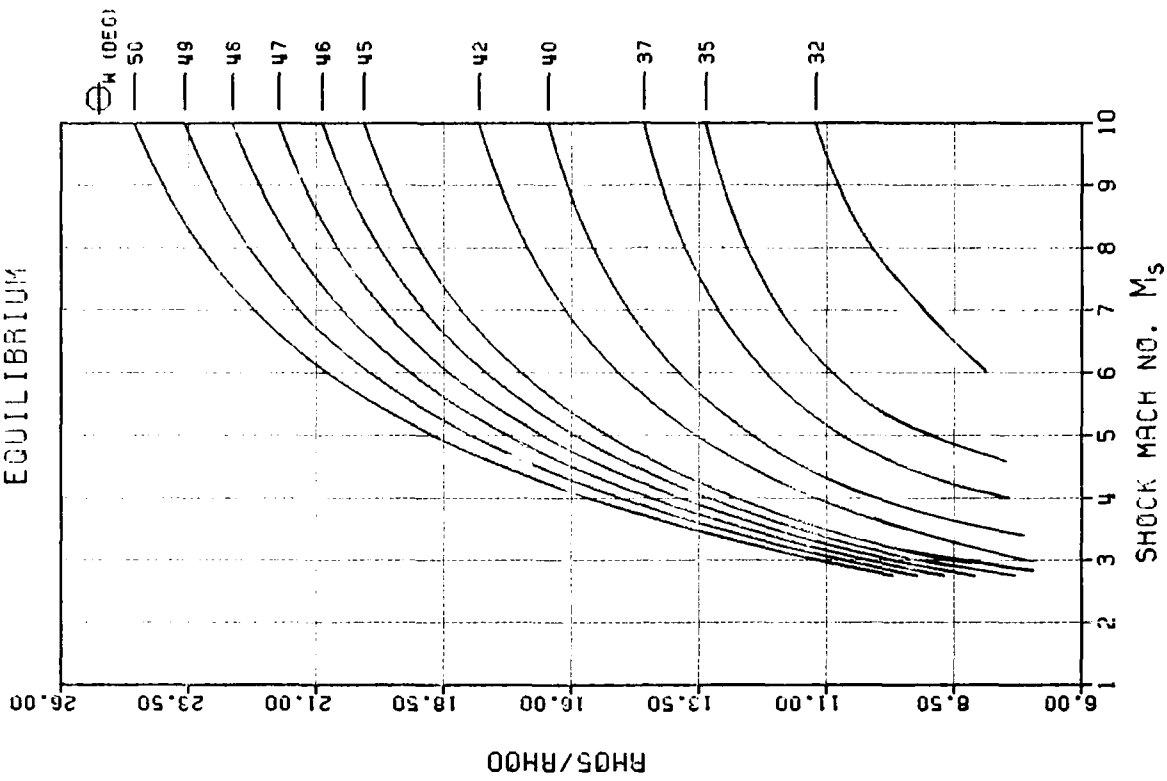
AIR-02 VIBRATIONAL EQUILIBRIUM DMR



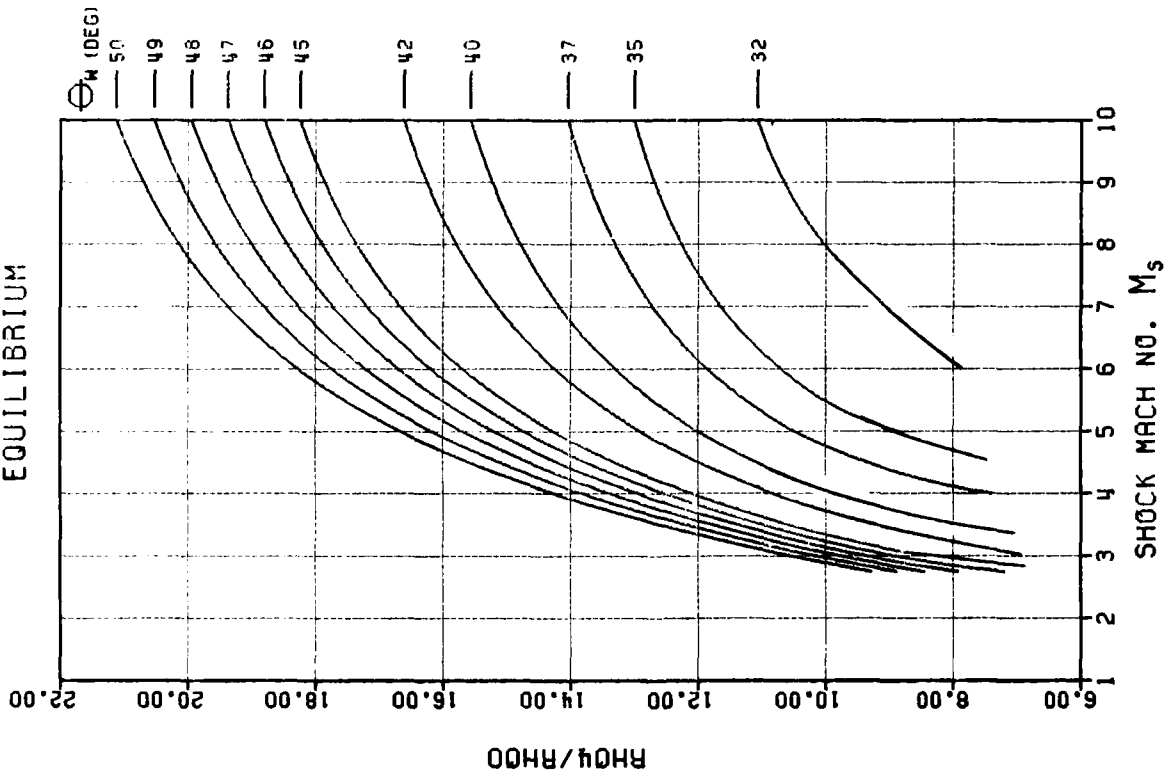
AIR-02 VIBRATIONAL EQUILIBRIUM DMR



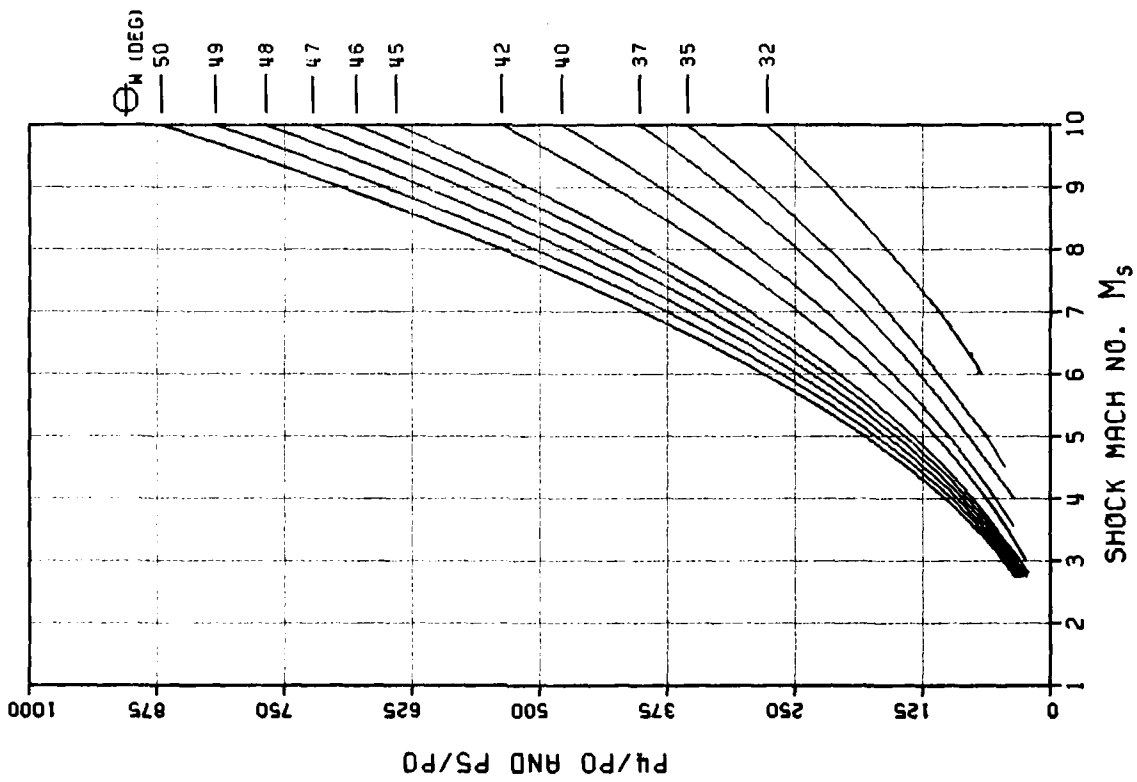
AIR-02 VIBRATIONAL EQUILIBRIUM DMR



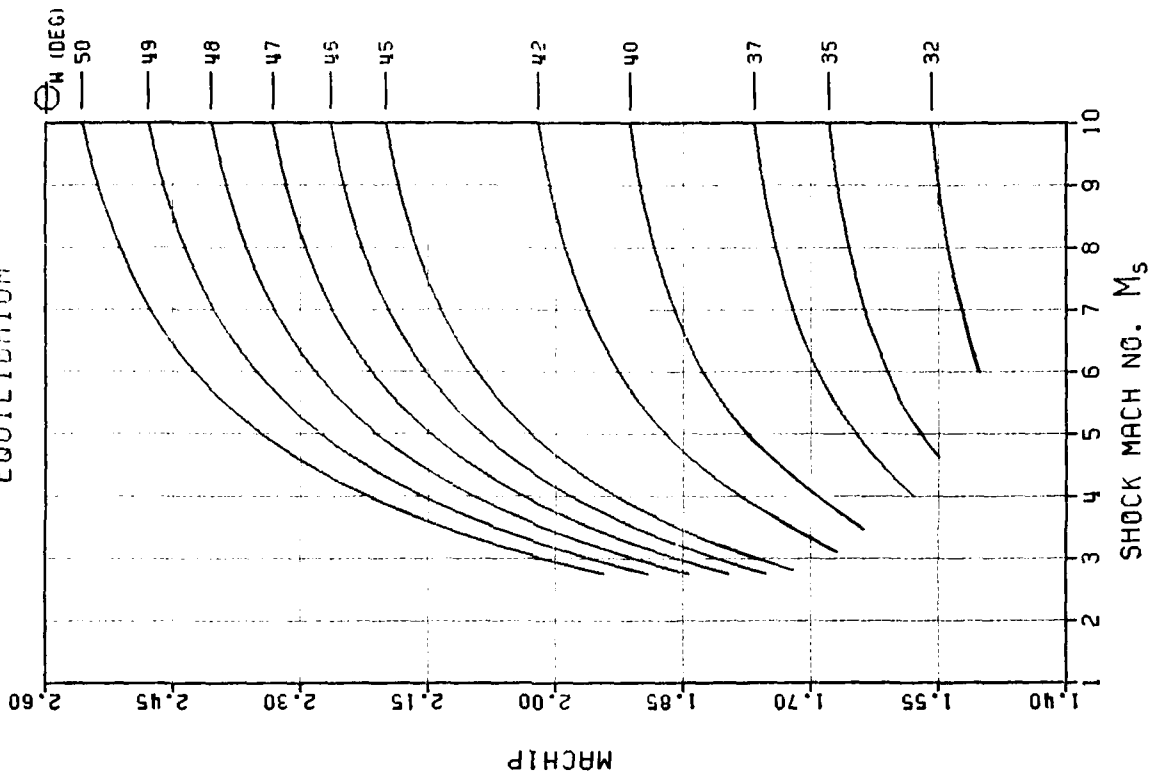
AIR-02 VIBRATIONAL EQUILIBRIUM DMR



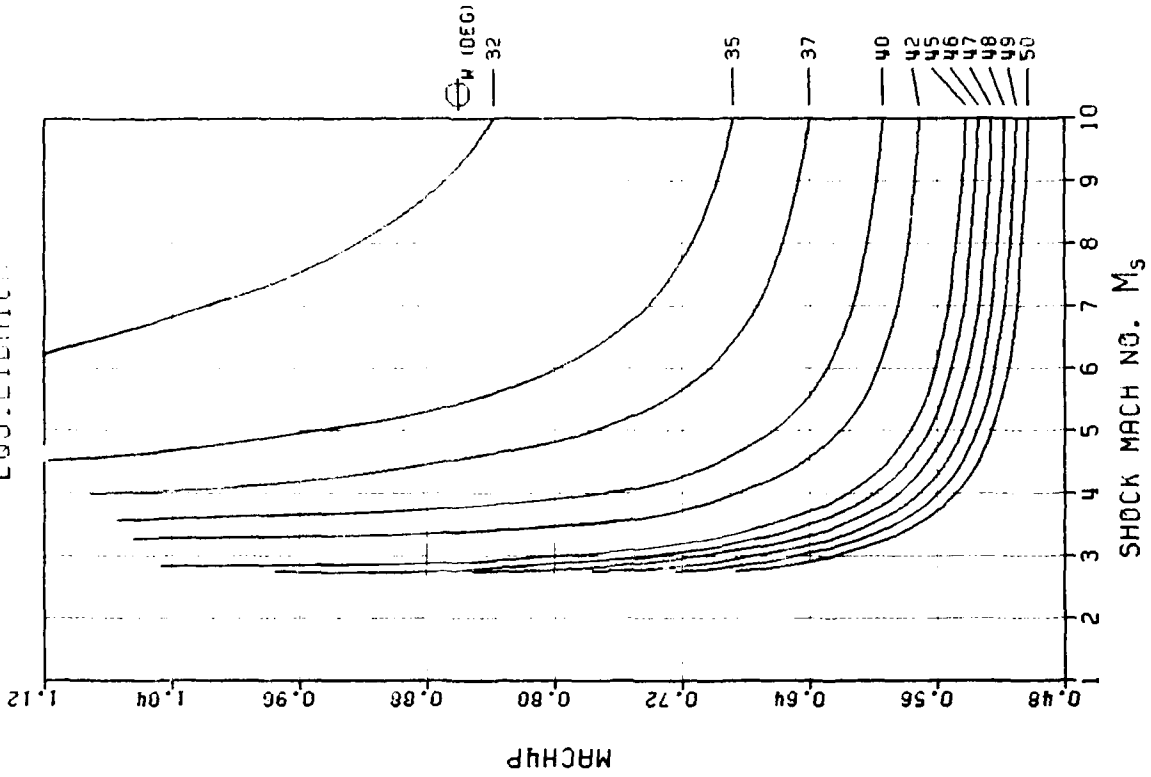
AIR-02 VIBRATIONAL EQUILIBRIUM DMR



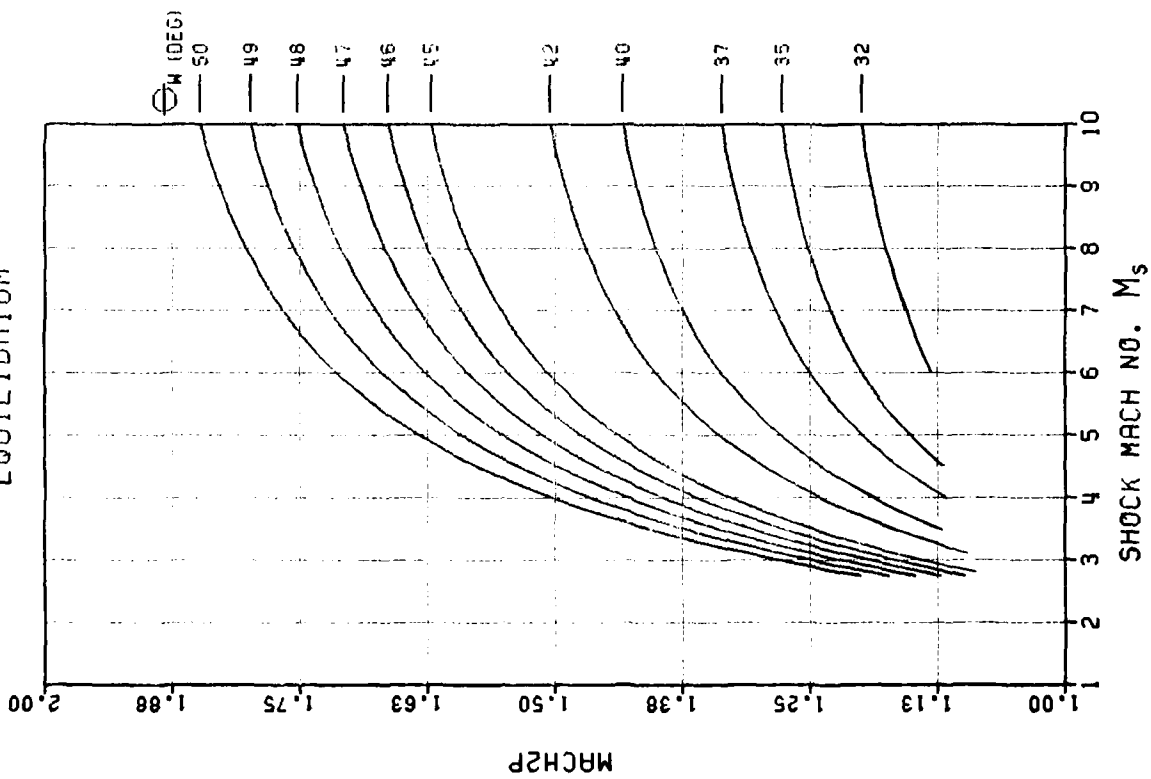
AIR-02 VIBRATIONAL EQUILIBRIUM DMR



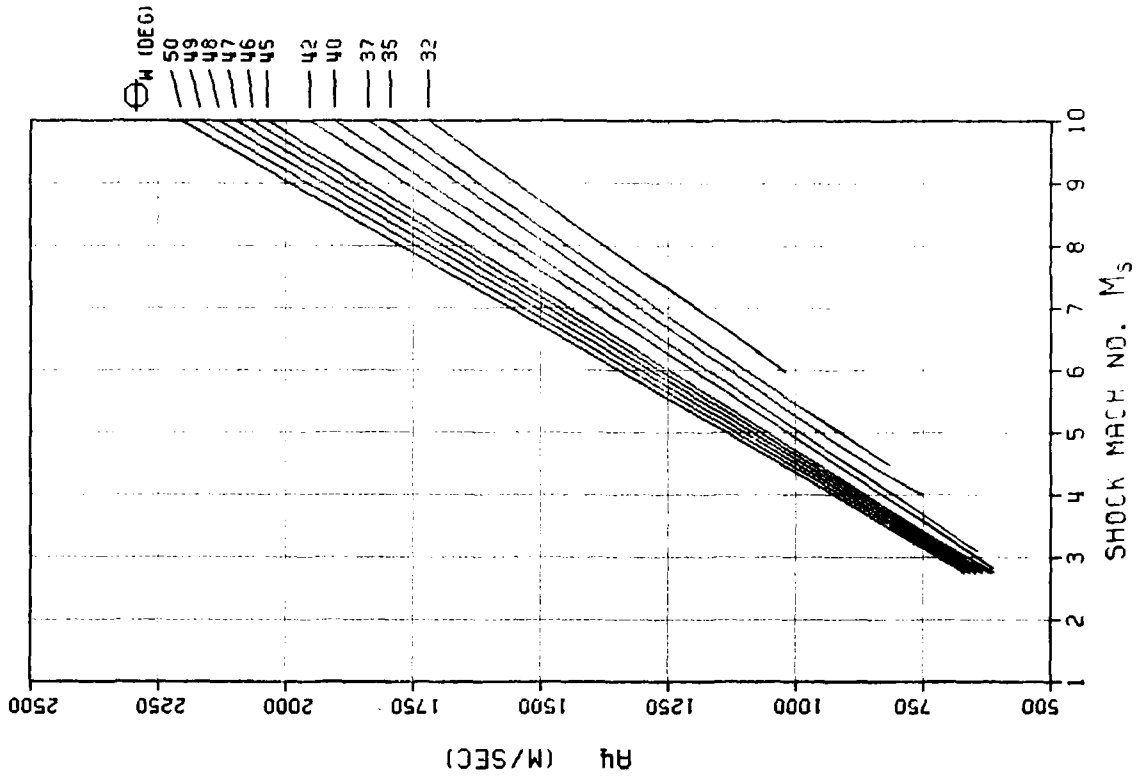
AIR-02 VIBRATIONAL DMR EQUILIBRIUM



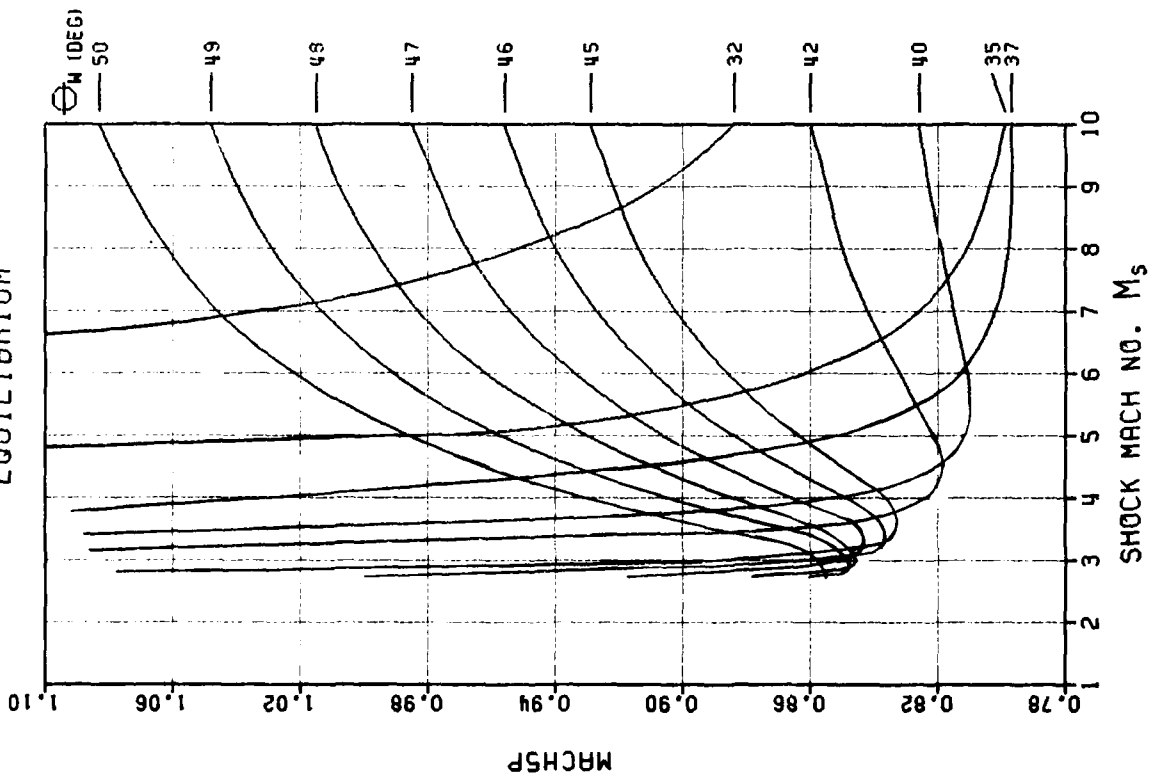
AIR-02 VIBRATIONAL DMR EQUILIBRIUM



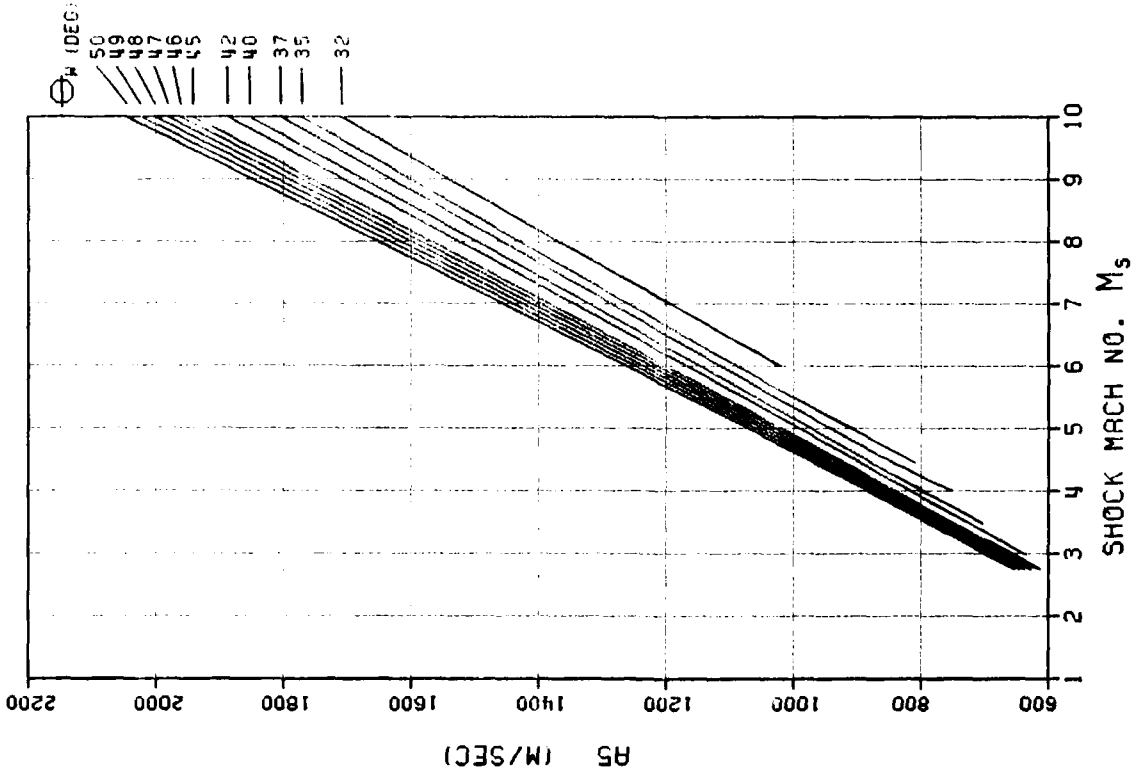
AIR-02 VIBRATIONAL EQUILIBRIUM DMR



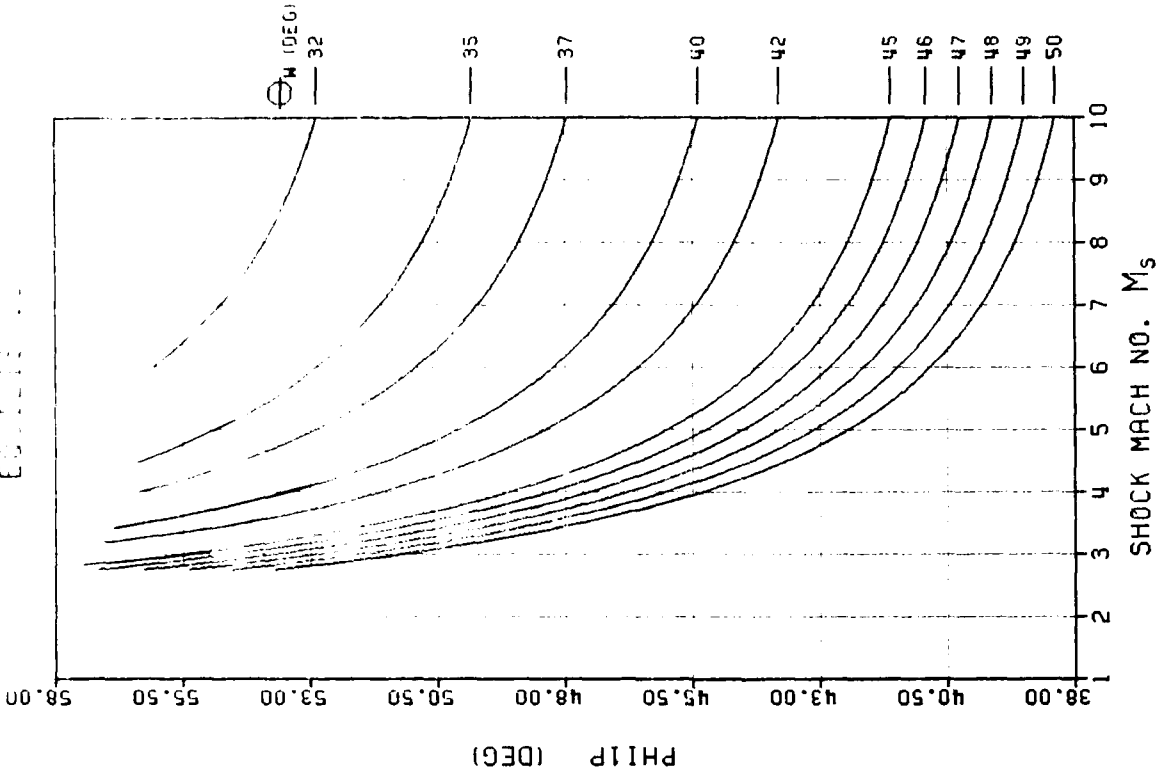
AIR-02 VIBRATIONAL EQUILIBRIUM DMR



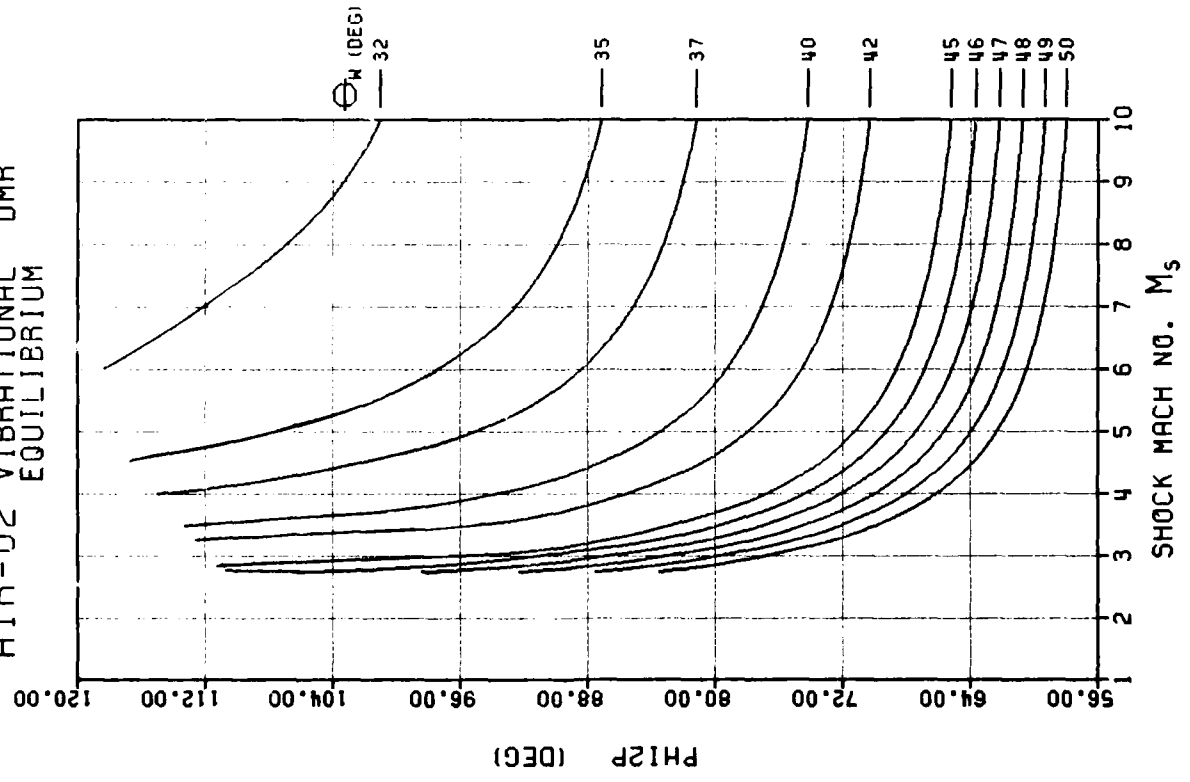
AIR-02 VIBRATIONAL EQUILIBRIUM DMR



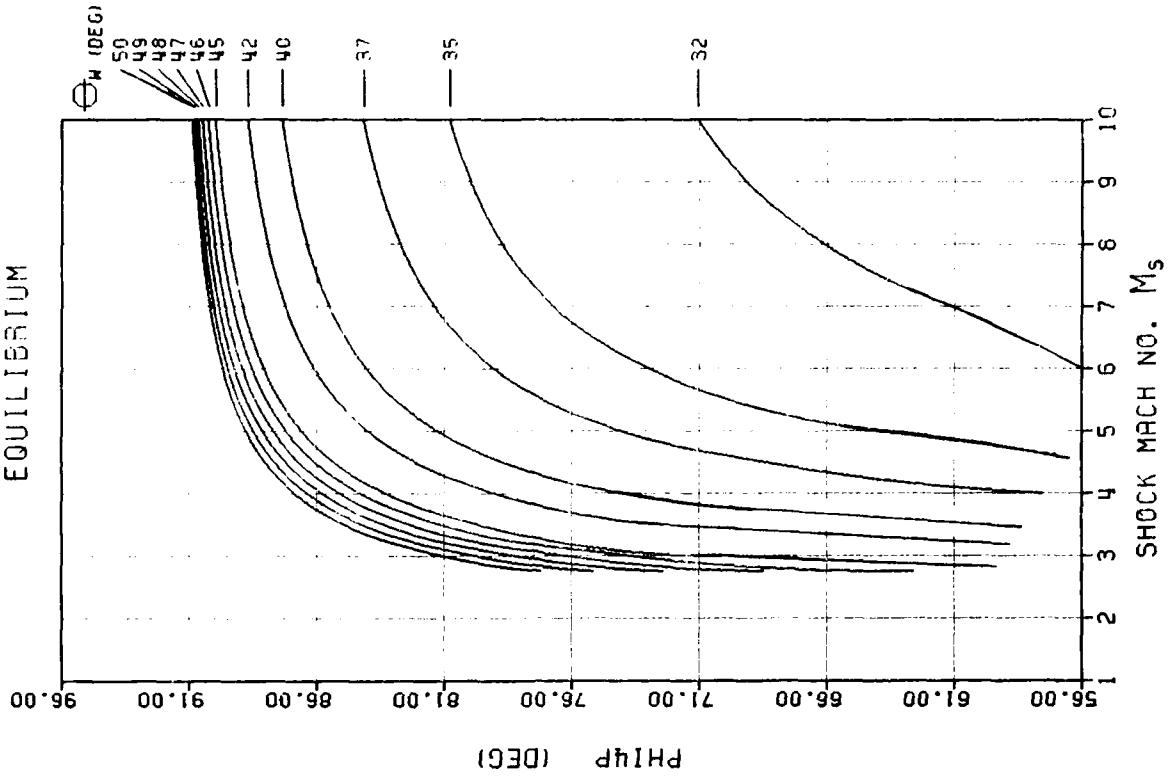
AIR-02 VIBRATIONAL EQUILIBRIUM DMR



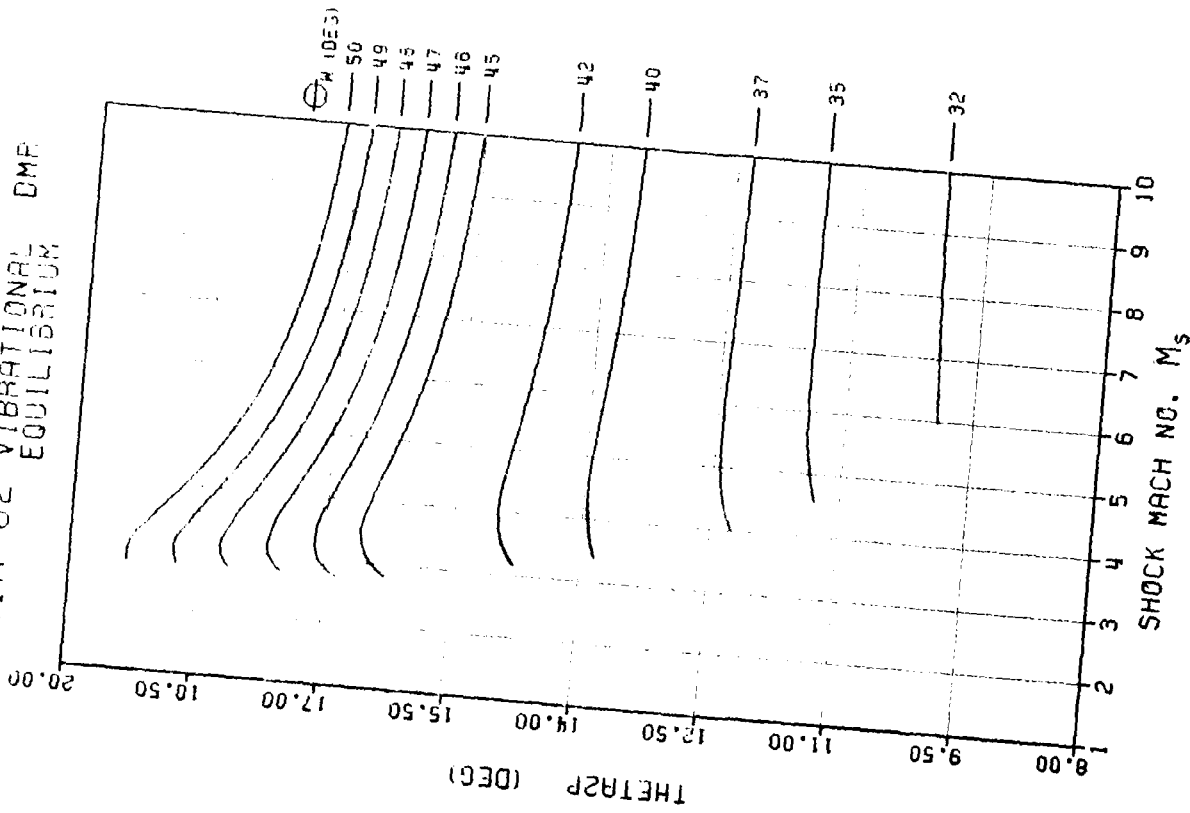
AIR-02 VIBRATIONAL DMR EQUILIBRIUM



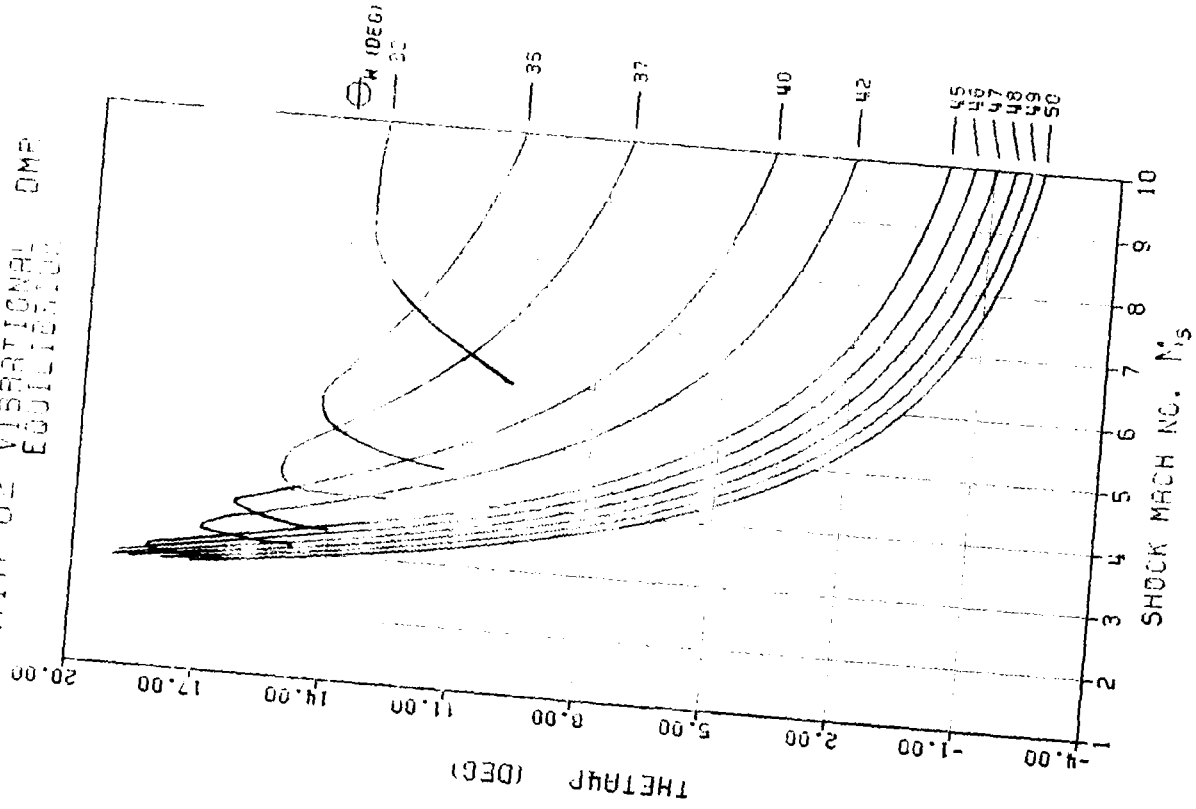
AIR-02 VIBRATIONAL DMR EQUILIBRIUM



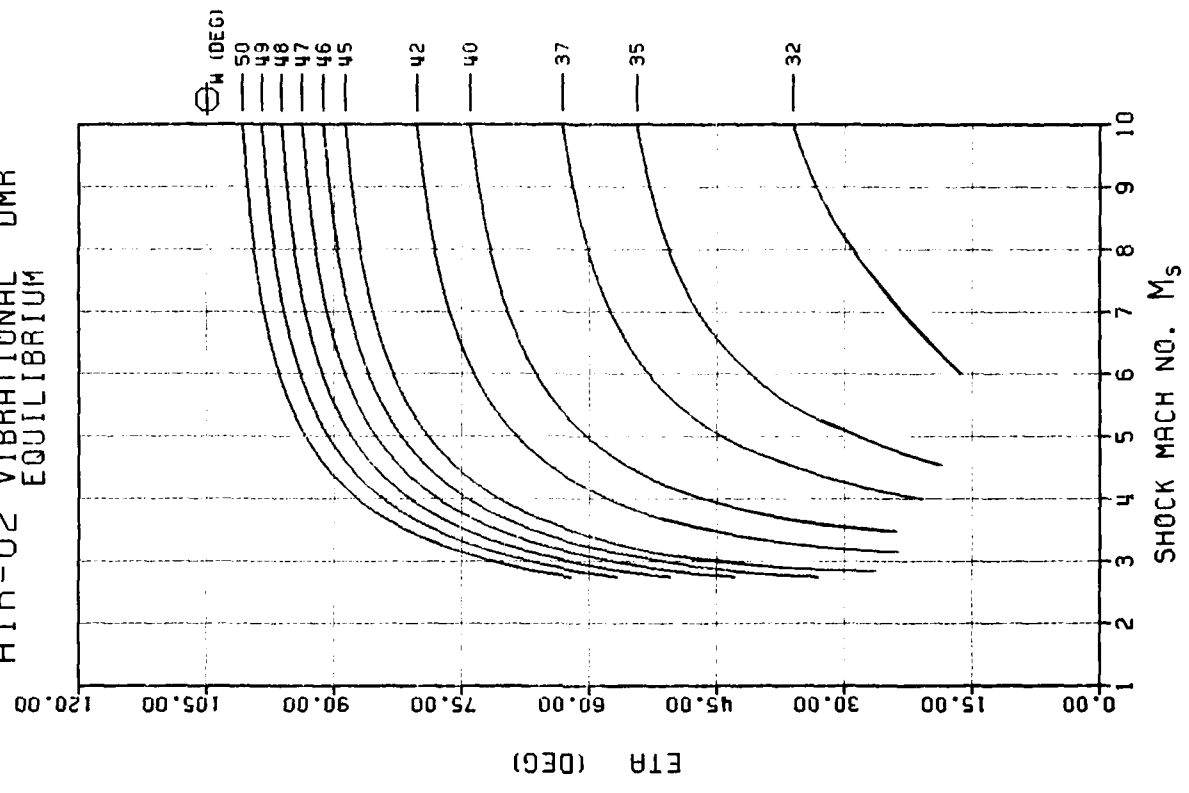
AIR-02 VIBRATIONAL EQUILIBRIUM



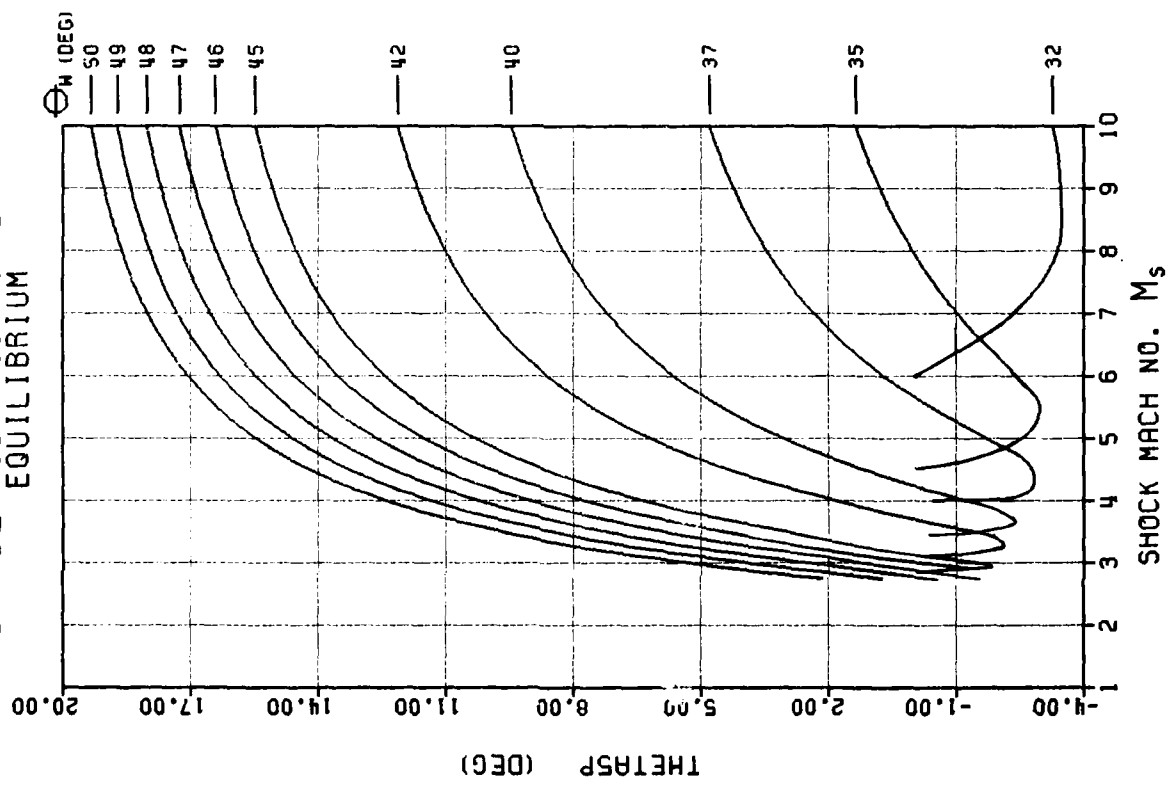
AIR-02 VIBRATIONAL EQUILIBRIUM



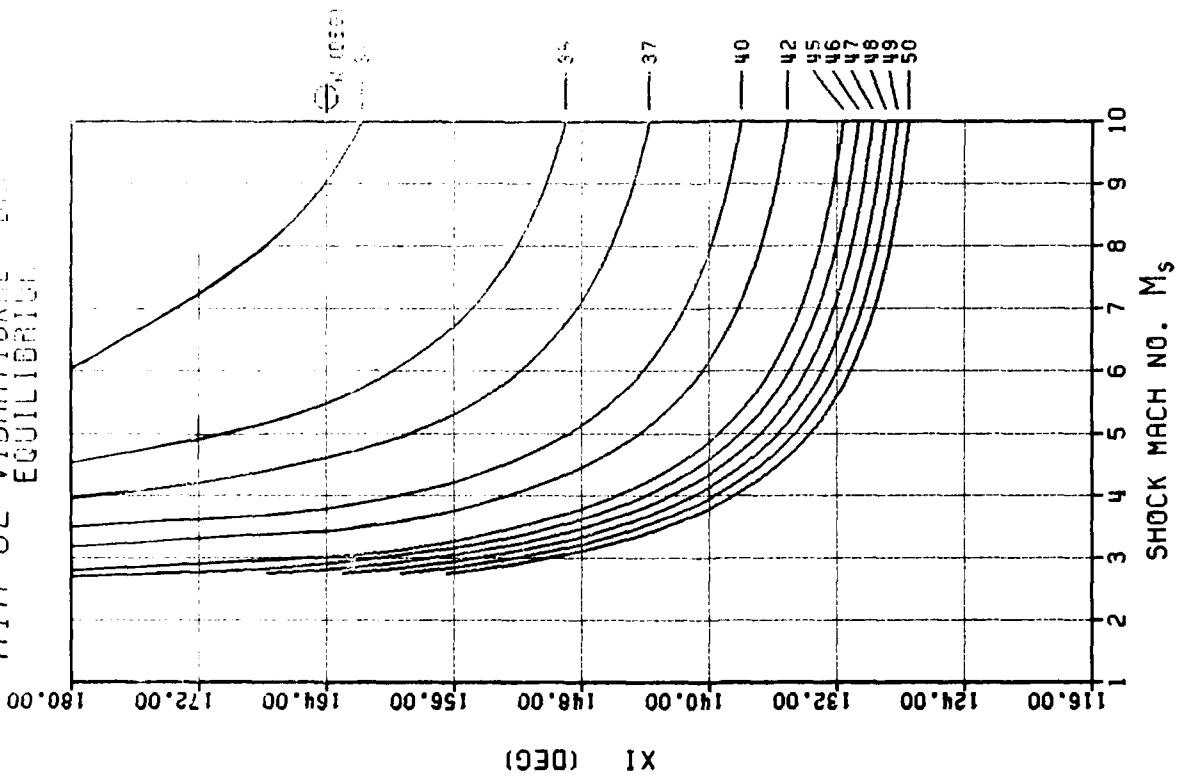
AIR-02 VIBRATIONAL EQUILIBRIUM DMR

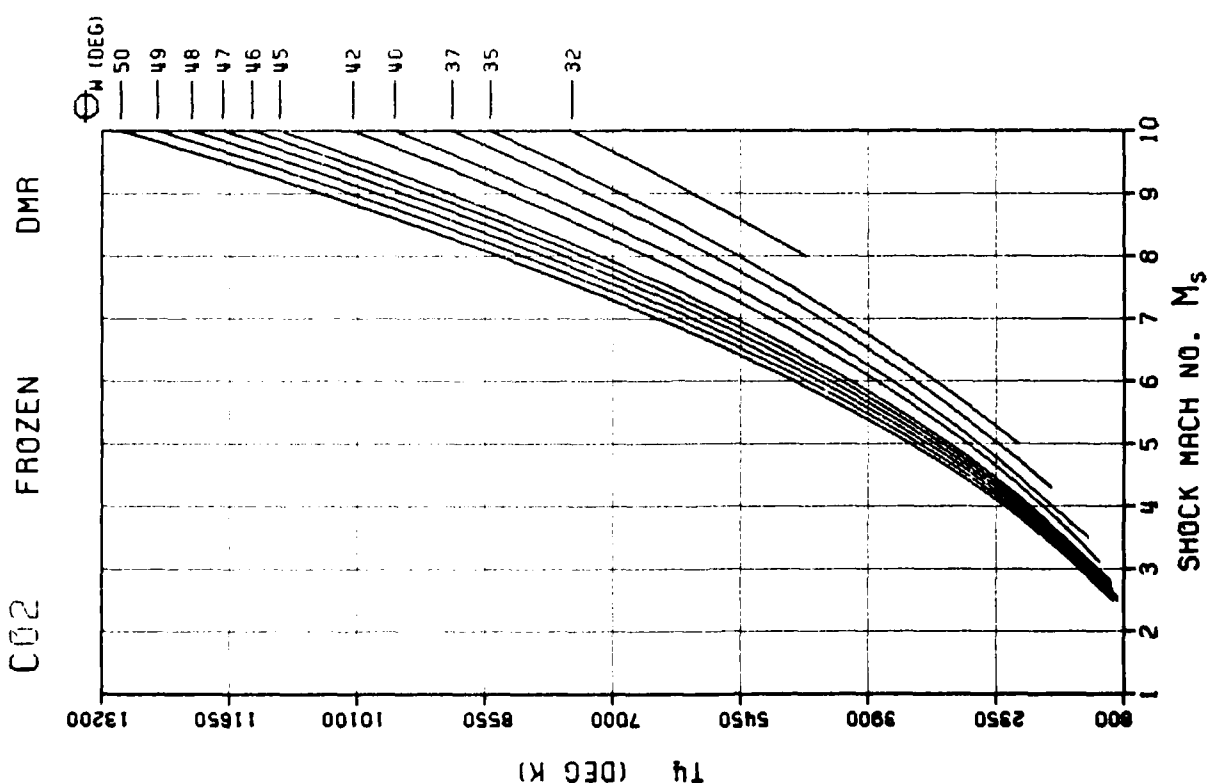
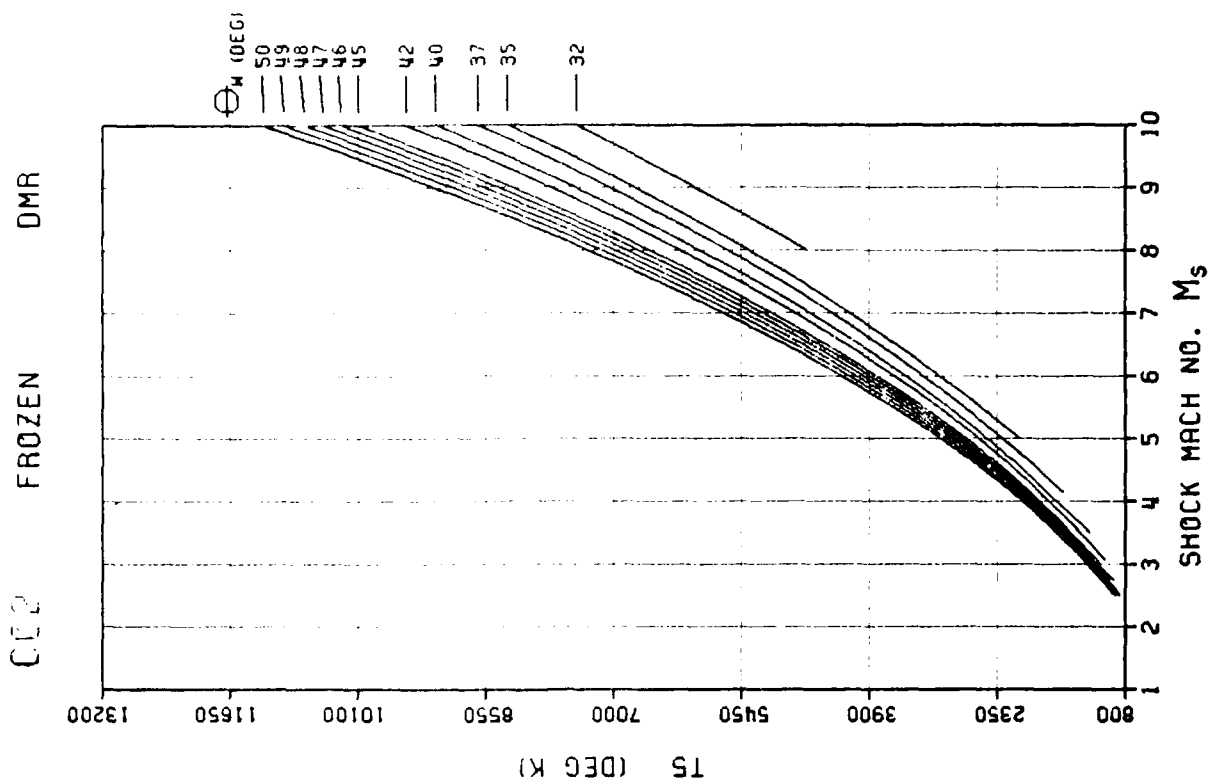


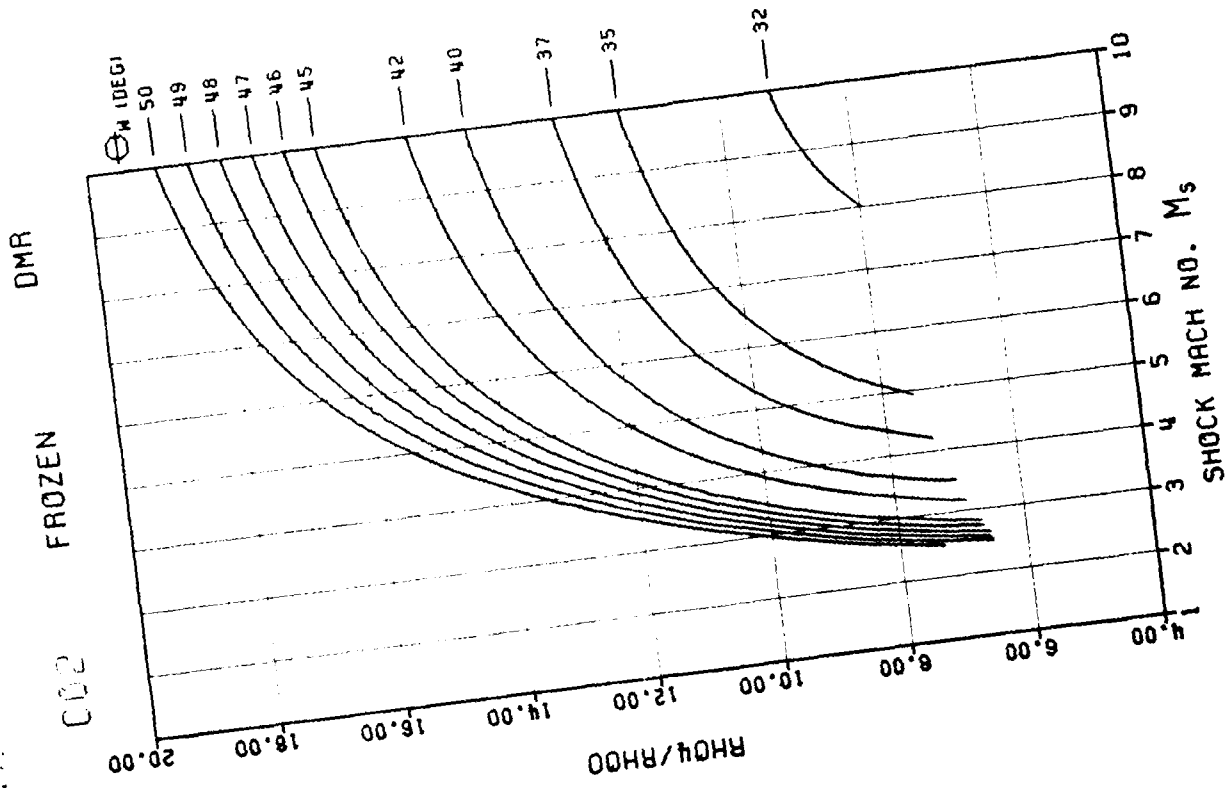
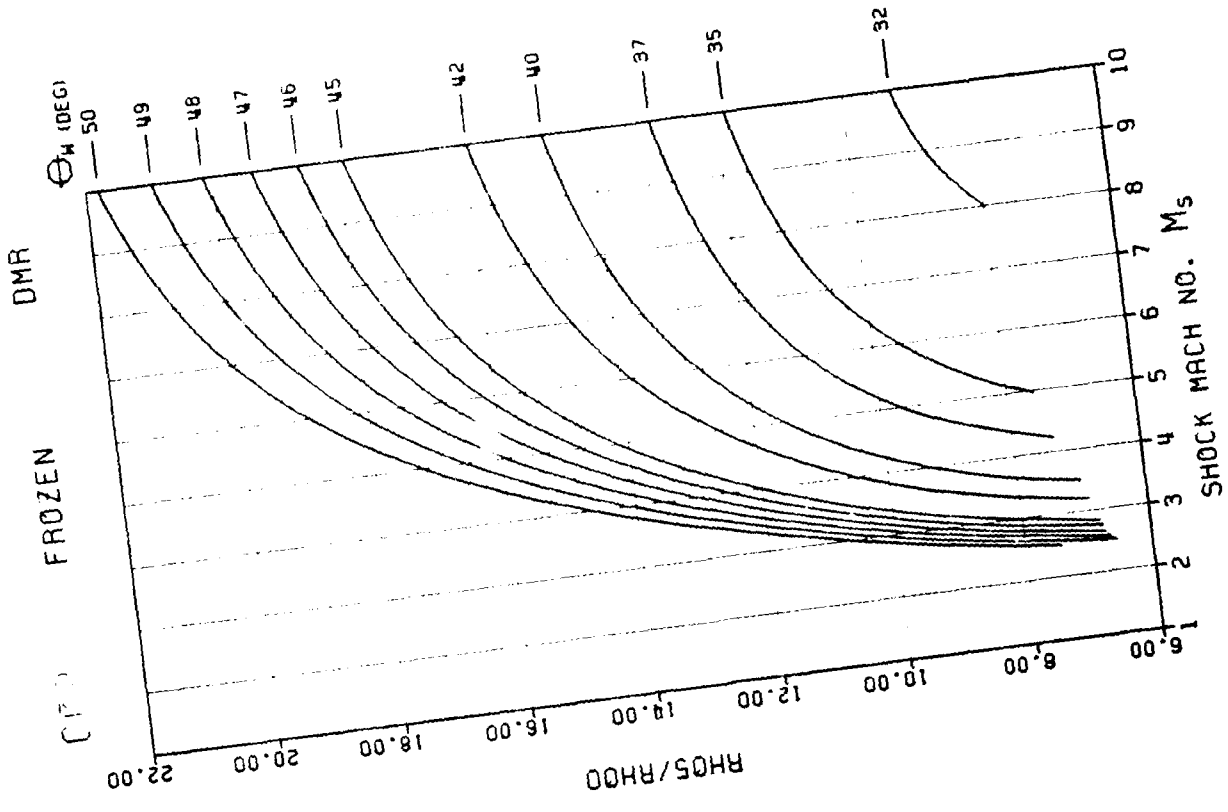
AIR-02 VIBRATIONAL EQUILIBRIUM DMR



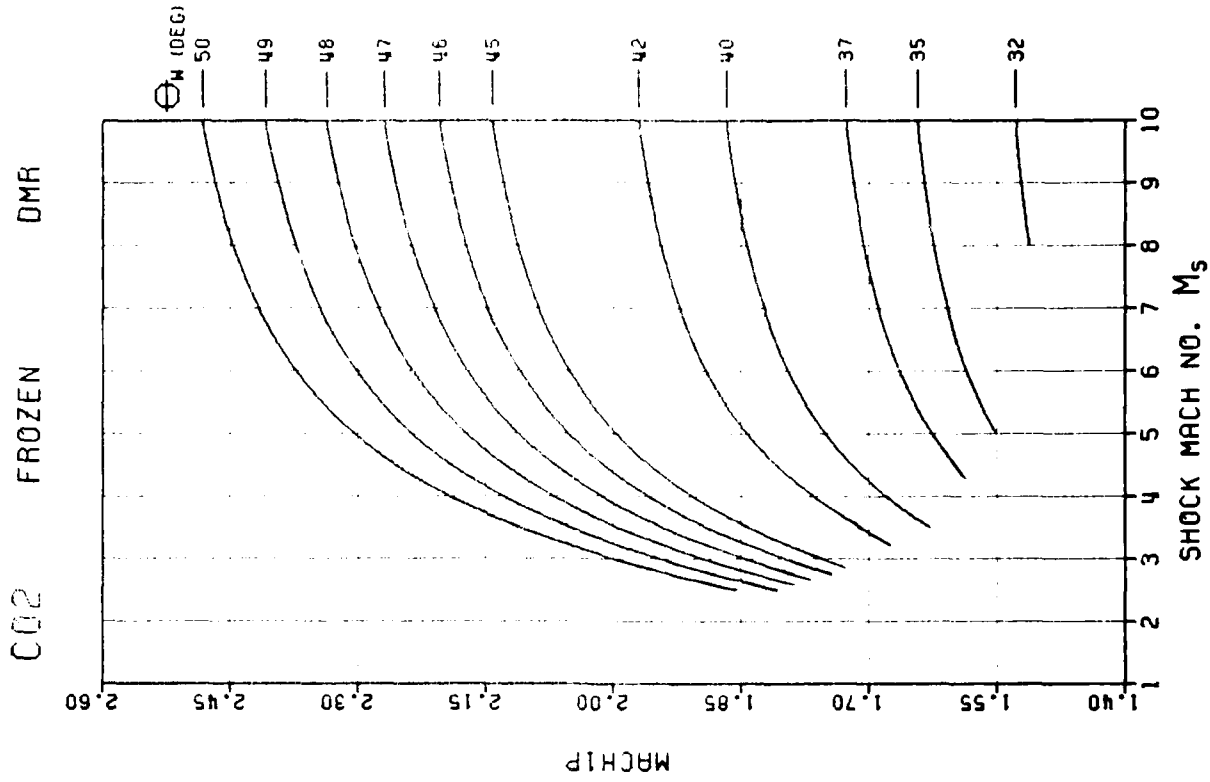
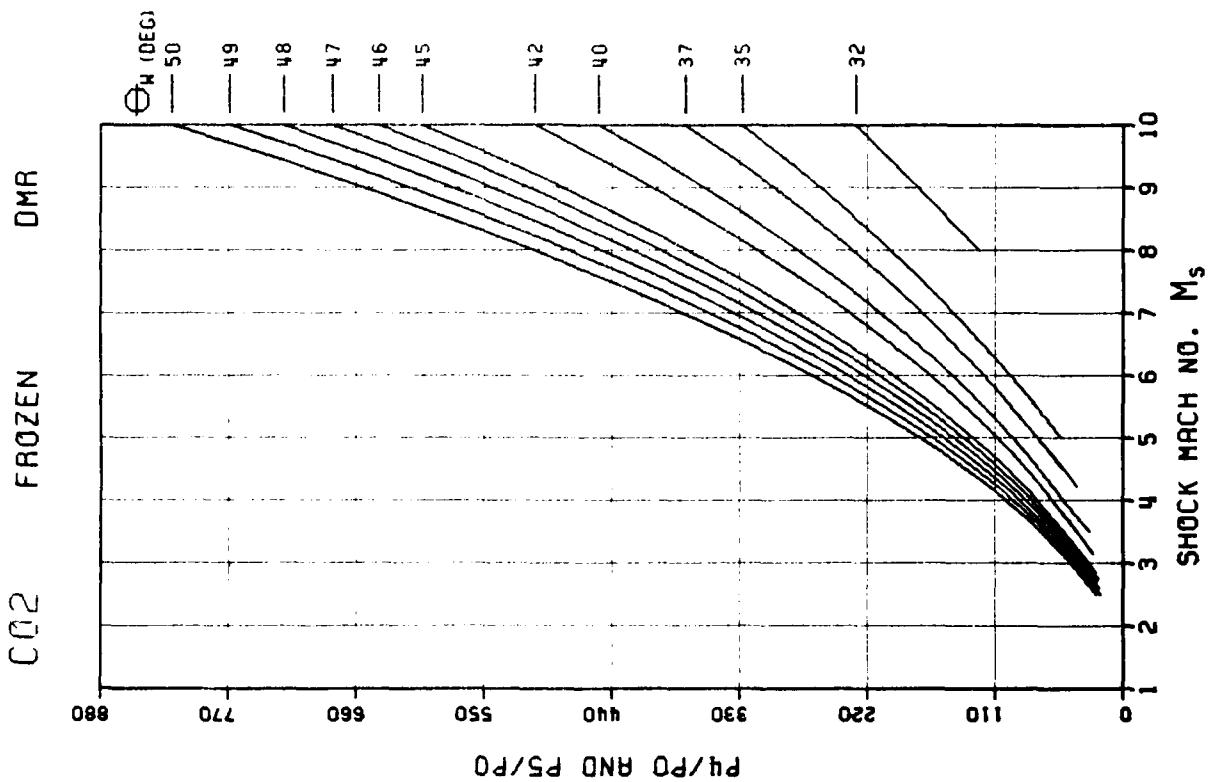
AIR-02 VIBRATIONEL DMS
EQUILIBRIUM

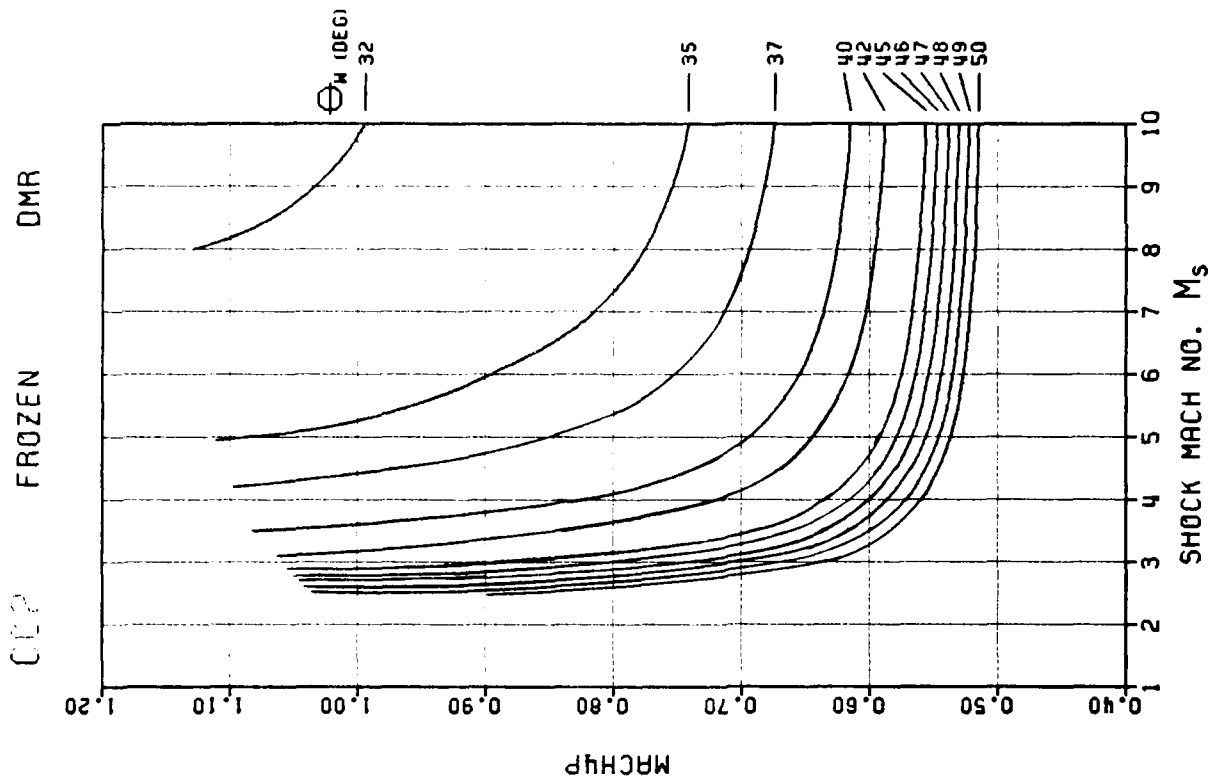
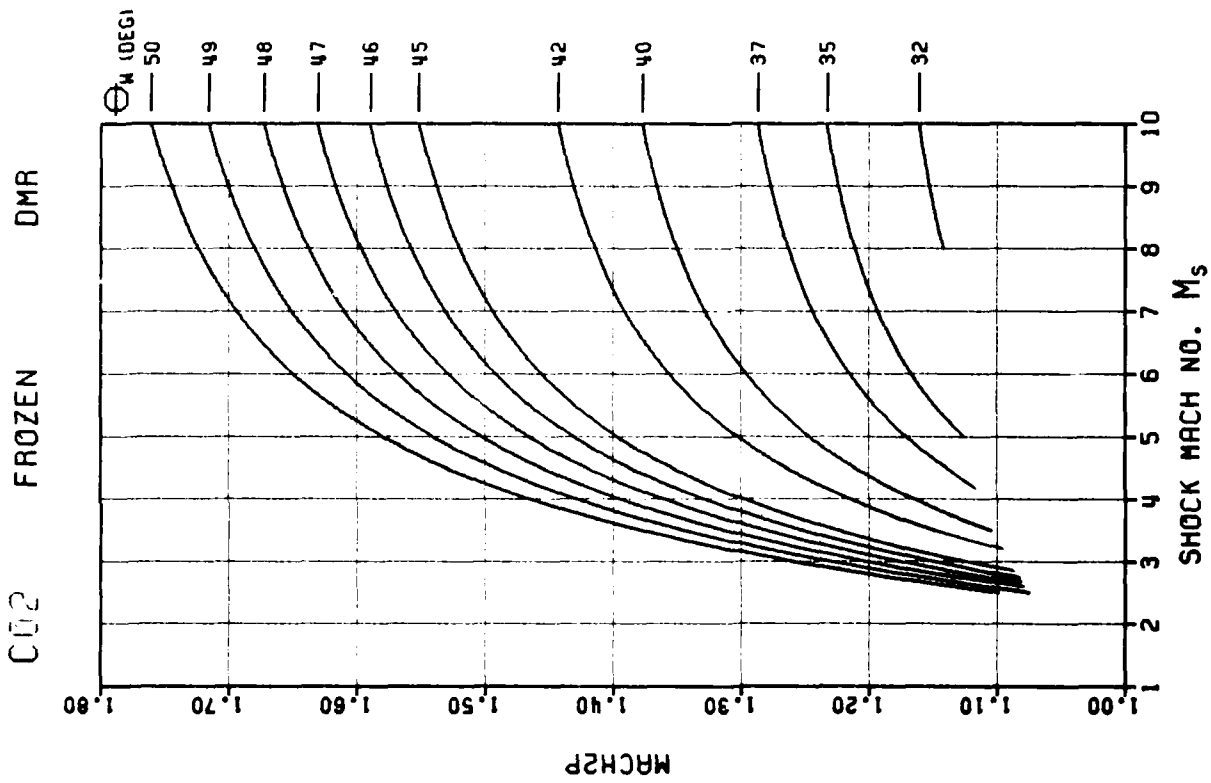


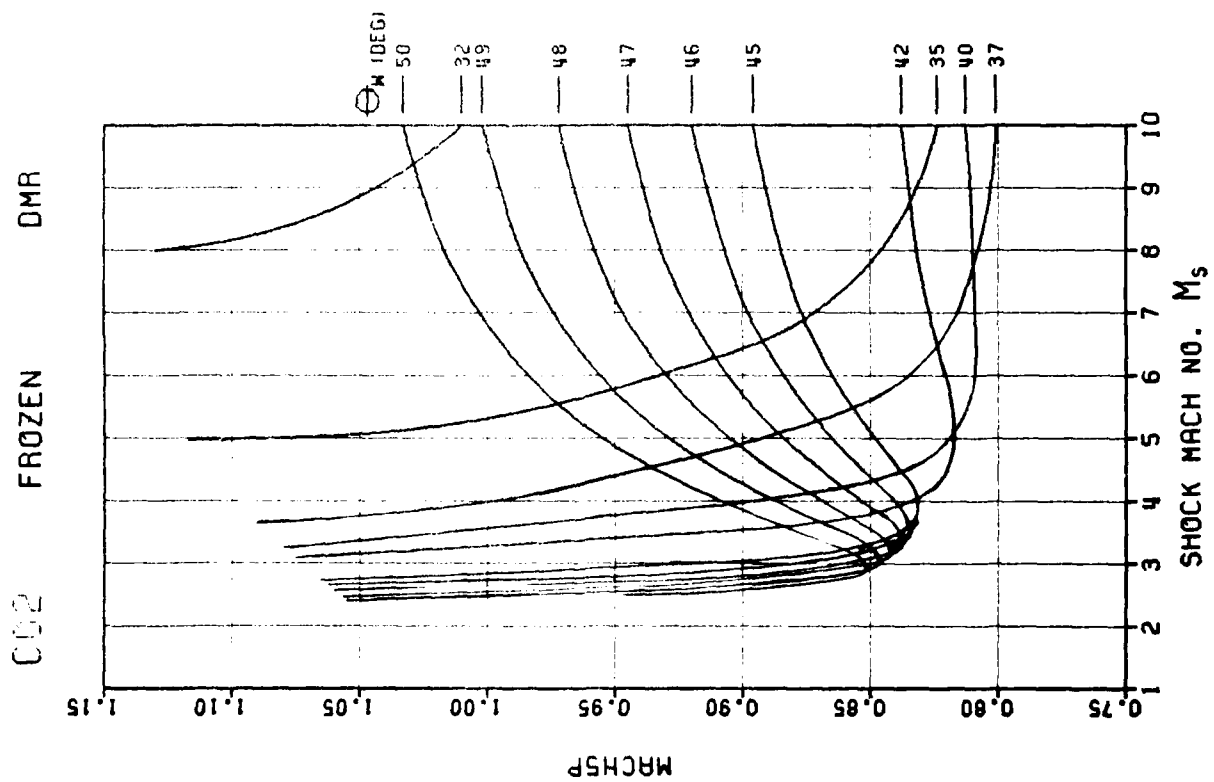
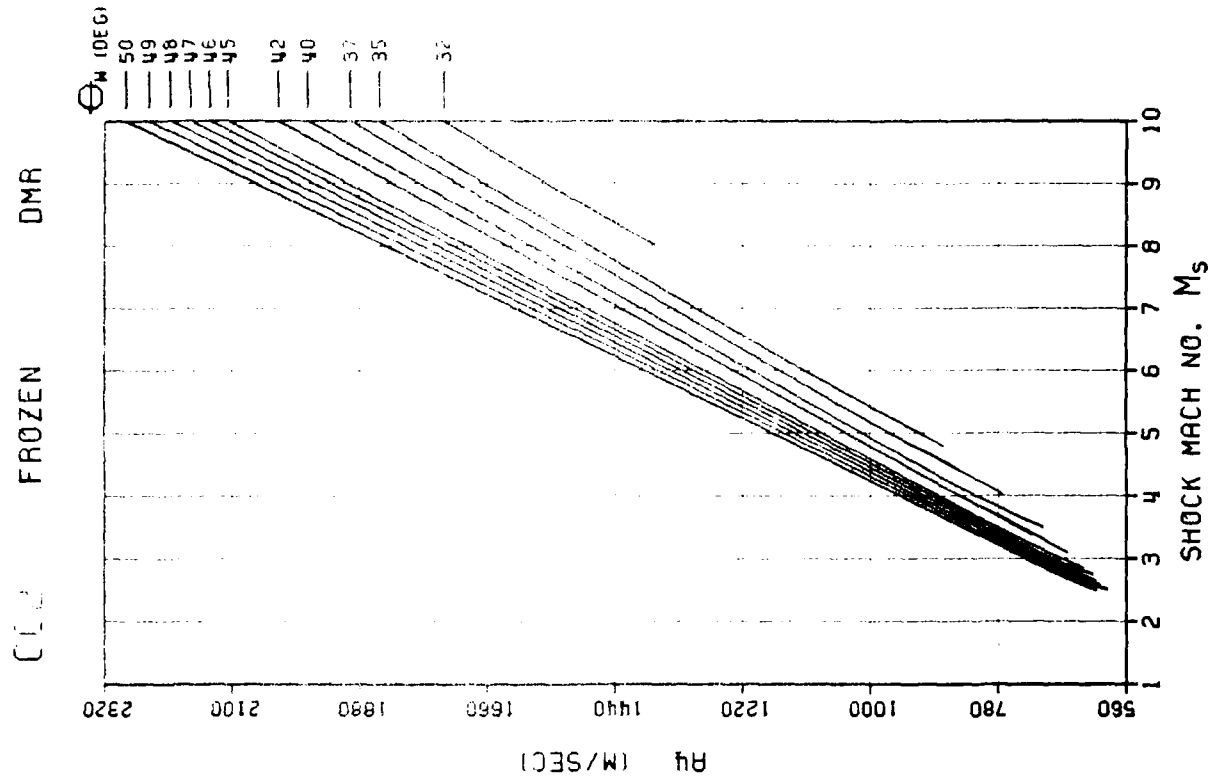


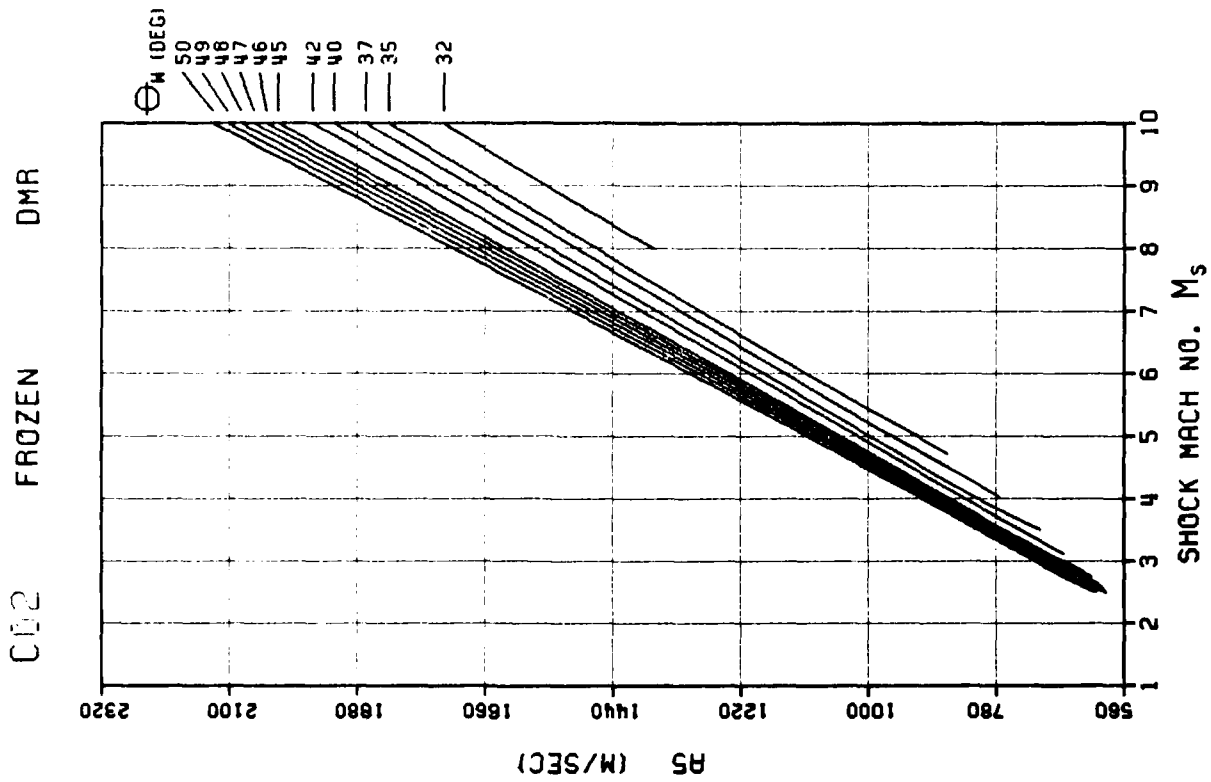
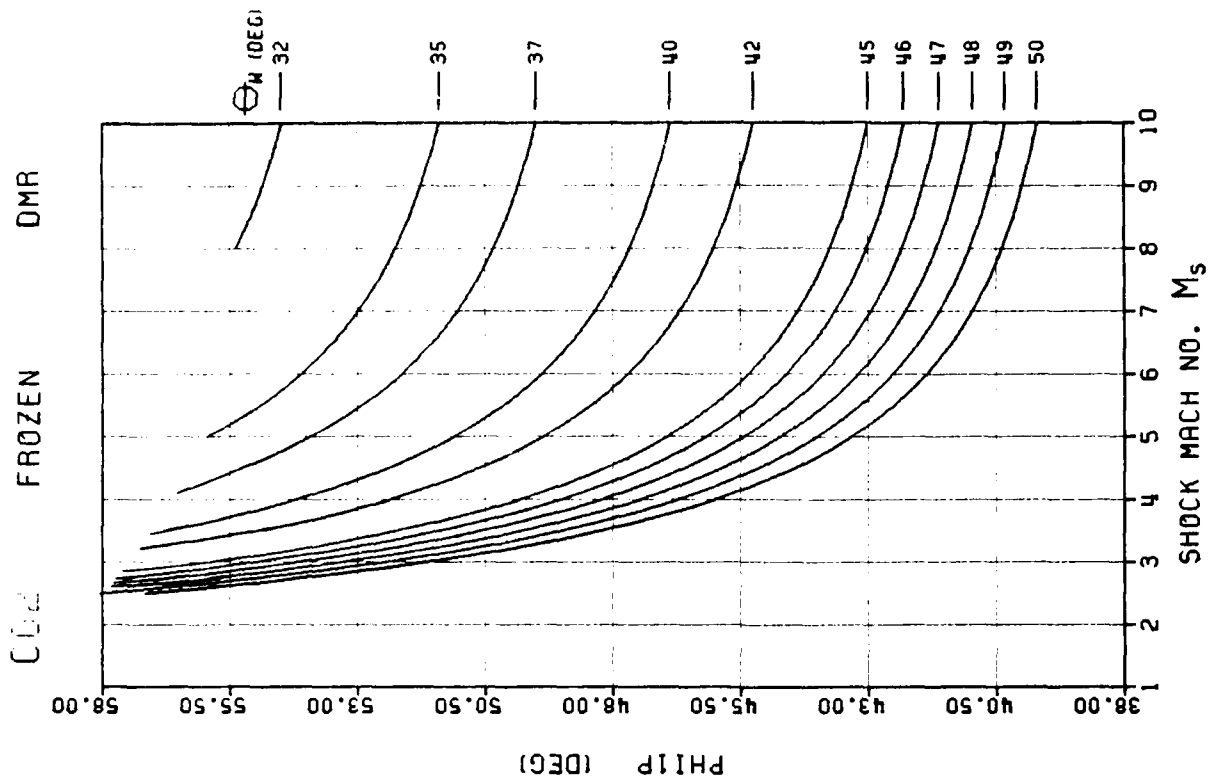


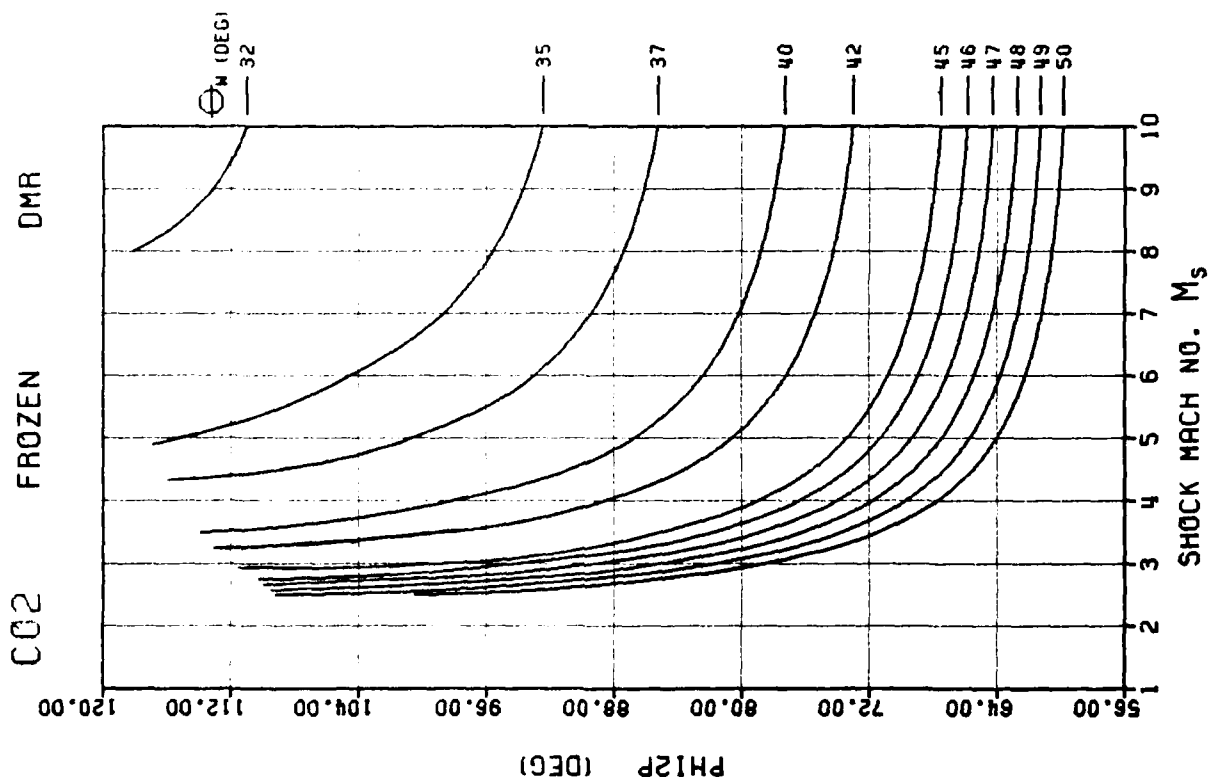
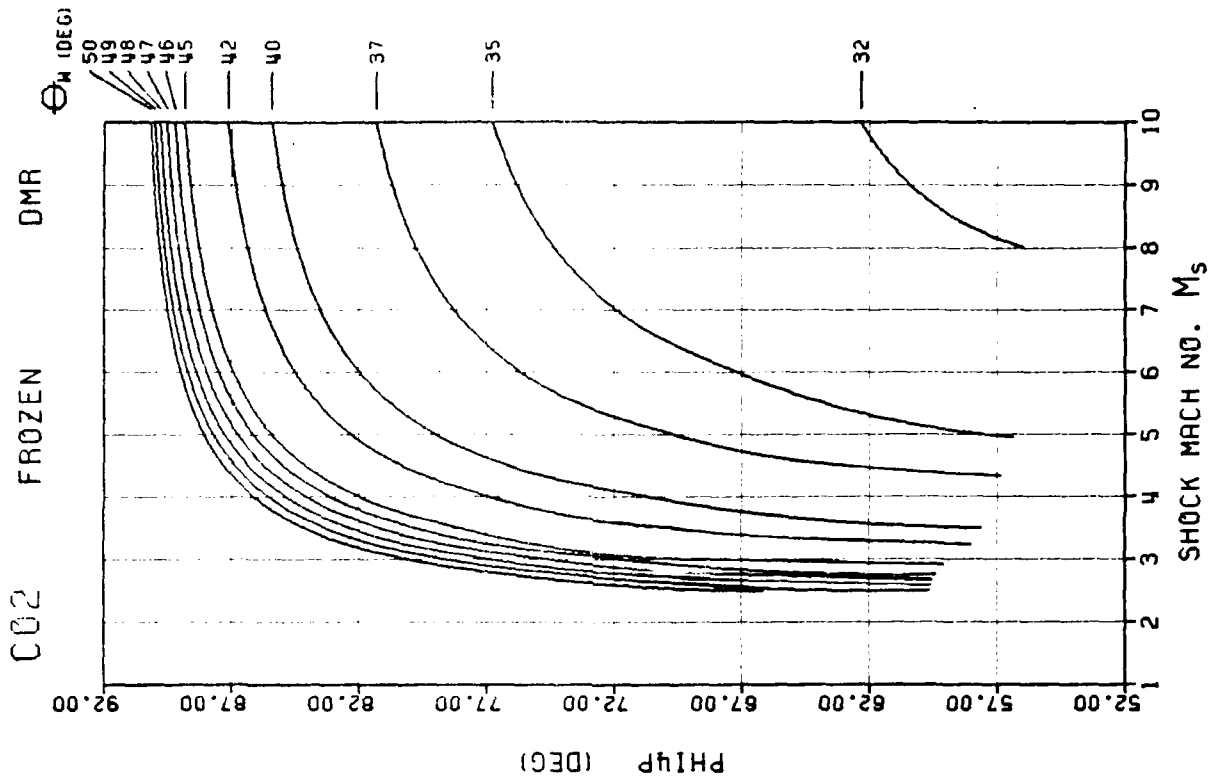
F - 282

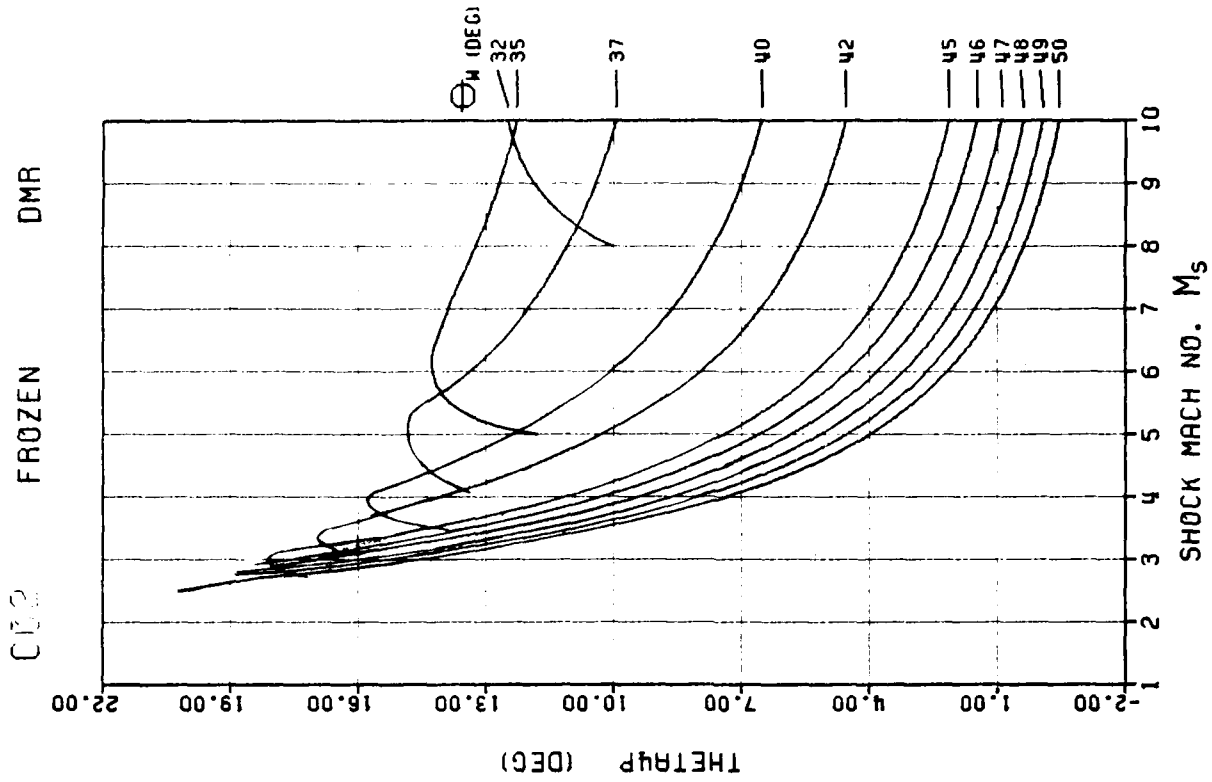
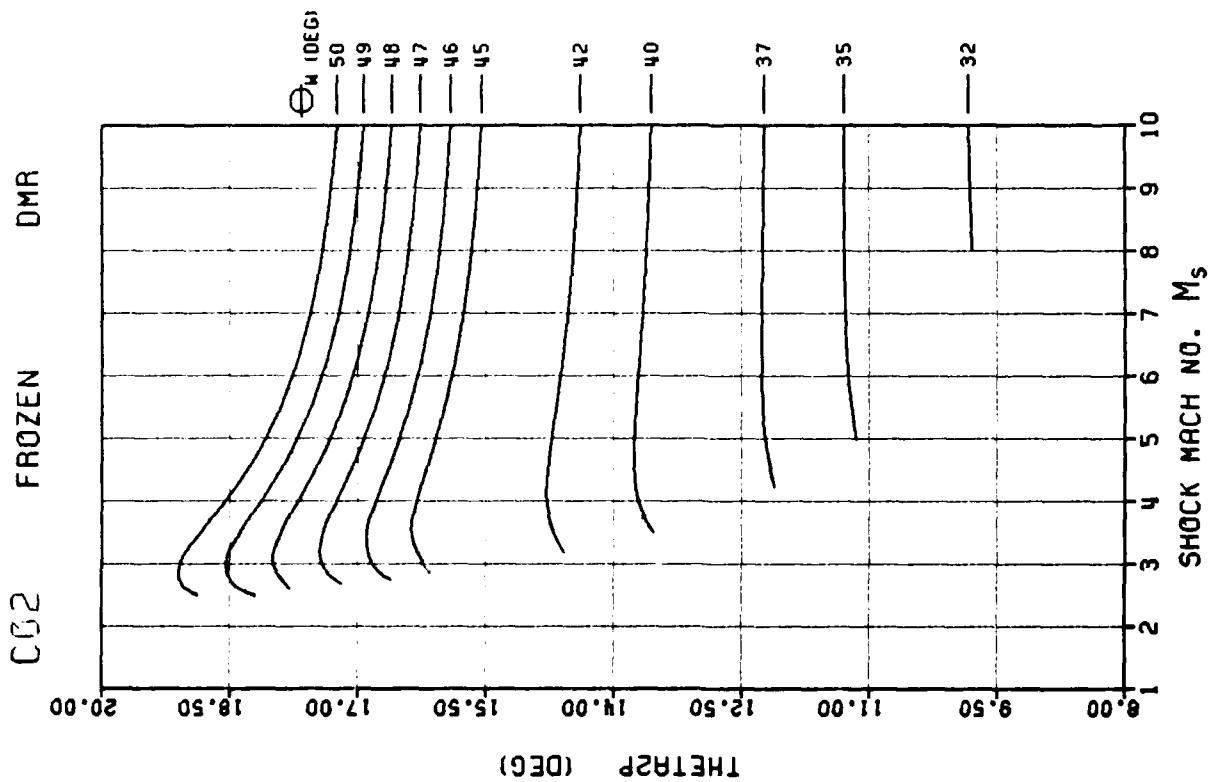


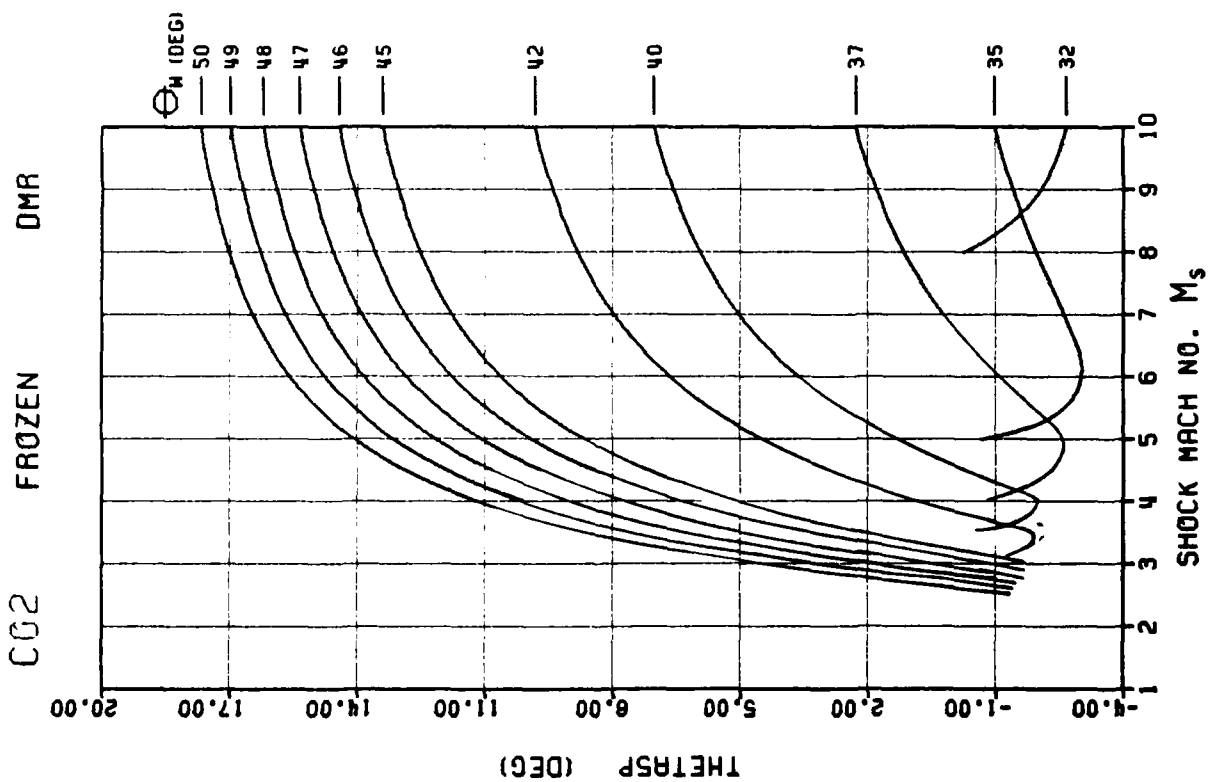
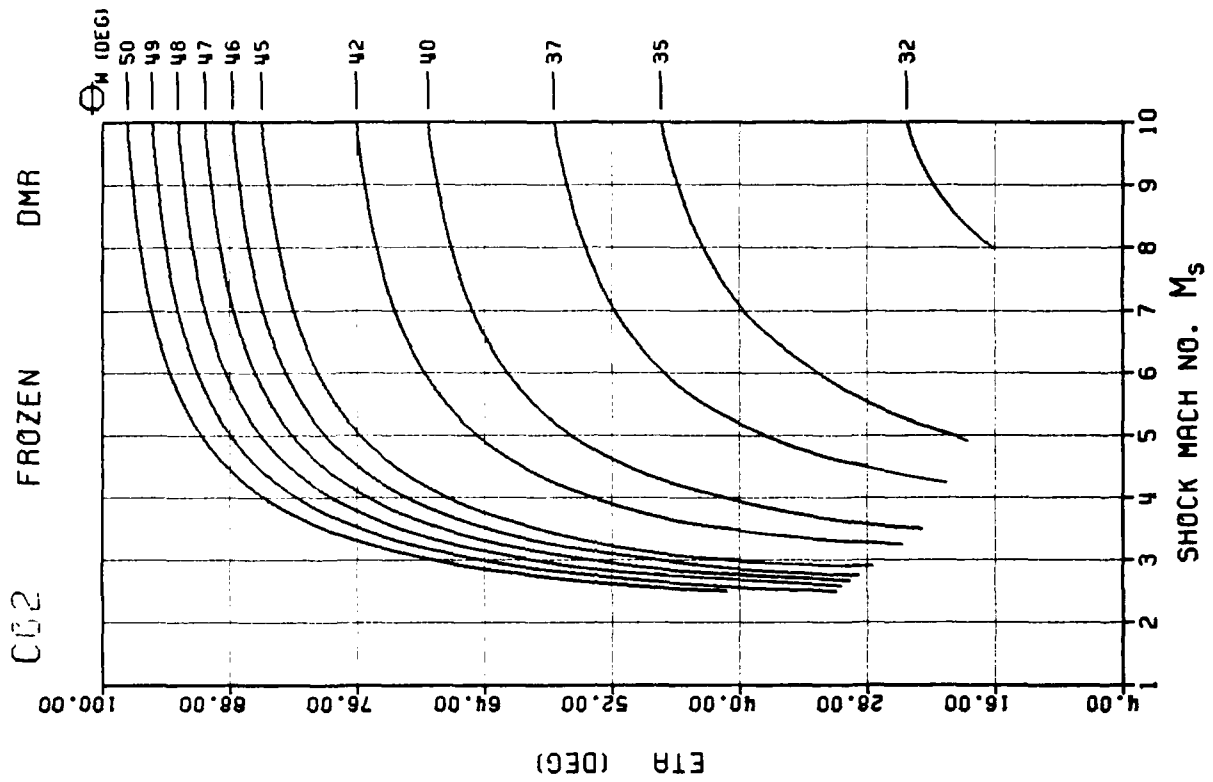


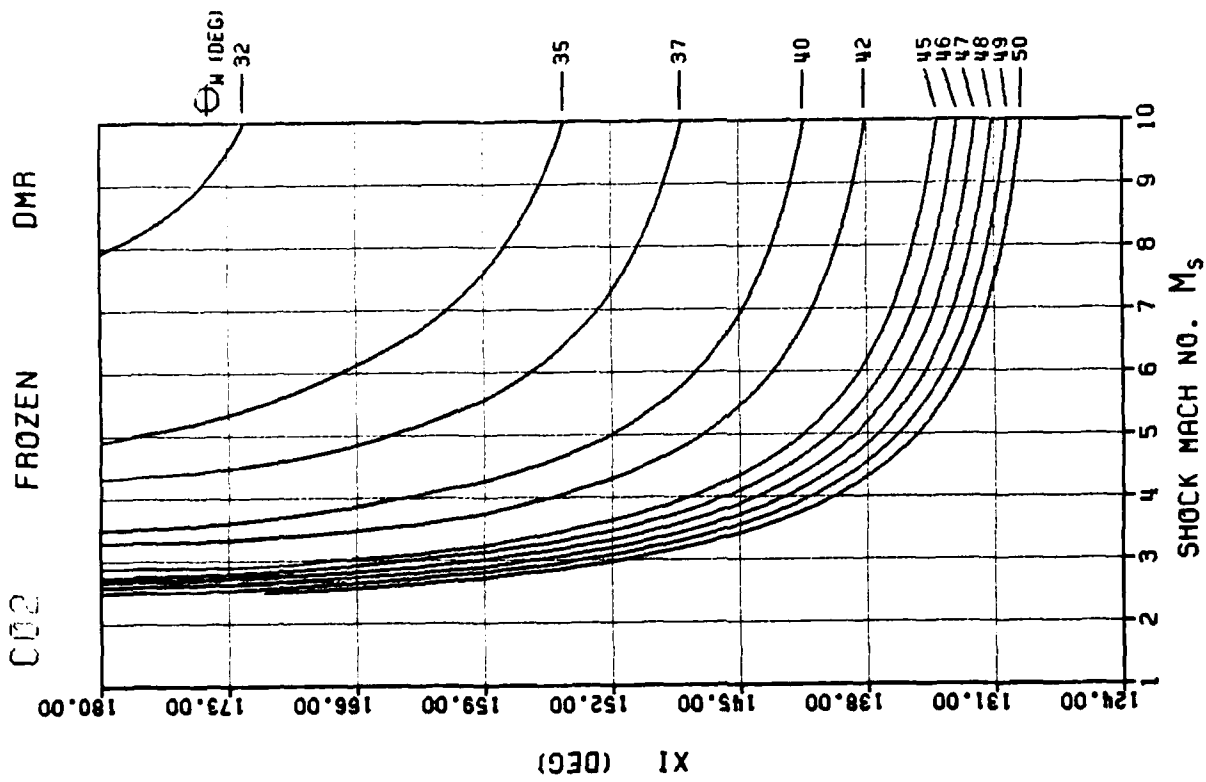




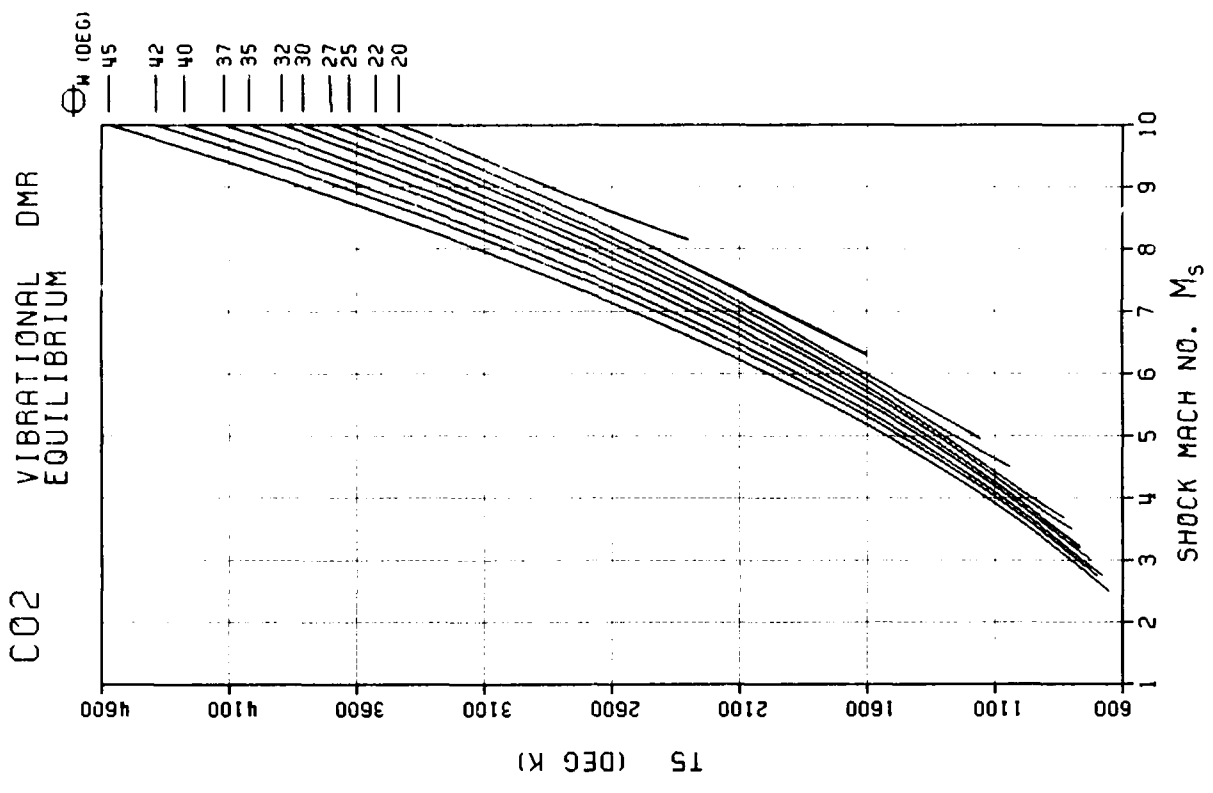
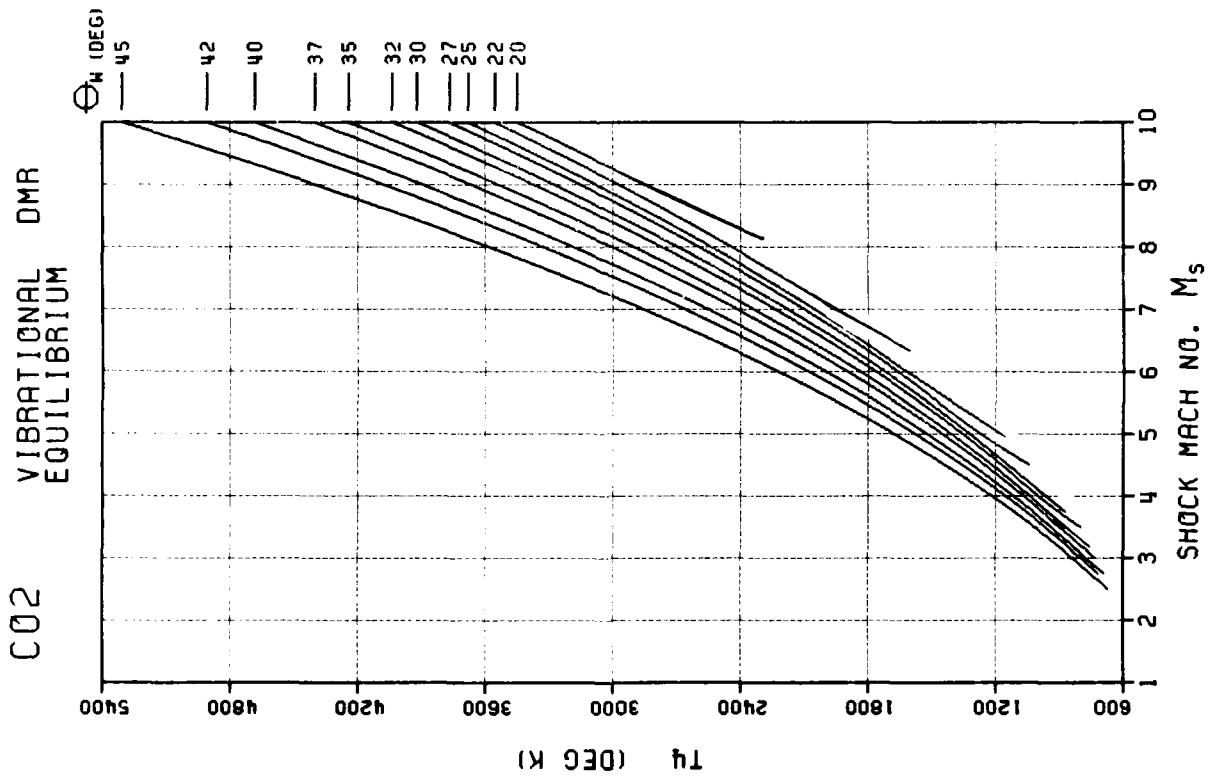


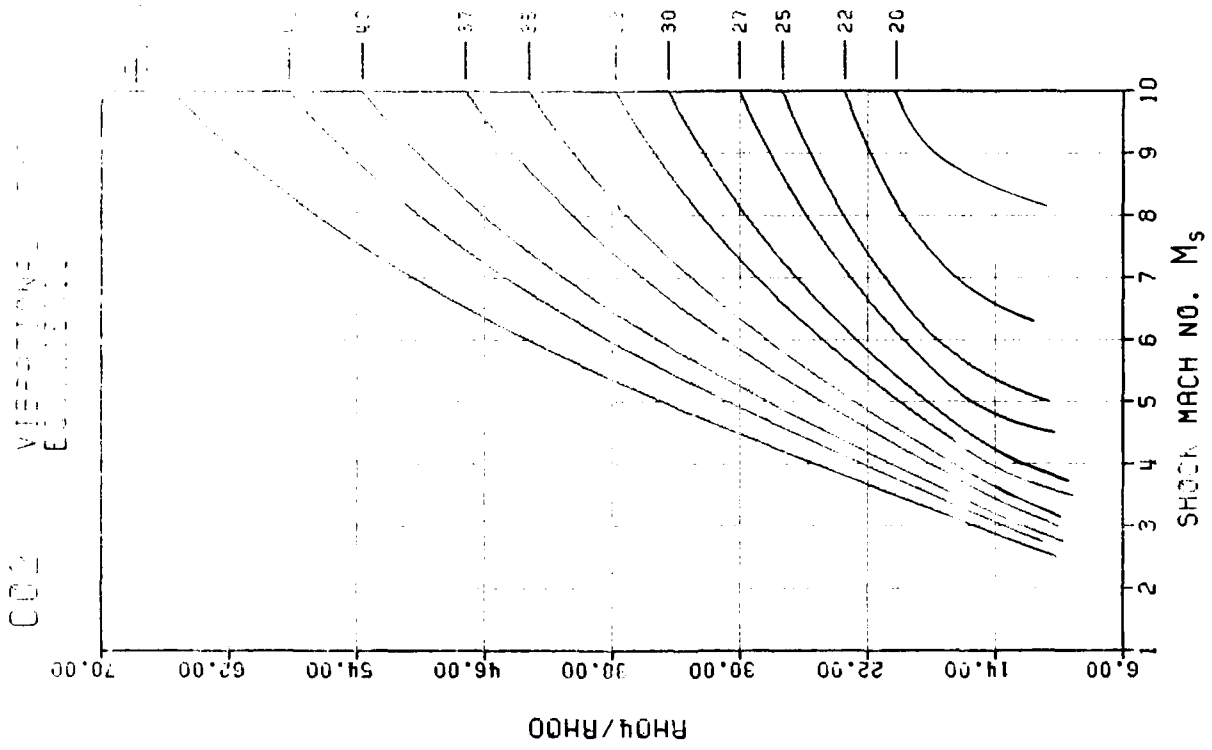
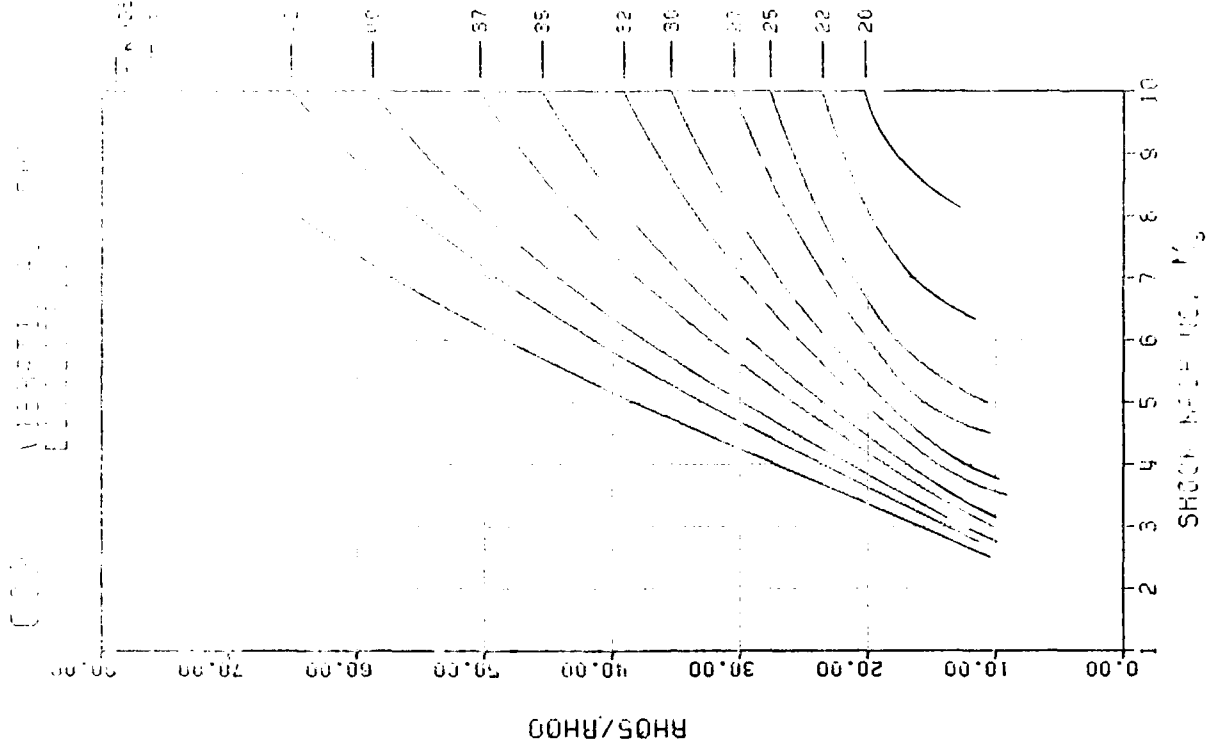


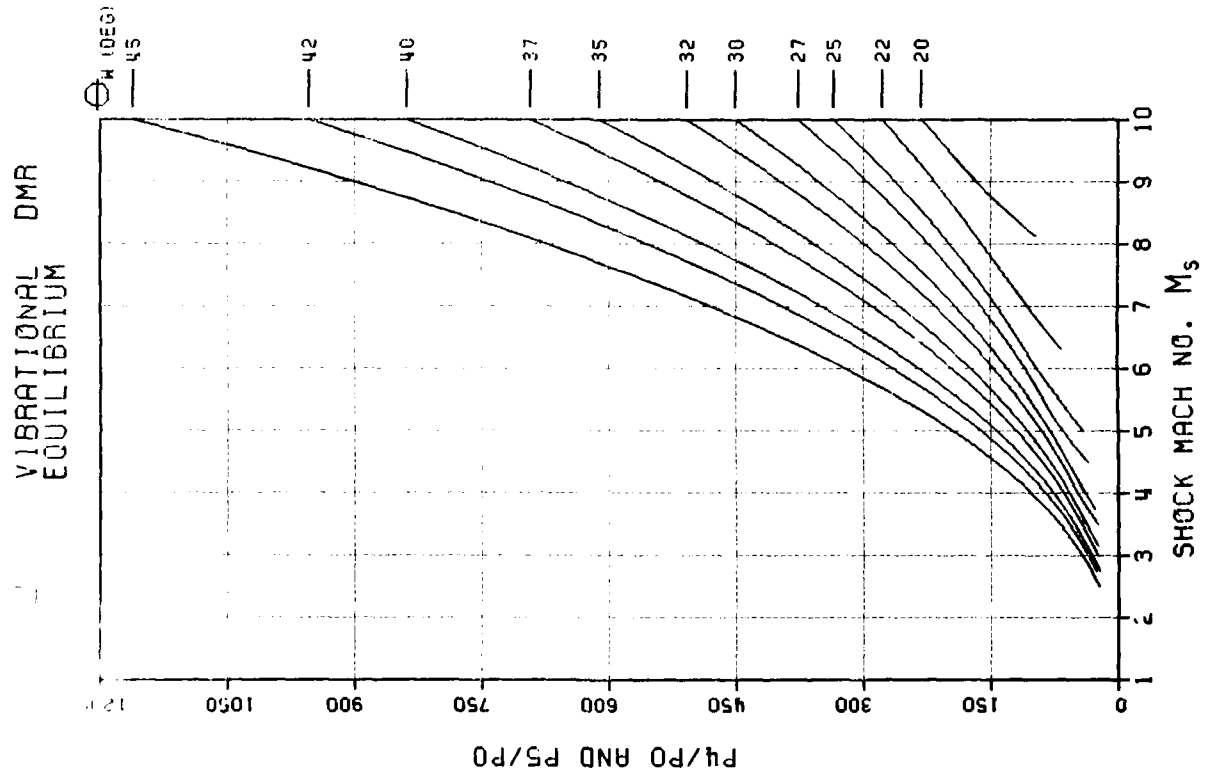
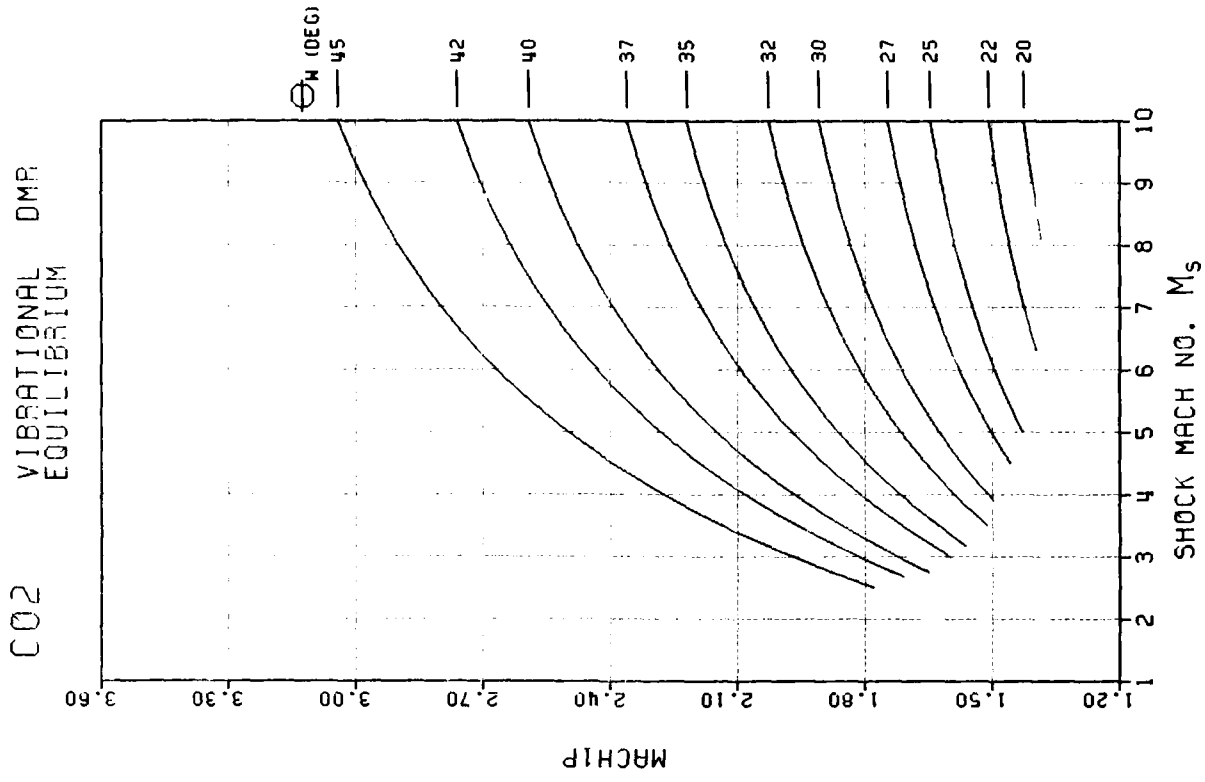


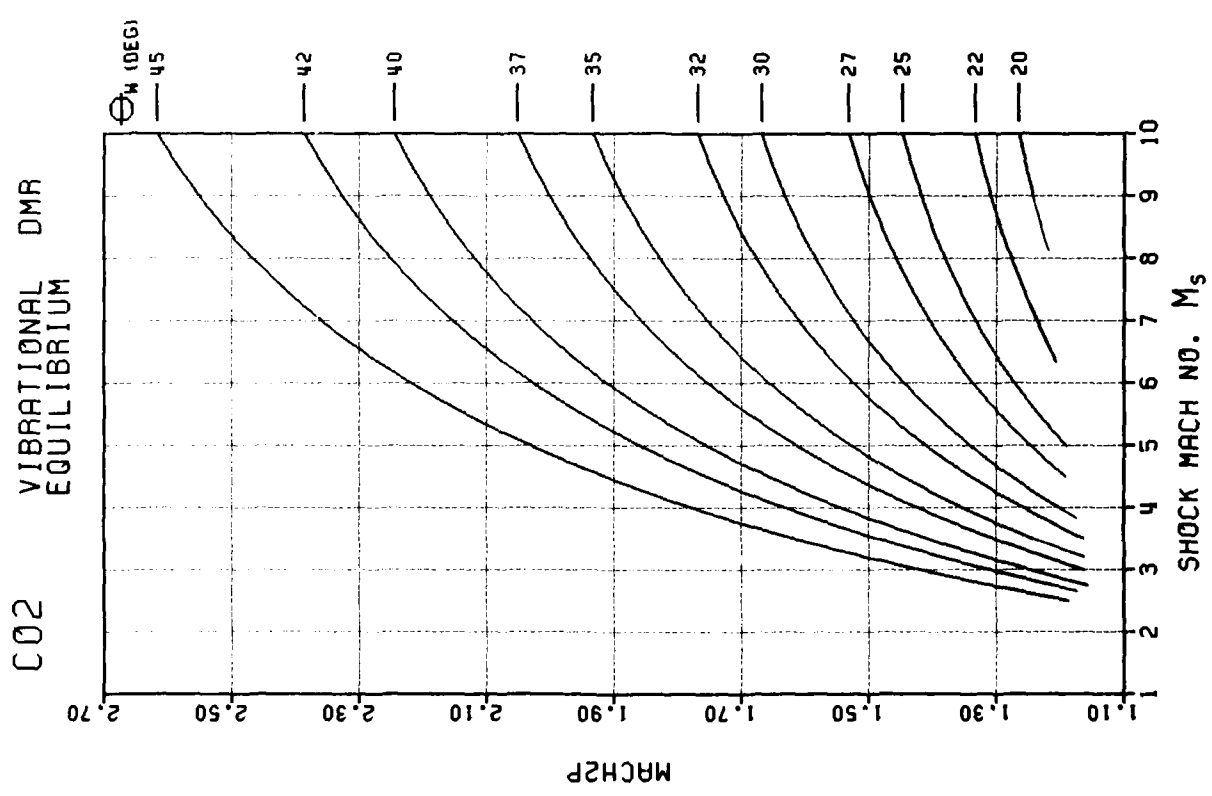
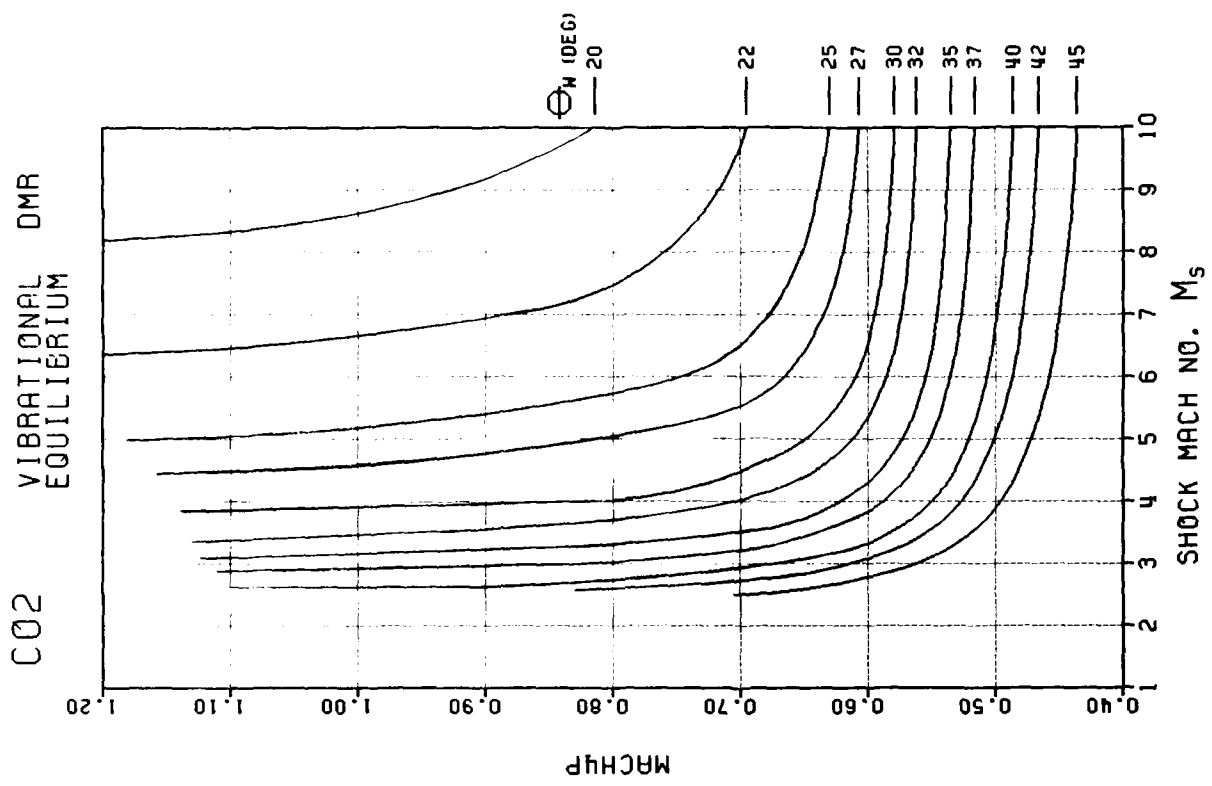


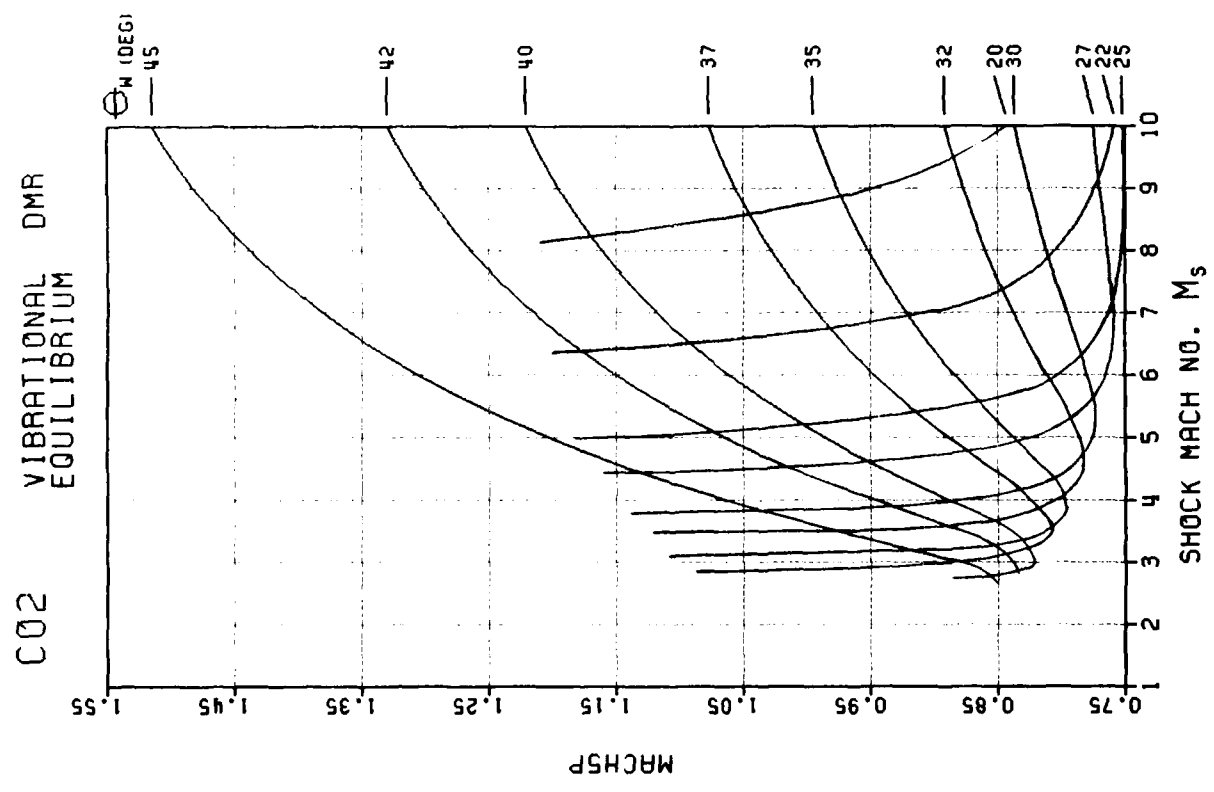
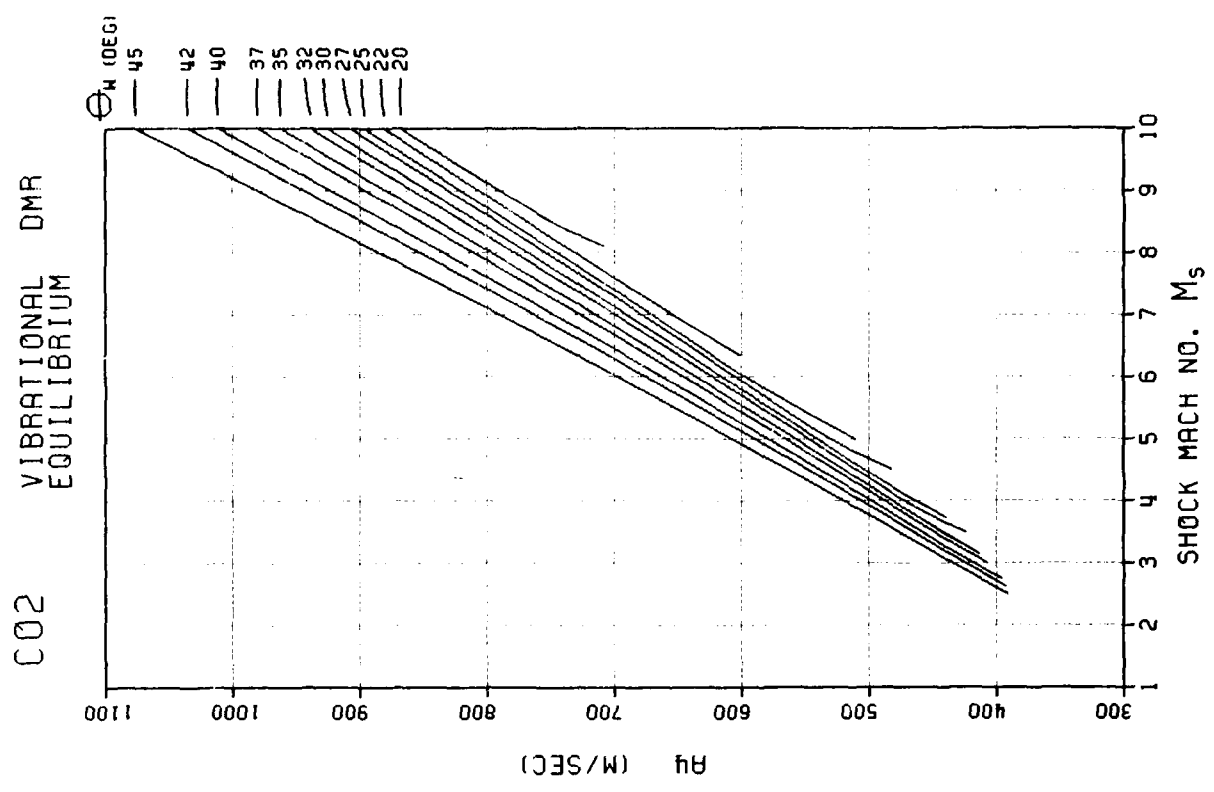
F - 290

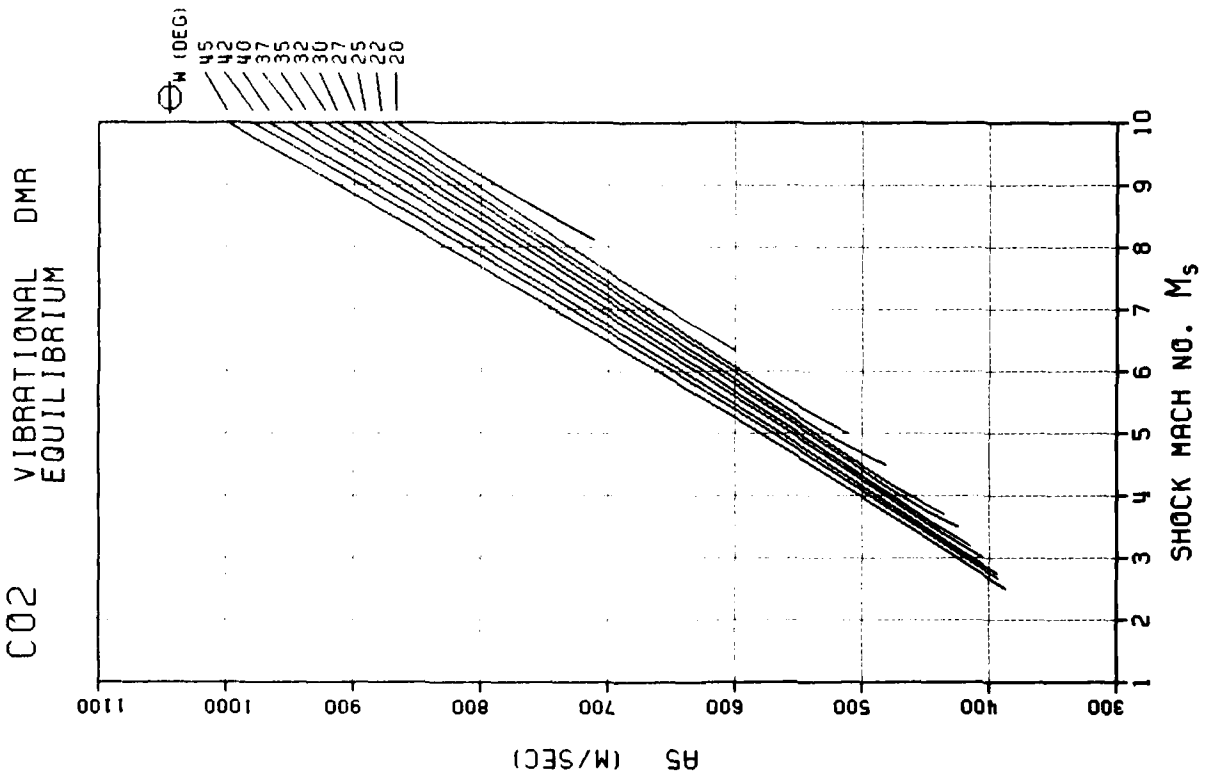
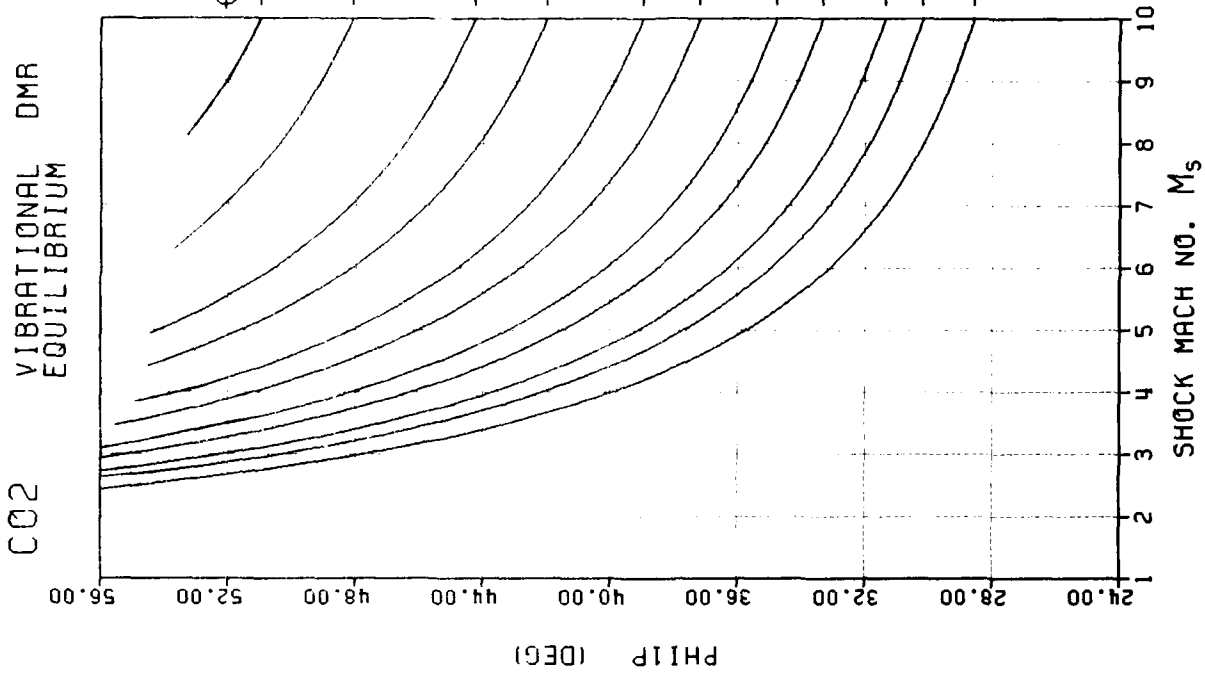


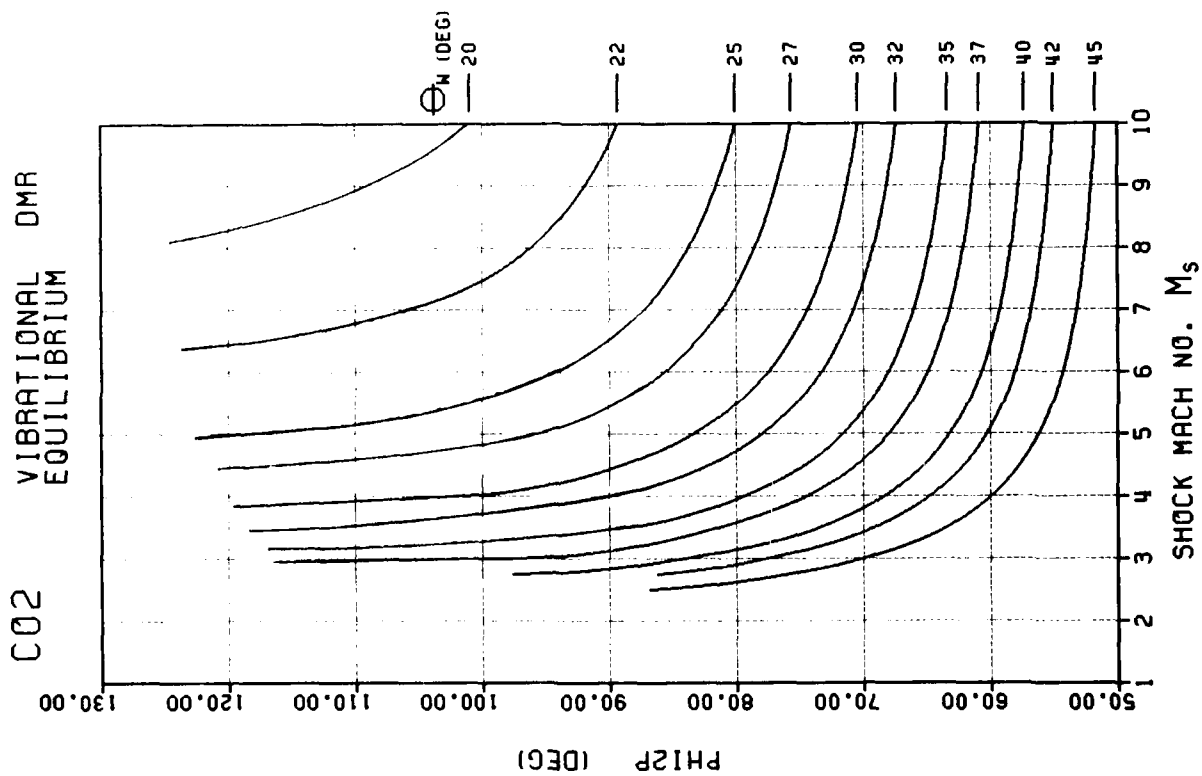
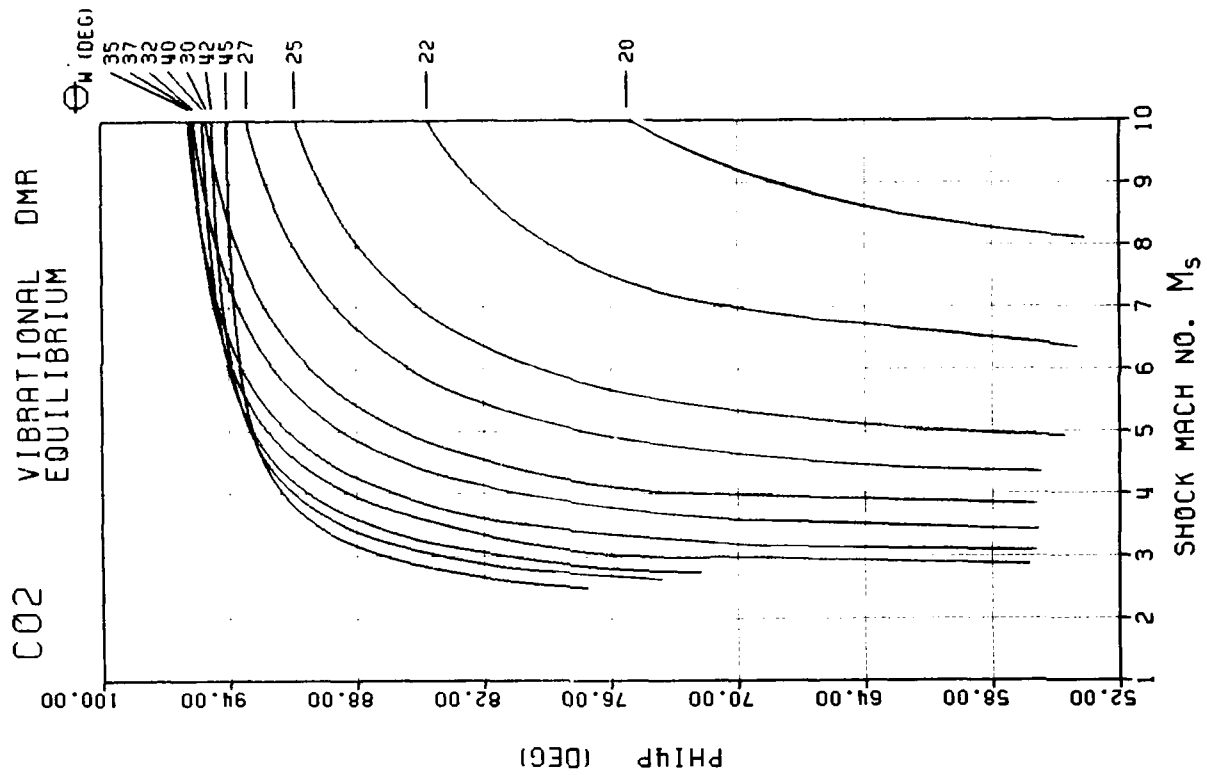


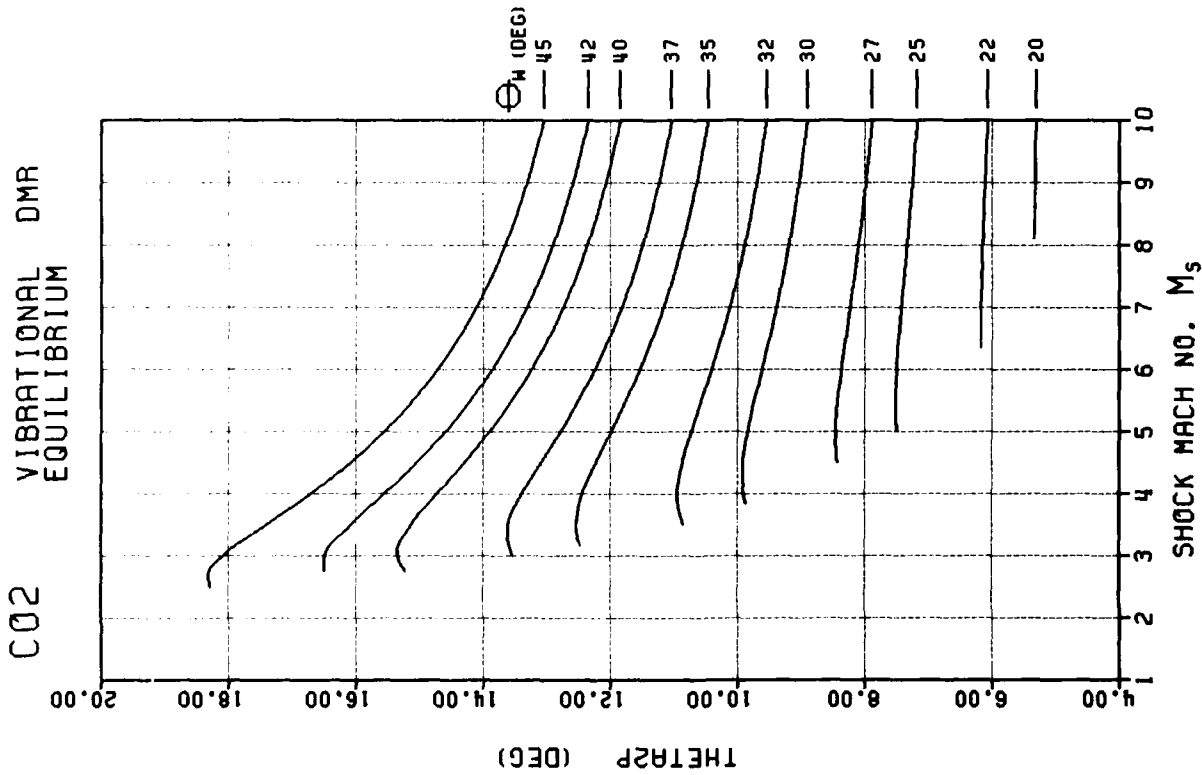
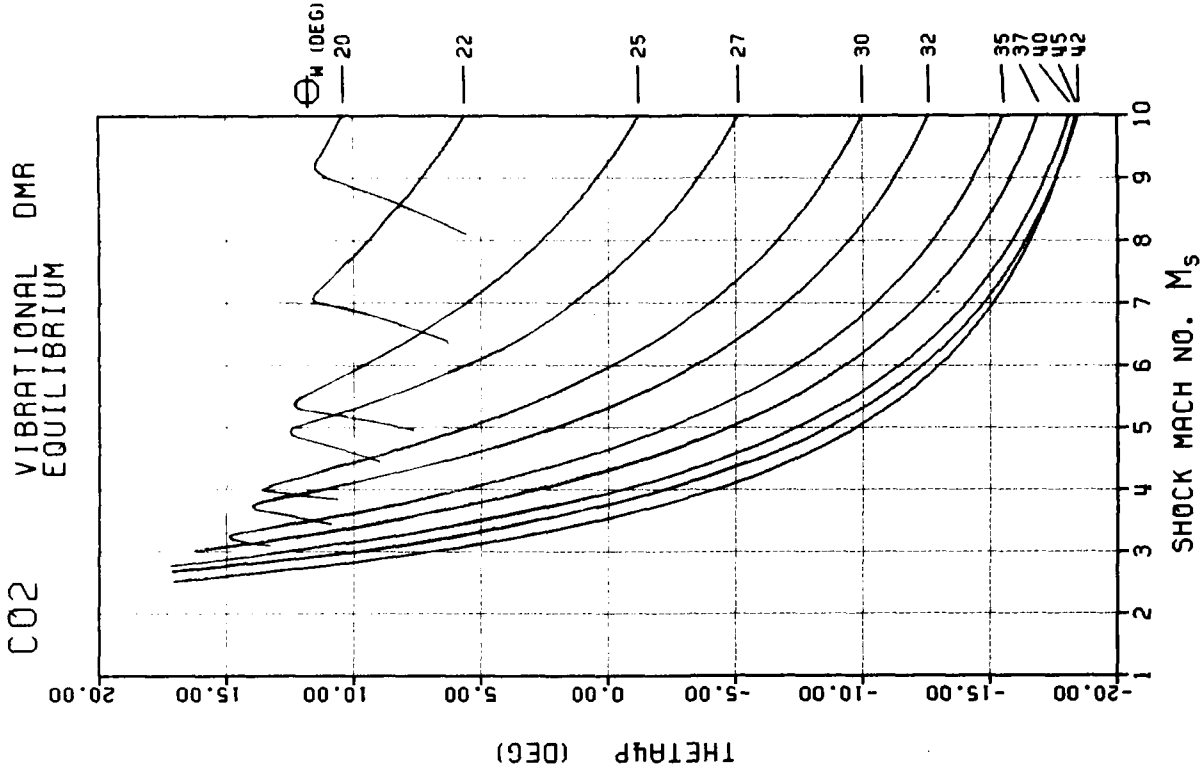


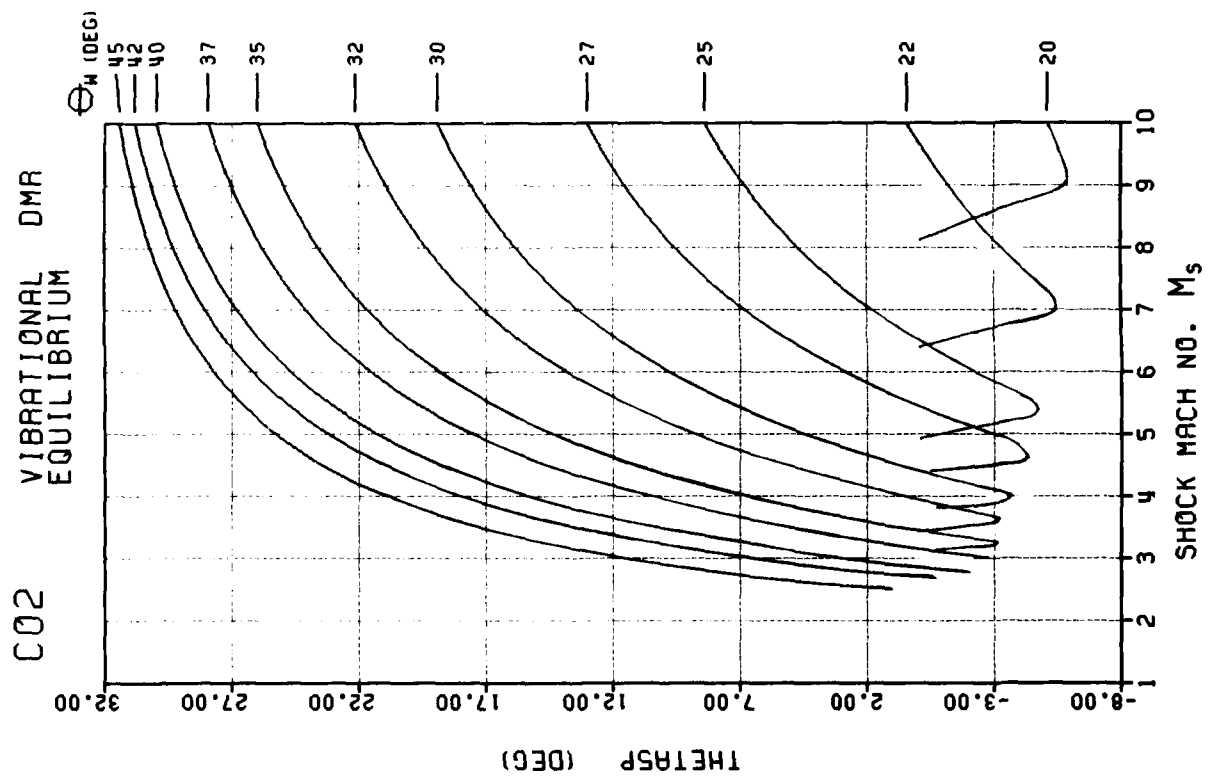
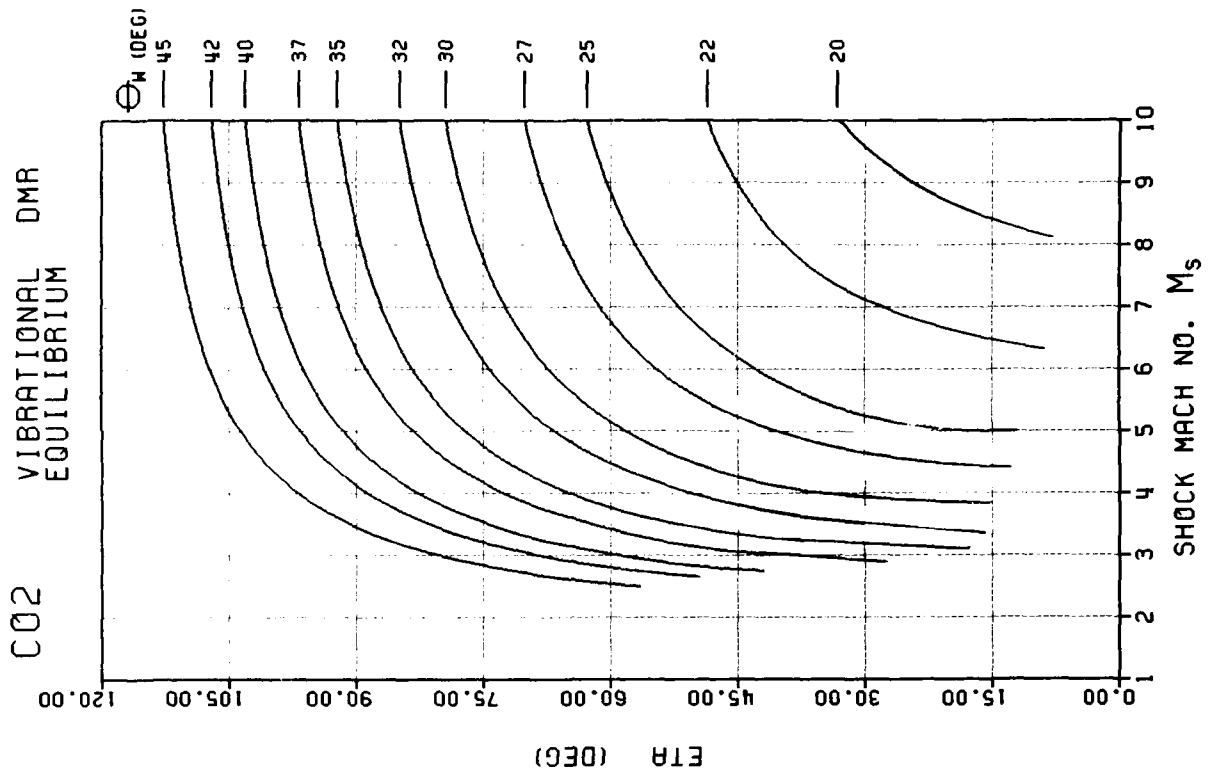


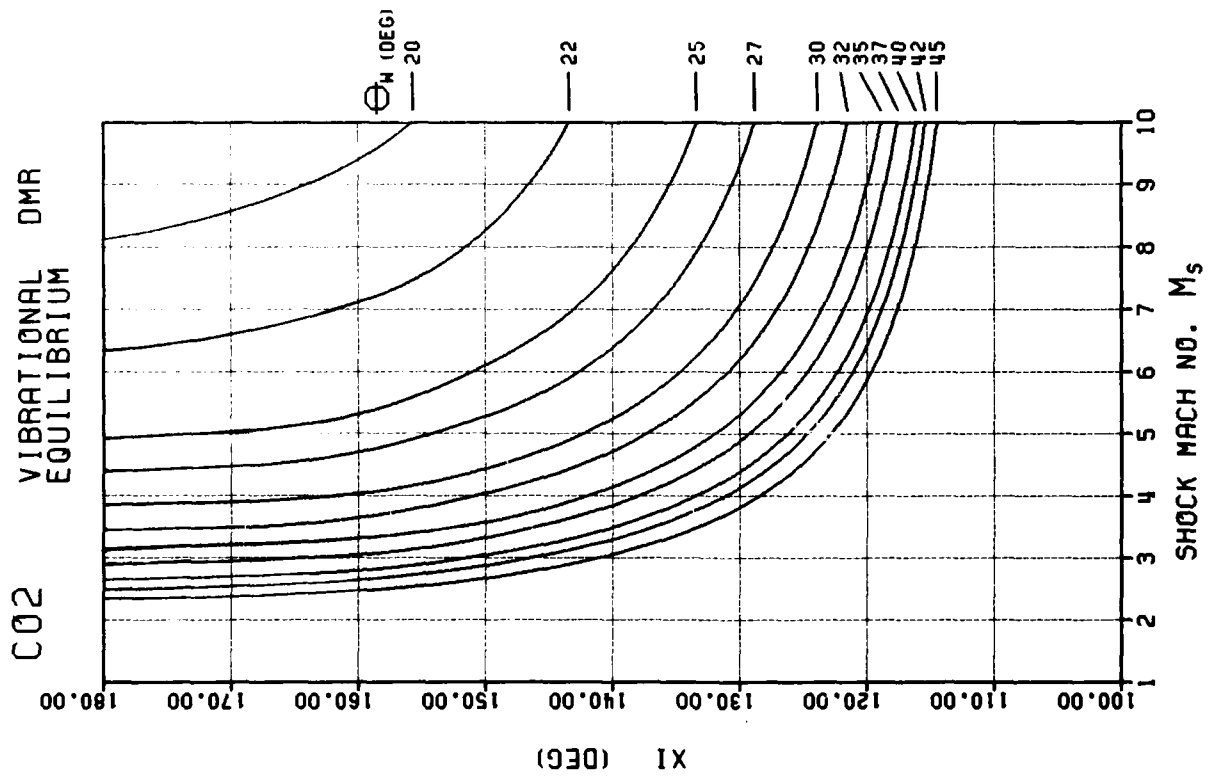


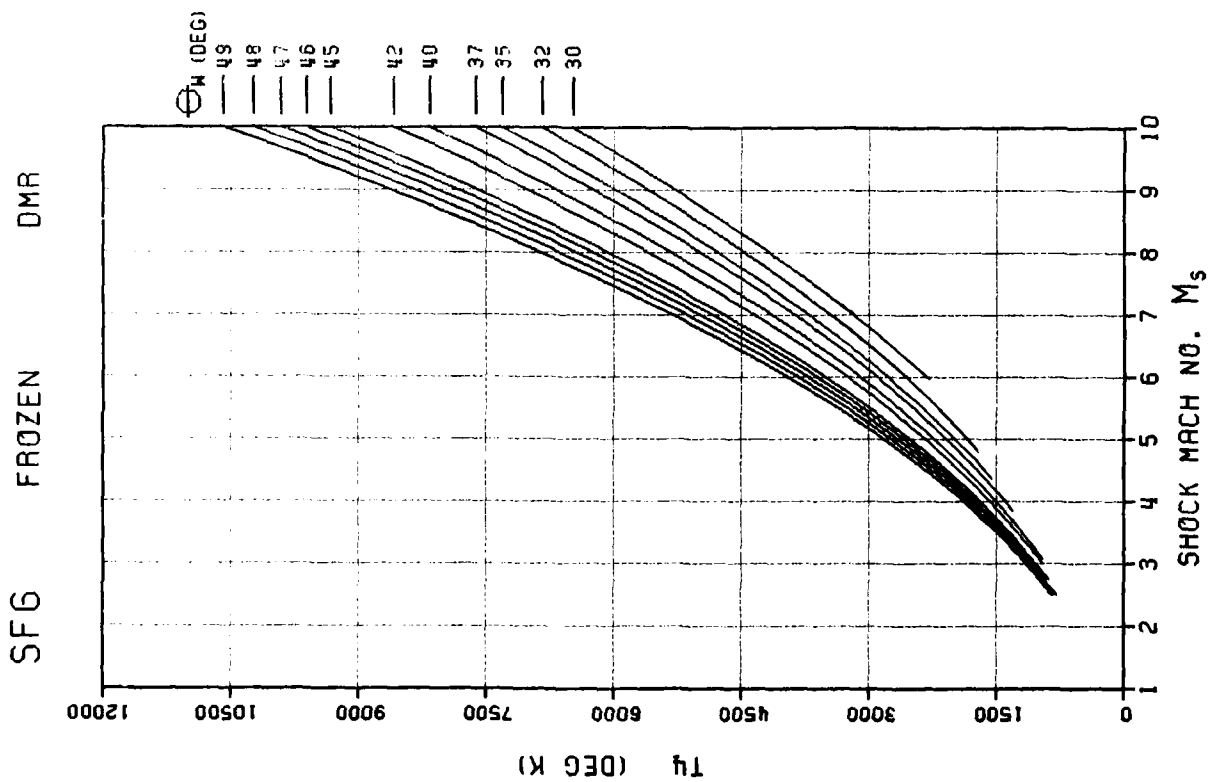
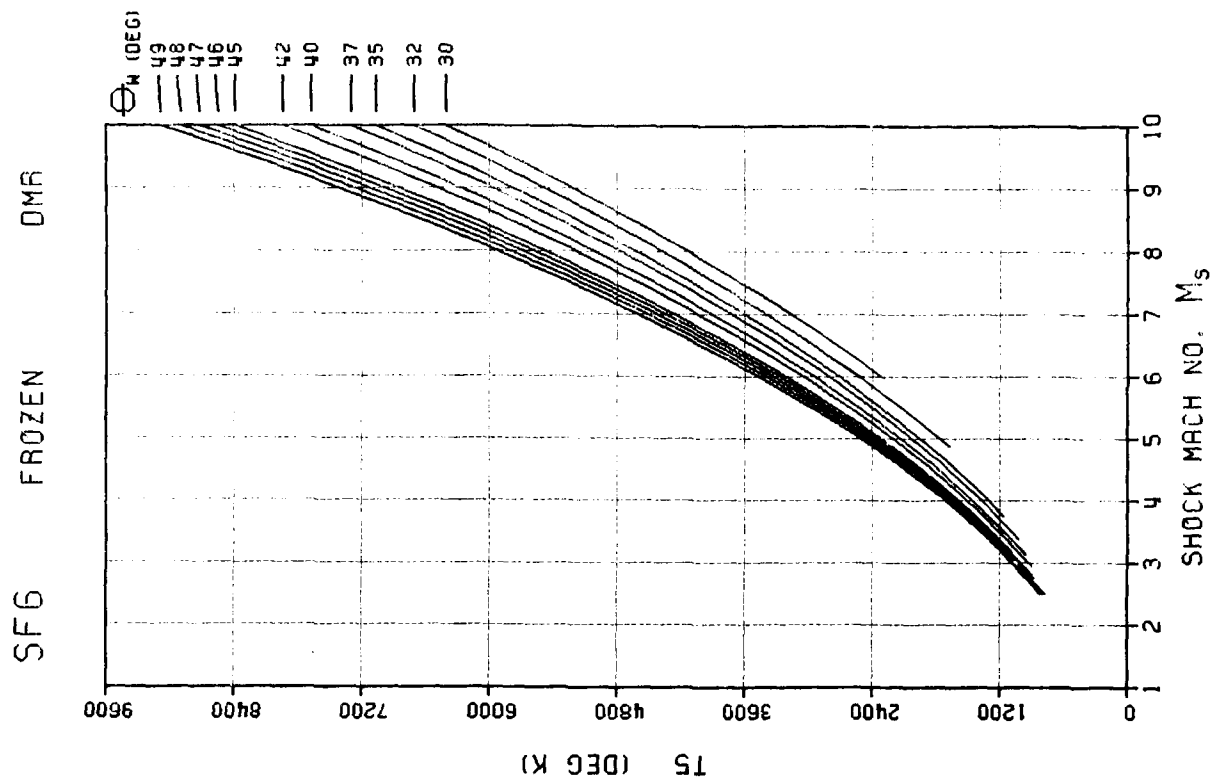


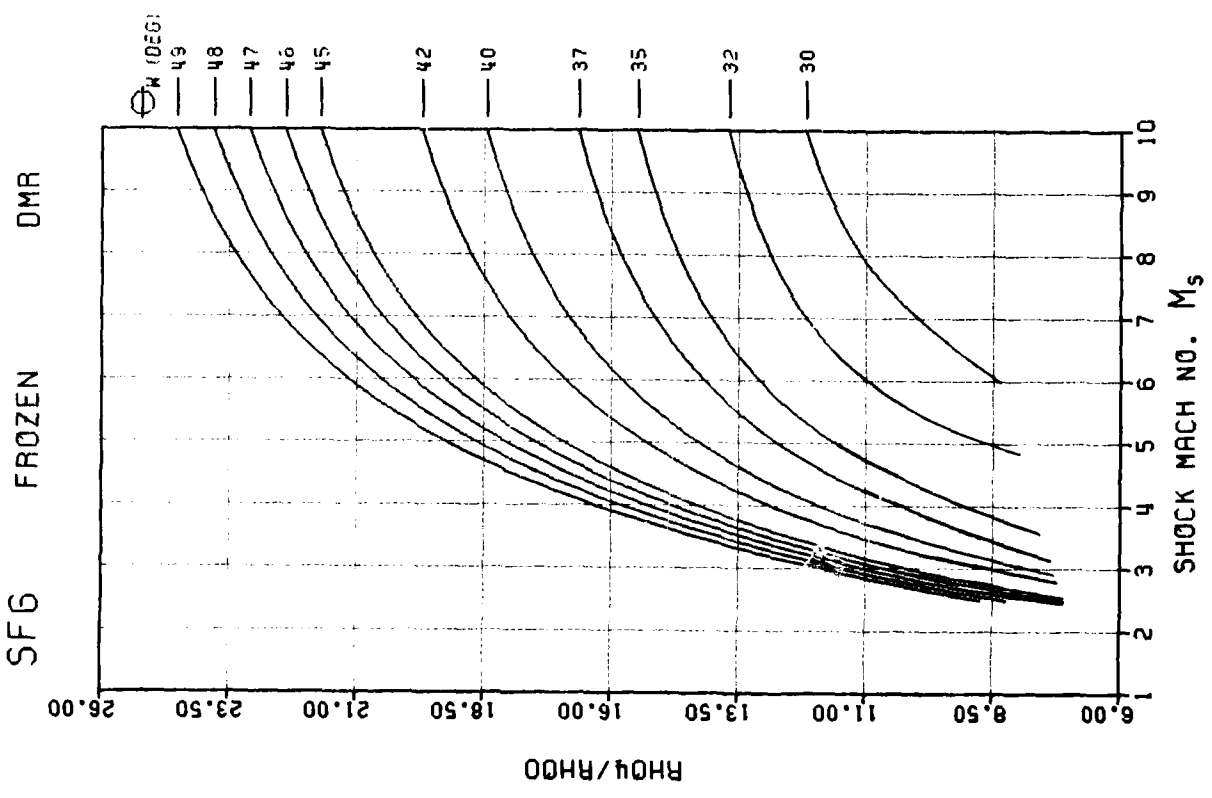
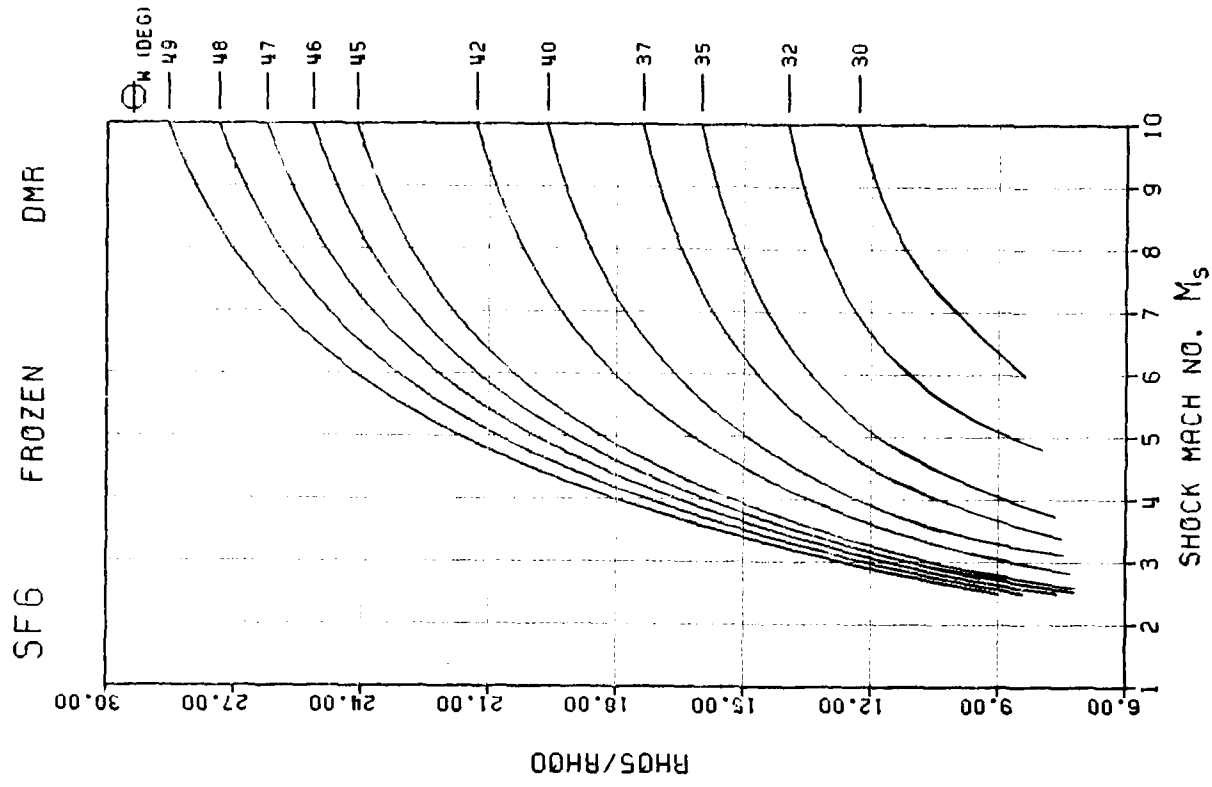


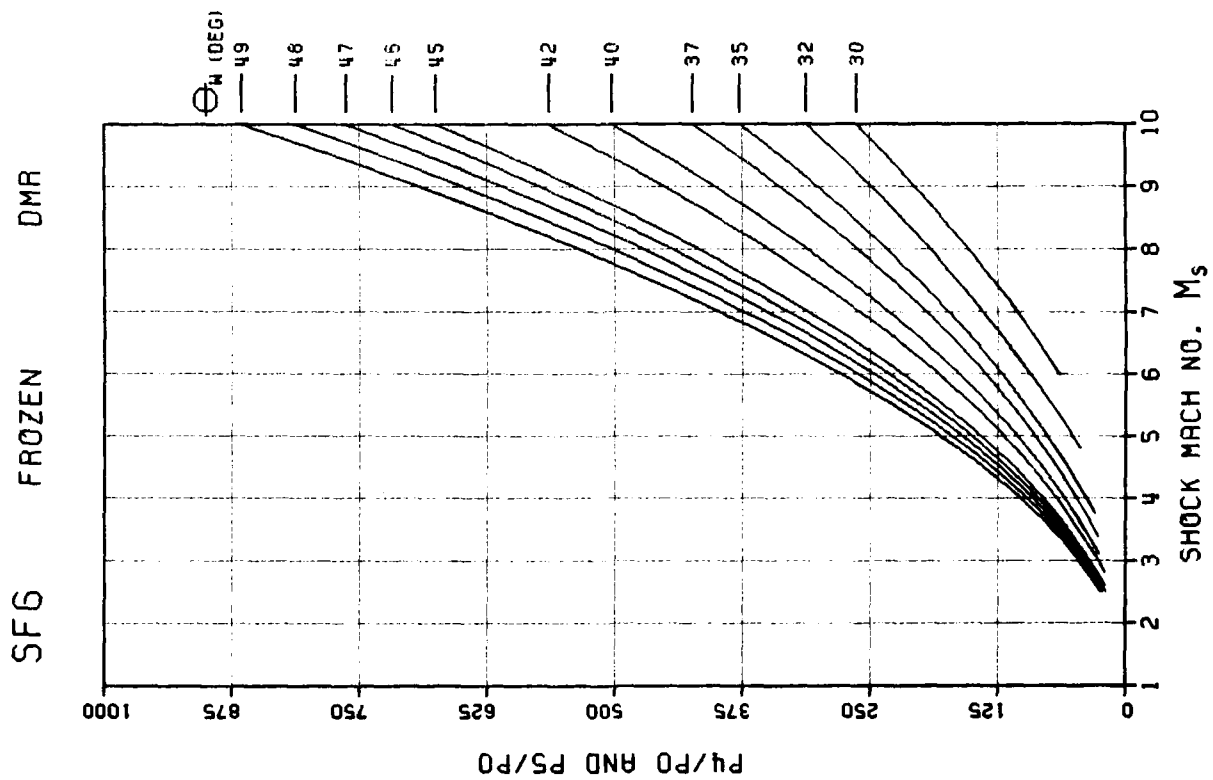
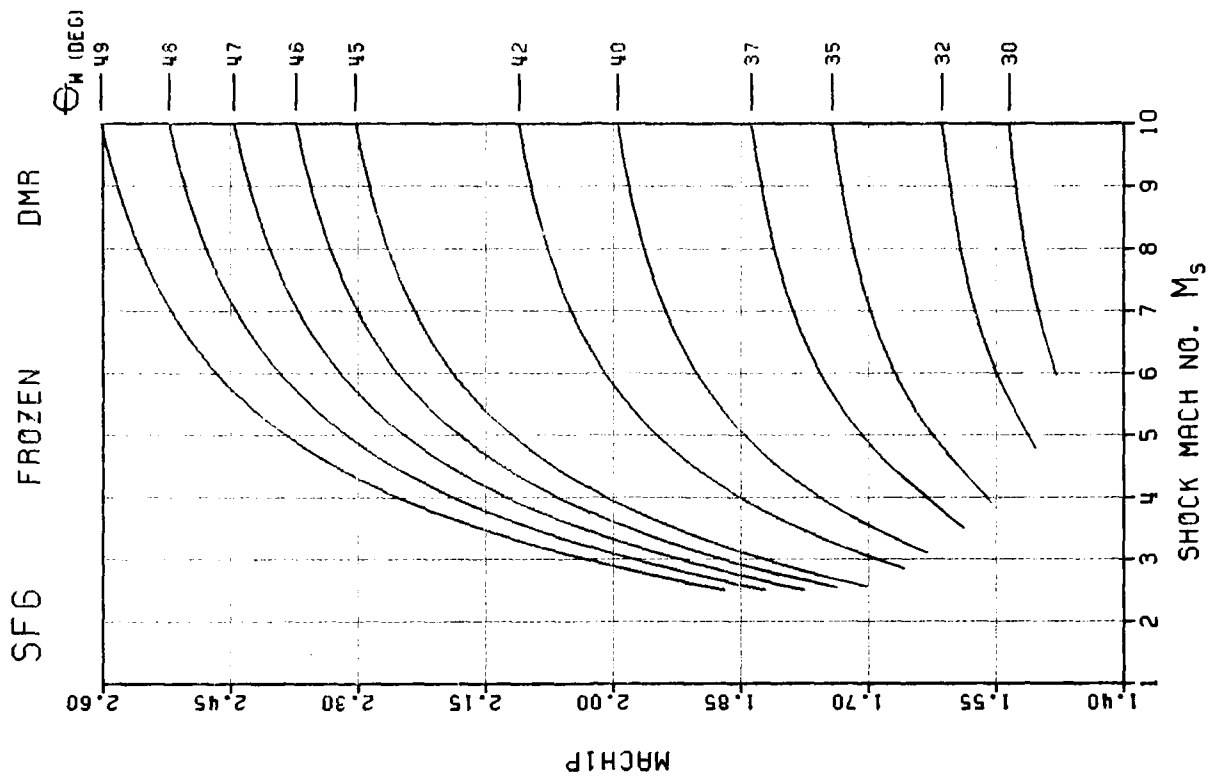


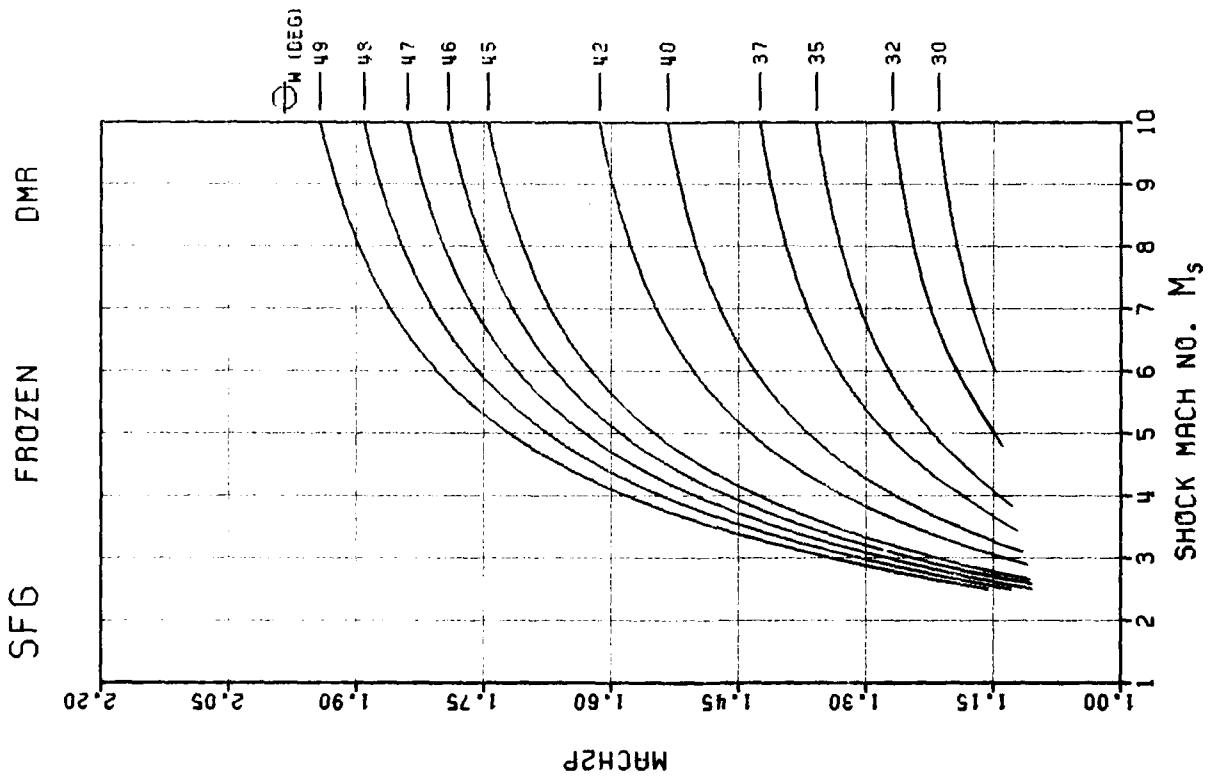
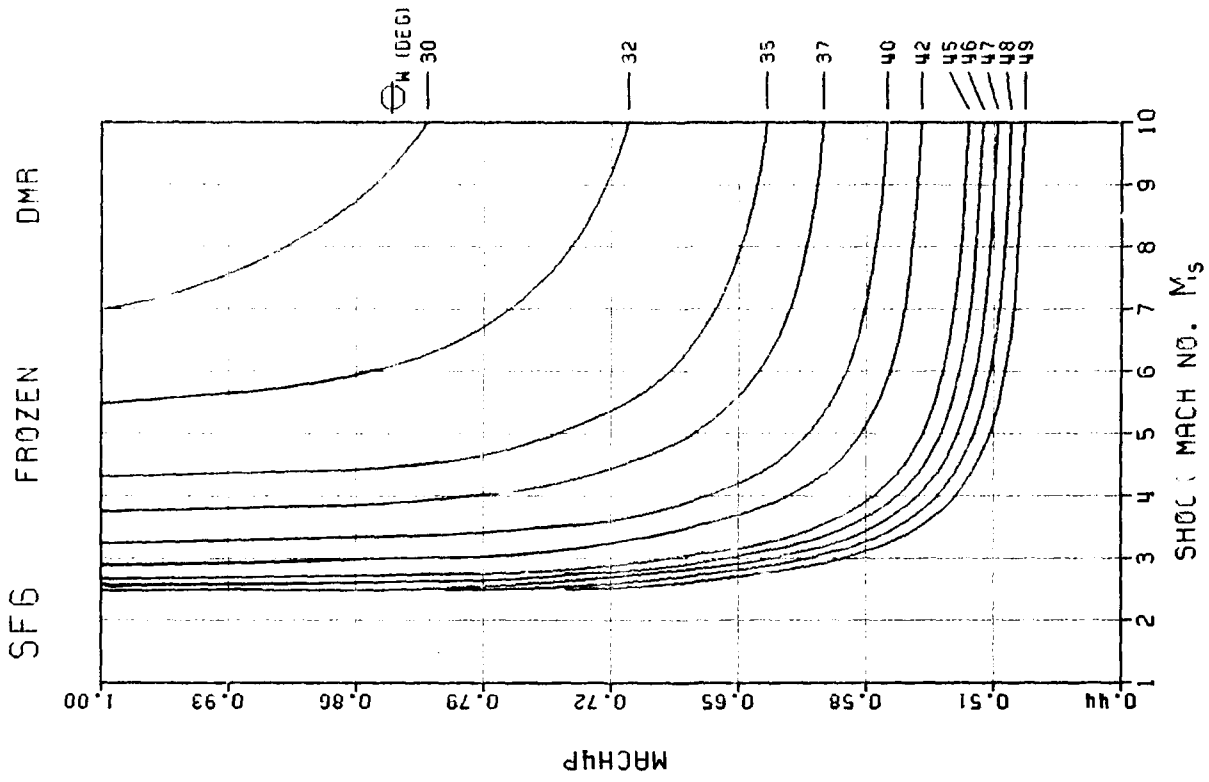


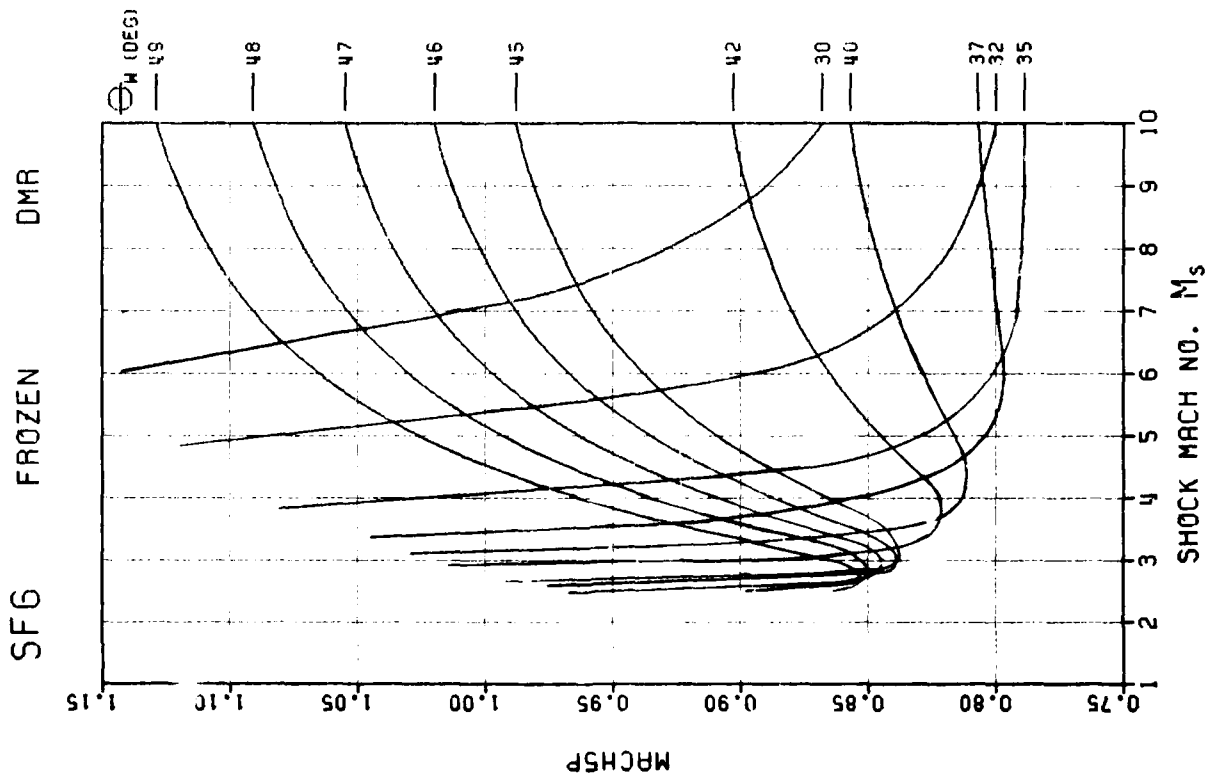
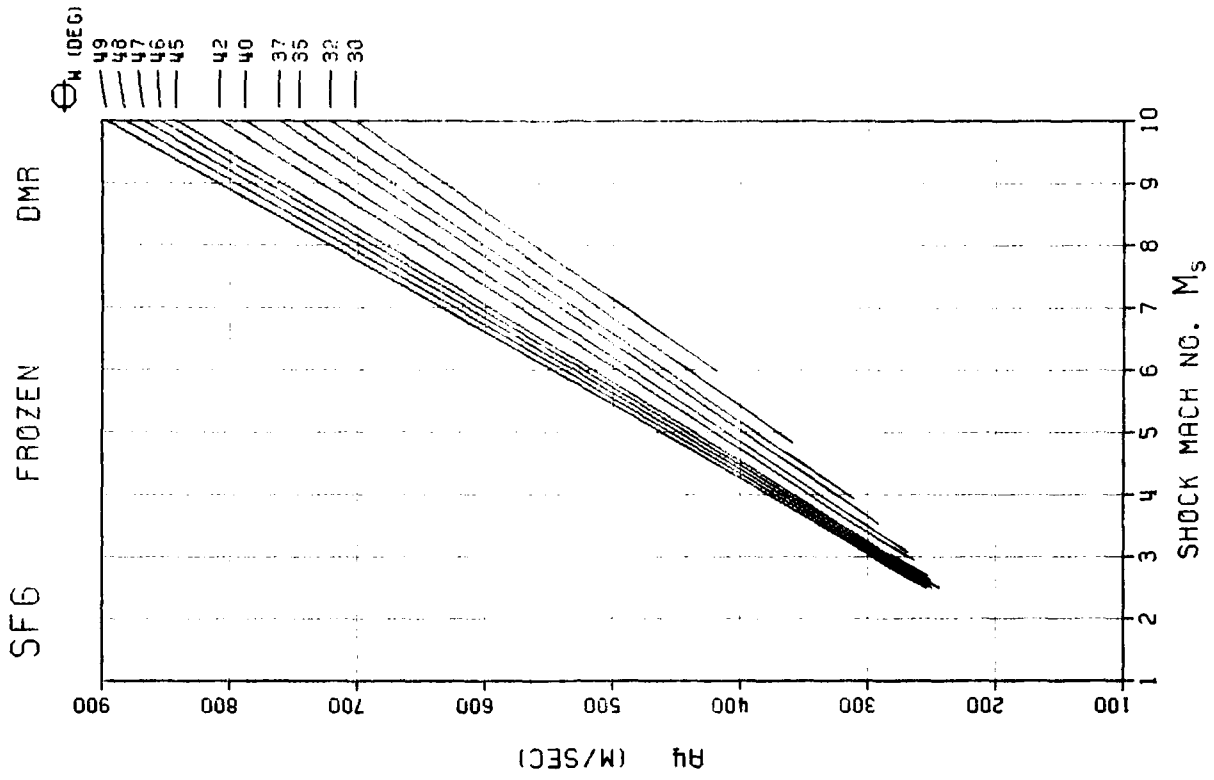


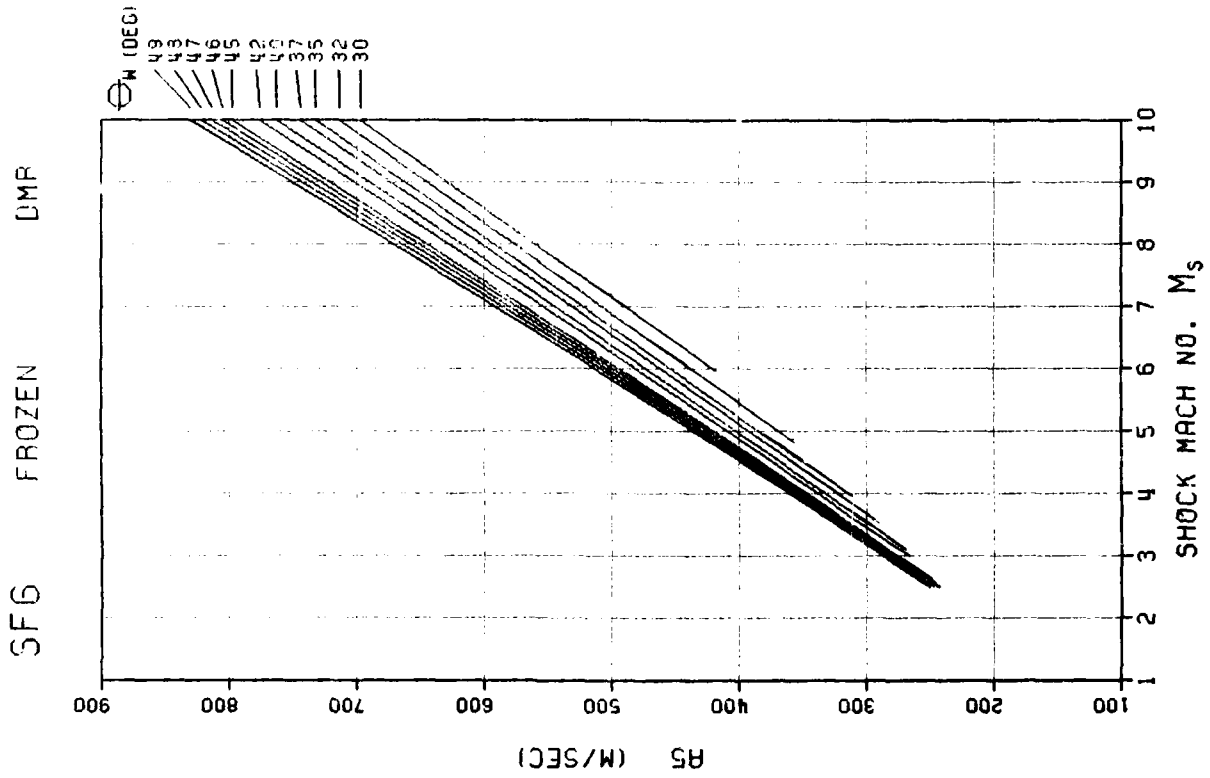
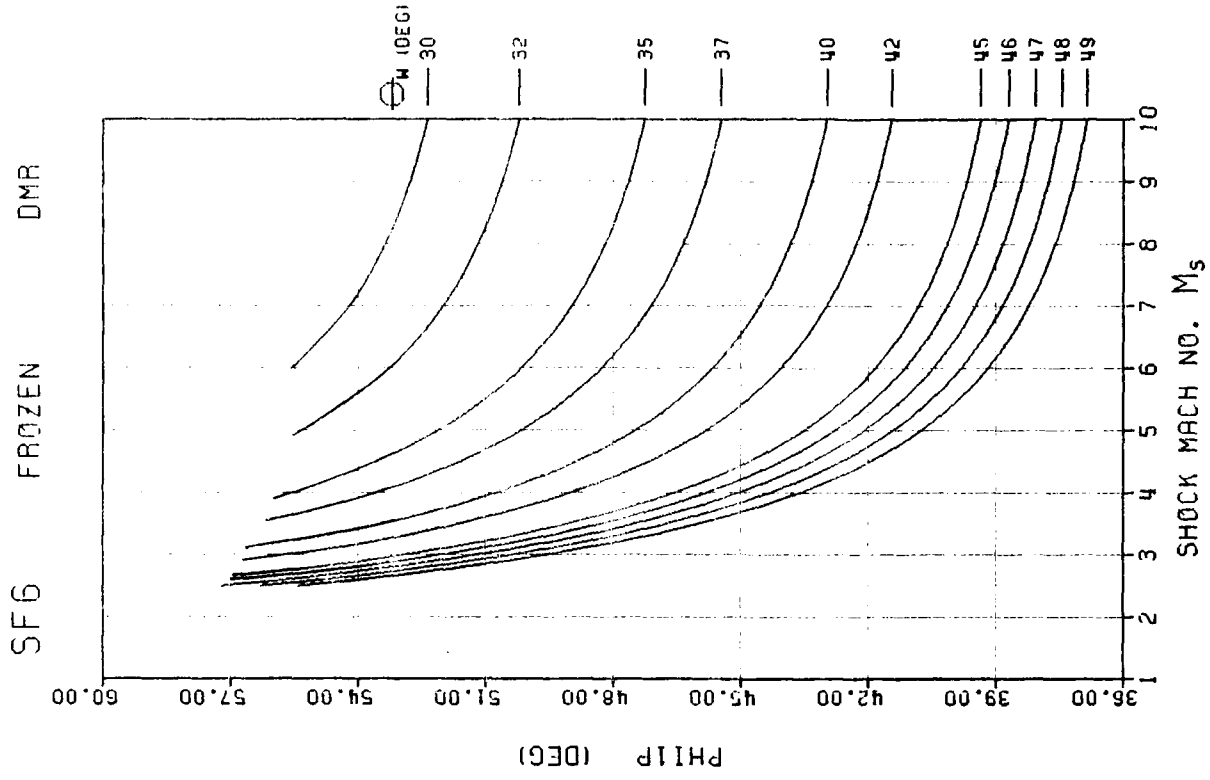


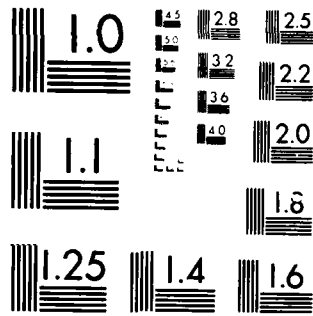




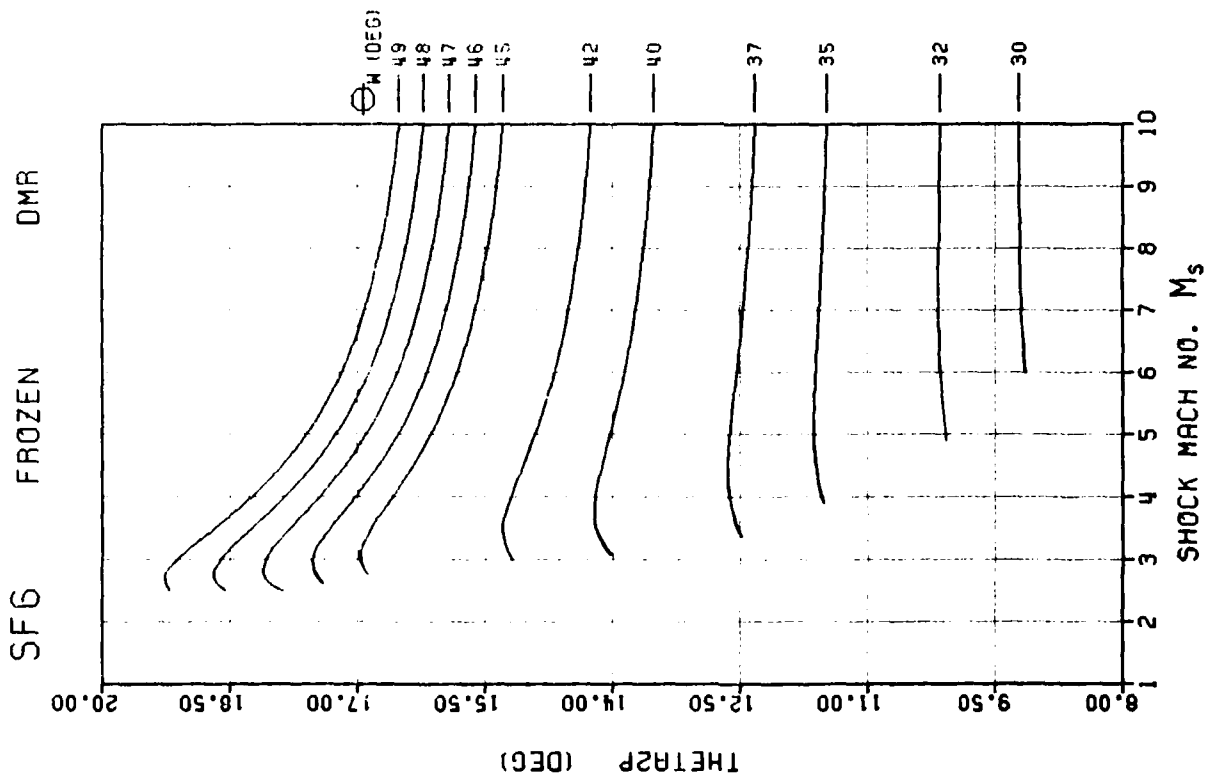
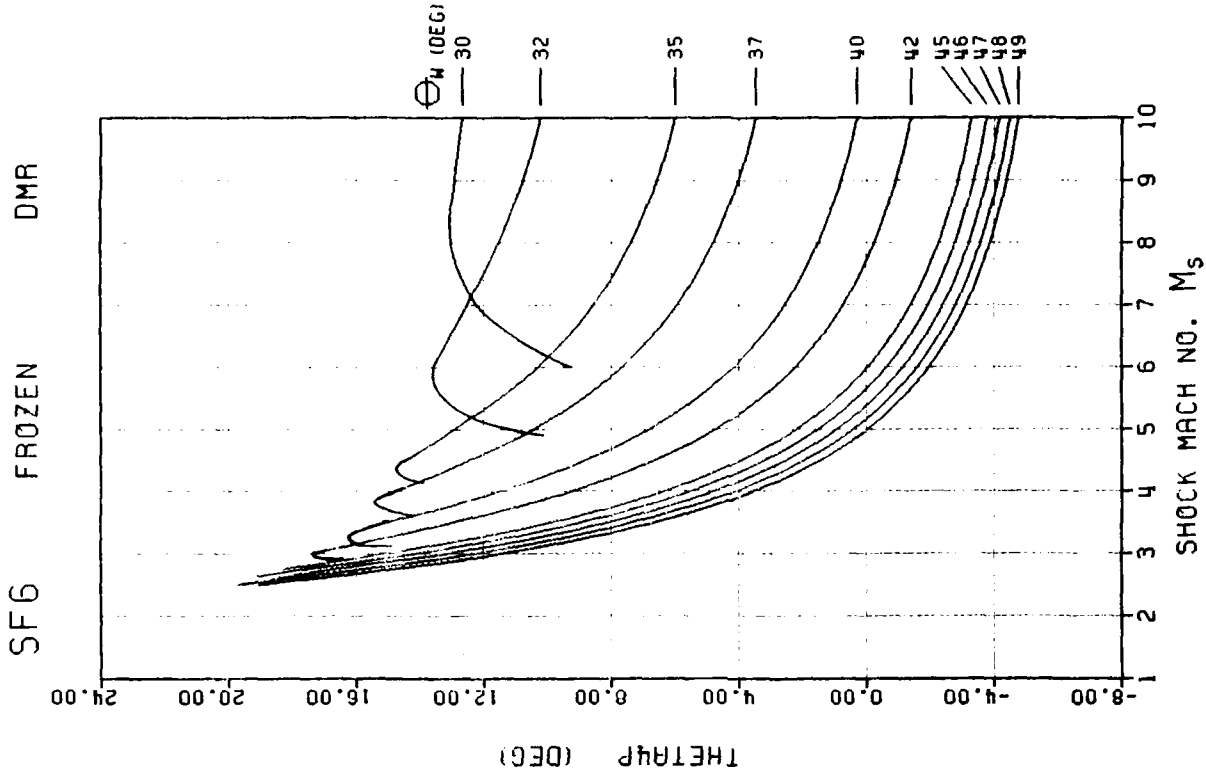


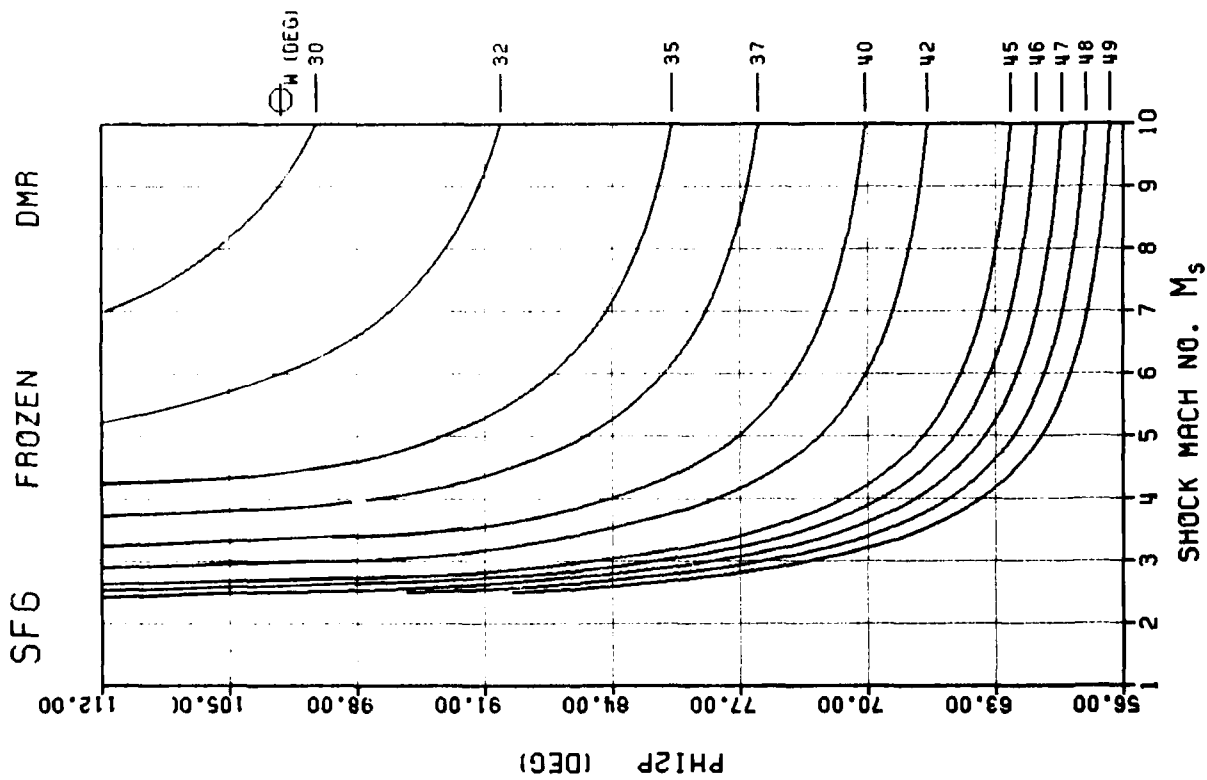
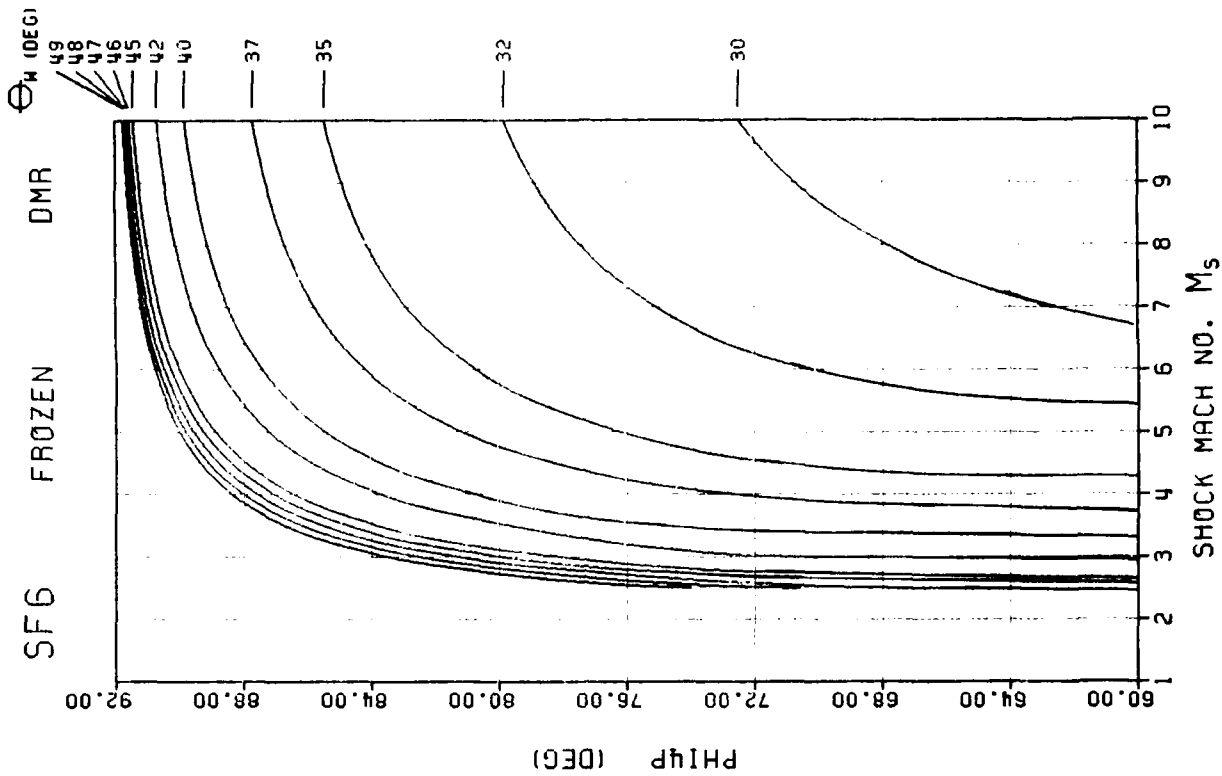


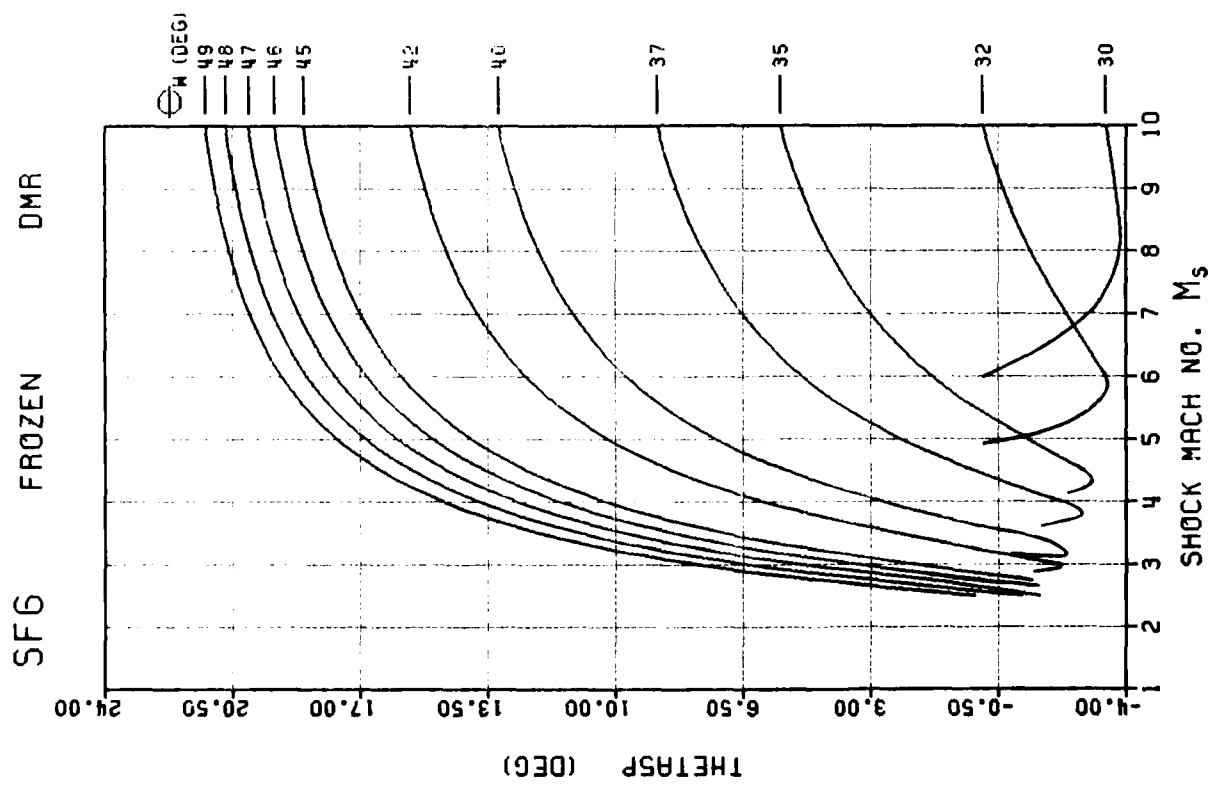
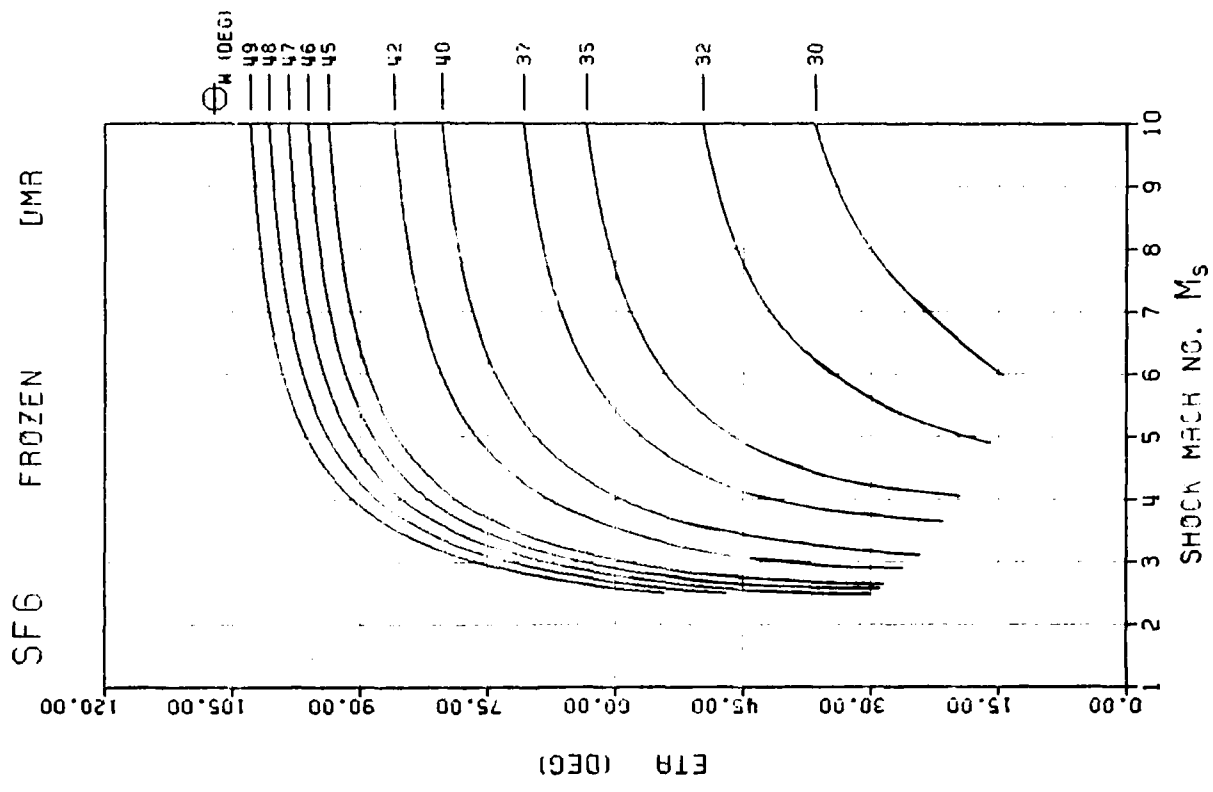


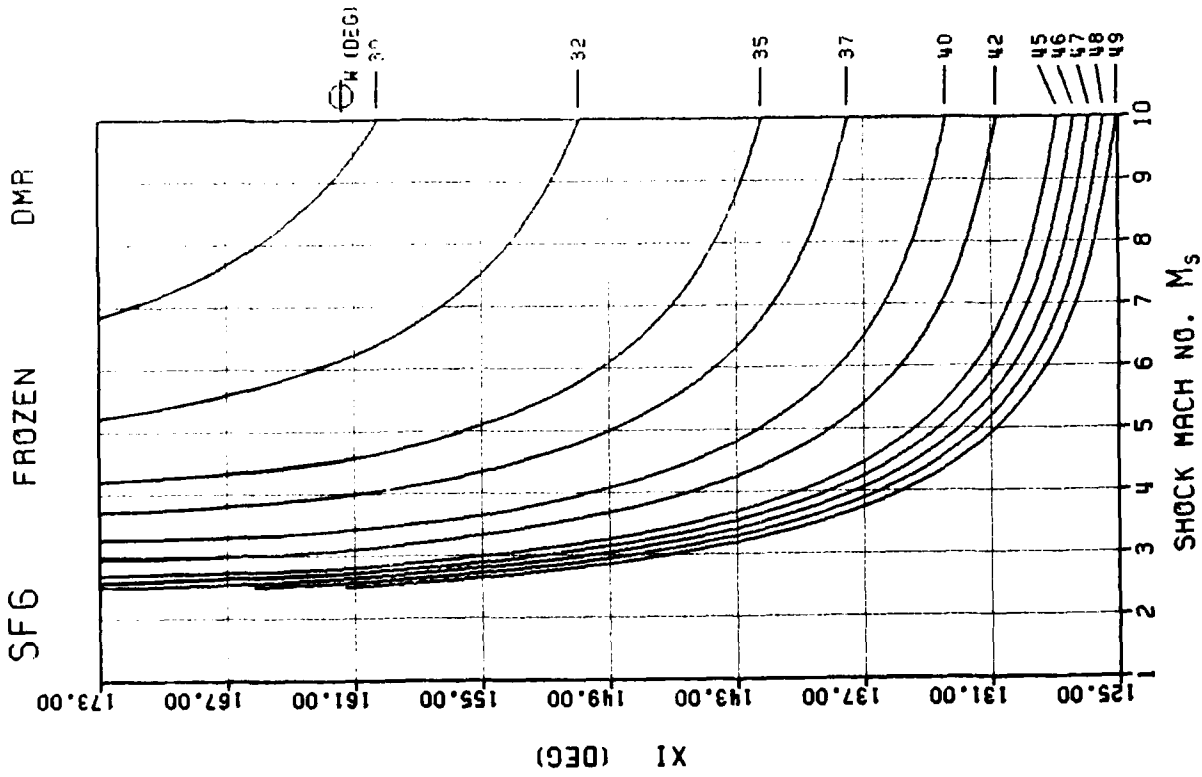


MICROCOPY RESOLUTION TEST CHART
NATIONAL BUREAU OF STANDARDS-1963-A

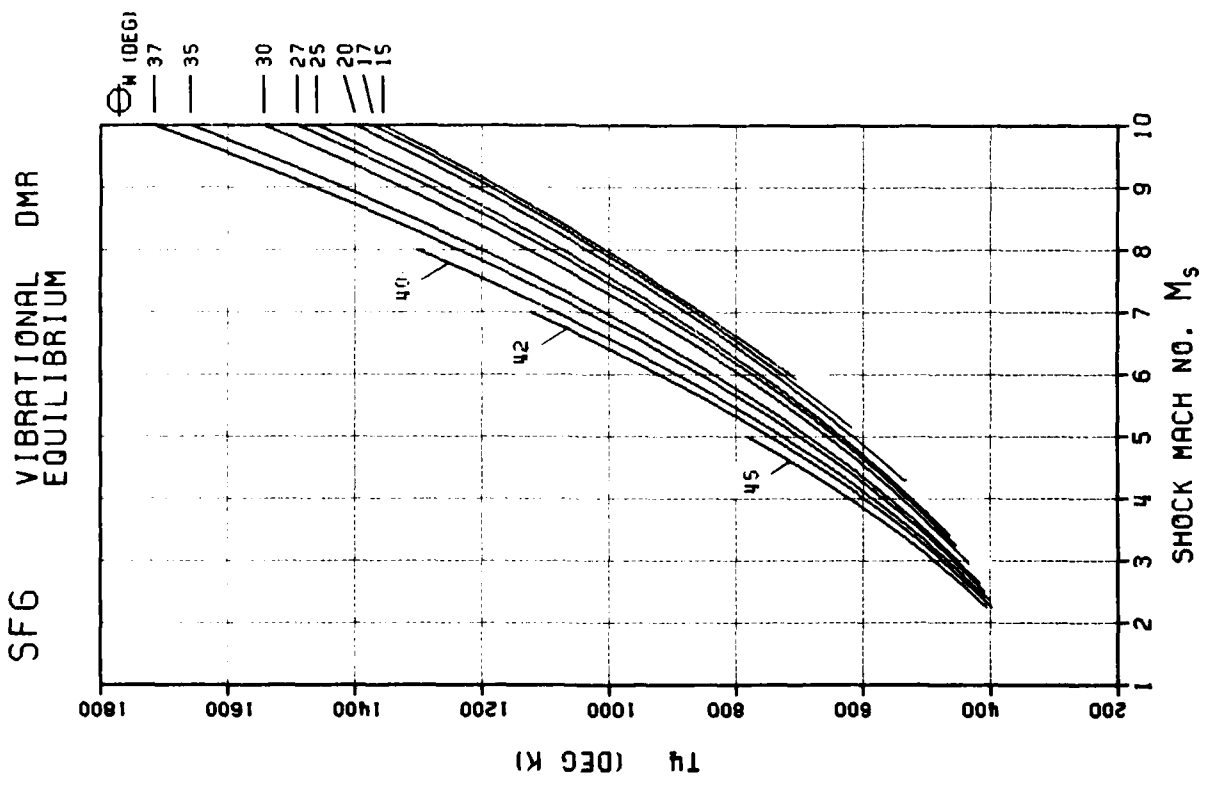
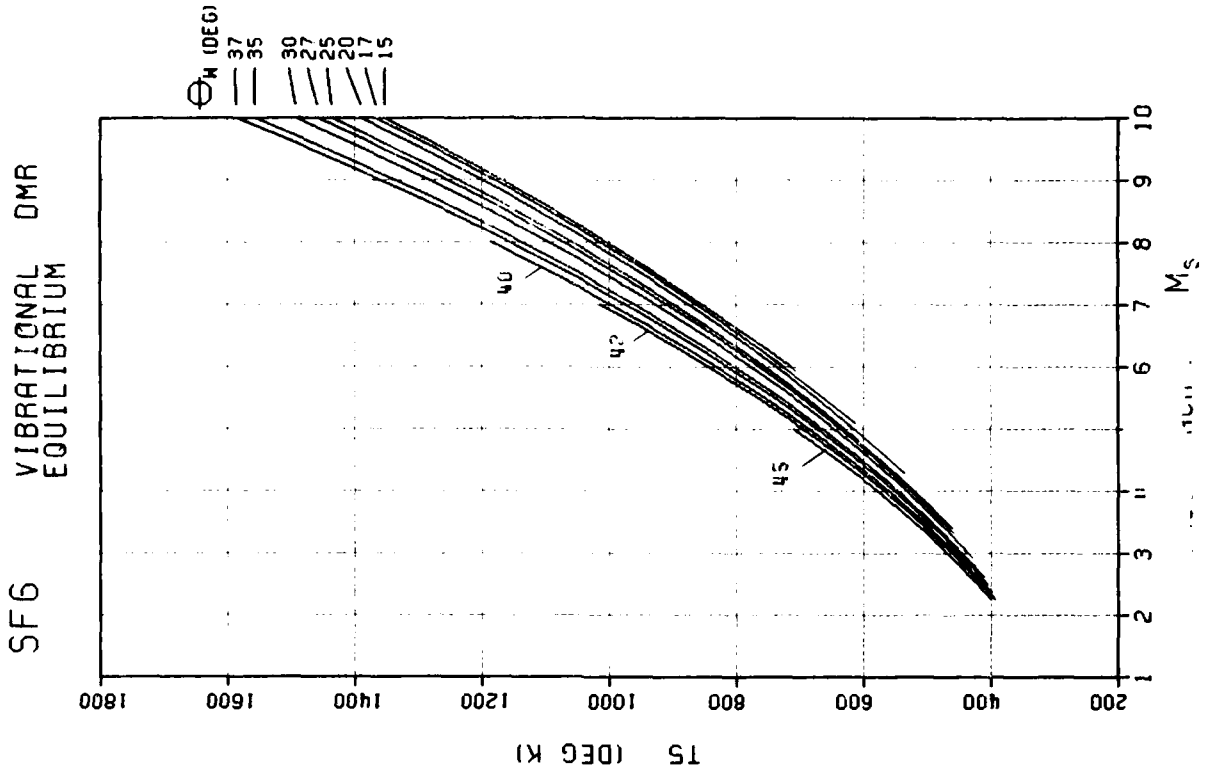


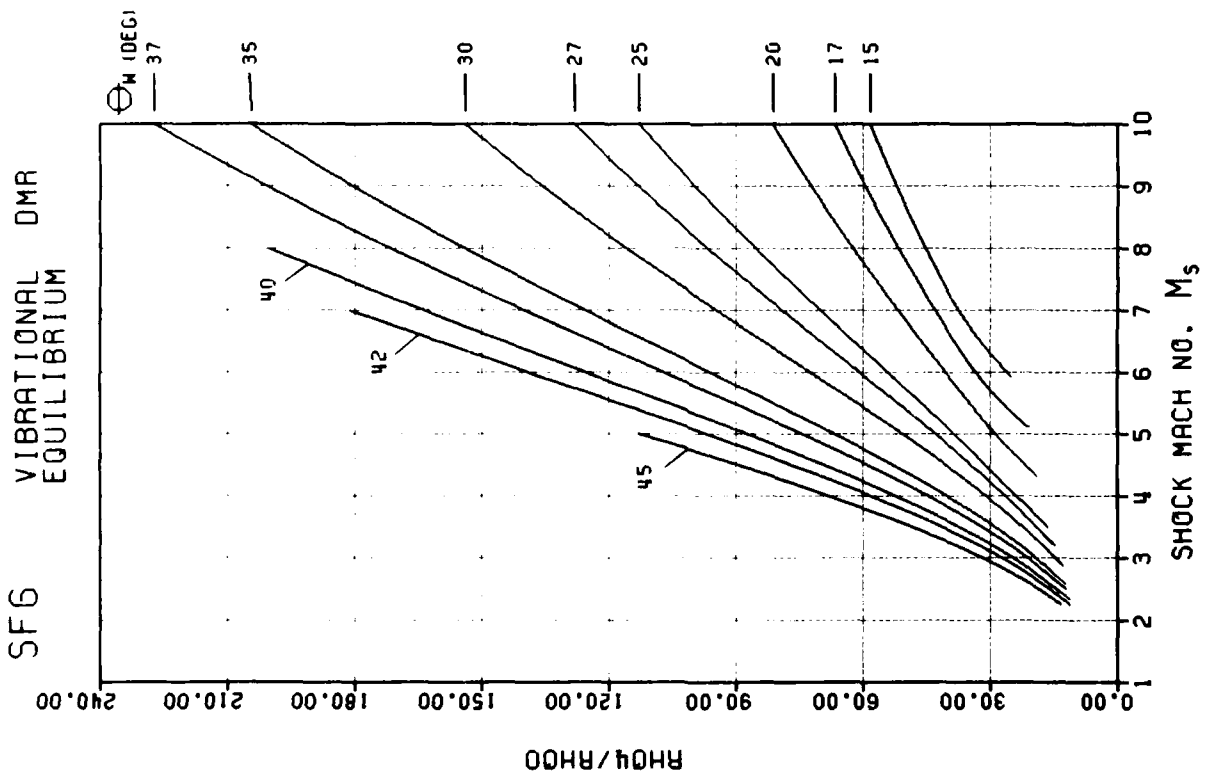
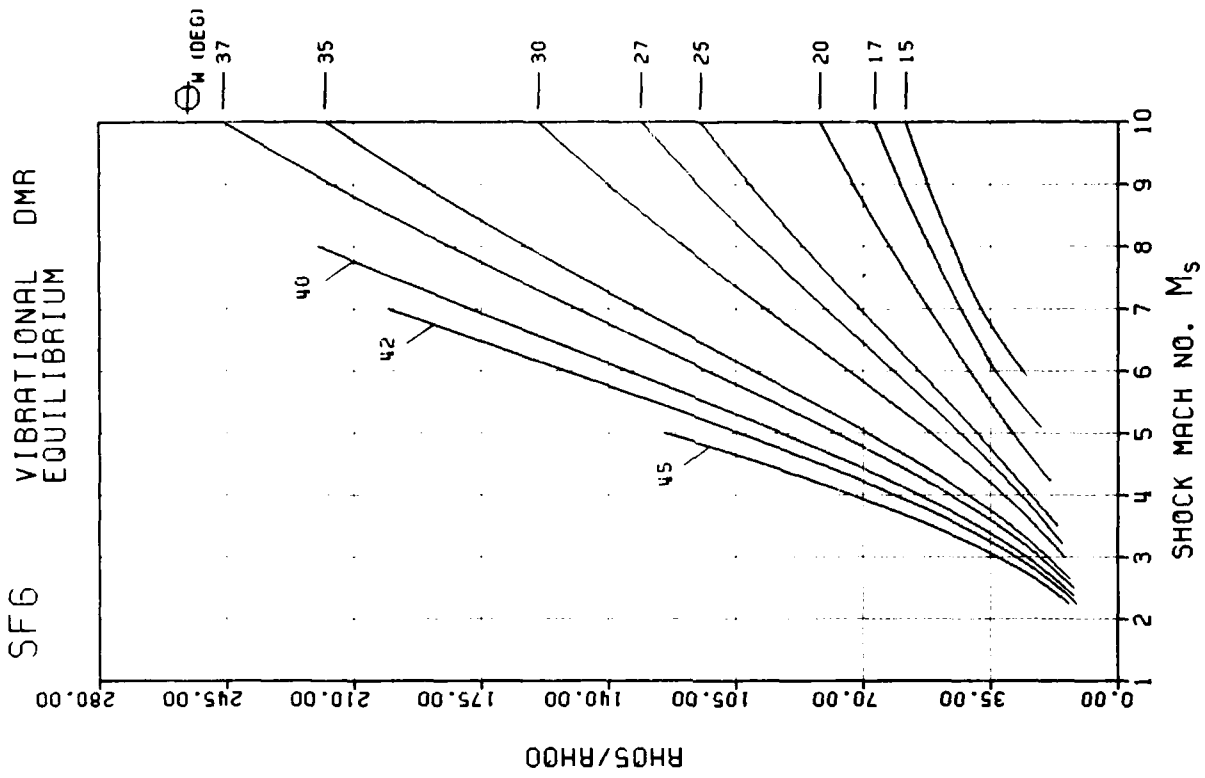


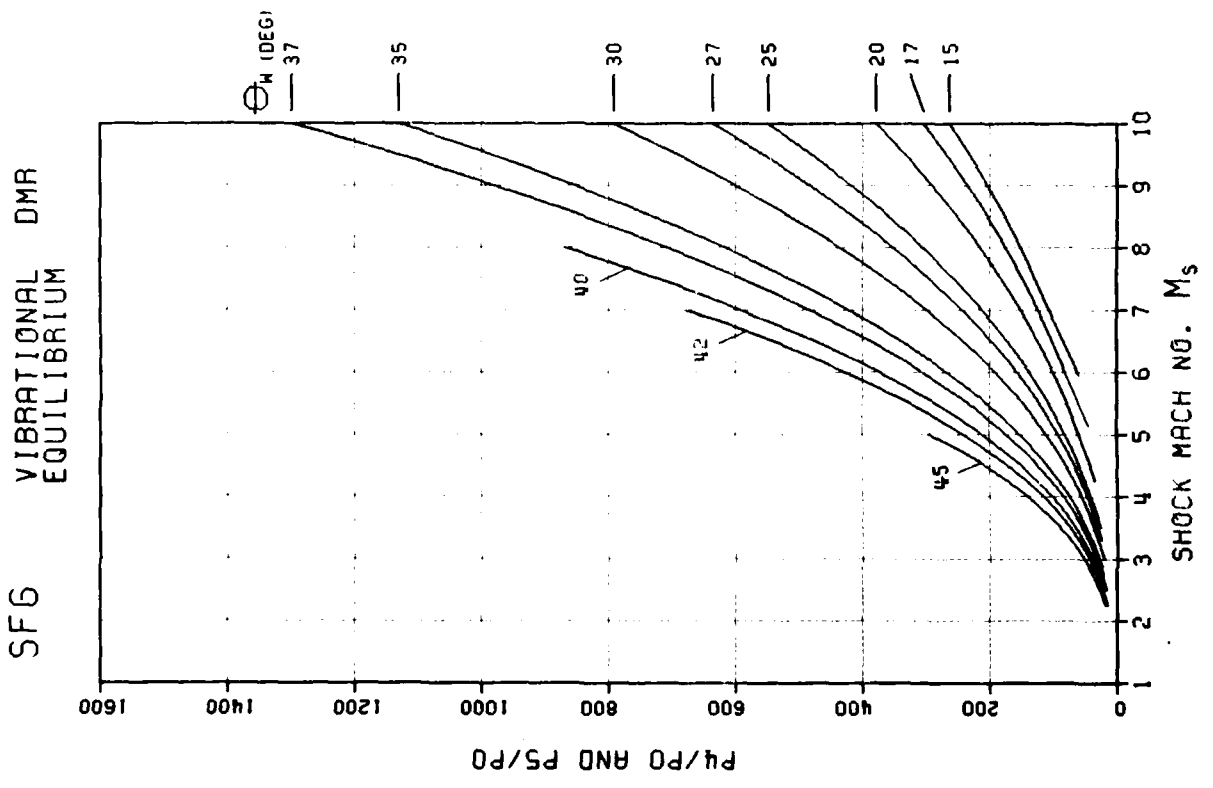
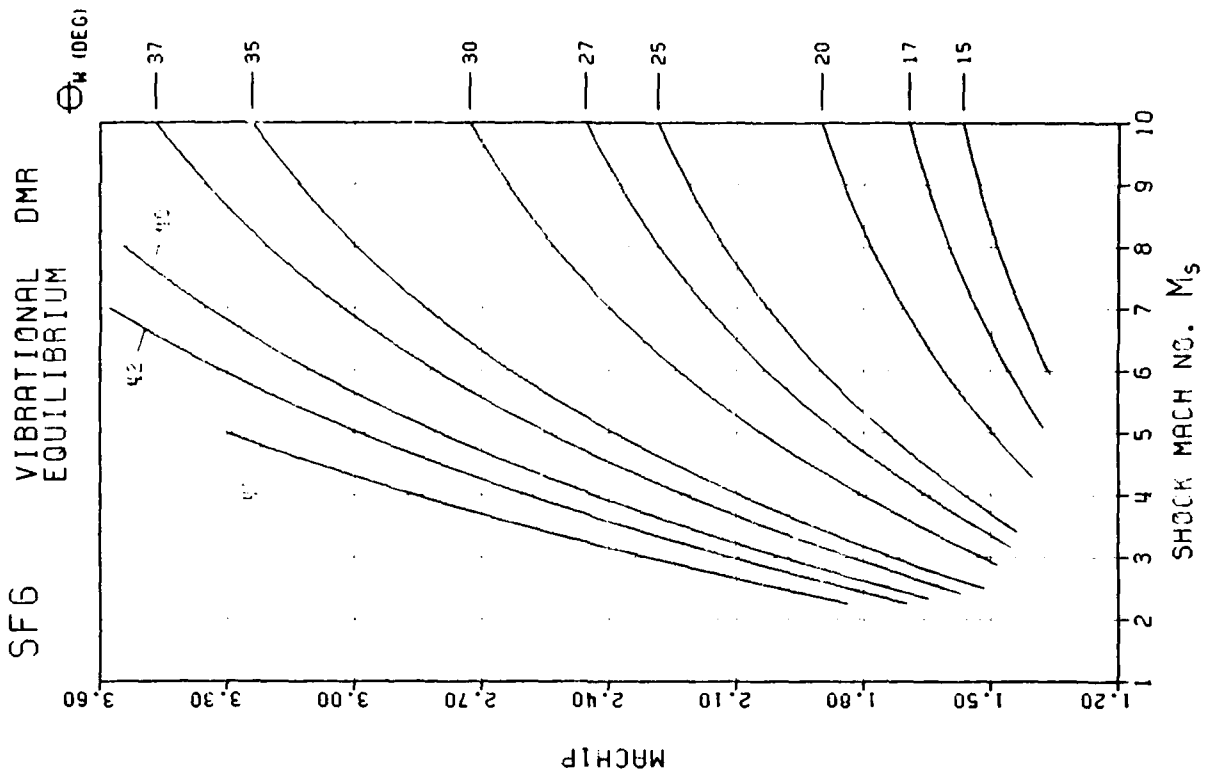


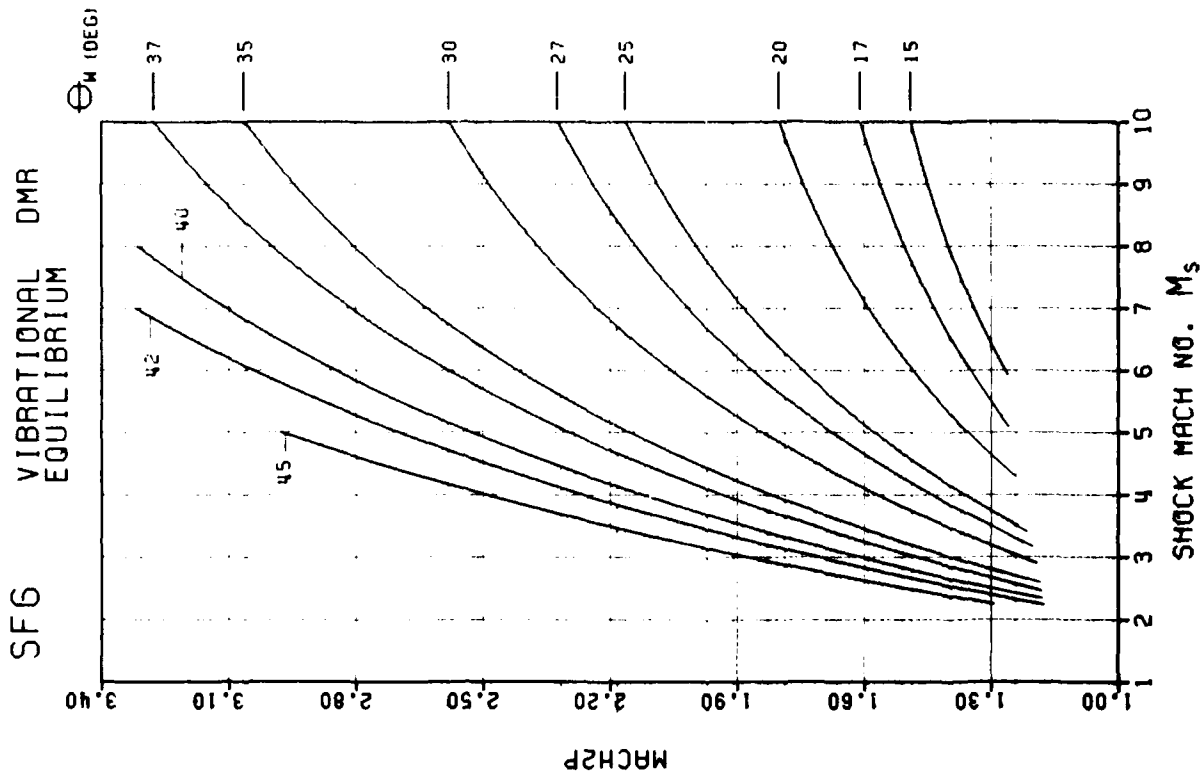
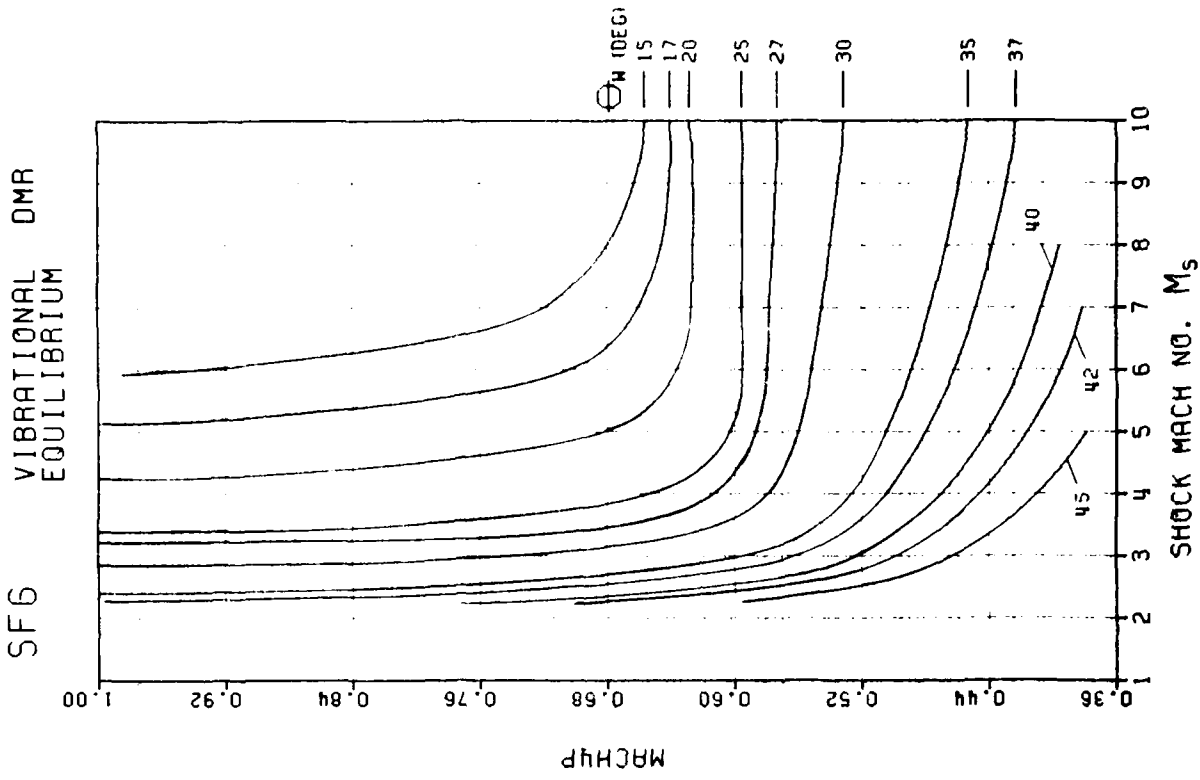


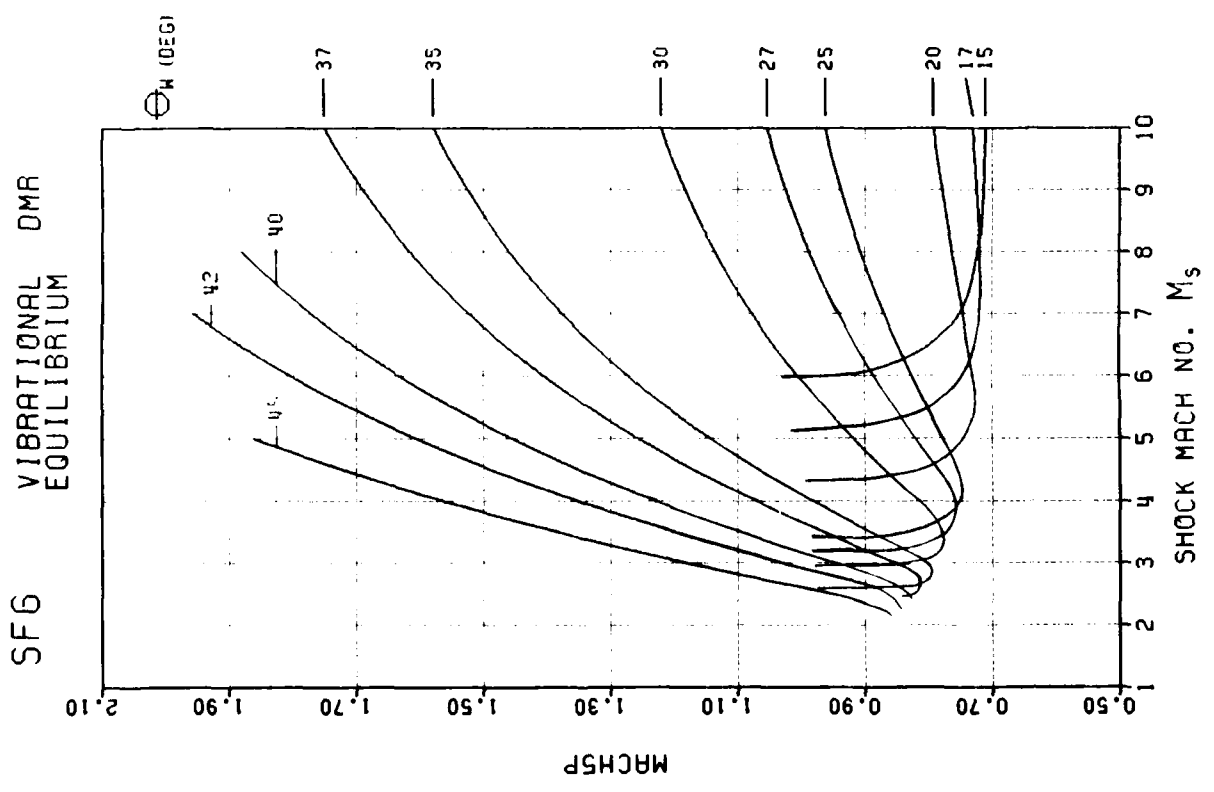
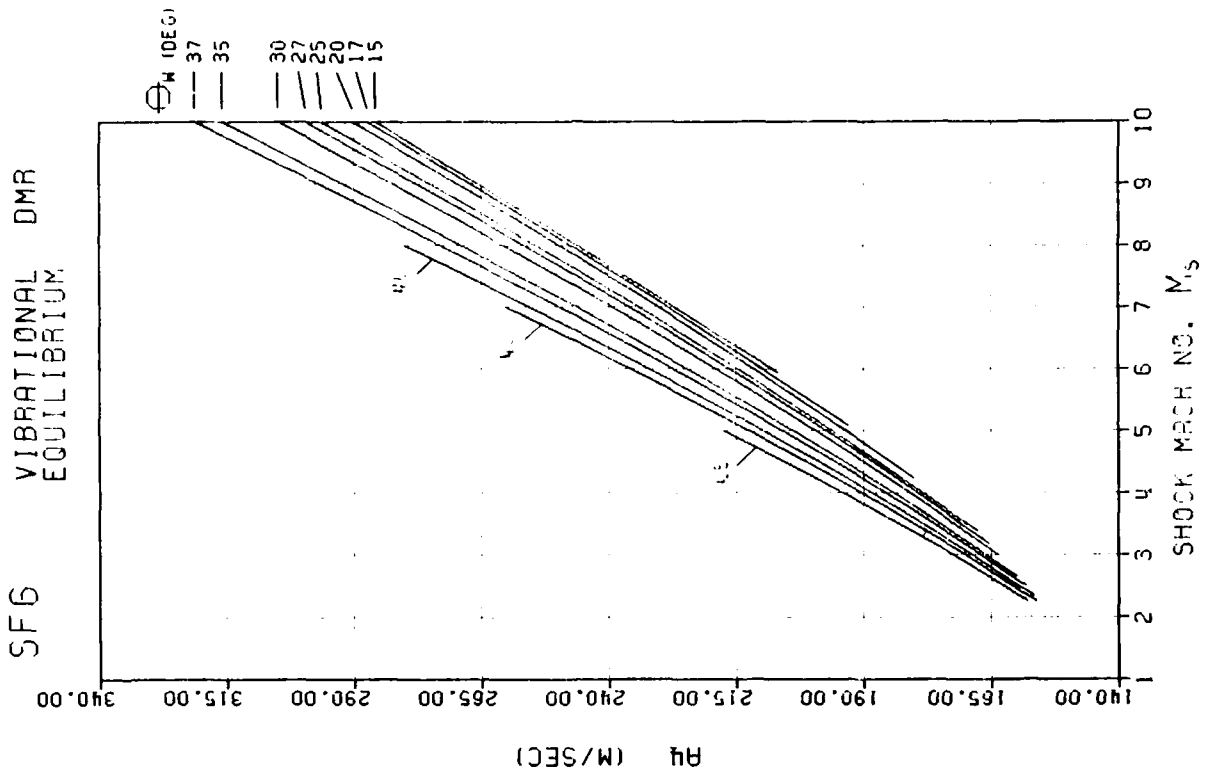
F - 310

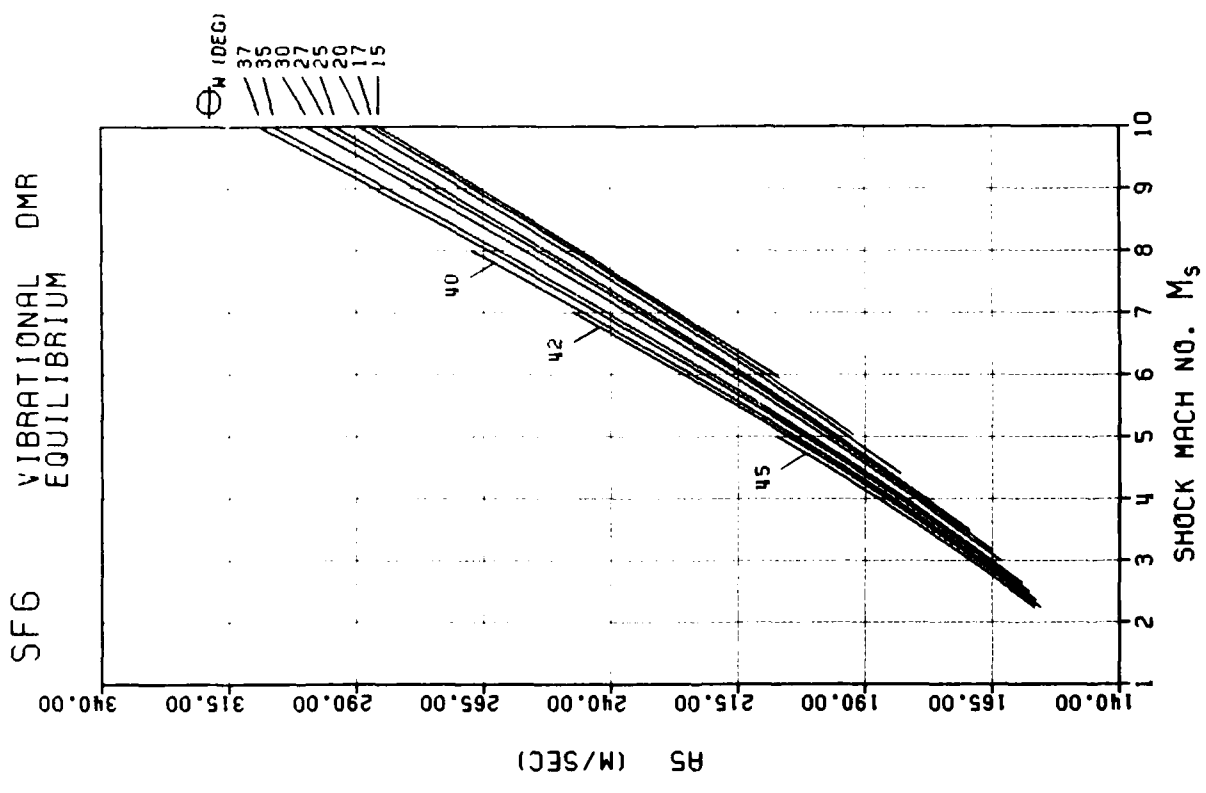
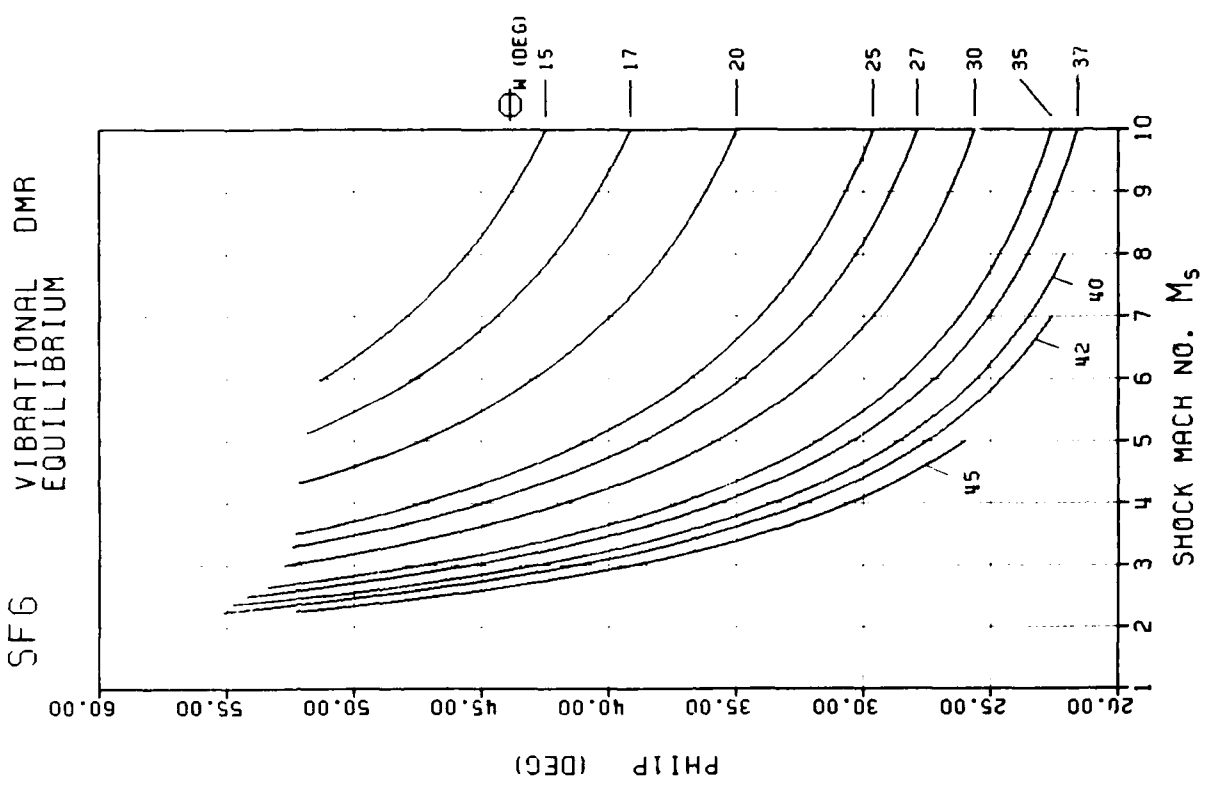


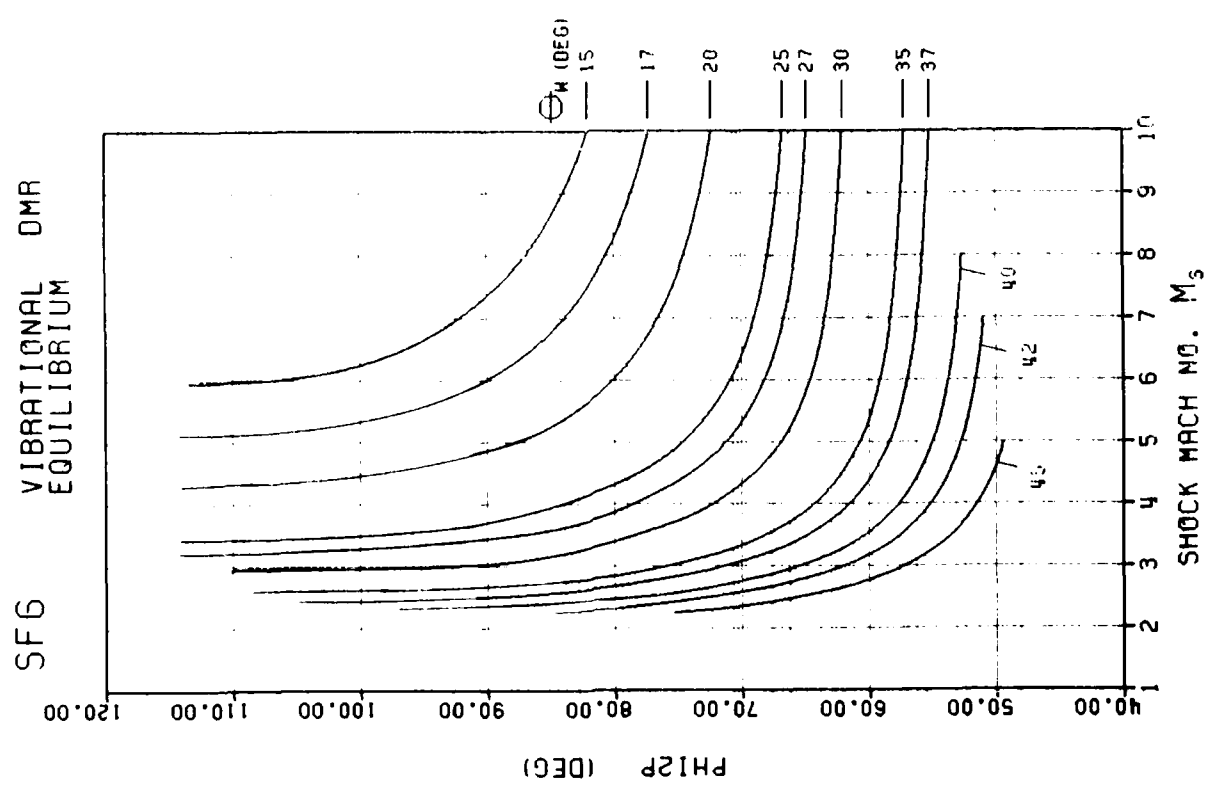
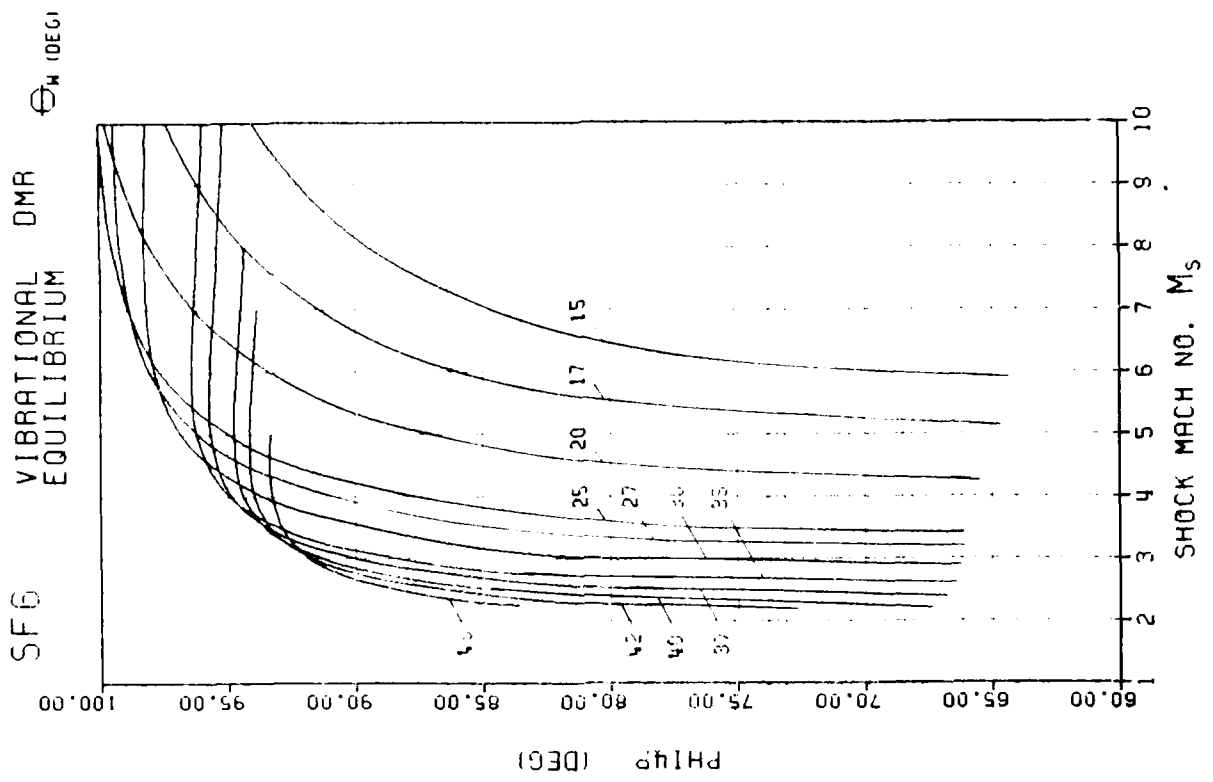


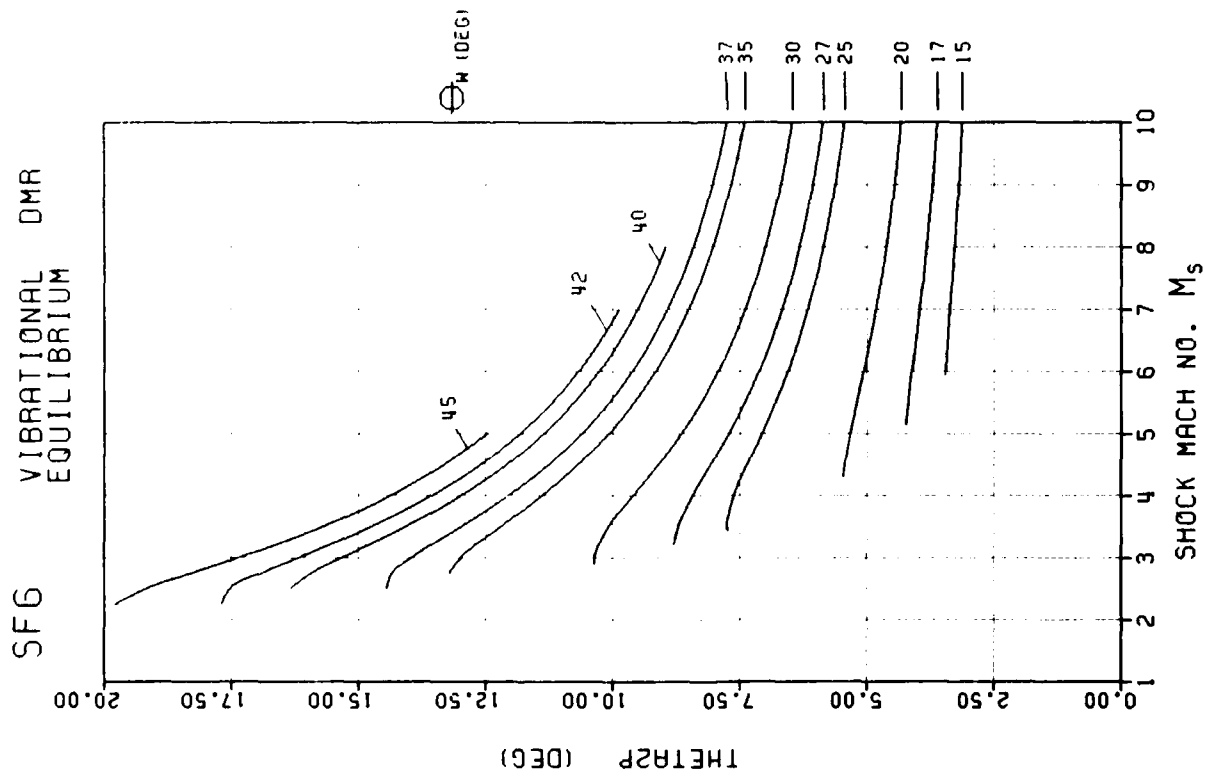
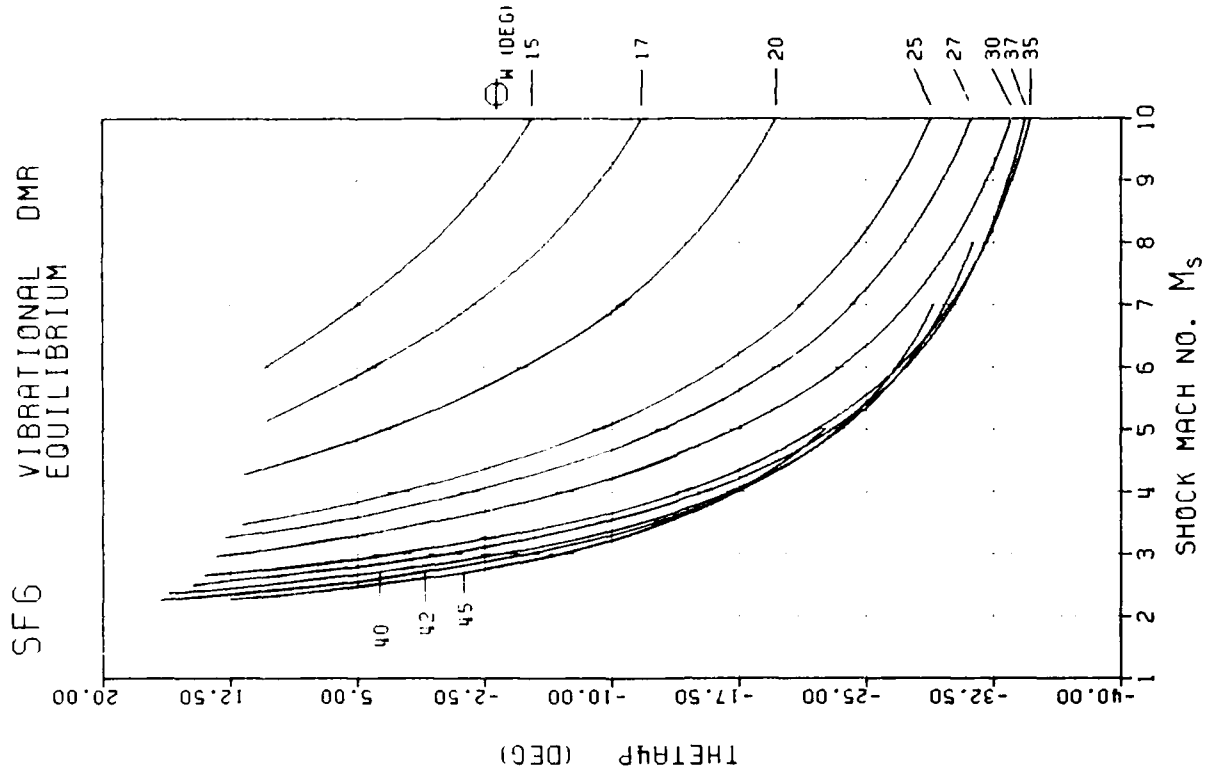


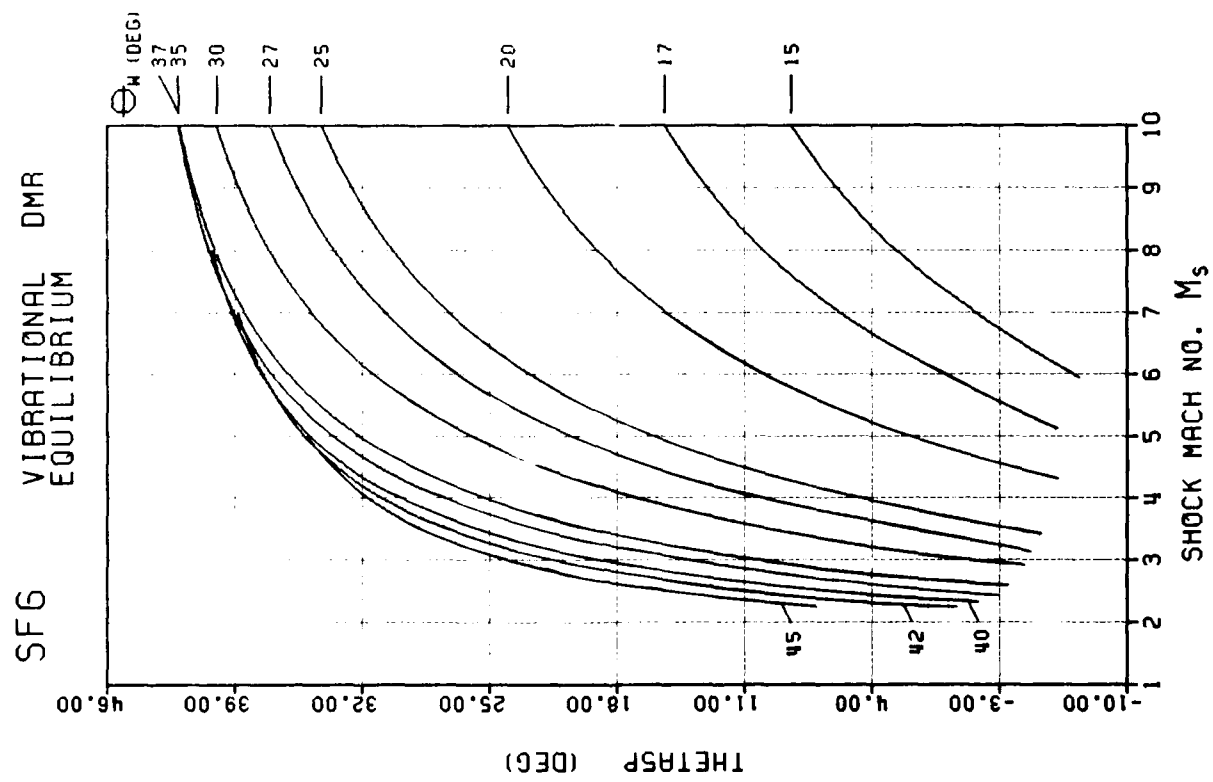
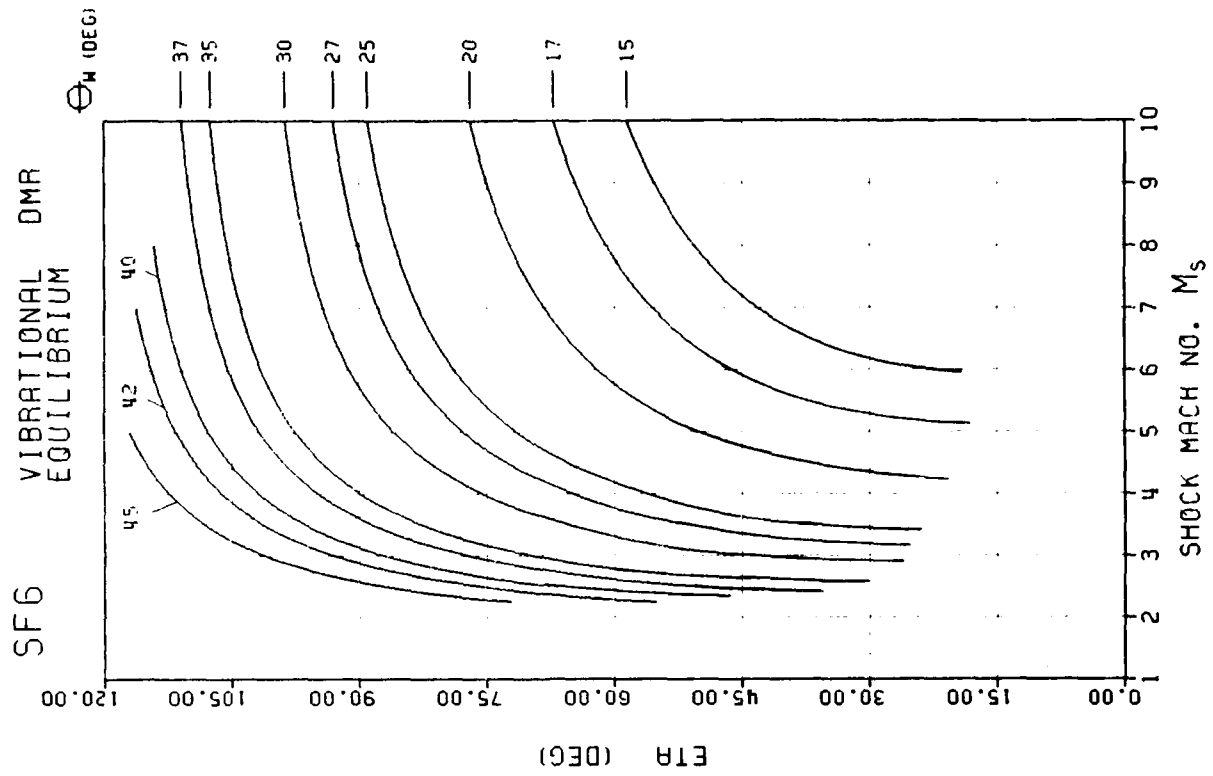


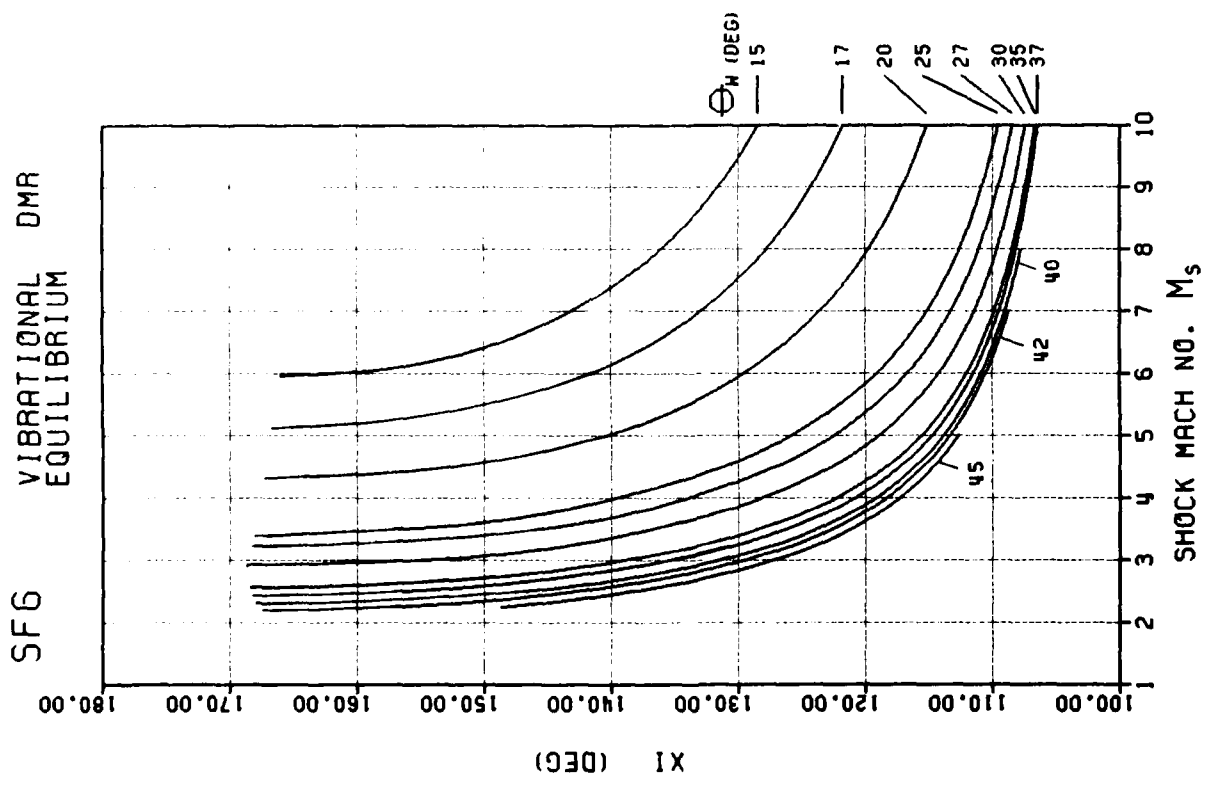












F - 320

APPENDIX A

ACTUAL SIDEWALL PRESSURE HISTORY AND NUMERICAL RESULTS

Recently, Deschambault (Ref. 11) measured the pressure history on and above a 40° wedge for the four types of pseudo-stationary oblique-shock-wave reflection in air. The numerical results generated by the present work are compared with the experimental pressure histories recorded by Deschambault and the results from the numerical simulation done by Glaz (Ref. 12) for a case of DMR in air. The comparison is applied only to the regions around the two triple points due to the limitations of the three-shock theory. Hence, only the sidewall pressure histories are considered. The wedge surface and sidewall pressure histories can be found in Ref. 11. Figure A-1 illustrates the sidewall pressure gauge positions used in the experiments by Deschambault.

Initial conditions : $M_s = 3.72$, $\theta_w = 40^\circ$, $P_0 = 45$ torr (6 kPa) and
 $T_0 = 21.94^\circ\text{C}$

The infinite-fringe interferogram is presented in Fig. A-2. Since the flow is self-similar, the position of the gauge "path" across the wave system can be traced by superimposing Fig. A-1 onto Fig. A-2. The traced positions of the gauges in the reflection system are shown schematically in Fig. A-3. In this run, both gauges 6 and 7 were below the first triple-point trajectory. Gauge 6 measured the pressure jumps across the Mach stem M from state (0) to state (3) close to the wedge surface, across the rolled up slipstream and across the tip of the second Mach stem M' to state (5). Gauge 7 is located slightly above gauge 6 and it recorded the pressure across the primary Mach stem M, across the upper portion of the rolled up slipstream S and across the second Mach stem M' from state (2) to state (5). Gauge 8 was located above the first triple-point trajectory but below the second triple-point trajectory. Gauge 8 was able to measure the pressure jumps across the incident shock wave I to state (1), across the primary reflected shock wave R to state (2), and across the second triple point T' to state (5). Gauge 9 was positioned above the first and second triple-point trajectories. It recorded the pressure jumps across the incident shock wave I to state (1) and across the second reflected shock wave R' to state (4) just behind the second triple point T'. The experimental sidewall pressure histories are shown in Fig. A-4. The measured pressures of the various flow states are indicated in Fig. A-4 and the various states in Fig. A-7.

The corresponding pressure histories at the four gauge locations given by the numerical simulation of Glaz (Ref. 12) are presented in Fig. A-5. Since each station is merely a mesh point on the numerical grid network, the time resolution of the numerical simulation is much greater than that of the pressure gauge. In addition, the numerical records have infinite rise times, whereas physically the gauge has a finite dimension and rise times limited to about $4 \mu\text{s}$. The pressure histories generated by the numerical code trace the local and instantaneous pressure variations ideally at a point station. Experimentally, a pressure gauge provides the average pressure over its finite recording area and the peak signals are

smoothed out because of the limited transient response time. The pressure jump across each shock wave is indicated in torr and kPa units on the plots. The lower pressure experienced at station 6 than at station 7 across the rolled up slipstream is clearly shown in Fig. A-5 by the sharp dip immediately behind the jump across the primary Mach stem M at station 6 here. The pressure jumps recorded by gauge 8 across the incident shock, first reflected shock and the second Mach stem are not as sharp and definite as shown by the simulated results. In the measured pressure history, the rise from P_2 to P_5 are continuous. However the simulation has a pressure peak at P_2 , then the pressure dips slightly before rising up to P_5 . Gauge 8 and 9 both measured about the same P_1 , but gauge 9 has a longer record of P_1 than gauge 8 because gauge 9 went from state (1) to state (4) above T' , whereas gauge 8 went from state (1) through state (2) to state (5) below T' . Due to the limited time record of the simulated pressure history given at station 9, the shape of the pressure history and the value of P_4 cannot be read and compared with the measured value. However P_4 can be read out from the isobaric contours of the entire reflection configuration (Fig. A-6).

The isobaric contours of the entire flow field (Ref. 12) and the enlargement of the flow regions around the two triple points are presented in Fig. A-6. From Fig. A-6(b), both P_2 and P_3 behind the first triple point are 2×10^6 dynes/cm² or 200 kPa (1500 torr), and both P_4 and P_5 behind the second triple point are 3×10^6 dynes/cm² or 300 kPa (2250 torr). Besides extracting the pressure information from the isobaric contour plots, several reflection angles can also be measured from this figure for comparing with the experimental values. The angles of interest are: (1) angle between incident shock wave and reflected shock wave at the first triple point δ , (2) angle between first reflected and second reflected shock η , (3) angle between first reflected shock and second Mach stem ξ , (4) first triple-point trajectory angle χ , and (5) second triple-point trajectory angle χ' . Refer to Fig. A-7 for the definition of these angles.

The computer program that calculates the various thermodynamic states was modified so that a unique thermodynamic of state could be specified for each flow region. This is seen to be important for doing analysis in air where several flow regions may still be frozen while the rest of the flow regions may be in equilibrium. Concerning equilibrium flow in air, there may be some circumstances where only the oxygen molecules are in vibrational equilibrium, or in some other cases, both oxygen and nitrogen molecules are in vibrational equilibrium. Since the incident shock Mach number is low in this case, no dissociation needs to be included in the analysis. To determine whether the flow is frozen or in equilibrium, relaxation length concepts are used. If the relaxation length of an internal degree of freedom is considerably shorter than a characteristic length, the state is considered to be in equilibrium. Otherwise, it is assumed to be frozen. The vibrational relaxation length of N_2 is calculated according to the data reported by White and Millikan (Ref. 13) which shows that below a temperature of 3000 K at a pressure of one atmosphere, N_2 is excited more rapidly in air than in pure N_2 . The vibrational relaxation length of O_2 in air is calculated using the relation given by Lutz and Kiefer (Ref. 14) for pure O_2 . Also included is the correction factor introduced by Vincenti (Ref. 15). This takes into

account the experimental findings of Blackman (Ref. 16) that O_2-N_2 collisions in air are only 40% as effective as O_2-O_2 collisions in transferring energy for vibrational readjustment of O_2 . According to this analytical model, states (0), (1) and (2) are frozen, whereas the flow in states (3), (4) and (5) are in O_2 vibrational equilibrium. The vibrational relaxation length calculated by the present program is 38 mm in state (1), 16 mm in state (2), 3 mm in state (3), 7 mm in state (4) and 9 mm in state (5). Results of this model are listed in Table A-1 under present analysis (A).

Glaz used in his simulation the real-gas equation of state for air by Deschambault (Ref. 17), which was originally developed by Hansen (Ref. 18). Glaz's results indicated that all flow regions of the reflection system should be in equilibrium and a frozen gas assumption would not be valid. Another run was done using the present program based on the assumption that all five flow regions are in vibrational equilibrium and the results are listed in Table A-1 under present analysis (B). The pressure of each flow region and the reflection angles measured or calculated from experiment, numerical simulation and analysis are all tabulated in Table A-1. Both the numerical simulation (Ref. 12) and the analysis from the present work give extremely good results for pressures in the flow regions (1) to (3) with a maximum discrepancy of 2.5%. The measured P_3 of gauge 7 was used for comparison since gauge 6 gave a lower value because the vortical flow of the rolled up primary slipstream went past gauge 6. Behind the second triple point T', the pressures P_4 and P_5 given by Glaz are consistently higher than the measured values by 13.6% and 10.5%, respectively. However, the numerical results from the present study gave similar results to the experimental P_4 and P_5 values with the maximum deviation only 3.6% for set (A) and 7.1% for set (B).

The pressures predicted by the present analysis (A) agree very well with the measured pressures from the experiment. However, the pressures predicted by the present analysis (B) agree better with the numerical simulation results than with the measurements from experiment.

The first triple-point-trajectory angle χ was predicted very well by Glaz and the present work with a maximum deviation of 0.5° . The second triple-point-trajectory angle χ' was very well predicted by the present analysis (A). Numerical simulation and present analysis (B) give slightly smaller values of χ' than the measured experimental value. The present analyses (A) and (B) give values of the reflection angles δ , ξ and η to within 1.6° and 3.5° respectively that of the experimental value for this case. Glaz predicted the angles δ and η being 4° and 3.5° respectively too high, whereas the angle ξ had a value of 9.5° too low. Present analysis (A) agrees best with experiment on physical quantities. Present analysis (B) give very reasonable physical angles except the value of χ' is slightly low. Numerical simulation predicts triple point trajectory angles well but not so for the reflection angles.

A comparison of the values of δ shows how well the numerical work from the present study can predict the orientation of the reflected shock wave R at the first triple point T relative to the incident shock wave I. Similarly, comparisons of the angle ξ and η indicates the accuracy of the numerical work in predicting the orientation of the second reflected shock

wave R' and the second Mach stem M' relative to the primary reflected shock wave K . The numerical simulation by Glaz predicts a smaller angle ξ and a larger angle η than the experimental and analytical values, and it gives larger values of P_4 and P_5 . This is because decreasing ξ will place the second reflected shock R' more normal to the incoming flow, subsequently increasing the pressure P_4 behind it in region (4). Similarly, as the second Mach stem M' becomes stronger, the angle η gets larger and the incoming flow in region (2) is now more normal to the second Mach stem M' , thus resulting in a higher pressure P_5 in region (5).

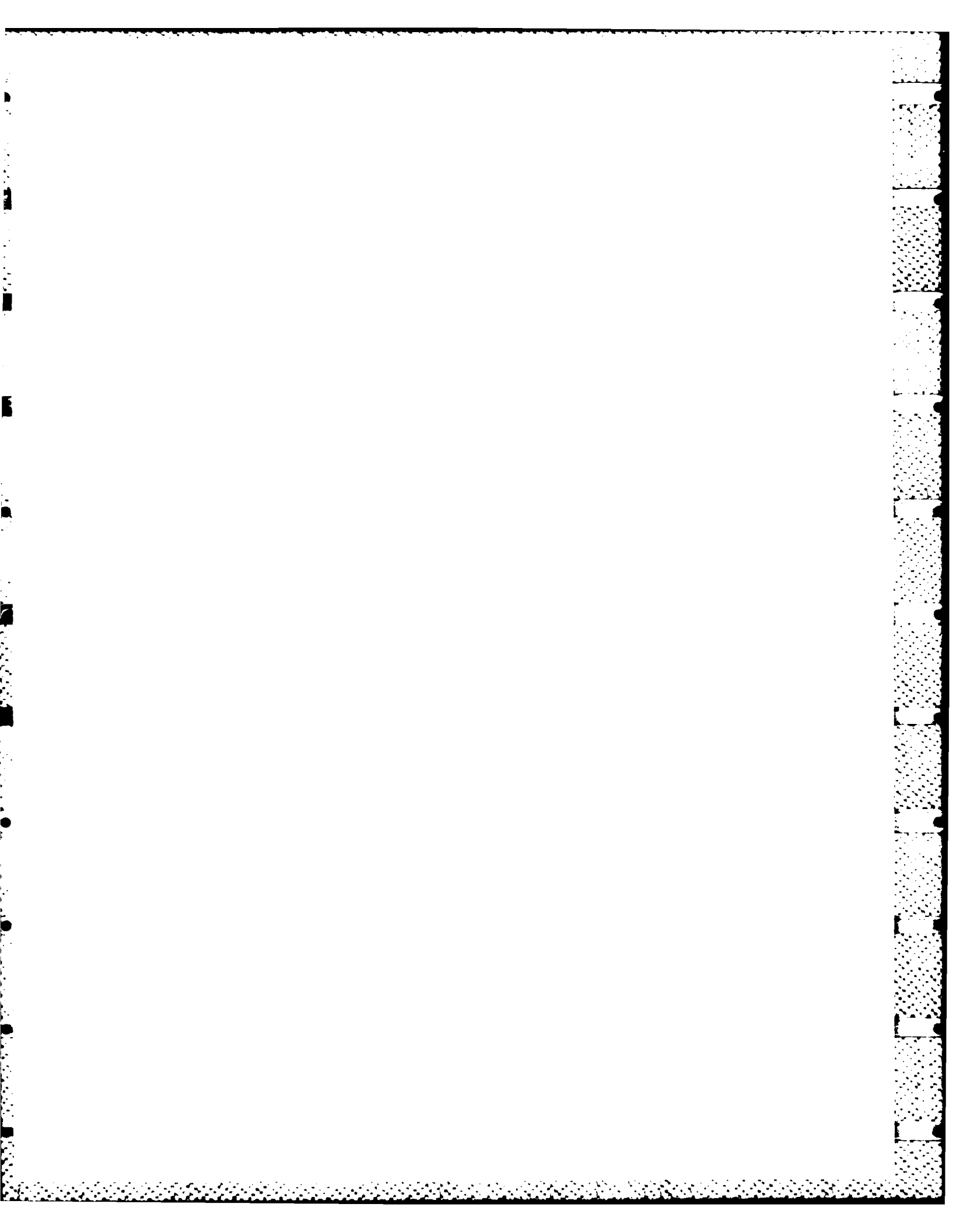
Present analysis (A) has given results for the pressure at all five states (1) to (5) showing good agreement with experiment. It can predict accurately the orientations of the shock waves around the two triple points. The good agreement indicates that the application of different equations of state to each region is justified based on relaxation length concepts. The numerical simulation by Glaz provides more detailed information about the entire flow field in contrast to the present work. However, his results show larger deviations in the pressures behind the second triple point and in the reflection angles when compared to the experimental results.

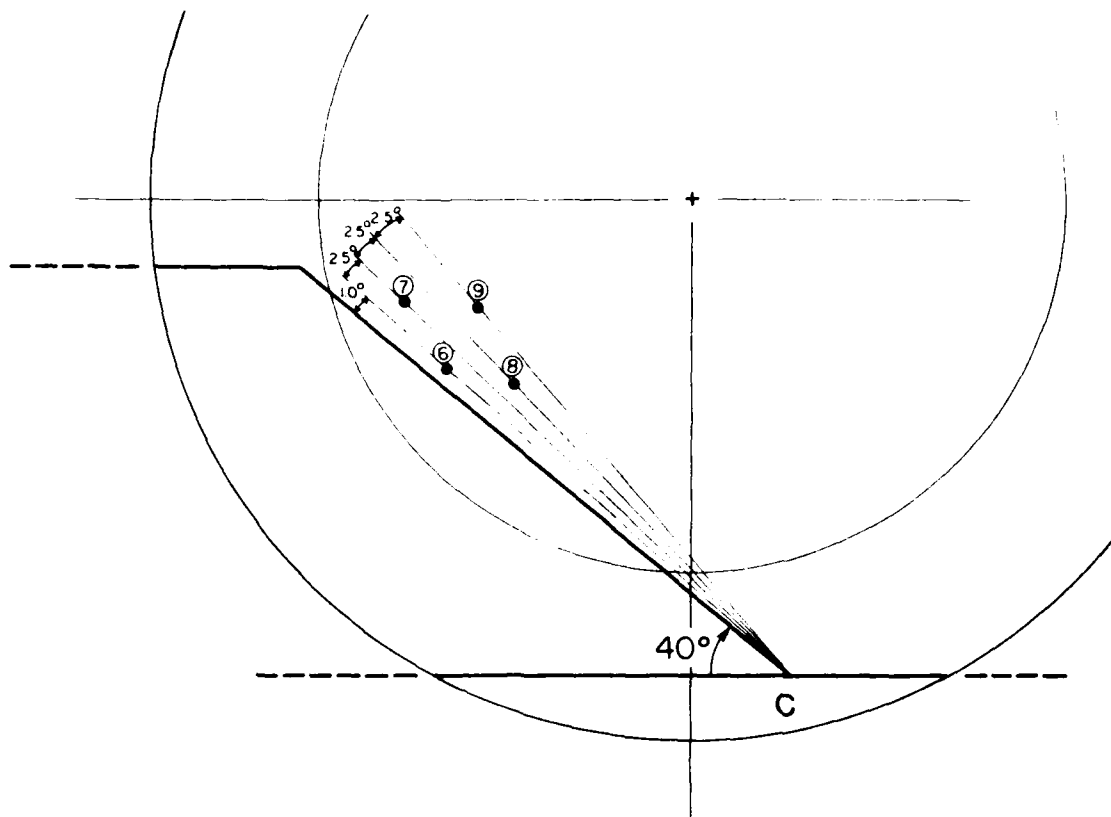
TABLE A-1

Comparison of Pressures and Physical Angles between
Experiment and Numerical Results for a DMR in Air.

$M_s = 3.72$, $\theta_w = 40^\circ$, $P_0 = 45$ torr (6 kPa), $T_0 = 21.94^\circ\text{C}$.

Parameter	Experiment (Ref. 11)		Numerical Simulation (Ref. 12)		Present Analysis (A)		(B)	
	Torr	kPa	Torr	kPa	Torr	kPa	Torr	kPa
P ₁	716	95.5	728	97.1	719	95.9	730	97.3
	722	96.3	728	97.1				
P ₂	1456	194.1	1455	194.0	1439	191.9	1449	193.2
P ₃	1476	196.8	1506	200.8	1439	191.9	1449	193.2
	1396	186.1	1542	205.6				
P ₄	1981	264.1	2250	300.0	2052	273.6	2122	282.9
P ₅	2045	272.6	2259	301.2	2052	273.6	2122	282.9
χ		5.0°		5.5°		4.8°		4.5°
χ'		7.8°		7.0°		7.4°		6.5°
δ		123.0°		127.0°		124.0°		126.2°
ξ		162.5°		153.0°		160.9°		159.0°
η		46.5°		50.0°		45.4°		47.7°





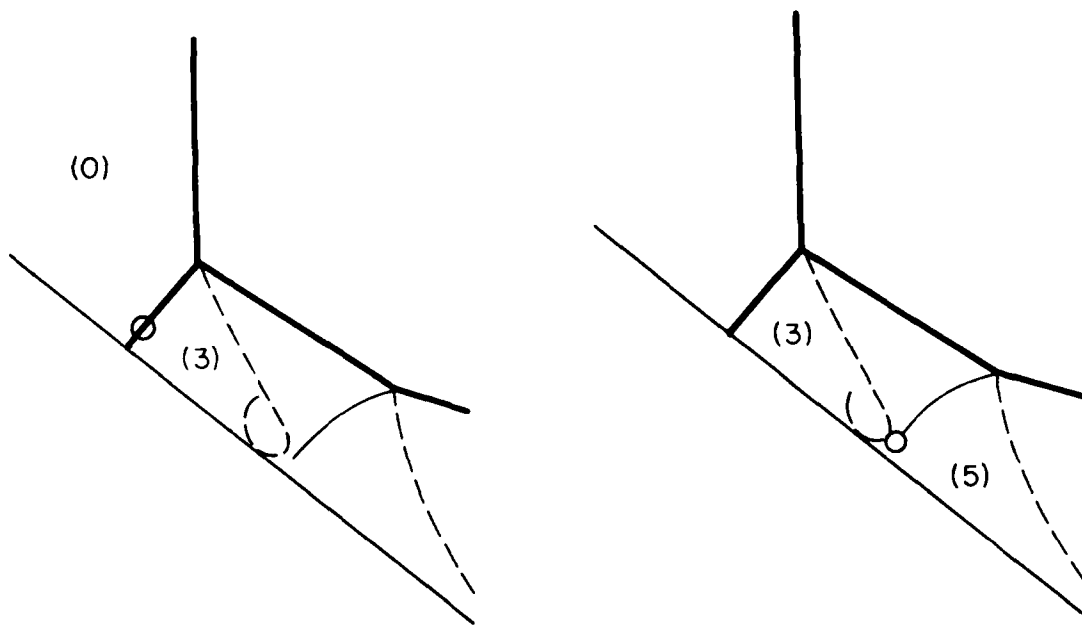
Gauge 6 is 8.56 cm from C
 Gauge 7 is 9.65 cm from C
 Gauge 8 is 7.75 cm from C
 Gauge 9 is 8.76 cm from C

Fig. A-1 Schematic diagram of gauge positions on the specially constructed steel window.



Fig. A-2 Infinite-fringe interferogram of double-Mach reflection in air (Ref. 11). $M_S = 3.72$, $\theta_w = 40^\circ$, $P_0 = 45$ torr (6 kPa), $T_0 = 21.94$ °C and $\lambda = 6943$ Å.

Gauge 6



Gauge 7

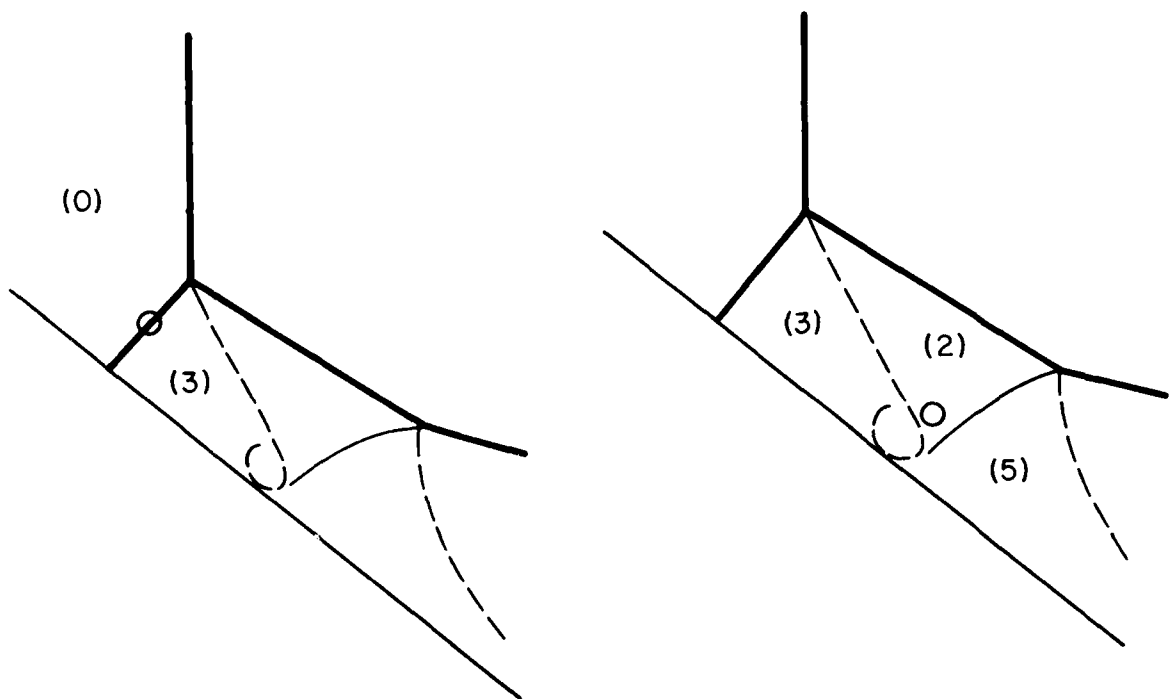
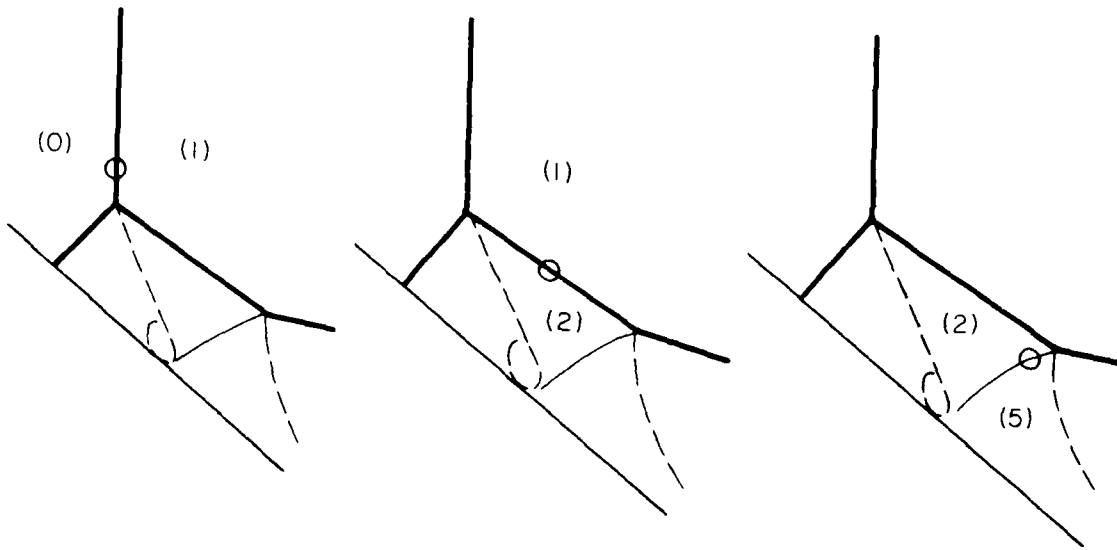


Fig. A-3 Positions of the gauge path across the reflection system traced by superimposition.

Gauge 8



Gauge 9

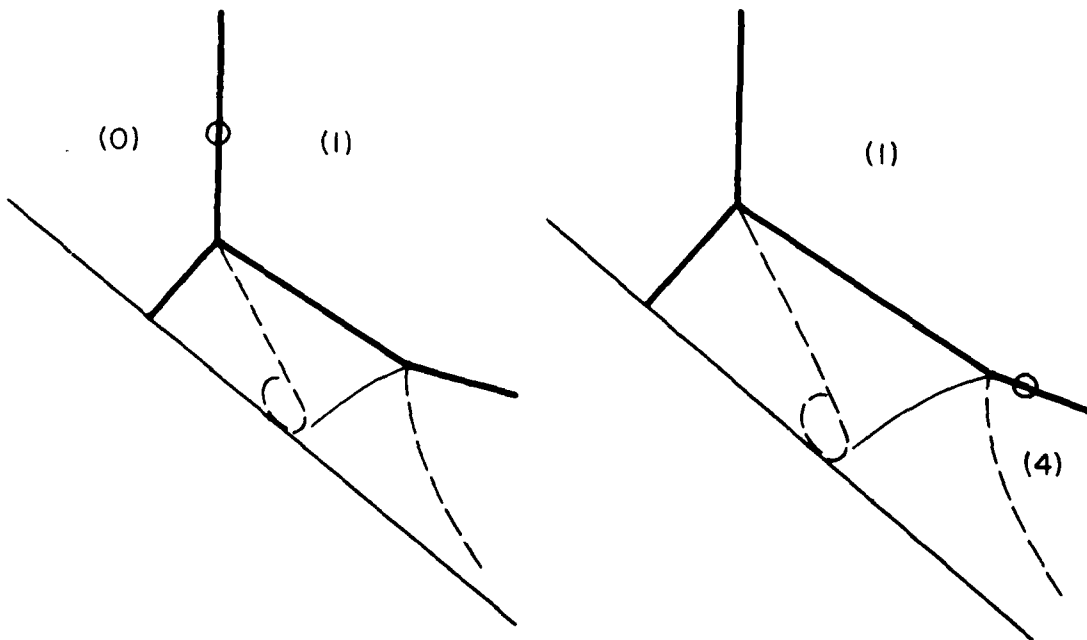
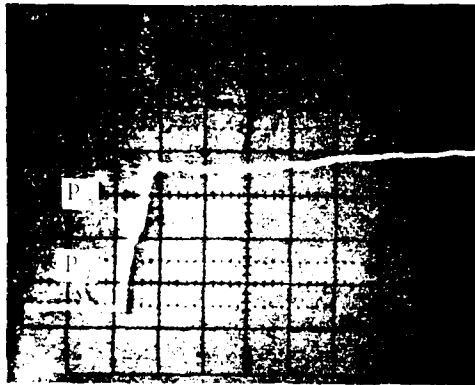


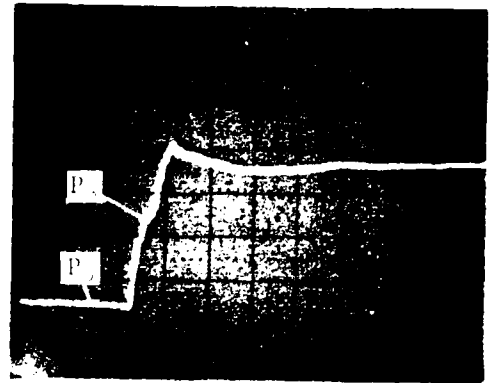
Fig. A-3 (Continued) Positions of gauge path across the reflection system by superimposition.

GAUGE 6



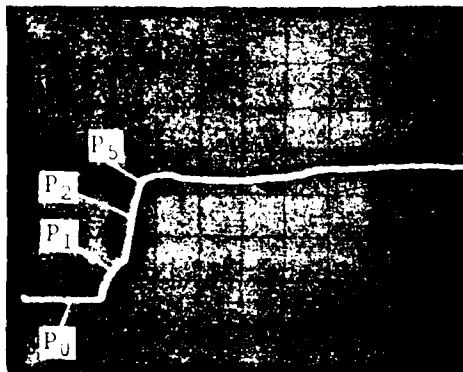
90.80 kPa/div (vertical)
 20 μ s/div (horizontal)
 P_0 45 torr (6 kPa)
 P_3 1396 torr (186.1 kPa)

GAUGE 7



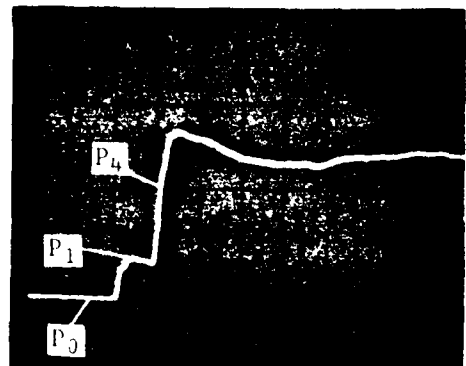
95.42 kPa/div (vertical)
 20 μ s/div (horizontal)
 P_0 45 torr (6 kPa)
 P_3 1476 torr (196.8 kPa)

GAUGE 8



98.80 kPa/div (vertical)
 20 μ s/div (horizontal)
 P_0 45 torr (6 kPa)
 P_1 716 torr (95.55 kPa)
 P_2 1456 torr (194.1 kPa)
 P_5 2045 torr (272.6 kPa)

GAUGE 9



98.18 kPa/div (vertical)
 20 μ s/div (horizontal)
 P_0 45 torr (6 kPa)
 P_1 722 torr (96.3 kPa)
 P_4 1981 torr (264.1 kPa)

Fig. A-4 Pressure history measurements along the sidewall and at the wedge surface for the case of double-Mach reflection in air by Deschambault (Ref. 11). $M_S = 3.72$, $\theta_w = 40^\circ$, $P_0 = 45$ torr (6.119), $T_0 = 21.94^\circ\text{C}$.

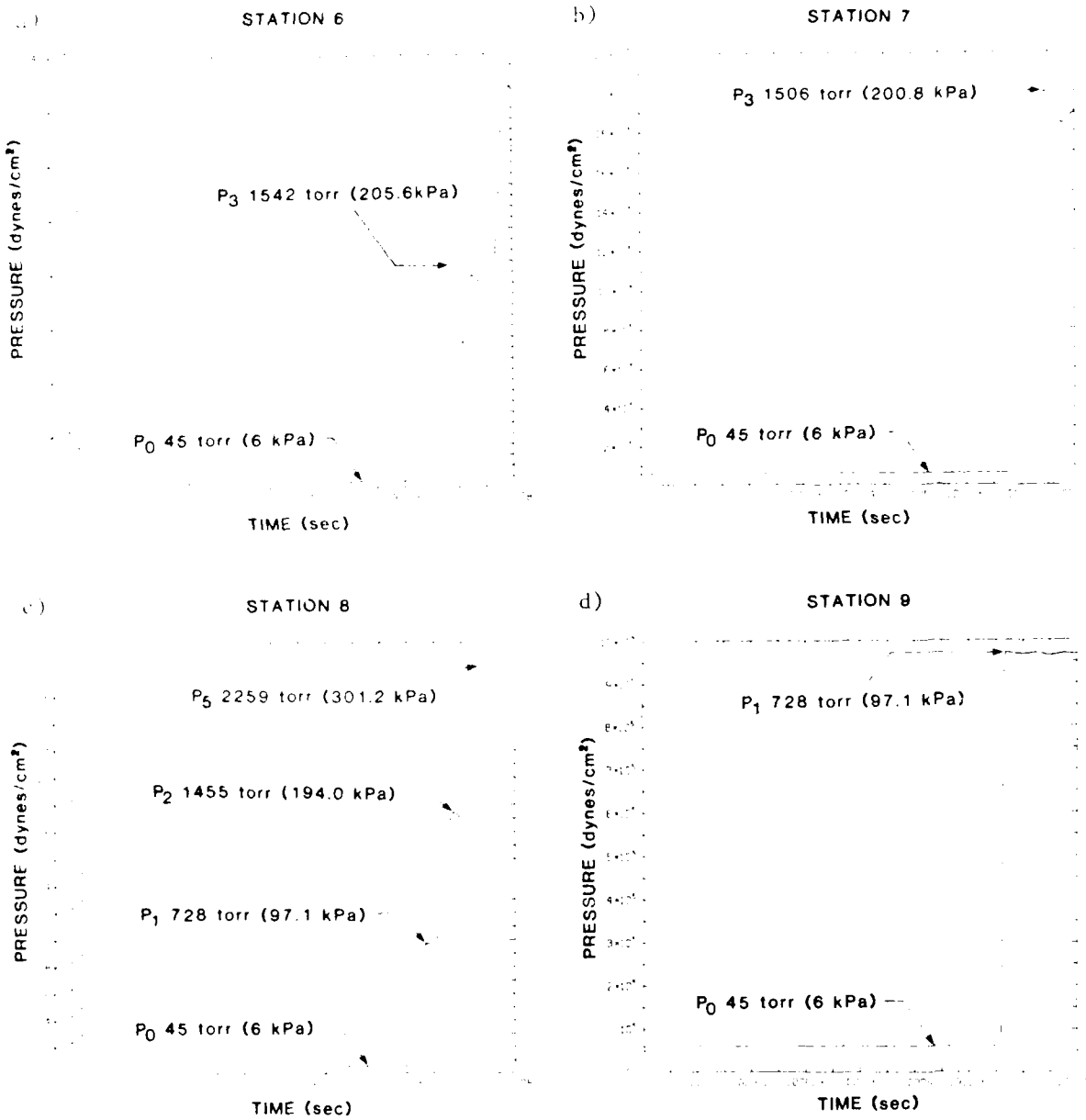
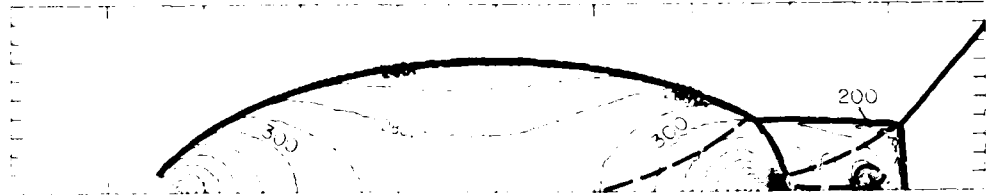


Fig. A-5 Numerical simulation of pressure history by Glaz (Ref. 12).
 for the case of double-Mach reflection in air. $M_S = 3.72$,
 $\theta_w = 40^\circ$, $P_0 = 45$ torr (6 kPa), $T_0 = 21.94$ °C.

a) Isobaric contours of the entire flow field



b) Isobaric contours of the flow regions around the two triple points

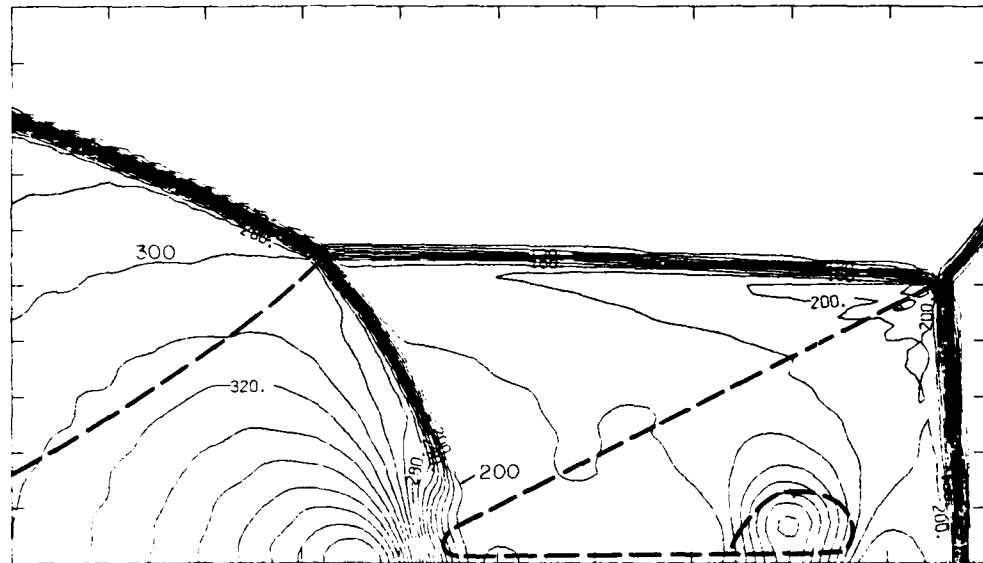


Fig. A-6 Numerical simulation of pressure contours by Glaz (Ref. 12) for the case of double-Mach reflection in air. $M_S = 3.72$, $\theta_w = 40^\circ$, $P_0 = 45$ torr (6 kPa), $T_0 = 21.94$ °C and $\gamma = 1.4$. Contours are shown from 0.0 to 3.8×10^6 dynes/cm² with an interval of 1.0×10^5 and labels are scaled by 1.0×10^{-4} .

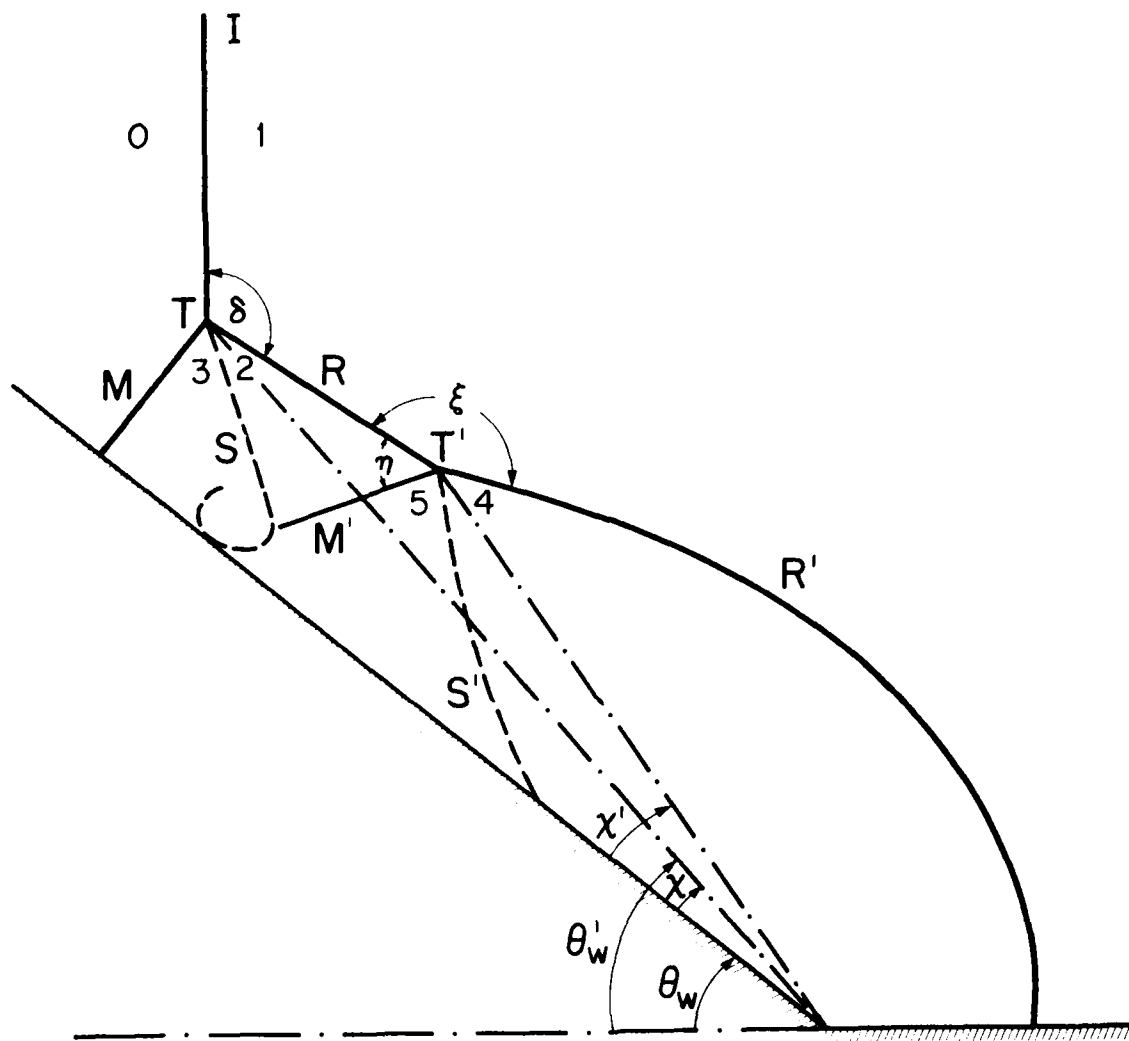


Fig. A-7 Schematic diagram of double-Mach reflection.

APPENDIX B

COMPUTER-PROGRAM LISTING FOR THE ANALYTICAL SOLUTION

OF REGULAR AND MACH REFLECTIONS

The computer program listed here follows the method of calculation discussed in Section 2. The program is very general and is used for argon, nitrogen, air, carbon dioxide and sulfur hexafluoride. It allows a choice of frozen, perfect or vibrational equilibrium thermodynamic states. It can be easily modified to include any other gas by changing SUBROUTINE GAS.

The program will first check whether the input flow conditions can give regular reflection by calling SUBROUTINE RR. If it fails to obtain a solution, the program will proceed to call SUBROUTINE SIMMR to calculate Mach reflection case. If the actual wedge angle has been chosen as the parameter, the program will predict a trajectory angle for the first triple point. However, if the effective wedge angle has been chosen as the parameter, the program will iterate the wedge angle until the calculated effective wedge angle is the same as the input one. After solving for the first triple-point system, a check of the flow Mach number in region (2) with respect to the kink is done. If that is a supersonic flow, the second triple-point system will be solved by calling SUBROUTINE TRPL2. The subroutines are listed following the main program alphabetically. Input data are explained in the main program. The program is run on the Perkin Elmer 3250 Computer System at UTIAS.


```

C     *** SUBROUTINE SUB-PROGRAM MAXTHE ***
C     -----
C
SUBROUTINE MAXTHE(MACH1, PRS1, TMP1, PH11, THETA1, MACH2, PRS2, TMP2, ILL)
  DIMENSION THETA(3), G(2)
  REAL MACH1, MACH2
  FACT21 = 0.005
  FACT22 = 1.0E-5
  Q2 = 0.017453293
C
C     --- SET THE INITIAL VALUE FOR PH1 ---
C
  TRR = 0.0
  DO 5 I = 1, 4
    PP = (45.0+I*10.0)*Q2
    CALL SVFS(MACH1, PRS1, TMP1, PP, MACH2, PRS2, TMP2, PH112, I, ILL, 2)
    IF(ILL.NE.0) GO TO 102
    IF(PP-PH112.LT.TRR) GO TO 5
    TRR = PP-PH112
  TPHI = PP
  5 CONTINUE
  TPHIF = TPHI
  STEP = 3.0*Q2
  K = 0
C
C     --- START ITERATION ---
C
  10 IF(MACH1*SIN(TPHI-STEP).GT.1.0) GO TO 11
  STEP = 0.4*TPHIF
  TPHI = TPHIF*0.44
  TPHIF = TPHI
  11 DO 20 I = 1, 3
    PP = TPHI+(I-2)*STEP
    CALL SVFS(MACH1, PRS1, TMP1, PP, MACH2, PRS2, TMP2, PH112, I, ILL, 2)
    IF(ILL.NE.0) GO TO 101
    THETA(1) = PP-PH112
  20 CONTINUE
C
  G(1) = THETA(2)-THETA(1)
  G(2) = THETA(3)-THETA(2)
C
  IF(G(1)*G(2).GT.0.0) GO TO 21
  IF(STEP.LT.FACT22) GO TO 30
  IF(ABS(G(1)).LT.STEP*FACT21.AND.ABS(G(2)).LT.STEP*FACT21) GO TO 30
  GO TO 22
C
  21 IF(ABS(G(1)-G(2)).LE.ABS(G(2)*STEP/1.67)) GO TO 22
C
  TPHIF = TPHI
  TPHI = TPHI+(G(1)+G(2))/2.0/(G(1)-G(2))*STEP
  STEP = ABS((G(1)+G(2))/2.0/(G(1)-G(2))*STEP)
  22 STEP = STEP*0.30
  K = K+1
C
IF(K.GT.20) GO TO 40
GO TO 10
C
  30 ILL = 0
  PH11 = TPHI
  THETA1 = THETA(2)
  RETURN
C
  40 ILL = 999
  RETURN
C
  101 WRITE(6,601)
  601 FORMAT(1H, '(STOPPED AT MAXTHE 101)')
  GO TO 1000
  102 WRITE(6,602)
  602 FORMAT(1H, '(STOPPED AT MAXTHE 102)')
  RETURN
  END
C
C     *** SUBROUTINE SUB-PROGRAM NR ***
C     -----
C
SUBROUTINE NR(MACHS, PRSO, TMP0, THEM1N, IC, IOUT, ILL)
  REAL MACH0, MACHS, MACH1
  DIMENSION AM(3)
  Q2 = 0.017453293
  FACT = 1.0E-4
  GO TO (10,50), IC
C
  10 TTHE = 30.0*Q2
  STEP = 0.2*TTHE
  K = 0
C
C     --- START ITERATION ---
C
  20 DO 30 I = 1, 3
    TT = TTHE+(I-2)*STEP
    PH10 = 90.0*Q2-TT
    MACH0 = MACHS/SIN(PH10)
    CALL SVFS(MACH0, PRSO, TMP0, PH10, MACH1, PRS1, TMP1, PH101, 2, ILL, 1)
    IF(ILL.NE.0) GO TO 101
    AM(1) = MACH1
  30 CONTINUE
C
  IF(ABS(AM(2)-1.0).LT.FACT) GO TO 40
  TTHE = TTHE*(AM(2)-1.0)*STEP*2.0/(AM(1)-AM(3))
  STEP = 0.3*ABS(AM(2)-1.0)*STEP*2.0/(AM(1)-AM(3))
  IF(STEP.GT.20.0*Q2) GO TO 102
  K = K+1
  IF(K.GT.25) GO TO 103

```

```

C
GO TO 20
40 ILL = 0
THEMIN = ITNE
PRTHE = ITNE/Q2
IF(IOUT.EQ.0) RETURN
WRITE(6,604) MACHS,PRTHE
1 WALL PRIME = ,F8.4, (DEG)'
RETURN
604 FORMAT(1H ,//, '***** NR-MR BOUNDARY AT MACHS= ,F5.2, IS AT THETA
14, (DEG)'
ILL = 0
RETURN
C
50 THETA = MACHS
PRTHE = THETA/Q2
PHIO = 90.0*Q2-THETA
MACH0 = 1.5/SIN(PHIO)
CALL SVFS(MACH0,PRS0,TMP0,PHIO,MACH1,PRSI,TMP1,PHI01,2,ILL,1)
IF(ILL.NE.0) GO TO 102
IF(MACH1.LT.1.0) GO TO 60
THEMIN = 1.5
IF(IOUT.EQ.0) RETURN
WRITE(6,605) PRTHE
605 FORMAT(1H ,//, '***** NO NR-MR BOUNDARY AT THETA WALL PRIME = ,F8.
14, (DEG)'
ILL = 0
RETURN
C
60 RM = 1.2
RMF = RM
STEP = 0.05
PHIO = 90.0*Q2-THETA
K = 0
C --- START ITERATION ---
70 DO 80 I = 1,3
RM = RM+(1-2)*STEP
MACH0 = RM/SIN(PHIO)
CALL SVFS(MACH0,PRS0,TMP0,PHIO,MACH1,PRSI,TMP1,PHI01,2,ILL,1)
IF(ILL.NE.0) GO TO 101
AM(1) = MACH1
80 CONTINUE
C
IF(ABS(AM(2)-1.0).LT.FACT) GO TO 90
RM = RM+(AM(2)-1.0)*STEP+2.0/(AM(1)-AM(3))
STEP = 0.3*ABS((AM(2)-1.0)*STEP+2.0/(AM(1)-AM(3)))
IF(RM*STEP.LT.1.5) GO TO 85
STEP = 0.4*(1.5-RMF)
RM = 1.5-STEP*1.1
85 IF(RM*STEP.GT.1.0) GO TO 86
STEP = 0.4*(RMF-1.0)
RM = 1.0+1.1*STEP
86 RMF = RM
K = K+1
IF(K.GT.25) GO TO 103
GO TO 70
C
90 ILL = 0
THEMIN = RM
IF(IOUT.EQ.0) RETURN
WRITE(6,606) PRTHE,RM
606 FORMAT(1H ,//, '***** NR-MR BOUNDARY AT THETA WALL PRIME = ,F8.3,
1(DEG) IS AT MACHS = ,F6.3)
RETURN
C
101 WRITE(6,601)
601 FORMAT(1H ,(STOPPED AT NR 101)')
GO TO 1000
102 WRITE(6,602)
602 FORMAT(1H ,(STOPPED AT NR 102)')
GO TO 1000
103 WRITE(6,603)
603 FORMAT(1H ,(STOPPED AT NR 103)')
1000 ILL = 999
RETURN
C
END
C --- SUBROUTINE SUB-PROGRAM RR ***
C
SUBROUTINE RR(MACHS,THETA,MACH0,PRS0,TMP0,PHIO,MACH1,PRSI,TMP1,PHI01,PHI12,MACH2,PRS2,TMP2,DISP,ISOL,IOUT,ILL)
DIMENSION T(3)
REAL MACHS,MACH0,MACH1,MACH2
Q2 = 0.017453293
FACT = 0.01*Q2
C --- SET INITIAL VALUE FOR PHII ---
MACH0 = MACHS/COS(THETA)
PHIO = 90.0*Q2-THETA
CALL SVFS(MACH0,PRS0,TMP0,PHIO,MACH1,PRSI,TMP1,PHI01,1,ILL,1)
IF(ILL.NE.0) GO TO 101
CALL MAXTHE(MACH1,PRSI,TMP1,PHI01,THETA,MACH2,PRS2,TMP2,ILL)
IF(ILL.NE.0) GO TO 102
THETAI = PHIO-PHI01
PHEI = THETA/Q2
PTHEM = THETA/Q2
PDISP = DISP/Q2
ILL = 100
IF(IOUT.EQ.0) RETURN
WRITE(6,610) PHEI,PTHEM,PDISP
RETURN
C
5 PHEI = PHI01-2.0*Q2
STEP = 0.3*Q2

```



```

PHI1 = APHI1(2)
CALL SVFS(MACH0, PRS0, TMP0, PHIO, MACH1, PRS1, TMP1, PHI01, 1, ILL, 1)
CALL SVFS(MACH1, PRS1, TMP1, PH11, MACH2, PRS2, TMP2, PHI12, 1, ILL, 2)
THETW0 = 90.0*Q2-PHI0
RETURN

```

```

C 40 PHIO = 90.0*Q2-THETW0
MACHX = THEMIN

```

```

C --- SET INITIAL VALUE FOR MACHS ---

```

```

C TM = 1.2/SIN(PHI0)
TMF = TM
STEP = 0.03/SIN(PHI0)
K = 0

```

```

C --- START THE ITERATION ---

```

```

C 50 IF((TM-STEP)*SIN(PHI0).GT.1.0) GO TO 51
STEP = (TMF-1.0/SIN(PHI0))*0.4

```

```

C TM = 1.0/SIN(PHI0)+1.1*STEP

```

```

C 51 IF(TM+STEP.LT.MACHX/SIN(PHI0)) GO TO 52
STEP = (MACHX/SIN(PHI0)-TMF)*0.4

```

```

C TM = MACHX/SIN(PHI0)-1.1*STEP

```

```

C 52 TMF = TM

```

```

C DO 60 I = 1,3

```

```

C TM = TM*(1-2)*STEP

```

```

C CALL SVFS(TM, PRS0, TMP0, PHIO, MACH1, PRS1, TMP1, PHI01, 1, ILL, 1)

```

```

C IF(ILL.NE.0) GO TO 101

```

```

C CALL MAXTHE(MACH1, PRS1, TMP1, PH11, THETAM, MACH2, PRS2, TMP2, ILL)

```

```

C IF(ILL.NE.0) GO TO 102

```

```

C T(1) = THETAM-(PHIO-PHI0)

```

```

C APHI1(1) = PHI1

```

```

C 60 CONTINUE

```

```

C IF(ABS(T(2)).LT.FACT02) GO TO 70

```

```

C IF((T(3)-T(1)).EQ.0.0) GO TO 65

```

```

C TM = TM+STEP*2.0*(2)/(T(1)-T(3))

```

```

C STEP = ABS(STEP*2.0*(2)/(T(1)-T(3)))

```

```

C 65 STEP = 0.30*STEP

```

```

C IF(STEP.GT.0.2) GO TO 104

```

```

C K = K+1

```

```

C IF(K.GT.25) GO TO 103

```

```

C GO TO 50

```

```

C 70 ILL = 0

```

```

C MACH0 = TM

```

```

C MACHS = TM*SIN(PHI0)

```

```

C PHI1 = APHI1(2)

```

```

C CALL SVFS(MACH0, PRS0, TMP0, PHIO, MACH1, PRS1, TMP1, PHI01, 1, ILL, 1)

```

```

C CALL SVFS(MACH1, PRS1, TMP1, PH11, MACH2, PRS2, TMP2, PHI12, 1, ILL, 2)

```

```

C RETURN

```

```

C 101 WRITE(6,602)

```

```

C 602 FORMAT(1E, '(STOPPED AT REHR 101)')

```

```

C GO TO 1000

```

```

102 WRITE(6,603)
603 FORMAT(1E, '(STOPPED AT REHR 102)')
GO TO 1000
103 WRITE(6,604)
604 FORMAT(1E, '(STOPPED AT REHR 103)')
GO TO 1000
104 WRITE(6,608)
608 FORMAT(1E, '(STOPPED AT REHR 104)')
1000 ILL = 999

```

```

RETURN

```

```

END

```

```

C --- SUBROUTINE SUB-PROGRAM SIMMR ---

```

```

SUBROUTINE SIMMR(NUM,MACHS,PRS0,TMP0,PTHWP)

```

```

REAL MACH0,MACHS,MACH1,MACH2,MACH3,MACHX,MA(3)

```

```

DOUBLE PRECISION ALPHA,BETA,GO,DPI,DP2,DP3,DT1,DT2,DT3,PRO,DR1,

```

```

IDR2,DR3,DA1,DA2,DA3,DPR,DTM,AS

```

```

DIMENSION PR(3),TM(3),PH(3),TH(3),IST(3),VRL(3)

```

```

COMMON IREAL,IGAS,GO,ALPHA,BETA,IP,IQ

```

```

COMMON /CI/SLIP

```

```

COMMON /ST/ISTAT0,ISTAT1,ISTAT2,ISTAT3,ISTAT4,ISTAT5

```

```

C Q1 = 13.6*9.806

```

```

C Q2 = 0.017453293

```

```

C SLIP = 0.0

```

```

C ALPHA = 0.0

```

```

C BETA = 0.0

```

```

C L=0

```

```

C IF(IQ.EQ.1) GO TO 5

```

```

C IQ = 0, THETA WALL AS THE PARAMETER

```

```

C PTHW=PTHWP

```

```

C THETAW=PTHW*Q2

```

```

C CALL NR(MACHS,PRS0,TMP0,THEMIN,1,0,ILL)

```

```

C CALL TRPLI(THETAW,MACHS,PRS0,TMP0,CHI,PHI,MACH2,MACHX,PHIK,

```

```

ITHEMIN,DELTA,PHI3,CHIP,2,ILL)

```

```

C GO TO 55

```

```

C IQ = 1, THETA WALL PRIME AS THE PARAMETER

```

```

C THEWP=PTHWP*Q2

```

```

C CALL NR(MACHS,PRS0,TMP0,THEMIN,1,0,ILL)

```

```

C CALL RMR(MACHS,MACH0,PRS0,TMP0,PHIO,MACH1,PRS1,TMP1,PHI01,

```

```

IMACH2,PRS2,TMP2,PHI1,PHI12,THETW0,THEMIN,0.0,K,1,ILL)

```

```

C THETW1=2.*Q2

```

```

C THETW3=THETW0

```

```

C CALL TRPLI(THETW1,MACHS,PRS0,TMP0,CHI1,PHI,MACH2,MACHX,PHIK,

```

```

ITHEMIN,DELTA,PHI3,CHIP,2,ILL)

```

```

C CALL TRPLI(THETW3,MACHS,PRS0,TMP0,CHI3,PHI,MACH2,MACHX,PHIK,

```

```

ITHEMIN,DELTA,PHI3,CHIP,2,ILL)

```

```

1 PCHI,PTHW,PCHIP,PDELTA,PMP,MACHK
WRITE(6,608) ISTAT1, ISTAT2, ISTAT3
WRITE(6,604) MACH1, MACH2, MACH3
WRITE(6,602) P1, P2, P3
WRITE(6,605) TMP1, TMP2, TMP3
WRITE(6,607) DR1, DR2, DR3
WRITE(6,610) DAI, DAA2, DAA3
WRITE(6,603) T1, T2, T3
WRITE(6,606) PH0, PH1, PH3
THEWPP=THETAW+CHIP
MA(1)=MACH1
MA(2)=MACH2
MA(3)=MACH3
PR(1)=PRS1
PR(2)=PRS2
PR(3)=PRS3
TM(1)=TMP1
TM(2)=TMP2
TM(3)=TMP3
PH(1)=PH0
PH(2)=PH1
PH(3)=PH3
TH(1)=T1
TH(2)=T2
TH(3)=T3
IST(1)=ISTAT1
IST(2)=ISTAT2
IST(3)=ISTAT3
DO 60 I=1,3
CALL VIB(IGAS,PR(1),TM(1),TAU)
DPR=PR(1)
DTM=TM(1)
60 CONTINUE
WRITE(6,609)(VRL(I),I=1,3)
CALL TRPL2(MACH1,PRS1,TMP1,PH11,PH101,THEWPP)
503 FORMAT(5X,'ILL IN TRPL1 IS NOT ZERO')
505 FORMAT(5X,'ITERATION MORE THAN 25 TIMES')
C 506 FORMAT(5X,THEWPP,THEW2 : ',2F10.5)
601 FORMAT(/,1H,'EXP=',I4.3X,'***** MR-SOLUTION AT MACHS=',F7.3,3X,
1'THETAW=',F6.2,3X,'ILL=',I3.3X,'REAL=',I2.3X,'IGAS=',I2,
23X,'P0=',F8.2,'(TORR)',3X,'T0=',
1F8.2,'(DEG)',3X,'RHO0=',F10.7,'(KG/M**3)',/9X
1'CHI=',F7.3,3X,'THETAW=',F6.2,3X,'CHIP=',F7.3,3X,'DELTA=',F8.3,
13X,'OMEGA PRIME=',F8.3,3X,'MACHK=',F7.3,
1//,9X,'** REGION **',9X,'1',11X,'2',
111X,3')
602 FORMAT(1H,10X,'PRESSURE',6X,3(F9.2,3X))
605 FORMAT(1H,10X,'TEMPERATURE',3X,3(F9.2,3X))
604 FORMAT(1H,10X,'MACH',11X,3(F7.3,5X))
603 FORMAT(1H,10X,'THETA',10X,3(F7.3,5X))
606 FORMAT(1H,10X,'PHI',12X,3(F7.3,5X))
607 FORMAT(1H,8X,'DENSITY (KG/M**3)',3(F10.7,2X))
608 FORMAT(1H,8X,'** STATE **',9X,11,11X,11,11X,11,1)

THEW1=THETW1+CHI1
THEW3=THETW3+CHI3
THEW2=0.5*(THEW1+THEW3)
CALL TRPL1(THETW2,MACHS,PRS0,TMPO,CHI2,PHI,MACH2,MACHK,PHIK,
1THEMIN,DELTA,PHI3,CHIP,2,ILL)
THEW2=THEW2+CHI2
WRITE(6,506)THEWPP,THEW2
IF(ABS(THETW2-THEWPP).LT.0.1*Q2) GOTO 50
IF(THETWPP.GT.THEW2) GOTO 30
THEW3=THEW2
GOTO 40
30 THEW1=THEW2
40 THEW2=0.5*(THEW1+THEW3)
L=L+1
IF(L.GT.25) WRITE(6,505)
IF(L.GT.25) GOTO 60
GOTO 10
50 THETAW=THEW2
CHI=CHI2
PTHW=THETAW/Q2
55 IF(ILL.NE.0) WRITE(6,503)
IF(ILL.NE.0) GOTO 70
PCHI = CHI/Q2
PCHIP=CHIP/Q2
PTHWPP=PTHW+PCHI
PDELTA = DELTA/Q2
PWP = 90.0-(DELTA-THETAW-CHI)/Q2
PHI0 = 90.0*Q2-THEWPP-CHI
PHI3 = 90.0*Q2-CHI
PHI1 = PHI
MACH0 = MACHS/SIN(PHI0)
CALL SVFS(MACH0,PRS0,TMPO,PHI0,MACH1,PRS1,TMP1,PHI01,2,ILL,1)
CALL SVFS(MACH1,PRS1,TMP1,PHI1,MACH2,PRS2,TMP2,PHI12,2,ILL,2)
CALL SVFS(MACH0,PRS0,TMPO,PHI3,MACH3,PRS3,TMP3,PHI33,2,ILL,3)
DP1= PRS1
DP2= PRS2
DP3= PRS3
DT1= TMP1
DT2= TMP2
DT3= TMP3
CALL GAS(PRS0,TMPO,DIM,DR0,DUM,DUM,DUM,ISTATO)
CALL GAS(DP1,DT1,DUM,DR1,DUM,DA1,DUM,ISTAT1)
CALL GAS(DP2,DT2,DUM,DR2,DUM,DA2,DUM,ISTAT2)
CALL GAS(DP3,DT3,DUM,DR3,DUM,DA3,DUM,ISTAT3)
P1 = PRS1/Q1
P2 = PRS2/Q1
P3 = PRS3/Q1
T1 = (PHI0-PHI01)/Q2
T2 = (PHI1-PHI12)/Q2
T3 = (PHI3-PHI33)/Q2
PH0 = PHI0/Q2
PH1 = PH1/Q2
PH3 = PH3/Q2
PRS0= PRS0/Q1
WRITE(6,601)NUM,MACHS,PTHEWPP,ILL,IREAL,IGAS,PRS0,TMPO,DR0,

```

```

609 FORMAT(1H,'VIB. R.L.L.(MM) IN REGIONS 1, 2 & 3 = ',3(F10.4,2X))
610 FORMAT(1H,'SOUND SPEED',4X,3(F8.2,4X))
70 RETURN
END

C ----- SUBROUTINE SUB-PROGRAM SVFS ***
C
C
SUBROUTINE SVFS(SMACHI, SPRS1, STMPI, SPH11, SMACH2, SPRS2, STMP2, SPH12,
11C, ILL, IREGIN)
IMPLICIT REAL*8(A-H,M,O-R,T-Z)
DOUBLE PRECISION A3(3,2), A4(3,2)
COMMON IREAL, IGAS, GO, ALPHA, BETA, IP
COMMON /ST/ISTATO, ISTAT1, ISTAT2, ISTAT3, ISTAT4, ISTAT5
C IREGIN 1 FLOW REGIONS (0) & (1)
C IREGIN 2 FLOW REGIONS (1) & (2)
C IREGIN 3 FLOW REGIONS (0) & (3)
C IREGIN 4 FLOW REGIONS (1) & (4)
C IREGIN 5 FLOW REGIONS (2) & (5)
C IFORE FLOW STATE IN FRONT OF THE SHOCK WAVE
C IHIND FLOW STATE BEHIND THE SHOCK WAVE
C
MACHI = DBLE(SMACHI)
SPRS1 = DBLE(SPRS1)
TMP1 = DBLE(STMP1)
PHI1 = DBLE(SPH11)
ICOUNT=0
15 ICOUNT=ICOUNT+1
C DEFINE THE STATE OF FLOW
C IF(IREAL.EQ.2) GOTO 6
GOTO (1,2,3,4,5), IREGIN
C REGIONS (0) & (1)
C IFORE=ISTATO
C IHIND=ISTAT1
GOTO 7
C REGIONS (1) & (2)
C IFORE=ISTAT1
C IHIND=ISTAT2
GOTO 7
C REGIONS (0) & (3)
C IFORE=ISTATO
C IHIND=ISTAT3
GOTO 7
C REGIONS (1) & (4)
C IFORE=ISTAT1
C IHIND=ISTAT4
GOTO 7
C REGIONS (2) & (5)
C IFORE=ISTAT2
C IHIND=ISTAT5

```

```

GOTO 7
ALREADY DEFINED VIB. EQUILIBRIUM
IFORE=1
IHIND=1
RR = 8.3201D3
FACT11 = 1.0D-5
IF(1C.EQ.2) FACT11 = FACT11*DCOS(PHI1)**2/1.51M
IF(DABS(PHI1)-1.57079632).LT.1.0D-7) PHI1 = 1.:707963
CALL GAS(PRS1, TMPI, GMM1, RH01, H1, A1, MASS, IFORE)
U1 = MACHI*A1
C1 = RH01*DTAN(PHI1)
C2 = RH01*U1*DSIN(PHI1)
C3 = PRS1+RH01*U1**2*DSIN(PHI1)**2
C4 = H1+0.5*U1**2*DSIN(PHI1)**2
CC = C3**2-2.*C2**2+C4*(GMM1**2-1.0)/(GMM1**2
IF(CC.LE.0.0D0) CC = 0.0D0
TRHO = (C3+DSQRT(CC))/(2.*C4*(GMM1-1.0)/(GMM1)
TPRS = C3-C2**2/TRHO
TPRS = TPRS/TRHO/RR*MASS
TSTEP = 0.3*TMP
PSTEP = 0.2*TPRS
K = 0
C --- START ITERATION ---
10 DO 20 I = 1,3
DO 30 J = 1,2
TP = TPRS*(I-2)*(2-J)*PSTEP
TT = TTMP*(I-2)*(J-1)*TSTEP
CALL GAS(TP, TT, TGM, TRHO, TH, TA, MASS, IHIND)
A3(I,J) = (C3-C2**2/TRHO-TP)/C3
A4(I,J) = (C4-0.5*C2**2/TRHO**2-TH)/C4
30 CONTINUE
20 CONTINUE
C IF(DABS(A3(2,1)).LT.FACT11.AND.DABS(A4(2,1)).LT.FACT11) GO TO 40
IF(K.GE.25) GO TO 50
C
C
B1 = (A3(3,1)-A3(1,1))/FSTEP/2.0
B2 = (A4(3,1)-A4(1,1))/FSTEP/2.0
A1 = (A3(3,2)-A3(1,2))/TSTEP/2.0
A2 = (A4(3,2)-A4(1,2))/TSTEP/2.0
B3 = (A1*A4(2,1)-A2*A3(2,1))/BB
TS = (B1*A4(2,1)-B2*A3(2,1))/BB
IF(DABS(P3/TPRS).GT.0.2) P3 = TPRS*0.2*PS/DABS(P3)
IF(DABS(TS/TMP).GT.0.2) TS = TMP*0.2*TS/DABS(TS)
TPRS = TPRS-PS
TMP = TMP+TS
PSTEP = 0.3*DABS(P3)
TSTEP = 0.3*DABS(TS)
K = K+1
GO TO 10

```



```

COMMON /CL/SLIP,EPSLN
COMMON /ST/ISTAT0,ISTAT1,ISTAT2,ISTAT3,ISTAT4,ISTAT5

C      FACT1 = 1.0E-4
C      FACT2 = 1.0E-4
C      Q2 = 0.017453293

C      --- SET INITIAL VALUE FOR CHI AND PHII ---
C
C      CALL INTL(PRSO,TMPO,THEIAW,MACHS,TCHI,CSTEP,TPH1,PSTEP)
C      TCHI = TCHI*EPSLN
C      TPH1 = TPH1*EPSLN
C      IF(TCHI-CSTEP.IT.THEMIN-THEIAW) TCHI = THEMIN-THEIAW+CSTEP*1.1
C      TCHIF = TCHI
C      MACHO = MACHS/SIN(90.0*Q2-THEIAW-TCHI+CSTEP)
C      CALL SVFS(MACHO,PRS0,TMPO,90.0*Q2-THEIAW-TCHI+CSTEP,MACHI,PRS1,TPM
C      11,PHI01,2,ILL,1)
C      IF(ILL.NE.0) GO TO 105
C      IF(.NCHI*SIN(TPH1-PSTEP).IT.1.0) TPH11 = ASIN(1.0/MACHI)+1.1*PST
C      IEP
C      TPH11F = TPH11
C      K = 0
C
C      --- START ITERATION ---
C
C      10 IF(TCHI-CSTEP.GT.THEMIN-THEIAW+0.02*Q2.AND.TCHI-CSTEP.GT.0.0) GO 1
C      10 11
C      CSTEP = 0.3*(TCHIF-AMAXI(THEMIN-THEIAW+0.02*Q2,0.0))
C      TCHI = 1.2*CSTEP+AMAXI(THEMIN-THEIAW+0.02*Q2,0.0)
C      TCHIF = TCHI
C      11 MACHO = MACHS/SIN(90.0*Q2-THEIAW-TCHI+CSTEP)
C      CALL SVFS(MACHO,PRS0,TMPO,90.0*Q2-THEIAW-TCHI+CSTEP,MACHI,PRS1,TPM
C      11,PHI01,2,ILL,1)
C      IF(ILL.NE.0) GO TO 104
C      IF(TPH11.GT.90.0*Q2) GO TO 12
C      IF(MACHI*SIN(TPH11-PSTEP).GT.1.0) GO TO 14
C      PSTEP = 0.4*ABS(TPH11F-ASIN(1.0/MACHI))
C      TPH11 = ASIN(1.0/MACHI)+PSTEP*1.1
C      TPH11F = TPH11
C      GO TO 14
C      12 IF(TPH11+PSTEP.GT.180.0*Q2-PHI01) TPH11 = 180.0*Q2-PHI01-PSTEP*1.1
C      IF(MACHI*SIN(TPH11+PSTEP).GT.1.0) GO TO 14
C      PSTEP = 0.4*ABS(180.0*Q2-ASIN(1.0/MACHI))-TPH11F
C      TPH11 = 180.0*Q2-ASIN(1.0/MACHI)-PSTEP*1.1
C      14 IF(TPH11.GT.124.0*Q2) TPH11 = 100.0*Q2
C      TPH11F = TPH11
C      DO 20 I = 1,3
C      DO 30 J = 1,2
C      IF(I+J.EQ.4) GO TO 30
C      TC = TCHI+(1-2)*(2-J)*CSTEP
C      TP = TPH11+(1-2)*(J-1)*PSTEP
C      PHIO = 90.0*Q2-(THEIAW+TC)
C      MACHO = MACHS/SIN(PHIO)
C      PHI3 = 90.0*Q2-TC+EPSLN
C      CALL SVFS(MACHO,PRS0,TMPO,PHIO,MACHI,PRS1,TPM1,PHI01,2,ILL,1)
C      IF(ILL.NE.0) GO TO 101

```

```

C      50 ILL = 999
C      RETURN
C
C      40 ILL = 0
C      PRS2 = TPRS
C      TMP2 = TMP
C      CALL GAS(PRS2,TMP2,CMM2,RHO2,H2,A2,MASS,IHND)
C      PHI2 = DATAN(CI/RHO2)
C      IF(CL.IT.0.0) PHI2 = PHI2+3.14159265359
C      U2 = C2/RHO2/DSIN(PHI2)
C      MACH2 = U2/A2
C      IP = 1, THERMODYN. STATES ARE AS GIVEN
C      IP = 2, THERMODYN. STATES ARE TO BE DETERMINED BY THE PROGRAM
C      IF(ICOUNT.EQ.IP) GOTO 1050
C
C      DEFINE THE STATE OF THE FLOW REGION
C      CALL VIB(IGAS,PRS2,TMP2,TAU)
C      V2=U2*DSIN(PHI2)
C      VRL=TAU*V2*1.D-06
C      IF(IP.EQ.2.AND.VRL.GT.0.001) GOTO 1025
C
C      FOR VIB. EQUILIBRIUM
C      IF(IREGIN.EQ.1) ISTAT1=1
C      IF(IREGIN.EQ.2) ISTAT2=1
C      IF(IREGIN.EQ.3) ISTAT3=1
C      IF(IREGIN.EQ.4) ISTAT4=1
C      IF(IREGIN.EQ.5) ISTAT5=1
C      GOTO 15
C
C      1050 RESET ISTATE IF NOT IN VIB. EQUILIBRIUM
C      IF(IREGIN.EQ.1) ISTAT1=0
C      IF(IREGIN.EQ.2) ISTAT2=0
C      IF(IREGIN.EQ.3) ISTAT3=0
C      IF(IREGIN.EQ.4) ISTAT4=0
C      IF(IREGIN.EQ.5) ISTAT5=0
C
C      SMACH2 = SNGL(MACH2)
C      SPRS2 = SNGL(PRS2)
C      STMP2 = SNGL(TMP2)
C      SPHI2 = SNGL(PHI2)
C      RETURN
C      END
C
C      --- SUBROUTINE SUB-PROGRAM TRPL1 ---
C
C      SUBROUTINE TRPL1(THEIAW,MACHS,PRS0,TMPO,CHI,PHI1,MACH2,MACHK,PHIK,
C      ITHETA,DELTA,PHI3,CHIP,IC,ILL)
C
C      REAL MACHS,MACHO,MACHI,MACH2,MACH3,MACHK
C      DIMENSION AP(3,2),AT(3,2),AM(3),APHI(3,3)
C      DOUBLE PRECISION DPRS(3,2),DTMP(3,2),DRHO0,DRHO1,DUM,DPRS0,DTMPO,D
C      LA0,DA2

```

```

CALL GAS(DPRS, P, P, DRH00, DIM, DUM, DUM, DUM, DUM, DUM, DUM, DUM, DUM)
RH00 = DRH00
RH01 = DRH01
AO = DAO
AZ = DAC
VZ1 = RHO0/RH01/SIN(THETA)
VZ2 = MACH2*AZ
MACHIP = MACH*SQRT(1.0+(VKTA/D)**2)
PHIK = ATAN(0.0-KR06/RH01)/(0.0+VKTA/D)**2
ITAN(TPH1+PHI1, 1, 1)
CHIP = 90.*Q2-THETA-M-PIK
WRITE(6, *) THETA, CHI, PHIK, CHIP
RETURN

```

```

101 WRITE(6, 601)
601 FORMAT(1H, '(STOPPED AT TRPL1 101)')
GO TO 1000
102 WRITE(6, 602)
602 FORMAT(1H, '(STOPPED AT TRPL1 102)')
GO TO 1000
103 WRITE(6, 603)
603 FORMAT(1H, '(STOPPED AT TRPL1 103)')
GO TO 1000
104 WRITE(6, 604)
604 FORMAT(1H, '(STOPPED AT TRPL1 104)')
GO TO 1000
105 WRITE(6, 605)
605 FORMAT(1H, '(STOPPED AT TRPL1 105)')
1000 ILL = 999
RETURN
END

```

```

C
C
C *** SUBROUTINE SUB-PROGRAM TRPL2 ***
C

```

```

SUBROUTINE TRPL2(MACH1, PRSI, TMP1, PHI1, PHIO1, THEMPP)
DOUBLE PRECISION DP2P, DP4, DP5, DT2P, DT4, DT5, GMM1, GMM2P, GMM4,
.GMM5, DR2P, DR4, DR5, DA1, DA2P, DA4, DA5, DPR, DTM, AS
REAL MACH1, MACHIP, MACH2P, MACH4, MACH5, MA(3)
DIMENSION AP(3,2), AT(3,2), AM(3), PR(3), TM(3), TH(3),
.IST(3), VRL(3)
COMMON IREAL, IGAS, GO, ALPHA, BETA
COMMON /SI/ISTAT0, ISTAT1, ISTAT2, ISTAT3, ISTAT4, JSTAT5
COMMON /GUESS/GT2, GT4

```

```

FACT1=1.0E-4
FACT2=1.0E-4
Q1=13.6*9.806
Q2=0.017453293

```

```

PHIP=PHI1+PHIO1
MACHIP=MACH1*(1.+SIN(PHI01)*SIN(PHI01))/(SIN(PHIP)*SIN(PHI1P))

```

```

CALL SVFS(MACH1, PRSI, TMP1, TP, MACH2, PRS2, TMP2, PRSI2, P, ILL, 2)
IF(ILL.NE.0) GO TO 102
CALL SVFS(MACH0, PRS0, TMP0, PHI0, MACH3, PRS3, TMP3, PHI33, 2, ILL, 3)
IF(ILL.NE.0) GO TO 103
AP(I, J) = (PRS3-PRS2)/PRS2
AT(I, J) = (PHI3-PHI33)-(PHIO-PHI01)*(TP-TH12)/SLIP
AM(I) = PRS0
DPRS0 = PRS0
DPRS(1,1) = PRSI
DPRS(1,2) = PRS2
DTMP0 = TMP0
DTMP(1,1) = TMP1
DTMP(1,2) = TMP2
APHI(1,1) = PHIO
APHI(1,2) = PHI01
APHI(1,3) = PHI02
30 CONTINUE
20 CONTINUE

```

```

IF(ABS(AP(2,1))-LT.FACT1.AND.ABS(AT(2,1))-LT.FACT2) GO TO 40
IF(K.GT.25) GO TO 50

```

```

IF((AP(3,2)-AP(1,2))*AT(3,2)-AT(1,2)).EQ.0.0) GO TO 42
B1 = (AP(3,1)-AP(1,1))/GSTEP/2.0
B2 = (AT(3,1)-AT(1,1))/GSTEP/2.0
A1 = (AP(3,2)-AP(1,2))/PSTEP/2.0
A2 = (AT(3,2)-AT(1,2))/PSTEP/2.0
BB = A1*B2-A2*B1
PP = (B1*AT(2,1)-B2*AP(2,1))/BB
IF(ABS(PP).GT.20.0*Q2) PP = 20.0*Q2*PP/ABS(PP)
TPH1F = TPH1
TPH1 = TPH1+PP
PSTEP = 0.3*ABS(PP)
CC = (A1*AT(2,1)-A2*AP(2,1))/BB
IF(ABS(CC).GT.10.0*Q2) CC = 5.0*Q2*CC/ABS(CC)
TCHF = TCHI
TCHI = TCHI-CC
CSTEP = ABS(CC)
GO TO 41

```

```

42 TCHF = TCHI
TCHI = TCHI+2.0*CSTEP*AT(2,1)/(AT(1,1)-AT(3,1))
CSTEP = 0.3*ABS(2.0*CSTEP*AT(2,1)/(AT(1,1)-AT(3,1)))
41 K = K+1
GO TO 10

```

```

C
50 ILL = 999
RETURN

```

```

C
40 ILL = 0
CHI = TCHI
PHI1 = TPH1
DELTA = 180.0*Q2-(APHI(2,2)+TPH1)
MACH2 = AM(2)
IF(IC.EQ.1) RETURN
CALL GAS(DPRS0, TMP0, DIM, DRH00, DIM, DAO, DIM, ISTAT0)
CALL GAS(DPRS(2,1), DTRP(2,1), DUM, DRH01, DUM, DUM, ISTAT1)

```

```

-2.*SIN(PHI01)*COS(PHI1)/SIN(PHI1P))*0.5
CALL SVFS(MACHP, PRS1, TMP1, PH1P, MACH2P, PRS2P, TMP2P, PH112P, 2,
.ILL, 2)
WRITE(6, 511)MACHIP
FORMAT(/ ' MACHP = ', F10.4)
IF(ILL.NE.0) GO TO 101
NOT DMR CASE
IF(MACH2P.LT.1.0) GOTO 1000

511
C
C SET INITIAL VALUES FOR PHI4 AND PH12
TPHI4=GT4*Q2
P4STEP=2.*Q2
TPHI2=GT2*Q2
P2STEP=2.*Q2
IF(MACH2P*SIN(TPHI2-P2STEP).LT.1.0) TPHI2=ASIN(1.0/MACH2P)
+.1.1*P2STEP
TPHI2F=TPHI2
TPHI4F=TPHI4
K=0

C START ITERATION
10 IF(TPHI4+P4STEP.GT.(PH1P-5.*Q2).AND.TPHI4+P4STEP.GT.0.0)GOTO 11
P4STEP=1.1*TPHI4F
TPHI4=1.2*TPHI4+P4STEP
TPHI4F=TPHI4
CALL SVFS(MACHIP, PRS1, TMP1, TPHI4, MACH4, PRS4, TMP4, PH114, 2, ILL, 4)
IF(ILL.NE.0) GO TO 102
IF(TPHI2.GT.90.*Q2) GO TO 12
IF(MACH2P*SIN(TPHI2-P2STEP).GT.1.0) GO TO 14
P2STEP=0.4*ABS(TPHI2F-ASIN(1.0/MACHIP))
TPHI2=ASIN(1.0/MACHIP)+P2STEP*1.1
TPHI2F=TPHI2
GO TO 14

12 IF(TPHI2+P2STEP.GT.180.*Q2-PHI12P) TPHI2=180.*Q2-PHI12P-P2STEP*1.1
IF(MACHIP*SIN(TPHI2+P2STEP).GT.1.0) GO TO 14
P2STEP=0.4*ABS(180.*Q2-ASIN(1.0/MACHIP)-TPHI2F)
TPHI2=180.*Q2-ASIN(1.0/MACHIP)-P2STEP*1.1
IF(TPHI2.GT.175.*Q2) TPHI2=175.*Q2
TPHI2F=TPHI2
DO 20 I=1,3
DO 30 J=1,2
IF(I=J.EQ.4) GO TO 30
TP4=TPHI4+(I-2)*(2-J)*P4STEP
TP2=TPHI2+(I-2)*(J-1)*P2STEP
PHI4=TP4
PHI2=TP2
CALL SVFS(MACH2P, PRS2P, TMP2P, PH2, MACH5, PRS5, TMP5, PH125, 2, ILL, 5)
IF(ILL.NE.0) GO TO 103
CALL SVFS(MACHIP, PRS1, TMP1, PH14, MACH4, PRS4, TMP4, PH114, 2, ILL, 4)
IF(ILL.NE.0) GO TO 104
AP(I, J)=(PRS4-PRS5)/PRS5
AT(I, J)=(PH14-PHI14)-(PH1P-PHI12P)+(TP2-PHI25)
AM(1)=MACH5
IF(I.NE.2) GOTO 30
IF(J.NE.1)GOTO 30

-2.*SIN(PHI01)*COS(PHI1)/SIN(PHI1P))*0.5
CALL SVFS(MACHP, PRS1, TMP1, PH1P, MACH2P, PRS2P, TMP2P, PH112P, 2,
.ILL, 2)
WRITE(6, 511)MACHIP
FORMAT(/ ' MACHP = ', F10.4)
IF(ILL.NE.0) GO TO 101
NOT DMR CASE
IF(MACH2P.LT.1.0) GOTO 1000

511
C
C SET INITIAL VALUES FOR PHI4 AND PH12
TPHI4=GT4*Q2
P4STEP=2.*Q2
TPHI2=GT2*Q2
P2STEP=2.*Q2
IF(MACH2P*SIN(TPHI2-P2STEP).LT.1.0) TPHI2=ASIN(1.0/MACH2P)
+.1.1*P2STEP
TPHI2F=TPHI2
TPHI4F=TPHI4
K=0

C START ITERATION
10 IF(TPHI4+P4STEP.GT.(PH1P-5.*Q2).AND.TPHI4+P4STEP.GT.0.0)GOTO 11
P4STEP=1.1*TPHI4F
TPHI4=1.2*TPHI4+P4STEP
TPHI4F=TPHI4
CALL SVFS(MACHIP, PRS1, TMP1, TPHI4, MACH4, PRS4, TMP4, PH114, 2, ILL, 4)
IF(ILL.NE.0) GO TO 102
IF(TPHI2.GT.90.*Q2) GO TO 12
IF(MACH2P*SIN(TPHI2-P2STEP).GT.1.0) GO TO 14
P2STEP=0.4*ABS(TPHI2F-ASIN(1.0/MACHIP))
TPHI2=ASIN(1.0/MACHIP)+P2STEP*1.1
TPHI2F=TPHI2
GO TO 14

12 IF(TPHI2+P2STEP.GT.180.*Q2-PHI12P) TPHI2=180.*Q2-PHI12P-P2STEP*1.1
IF(MACHIP*SIN(TPHI2+P2STEP).GT.1.0) GO TO 14
P2STEP=0.4*ABS(180.*Q2-ASIN(1.0/MACHIP)-TPHI2F)
TPHI2=180.*Q2-ASIN(1.0/MACHIP)-P2STEP*1.1
IF(TPHI2.GT.175.*Q2) TPHI2=175.*Q2
TPHI2F=TPHI2
DO 20 I=1,3
DO 30 J=1,2
IF(I=J.EQ.4) GO TO 30
TP4=TPHI4+(I-2)*(2-J)*P4STEP
TP2=TPHI2+(I-2)*(J-1)*P2STEP
PHI4=TP4
PHI2=TP2
CALL SVFS(MACH2P, PRS2P, TMP2P, PH2, MACH5, PRS5, TMP5, PH125, 2, ILL, 5)
IF(ILL.NE.0) GO TO 103
CALL SVFS(MACHIP, PRS1, TMP1, PH14, MACH4, PRS4, TMP4, PH114, 2, ILL, 4)
IF(ILL.NE.0) GO TO 104
AP(I, J)=(PRS4-PRS5)/PRS5
AT(I, J)=(PH14-PHI14)-(PH1P-PHI12P)+(TP2-PHI25)
AM(1)=MACH5
IF(I.NE.2) GOTO 30
IF(J.NE.1)GOTO 30

```

```

T2P=PH1P-PH12P
T4=PH14-P14
T5=PH12-P25
DELTA=180.*Q2-(PH101+PH11)
PSI=DELTA+PH1P+PH12-T2P-THEWPP-90.*Q2
SIGMA=90.*Q2+THEWPP+PH14-PH11P-DELTA
ETA=180.*Q2-(PH12+PH112P)
X1=180.*Q2+(PH1P-PH14)
WRITE(6,610)
WRITE(6,619) ISTAT2,ISTAT4,ISTAT5
WRITE(6,611)MACH2P,MACH4,MACH5
WRITE(6,612)P2P,P4,P5
WRITE(6,613)TMP2P,AT4,AT5
WRITE(6,614)DR2P,DR4,DR5
WRITE(6,618)DA2P,DA4,DA5
WRITE(6,615)T2P/Q2,T4/Q2,T5/Q2
WRITE(6,616)PH1P/Q2,PH14/Q2,PH12/Q2
WRITE(6,617)PSI/Q2,SIGMA/Q2,ETA/Q2,X1/Q2
MA(1)=MACH2P
MA(2)=MACH4
MA(3)=MACH5
PR(1)=PRS2P
PR(2)=AP4
PR(3)=AP5
TH(1)=TMP2P
TH(2)=AT4
TH(3)=AT5
PH(1)=PH1P/Q2
PH(2)=PH14/Q2
PH(3)=PH12/Q2
TH(1)=T2P/Q2
TH(2)=T4/Q2
TH(3)=T5/Q2
IST(1)=ISTAT2
IST(2)=ISTAT4
IST(3)=ISTAT5
DO 60 I=1,3
CALL VIB(IGAS,PR(1),TH(1),TAU)
DPR=PR(1)
DTH=TH(1)
CALL GAS(DPR,DTH,DUM,DUM,AS,DUM,IST(1))
V2=MA(1)*AS*SIN((PH(1)-TH(1))*3.14159/180.)
VRL(1)=TAU*V2*1.E-06*1000.
CONTINUE
60 WRITE(6,621)(VRL(1),I=1,3)
RETURN
C
101 WRITE(6,601)
601 FORMAT(' STOPPED AT TRPL2 101')
GO TO 1000
102 WRITE(6,602)
602 FORMAT(' STOPPED AT TRPL2 102')
GO TO 1000
103 WRITE(6,603)
603 FORMAT(' STOPPED AT TRPL2 103')
GO TO 1000

```

```

104 WRITE(6,604)
604 FORMAT(' STOPPED AT TRPL2 104')
610 FORMAT(/3X,'SECOND TRIPLE POINT: '//10X,'** REGION **',9X,2H2',
.10X,'4',11X,'5')
611 FORMAT(1H,10X,'MACH',10X,3(F8.4,4X))
612 FORMAT(1H,10X,'PRESSURE',5X,3(F10.2,2X))
613 FORMAT(1H,10X,'TEMPERATURE',2X,3(F10.2,2X))
614 FORMAT(1H,8X,'DENSITY (KG/M**3)',3(F10.7,2X))
615 FORMAT(1H,10X,'THETA',10X,3(F7.3,5X))
616 FORMAT(1H,10X,'PHI',12X,3(F7.3,5X))
617 FORMAT(/11X,'PSI = ',F7.2,3X,'SIGMA = ',F7.2,3X,'ETA = ',F7.3,
3X,'X1 = ',F7.3)
618 FORMAT(1H,10X,'SOUND SPEED',2X,3(F10.2,2X))
619 FORMAT(1H,9X,'** STATE **',9X,11,11X,11,11X,11,11)
621 FORMAT(7X,'VIB. R.I.(MP) IN REGIONS 2, 4 & 5 = ',3(F10.4,2X))
1000 ILL=999
RETURN
END

```

```

C -----
C *** SUBROUTINE SUB-PROGRAM VIB ***
C -----

```

```

SUBROUTINE VIB(IGAS,PRS,TMP,TAU)
IMPLICIT REAL*8(A-H,O-Z)
DEFINE THE STATE OF FLOW
GOTO (100,200,300,400,500,600,700),IGAS
AIR (N2 IN AIR) REF. [WHITE & MILLIKAN]
100 TAU=10.**(-213.5973*TMP**(-2./3.)+82.3374*TMP**(-1./3.)
1-9.0463)*1.E+06/PRS*101325.
C TAU=(2.9D-04*DEXP(126.*TMP**(-1./3.))
C 1+6.22D-05*DEXP(202.*TMP**(-1./3.)))*1./PRS*101325.
RETURN
C NITROGEN
200 TAU=(6.22D-05*DEXP(202.*TMP**(-1./3.)))*1./PRS*101325.
RETURN
C ARGON
300 TAU=9999.
RETURN
C CARBON DIOXIDE
400 TAU=DEXP(36.5*TMP**(-1./3.)-3.9)*1./PRS*101325.
RETURN
C SULPHUR HEXAFLUORIDE (SF6)
500 TAU=2.92D-03*DEXP(38.*TMP**(-1./3.)))*1./PRS*101325.
RETURN
C GAMMA = 1.3333
600 TAU=9999.
RETURN
C ONLY OXYGEN IS EXCITED IN AIR -- REF. [BLACKMAN, VINCENTI]
700 TAU=2.92D-04*DEXP(126.*TMP**(-1./3.))/0.527*101325./PRS
RETURN
END
C *****

```

UTIAS Report No. 283

Institute for Aerospace Studies, University of Toronto (UTIAS)
4925 Battershall Street, Downsview, Ontario, Canada, M3H 5T6

TABULAR AND GRAPHICAL SOLUTIONS OF REGULAR AND MACH REFLECTIONS
IN PSEUDO-STATIONARY FROZEN AND VIBRATIONAL-EQUILIBRIUM FLOWS

Hu, T. C. J. and Shirouzu, M.

1. Oblique-shock-wave reflections
2. Regular reflection
3. Mach reflection
4. Numerical and graphical solutions
5. Frozen and equilibrium flows

I. Hu, T. C. J., Shirouzu, M. II. UTIAS Report No. 283

Flow properties of pseudo-stationary oblique-shock-wave reflections are given as solutions of two-shock and three-shock theories. The calculations were performed for Ar, air, CO_2 and SF_6 using both frozen and vibrational equilibrium gas assumptions. The flow properties are tabulated for initial shock Mach numbers $1.2 < M_0 < 10.0$ and wedge angles $1^\circ < \theta_0 < 85^\circ$. The flow properties are plotted as a function of the incident shock Mach number for a series of wedge angles for both regular and Mach reflections. Another set of graphs is presented for Mach reflection with the flow properties plotted against the effective wedge angle θ_0 for a series of shock Mach numbers. The latter set is used when the effective wedge angle is chosen as the parameter for comparison. The second triple-point system, which exists only in double-Mach reflection, is solved numerically for the first time, and the solutions are presented both in tabular and graphical forms. The tables and graphs are designed to serve the analyst and experimenter working on oblique-shock-wave reflections.

Available copies of this report are limited. Return this card to UTIAS, if you require a copy.

UTIAS Report No. 283

Institute for Aerospace Studies, University of Toronto (UTIAS)
4925 Battershall Street, Downsview, Ontario, Canada, M3H 5T6

TABULAR AND GRAPHICAL SOLUTIONS OF REGULAR AND MACH REFLECTIONS
IN PSEUDO-STATIONARY FROZEN AND VIBRATIONAL-EQUILIBRIUM FLOWS

Hu, T. C. J. and Shirouzu, M.

1. Oblique-shock-wave reflections
2. Regular reflection
3. Mach reflection
4. Numerical and graphical solutions
5. Frozen and equilibrium flows

I. Hu, T. C. J., Shirouzu, M. II. UTIAS Report No. 283

Flow properties of pseudo-stationary oblique-shock-wave reflections are given as solutions of two-shock and three-shock theories. The calculations were performed for Ar, air, CO_2 and SF_6 using both frozen and vibrational equilibrium gas assumptions. The flow properties are tabulated for initial shock Mach numbers $1.2 < M_0 < 10.0$ and wedge angles $1^\circ < \theta_0 < 85^\circ$. The flow properties are plotted as a function of the incident shock Mach number for a series of wedge angles for both regular and Mach reflections. Another set of graphs is presented for Mach reflection with the flow properties plotted against the effective wedge angle θ_0 for a series of shock Mach numbers. The latter set is used when the effective wedge angle is chosen as the parameter for comparison. The second triple-point system, which exists only in double-Mach reflection, is solved numerically for the first time, and the solutions are presented both in tabular and graphical forms. The tables and graphs are designed to serve the analyst and experimenter working on oblique-shock-wave reflections.

Available copies of this report are limited. Return this card to UTIAS, if you require a copy.

UTIAS Report No. 283

Institute for Aerospace Studies, University of Toronto (UTIAS)
4925 Battershall Street, Downsview, Ontario, Canada, M3H 5T6

TABULAR AND GRAPHICAL SOLUTIONS OF REGULAR AND MACH REFLECTIONS
IN PSEUDO-STATIONARY FROZEN AND VIBRATIONAL-EQUILIBRIUM FLOWS

Hu, T. C. J. and Shirouzu, M.

1. Oblique-shock-wave reflections
2. Regular reflection
3. Mach reflection
4. Numerical and graphical solutions
5. Frozen and equilibrium flows

I. Hu, T. C. J., Shirouzu, M. II. UTIAS Report No. 283

Flow properties of pseudo-stationary oblique-shock-wave reflections are given as solutions of two-shock and three-shock theories. The calculations were performed for Ar, air, CO_2 and SF_6 using both frozen and vibrational equilibrium gas assumptions. The flow properties are tabulated for initial shock Mach numbers $1.2 < M_0 < 10.0$ and wedge angles $1^\circ < \theta_0 < 85^\circ$. The flow properties are plotted as a function of the incident shock Mach number for a series of wedge angles for both regular and Mach reflections. Another set of graphs is presented for Mach reflection with the flow properties plotted against the effective wedge angle θ_0 for a series of shock Mach numbers. The latter set is used when the effective wedge angle is chosen as the parameter for comparison. The second triple-point system, which exists only in double-Mach reflection, is solved numerically for the first time, and the solutions are presented both in tabular and graphical forms. The tables and graphs are designed to serve the analyst and experimenter working on oblique-shock-wave reflections.

Available copies of this report are limited. Return this card to UTIAS, if you require a copy.

UTIAS Report No. 283

Institute for Aerospace Studies, University of Toronto (UTIAS)
4925 Battershall Street, Downsview, Ontario, Canada, M3H 5T6

TABULAR AND GRAPHICAL SOLUTIONS OF REGULAR AND MACH REFLECTIONS
IN PSEUDO-STATIONARY FROZEN AND VIBRATIONAL-EQUILIBRIUM FLOWS

Hu, T. C. J. and Shirouzu, M.

1. Oblique-shock-wave reflections
2. Regular reflection
3. Mach reflection
4. Numerical and graphical solutions
5. Frozen and equilibrium flows

I. Hu, T. C. J., Shirouzu, M. II. UTIAS Report No. 283

Flow properties of pseudo-stationary oblique-shock-wave reflections are given as solutions of two-shock and three-shock theories. The calculations were performed for Ar, air, CO_2 and SF_6 using both frozen and vibrational equilibrium gas assumptions. The flow properties are tabulated for initial shock Mach numbers $1.2 < M_0 < 10.0$ and wedge angles $1^\circ < \theta_0 < 85^\circ$. The flow properties are plotted as a function of the incident shock Mach number for a series of wedge angles for both regular and Mach reflections. Another set of graphs is presented for Mach reflection with the flow properties plotted against the effective wedge angle θ_0 for a series of shock Mach numbers. The latter set is used when the effective wedge angle is chosen as the parameter for comparison. The second triple-point system, which exists only in double-Mach reflection, is solved numerically for the first time, and the solutions are presented both in tabular and graphical forms. The tables and graphs are designed to serve the analyst and experimenter working on oblique-shock-wave reflections.

Available copies of this report are limited. Return this card to UTIAS, if you require a copy.

END

FILMED

4-86

DTIC